DISS. ETH NO. 23711

I. Total Synthesis of Pallambins A and B
II. Ti(III)-Mediated Regioselective Epoxide Opening
III. Synthesis of Raman-Active Epoxyisoprostane Analogs

A dissertation submitted to

ETH ZURICH

for the degree of

DOCTOR OF SCIENCES

presented by

CHRISTIAN EBNER

M.Sc. ETH Zurich

born on 05.05.1988

Citizen of the Federal Republic of Germany

Accepted on the recommendation of

Prof. Dr. Erick M. Carreira, examiner

Prof. Dr. Karl-Heinz Altmann, co-examiner

2016

Acknowledgements

I am grateful to Prof. Dr. ERICK M. CARREIRA for supervising my graduate studies. I am indebted to him for his constant trust in me and the projects I was working on as well as the scientific freedom I enjoyed during the last four years. I want to thank him for entrusting me with the organization of lectures, exercises and exams as well as with the *Synfacts* team. His constructive and critical input provided the basis for the success of my graduate studies.

I would like to express my sincere gratitude to Prof. Dr. KARL-HEINZ ALTMANN for accepting the co-examination of my thesis. His valuable comments and corrections are highly appreciated.

A special thank goes to the proofreaders of this thesis, Dr. HANNES ZIPFEL, MATTHIAS WESTPHAL, STEFAN FISCHER, ADRIEN JOLITON, JOHANNES BOSHKOW and SARA DA ROS for their effort and time to thoroughly proofread this manuscript. Their suggestions, comments and corrections substantially improved my thesis.

I am grateful to my chemistry mentors, Dr. TINA VOCI, Dr. STEFAN DIETHELM and Dr. CHRISTIAN NILEWSKI for their constant effort to teach me invaluable experimental and theoretical skills, for their time and patience and all their enthusiasm during my education.

Furthermore, I want to thank Dr. SÉBASTIEN GOUDREAU, Dr. NIKOLAS HUWYLER, Dr. SIMON BREITLER, ADRIEN JOLITON, STEFAN FISCHER, LEONARDO NANNINI and MICHAEL IMHOF of the I. B. in G338 for the fantastic time we spent together. I cannot express how important it was to me to be able to work with such an outstanding group of people over the last four years. Your support and friendship is invaluable to me.

Additionally, I want to thank all past and present members of the *Carreira* group. It was highly inspiring for me to collaborate with such talented, friendly and helpful people. The scientific environment in this group is inimitable. I highly appreciated that there was always an open ear and helpful advice for every chemical problem I had over the time. Special thanks goes to Prof. Dr. DAVID SARLAH for all his time, enthusiasm and valuable advice. Furthermore, I want to thank STEFAN FISCHER, ADRIEN JOLITON, LEONARDO NANNINI, MARCO BRANDSTÄTTER, Dr. ERIK DA FUNDER, Prof. Dr. DAVID SARLAH, ANDREJ SHEMET, JOHANNES BOSHKOW, Dr. HANNES ZIPFEL and MATTHIAS WESTPHAL for the amazing time outside the lab during the *Wine-Hikes*, the *Yugo-Trips*, the *Munich-Soccer-Trips* and all the numerous awesome nights we spent together.

I consider myself fortunate that I was allowed to supervise ALEXANDRA EBERLE during her three-year apprenticeship as a laboratory technician. I want to thank her not only for the valuable synthetic support but also for her unique character with which she was able to cheer up all our moods in G338. I am sure no matter how much she thinks she learned from me, I have certainly learned more from her.

ANKE KLEINT is acknowledged for taking care of organizational and administrative issues.

This thesis would have never been possible without the excellent infrastructure at ETH Zurich. Accordingly, I want to thank the MS service with LOUIS BERTSCHI, OSWALD GRETER, ROLF HÄFLIGER and Dr. XIANGYANG ZHANG, the NMR service with RENÉ ARNOLD, RAINER FRANKENSTEIN, PHILIPP ZUMBRUNNEN, STEPHAN BURKHARDT and Dr. MARC-OLIVER EBERT and the SMoCC-team with Dr. NILS TRAPP and MICHAEL SOLAR. Furthermore, I am thankful to the whole *Schalter*- and *Entsorgungs* team.

Vorrei ringraziare la famiglia Stra per la loro incredibile ospitalità e iminensa generosità. Il tempo trascorso a Novello mi ha sempre dato nuovo forze – Grazie mille.

Besonders möchte ich mich bei PHILIP JÜTTNER für die tiefe Freundschaft der letzten 16 Jahre bedanken. Immer wenn mir die Dinge während des Doktorats drohten über den Kopf zu wachsen konnte ich mich an dich wenden und mich wieder über das Schöne und Wesentliche im Leben freuen. Danke fürs Aufheitern, die zahlreichen Trainings, die vielen unvergesslichen Abende, die geniale Thailand-Reise und für die ganzen tollen Jahre – auf das noch viele Weitere folgen mein Freund.

Mein besonderer Dank gilt meinen Eltern. Erst eure bedingungslose Unterstützung und euer Glaube an mich, brachte mich an den Punkt an dem ich heute stehe – Danke!

Zuletzt möchte ich mich bei SARA DA ROS für die unglaublich schöne Zeit und die grenzenlose Unterstützung bedanken. Ich bin dankbar für deine Liebe und Zuneigung und freue mich auf unsere gemeinsame Zukunft. Ich liebe dich!

Publications

K. C. Nicolaou, C. R. H. Hale, C. Ebner, C. Nilewski, C. F. Ahles, D. Rhoades

Synthesis of Macroheterocycles through Intramolecular Oxidative Coupling of Furanoid β-Ketoesters

Angew. Chem. Int. Ed. **2012**, *51*, 4726-4730.

K. C. Nicolaou, C. Nilewski, C. R. H. Hale, C. F. Ahles, C. A. Chiu, C. Ebner, A. ElMarrouni, L. Yang, K. Stiles, D. Nagrath

Synthesis and Biological Evaluation of Dimeric Furanoid Macroheterocycles: Discovery of New Anticancer Agents

J. Am. Chem. Soc. **2015**, *137*, 4766-4770.

C. Ebner, E. M. Carreira

Pentafulvene for the Synthesis of Complex Natural Products: Total Syntheses of (±)-Pallambins A and B

Angew. Chem. Int. Ed. **2015**, *54*, 11227-11230.

Poster and Oral Presentations

Speaker at the 4th SSCI-Symposium

ETH Zurich, December 2013

Poster Contribution to the 5th SSCI-Symposium

ETH Zurich, January 2015

Poster Contribution to the Novartis-Day

ETH Zurich, September 2015

Table of Contents

Abstract vi

Zusammenfassung viii

List of Abbreviations, Acronyms and Symbols x

Part I Total Synthesis of Pallambins A and B 1

1 Introduction 3

1.1 Natural Products Isolated from *Pallavicinia* 3

1.2 Other Syntheses of *Pallavicinia* Terpenoids 7

2 Synthetic Strategy 17

2.1 General Considerations 17

2.2 Retrosynthetic Analysis 18

2.3 Conclusion 19

3 Results and Discussion 21

3.1 Fulvene as a Diene in Diels–Alder Reactions 21

3.2 C(3)-Ketone Formation and α-Functionalization 26

3.3 C(9)–C(10) Bond Formation 31

3.4 Cyclopropanation of the *endo* Olefin 39

3.5 Revision of the Synthetic Strategy 41

3.6 Selective Cyclopropanation and Hydrogenation 42

3.7 C(3)-Ketone Generation and Modified α-Functionalization 45

3.8 C(9)–C(10) Bond Formation *via* C–H Insertion 51

3.9 Stereoselective Functionalization of C(8) and C(9) 53

3.10 Elaboration of the Bromoisoxazoline 55

3.11 Alkoxycarbonylation and Completion of the Synthesis 62

4 Conclusion 67

Part II Regioselective Ti(III)-Mediated Epoxide Opening 71

5 Introduction 73

5.1 Established Methods for Reductive Epoxide Openings 73

6 Aim of the Project 81

6.1 Total Synthesis of Microcin SF608 81

6.2 Studies on the Origin of Selectivity 82

7 Results and Discussion 85

7.1 Substrate Design and Preparation 85
7.2 Exploration of the Substrate Scope 88

8 Conclusion 93

Part III Synthesis of Raman-Active Epoxyisoprostane Analogs 95

9 Introduction 97

9.1 Investigation of the Role of Oxidized Phospholipids in Inflammatory Diseases 97

10 Aim of the Project 103

10.1 Mode of Action of EC and CycloEC 103
10.2 Imaging of Alkyne-Tagged Biomolecules in Living Cells by Raman Spectroscopy 104
10.3 Conclusion 107

11 Synthetic Strategy 109
12 Results and Discussion 111

12.1 Synthesis of PDEC and PDCycloEC 111
12.2 Conclusion and Outlook 113

Part IV Experimental Section 115

13 Experimental Procedures 117

13.1 General Methods 117
13.2 Chemicals 117
13.3 Analytics 118
13.4 Experimental Procedures 119
13.5 X-Ray Chrystallographic Data 177
13.6 NMR Spectra 201

Abstract

In 2012, the two cyclopropane-containing diterpenoids pallambins A (**I**) and B (**II**) were isolated by LOU and co-workers from the Chinese liverwort *Pallavicinia ambigua* (Figure I). Additionally, the structurally related pallambins C (**III**) and D (**IV**) were also present in the extracts. Pallambins A (**I**) and B (**II**) are endowed with thus far unprecedented tetracyclo[4.4.0^{3,5}.0^{2,8}]decane core structures, embedding cyclopropanes in a sterically encumbered environment. Furthermore, these natural products possess ten contiguous stereocenters, two of which are quaternary. These challenging structural aspects render pallambins A and B intriguing targets for total synthesis. The first part of this thesis describes the development of a synthetic strategy, which ultimately culmintated in the first total synthesis of **I** and **II**.

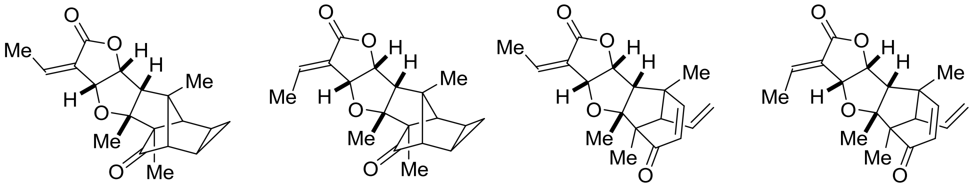

pallambin A (**I**) pallambin B (**II**) pallambin C (**III**) pallambin D (**IV**)

Figure I: Structures of pallambins A-D (**I-IV**) isolated by LOU and co-workers.

Due to the challenges associated with the preparation of the highly congested tetracyclic core of the pallambins A and B, our synthetic strategy focused on the development of an efficient entry towards key intermediate **VIII** (Scheme I).

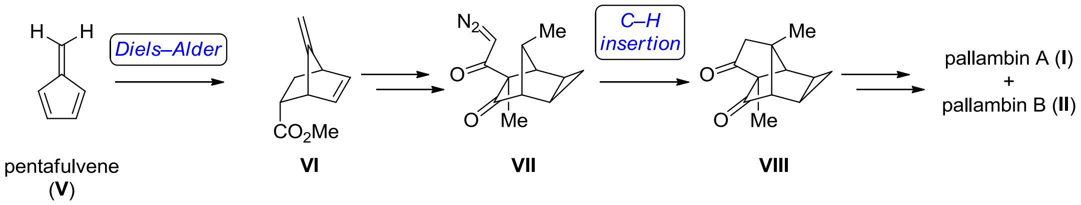

Scheme I: Total synthesis of pallambins A (**I**) and B (**II**).

Upon thorough analysis of the latter, we became intrigued by the idea to generate the bicyclo[2.2.1]heptane moiety *via* a Diels–Alder reaction between pentafulvene (**V**) and a suitable dienophile. Due to the lack of precedents, extensive optimization studies were necessary to enable this reaction. Ultimately, methyl acrylate was found to be a dienophile, leading to ester **VI**. Further transformations into diazo ketone **VII** included oxidative decarboxylation, regio- and diastereoselective cyclopropanation and diastereoselective hydrogenation of the *exo* olefin. A highly efficient C–H insertion then completed the

synthesis of tetracycle **VIII**, which was further converted into the targeted diterpenoids within several additional steps. Pallambins A and B were obtained in a total of 22 steps and 0.5% (pallambin A) respectively 3.8% (pallambin B) overall yield from pentafulvene (**V**).

In the second part of this thesis, a Ti(III)-mediated epoxide opening showing remarkable regioselectivities due to intramolecular hydrogen atom transfer was investigated (Scheme II). The results obtained suggest that this reaction proceeds *via* a S_H2 mechanism including the transfer of a proximal heteroatom bound hydrogen atom (**X**) leading to radical **XI**. The latter then subsequently undergoes one electron reduction to **XII**. In addition to the exploration of the substrate scope, this transformation could be rendered catalytic using manganese as the stoichiometric reductant.

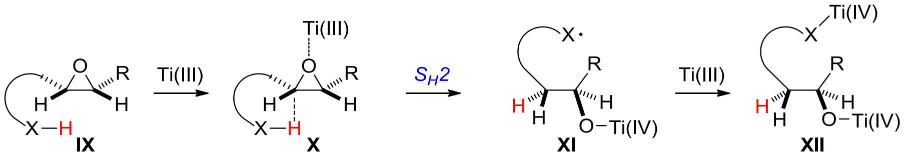
O
R
H
H
X–H
IX
Ti(III)
Ti(III)
O
R
H
H
X–H
X
S_H2
X·
R
H
H
H
O–Ti(IV)
XI
Ti(III)
Ti(IV)
X
R
H
H
H
O–Ti(IV)
XII

Scheme II: Ti(III)-mediated regioselective epoxide opening *via* intramolecular hydrogen atom transfer.

The last part of this thesis describes the synthesis of phenyldiyne-tagged Raman active analogs of epoxyisoprostane EC (**XIII**) and CycloEC (**XV**) for live cell imaging of these anti-inflammatory agents (Scheme III). The synthetic strategy is widely based on the total synthesis of CycloEC (**XV**) developed previously in our group. The crucial phenyldiyne moiety was introduced by a late-stage palladium-catalyzed C(sp)–C(sp) coupling reaction.

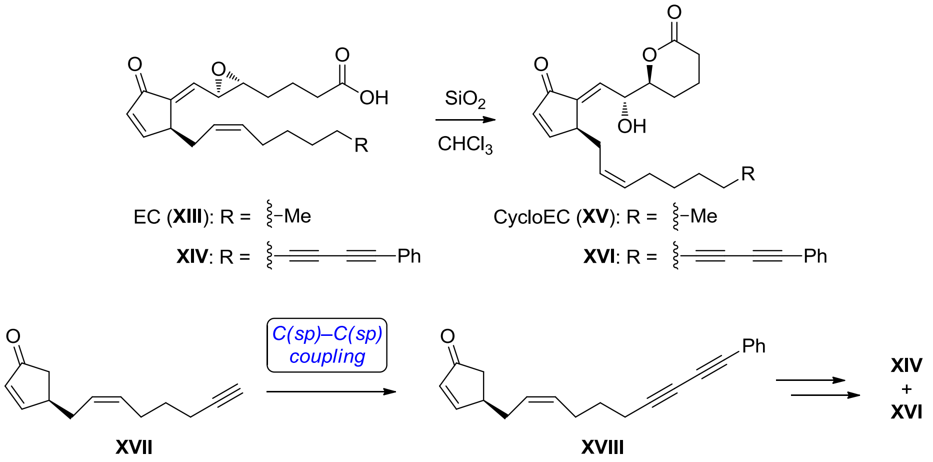
O
O
O
OH
R
SiO_2
$CHCl_3$
O
O
O
OH
R
EC (XIII): R = Me
XIV: R = Ph
CycloEC (XV): R = Me
XVI: R = Ph
O
XVII
C(sp)–C(sp) coupling
O
Ph
XVIII
XIV
+
XVI

Scheme III: Synthesis of phenyldiyne-tagged Raman active analogs of EC (**XIV**) and CycloEC (**XV**).

Zusammenfassung

Im Jahre 2012 wurden die zwei Cyclopropan-Diterpenoide Pallambine A (**I**) und B(**II**) von LOU und Mitarbeitern aus dem chinesischen Moos *Pallavicinia ambigua* isoliert (Abbildung I). Des Weiteren waren auch die strukturell verwandten Pallambine C (**III**) und D (**IV**) in den Extrakten vorhanden. Die Pallambine A (**I**) und B (**II**) sind mit bislang unbekannten Tetracyclo[4.4.$0^{3,5}$.$0^{2,8}$]decan-Kernen ausgestattet, welche Cyclopropane in sterisch sehr gehinderter Umgebung enthalten. Zusätzlich besitzen diese Naturstoffe zehn aufeinanderfolgende Stereozentren, von denen zwei quaternärer Natur sind. Diese strukturellen Aspekte machen die Pallambine A und B zu faszinierenden Zielmolekülen für die Totalsynthese. Der erste Teil dieser Dissertation behandelt die Entwicklung einer Synthesestrategie, welche schlussendlich zur ersten Totalsynthese von **I** und **II** führte.

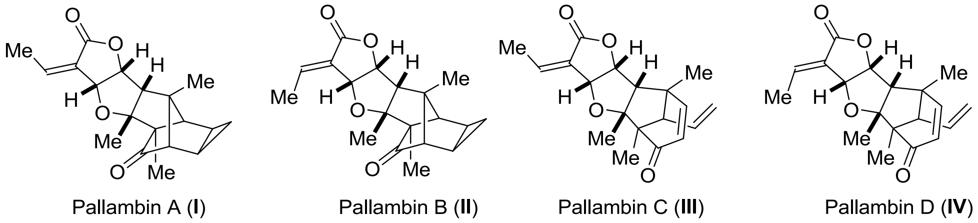

Abbildung I: Struktur der Pallambine A-D (**I-IV**), isoliert von LOU und Mitarbeitern.

Aufgrund der Schwierigkeiten im Zusammenhang mit der Herstellung des hochgradig geballten tetracyclischen Kerns der Naturstoffe, zielte unsere Synthesestrategie auf die Entwicklung eines effizienten Zugangs zu Schlüsselintermediat **VIII** (Schema I).

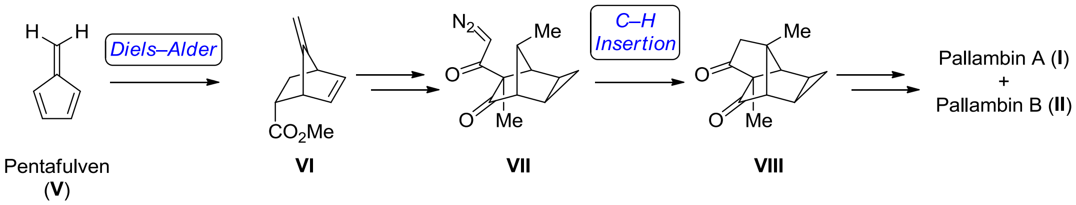

Schema I: Totalsynthese der Pallambine A (**I**) und B (**II**).

Eine gründliche Analyse der Pallambine A und B hat uns von der Idee begeistert, die Bicyclo[2.2.1]heptan-Grundstruktur mittels einer Diels–Alder Reaktion zwischen Pentafulven (**V**) und einem passenden Dienophil aufzubauen. Wegen des Fehlens von Präzedenzfällen waren umfassende Optimierungsstudien nötig um diese Reaktion zu ermöglichen. Letztendlich wurde Methylacrylat als Dienophil benutzt um Ester **VI** zu erhalten. Weitere Transformationen, die zu Diazoketon **VII** führten, waren unter anderem eine oxidative Decarboxylierung, eine regio- und diastereoselektive Cyclopropanierung, sowie die Hydrierung des *exo* Olefins. Eine hocheffiziente C–H Insertion vollendete die Synthese des wichtigen Tetracycluses **VIII**, von wo aus die Synthese in weiteren Schritten beendet wurde. Die Pallambine A und B wurden auf diesem Wege in einer Gesamtzahl von 22 Schritten und 0.5% (Pallambin A), beziehungsweise 3.8% (Pallambin B), Gesamtausbeute ausgehend von Pentafulven (**V**) erhalten.

Der zweite Teil dieser Dissertation, behandelt die Erforschung einer Ti(III)-vermittelten Epoxidöffnung, welche bemerkenswerte Regioselektivitäten aufgrund intramolekularen Wasserstoffatomtransfers zeigt (Schema II). Die Resultate dieser Studie legen nahe, dass diese Reaktion *via* eines S_H2 Mechanismus eines intramolekular übertragenen heteroatomgebundenen Wasserstoffatoms abläuft, was zur Bildung von Radikal **XI** führt. Dieses wird dann durch eine Ein-Elektronen-Reduktion zu **XII** umgesetzt. Zusätzlich zur Erforschung des einsetzbaren Substratbereichs, wurde diese Transformation auch katalytisch durchgeführt, wobei Mangan als stöchiometrisches Reduktionsmittel benutzt wurde.

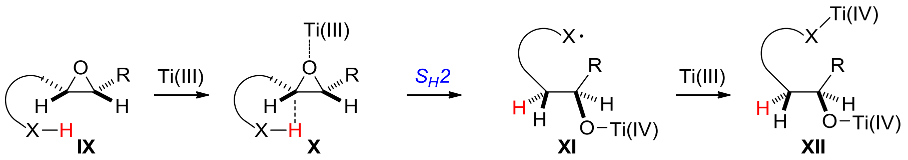

Schema II: Ti(III)-vermittelte regioselektive Epoxidöffnung *via* intramolekularem Wasserstoffatomtransfer.

Der letzte Teil dieser Dissertation beschreibt die Synthese von Phenyldiin-markierten ramanaktiven Analoga der Epoxyisoprostanoide EC (**XIII**) und CycloEC (**XV**) zur Untersuchung dieser entzündungshemmenden Reagenzien in der lebenden Zelle (Schema III). Die Strategie beruht weitgehend auf der Totalsynthese von CycloEC (**XV**), welche in unserer Gruppe entwickelt wurde. Die ausschlaggebende Phenyldiin-Gruppe wurde auf einer späten Stufe durch eine Palladium-katalysierte C(sp)–C(sp) Kupplungsreaktion eingeführt.

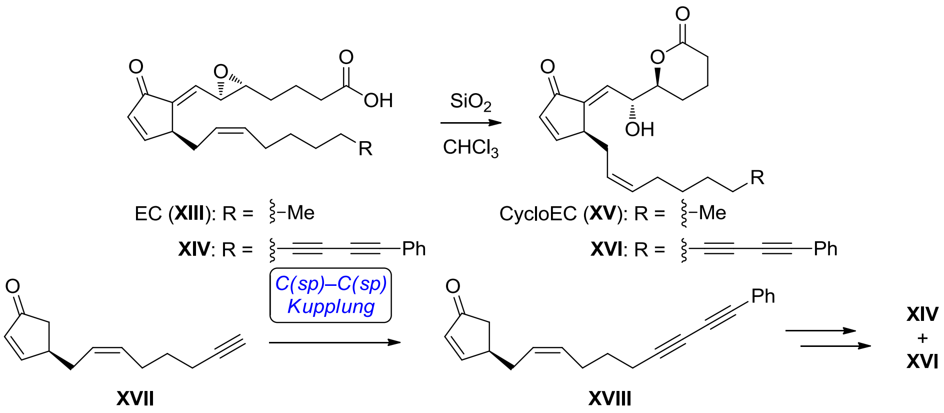

Schema III: Synthese von Phenyldiin-markierten ramanaktiven Analoga von EC (**XIV**) und CycloEC (**XV**).

List of Abbreviations, Acronyms and Symbols

Abbreviations and Acronyms

9-BBN	9-borabicyclo[3.3.1]nonane
ABSA	acetamidobenzenesulfonyl azide
Ac	acetyl
acac	acetylacetonato
AIBN	azobisisobutyronitrile
app	apparent
atm	atmosphere
b	broad
BHT	2,6-di-*tert*-butyl-4-methylphenol
BMDC	bone marrow-derived dendritic cells
Bn	benzyl
Boc	*tert*-butoxycarbonyl
Bu	butyl
Bz	benzoyl
C	Celsius
c	concentration, centi
cal	calorie
calcd	calculated
CAM	cerium ammonium molybdate
cat	catalytic
Cbz	carboxybenzyl
CD	circular dichroism
cf	*confer*
COSY	correlation spectroscopy
Cp	cyclopentadienyl
CPBA	chloroperoxybenzoic acid
CSA	camphor-10-sulfonic acid
d	doublet
d.r.	diastereomeric ratio
dba	dibenzylideneacetone
DBU	1,8-diazabicyclo[5.4.0]undec-7-ene

DEPT	distortionless enhancement by polarization transfer
DIBAL	diisobutylaluminum hydride
DMAP	4-dimethylaminopyridine
DME	dimethyl ether
DMF	*N*,*N*-dimethylformamide
DMP	Dess–Martin periodinane
DMPU	1,3-dimethyl-3,4,5,6-tetrahydro-2(1*H*)-pyrimidinone
DMSO	dimethylsulfoxide
DQF	double-quantum filtered
EC	epoxycyclopentenone isoprostanes
ee	enantiomeric excess
EI	epoxyisoprostane, impact ionization
equiv	equivalents
ESI	electron spray ionization
esp	α,α,α’,α’-tetramethyl-1,3-benzenedipropionate
Et	ethyl
ETH	*Eidgenössische Technische Hochschule*
FT	fourier transform
g	gram
h	hour
HMBC	heteronuclear multiple bond coherence
HMDS	hexamethyldisilazide
HMPA	hexamethylphosphortriamide
HRMS	high resolution mass spectrometry
HSQC	heteronuclear single quantum coherence
Hz	Hertz
i	*iso*
IBX	2-iodoxybenzoic acid
IC_{50}	half maximal inhibitory concentration
IL	Interleukin
IPr	*N*,*N*’-bis(2,6-diisopropylphenyl)-imidazol-2-ylidiene
IR	infrared
J	coupling constant
k	kilo

Keap1	Kelch-like ECH-associated protein 1
L	liter
M	molar, mega
M	molecular ion
m	milli, meter, multiplet or unresolved
m	*meta*
MALDI	matrix-assisted laser desorption/ionization
Me	methyl
min	minute
MOM	methoxymethyl acetal
MS	molecular sieves
Ms	methanesulfonyl
n	nano
n	*normal*
NBS	*N*-bromosuccinimide
NCS	*N*-chlorosuccinimide
NMR	nuclear magnetic resonance
NOE	nuclear *Overhauser* effect
Nrf2	Nuclear factor-erythroid-2-related factor 2
o	*ortho*
ORTEP	oak ride thermal ellipsoid plot
OxPL	oxidized phospholipid
p	*para*
PC	phosphatidylcholine
PDC	pyridinium dichromate
PECPC	epoxycyclopentenone isoprostane phospholipid
PEIPC	epoxyisoprostane phospholipid
pH	negative decadic logarithm of hydrogen ion concentration
Ph	phenyl
Piv	pivaloyl
pK_a	negative decadic logarithm of the acid dissociation constant
pmdba	bis(4-methoxybenzylidene)acetone
PPAR-γ	peroxisome proliferator-activated receptor gamma
ppm	parts per million

PPTS	pyridinium *p*-toluenesulfonate
Pr	propyl
PTAD	(1-adamantyl)-(*N*-phtalimido)acetate
q	quartet
quant	quantitative
Ra–Ni	Raney nickel
R_f	retention factor
RT	room temperature
s	singlet, second
T	temperature
t	triplet
t	*tert*
TBAF	tetra-*n*-butylammonium fluoride
TBDPS	*tert*-butyldiphenylsilyl
TBS	*tert*-butyldimethylsilyl
TC	thiophene-2-carboxylate
TES	triethylsilyl
TFA	trifluoroacetic acid
THF	tetrahydrofuran
TLC	thin layer chromatography
TMP	2,2,6,6-tetramethylpiperidine
TMS	trimethylsilyl
TMTU	tetramethylthiourea
Ts	*p*-toluenesulfonyl
UV	ultraviolet
X	halogen atom

Symbols

°	degree
Å	Ångström
$[\alpha]^{T}_{D}$	specific rotation at temperature T at the sodium D line
δ	chemical shift in ppm
µ	micro
ν	wavenumber

Part I

Total Synthesis of Pallambins A and B

1 Introduction

1.1 Natural Products Isolated from *Pallavicinia*

1.1.1 Background

Bryophytes are all-green, seedless embryophyta, which lack vascular tissue (Figure 1.1). They belong to the most primitive land plants, grow on rocks, trees and soil and are distributed all over the world. To date, about 24 000 species are known. Bryophytes are further divided into three classes, Marchantiophyta (liverwort), Bryophyta (moss) and Anthocerotophyta (hornwort).[1] On the basis of their secondary metabolites, liverworts are classified into two subclasses, Jungermannidae and Marchantiidae.[2] Both subclasses comprise of numerous orders and species.

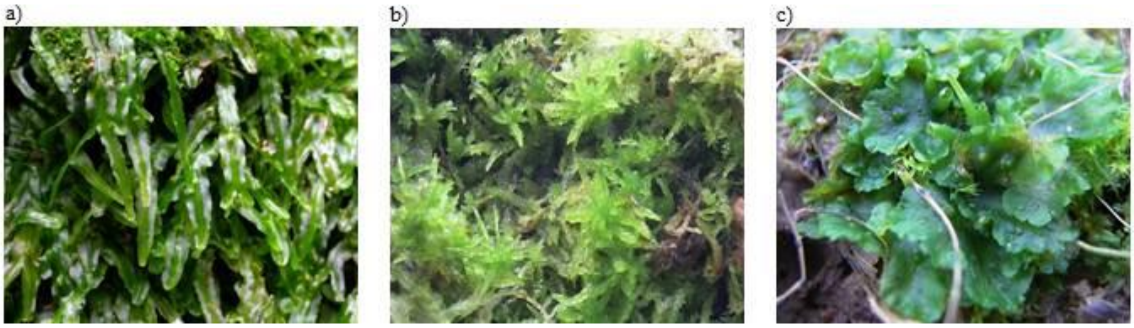

Figure 1.1: Selected examples of bryophytes: a) Liverwort (*Pallavicinia subciliata*); b) Moss (*Sphagnum sp.*); c) Hornwort (*Phaeoceros laevis*).[3]

Due to their antibacterial activity, mosses have been used in traditional Chinese folk medicine to treat burns, eczemas and external wounds. These features have also been exploited to dress wounds during World War I, when material supply was impeded. Despite this inarguably interesting biological profile, phytochemical investigations of liverworts only started in the last decades. A reason for this might have beeen the difficulties associated with species classification and collection of larger amounts of pure samples.[1a)]

---

[1] a) Y. Asakawa, A. Ludwiczuk, F. Nagashima, M. Toyota, T. Hashimoto, M. Tori, Y. Fukuyama, L. Harinantenaina, *Heterocycles* **2009**, *77*, 99-150; b) Y. Asakawa, *Pure Appl. Chem.* **2007**, *79*, 557-580.

[2] Y. Asakawa, *Phytochemistry* **2004**, *65*, 623-669.

[3] Picture a) taken with permission from http://bryophytes.plant.siu.edu/imPallaviciniaSubciliata.html, downloaded on 07.05.2015, photographed by Dr. LI ZHANG.
Picture b) taken from https://de.wikipedia.org/wiki/Laubmoose#/media/File:Sphagnum_moos.jpg, downloaded on 07.05.2015.
Picture c) taken from: https://en.wikipedia.org/wiki/Phaeoceros_laevis#/media/File:Phaeoceros_laevis.jpg, downloaded on 07.05.2015.

1.1.2 Phytochemical Investigations

Phytochemical investigations of bryophytes revealed a variety of natural product classes, namely flavonoids, phenolic compounds and most relevant for biological activity, terpenes and terpenoids (Figure 1.2).[4]

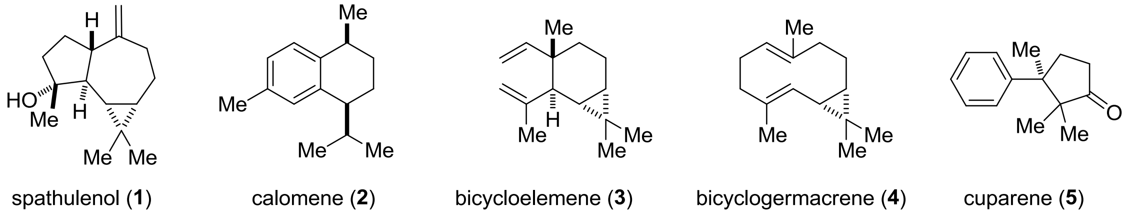

Figure 1.2: Selected natural products isolated from different bryophytes.

1.1.2.1 *Pallavicinia Subciliata*

Although liverworts synthesize a variety of intriguing natural products, a first study on *Pallavicinia* species, *P. subciliata* and *P. lyelli* revealed already known compounds, such as terpenes, fatty acids and sterols.[5] However, during their investigation of *P. subciliata*, collected near Taipei City, WU *et al.* identified a novel 7,8-secolabdanoid diterpene with the molecular formula $C_{20}H_{26}O_4$ and named it pallavicinin (**6**, Figure 1.3). In 1999, the same authors also found neopallavicinin (**7**), a diastereomer of pallavicinin (**6**).[6] The structural assignments of both natural products were based on NMR studies (^{1}H, ^{13}C, COSY, ^{13}C-DEPT, HMBC, NOE), which revealed the presence of two olefins, four tetrasubstituted carbons, a ketone and a lactone. The final structure and relative configuration could be established by X-ray diffractometry.

In 1998, ASAKAWA and co-workers isolated five novel terpenoids **8-13** (Figure 1.3).[4d)] Structurally, **8** is an oxidized version of pallavicinin (**6**), while **9** suffered from ether bond cleavage. Lactone **10**, which was only later entitled pallambin D,[7] possesses an additional site of unsaturation within the bicyclo[3.2.1]octane core. Noteworthy, the γ-lactone is endowed with a β,γ-olefin, which is a recurring structural feature of the terpenoid natural products shown in Figure 1.3.

---

[4] a) Y. Asakawa in *Progress in the Chemistry of Organic Natural Products* (Eds.: W. Herz, H. Grisebach, G. W. Kirby), Springer-Verlag, Vienna, **1982**, pp. 1-285; b) Y. Asakawa, M. Toyota, R. Takeda, C. Suire, T. Takemoto, *Phytochemistry* **1981**, *20*, 725-728; c) Y. Asakawa, R. Matsuda, T. Takemoto, S. Hattori, M. Mizutani, H. Inoue, C. Suire, S. Huneck, *J. Hattori Bot. Lab.* **1981**, *50*, 107; d) M. Toyota, T. Saito, Y. Asakawa, *Chem. Pharm. Bull.* **1998**, *46*, 178-180.

[5] C. L. Wu, H. J. Liu, H. L. Uang, *Phytochemistry* **1994**, *35*, 822-824.

[6] H. J. Liu, C. L. Wu, *J. Asian Nat. Prod. Res.* **1999**, *1*, 177-182.

[7] L. N. Wang, J. Z. Zhang, X. Li, X. N. Wang, C. F. Xie, J. C. Zhou, H. X. Lou, *Org. Lett.* **2012**, *14*, 1102-1105.

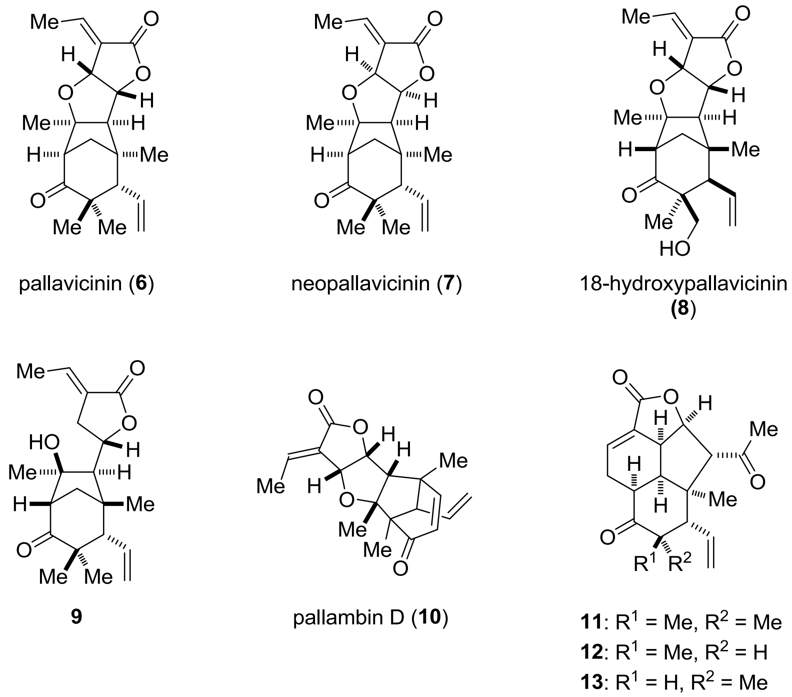

pallavicinin (**6**)

neopallavicinin (**7**)

18-hydroxypallavicinin (**8**)

9

pallambin D (**10**)

11: R^1 = Me, R^2 = Me
12: R^1 = Me, R^2 = H
13: R^1 = H, R^2 = Me

Figure 1.3: Terpenoid natural products isolated from *Pallavicinia subciliata* by WU and ASAKAWA.

1.1.2.2 *Pallavicinia Ambigua*

In 2005, LI *et al.* isolated the already known (+)-pallavicinin (**6**), (–)-neopallavicinin (**7**) and (–)-18-hydroxypallavicinin (**8**) also from a different species, *Pallavicinia ambigua* and determined the absolute configurations using a combination of NMR and CD studies.[8]

In 2012, LOU and co-workers discovered four norditerpenoid natural products and named them pallambins A-D (**10** and **14-16**, Figure 1.4).[7] While one of them turned out to be the previously reported compound **10**, the remaining three, pallambins A-C (**14-16**), were unknown. The researchers collected the liverworts from Zunyi, Guizhou province, P. R. China. After authentication of the species, grinding, gel column chromatography and high performance liquid chromatography, pallambins A-D could be obtained in pure form. High resolution electrospray ionization mass spectrometry revealed that all four compounds possess the same molecular formula $C_{19}H_{22}O_4$. Initial inspection of the ^{1}H- and ^{13}C-NMR spectroscopy indicated that pallambins A (**14**) and B (**15**) as well as pallambins C (**16**) and D (**10**) must be pairs of geometric isomers. Since **10** was already known, the structural assignment of pallambin C (**16**) was rather straightforward. After the structure was confirmed by ^{1}H-, ^{13}C-NMR, HSQC, COSY and HMBC, X-ray analysis disclosed that **10** and **16** only differ in the ethylidene olefin geometry.

---

[8] Z. J. Li, H. X. Lou, W. T. Yu, P. H. Fan, D. M. Ren, B. Ma, M. Ji, *Helv. Chim. Acta* **2005**, *88*, 2637-2640.

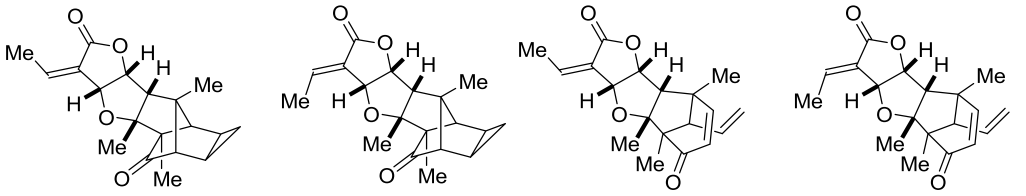

pallambin A (**14**) pallambin B (**15**) pallambin C (**16**) pallambin D (**10**)

Figure 1.4: Pallambins A-D isolated by LOU and co-workers from *Pallavicinia ambigua*.

Structural assignment of pallambins A (**14**) and B (**15**) proved to be more challenging. The ^{13}C-NMR spectrum displayed the presence of a ketone and an ester carbonyl group as well as a single olefin. Given the molecular formula of $C_{19}H_{22}O_4$, this finding implied a hexacyclic structure to achieve the degree of unsaturation of nine. Analysis of the HSQC spectrum showed four tetrasubstituted carbons in addition to the two carbonyl groups. Furthermore, the COSY and HMBC spectra revealed the presence of a cyclopropane incorporated in a norbornane fragment. The common tetrahydrofuran *γ*-lactone motif equipped with an ethylidene side chain was established by comparison to known natural products **6**, **7**, **10** and **16** and further proven by HMBC correlations. Taken these information together, pallambins A (**14**) and B (**15**) possess a tetracyclo[4.4.0^{3,5}.0^{2,8}]decane core. Detailed NOE spectroscopy enabled the assignment of the relative structure, which was further confirmed by X-ray diffractometry.

1.2 Other Syntheses of *Pallavicinia* Terpenoids

1.2.1 Total Synthesis of (±)-Pallavicinin and (±)-Neopallavicinin

In 2006, PENG and WONG reported the total synthesis of (±)-pallavicinin (**6**) and (±)-neopallavicinin (**7**).[9] As depicted in Scheme 1.1, their retrosynthetic analysis relies on a 1,4-conjugate addition to butenolide **17**, which is envisioned to be generated from furan **18**. Additionally, an aldol reaction would trigger the formation of the tricyclo[3.2.1]octane core. The Wieland–Miescher ketone (**19**) was chosen as starting material.[10]

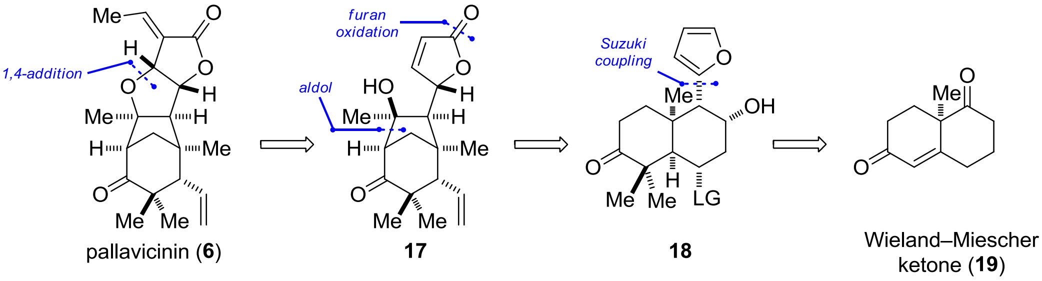

Scheme 1.1: Retrosynthetic analysis of (±)-pallavicinin (**6**) by PENG and WONG.

The Wieland–Miescher ketone (**19**) was first selectively reduced and protected. Introduction of the geminal dimethyl group furnished **20**. Oxidation with PDC, followed by reduction and protecting group exchange yielded alcohol **21**. The crucial furan moiety was installed *via* Suzuki coupling. Hydroboration and a sequence of protecting group manipulations provided the precursor for a Grob fragmentation. The latter occurred upon treatment of TBS ether **24** with TBAF, followed by KO*t*Bu in 56% overall yield. The stage was now set for the construction of the tricyclo[3.2.1]octane core *via* an intramolecular aldol reaction. Thus, the ketal of **25** was cleaved under acidic conditions and subsequently treated with NaO*t*Bu to yield diketone **26** after oxidation with IBX. The selectively reprotected ketone was exposed to excess MeLi, which not only installed the tertiary alcohol, but also deprotonated the furan 2-position. The thus formed anion was trapped with TMSCl and the furan oxidized to butenolide **28**. Base-mediated 1,4-conjugate addition occurred in only moderate yield (43% for **29** and 10% for **30**). After separation of the diastereomers, **29** and **30** were separately carried through a three-step sequence to install the ethylidene side chain and to deprotect the remaining ketal. In conclusion, (±)-pallavicinin (**6**) and (±)-neopallavicinin (**7**) were obtained in 32 steps and 0.0006% (**6**), respectively 0.00004% (**7**), overall yield.

---

[9] X. S. Peng, H. N. C. Wong, *Chem. Asian J.* **2006**, *1*, 111-120.

[10] P. Wieland, K. Miescher, *Helv. Chim. Acta* **1950**, *33*, 2215-2228.

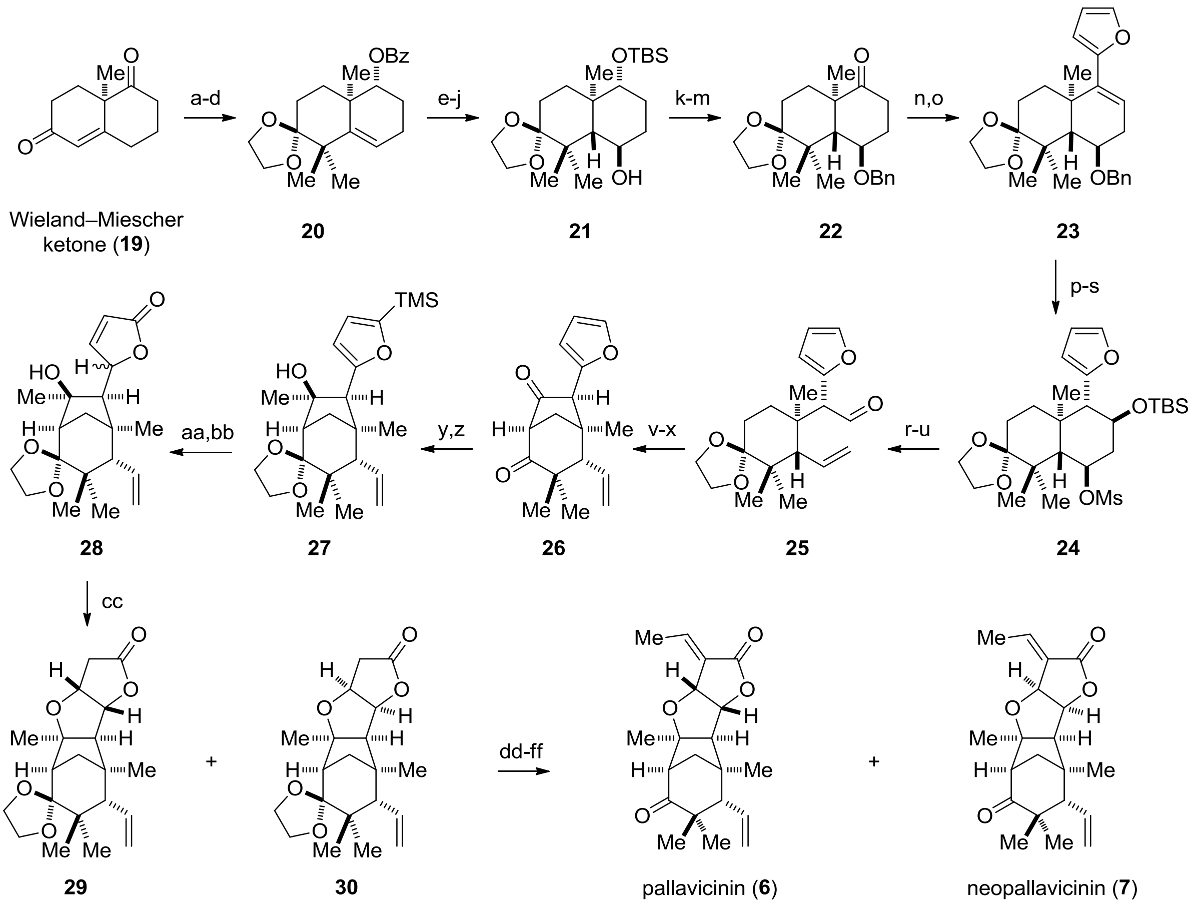

Scheme 1.2: WONG’s total synthesis of (±)-pallavicinin (**6**) and (±)-neopallavicinin (**7**). Reagents and conditions: a) $NaBH_4$, EtOH, 0 °C, 95%; b) BzCl, pyridine, 96%; c) KO*t*Bu, MeI, *t*BuOH, 74%; d) ethylene glycol, TsOH (10 mol%), C_6H_6, reflux, 98%; e) KOH, MeOH, reflux, 96%; f) TBSCl, imidazole, CH_2Cl_2, 92%; g) $BH_3{\cdot}THF$, CH_2Cl_2, 0 °C to RT; h) PDC, CH_2Cl_2; i) NaOMe, THF, 56% over three steps; j) Na, NH_3, THF–MeOH (4:1), −78 °C, 79%; k) NaH, BnBr, *n*Bu_4NI, THF, reflux, 92%; l) TBAF, THF, reflux, 93%; m) PDC, CH_2Cl_2, 85%; n) *i*Pr_2NLi, $PhNTf_2$, THF, –78 °C, 86%; o) $Pd(PPh_3)_4$ (4 mol%), K_2CO_3, 2-furylboronic acid, THF, reflux, 84%; p) 9-BBN, CH_2Cl_2, then NaOH, H_2O_2, 76%; q) TBSCl, imidazole, DMF, 84%; r) H_2 (1 atm), Pd/C (10% w/w), MeOH, 97%; s) MsCl, NEt_3, DMAP, CH_2Cl_2, 77%; t) TBAF, THF; u) KO*t*Bu, 18-crown-6, *t*BuOH, 40 °C to 50 °C, 56% over two steps; v) TsOH (10 mol%), Me_2CO; w) *t*BuONa, *t*BuOH, 60 °C; x) IBX, CH_2Cl_2, 56% over three steps; y) ethylene glycol, TsOH (10 mol%), C_6H_6, reflux, 72%; z) MeLi, THF –78 °C to RT, then TMSCl, 0 °C, 54%; aa) $MeCO_3H$, NaOAc, CH_2Cl_2, 0 °C to RT; bb) *i*Pr_2NLi, THF, 0 °C, then AcOH, 56% over two steps; cc) DBU, toluene, reflux, 43% for **29**, 10% for **30**; dd) *i*Pr_2NLi, MeCHO, –78 °C; ee) NEt_3, MsCl, CH_2Cl_2, 0 °C to RT; ff) TsOH (10 mol%), Me_2CO, 0 °C to RT, 30% over three steps for (±)-pallavicinin (**6**), 9% over three steps for (±)-neopallavicinin (**7**).

Shortly after publication of our work on the total synthesis of pallambins A and B, JIA and co-workers reported an asymmetric approach towards (–)-pallavicinin (**6**) and (+)-neopallavicinin (**7**).[11] As presented in Scheme 1.3 their synthetic strategy also relies on an intramolecular 1,4-addition of a tertiary alcohol to a butenolide. Furthermore, a serendipitously discovered $LiBHEt_3$ induced fragmentation would provide diketone **31** from hydroxy epoxide **32**.

---

[11] B. Huang, L. Guo, Y. Jia, *Angew. Chem. Int. Ed.* **2015**, *54*, 13599-13603.

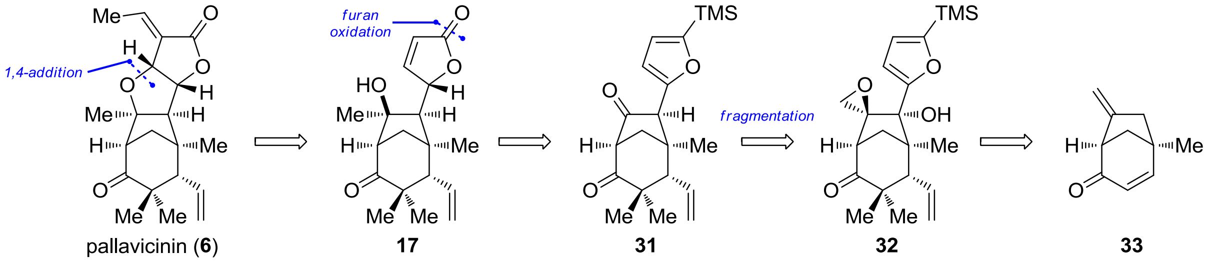

Scheme 1.3: Retrosynthetic analysis of (–)-pallavicinin (**6**) and (+)-neopallavicinin (**7**) according to JIA and co-workers.

The synthesis commences with an enantioselective palladium-catalyzed decarboxylative allylation of **34** as developed by STOLTZ and co-workers.[12] **34** could be prepared in three steps following a procedure described by TROST *et al.*[13] After reduction and elimination, enone **37** was converted into the corresponding TBS enol ether and underwent oxidative cyclization upon treatment with catalytic amounts of $Pd(OAc)_2$ in the presence of molecular oxygen. Subsequent conjugate addition and allylic oxidation gave access to allylic alcohol **38** in 88% yield. Stereoselective vanadium-mediated epoxidation and Dess–Martin oxidation yielded diketone **39**. Although the following addition of 2-trimethylsilyl-5-lithiofuran occurred from the undesired *Si* face to produce **40**, an intriguing $LiBHEt_3$-mediated fragmentation took place, converting **40** into ketone **41** in excellent yield (84%).[14] After reoxidation and 1,2-addition, furan **42** was oxidized in the presence of *m*CPBA to give unstable butenolide **17**. Treatment of **17** with DBU produced 30% of **43** along with 15% of **44**. The synthesis was completed after a two-step aldol condensation, providing (–)-pallavicinin (**6**) and (+)-neopallavicinin (**7**). In conclusion, these first enantioselective syntheses provided the natural products in 20 steps and 0.8% (pallavicinin) respectively 0.09% (neopallavicinin) overall yield.

---

[12] S. R. Levine, M. R. Krout, B. M. Stoltz, *Org. Lett.* **2009**, *11*, 289-292.
[13] B. M. Trost, R. N. Bream, J. Xu, *Angew. Chem. Int. Ed.* **2006**, *45*, 3109-3112.
[14] For a mechanistic hypothesis see ref. 11.

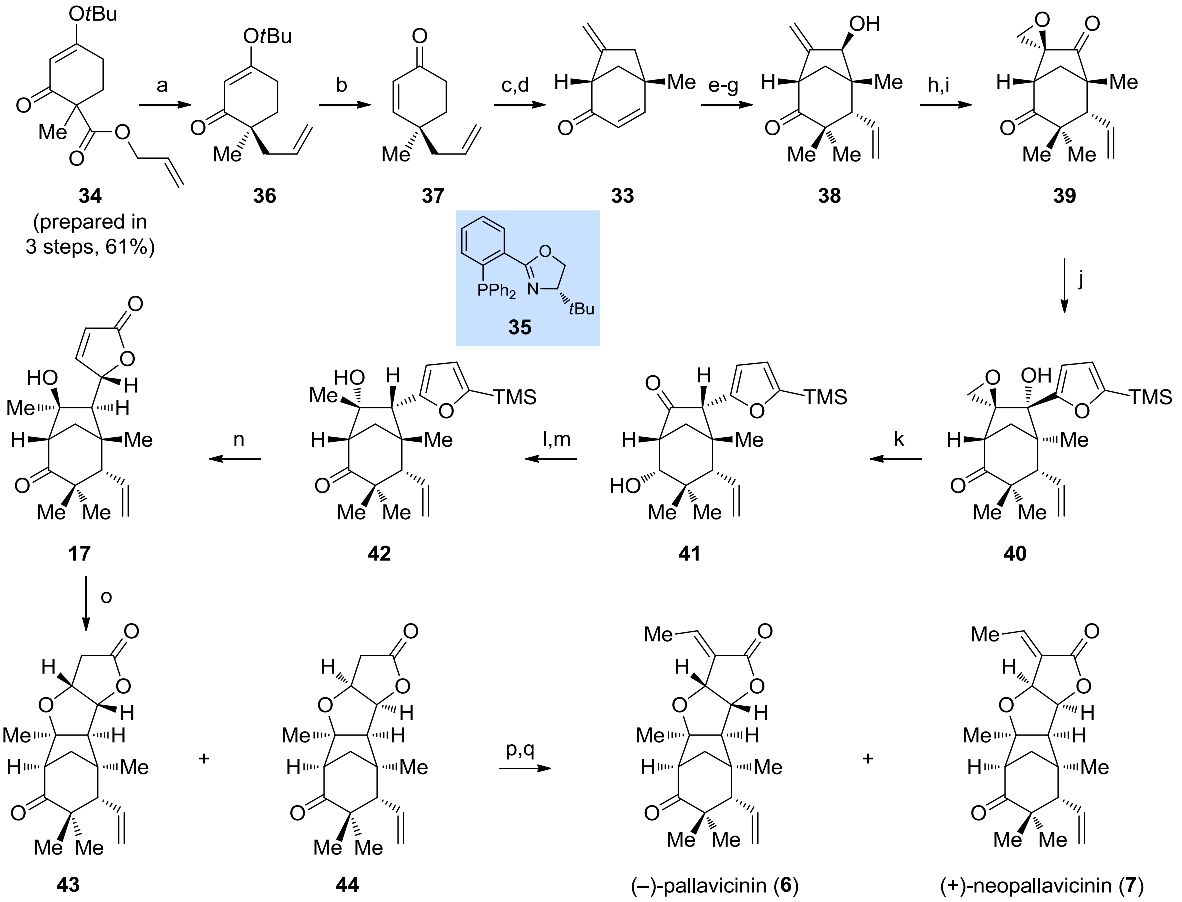

Scheme 1.4: Asymmetric total synthesis of (–)-pallavicinin (**6**) and (+)-neopallavicinin (**7**) by JIA and co-workers. Reagents and conditions: a) **35** (6 mol%), $Pd_2(pmdba)_3$ (2.5 mol%), toluene, 50 °C, 79%, 85% *ee*; b) $LiAlH_4$, Et_2O, then H_2SO_4, 90%; c) iPr$_2$NLi, THF, –78 °C, then TBSCl, HMPA; d) $Pd(OAc)_2$ (10 mol%), DMSO, O_2 (1 atm), 65 °C; e) vinylmagnesium bromide, CuBr·SMe$_2$, THF, –40 °C, d.r. = 10:1, 73% over three steps; f) NaH, MeI, DME, 93%; g) SeO_2, tBuO$_2$H, CH_2Cl_2, 75%; h) VO(acac)$_2$ (15 mol%), tBuO$_2$H, CH_2Cl_2, 64%; i) DMP, CH_2Cl_2, 79%, 99% *ee* after recrystallization; j) 2-trimethylsilyl-5-lithiofuran, Et_2O, 40 °C, 72%; k) LiBHEt$_3$, THF, 60 °C, 84%; l) DMP, CH_2Cl_2, 89%; m) MeMgBr, THF, –40 °C, 80%; n) *m*CPBA, CH_2Cl_2; o) DBU, CH_2Cl_2, from **42** 7% of **43**, 15% of **44**; p) iPr$_2$NLi, THF, –78 °C, then MeCHO, –78 °C; q) MsCl, NEt$_3$, DMAP, CH_2Cl_2, from **43** 55% of (–)-pallavicinin (**6**), from **44** 12% of (+)-neopallavicinin.

1.2.2 Total Synthesis of Pallambins C and D

In 2012, WONG and co-workers reported the first total synthesis of (±)-pallambins C and D.[15] As for (±)-pallavicinin and (±)-neopallavicinin, their route relies on the Wieland–Miescher ketone (**19**) as the starting material. However, as shown in Scheme 1.5, the researchers envisioned to employ a palladium-catalyzed alkoxycarbonylation for the installation of the γ-lactone-tetrahydrofuran bicycle. The tricyclo[3.2.1]octane core should again be generated by an intramolecular aldol reaction.

---

[15] X.-S. Xu, Z.-W. Li, Y.-J. Zhang, X.-S. Peng, H. N. C. Wong, *Chem. Commun.* **2012**, *48*, 8517-8519.

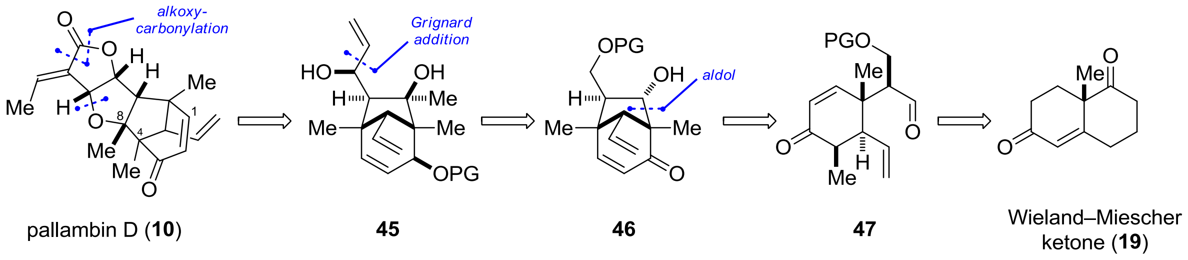

Scheme 1.5: WONG's retrosynthetic analysis of pallambin D (**10**).

The Wieland–Miescher ketone (**19**) firstly needed to be decorated with additional substituents. Therefore, both ketones were reduced and the resulting hydroxy groups protected as its benzyl ethers (Scheme 1.6). Subsequent epoxidation and nucleophilic opening with MeMgI installed the C(4)-Me group. The remaining tertiary alcohol was eliminated and the corresponding olefin exposed to standard hydroboration/oxidation conditions. After several functional group interconversions, WONG and co-workers arrived at vinyl iodide **51**, which underwent Pd-catalyzed carboxylation in the presence of CO and MeOH. Reduction with DIBAL and subsequent protection was followed by another hydroboration/oxidation sequence. After additional functional group interconversions, acetate **53** could be obtained. Cleavage of the acetate followed by treatment with KO*t*Bu at elevated temperature mediated both, a Grob fragmentation and the envisioned intramolecular aldol reaction to furnish **54**. Furthermore, the oxidation states of the newly formed alcohol and the ketone needed to be inverted. Thus, oxidation to the diketone was followed by a moderately selective reduction and protection. Since nucleophilic addition of methyl nucleophiles led to the incorrect configuration at C(8), a detour had to be taken. Hence, Ti-mediated olefination followed by hydroxyl directed VO(acac)$_2$ epoxidation provided epoxide **56**. Regioselective opening of the epoxide was effected by LiAlH$_4$. The remaining primary alcohol was oxidized and treated with vinylmagnesium bromide to yield the precursor for the palladium-catalyzed alkoxycarbonylation. Exposure of **58** to established conditions generated the γ-lactone-tetrahydrofuran **59** in 78% yield.[16] The ethylidene side chain was then introduced by an aldol reaction with acetaldehyde and subsequent treatment with MsCl and NEt$_3$ in the presence of catalytic amounts of DMAP. After separation of the olefin isomers, the same deprotection, oxidation sequence was used for the conversion into pallambins C (**16**) and D (**10**) in 37 steps and 0.2% (**16**), respectively 0.1% (**10**), overall yield.

---

[16] a) Z. Li, Y. Gao, Y. Tang, M. Dai, G. Wang, Z. Wang, Z. Yang, *Org. Lett.* **2008**, *10*, 3017-3020; b) Z. Li, Y. Gao, Z. Jiao, N. Wu, D. Z. Wang, Z. Yang, *Org. Lett.* **2008**, *10*, 5163-5166.

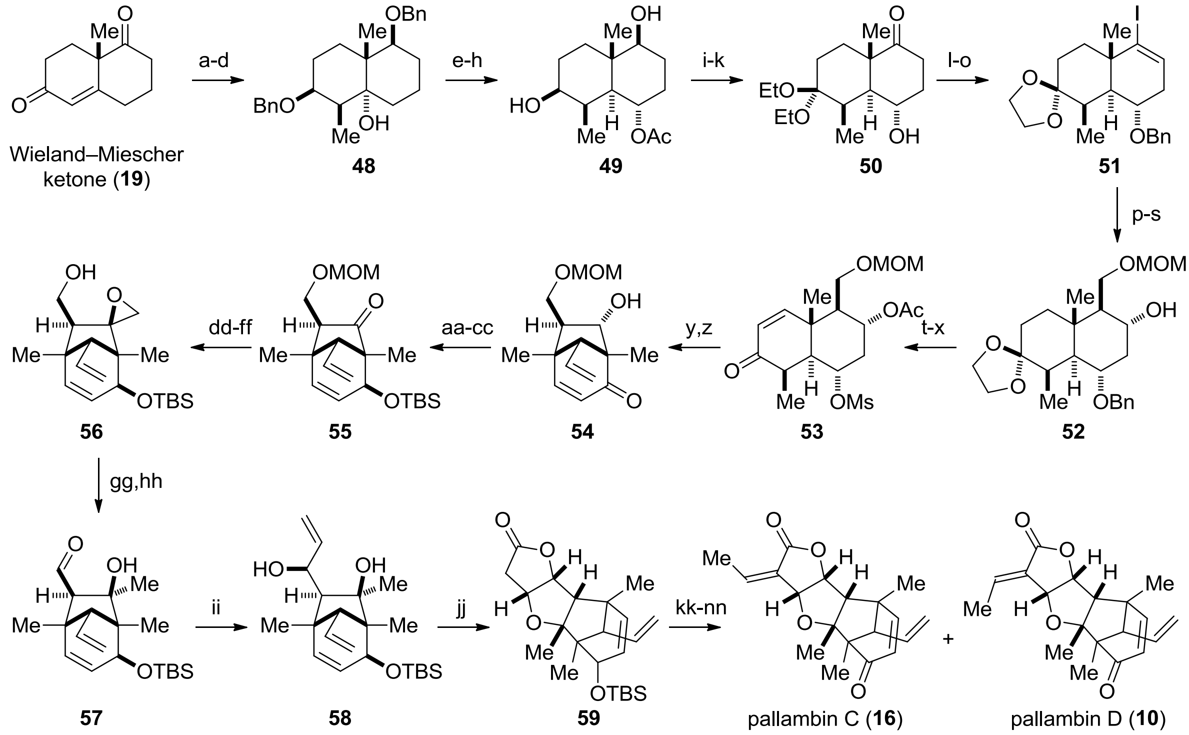

Scheme 1.6: WONG's total synthesis of (±)-pallambins C (**16**) and D (**10**). Reagents and conditions: a) $NaBH_4$, $CeCl_3{\cdot}7H_2O$, MeOH, –78 °C, 86%; b) BnBr, NaH, DMF, 95%, c) *m*CPBA, $NaHCO_3$, CH_2Cl_2, 86%; d) MeMgI, C_6H_6, reflux, 89%; e) $SOCl_2$, pyridine, CH_2Cl_2, 0 °C, 92%; f) $BH_3{\cdot}SMe_2$, Et_2O, then THF–H_2O (1:1), H_2O_2, NaOH, 82%; g) Ac_2O, pyridine, DMAP (13 mol%), CH_2Cl_2, 99%; h) Pd/C (10% w/w), H_2 (1 atm), EtOH, 95%; i) CrO_3, H_2SO_4, Me_2CO, 0 °C, 92%; j) $CH(OEt)_3$, $TsOH{\cdot}H_2O$, EtOH, 61%; k) K_2CO_3, MeOH; l) $H_2NNH_2{\cdot}H_2O$, NEt_3, EtOH, reflux; m) I_2, 1,1,3,3-tetramethylguanidine, THF, 84% over three steps; n) BnBr, NaH, DMF, 0 °C to RT; o) $TsOH{\cdot}H_2O$ (20 mol%), ethylene glycol, C_6H_6, reflux, 89% over two steps; p) $Pd(OAc)_2$ (10 mol%), NEt_3, CO (1 atm), MeOH–DMF (7:1), 55 °C, 81%; q) DIBAL, CH_2Cl_2, –78 °C, 97%; r) MOMCl, pyridine, DMAP (1 mol%), toluene, RT to 70 °C; 96%; s) $BH_3{\cdot}SMe_2$, Et_2O, then THF–H_2O (1:1), H_2O_2, NaOH, 77%; t) Ac_2O, pyridine, DMAP (20 mol%), CH_2Cl_2, 95%; u) Pd/C (10% w/w), H_2 (1 atm), EtOH, 50 °C; v) MsCl, NEt_3, CH_2Cl_2, 92% over two steps; w) PPTS (10 mol%), Me_2CO–H_2O (9:1), reflux, 85%; x) PhSeCl, $TsOH{\cdot}H_2O$, EtOAc, then CH_2Cl_2, pyridine, H_2O_2, 71%; y) K_2CO_3, MeOH, 98%; z) KO*t*Bu, *t*BuOH, 70 °C, 61%; aa) DMP, CH_2Cl_2, 90%; bb) $NaBH_4$, $CeCl_3{\cdot}7H_2O$, MeOH, –78 °C, 3 × recycled, 78%; cc) TBSOTf, NEt_3, CH_2Cl_2, 0 °C, 90%; dd) Mg, $TiCl_4$, CH_2Cl_2–THF (7:2), 77%; ee) PPTS, NaI, butanone–H_2O (10:1), reflux, 56%; ff) $VO(acac)_2$ (2 mol%), *t*BuOOH, C_6H_6, 86%; gg) $LiAlH_4$, Et_2O, reflux, 90%, hh) DMP, $NaHCO_3$, CH_2Cl_2, 88%; ii) vinylmagnesium bromide, THF, 0 °C, 48%; jj) $Pd(OAc)_2$ (10 mol%), $CuCl_2$, TMTU (10 mol%), propylene oxide, NH_4OAc (10 mol%), CO (1 atm), THF, 50 °C, 78%; kk) *i*Pr_2NLi, MeCHO, THF, –78 °C; ll) MsCl, NEt_3, DMAP (cat.), CH_2Cl_2, 35 °C; mm) HF (aqueous), MeCN, 90%, nn) DMP, $NaHCO_3$ CH_2Cl_2, 44% over three steps for pallambin C (**16**), 24% over three steps for pallambin D (**10**).

One year after the publication of our work on the total synthesis of pallambins A and B, BARAN and co-workers reported another approach towards pallambins C and D.[17] Their retrosynthetic analysis is shown in Scheme 1.7. An aldol condensation with acetaldehyde and a iodomalonation would trace pallambins C and D back to enol ether **60**. The latter was envisioned to be generated by an acetalization between a tertiary alcohol and an aldehyde followed by elimination. The remaining cyclopentane in **61** would be generated by an aldol reaction leading to ketoaldehyde **62**.

---

[17] L. R. Martinez, S. Umemiya, S. E. Wengryniuk, P. S. Baran *J. Am. Chem. Soc.* **2016**, *138*, 7536-7539.

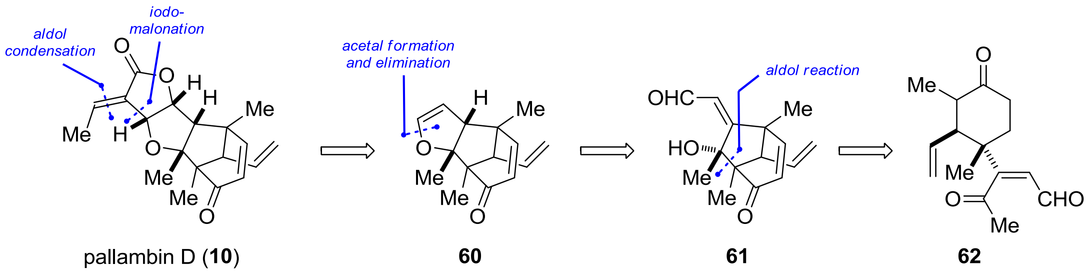
aldol condensation
iodo-malonation
acetal formation and elimination
aldol reaction
pallambin D (10)
60
61
62
Me
H
O
OHC
HO
CHO

Scheme 1.7: BARAN's retrosynthetic analysis of pallambin D (**10**).

The synthesis commenced with an Eschenmoser–Claisen rearrangement between furfuryl alcohol and amine **64**, followed by a reduction of the resulting amide to furnish aldehyde **65** in 75% yield. A Robinson annulation with ethyl vinyl ketone then produced cyclohexenone **66**.

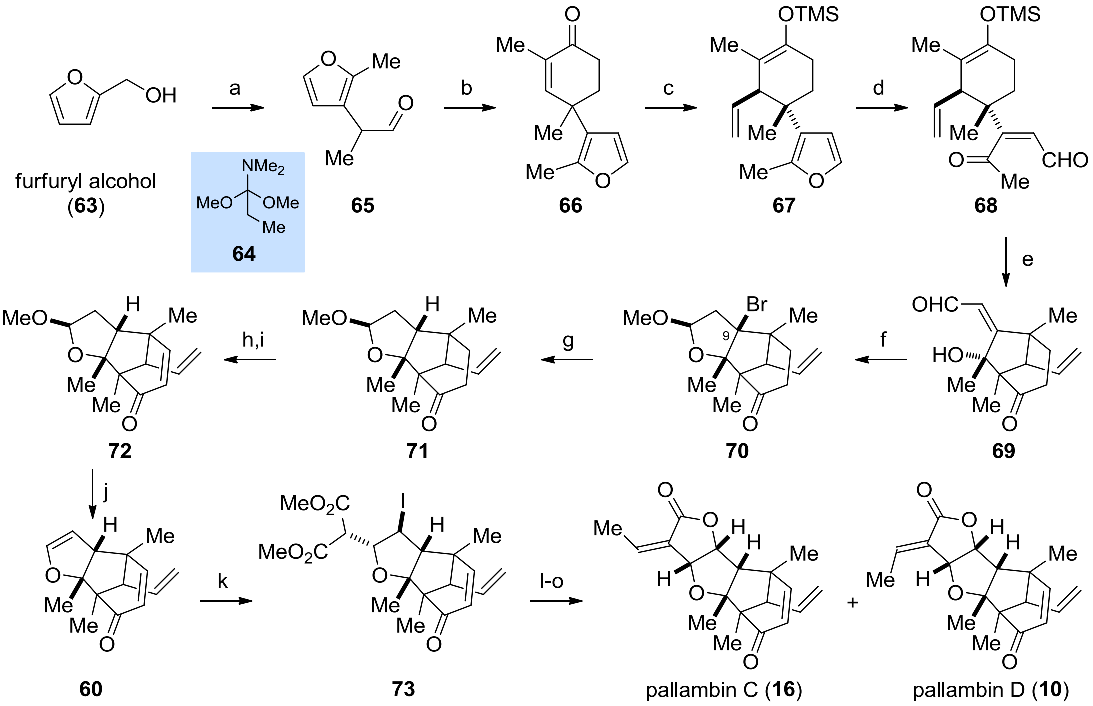
furfuryl alcohol (63)
NMe2
MeO
OMe
Me
64
65
66
OTMS
67
68
69
70
71
72
60
73
pallambin C (16)
pallambin D (10)
a
b
c
d
e
f
g
h,i
j
k
l-o
+
MeO2C
I
Br
9
OHC
HO
CHO

Scheme 1.8: BARAN's total synthesis of pallambins C and D. Reagents and conditions: a) **64**, toluene, 110 °C, then $(Me_2HSi)_2O$, $Ti(OiPr)_4$, 50 °C, 75%; b) ethyl vinyl ketone, Bu_4NBr (10 mol%), KOH (aqueous, 60%), toluene, 68%; c) vinylmagnesium bromide, $CuBr\cdot SMe_2$ (20 mol%), HMPA, TMSCl, THF, –78 °C, 75%; d) O_2 (bubbling), methylene blue, hν, CH_2Cl_2, –10 °C, then thiourea, RT; e) $TiCl_4$, Et_2O, –78 °C, 58% over two steps; f) $CH(OMe)_3$, $BF_3\cdot OEt_2$, $MgSO_4$, CH_2Cl_2, 0 °C then AcBr, 0 °C to RT 57%; g) Bu_3SnH, AIBN, toluene, 110°C, 90%, h) LiHMDS, PhSeCl, THF, –78 °C; i) H_2O_2, CH_2Cl_2, 0 °C, 60% over two steps; j) PPTS, pyridine, PhCl, 130 °C; k) dimethyl malonate, $SnCl_4$, DBU, I_2, CH_2Cl_2, 87% over two steps; l) NaOH (2.0 M, aqueous), MeOH; m) NEt_3, MeCN, 60 °C; n) LiHMDS, THF, –78 °C, then MeCHO; o) NEt_3, MsCl, DMAP, CH_2Cl_2, 94% over four steps for a 1:2 mixture of pallambins C and D.

Conjugate addition followed by enolate trapping with TMSCl gave silyl enol ether **68** in 75% yield. The furan ring was then cleaved by singlet oxygen followed by a titanium-mediated intramolecular Mukaiyama aldol reaction providing aldehyde **69** in 58% yield over two steps. After extensive experimentation, acetalization could be effected by treatment of the latter with $HC(OMe)_3$ in the presence of $BF_3{\cdot}OEt_2$. Since the obtained C(9)-methoxy derivative of **70** could not be converted into reduced acetal **71**, methoxide–bromide exchange had to be carried out. Thus, the initial acetalization product was treated with AcBr affording **70** in 57% overall yield. The subsequent radical dehalogenation finally furnished mixed acetal **71**. The required enone moiety was introduced next *via* two-step selenoxide elimination. In order to install the remaining *γ*-lactone, the methoxide in **72** was eliminated to produce enol ether **60**. The tin enolate of dimethyl malonate was then added to the corresponding iodonium ion of **60**, leading to iodide **73** in high yield. The two ester functionalities were subsequently hydrolyzed and the obtained diacid underwent monodecarboxylation and iodide displacement upon heating to 60 °C in acetonitrile. Finally, the ethylidene side chain was introduced by a two step aldol condensation with acetaldehyde. In conclusion, pallambins C and D have been obtained in 15 steps and 5.6% overall yield.

1.2.3 Conclusion

In summary, both synthetic approaches which appeared before the initiation of our project that are described in the previous chapters 1.2.1 and 1.2.2 rely on the employment of the Wieland–Miescher ketone (**19**) as entrance point to the targeted *Pallavicinia* terpenoids. However, the two syntheses differ in the construction of the common *γ*-lactone-tetrahydrofuran bicycle. While a 1,4-conjugate addition of a tertiary alcohol onto a butenolide is used in the course of the synthesis of (±)-pallavicinin and (±)-neopallavicinin, a palladium-catalyzed alkoxycarbonylation is employed in the synthesis of (±)-pallambins C and D. Importantly, the conjugate addition favors isomer **29**, which would lead to the undesired isomer in the pallambins C and D synthesis. Comparing the two methods, the alkoxycarbonylation is to be preferred not only because of the higher yield (78% vs. 53% of the combined isomers **29** and **30**), but also because of the tedious installation and oxidation of the furan moiety.

Additionally, both syntheses described, require 33 (pallavicinin and neopallavicinin), respectively 37 (pallambins C and D) steps. This large number is mainly due to the necessity of exhaustive protections, deprotections and reprotections as well as various oxidation state adjustments.[18] Several of these additional steps are necessary because of the use of the Wieland-Miescher ketone (**19**) as the starting material. While this compound has the advantage of being a cheap and easily accessible advanced bicycle with various sites for functionalization, it must not create laborious steps to force it into the overall synthetic strategy.

While these approaches present a solution for the generation of the *γ*-lactone-tetrahydrofuran bicycle, a more efficient approach to the tricyclic core fragments would be of interest to the synthetic community.

---

[18] Although the author of this thesis (C. E.) does not agree that syntheses can be simply judged by the following concepts, they nevertheless can serve as indicators. a) For the concept of step economy see: P. A. Wender, V. A. Verma, T. J. Paxton, T. H. Pillow, *Acc. Chem. Res.* **2008**, *41*, 40-49; b) For the concept of atom economy see: B. M. Trost, *Science* **1991**, *254*, 1471-1477; c) For the concept of redox economy see: N. Z. Burns, P. S. Baran, R. W. Hoffmann, *Angew. Chem. Int. Ed.* **2009**, *48*, 2854-2867; d) For a review see: T. Newhouse, P. S. Baran, R. W. Hoffmann, *Chem. Soc. Rev.* **2009**, *38*, 3010-3021.

2 Synthetic Strategy[19]

2.1 General Considerations

Pallambins A (**14**) and B (**15**) were chosen as the primary targets for total synthesis due to the increased structural complexity emanating from the additional cyclopropane. Moreover, the absence of any synthetic method towards the unprecedented tetracyclo[4.4.$0^{3,5}$.$0^{2,8}$]decane core allowed for an unbiased analysis.

This core fragment contains a double-gauche pentane-like arrangement of the cyclopropane and the C(10) methyl group.[20] Additionally, pallambins A (**14**) and B (**15**) comprise ten contiguous stereocenters, two of which are quaternary. At the outset of this project, it appeared reasonable to primarily focus on the construction of the tetracyclic core, before investigating additional methods to generate the γ-lactone-tetrahydrofuran bicycle (*cf.* Chapter 1.2.3).

Among the analytical tools available for developing a synthetic strategy, the retrosynthetic analysis developed by E. J. COREY *et al.* is the most widely used approach to date and thus regarded as the method of choice.[21] Therein, the chosen complex target molecule is iteratively disconnected into simpler intermediates, until easily accessible starting materials are reached. Of particular interest to our analysis of pallambins A (**14**) and B (**15**) were the aforementioned characteristic stereochemical features, which dictate an optimal synthetic tactic (Figure 2.1).

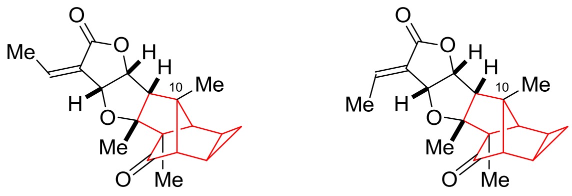

pallambin A (**14**)　pallambin B (**15**)

- ten contiguous stereocenters
- two quaternary carbon atoms
- unprecedented tetracyclo[4.4.$0^{3,5}$.$0^{2,8}$]decane core

Figure 2.1: Structure of targeted pallambins A (**14**) and B (**15**).

---

[19] Parts of this work have been published: C. Ebner, E. M. Carreira, *Angew. Chem. Int. Ed.* **2015**, *54*, 11227-11230.

[20] Throughout this thesis, pallambin A and B numbering is used (*cf.* ref. 7).

[21] a) E. J. Corey, X.-M. Cheng, in *The Logic of Chemical Synthesis*, John Wiley: New York, **1989**; b) S. Hanessian, in *Total Synthesis of Natural Products, the "Chiron" Approach*, 1st, Organic Chemistry series, 3, Pergamon Press: Oxford Oxfordshire, New York, **1983**; c) D. A. Evans in *An Organizational Format for the Classification of Functional Groups. Application to the Construction of Difunctional Relationships* (Chemistry 206: Advanced Organic Chemistry, Handout 27A), Harvard University, **2001**.

2.2 Retrosynthetic Analysis

Scheme 2.1 illustrates our first generation retrosynthetic analysis. Since the palladium-catalyzed alkoxycarbonylation proved to be reliable during the total synthesis of pallambins C and D by WONG an co-workers,[15] we decided to incorporate this method into our strategic plan. Thus, after retrosynthetic scission of the ethylidene side chain and *γ*-lactone-tetrahydrofuran formation, diol **74** evolved as a first simplified intermediate. The tertiary alcohol at C(8) could thereby be derived from the corresponding diketone **75** by aldol addition of the only enolizable ketone.

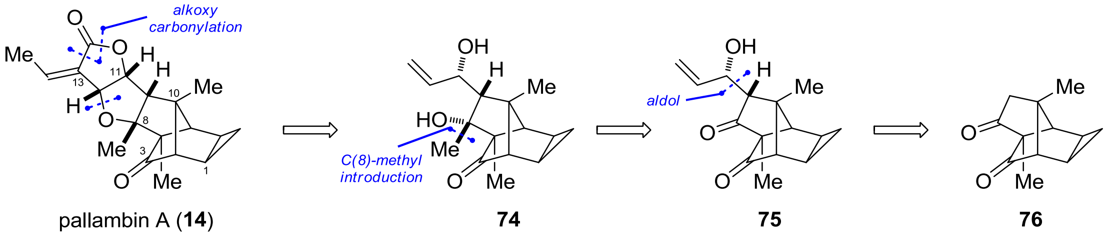
alkoxy carbonylation
O
Me
H
13
11
10
8
3
1
pallambin A (**14**)
C(8)-methyl introduction
HO
OH
74
aldol
75
76

Scheme 2.1: First generation retrosynthetic analysis of pallambin A (**14**).

At this stage, we were optimistic that the cyclopentanone containing C(4) and C(5) would induce sufficient strain on the norbornene system, thereby widening the angle between the olefin in **77** and the C(10) methyl group and consequently enable a cyclopropanation reaction (Scheme 2.2).

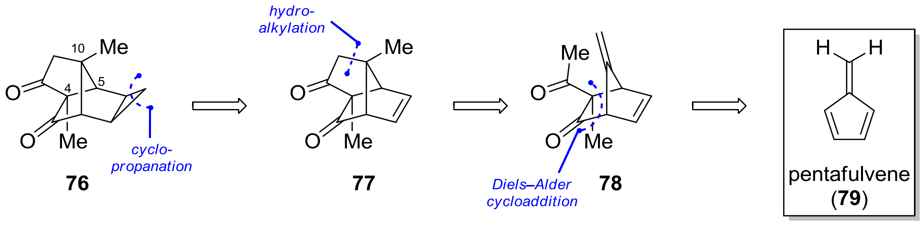
10
Me
4
5
O
cyclo-propanation
76
hydro-alkylation
77
Diels–Alder cycloaddition
78
H
pentafulvene (**79**)

Scheme 2.2: First generation retrosynthetic analysis of key intermediate **76**.

The envisioned key-disconnection was a transition metal-catalyzed intramolecular hydroalkylation reaction between the methyl ketone and the exocyclic disubstituted olefin to generate the quaternary center at C(10). We became aware of recent studies by CHE and co-workers, who reported the Au(I)-catalyzed intramolecular hydroalkylation of alkenes with 1,3-dicarbonyl compounds as well as unactivated ketones.[22] Additional considerations included acid-mediated enol formation with concomitant alkene protonation and trapping of the tertiary carbocation.

---

[22] a) C.-Y. Zhou, C.-M. Che, *J. Am. Chem. Soc.* **2007**, *129*, 5828-5829; b) Y.-P. Xiao, X.-Y. Liu, C.-M. Che, *Angew. Chem. Int. Ed.* **2011**, *50*, 4937-4941.

While analyzing diketone **78**, we became intrigued by the possibility of using pentafulvene (**79**), the simplest representative of the fulvene class, as a diene in the course of a Diels–Alder cycloaddition. The investigation of pentafulvene in such a transformation is beneficial due to three salient features. Firstly, unlike substituted cyclopentadienes, fulvene is not susceptible to isomerization through thermally allowed 1,5-hydrogen shifts (Scheme 2.3, A and ref. 19). Secondly, the sp^2-hybridized bridge carbon enables a wide variety of possibilities for functionalization. Consequently, the use of fulvene in a [4+2] cycloaddition creates significantly higher strategic flexibility for further elaboration. Thirdly, the successful realization of the cycloaddition would constitute the first use of pentafulvene in complex natural product synthesis.

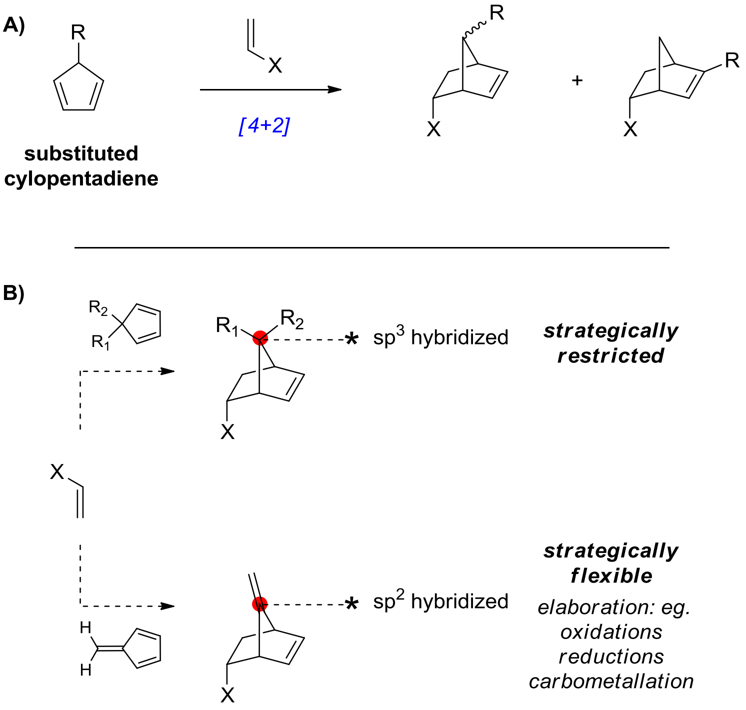
A)
R
substituted
cylopentadiene
X
[4+2]
R
X
+
R
X
B)
R2
R1
R1
R2
sp3 hybridized
strategically
restricted
X
X
H
H
sp2 hybridized
strategically
flexible
elaboration: eg.
oxidations
reductions
carbometallation
X

Scheme 2.3: A) Isomerization in [4+2] cycloadditions with mono-substituted cyclopentadienes; B) Strategic consequences of sp^3- vs. sp^2-substituted bridge carbons. Picture taken with permission from ref. 19.

2.3 Conclusion

The presented retrosynthetic analysis would provide a short and efficient route towards (±)-pallambins A (**14**) and B (**15**). The first critical issue to address was the development of a Diels–Alder reaction between pentafulvene (**79**) and a suitable dienophile, an endeavor, which is described in the following chapter. Additionally, total synthesis marks the gold standard to test the reliability and versatility of any reported methodology, such as the envisioned key hydroalkylation reaction.

3 Results and Discussion

3.1 Fulvene as a Diene in Diels–Alder Reactions

3.1.1 Introduction

Fulvenes are a class of hydrocarbons consisting of a cyclopentadiene equipped with an *exo* olefin (*cf.* Scheme 3.1). Pentafulvene (**79**), an isomer of benzene, has been synthesized for the first time in 1956 by THIEC and WIEMANN *via* condensation of sodium cyclopentadienide with formaldehyde.[23,24] Only four years later, ANGUS *et al.* discovered that this bright yellow oil can also be obtained by irradiation of benzene.[25] However, it was not possible to obtain pentafulvene (**79**) in pure form. Due to its challenging physical and chemical properties, including the high volatility and reactivity, the extraordinary Lewis and Brønsted acid sensitivity as well as its tendency to rapidly polymerize at room temperature, the handling and purification of **79** is highly demanding.[26,27] In neat form, pentafulvene is only stable for a few weeks, if excluded from air and stored below –70 °C. Of particular interest is, that only pentafulvene, the simplest representative of its class, and a limited number of exotic derivatives are endowed with these characteristics. For example, dimethylfulvene is a bench-stable and commercially available orange oil.

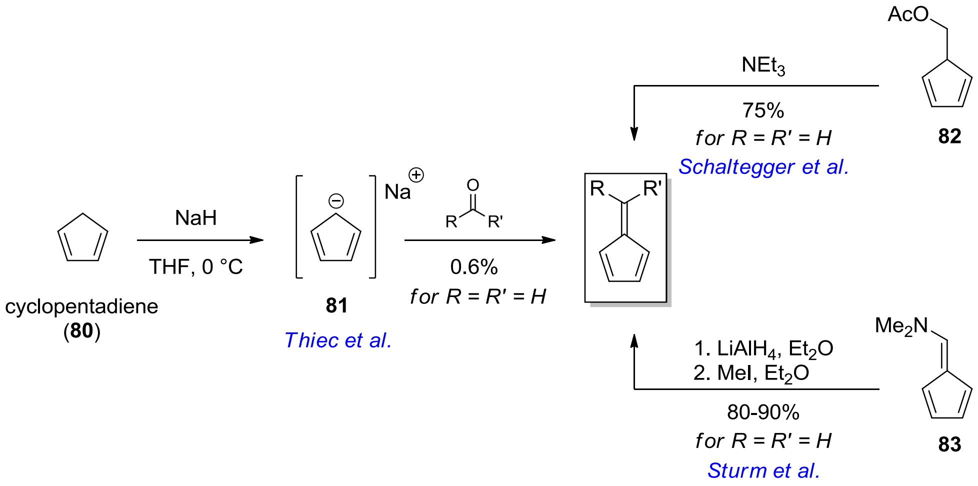

Scheme 3.1: General structure of fulvenes and synthetic strategies for the generation of pentafulvene.

While the condensation between sodium cyclopentadienide (**81**) and the vast majority of ketones proceeds generally without difficulties and in high yields, pentafulvene could only be

---

[23] a) J. Thiec, J. Wiemann, *Bull. Soc. Chim. Fr.* **1956**, 177-180; b) J. Thiec, J. Wiemann, *Bull. Soc. Chim. Fr.* **1960**, 1066-1067.
[24] a) J. Thiele, H. Balhorn, *Liebigs Ann. Chem.* **1906**, *348*, 1-15; b) J. Thiele, *Ber. Dtsch. Chem. Ges.* **1900**, *33*, 666-673.
[25] H. J. F. Angus, J. M. Blair, D. Brycesmith, *J. Chem. Soc.* **1960**, 2003-2016.
[26] D. Meuche, M. Neuenschwander, H. Schaltegger, H. U. Schlunegger, *Helv. Chim. Acta* **1964**, *47*, 1211-1215.
[27] C. Rentsch, M. Slongo, S. Schonholzer, M. Neuenschwander, *Makromol. Chem.* **1980**, *181*, 19-29.

obtained in 0.6% yield.[26,28] The demand for a milder and in particular higher yielding route for the synthesis of pentafulvene (**79**) prompted two research groups to seek for better solutions. In 1965, SCHALTEGGER *et al.* published the NEt_3-mediated elimination of acetoxymethyl-cyclopentadiene (**82**).[29] This process provided, after distillation, pentafulvene (**79**) in 75% yield. Moreover, STURM and HAFNER employed a $LiAlH_4$-mediated reduction, followed by Hofmann degradation of dimethylamino fulvene (**83**) and obtained pentafulvene (**79**) in 80% to 90% yield.[30]

Due to its instability, the reactivity profile of pentafulvene (**79**) is rather unexplored. However, already in 1956, THIEC and WIEMANN trapped pentafulvene with maleic anhydride in a Diels–Alder reaction in order to verify its generation.[23] Several years later, UEBERSAX *et al.* investigated the Diels–Alder dimerization of pentafulvene at room temperature.[31] In the course of a theoretical study, TROST and CORY generated the Diels–Alder adduct of fulvene (**79**) with diethyl azodicarboxylate (**86**) (Scheme 3.2).[32] Therein, pentafulvene was generated according to a modified procedure of STURM and HAFNER.[30] After reduction, the crude amines (**84** and **85**) were loaded on an alumina column and pentafulvene (**79**) was eluted under nitrogen. Refluxing an ethereal solution of **79** in the presence of excess diethyl azodicarboxylate (**86**) provided adduct **87** in 95% yield, albeit on small scale.

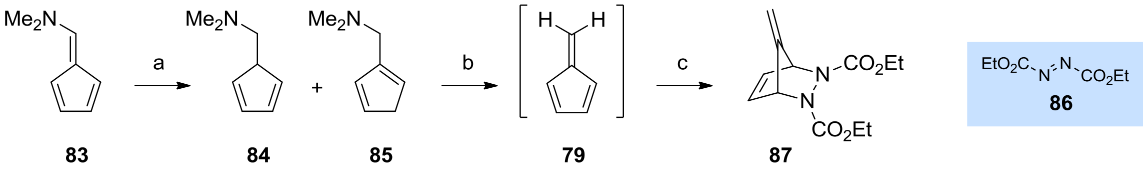

Scheme 3.2: TROST's Diels–Alder reaction between pentafulvene (**79**) and diethyl azodicarboxylate (**86**). Reagents and conditions: a) $LiAlH_4$, Et_2O, –5 °C to 0 °C, 78%; b) alumina, pentane, 77%; c) **86**, Et_2O, reflux, 95%.

Later, the TROST group optimized the generation of pentafulvene by returning to the original method of STURM and HAFNER[30], however removing the ammonium salt generated during the Hofmann degradation by simple filtration.[33] Thereby, the conversion from amines **84** and **85** to **79** was >99%, as determined by NMR spectroscopy.

---

[28] E. D. Bergmann, *Chem. Rev.* **1968**, *68*, 41-84.
[29] H. Schaltegger, M. Neuenschwander, M, D. Meuche, *Helv. Chim. Acta* **1965**, *48*, 955-961.
[30] E. Sturm, K. Hafner, *Angew. Chem.* **1964**, *76*, 862-863.
[31] B. Uebersax, M. Neuenschwander, H. P. Kellerhals, *Helv. Chim. Acta* **1982**, *65*, 74-88.
[32] B. M. Trost, R. M. Cory, *J. Org. Chem.* **1972**, *37*, 1106-1110.
[33] R. D. J. Froese, M. G. Organ, J. D. Goddard, T. D. P. Stack, B. M. Trost, *J. Am. Chem. Soc.* **1995**, *117*, 10931-10938.

3.1.2 Fulvene Diels–Alder Reaction for the Total Synthesis of Pallambins A and B

As previously established in our retrosynthetic analysis in Chapter 2.2, diketone **78** emerged as the first key intermediate (Scheme 3.3). This ketone was envisioned to be accessible *via* a Diels–Alder reaction of pentafulvene (**79**) and ketene (**89**). Importantly, a masked equivalent of the latter must be employed, since ketene is known to undergo [2+2] rather than [4+2] cycloadditions with fulvenes.[34] Additionally, this dienophile must be reactive enough to undergo the cycloaddition under conditions which do not trigger polymerization reactions of fulvene. Thus, strong acids, high temperatures, and prolonged reaction times should be avoided.

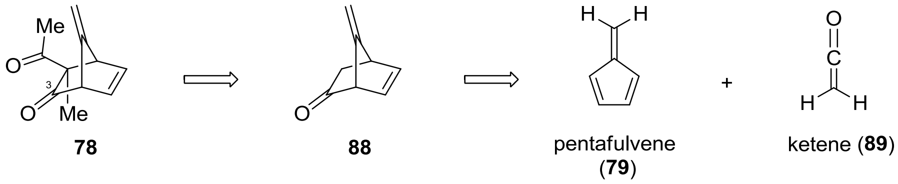

Scheme 3.3: Retrosynthetic analysis of intermediate diketone **78**.

Due to the availability of the starting materials, the higher overall yield and the facile purification, we chose to employ the method of STURM and HAFNER[30] for the generation of pentafulvene. Dimethylaminofulvene (**83**) was prepared according to a literature procedure from cyclopentadiene and DMF and then reduced with $LiAlH_4$ (Table 3.1).[35] After a modified work-up procedure the crude amines **84** and **85** were directly dissolved in the given solvent. Hofmann degradation was then effected by addition of methyl iodide and the ammonium salt formed was removed by filtration. The crude pentafulvene (**79**) was then subjected to various ketene equivalents to mediate a Diels–Alder reaction. We commenced our investigation with 2-chloroacrylonitrile (**91**) in refluxing toluene (Table 3.1, Entry 1). The desired Diels–Alder adduct could indeed be isolated, albeit 22% yield. At the bottom of the reaction flask, a rubber-like polymeric tar was formed indicating polymerization of pentafulvene. In order to suppress polymerization reactions the temperature was decreased. Hence, diethyl ether was employed to generate the fulvene and after filtration and addition of **91**, the desired product was obtained in slightly improved yield (27%, Entry 2).

---

[34] H. Stadler, M. Rey, A. S. Dreiding, *Helv. Chim. Acta* **1984**, *67*, 1854-1858.
[35] K. Hafner, K. H. Vöpel, G. Ploss, C. König, *Org. Syn. Coll. Vol. 5*, **1973**, 431.

Table 3.1: Initial screening of ketene equivalents in the Diels–Alder reaction with pentafulvene (**79**). Reagents and conditions: a) $LiAlH_4$, Et_2O, –17 °C, 88%; b) MeI, solvent, 0 °C, quant.

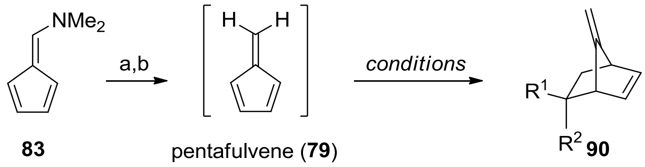

Entry	Dienophile	Additive	Solvent	Temperature	Yield[a]-[c]
1	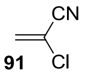 **91**	-	toluene	111 °C	22%
2	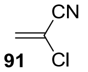 **91**	-	Et_2O	35 °C	27%
3	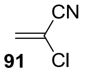 **91**	$Cu(BF_4)_2$ (0.30 equiv)	THF	0 °C	19%
4	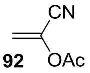 **92**	ZnI_2 (0.30 equiv)	Et_2O	40 °C	10%
5	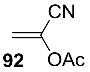 **92**	-	Et_2O	40 °C[d]	n.d.
6	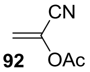 **92**	ZnI_2 (0.35 equiv)	Et_2O	4 °C	8 to 18%
7	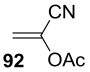 **92**	Me_2AlCl (0.20 equiv)	Et_2O	4 °C	n.d.
8	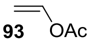 **93**	-	vinyl acetate– Et_2O (7:1)	50 °C to 80 °C	n.d.
9	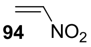 **94**	-	Et_2O–C_6H_6 (7:1)	4 °C	3%

[a] Yields refer to spectroscopically and chromatographically homogenous materials. [b] Since the d.r. is irrelevant for the C(3) position, it was not determined. [c] n.d. = Product not detected. [d] Reaction performed in a sealed vessel.

In order to allow even lower reaction temperatures, a potent catalyst was needed. In 1971, during their prostaglandin synthesis, COREY and co-workers reported $Cu(BF_4)_2$ to be an efficient catalyst for the Diels–Alder reaction between substituted cyclopentadienes and 2-chloroacrylonitrile (**91**).[36] However, performing the cycloaddition under these conditions gave only 19% of product (Entry 3). We next examined the related 2-acetoxyacrylonitrile (**92**), which has been used by VOGEL and co-workers in combination with ZnI_2 to catalyze the Diels–Alder reaction with furan.[37] Applying 30 mol% of ZnI_2 to pentafulvene in refluxing Et_2O provided the desired cycloadduct, unfortunately in only 10% yield (Entry 4). Lowering the reaction temperature to 4 °C increased the yield up to 18% (Entry 6), while no product could be detected in the absence of a Lewis acid catalyst (Entry 5). Switching to the more reactive Lewis acid Me_2AlCl did not lead to product formation (Entry 7). An attempt of an inverse electron demand Diels–Alder reaction of pentafulvene in refluxing vinyl acetate did also not yield the corresponding cycloadduct (Entry 8). With nitroethylene (**94**), a highly reactive dienophile, only traces of product could be obtained (3%, Entry 9). Noteworthy, solely the Diels–Alder adduct of 2-acetoxyacrylonitrile could be converted into targeted ketone **88**, while the chloro-equivalent did not undergo any further reaction.

---

[36] E. J. Corey, U. Koellike, J. Neuffer, *J. Am. Chem. Soc.* **1971**, *93*, 1489-1490.
[37] K. A. Black, P. Vogel, *Helv. Chim. Acta* **1984**, *67*, 1612-1615.

In summary, the results presented in Table 3.1 indicate that decreasing the temperature does indeed abet to decrease polymerization reactions, but that the 2-substituted acrylonitriles are not reactive enough to permit an efficient reaction. Even under the action of otherwise powerful catalysts, the reaction rate is too slow to entirely outcompete polymerization. A possible solution to prevent pentafulvene side reactions with itself would be to run the reaction in presence of a huge excess of dienophile. However this demands for a cheap and volatile reaction partner.

Having the above findings in mind, we next turned our attention to the use of acrylates. These unsaturated esters served as powerful dienophiles in countless [4+2] cycloadditions. Importantly, while thermal conditions should be avoided, a variety of different Lewis acids can be employed. Hence, pentafulvene was generated directly in methyl acrylate by the addition of methyl iodide. The generated ammonium salt was removed by filtration leaving a bright yellow solution. Then, two equivalents of Me_2AlCl were added at –20 °C. Gratifyingly, after stirring overnight, the yellow color vanished without the formation of polymeric tar. Indeed, after workup and purification, the desired adduct **95** was isolated in excellent yield of 89% (Scheme 3.4).

Finally, the scalability of the newly established Diels–Alder reaction needed to be investigated. In order to simplify the reaction handling and the work-up procedure, catalytic amounts of Et_2AlCl (0.3 equiv) were used on a 25 g scale. To our delight **95** was still the only observed product, albeit in slightly lower yield of 62%.

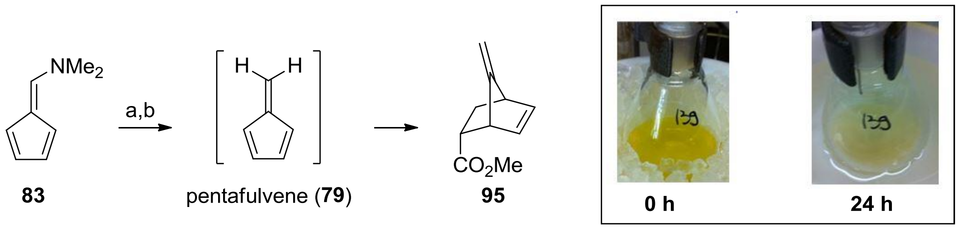

Scheme 3.4: Diels–Alder reaction between pentafulvene (**79**) and methyl acrylate. Reagents and conditions: a) $LiAlH_4$, Et_2O, –17 °C, 88%; b) MeI, methyl acrylate, 0 °C, then Me_2AlCl (2.0 equiv), –20 °C, 89% or MeI, methyl acrylate, then Et_2AlCl (0.3 equiv), –20 °C to 5 °C, 62%.

3.2 C(3)-Ketone Formation and α-Functionalization

3.2.1 Oxidative Decarboxylation

Having established a reliable access to diene **95** *via* Diels–Alder reaction of pentafulvene (**79**), we next turned our attention to the generation of the C(3) ketone. Such a transformation requires not only an oxidation, but also a decarboxylation of the methyl ester. A literature survey revealed a few direct methods for the oxidative decarboxylation of different carbonyl groups. In the course of a formal synthesis of platensimycin, YAMAMOTO employed such a transformation by firstly generating the nitroso-aldol product between ester **96** and nitrosobenzene (Scheme 3.5, A).[38] The oxidative decarboxylation was then effected by treatment with LiOH to give ketone **98** in high overall yield of 75%. However, when applying this procedure to our system, only minor amounts of product could be isolated (30% yield, Scheme 3.5, B). A closer reaction survey, in which the nitroso-aldol product **100** was isolated and purified before subjected to lithium hydroxide, revealed that this part of the transformation was very low yielding (32%). Attempts to improve the yield by lowering the temperature or performing an inverse addition were met with failure.

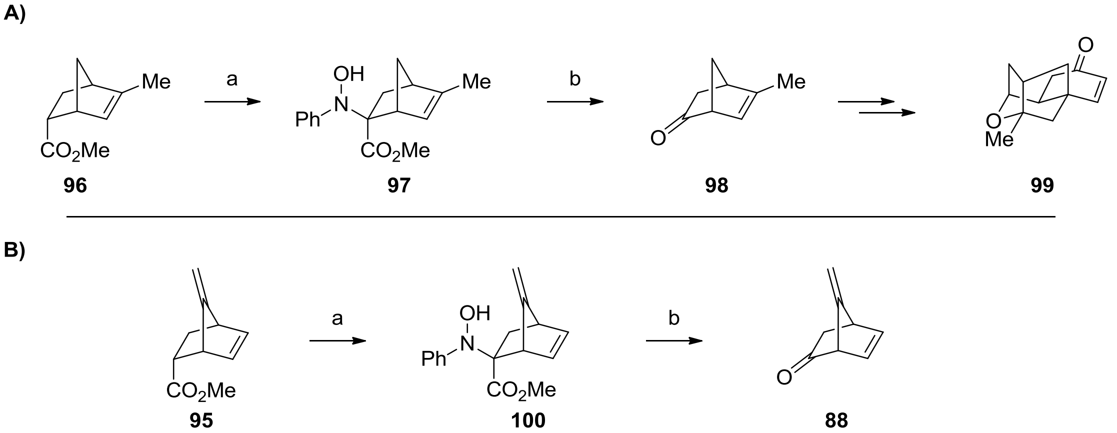

Scheme 3.5: A) YAMAMOTO's oxidative decarboxylation using nitrosobenzene during a formal synthesis of platensimycin; B) Attempted transformation of ester **95** into ketone **88** using this method. Reagents and conditions: a) *i*Pr_2NLi, THF, –78 °C, then PhNO, –78 °C, 32% for **100**; b) LiOH·H_2O, H_2O–dioxane (7:6), 35 °C, 75% for **98**, 30% for **88** (over two steps).

---

[38] P. F. Li, J. N. Payette, H. Yamamoto, *J. Am. Chem. Soc.* **2007**, *129*, 9534-9535.

A related transformation was reported by TROST and TAMARU in 1975.[39] Thereby, the dianion of a carboxylic acid is reacted with dimethyl disulfide. Upon treatment with *N*-chlorosuccinimide and subsequent hydrolysis, the corresponding ketones are isolated in 44–78% overall yield. Unfortunately, when applied to our system, no product could be detected.

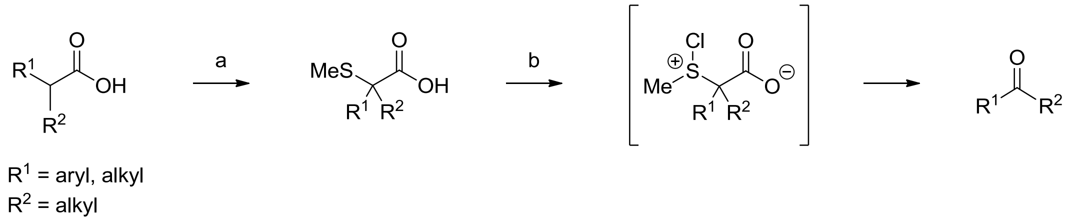

Scheme 3.6: TROST's oxidative decarboxylation using dimethyl disulfide. Reagents and conditions: a) *i*Pr_2NLi, THF–HMPA (5:1), 0 °C, then Me_2S_2, 0 °C; b) $NaHCO_3$, MeOH, then NCS, 0 °C, 44–78% over two steps.

Since both established oxidative decarboxylation protocols failed, stepwise *α*-hydroxylation followed by ester reduction and subsequent diol cleavage was considered as an efficient alternative to this end. While initial oxidation attempts employing Davis oxaziridine[40] or Rubottom oxidation[41] of the silyl ketene acetal derived from **95** were met with failure, quenching of the corresponding lithium enolate with molecular oxygen and concomitant peroxide reduction provided alcohol **102** in moderate yield of 59% (Scheme 3.7).[42]

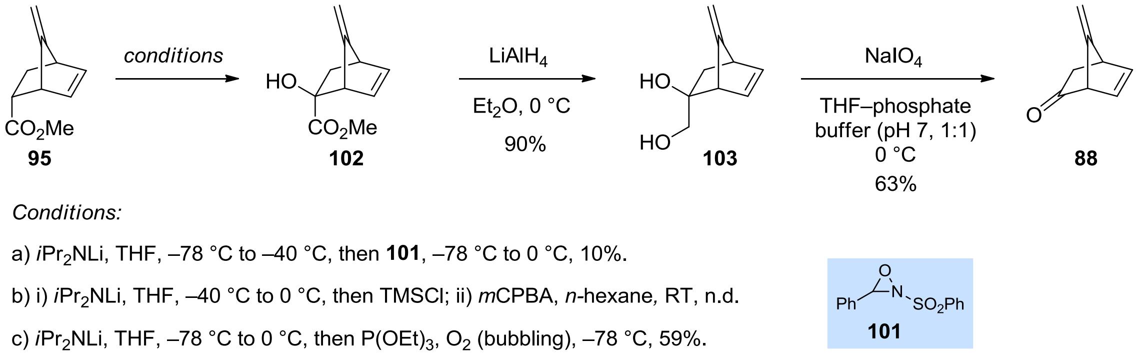

Conditions:

a) *i*Pr_2NLi, THF, –78 °C to –40 °C, then **101**, –78 °C to 0 °C, 10%.

b) i) *i*Pr_2NLi, THF, –40 °C to 0 °C, then TMSCl; ii) *m*CPBA, *n*-hexane, RT, n.d.

c) *i*Pr_2NLi, THF, –78 °C to 0 °C, then $P(OEt)_3$, O_2 (bubbling), –78 °C, 59%.

Scheme 3.7: *α*-Hydroxylation of ester **95** and further transformation into ketone **88**.

Hydroxyester **102** could be smoothly reduced to diol **103** in 90% yield. Subsequent sodium periodate-mediated cleavage gave ketone **88** in satisfactory yield of 63%. We later discovered that ketone **88** proved to be extremely volatile and careful evaporation of solvents was necessary.

---

[39] B. M. Trost, Y. Tamaru, *J. Am. Chem. Soc.* **1975**, *97*, 3528-3530.
[40] F. A. Davis, L. C. Vishwakarma, J. M. Billmers, J. Finn, *J. Org. Chem.* **1984**, *49*, 3241-3243.
[41] G. M. Rubottom, M. A. Vazquez, Pelegrin.Dr, *Tetrahedron. Lett.* **1974**, 4319-4322.
[42] J. L. Belletire, D. F. Fry, *J. Org. Chem.* **1988**, *53*, 4724-4729.

3.2.2 α-Functionalization of Ketone 88

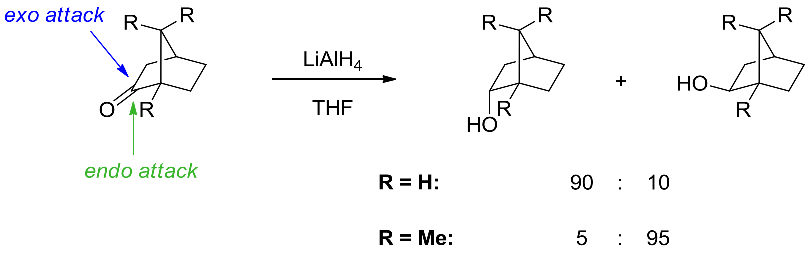

Scheme 3.8: Observed selectivity during the reduction of norbornanone and camphor.

With a reliable route to key intermediate **88** in hand, the challenge of generating the C(4) quaternary center by electrophilic α-functionalization was tackled next. Since it dictated the order of events, the question of stereoselectivity needed to be addressed first. As shown in Scheme 3.8, it is well known that $LiAlH_4$-mediated reduction of norbornanone (R = H) selectively provides the *endo* alcohol.[43] For camphor (R = Me) on the other hand, the *exo* attack is disfavored due to the steric shielding of the bridge substituents. This finding leads to the conclusion, that nucleophiles, as well as potential electrophiles for the corresponding enolates, favor *exo* attack. Since ketone **88** bears an *exo* methylene moiety at the bridge carbon, we surmised that this compound would behave similar to norbornanone and thus favor *exo* functionalization. Hence, the first transformation *en route* to diketone **78** should be the α-methylation, followed by α-acylation.

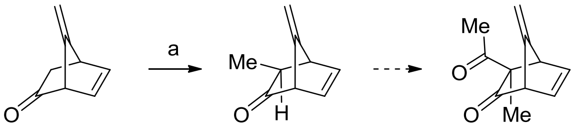

88 **104** **78**

Scheme 3.9: α-Methylation of ketone **88**. Reagents and conditions: a) iPr$_2$NLi, THF, –78 °C, then MeI, –78 °C to RT, 86%.

In a first experiment, ketone **88** was deprotonated with iPr$_2$NLi, and reacted with MeI to furnish methyl ketone **104** in 86% yield. The product was obtained as a single diastereomer, thus confirming our assumption of selective *exo* functionalization. Unfortunately, when the experiment was repeated several times, a vast fluctuation of yield was observed. Under identical conditions, 32 to 86% of product were obtained. At this stage, we reasoned, that the volatility of **104** might be the reason for this issue, in combination with undefined side reactions. However, the search for an answer to this problem was postponed, since the envisioned key hydroalkylation of diketone **78** was in reach with the material available.

---

[43] For an overview, see for example: J. Clayden, N. Greeves, S. Warren, P. Wothers, *Organic Chemistry*, Oxford University Press, **2001**, p. 862.

The stage was now set to introduce the acyl moiety. Since O- vs. C-acylation is always an issue to address during such transformations, the use of acetyl chloride was avoided and 1-acetylimidazole was chosen as an alternative.

Table 3.2: Functionalization of ketone **104** to obtain a 1,3-dicarbonyl product.

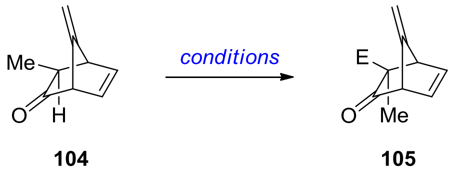

Entry	Electrophile	Base	Solvent	Temperature	Yield[a],[b]
1	1-acetyl-imidazole	*i*Pr$_2$NLi	THF	–78 °C to RT	6%
2[c]	1-acetyl-imidazole	*i*Pr$_2$NLi	THF	–78 °C	22%
3	(MeO)$_2$CO	NaH	THF	66 °C	n.d.
4	(MeO)$_2$CO	*i*Pr$_2$NLi	THF	–78 °C to RT	n.d.

[a] Yields refer to spectroscopically and chromatographically homogenous materials. [b] n.d. = Product not detected. [c] Electrophile added fast (t < 1s).

In a first attempt, the desired product could be obtained, although in poor yield of 6% with 40% recovered starting material (Table 3.2, Entry 1). Protonation of the enolate of **104** by 1-acetylimidazole might be a reason for the observed low conversion. Thus, fast addition of an excess acylating reagent was tested (Table 3.2, Entry 2). Indeed, the yield increased to 22%. The weaker electrophile dimethyl carbonate did not produce any product (Table 3.2, Entries 3 and 4).

Due to the discouraging results obtained with enolates, we switched to silyl enol ethers. A recent report from REIM *et al.* described the reaction between silyl enol ethers and methyl malonyl chloride in the presence of substoichiometric amounts of TMSOTf.[44] However, when applied to our system, the expected *β,δ*-diketoester **106** was not isolated, but diester **107** (Scheme 3.10). One logical explanation for the formation of the latter is the presence of water in the reaction mixture, which hydrolyzed the methyl malonyl chloride and led to the formation of triflic acid from TMSOTf. Subsequent protonation of the exocyclic olefin and trapping of the corresponding tertiary carbocation by methyl malonic acid would then provide **107**.

---

[44] S. Reim, D. Michalik, K. Weisz, Z. Xiao, P. Langer, *Org. Biomol. Chem.* **2008**, *6*, 3079-3084.

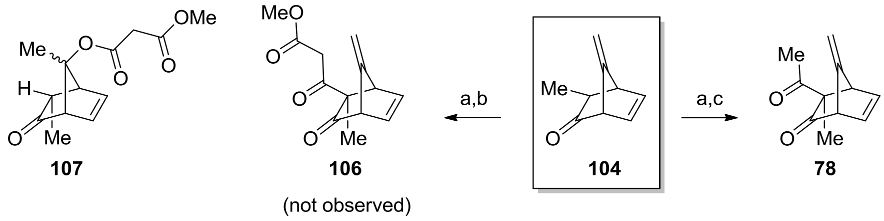
OMe
Me
O
H
O
Me
107
MeO
O
O
O
Me
106
(not observed)
a,b
Me
O
104
a,c
Me
O
O
Me
78

Scheme 3.10: Functionalization of ketone **104** *via* the corresponding silyl enol ether. Reagents and conditions: a) TMSOTf, NEt_3, CH_2Cl_2, 0 °C to RT, quant; b) Methyl malonyl chloride, TMSOTf, toluene, yield not determined; c) AcCl, $ZnCl_2$, Et_2O, CH_2Cl_2, 0 °C, 58%.

In 1982, TIRPAK and RATHKE reported the acylation of silyl enol ethers with acid chlorides in presence of $ZnCl_2$ or $SbCl_3$.[45] Gratifyingly, when the trimethylsilyl enol ether of ketone **104** was reacted with acetyl chloride and $ZnCl_2$, the desired diketone **78** was isolated in 58% yield along with 26% of α-isomerized **104** (Scheme 3.10). Attempts to further increase the conversion by using more stable silyl enol ethers (TES and TBS) were unfruitful.

3.2.3 Conclusion

In summary, an efficient route to diketone **78** from fulvene Diels–Alder adduct **95** has been established (Scheme 3.11). The sequence relies on α-hydroxylation of ester **95** with molecular oxygen, followed by reduction and diol cleavage. The thus obtained ketone **88** was selectively *exo* methylated to give **104** in varying yields.

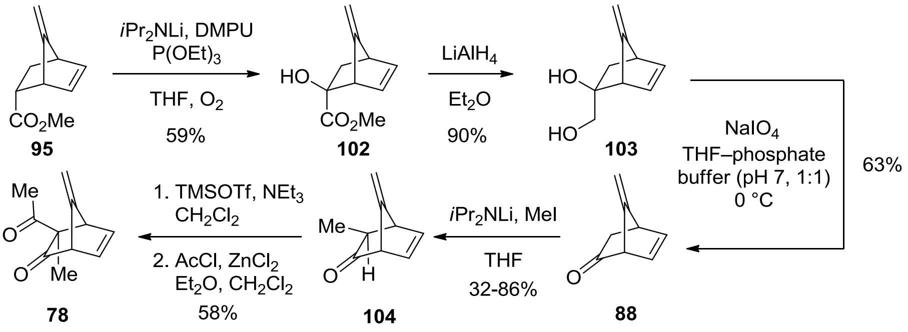
CO2Me
95
iPr2NLi, DMPU
P(OEt)3
THF, O2
59%
HO
CO2Me
102
LiAlH4
Et2O
90%
HO
HO
103
NaIO4
THF–phosphate
buffer (pH 7, 1:1)
0 °C
63%
O
88
iPr2NLi, MeI
THF
32-86%
Me
O
H
104
1. TMSOTf, NEt3
CH2Cl2
2. AcCl, ZnCl2
Et2O, CH2Cl2
58%
Me
O
O
Me
78

Scheme 3.11: Synthetic sequence from diene **95** to diketone **78**.

While direct enolate acylation failed, the use of the corresponding silyl enol ether provided valuable insights into the chemical behavior of this system. Even though the reaction with methyl malonyl chloride did not provide the desired product, it opened further alternatives for subsequent functionalization of **78** by olefin protonation and intramolecular enol trapping. Exposure of the trimethylsilyl enol ether of **104** to acetyl chloride in presence of $ZnCl_2$ ultimately provided access to diketone **78** in 58% overall yield.

---

[45] R. E. Tirpak, M. W. Rathke, *J. Org. Chem.* **1982**, *47*, 5099-5102.

3.3 C(9)–C(10) Bond Formation

With sufficient material of diketone **78** in hand, the crucial C(9)–C(10) bond formation was approached next. As described during the retrosynthetic analysis (*cf.* Chapter 2.2), an intramolecular hydroalkylation reaction of **78** was envisioned as the key step to form the tricyclic core of pallambins A and B (Scheme 3.12).

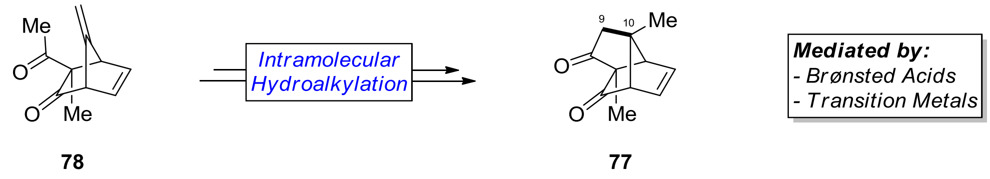
Me
O
O
Me
78
Intramolecular
Hydroalkylation
9
10
Me
O
O
Me
77
Mediated by:
- Brønsted Acids
- Transition Metals

Scheme 3.12: Envisioned hydroalkylation key step to form the C(9)–C(10) bond.

3.3.1 Au(I)-Mediated Hydroalkylation

In 2001, the WIDENHOEFER group reported the first efficient transition metal-mediated addition of stabilized carbon nucleophiles to unactivated olefins.[46] When dione **108** was exposed to one equivalent of $PdCl_2(MeCN)_2$ in THF, full conversion was reached after only 15 min to give cyclohexanone **109** in 70% yield (Scheme 3.13).

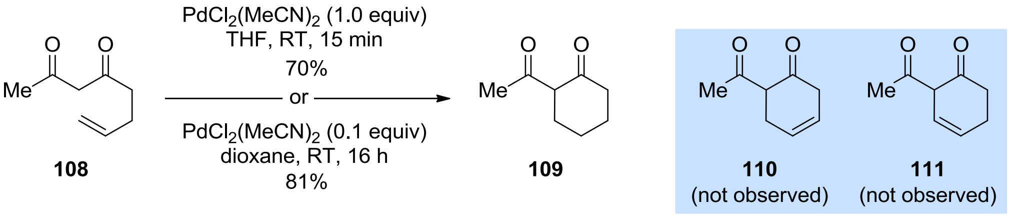
O
O
Me
108
PdCl2(MeCN)2 (1.0 equiv)
THF, RT, 15 min
70%
or
PdCl2(MeCN)2 (0.1 equiv)
dioxane, RT, 16 h
81%
O
O
Me
109
O
O
Me
110
(not observed)
O
O
Me
111
(not observed)

Scheme 3.13: Pd(II)-mediated hydroalkylation developed by WIDENHOFER and co-workers.

Surprisingly, no olefinic bond was present in the obtained product, suggesting that no oxidation occurred. Although alkyl Pd(II) complexes are typically unstable towards β-hydride elimination,[47] it has been shown, that in the present case, a protodepalladation occurred instead.[48] This finding proved to be crucial, since it opened the possibility to perform this reaction under catalytic conditions. Indeed, upon employment of only 10 mol% $PdCl_2(MeCN)_2$ the desired product **107** was obtained in 81% yield. Notably, the 6-*endo-trig* cyclized product was the only isolated product, while no 5-*exo-trig* cyclization occurred.

---

[46] T. Pei, R. A. Widenhoefer, *J. Am. Chem. Soc.* **2001**, *123*, 11290-11291.

[47] a) L. S. Hegedus *Transition Metals in the Synthesis of Complex Organic Molecules*, University Science Books, Mill Valley, CA, **1999**, pp. 188-204; b) L. S. Hegedus in *Organometallics in Synthesis* (Ed: M. Schlosser), John Wiley & Sons, Chichester, UK, **1994**, pp. 388-397.

[48] For a detailed mechanistic study, see H. Qian, R. A. Widenhoefer, *J. Am. Chem. Soc.* **2003**, *125*, 2056-2057.

Six years later, ZHOU and CHE published a related transformation using cationic gold(I) catalysts for the cyclization of β-ketoamides.[22a)] Upon exposure of various β-ketoamides to [Au(P(*t*Bu)$_2$-*o*-biphenyl]Cl (**112**) at 50 °C in toluene, 5-*exo-trig* cyclized lactams were obtained in high yields (90-99%). As for the Pd(II)-catalyzed hydroalkylation of WIDENHOEFER, the transformation is enabled by the favorable ketone/enol equilibrium of β-dicarbonyls. After initial activation of the alkene by the cationic gold(I) complex, the olefin is attacked by the enol tautomer and the thus formed C–Au bond undergoes protodeauration to regenerate the catalyst and liberate the cyclized product as a single *anti* diastereomer (Scheme 3.14).

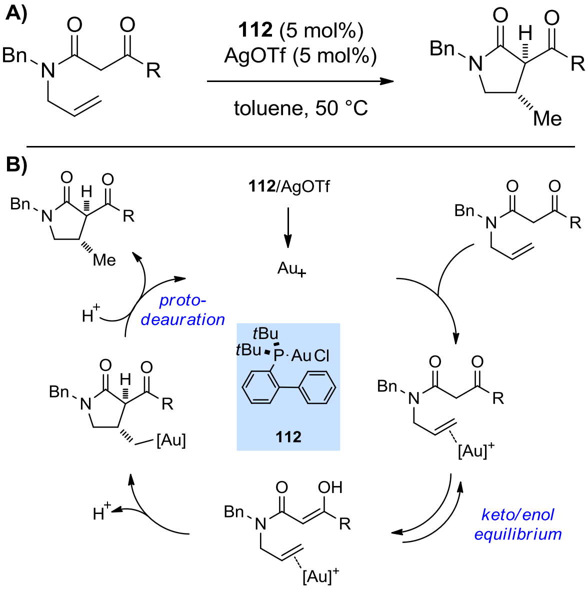

Scheme 3.14: A) Au(I)-catalyzed hydroalkylation of ketoamides by CHE; B) Proposed mechanism.

CHE and co-workers further investigated this transformation with the intention to enable the use of simple aliphatic ketones as carbon nucleophiles.[22b)] The two main problems which arise are firstly the lower acidity of the α-proton (p$K_a \approx 27$ for aliphatic ketones vs. p$K_a \approx 13$ for β-dicarbonyls)[49] and secondly the unfavorable enol/ketone equilibrium.[50] Nevertheless, these difficulties could be resolved by employing higher reaction temperatures (111 °C) and a different gold(I) catalyst (IPrAuCl)[51] providing the desired cyclized products in high yields (71-99%). Noteworthy, even 1,1-disubstituted olefins could be employed.

In order to perform the envisioned intramolecular hydroalkylation reaction of ketone **78**, we decided to start our investigation with the conditions described by CHE. Due to the commercial availability of **112** and the reported only slightly diminished yields, this complex was used as Au(I) source. When diketone **78** was added to a solution of **112** in toluene, followed by addition of $AgClO_4$, immediate precipitation of AgCl was observed (Scheme 3.15). The heterogeneous mixture was gradually warmed to 90 °C, but no conversion could be detected. Disappointingly, upon refluxing the reaction overnight, only decomposition of the starting material was observed.

---

[49] Values measured in DMSO, taken from the Evans pK_a table: http://evans.harvard.edu/pdf/evans_pKa_table.pdf

[50] Reported values of $K_{enol/ketone}$ for representative compounds: a) J. P. Guthrie, P. A. Cullimore, *Can. J. Chem.* **1979**, *57*, 240-248; b) J. P. Guthrie *Can. J. Chem.* **1979**, *57*,1177-1185; c) M. Bassetti, G. Cerichelli, B. Floris, *Tetrahedron* **1988**, *44*, 2997-3004.

[51] IPr = *N*,*N*'-bis(2,6-diisopropylphenyl)-imidazol-2-ylidiene

Based on this result and being aware of the higher reactivity of *β*-ketoesters in hydroalkylation reactions, ketone **78** was transformed into diketoester **113**. It should be noted, that an additional carbonyl group in this position could potentially be used later in the synthesis for the generation of the C(11) oxygen functionality (*cf.* **75**, Scheme 2.1) Following MANDER's protocol for selective C-acylation, the corresponding lithium enolate was reacted with methyl cyanoformate (Mander's reagent).[52] Although this reaction proceeded extremely sluggishly and provided the desired product **113** in only 7% yield, sufficient material could be produced to test the hydroalkylation reaction. Disappointingly, subjecting *β*-ketoester **113** to CHE's conditions resulted only in decomposition of the starting material.

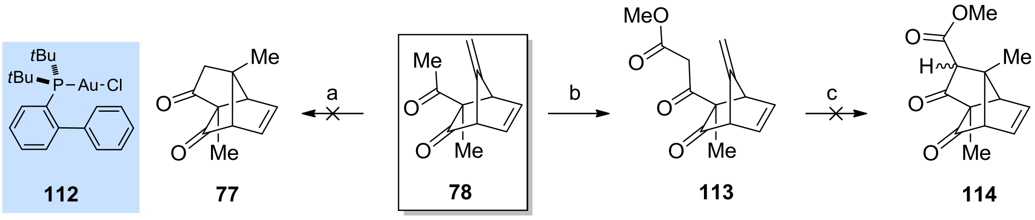

Scheme 3.15: Attempts to generate the C(9)–C(10) bond by a gold(I)-catalyzed intramolecular hydroalkylation. Reagents and conditions: a) **112** (15 mol%), $AgClO_4$ (15 mol%), toluene, RT to 111 °C, decomposition; b) *i*Pr_2NLi, THF, –78 °C, then $MeO_2C(CN)$, –78 °C to 0 °C, 7%; c) **112** (15 mol%), AgOTs (15 mol%), toluene, RT to 111 °C, decomposition.

3.3.2 Brønsted and Lewis Acid-Mediated Ring Closure

Due to the discouraging results obtained in the gold(I)-catalyzed hydroalkylation, an alternative method for the key C–C bond closure was deemed necessary. TRAUNER and co-workers realized the intramolecular attack of the *β*-ketolactone in **115** onto a tertiary carbocation, generated by olefin protonation with a strong acid (Scheme 3.16, A).[53] When *β*-ketoester **113** was subjected to 5 mol% of triflic acid in deuterated toluene, no reaction was observed upon gradual heating to 60 °C (Scheme 3.16, B). However, increasing the temperature to 90 °C entailed only decomposition of the starting material.

---

[52] S. R. Crabtree, W. L. A. Chu, L. N. Mander, *Synlett* **1990**, 169-170.
[53] V. Sofiyev, G. Navarro, D. Trauner, *Org. Lett.* **2008**, *10*, 149-152.

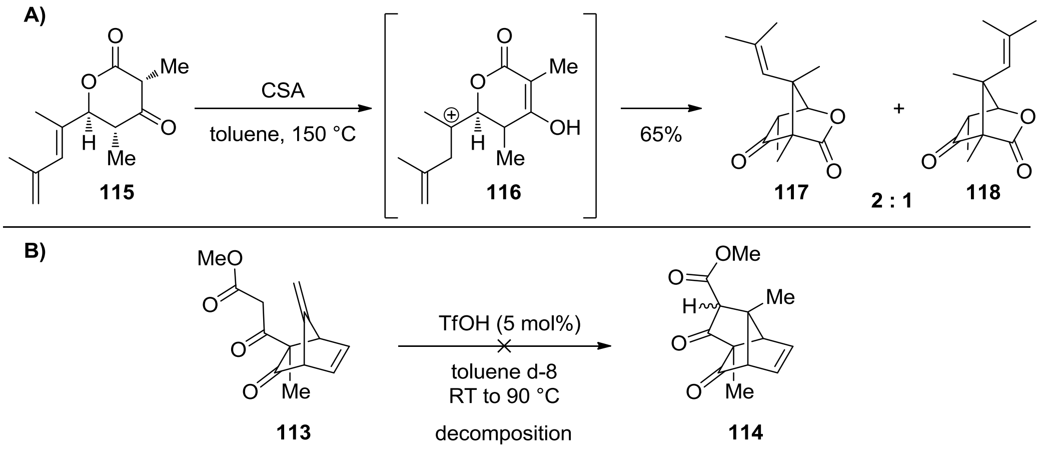

Scheme 3.16: A) Cyclization enabled by olefin protonation employed by TRAUNER and co-workers during the total syntheses of shimalactones; B) Attempted protonation and cyclization of *β*-ketoester **113**.

We then turned our attention to the use of Lewis acids, which could potentially coordinate to the *β*-ketoester, thereby mediate enolization with concomitant formation of H–X. The thus *in situ* liberated acid could then protonate the double bond and cyclization might occur. Indeed, a literature survey provided valuable examples by REETZ and co-workers, who undertook a detailed study of this transformation (Scheme 3.17, A).[54] When *β*-ketoester **113** was exposed to the reported conditions, a new spot on TLC appeared, indicating the formation of at least one new compound (Scheme 3.17, B). Unfortunately, despite extensive attempts to isolate this product only decomposition was observed upon workup. Hence, it was reasoned that the electron withdrawing effect of the *β*,*γ*-tricarbonyl fragment might cause side reactions (i.e. retro Claisen reaction). In order to circumvent such an event, the C(3) ketone was thus reduced and protected by the following sequence: protection of the C(8) ketone by conversion into the corresponding silylenol ether followed by selective *exo* reduction and protection provided **123**. Selective desilylation gave ketone **124** in a high overall yield of 57% from **78**. Conversion into *β*-ketoester **125** again proved to be difficult and proceeded in only 10% yield. Exposure of this material to $SnCl_4$ provided a new product, which could be isolated without difficulties. Unfortunately, this new compound was not identified as desired tricycle **126**, but as silylenol ether **127**. This product is presumed to arise from a retro Diels–Alder reaction of **125** to give **127** and volatile pentafulvene.

---

[54] M. T. Reetz, I. Chatziiosifidis, K. Schwellnus, *Angew. Chem. Int. Ed.* **1981**, *20*, 687-689.

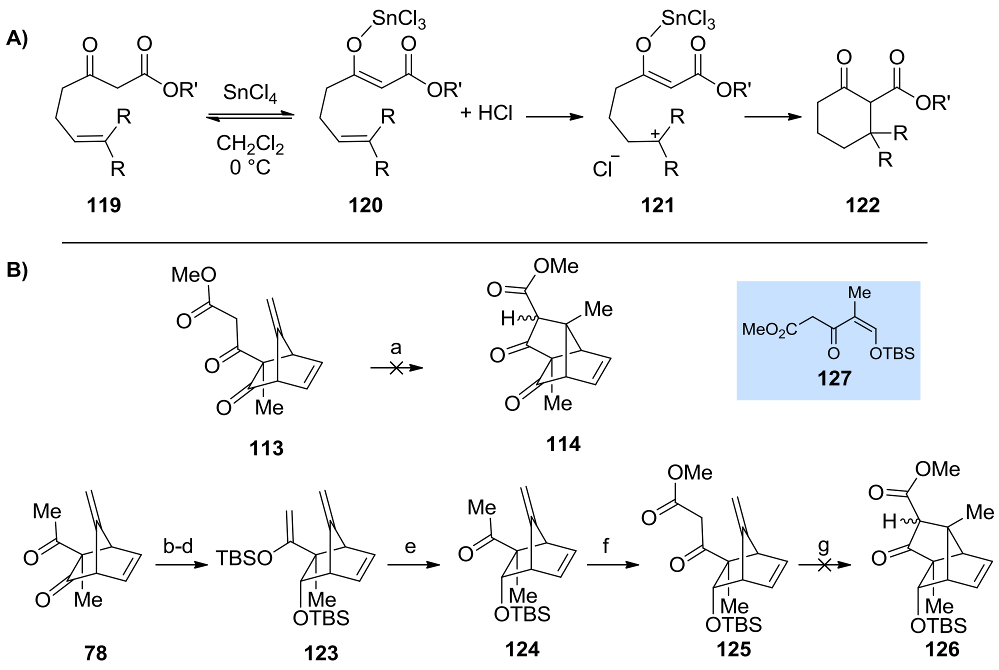

Scheme 3.17: A) Study by REETZ and co-workers on the cyclization of *β*-ketoesters and olefins in the presence of strong Lewis acids; B) Attempted cyclization of **113** and **125**. Reagents and conditions: a) $SnCl_4$ (0.5 equiv), CH_2Cl_2, 0 °C to RT, decomposition; b) TBSOTf, NEt_3, CH_2Cl_2, 0 °C to RT; c) $LiAlH_4$, Et_2O, −42 °C, 61% over two steps; d) TBSOTf, NEt_3, CH_2Cl_2, 0 °C, 94%; e) AcOH, CH_2Cl_2, quant.; g) *i*Pr_2NLi, Et_2O, –78 °C to –20 °C, then $MeO_2C(CN)$, 10%; g) $SnCl_4$ (0.5 equiv), CH_2Cl_2, 0 °C to RT, 68% of **127**.

3.3.3 Radical-Mediated Ring Closure

Due to the failure of mediating the key C(9)–C(10) bond formation *via* ionic pathways, i.e. protonation of the *exo* double bond, radical reactions were investigated next. In order to generate a radical at the C(9) carbon, a suitable leaving group is required. Thus, bromination of ketone **78** was performed by reacting the corresponding lithium enolate with NBS (Scheme 3.18, A). Bromide **128** was obtained in only 26% yield, along with various side products including the respective tribromide. In an initial attempt **128** was treated with *n*Bu_3SnH and AIBN in refluxing benzene.[55] Unfortunately, only decomposition of the starting material was observed and milder conditions were deemed necessary. A report by STEPHENSON and co-workers describes the generation of radicals in the *α*-position of carbonyl groups from bromides under the influence of photoredox-catalysis.[56] Therein, the radical is generated by single electron transfer from a Ru(III) or Ir(II) complex to the substrate. The thus generated radical subsequently reacts with an olefin or alkyne to give the desired cyclized products in high yields (Scheme 3.18, B). However, applying these conditions to bromide **128** only led to the formation of multiple unidentified products.

---

[55] For an excellent review, see C. P. Jasperse, D. P. Curran, T. L. Fevig, *Chem. Rev.* **1991**, *91*, 1237-1286.

[56] J. W. Tucker, J. D. Nguyen, J. M. R. Narayanam, S. W. Krabbe, C. R. J. Stephenson, *Chem. Commun.* **2010**, *46*, 4985-4987.

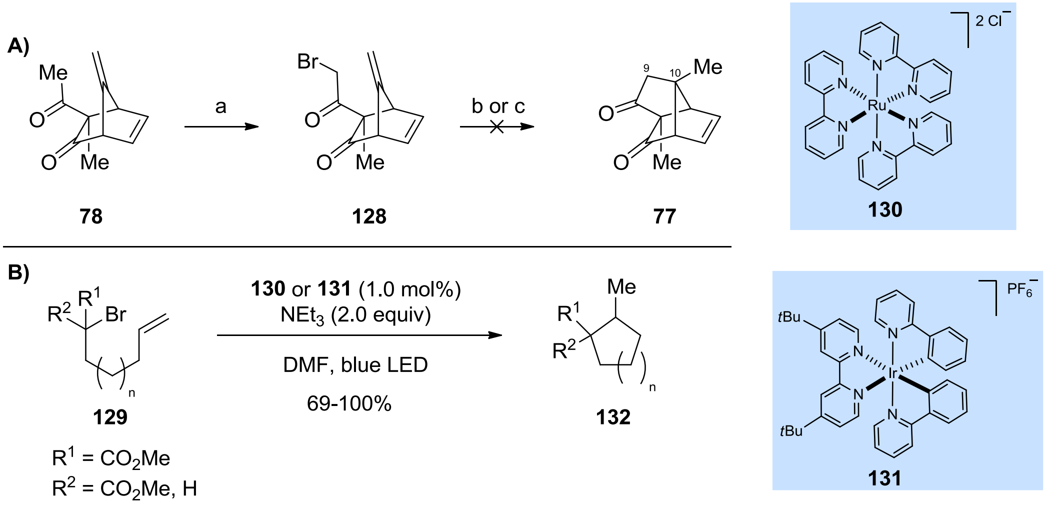

Scheme 3.18: A) Attempted radical cyclization to generate the key C(9)–C(10) bond. Reagents and conditions: a) *i*Pr_2NLi, THF, –78 °C, then NBS, THF, –78 °C, 22%; b) AIBN (5 mol%), Bu_3SnH, C_6H_6, decomposition; c) **131** (5 mol%), NEt_3, DMF, visible light, decomposition; B) Radical cyclization of *α*-bromoesters by STEPHENSON and co-workers *via* photoredox-catalysis.

3.3.4 Pd(II)-Mediated Ring Closure

Although gold(I) complexes could not effectively activate the desired *exo* double bond of ketone **78** (*cf.* Chapter 3.3.1), switching to another, more suitable metal might enable the desired cyclization reaction.[57] Due to its affinity to coordinate to olefins, a feature which is exceedingly used in various catalytic processes, palladium was chosen as an adequate replacement. In 1979, the SAEGUSA group reported a novel cyclization upon exposing *ω*-vinyl silylenol ethers such as **133** to $Pd(OAc)_2$ yielding cyclized enones (*cf.* **137,** Scheme 3.19, A).[58,59]A few years later, KENDE *et al.* proposed a mechanism involving activation of the *ω*-olefin followed by nucleophilic attack of the silylenol ether.[60] The thus formed organopalladium species **135** then suffers from *β*-hydride elimination to liberate the product and Pd(0). In most cases, the thermodynamically favored isomerization to *α,β*-unsaturated ketones occurred. In order to overcome the disadvantageous use of stoichiometric Pd(II), TOYOTA and co-workers developed a catalytic variant of this transformation (Scheme 3.19, A).[61]

Noteworthy, in contrast to the previously described examples, which are terminated by a *β*-hydride elimination and are hence of oxidative nature, the transformation of **78** to **77** demands a reductive Heck-type cyclization. After olefin coordination and nucleophilic attack, an organopalladium species adjacent to a quaternary center would be generated and thus cannot undergo *β*-hydride elimination (*cf.* **139** Scheme 3.19, B). If such a species was long-lived enough, an external reductant might be added after cyclization occurred. If successful, a screening of reductants might provide a suitable reagent, which does not interfere with TOYOTA's conditions, developed to reoxidize Pd(0) to Pd(II) by molecular oxygen and hence enable a catalytic process.

---

[57] F. Dénès, A. Pérez-Luna, F. Chemla, *Chem. Rev.* **2010**, *110*, 2366-2447.

[58] Y. Ito, T. Hirao, T. Saegusa, *J. Org. Chem.* **1978**, *43*, 1011-1013.

[59] Y. Ito, H. Aoyama, T. Hirao, A. Mochizuki, T. Saegusa, *J. Am. Chem. Soc.* **1979**, *101*, 494-496.

[60] a) A. S. Kende, B. Roth, P. J. Sanfilippo, *J. Am. Chem. Soc.* **1982**, *104*, 1784-1785; b) A. S. Kende, B. Roth, P. J. Sanfilippo, T. J. Blacklock, *J. Am. Chem. Soc.* **1982**, *104*, 5808-5810.

[61] a) M. Toyota, T. Wada, K. Fukumoto, M. Ihara, *J. Am. Chem. Soc.* **1998**, *120*, 4916-4925; b) M. Toyota, M. Ihara, *Synlett* **2002**, 1211-1222; c) See also: O. F. Jeker, Diss. ETH No. 21437.

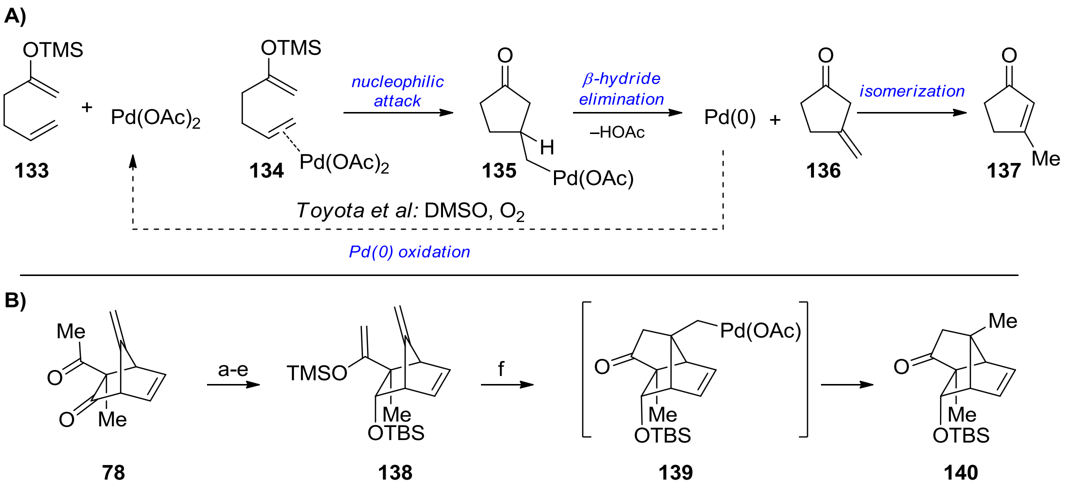

Scheme 3.19: A) Pd(II)-mediated intramolecular cyclization of silylenol ethers and *ω*-olefins discovered by SAEGUSA and co-workers including the mechanistic proposal by KENDE; B) Pd(II)-mediated cyclization of silylenol ether **138**. Reagents and conditions: a) TBSOTf, NEt_3, CH_2Cl_2, 0 °C to RT; b) $LiAlH_4$, Et_2O, –42 °C, 61% over two steps; c) TBSOTf, NEt_3, CH_2Cl_2, 0 °C, 94%; d) AcOH, CH_2Cl_2, quant.; e) TMSOTf, NEt_3, CH_2Cl_2, 0 °C to RT; f) $Pd(OAc)_2$ (1.05 equiv), DMSO, 50 °C, 9 h, then HCO_2H, 68%.

Due to the widespread use of trimethylsilylenol ethers in the Pd(II)-mediated oxidative Heck-type cyclizations, **138** was investigated first. The synthetic sequence for its preparation is in accordance with the preparation of **123** (*cf.* Scheme 3.17). Upon exposure to $Pd(OAc)_2$ in DMSO at 50 °C for 9 h disappearance of the starting material was observed, as judged by TLC. The reaction mixture was then quenched by the addition of formic acid, which resulted in immediate precipitation of palladium black. To our delight, only a single novel compound was formed, which proved to be the desired tricyclic diketone **140** obtained in 68% yield. Additionally, the more stable *tert*-butyldimethylsilylenol ether **123** (*cf.* Scheme 3.17, B) cyclized in a slightly improved yield of 71%.

3.3.5 Conclusion

During our investigation of the key C(9)–C(10) bond formation, several important features of diene **78** have been revealed. Firstly, radical reactions as well as strong Brønsted acids seem to be incompatible with this system and the reactions investigated led only to decomposition of the starting material. A likely explanation for this finding might be the unstable nature of norbornenes due to various rearrangement processes.[62] Such rearrangements might be even more facilitated by the presence of an additional 1,1-disubstitued double bond, which can lead to relatively stable tertiary radicals and carbocations. Furthermore, gold(I) catalysis did not mediate the desired cyclization. This is rather surprising, since **78** does not contain any functional groups, which were not tolerated during the screening of CHE and co-workers. Additionally, the methyl ketone is in close spatial proximity to the *exo* olefin and should therefore easily undergo C–C bond formation.[63] When replacing gold(I) by palladium(II), olefin activation smoothly occurred, providing the desired tricyclic diketone **140** in high yield.

---

[62] For examples see: a) J. K. Crandall, *J. Org. Chem.* **1964**, *29*, 2830-2833; b) H. C. Brown, *Acc. Chem. Res.* **1973**, *6*, 377-386; c) H. C. Brown, *Acc. Chem. Res.* **1983**, *16*, 432-440.

[63] It should be noted, that even when exposing silylenol ether **123** to gold(I) catalyst [P(*t*Bu$_2$-2-biphenyl)Au(MeCN)]PF$_6$ no cyclization occurred, indicating, that no effective *exo* olefin activation by Au(I) was achieved.

3.4 Cyclopropanation of the *endo* Olefin

With the key C(9)–C(10) bond formed, the introduction of the cyclopropane to complete the tetracyclo[4.4.$0^{3,5}$.$0^{2,8}$]decane core of pallambins A and B was tackled next. As indicated in Scheme 3.20 several challenges emerged while planning this transformation. Firstly, the majority of the numerous published methodologies for cyclopropanation employ activated olefins such as styrenes, enol ethers or enamines. Alkene **140** on the other hand is an isolated aliphatic alkene lacking such a beneficial increased reactivity. However, we were hoping that the ring strain associated with norbornene double bonds (14.4 kcal/mol for norbornane vs. 19.2 kcal/mol for norbornene)[64] would enhance the reactivity of this particular olefin towards electrophilic carbenoid reagents.

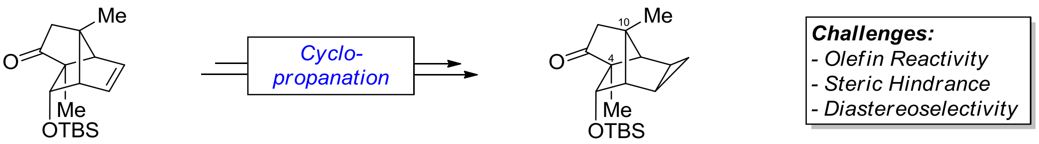

140 **141**

Scheme 3.20: Envisioned cyclopropanation to complete the tetracyclic core structure of pallambins A and B.

Secondly, the high steric encumbrance of the olefin has to be considered. While the *endo* face is shielded by the C(4) methyl group and the TBS ether, the *exo* face is covered by the C(10) methyl group. As mentioned in Chapter 2.1, it was presumed that the newly formed cyclopentanone containing C(4) and C(10) might entail an increase of the angle between the C(10) bridge and the corresponding olefin. This assumption would also provide a positive indication for the third challenge, the question of diastereoselectivity during the cyclopropanation reaction.

A powerful carbenoid for the cyclopropanation of even unactivated olefins was described by SHI and co-workers in 2004.[65] The researchers hypothesized, that if the nucleophilicity of the double bond cannot be increased, better results could be obtained by employing a more electrophilic carbenoid species. Along these lines, SHI and co-workers discovered that the properties of a (halomethyl)zinc reagent ($XZnCH_2Y$, where X are halogen atoms and Y are either halogens or alkylgroups) can be altered by treatment with protic reagents. A laborious screening revealed that the zinc carbenoid $(F_3CCO_2)ZnCH_2I$, generated from equimolar amounts of $ZnEt_2$, trifluoroacetic acid and CH_2I_2, is a very powerful cyclopropanation reagent, providing the desired products in significantly shorter reaction times and higher yields. Due to the hypothesized decreased reactivity of **140**, this protocol was expected to be the most promising method to perform the desired cyclopropanation.[66]

---

[64] K. B. Wiberg, *Angew. Chem. Int. Ed.* **1986**, *25*, 312-322.
[65] J. C. Lorenz, J. Long, Z. Q. Yang, S. Xue, Y. Xie, Y. Shi, *J. Org. Chem.* **2004**, *69*, 327-334.

Upon exposure of olefin **140** to the conditions described by SHI no cyclopropanation occurred (Scheme 3.21). Instead, a mixture of starting material and another unidentified side product was obtained. Increasing the equivalents of the added zinc carbenoid species did also not provide any desired tetracycle **141**. We assume that the steric environment of the corresponding olefinic bond is too encumbered to be reached by the carbenoid species.

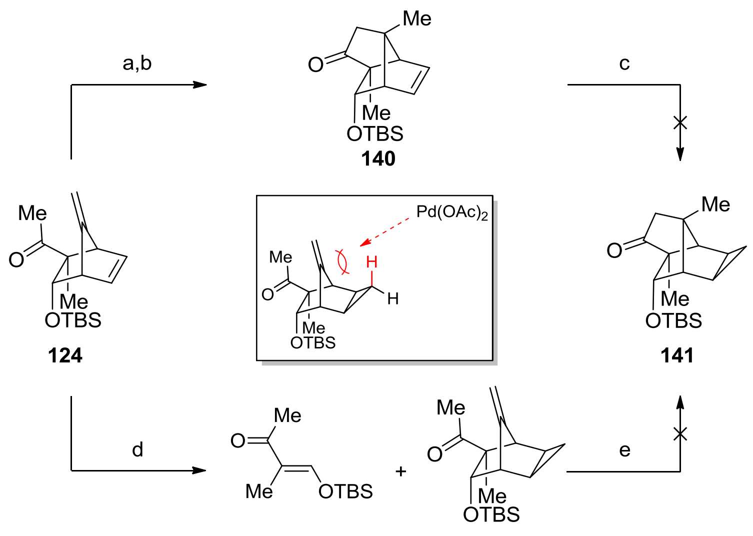

Scheme 3.21: Attempted synthesis of tetracycle **141** from **124** by Pd(II)-mediated cyclization and cyclopropanation. Reagents and conditions: a) TBSOTf, NEt_3, CH_2Cl_2, 0°C to RT; b) $Pd(OAc)_2$, DMSO, 50 °C, then HCO_2H, 71% over two steps; c) $ZnEt_2$, F_3CCO_2H, CH_2Cl_2, 0 °C to 30 °C, then CH_2I_2, 0 °C, then **140**, 0 °C to RT, no reaction; d) $ZnEt_2$, F_3CCO_2H, CH_2Cl_2, 0 °C to 30 °C, then CH_2I_2, 0 °C, then **124**, 73% for **142**, 26% for **143**; e) $Pd(OAc)_2$, DMSO, 50 °C then HCO_2H.

Based on this result, it was decided to reverse the order of events, i.e. first perform the cyclopropanation reaction on diene **124**, followed by the previously established palladium(II)-mediated ring closure. Accordingly, **124** was treated with two equivalents of SHI's carbenoid. Unfortunately expected cyclopropane **143** was only observed as the minor product (26% yield). In analogy to **125** (*cf.* Scheme 3.17), the predominant reaction was a retro Diels–Alder reaction to give volatile pentafulvene and silyl enol ether **142** in 73% yield. Nevertheless, we had sufficient material in hand to explore the palladium(II)-mediated ring closure. Disappointingly, no reaction occurred under the previously employed conditions ($Pd(OAc)_2$, DMSO, 50 °C). We surmised that the C–H bond (highlighted in red in Scheme 3.21) of the cyclopropane provides sufficient shielding of the *exo* olefin in order to prevent the crucial *anti* coordination of Pd(II).

---

[66] Dr. SÉBASTIEN GOUDREAU is gratefully acknowledged for helpful discussions about cyclopropanation reactions.

3.5 Revision of the Synthetic Strategy

Our initial synthetic strategy presented in the previous chapters revealed several important aspects for the generation of the tetracyclo[4.4.$0^{3,5}$.$0^{2,8}$]decane core. We started the synthetic sequence with pentafulvene in the course of a Diels–Alder reaction and were able to handle this highly unstable compound as well as render this cycloaddition useful on a preparative scale. During our attempts to introduce the cyclopropane motif, it became apparent that its introduction would have to precede the introduction of the C(10) quaternary center, since attempts to cyclopropanate **140** were met with failure (*cf*. Chapter 3.4). A direct consequence of this result and the failed cyclization attempt of cyclopropane **143** is that the established palladium(II)-mediated reductive Heck-type cyclization cannot be employed. Thus another reaction for the C(9)–C(10) bond formation must be explored. However, a very important consequence of **143** failing to cyclize, which we attributed to the steric shielding of the *exo* olefin by the cyclopropane, is that diastereoselective functionalization of the *Re* face of the double bond should be feasible (Scheme 3.22). Our quest for a novel cyclization reaction and a suitable olefin functionalization culminated in a strategy consisting of stereoselective hydrogenation of the *exo* double bond followed by an intramolecular C–H insertion to access the tetracyclic core **76**. In order to successfully perform these transformations, a chemo- and stereoselective cyclopropanation of ketone **88** is absolutely necessary. Scheme 3.23 summarizes the revised strategy that was envisaged to result in an efficient synthesis of the tetracyclic core **76** of pallambins A and B.

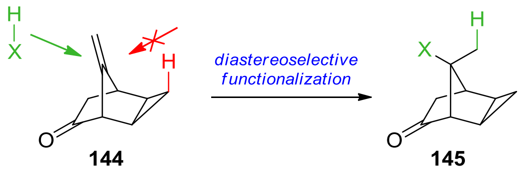

Scheme 3.22: Selective functionalization of **144**.

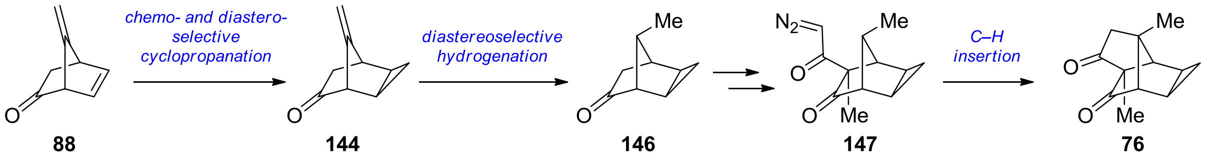
O
88
chemo- and diastereo-selective cyclopropanation
O
144
diastereoselective hydrogenation
Me
O
146
N2
Me
O
O
Me
147
C–H insertion
Me
O
O
Me
76

Scheme 3.23: Revised strategy for the construction of the tetracyclo[4.4.$0^{3,5}$.$0^{2,8}$]decane core **76** based on the results obtained in the previous chapters.

3.6 Selective Cyclopropanation and Hydrogenation

In the hope of increasing the modest overall yield during the generation of the C(3) ketone after Diels–Alder cycloaddition (*cf.* Scheme 3.7), we decided to perform the functionalization of the two olefins prior to the α-hydroxylation of ester **95**. Consequently, potential sensitive functional groups such as the strained *endo* olefin and the 1,1-disubstitued *exo* olefin would be converted into saturated hydrocarbon groups early in the synthesis.

The cyclopropanation of diene **95** bears several challenges. Firstly, as mentioned previously, both alkenes are not activated by electron donating groups and might thus not be reactive enough for various cyclopropanation methods. Secondly, a chemoselective transformation of the *endo* olefin must be achieved, since separation of the desired product from other cyclopropanated byproducts is, due to similar physical properties, tedious. Thirdly, if a chemoselective transformation of the desired olefin was achieved, the question of diastereoselectivity would arise. However, as shown in previous experiments, the desired *exo* attack should be favored (*cf.* Chapter 3.2.2). Our screening for conditions commenced with the already employed SHI modification of the Simmons–Smith reaction (Table 3.3, Entry 1).[65]

Table 3.3: Screening of cyclopropanation conditions of diene **95**.

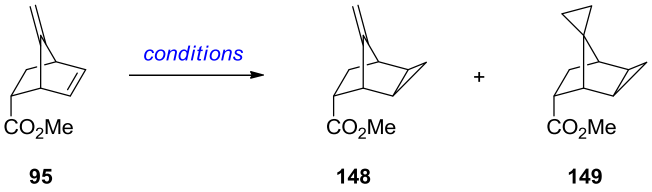

Entry	Reagents (equiv)	Temperature	Solvent	Products[a]	Yield of 148[b],[c]
1	$ZnEt_2$ (1.1), F_3CCO_2H (1.1) CH_2I_2 (1.1)	0 °C to RT	CH_2Cl_2	**148**, **149**, **95**[d]	44%
2	*i*Bu_3Al (1.0), CH_2I_2 (1.05)	0 °C to RT	CH_2Cl_2	**95**	n.r.
3	$ZnEt_2$ (1.05), CH_2I_2 (1.1)	60 °C	C_6H_6	**148**, **95**	36%
4	$ZnEt_2$ (5.0), CH_2I_2 (5.0)	60 °C	C_6H_6	**148**, **95**	48%
5	$ZnEt_2$ (1.4), CH_2I_2 (1.4) (*n*BuO)$_2$P(O)OH (1.4)	–15 °C to RT	CH_2Cl_2	**148**, **149**, **95**[d]	34%
6	$ZnEt_2$ (2.0), $ClCH_2I$ (4.0)	0 °C	CH_2Cl_2	**148**, **149**	78%

[a] Only products which could be identified are shown. [b] Yields refer to spectroscopically and chromatographically homogeneous materials. [c] n.r. = no reaction. [d] Other unidentified byproducts obtained.

Although desired product **148** was formed, it was only obtained in a moderate yield of 44% along with dicyclopropanated product **149**, recovered starting material and other unidentified side products. Noteworthy, the laborious isolation of spectroscopically pure **148** would be nearly impossible to perform on large scale. Next, an aluminum based carbenoid, introduced by YAMAMOTO, was investigated (Table 3.3, Entry 2).[67] However, upon exposure of diene **95** to the reported conditions, we were surprised to observe that no reaction took place and only starting material **95** was recovered. This lack of reactivity led us back to zinc carbenoid reagents. Since the highly reactive Shi carbenoid resulted in the formation of various byproducts including dicyclopropanated **149**, we reasoned that a carbenoid with decreased reactivity is necessary to achieve higher chemoselectivity and thus a higher yield. Indeed, when FURUKAWA's conditions ($ZnEt_2$ and CH_2I_2 in refluxing benzene) were employed, no byproducts were obtained (Table 3.3, Entry 3).[68] However the isolated yield was only 36% along with 38% of recovered starting material. Encouraged by this result, the equivalents of carbenoid species were increased in the hope to increase the conversion (Table 3.3, Entry 4). Unfortunately, the outcome was disappointing, since the isolated yield remained only moderate. Based on these results, we surmised that we would require a carbenoid which is more reactive than FURUKAWA's but less reactive than SHI's. A recently published method by CHARETTE and co-workers, employing a phosphoric acid, seemed to be promising.[69] Unfortunately, the yield could not be improved (Entry 5). Upon continuing our survey, we came over a report by DENMARK and EDWARDS describing the remarkable difference in reactivity upon substitution of CH_2I_2 in FURUKAWA's method by $ClCH_2I$.[70] A comparison of the methods revealed an increase in reactivity of the chloroiodomethane derived zinc carbenoid. Cyclodecene, which does not react with $ZnEt_2/CH_2I_2$ at 0 °C, provides the corresponding cyclopropanated species within 20 min in 87% yield upon exposure to $ZnEt_2/ClCH_2I$ at this temperature. Much to our delight, applying these conditions to diene **95** led to full conversion and the isolation of the desired product in 78% yield. The only byproduct formed was minor amounts of dicyclopropanated **149**, which could be separated by flash column chromatography. Noteworthy, this reaction proved to be smoothly scalable (14 g of product **148** prepared) with an even increased yield of 85%.

The task approached next was the hydrogenation of the remaining *exo* olefin to introduce the C(10) methyl group. Potential issues for this transformation are the chemoselectivity between the olefin and the newly installed cyclopropane as well as the desired diastereoselective *Re* side approach of the reductant. In an initial experiment, olefin **148** was reduced in presence of 5 mol% Pd/C and one atmosphere of H_2 in methanol (Scheme 3.24). Gratifyingly, a single product was obtained with full conversion. The ^{1}H-NMR indicated the presence of a new methyl group, appearing as a doublet and a new a C–H quartet with concomitant disappearance of the olefinic protons. In addition, a nuclear Overhauser effect was observed between the cyclopropane C–H and the newly formed methyl group thereby securing the structure of desired **150**. However, upon increasing the scale of the reaction to 5 g, an inseparable 1:1 mixture of desired product **150** and ring opened derivative **151** was obtained.[71]

---

[67] K. Maruoka, Y. Fukutani, H. Yamamoto, *J. Org. Chem.* **1985**, *50*, 4412-4414.

[68] a) J. Furukawa, N. Kawabata, J. Nishimura, *Tetrahedron Letters* **1966**, *7*, 3353-3354 ; b) J. Furukawa, N. Kawabata, J. Nishimura, *Tetrahedron* **1968**, *24*, 53-58.

[69] A. Voituriez, L. E. Zimmer, A. B. Charette, *J. Org. Chem.* **2010**, *75*, 1244-1250.

[70] S. E. Denmark, J. P. Edwards, *J. Org, Chem.* **1991**, *56*, 6974-6981.

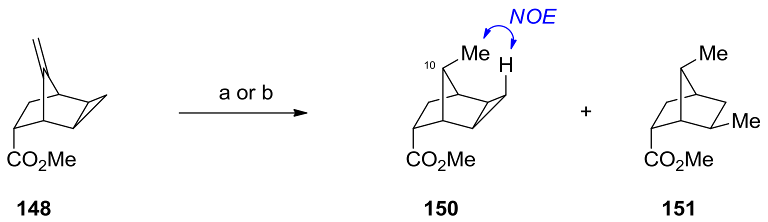

Scheme 3.24: Hydrogenation of olefin **148**. Reagents and conditions: a) Pd/C (5 mol%), H_2 (1 atm), MeOH, quant. for **150** up to 500 mg, 50% of **150**, 50% of **151** on 5 g scale; b) $ClRh(PPh_3)_3$ (4 mol%), H_2 (1 atm), CH_2Cl_2, 96% for **150**.

This finding is hypothesized to arise from the decreased catalyst surface/volume ratio and the thus prolonged reaction time. Certainly, a more reliable hydrogenation method was deemed necessary. A literature survey indicated no reported reductive cyclopropane opening in the presence of Wilkinson's catalyst under standard hydrogenation conditions. Accordingly, treatment of **148** with 4 mol% of $ClRh(PPh_3)_4$ and one atmosphere of hydrogen provided **150** in 96% yield reliably also on scales up to 15 g.

---

[71] Separation *via* flash column chromatography was possible after taking the mixture through the following two steps. See Chapter 3.7.1, intermediate **153**.

3.7 C(3)-Ketone Generation and Modified *α*-Functionalization

3.7.1 Oxidative Decarboxylation

With a reliable and scalabe route to cyclopropane **150** established, we turned our attention to the generation of the C(3) ketone. As described earlier, we were hoping that the presence of the diene was the reason for the failure of **95** to undergo oxidative decarboxylation upon exposure to YAMAMOTO's conditions (*i*Pr_2NLi, PhNO, then LiOH *cf.* Chapter 3.2.1).[38] However, fully saturated **150** also proved to be a delicate substrate for this transformation. Although desired ketone **146** was formed, the isolated yield was merely 17%. Therefore, the already established three-step sequence consisting of *α*-hydroxylation, reduction and diol cleavage was attempted next. Gratifyingly, compared to diene **95**, the overall yield could be improved from 33% to 82% for this sequence.

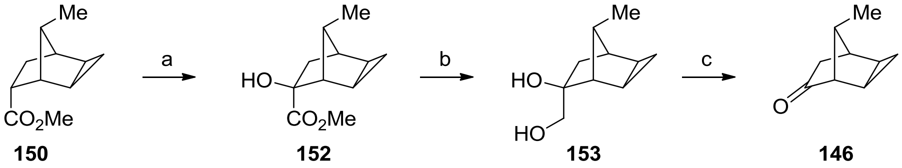

Scheme 3.25: Generation of the C(3) ketone. Reagents and conditions: a) *i*Pr_2NLi, THF, –78 °C, then $P(OEt)_3$, DMPU, O_2 (bubbling), –90 °C, 85%, d.r. = 10:1; b) $LiAlH_4$, Et_2O, 0 °C; c) $NaIO_4$, THF–phosphate buffer (aqueous, pH 7) (1:1), 0 °C, 97% over two steps.

3.7.2 C(4)-Methylation

The seemingly straightforward introduction of the C(4) methyl group from the corresponding enolate of ketone **146** proved to be extremely cumbersome (Scheme 3.26). In a first attempt on small scale (40 mg), following the procedure in Chapter 3.2.2, ketone **146** was deprotonated with *i*Pr_2NLi at –78 °C and a precooled solution of MeI in THF was added dropwise at this temperature. To our delight, the desired methyl ketone **154** was isolated in 91% yield. However, all attempts to reproduce this result failed. One problem observed was the widely varying conversion. We assumed that product **154** gets deprotonated by the enolate of **146** and hence inhibits the reaction. This hypothesis is strengthened by the finding that adding additional MeI after a certain time did not influence the conversion. Another, more serious problem was the formation of an inseparable byproduct in varying amounts. Up to 1:1 mixtures of the unknown compound and ketone **154** were obtained. Puzzled by this result, solutions to these problems were absolutely necessary. Varying the reaction temperature, concentration and increasing the amounts of methyl iodide did not lead to improvements. As a consequence, different reagents were emplyoed. At first, various bases and additives were investigated. However neither the addition of DMPU or HMPA,[72] reagents known to increase yields in enolate reactions, nor the employment of different bases such as *i*Pr_2NK or LiTMP suppressed byproduct formation. The alkylating reagent was exchanged by dimethyl sulfate and methyl trifluoromethanesulfonate. Disappointingly, no improvement could be achieved. Thus we surmised that the byproduct formation might occur during the usually performed aqueous workup using NH_4Cl. Due to the proportional dependence of the excess MeI employed and the byproduct formed, it was further hypothesized that the alkylating reagent might be responsible for byproduct formation. Consequently, two parallel reactions under equal conditions were set up. One reaction was quenched as previously described, whereas the other was quenched by adding equimolar amounts of triethylamine (relative to the MeI employed) to form the corresponding ammonium salt. Indeed, while the standard workup provided a mixture of product **154** and the unidentified byproduct, the triethylamine quenched reaction did not provide any side product. At last, we were able to increase the conversion by rapid addition of an excess of MeI at 0 °C. Applying the thus tediously developed experimental procedure, provided ketone **154** in excellent yield of 89% (Scheme 3.26).

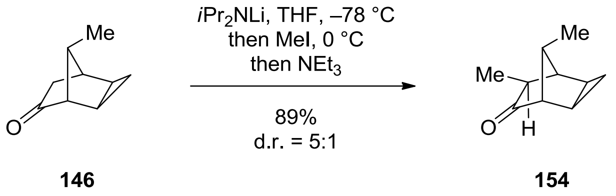

Scheme 3.26: Methylation of ketone **146**.

3.7.3 *α*-Acylation of Ketone 154

With a reliable and scalable entry towards methyl ketone **154** in hand, the generation of the C(4) quaternary center *via* *α*-acylation was examined next. To our surprise, only traces of product could be obtained under the previously established conditions from the corresponding TES enol ether **158** ($ZnCl_2$, AcCl, Table 3.4, Entry 1 *cf.* Chapter 3.2.2). We then employed the corresponding lithium enolate of **154** and exposed it to acetyl chloride (Entry 2). However, none of the desired product could be detected. Furthermore, the addition of HMPA did also not lead to any improvement (Entry 3).

---

[72] a) J. C. Stowell, *Carbanions in Organic Synthesis*; Wiley, New York, **1979**; b) H. O. House, *Modern Synthetic Reaction*, 2nd edition, Benjamin, New York, **1972**; c) T. Mukhopadhyay, D. Seebach, *Helv. Chim. Acta* **1982**, *65*, 385-391.

Table 3.4: Generation of the C(4) quaternary center.

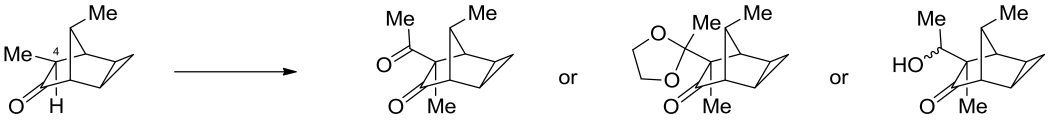
154 **155** **156** **157**

Entry	Nucleophile	Electrophile	Additive	Temperature	Yield[a]-[d]
1	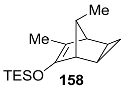 **158**	AcCl	$ZnCl_2$	0 °C	n.d.
2	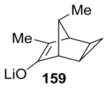 **159**	AcCl	-	–78 °C to RT	n.d.
3	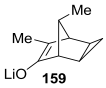 **159**	AcCl	HMPA	–78 °C to RT	n.d.
4	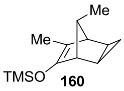 **160**	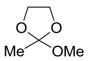 **161**	$BF_3{\cdot}OEt_2$	0 °C	n.d.
5	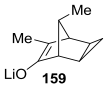 **159**	MeCHO	-	–78 °C	10 – 40%
6[e]	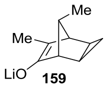 **159**	MeCHO	-	–78 °C	n.dt.
7	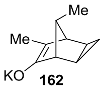 **162**	MeCHO	-	–15 °C	n.r.
8	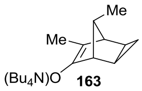 **163**	MeCHO	-	–78 °C	n.r.
9	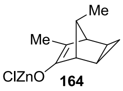 **164**	MeCHO	-	0 °C	n.dt.
10	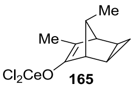 **165**	MeCHO	-	–15 °C	n.dt.
11	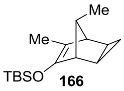 **166**	MeCHO	$TiCl_4$	–78 °C to RT	n.d.
12	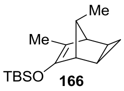 **166**	MeCHO	Ti(O*i*Pr)$_4$	–78 °C to RT	n.d.
13	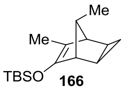 **166**	MeCHO	Me_2AlCl	–78 °C	traces
14	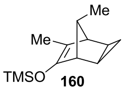 **160**	MeCHO	Gd(OTf)$_3$	RT	n.d.
15	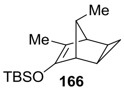 **166**	MeCHO	$BF_3{\cdot}OEt_2$	–90 °C	70%[f],[g]

[a] Yields refer to spectroscopically and chromatographically homogenous materials. [b] n.d. = product not detected. [c] n.dt. = yield not determined. [d] n.r. = no reaction observed. [e] Enolate generated from ***160*** *and MeLi. [f] Yield after three cycles. [g] exo/endo = 5:1, as determined later from the oxidized product.*

We hypothesized the failure of these reactions might be due to the following reasons. Firstly, due to the fact that no conversion of the starting material occurred, acetyl chloride might not be a suitable electrophile.[73] Additionally, deprotonation of the acylating reagent by the enolate of **154** might occur. In order to suppress this reaction, a formal acylating reagent bearing no acidic protons (**161**) was employed.[74] However upon exposure of TMS enol ether **160** to orthoester **161** in presence of $BF_3 \cdot OEt_2$, only methyl ketone **154** was recovered after aqueous workup (Entry 4).[75] The failure of this transformation might be associated with the sterically encumbered environment at C(4) and the relatively large electrophile. Interpreting these results, a relatively small, yet highly reactive electrophile was required, which would ultimately lead to targeted diketone **155**. Thus, acetaldehyde was chosen as the electrophilic reaction partner. A first attempt, employing the lithium enolate **159** and subsequent reaction with acetaldehyde, led to the desired aldol products **157** as a mixture of diastereomers (Entry 5). Unfortunately, the isolated yields were highly inconsistent and the reaction was accompanied by formation of acetaldehyde oligomers. This was problematic, since the oligomers could not be completely separated from the aldol products *via* flash column chromatography. Their formation might be effected by either deprotonation of acetaldehyde by enolate **159** or by condensation of acetaldehyde with the *in situ* generated $i\mathrm{Pr}_2\mathrm{NH}$. In order to exclude the latter event, enolate generation was performed under conditions excluding the formation of amine derivatives. Thus, TMS enol ether **160** was first treated with equimolar amounts of MeLi, generating only tetramethylsilane and the desired enolate (Entry 6). Disappointingly, exposure of the thus generated enolate produced only minute quantities of the desired aldol products. KO*t*Bu as well as TBAF have also been shown to enable the formation of enolates from TMS enol ethers.[76] Unfortunately, exposing TMS enol ether **160** to either of these conditions did not lead to any conversion and only methyl ketone **154** was recovered (Entries 7 and 8). As a consequence of the low conversion, we attempted to minimize proton exchange with acetaldehyde by employing less basic and more nucleophilic enolates such as cerium or zinc species (Entries 9 and 10).[77] Disappointingly, both zinc enolate **164** (generated from **159** and $ZnCl_2$) and cerium enolate **165** (generated from **159** and $CeCl_3$) provided various different products along with starting material **154**. We thus turned our attention to Lewis acid-catalyzed Mukaiyama aldol reactions.[78] A screening of various Lewis acids revealed the following: While $TiCl_4$, $Ti(O\textit{i}Pr)_4$ or $Gd(OTf)_3$[79] did not lead to any conversion, Me_2AlCl provided traces of the desired aldol products **157** (Entries 11-14). Gratifyingly, the conversion could be improved, by employing $BF_3{\cdot}OEt_2$ and rapid addition of the aldehyde (Entry 15). After three recycles, 70% yield for the generation of aldol products **157** could be achieved.

---

[73] Noteworthy, AcCl might have led to *O*-acylation, generating a labile enol acetate, which might be transformed back into **154** upon exposure to water or SiO_2.

[74] E. Akgun, M. Tunali, U. Pindur, *Monatsh. Chem.* **1987**, *118*, 363-367.

[75] It should be noted that ketone **154** was always recovered as a mixture of diastereomers due to competing *endo/exo* protonation.

[76] a) P. Duhamel, D. Cahard, J. M. Poirier, *J. Chem. Soc. Perkin Trans. 1* **1993**, 2509-2511; b) I. Kuwajima, E. Nakamura, *J. Am. Chem. Soc.* **1975**, *97*, 3257-3258.

[77] a) T. Imamoto, T. Kusumoto, M. Yokoyama, *Tetrahedron. Lett.* **1983**, *24*, 5233-5236; b) I. L. Jones, F. K. Moore, C. L. L. Chai, *Org. Lett.* **2009**, *11*, 5526-5529.

Having successfully generated the quaternary center at C(4), the task left to do was the oxidation of aldol products **157** to diketone **155**. Initial attempts of Dess–Martin oxidation led to diverse ratios of desired diketone **155** and methyl ketone **154** (Scheme 3.27, A).

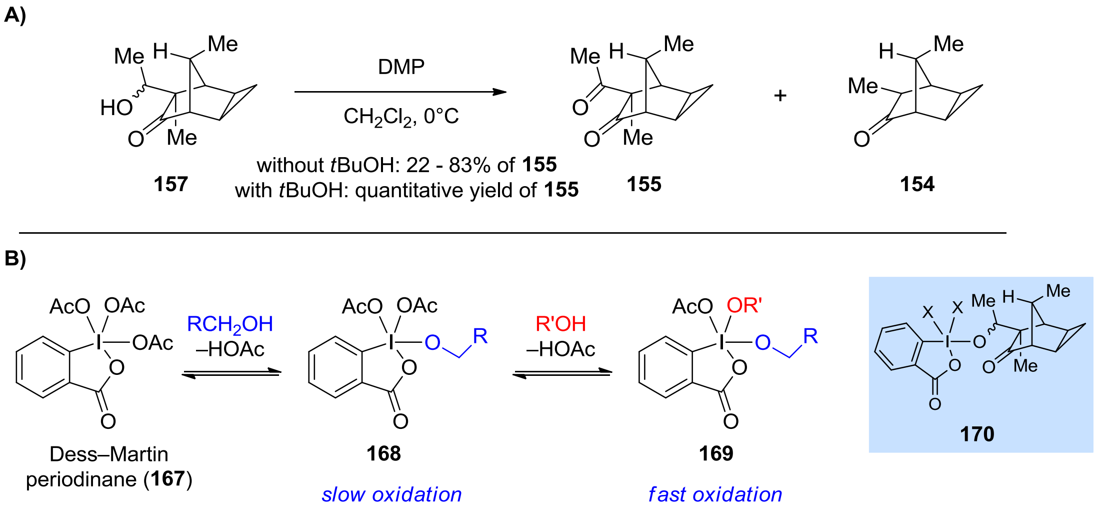
A)
DMP
CH2Cl2, 0°C
without tBuOH: 22 - 83% of 155
with tBuOH: quantitative yield of 155
157
155
154
B)
RCH2OH
–HOAc
R'OH
–HOAc
Dess–Martin periodinane (167)
168
169
170
slow oxidation
fast oxidation

Scheme 3.27: A) Oxidation of alcohols **157** with Dess–Martin periodinane. B) Mechanistic rationale for the *t*BuOH-accelerated Dess–Martin oxidation (taken from ref. 80 b).

This finding might be associated with the propensity of the aldol products to undergo a retro aldol reaction. We reasoned that the Lewis acidic nature of the Dess–Martin reagent might lead to a competitive scenario between oxidation and retro-aldol reaction. A literature survey revealed an explanation for the diverse product to byproduct ratio. After initial coordination of one equivalent of a hydroxy-substrate to **167**, the reagent thus formed only slowly oxidizes to the desired carbonyl product (Scheme 3.27, B). However, upon coordination of a second equivalent of alcohol, a labile compound **169** is formed, which undergoes rapid oxidation. In our case, compound **170** might be activated enough to suffer from competing retro-aldol reaction. In their original report, DESS and MARTIN found that the addition of equimolar amounts of a non-oxidizable alcohol such as *t*BuOH entails the formation of structures of type **169** and hence increases the overall reaction rate.[80] Indeed, applying this procedure to aldol products **157** led to rapid and quantitative oxidation without any detectable amounts of retro-aldol product **154**.

---

[78] For an excellent review on directed aldol reaction see: T. Mukaiyama, *Org. React.* **1982**, *28*, 203-331.
[79] S. Kobayashi, I. Hachiya, *Tetrahedron. Lett.* **1992**, *33*, 1625-1628.

3.7.4 Conclusion

Scheme 3.28 summarizes the synthetic sequence from cyclopropanated ketone **146** to diketone **155**. During our quest for a reliable route towards this key intermediate, several difficulties arose. Firstly, the α-methylation of ketone **146** proved to be highly delicate. The lack of reactivity of the corresponding lithium enolate had to be overcome by employing a relatively high alkylation temperature (0 °C) as well as an excess of methyl iodide (18 equiv). Furthermore, quenching of the residual alkylation reagent with NEt_3 prior to the aqueous workup proved to be crucial to exclude byproduct formation. Secondly, a direct acylation of the C(3) ketone failed, a result which was associated with the decreased reactivity of the corresponding enolate equivalent. However, after extensive experimentation, it was found that performing a Mukaiyama aldol reaction with acetaldehyde in the presence of $BF_3{\cdot}OEt_2$ at −90 °C provided the desired aldol products in 70% yield after three cycles. Thirdly, the envisioned oxidation of the aldol products proved to be surprisingly problematic. Inconsistent product yields were accompanied by the formation of retro aldol product **154**. Gratifyingly, upon premixing Dess–Martin periodinane with *t*BuOH and reacting the thus formed highly reactive oxidizing agent with the aldol products furnished diketone **155** in 70% over three steps from methyl ketone **154**.

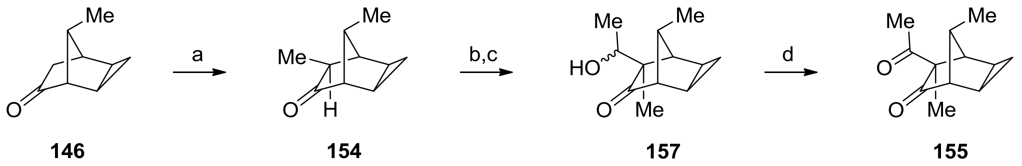

Scheme 3.28: Conversion of ketone **146** into key intermediate diketone **155**. Reagents and conditions: a) *i*Pr_2NLi, THF –78 °C, then MeI (18 equiv), 0 °C, then NEt_3 (18 equiv), 89%, d.r. = 5:1; b) TBSOTf, NEt_3, CH_2Cl_2, 0 °C; c) MeCHO, $BF_3{\cdot}OEt_2$, CH_2Cl_2, –90 °C, 3 x recycled; d) DMP, *t*BuOH, CH_2Cl_2, 0 °C, then **157**, 0 °C, 70% over three steps.

---

[80] a) D. B. Dess, J. C. Martin, *J. Org. Chem.* **1983**, *48*, 4155-4156; b) for an excellent overview see: M. Fernandez, G. Tojo in *Oxidation of Alcohols and Ketones: A Guide to Current Common Practice* (Ed.: E. Tojo), Springer, New York, **2006**, p. 194; c) S. D. Meyer, S. L. Schreiber, *J. Org. Chem.* **1994**, *59*, 7549-7552.

3.8 C(9)–C(10) Bond Formation *via* C–H Insertion

With an efficient route to diketone **155** in hand, the challenging key C(9)–C(10) bond formation was approached next. Since a C–H insertion reaction into the C(10) methine group was envisioned to complete the tetracyclo[4.4.0^{3,5}.0^{2,8}]decane core, a carbenoid precursor such as a diazo group was required. One of the most common methods to install a diazo group in the α-position of a carbonyl compound is the Regitz diazo-transfer reaction.[81] In the original publication from 1964, REGITZ depends on the use of active methylene compounds, such as β-dicarbonyls, which react with *p*-toluenesulfonyl azide under basic conditions (Scheme 3.29). Four years later, REGITZ reported an improvement of his method in which simple aliphatic ketones are firstly formylated with methyl formate.[82] The then activated ketone undergoes diazo transfer upon exposure to TsN_3 generating the diazo ketone and tosylformamide. Importantly, removal of the byproducts can be problematic. In order to overcome this issue, TABER *et al.* replaced TsN_3 by MsN_3.[83] The advantage of this substitution lies in the smooth removal of the formed mesylated byproducts during basic aqueous workup. A few years later, DANHEISER and co-workers further improved the diazotation of unactivated ketones.[84] Instead of performing a rather tedious formylation with methyl formate, 2,2,2-trifluoroethyltrifluoroacetate was employed in a Claisen condensation with the desired aliphatic ketone. The then formed diketone undergoes smooth diazotation upon exposure to MsN_3 and triethylamine. Noteworthy, a comparitive study with the formylation approach by REGITZ has been performed, exemplifying the superiority of this method.

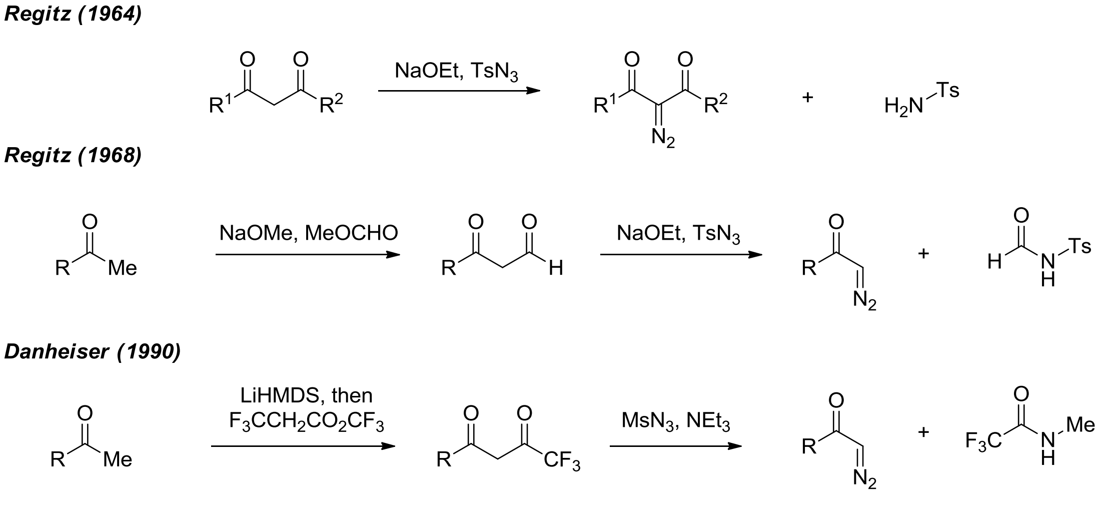

Scheme 3.29: Developments of the Regitz diazo-transfer reaction.

---

[81] M. Regitz, *Justus Liebigs Ann. Chem.* **1964**, *676*, 101-109.
[82] M. Regitz, F. Menz, *Chem. Ber.* **1968**, *101*, 2622-2632.
[83] D. F. Taber, R. E. Ruckle, M. J. Hennessy, *J. Org. Chem.* **1986**, *51*, 4077-4078.
[84] R. L. Danheiser, R. F. Miller, R. G. Brisbois, S. Z. Park, *J. Org. Chem.* **1990**, *55*, 1959-1964.

Due to the relatively non-activated nature of diketone **155**, the procedure reported by DANHEISER *et al.* was chosen as the starting point. Indeed, a single UV active spot appeared on TLC and a new peak in the crude ^{1}H NMR at 5.74 ppm indicated the formation of a diazo compound. However, upon attempted flash column chromatography, the novel product decomposed. Consequently, it was decided to directly employ crude diazo ketone **147** in the carbenoid C–H insertion step (Scheme 3.30).

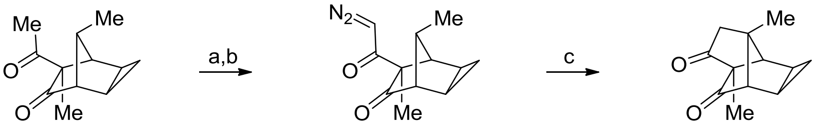

155 **147** **76**

Scheme 3.30: Diazotation and C–H insertion to generate tetracyle **76**. Reagents and conditions: a) LiHMDS, THF, –78 °C, then $F_3CCH_2CO_2CF_3$; b) MsN_3, NEt_3, MeCN; c) $Rh_2(OAc)_4$ (1.0 mol%), CH_2Cl_2, reflux, 76% over three steps.

To our delight, a single new compound could be isolated upon exposure to $Rh_2(OAc)_4$ in refluxing CH_2Cl_2. ^{1}H NMR analysis revealed the disappearance of the C(10) proton, as well as a new methyl singlet in addition to two diastereotopic methylene protons. Detailed 2D-NMR analysis in combination with high resolution mass spectrometry secured the structure of **76**. Noteworthy, the overall yield for the transformation of **155** into tetracycle **76** amounted to 76%.

3.9 Stereoselective Functionalization of C(8) and C(9)

With a scalable route towards the crucial tetracyclo[4.4.0^{3,5}.0^{2,8}]decane core successfully established, the challenge faced next was the stereoselective construction of the tertiary alcohol at C(8) as well as the generation of the C(9) stereocenter to ultimately access diol **74** (Scheme 3.31).

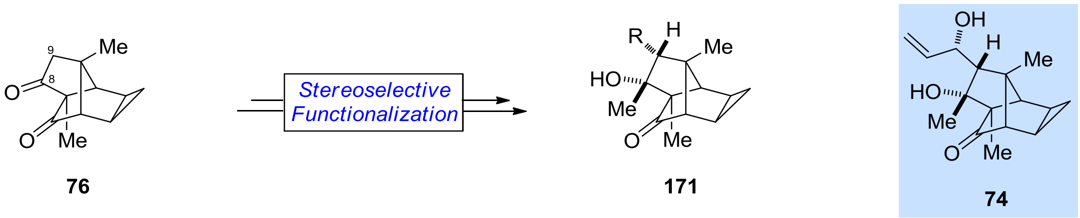

Scheme 3.31: Required stereoselective functionalization of C(8) and C(9).

An accurate stereochemical analysis of **76**, led us to the conclusion that the addition of organometallic methyl reagents towards the C(8) ketone would occur from the undesired *Re* face. However, it was realized that both substituents, the tertiary alcohol and the carbon chain, possess a *syn* relationship and hence would be advantageously introduced simultaneously. Thus, as indicated in Scheme 3.32 it was planned to generate the C(8) methyl group from the corresponding ketone. Subsequently, the tertiary alcohol as well as the C(9) substituent would be concomitantly introduced *via* a cycloaddition approach.

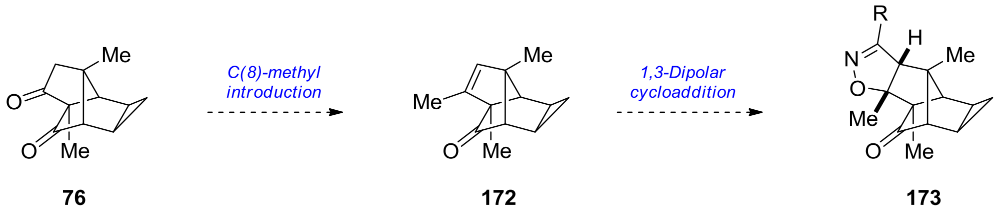

Scheme 3.32: Synthetic strategy for the simultaneous functionalization of positions C(8) and C(9).

In the event, diketone **76** was treated with *i*Pr$_2$NLi followed by the Hendrickson–McMurry reagent (PhNTf$_2$).[85] Subsequent Negishi coupling with ZnMe$_2$ smoothly provided trisubstituted olefin **172** in 64% overall yield (Scheme 3.33, B). Noteworthy, no reaction occurred upon exposure of the lithium enolate to Comins' reagent.[86] Even though reactivity problems might arise upon employing a trisubstituted olefin in a cycloaddition reaction, we were hoping that the high ring strain of the newly formed norbornene (*cf*. Chapter 3.4) and the associated strain release might enable such a transformation. In a first attempt Mukaiyama–Hoshino conditions were applied, starting from 1-nitropropene with the required olefin already incorporated.[87] However, due to the lack of reactivity, no conversion could be observed.[88] Consequently, a more reactive nitrile oxide, which would provide a flexible group for further functionalization was deemed necessary. During their synthesis of the diterpenoid natural product vinigrol, BARAN and co-workers needed to formally add the CH_3 and OH groups of methanol across the trisubstituted olefin in **174** (Scheme 3.33, A).[89] The problem was solved by performing a cycloaddition with bromonitrile oxide, a highly reactive reagent firstly reported by DEPAOLINI in 1936.[90]

---

[85] J. B. Hendrickson, R. Bergeron, *Tetrahedron. Lett.* **1973**, 4607-4610.; b) W. J. Scott, J. E. McMurry, *Acc. Chem. Res.* **1988**, *21*, 47-54.

[86] *N*,*N*-Bis(trifluoromethylsulfonyl)-5-chloro-2-pyridylamine, see: D. L. Comins, A. Dehghani, *Tetrahedron. Lett.* **1992**, *33*, 6299-6302.

Gratifyingly, olefin **172** smoothly underwent the desired 1,3-dipolar cycloaddition with bromonitrile oxide, generated *in situ* from dibromoformaldoxime and $KHCO_3$ to give isoxazoline **177** in excellent yield of 91% (Scheme 3.33, B). Remarkably, **177** was the only detected regio- and diastereomer. Recrystallization produced crystals suitable for X-ray diffractometry, thereby unambiguously confirming all stereochemical assignments.

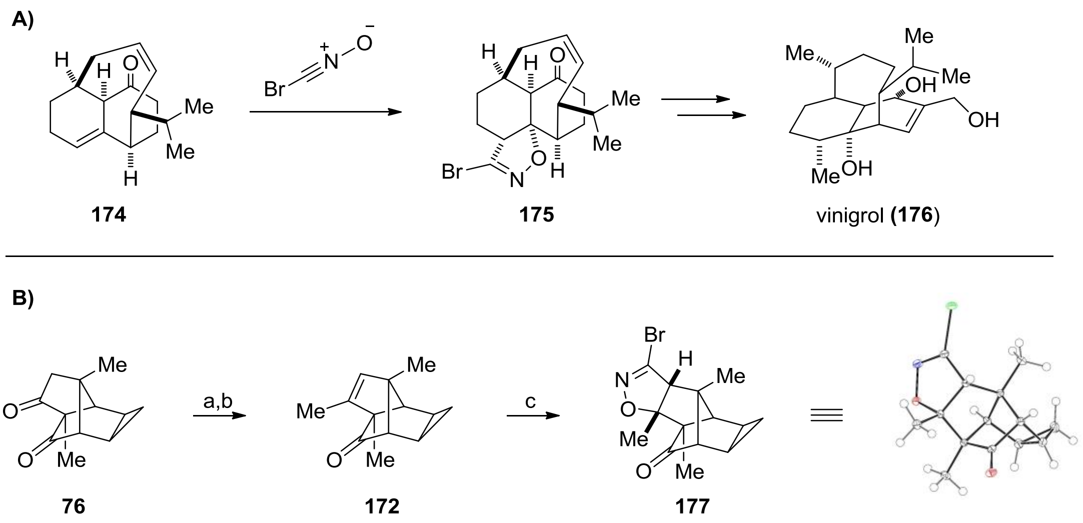

Scheme 3.33: A) BARAN's use of bromonitrileoxide during a 1,3-dipolar cycloaddition in the total synthesis of vinigrol (**176**). B) Synthesis of isoxazoline **177**. Reagents and conditions: a) iPr$_2$NLi, THF, –78 °C, then PhNTf$_2$, −78 °C to 5 °C, 64%; b) Pd(PPh$_3$)$_4$ (5 mol%), ZnMe$_2$, THF, 0 °C to RT, quant; c) Br$_2$CNOH, KHCO$_3$, EtOAc, 91%. ORTEP representation of **177**. Thermal ellipsoids are shown at 50% probability.

---

[87] T. Mukaiyama, T. Hoshino, *J. Am. Chem. Soc.* **1960**, *82*, 5339-5342.
[88] A control experiment with norbornene provided the corresponding cycloadduct.
[89] T. J. Maimone, J. Shi, S. Ashida, P. S. Baran, *J. Am. Chem. Soc.* **2009**, *131*, 17066-17067.
[90] I. DePaolini, *Gazz. Chim. Ital.* **1930**, *60*, 700-704.

3.10 Elaboration of the Bromoisoxazoline

With advanced isoxazoline **177** in hand, functionalization of this intermediate was investigated next. A close literature review however revealed that methods for the functionalization of bromoisoxazolines such as **177** are rare. Most commonly, reduction to the β-hydroxyamines or opening to the β-hydroxynitriles are performed.[91] In the present case, two general strategies could be employed to ultimately access targeted diol **74** (Scheme 3.34). On the one hand, vinylation *via* transition metal-catalyzed coupling or nucleophilic displacement could provide alkene **178**. The isoxazoline would then be reductively cleaved and the corresponding β-hydroxyketone selectively reduced under Evans–Saksena conditions.[92] On the other hand, suitable conditions might be identified to both reduce the N–O bond as well as the thus formed imidoyl bromide to aldehyde **179**. Alternatively, one of the established methods to generate the corresponding β-hydroxynitrile could be employed, followed by DIBAL-mediated reduction to aldehyde **179**. A chelation controlled 1,2-addition mediated by the tertiary alcohol would then lead to diol **74**.

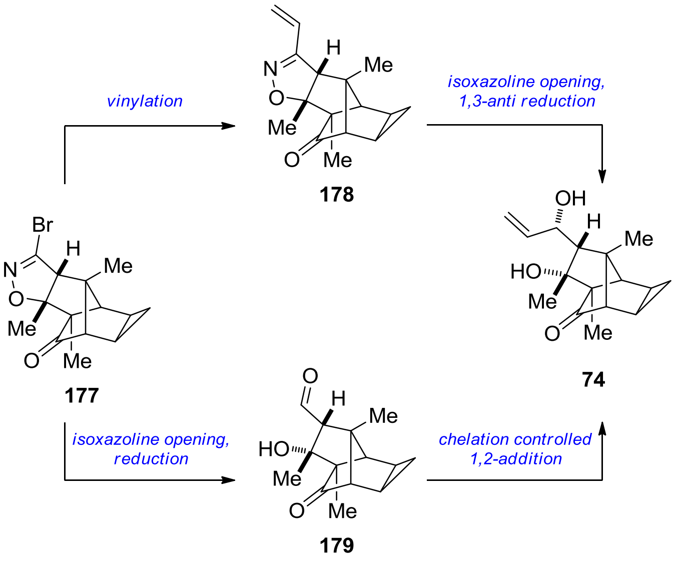
vinylation
isoxazoline opening, 1,3-anti reduction
isoxazoline opening, reduction
chelation controlled 1,2-addition
177
178
179
74
Br
H
Me
N
O
OH
HO

Scheme 3.34: Synthetic strategies to convert bromo-isoxazoline **177** into targeted diol **75**.

Due to the lack of literature precedence for the functionalization of 3-bromoisoxazolines in combination with the advanced nature of intermediate **177**, it was decided to first investigate novel transformations on model compound **180** (Table 3.5).[93] At first, vinylation of **180** was attempted *via* palladium-mediated cross couplings. Unfortunately, under Stille conditions, not the desired vinylisoxazoline **181** was formed, but ring opened β-hydroxynitrile **182** was isolated in 65% yield (Table 3.5, Entry 1).[94] FÜRSTNER described a modification of the original Stille protocol, allowing the coupling of highly challenging substrates, which failed to react under standard conditions.[95] However, also under these conditions, nitrile **182** was the only isolated product (Table 3.5, Entry 2). Additionally, Negishi cross-coupling with vinylzinc chloride, also produced the *β*-hydroxynitrile as the sole product (Table 3.5, Entry 3).

---

[91] a) M. H. Seo, Y. Y. Lee, Y. M. Goo, *Synth. Commun.* **1994**, *24*, 1433-1439; b) M. G. Kociolek, K. P. Kalbarczyk, *Synth. Commun.* **2004**, *34*, 4387-4394.

[92] a) A. K. Saksena, P. Mangiaracina, *Tetrahedron Lett.* **1983**, *24*, 273-276; b) D. A. Evans, K. T. Chapman, E. M. Carreira, *J. Am. Chem. Soc.* **1988**, *110*, 3560-3578.

[93] Although the author of this thesis (C. E.) agrees with the opinion that novel reactions should be performed on the real system, since suitable model compounds are usually difficult to prepare and the transfer of such a reaction to the real system is often problematic, **180** was chosen as a starting point of this investigation. **180** is easily prepared in a single step from norbornene and enables the investigation of novel transformations.

[94] Nitrile **182** is known in the literature: F. De Sarlo, A. Brandi, A. Goti, A. Guarna, P. Rovero, *Heterocycles*, **1983**, *20*, 511-518.

With these disappointing results in mind, we explored the direct nucleophilic attack onto the bromoisoxazoline. When only vinylmagnesium bromide was used, decomposition occurred upon prolonged exposure to the reagent at room temperature (Table 3.5, Entry 4). However, when the organocerium reagent, prepared from vinylmagnesium bromide and $CeCl_3$, was employed, 53% of the desired vinylated isoxazoline **181** could be isolated (Table 3.5, Entry 5). Attempts to increase the yield by Lewis acid assistance or generating the organocerium reagent from vinyllithium were met with failure (Table 3.5, Entries 6 and 7).

Table 3.5: Vinylation of model bromoisoxazoline **181**.

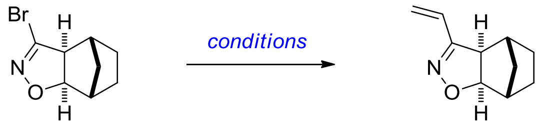

180 **181**

Entry	Vinyl Source	Additives	Solvent	Temperature	Product	Yield[a]-[d]
1	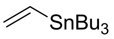 $SnBu_3$	$Pd(PPh_3)_4$ CsF	toluene	111 °C	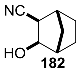 NC HO **182**	65%
2	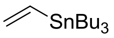 $SnBu_3$	CuTC, $Pd(PPh_3)_4$ $(Bu_4N)(O_2PPh_2)$,	DMF	RT	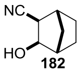 NC HO **182**	n.dt.
3	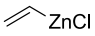 ZnCl	$Pd(PPh_3)_4$	THF	0 °C to RT	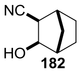 NC HO **182**	n.dt.
4	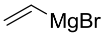 MgBr	-	THF	–15 °C to RT	-	n.d.
5	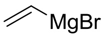 MgBr	$CeCl_3$	THF	–78 °C to 5 °C	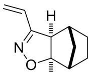 H N O H **181**	53%
6	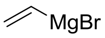 MgBr	$CeCl_3$, $BF_3 \cdot OEt_2$	THF	–78 °C to 5 °C	-	n.r.
7	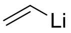 Li	$CeCl_3$	THF	–78 °C to –40 °C	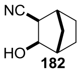 NC HO **182**	n.dt.

[a] Yields refer to spectroscopically and chromatographically homogenous materials. [b] n.d. = Product not detected. [c] n.dt. = Yield not determined. [d] n.r. = No reaction occurred.

Even though the addition of the organocerium reagent provided the desired vinyl isoxazoline **181**, the second strategy of reductive N–O bond cleavage with concomitant aldehyde formation (*cf.* Scheme 3.34) was also investigated (Table 3.6). Conditions, which are well known for the reductive cleavage of the N–O bond of isoxazolines are either zinc in protic media or hydrogenolysis mediated by palladium. Hence, bromoisoxazoline **180** was first subjected to these protocols. However in all cases examined, *β*-hydroxynitrile was the only product isolated (Table 3.6, Entries 1-3). Next, we explored the use of tin based radicals. Upon exposure of **180** to *n*Bu$_3$SnH and AIBN in refluxing benzene, indeed a novel product containing an aldehyde was formed (Table 3.6, Entry 4).

---

[95] A. Fürstner, J. A. Funel, M. Tremblay, L. C. Bouchez, C. Nevado, M. Waser, J. Ackerstaff, C. C. Stimson, *Chem. Commun.* **2008**, 2873-2875.

Table 3.6: Attempted reduction of bromoisoxazoline **180**.

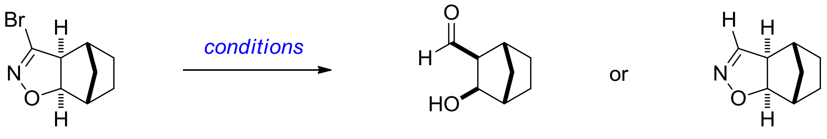

180 **183** **184**

Entry	Reagents	Solvent	Temperature	Product	Yield[a]-[c]
1	Zn	AcOH	RT	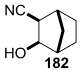 **182**	n.dt.
2	Zn, NH$_4$Cl	THF–H$_2$O (4:1)	RT	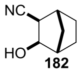 **182**	n.dt.
3	Pd/C, H$_2$	EtOAc	RT	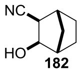 **182**	n.dt.
4[d]	*n*Bu$_3$SnH, AIBN	C$_6$H$_6$	80 °C	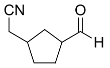 **185**	80%
5	*t*BuLi, then MeOH	THF	–78 °C	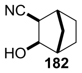 **182**	n.dt.
6	NaBH$_4$	*i*PrOH	RT	-	n.r.
7	DIBAL	THF	–78 °C to RT	-	n.r.

[a] Yields refer to spectroscopically and chromatographically homogenous materials. [b] n.dt. = Yield not determined. [c] n.r. = No reaction occurred. [d] The relative stereochemistry of ***185*** *was not established, however a single diastereomer was formed.*

Unfortunately, NMR analysis revealed that not desired *β*-hydroxyaldehyde **183** had been generated, but instead ring opening to aldehyde **185** had occurred. This product most probably forms upon radical debromination and subsequent nitrile formation with concomitant N–O bond rupture. The thus formed nitrile entails an O-centered radical, which cleaves the norbornane, a reaction facilitated by the release of ring strain. We then set out to explore reductive debromination methods. Disappointingly, while lithium halogen exchange only provided *β*-hydroxynitrile **182** (Table 3.6, Entry 5), no reaction was observed upon exposure to sodium borohydride or DIBAL (Table 3.6, Entries 6 and 7).

Due to the failure of all of the tested reductive conditions, the only successful method employing the vinylcerium reagent (*cf*. Table 3.5, Entry 5) was tested on bromoisoxazole **177** (Scheme 3.35). Unfortunately, the only isolated product was not the desired vinyl isoxazoline **178**, but *β*-hydroxynitrile **186**, obtained in 62% yield.

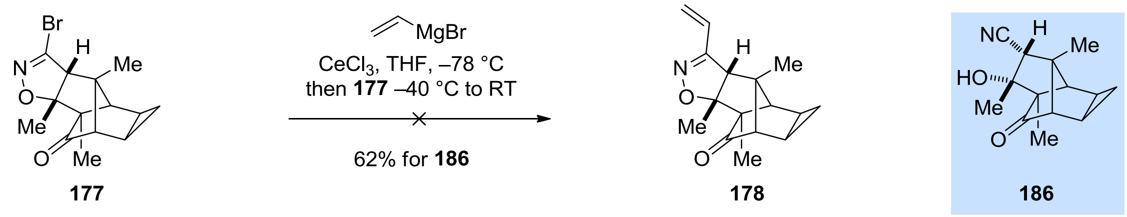

Scheme 3.35: Attempted vinylation of bromoisoxazoline **177** with a vinylcerium reagent.

This result in combination with the observed tendency of model substrate **180** to generate *β*-hydroxynitrile **182** under a variety of conditions prompted us to investigate the conversion of **177** to **186** followed by nitrile reduction to access aldehyde **179** (Table 3.7). Following the reports by SEO and KOCIOLEK, **177** was converted into nitrile **186** either by NaSEt in MeOH[91a)] or TMSCl and NaI in acetonitrile[91b)]. Even though the yields for both transformations were high, isomerization at C(9) occurred in presence of basic sodium ethylthiolate.

In an initial experiment, the generated *β*-hydroxynitrile was treated with diisobutylaluminum hydride at low temperature (Table 3.7, Entry 1). However, no conversion was visible upon TLC analysis. Hence, the reaction was warmed gradually to RT and more reducing agent was added. After stirring overnight, a new product formed, which unfortunately proved to be nitrile **187**, which suffered from C(3) ketone reduction. We surmised that after one equivalent of diisobutylaluminum hydride deprotonates the tertiary alcohol, a highly sterically demanding aluminum complex is formed, thereby shielding the nitrile and inhibiting the desired reduction. Consequently, Red-Al was employed, a reducing agent bearing two hydrides bound to aluminum.[96] We hypothesized that after deprotonation and ate complex formation the second hydride would be in close spatial proximity to the nitrile group and hence perform the reduction. Disappointingly, only decomposition of the starting material was observed (Table 3.7, Entry 2).

---

[96] It should be noted, that protection of the tertiray alcohol with TMSCl and subsequent attempted reduction wit DIBAL only led to slow decomposition of the starting material.

Table 3.7: Attempted conversion of bromoisoxazole **177** to aldehyde **179** *via* nitrile **186**. Reagents and conditions: a) NaSEt, MeOH, 78%, b) TMSCl, NaI, MeCN, 0 °C tor RT, 99%.

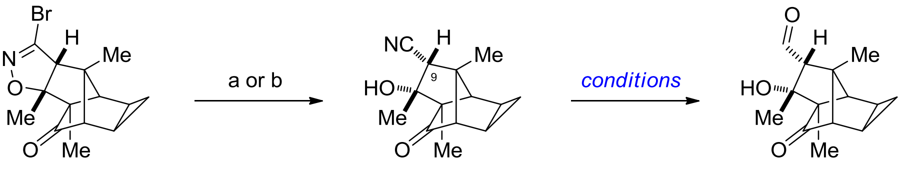

177 **186** **179**

Entry	Reagents	Solvent	Temperature	Product	Yield[a]-[d]
1	DIBAL	THF	–78 °C to RT	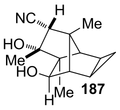	n.dt.
2	Red-Al	THF	–78 °C to RT	-	n.d.
3	$NaH_2PO_4 \cdot H_2O$, Ra–Ni	Py–AcOH–H_2O (2:1:1)	RT to 55 °C	-	n.r.
4	Li(*i*Bu)$_2$(*n*Bu)AlH	Et_2O	–40 °C to RT	-	n.d.
5	DIBAL·SMe_2	Et_2O	0 °C	-	n.d.
6	VO(O*i*Pr)$_3$, $(Me_2SiH)_2O$	toluene	60 °C	-	n.r.
7	$Cp_2Zr(H)Cl$	CH_2Cl_2	RT	-	n.d.

[a] Yields refer to spectroscopically and chromatographically homogenous materials. [b] n.dt. = Yield not determined. [c] n.d. = Product not detected. [d] n.r. = No reaction occurred.

Already in 1962, BACKEBARG and STASKUN reported a method for the conversion of nitriles into aldehydes mediated by Raney nickel in the presence of sodium hypophosphite.[97] However, upon applying this procedure to our system, no reaction was observed, even at elevated temperatures (Table 3.7, Entry 3).

The ate complex between DIBAL and *n*BuLi[98] has been shown to be an efficient reducing agent for the conversion of aliphatic nitriles to aldehydes.[99] However, applied to **186** only decomposition was observed (Table 3.7, Entry 4). In 1994, CHA *et al.* reported the beneficial use of DIBAL·SMe_2, generated from DIBAL and dimethyl sulfide, during the reduction of nitriles.[100] In the present case, rapid decomposition of **186** was observed (Table 3.7, Entry 5). Also other reported suitable reducing systems such as siloxanes in the presence of a vanadium complex[101] or Schwartz' reagent[102] did not provide the desired aldehyde **179** (Table 3.7, Entries 6 and 7).

---

[97] O. G. Backeberg, B. Staskun, *J. Chem. Soc.* **1962**, 3961-3962; for a review see: B. Staskun, T. van Es, *S. Afr. J. Chem.* **2008**, *61*, 144-156.
[98] S. Kim, K. H. Ahn, *J. Org. Chem.* **1984**, *49*, 1717-1724.
[99] T. Ritter, P. Zarotti, E. M. Carreira, *Org. Lett.* **2004**, *6*, 4371-4374.
[100] J. S. Cha, O. O. Kwon, M. K. Jeoung, E. J. Kim, *Bull. Kor. Chem. Soc.* **1994**, *15*, 1021-1023.

Concluding the described experiments, β-hydroxy nitrile **186** seemed to be a dead end and thus another strategy for the functionalization of bromoisoxazoline **177** was absolutely necessary, in order to maintain the advantage of simultaneous diastereoselective C(8) and C(9) functionalization by a 1,3-dipolar cycloaddition.

In 1986, DE MICHELI and co-workers reported the conversion of bromoisoxazolines into β-hydroxyesters *via* bromide-methoxide exchange upon exposure to LiOMe and subsequent hydrogenolysis with Ra–Ni and H_2.[103] To our delight, applying these conditions to isoxazoline **177**, methoxide **188** could be isolated in excellent 94% yield (Scheme 3.36). The subsequent N–O hydrogenolysis smoothly provided β-hydroxyester **189** in 91% yield.

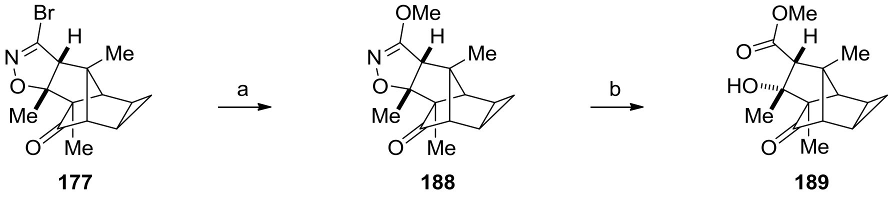

Scheme 3.36: Conversion of bromoisoxazoline **177** into β-hydroxyester **189**. Reagents and conditions: a) LiOMe, MeOH, reflux, 94%; b) $B(OH)_3$, Ra–Ni, H_2, MeOH–H_2O (5:1), 91%.

The synthetic sequence to access diol **74** from **189** was envisioned to comprise of reduction to the aldehyde and nucleophilic vinylation. Due to the sterically highly encumbered nature of the C(3) ketone, we surmised that selective reduction of the ester functionality should be possible. When ester **189** was exposed to 3.5 equivalents of DIBAL in THF, the conversion ceased at *circa* 50%. Noteworthy, when additional DIBAL was added and the reaction stirred overnight, decomposition was observed. Thus, it was attempted to expose **189** directly to an excess of reducing agent (6 equiv). Unfortunately, although desired diol **190** was formed, at least two side products were concomitantly produced. We hypothesized that the Lewis acidic nature of diisobutylaluminum hydride might cause side reactions such as retro aldol reaction between the tertiary alcohol and the C(3) ketone or the adjacent ester. Consequently, the ate complex between DIBAL and *n*BuLi, which does not possess a vacant coordination site, was tested as an alternative.[98] Indeed, upon treatment of **189** with three equivalents of freshly prepared $Li(iBu)_2(nBu)AlH$, diol **190** was isolated in excellent 89% yield (Scheme 3.37). Subsequent oxidation to the aldehyde with the Dess–

---

[101] S. Laval, W. Dayoub, L. Pehlivan, E. Metay, D. Delbrayelle, G. Mignani, M. Lemaire, *Tetrahedron. Lett.* **2014**, *55*, 23-26.

[102] V. Girjavallabhan, G. F. Njoroge, S. Bogen, V. Verma, F. Bennett, A. Kerekes, A. Arasappan, D. Pissarnitski, Q. Dan, I. Davies, D. B. Olsen, A. Stamford, J. P. Vacca EP2696681 (A1), **2012**.

[103] P. Caldirola, M. Ciancaglione, M. De Amici, C. De Micheli, *Tetrahedron. Lett.* **1986**, *27*, 4647-4650.

Martin periodinane was troublesome due to byproduct formation and incomplete conversion. However, this problem was easily solved by performing a Swern oxidation instead, furnishing aldehyde **179** in quantitative yield without any detectable byproducts.

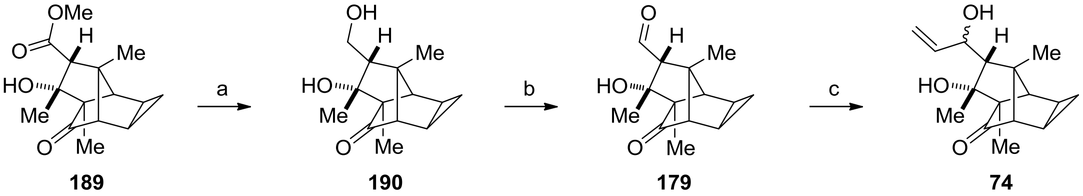

Scheme 3.37: Conversion of ester **189** into diol **74**. Reagents and conditions: a) DIBAL, *n*BuLi, THF, 0 °C then **189**, THF, –60°C to 0 °C, 89%; b) $(COCl)_2$, DMSO, CH_2Cl_2, –78 °C then **189**, CH_2Cl_2 –78 °C, then NEt_3, −78 °C to RT, quant.; c) $CeCl_3$, vinylmagnesium bromide, THF, –78 °C, then **179**, –78 °C to RT, 90%, d.r. = 60:40.

To our surprise, the subsequent Grignard addition of vinylmagnesium bromide did not yield the desired product. However, employing the organocerium reagent instead produced diol **74** in 90% yield as a 60:40 mixture of inseparable diastereomers. Attempts to increase the selectivity by prior chelation of the aldehyde and the tertiary alcohol with *n*Bu_2BOTf, indeed gave an increased diastereomeric ratio of 6:1, but resulted in a poor yield of 18%.

3.11 Alkoxycarbonylation and Completion of the Synthesis

With diol **74** in hand, the final alkoxycarbonylation could be approached next. In 1984, SEMMELHACK *et al*. reported the synthesis of pyran-lactones such as **196** *via* palladium(II)-mediated alkoxycarbonylation of **191**.[104] While initially carried out with stoichiometric amounts of $Pd(OAc)_2$, catalytic protocols have been developed by SEMMELHACK and YOSHIDA using $CuCl_2$ as the stoichiometric oxidant.[104,105] A detailed catalytic cycle is shown in Scheme 3.38.[16] After initial activation of the double bond by Pd(II), pyran formation occurs to yield **193**. After subsequent CO coordination, migratory insertion provides acyl palladium intermediate **195**. Lactone formation with concomitant generation of Pd(0) then produces pyran-lactone **196**. The final Cu(II)-mediated reoxidation to Pd(II) then completes the catalytic cycle.

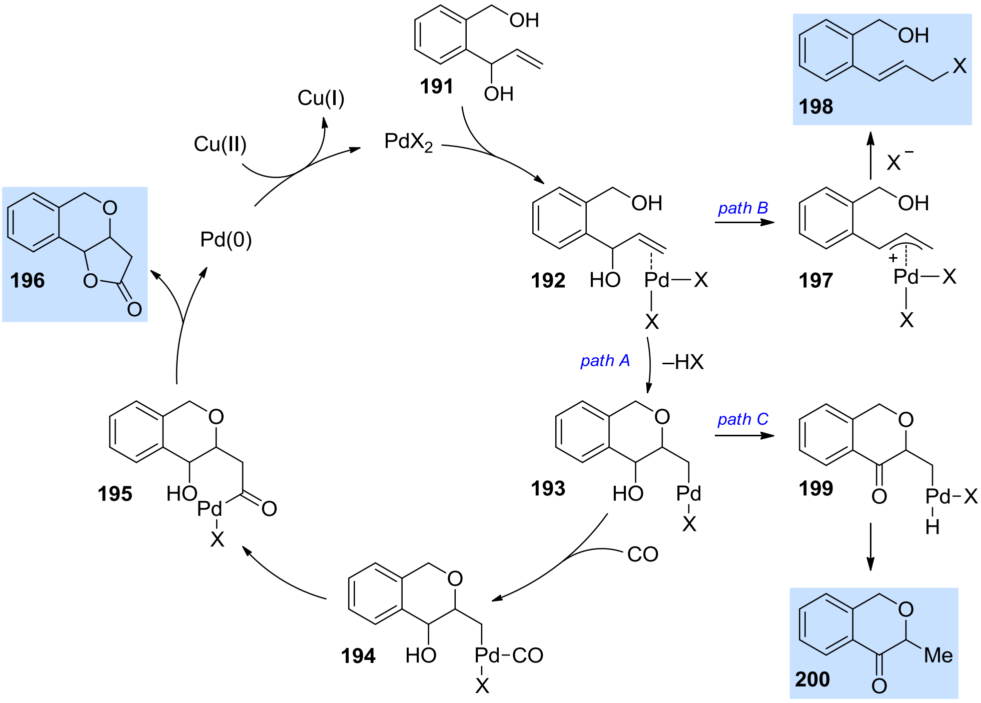

Scheme 3.38: Mechanistic hypothesis for the Pd(II)-mediated alkoxycarbonylation for the formation of pyran-lactones.

Noteworthy, several byproducts of the parent reaction have been discovered. Firstly, upon initial coordination of Pd(II) to the olefin, an alternative reaction pathway might occur (path B in Scheme 3.38). Instead of the desired pyran formation (path A), a cationic allylpalladium complex can be formed, which ultimately suffers from nucleophilic attack by chloride or acetate ions. Secondly, after the pyran is formed, the thus obtained alkylpalladium species **193** can undergo a hydride abstraction to ultimately give ketone **200** (path C). In 2008, YANG and co-workers undertook a detailed optimization study for the Pd(II)-catalyzed alkoxycarbonylation in order to overcome these limitations.[16] Allyl chloride formation (*cf.* Scheme 3.38, **198**) becomes problematic when stoichiometric $CuCl_2$ is employed. Consequently, in order to trap the chloride ions liberated during the reoxidation process, propylene oxide was added as a scavenger.[106] Additionally, the researchers hypothesized that the formation of ketone **200** might be affected by the base utilized. Indeed, while NaOAc and CsOAc were found to be inferior, the use of NH_4OAc completely shut down the formation of **200**. Additionally, tetramethylthiourea (TMTU) has been found to serve as a superior ligand for palladium(II) in the parent reaction.

---

[104] M. F. Semmelhack, C. Bodurow, M. Baum, *Tetrahedron Lett*. **1984**, *25*, 3171-3174.
[105] Y. Tamaru, T. Kobayashi, S. Kawamura, H. Ochiai, M. Hojo, Z. Yoshida, *Tetrahedron. Lett*. **1985**, *26*, 3207-3210.

Initially, it was decided to perform the alkoxycarbonylation with stoichiometric amounts of $Pd(OAc)_2$ under one atmosphere of carbon monoxide. To our delight, when a 60:40 mixture of diastereomeric diol **74** was treated with the conditions described by SEMMELHACK,[104] lactones **201** and **202** were isolated in 22% yield for each diastereomer, along with 7% of carbonate **203** (Scheme 3.39). Both, **201** and **203** provided crystals suitable for X-ray diffractometry, thereby unambiguously confirming their structural assignments.

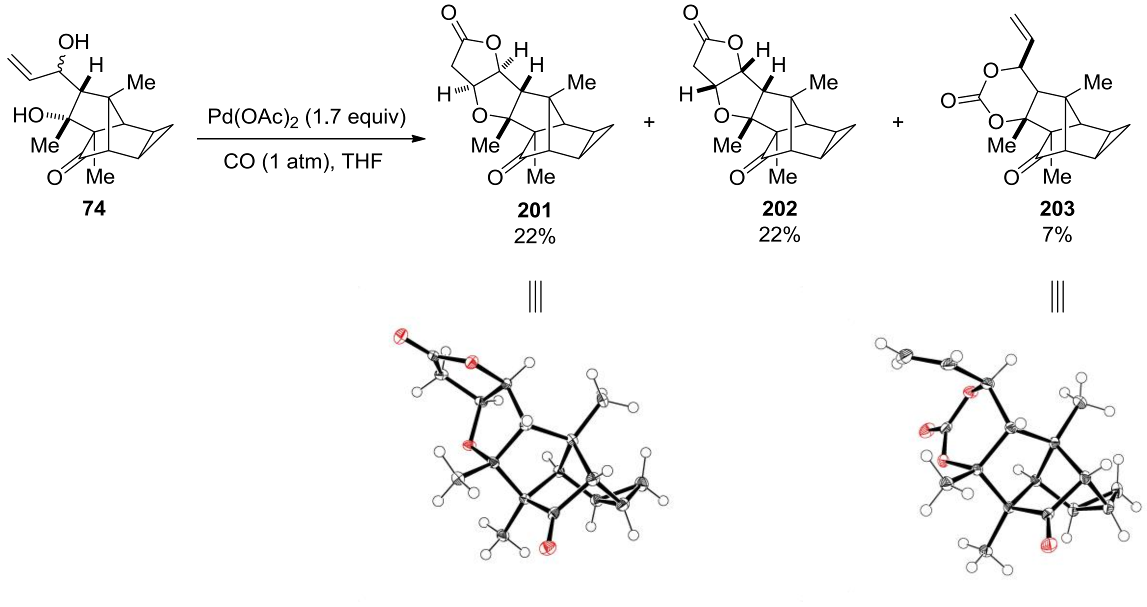

Scheme 3.39: Stoichiometric Pd(II)-mediated alkoxycarbonylation of diol **74**. ORTEP representations of **201** and **203**. Thermal ellipsoids at 50% probability.

While the mechanism of formation of carbonate **203** was not investigated, we surmised that performing the alkoxycarbonylation under catalytic conditions might not only suppress carbonate formation, but also increase the overall yield. Thus, the optimized catalytic conditions described by YANG and co-workers were tested next.[16] Noteworthy, this catalytic system already proved to be efficient during the total synthesis of pallambins C and D (*cf.* Chapter 1.2.2).[15]

---

[106] The beneficial addition of propylene oxide has been previously reported by TAMARU and WALKUP: a) Y. Tamaru, M. Hojo, Z. Yoshida, *J. Org. Chem.* **1991**, *56*, 1099-1105; b) R. D. Walkup, M. D. Mosher, *Tetrahedron* **1993**, *49*, 9285-9294.

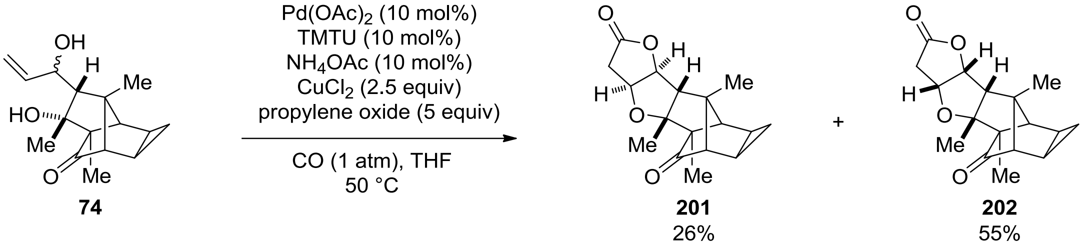
OH
H
Me
HO
Me
O
Me
74
Pd(OAc)$_2$ (10 mol%)
TMTU (10 mol%)
NH$_4$OAc (10 mol%)
CuCl$_2$ (2.5 equiv)
propylene oxide (5 equiv)
CO (1 atm), THF
50 °C
201
26%
+
202
55%

Scheme 3.40: Pd(II)-catalyzed alkoxycarbonylation of diol **74** under the conditions described by YANG and co-workers.

Indeed, as shown in Scheme 3.40, the use of the aforementioned conditions completely suppressed the formation of carbonate **203** and increased the yield of desired **202** to 55%. Noteworthy, the yield calculated based on the desired *anti* diastereomeric diol **74** constitutes 83%, thereby highlighting the efficiency of this synthetic method.

With a reliable route to lactone **202** in hand, the only remaining task was the introduction of the ethylidene moiety. A literature survey revealed two methods which have been successfully employed with γ-lactones. WIEMER and co-workers reported the reaction of diethyl phosphorochloridate in the presence of DMPU with the corresponding lithium enolates of lactones to ultimately access α-phosphono lactones.[107] A subsequent Horner–Wadsworth–Emmons reaction with acetaldehyde would then provide pallambins A and B. Furthermore, an aldol reaction with acetaldehyde followed by mesylation and base-mediated elimination would also furnish the natural products.

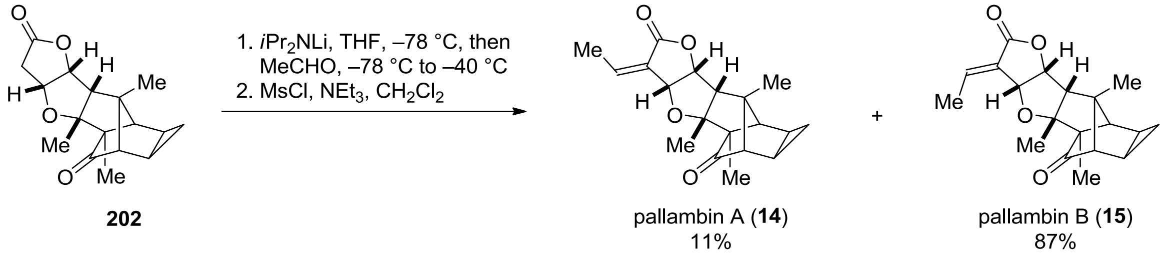
202
1. *i*Pr$_2$NLi, THF, –78 °C, then MeCHO, –78 °C to –40 °C
2. MsCl, NEt$_3$, CH$_2$Cl$_2$
pallambin A (14)
11%
+
pallambin B (15)
87%

Scheme 3.41: Aldol condensation of **202** providing pallambins A (**14**) and B (**15**).

While attempted generation of the α-phosphono lactone only led to decomposition of the starting material, exposure of the lithium enolate of **202** to acetaldehyde produced the desired aldol product, which was directly subjected to a mixture of MsCl and NEt$_3$ (Scheme 3.41). Gratifyingly, this two-step aldol condensation provided a mixture of pallambins A and B, which could be separated by preparative thin layer chromatography to yield 87% of pallambin B and 11% of pallambin A. As shown in Tables 3.8 and 3.9 all obtained spectral data were in good agreement with the values of the isolation report.[7]

---

[107] J. A. Jackson, G. B. Hammond, D. F. Wiemer, *J. Org. Chem.* **1989**, *54*, 4750-4754.

Table 3.8: Comparison of NMR spectroscopic data in $CDCl_3$ for natural vs. synthetic pallambin A.

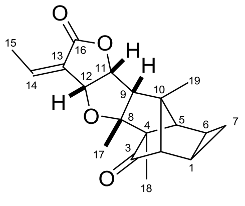

pallambin A (**14**)

Carbon	^{1}H natural[a]	^{1}H synthetic[b]	^{13}C natural[c]	^{13}C synthetic[d]
1	1.43 (m, 1H)	1.42 (m, 1H)	14.5	14.5
2	2.49 (br, 1H)	2.49 (br, 1H)	58.0	58.0
3	-	-	214.4	214.4
4	-	-	67.0[e]	67.0
5	2.48 (br, 1H)	2.48 (br, 1H)	54.9	54.9
6	0.87 (m, 1H)	0.88 (m, 1H)	15.0	15.0
7α	0.56 (dd, J = 13.8, 7.5 Hz 1H)	0.56 (m, 1H)	12.0	12.0
7β	1.40 (m, 1H)	1.40 (m, 1H)		
8	-	-	89.8	89.8
9	2.45 (d, J = 7.1 Hz, 1H)[f]	2.45 (d, J = 7.1 Hz, 1H)	60.9	60.8
10	-	-	44.6	44.6
11	4.95 (dd, J = 7.1, 3.5 Hz, 1H)	4.95 (dd, J = 7.1, 3.5 Hz, 1H)	84.7	84.7
12	4.75 (d, J = 3.5 Hz, 1H)	4.75 (dt, J = 3.5, 0.6 Hz, 1H)	80.1	80.1
13	-	-	126.0	126.0
14	6.69 (q, J = 7.3 Hz, 1H)	6.69 (qd, J = 7.3, 0.6 Hz, 1H)	144.8	144.9
15	2.27 (d, J = 7.3 Hz, 3H)	2.27 (d, J = 7.3 Hz, 3H)	14.2	14.2
16	-	-	168.3	168.4
17	1.11 (s, 3H)	1.11 (s, 3H)	19.4	19.5
18	1.18 (s, 3H)	1.18 (s, 3H)	7.3	7.3
19	1.34 (s, 3H)	1.34 (s, 3H)	21.5	21.5

[a] According to ref. 7, 600 MHz, referenced chloroform to 7.28 ppm; [b] 600 MHz, referenced chloroform to 7.26 ppm; [c] According to ref. 7, 150 MHz, referenced $CDCl_3$ to 77.0 ppm; [d] 150 MHz, referenced $CDCl_3$ to 77.16 ppm; [e] Although Table 1 in ref. 7 states this signal at 70.0 ppm, the reported ^{13}C NMR spectrum clearly shows this signal at 67.0 ppm. Therefore a typing error in the isolation report is assumed; [f] Although Table 1 in ref. 7 states this signal at 2.27 ppm, the reported ^{1}H NMR spectrum clearly shows this signal at 2.45 ppm. Therefore a typing error in the isolation report is assumed.

Table 3.9: Comparison of NMR spectroscopic data in $CDCl_3$ for natural vs. synthetic pallambin B.

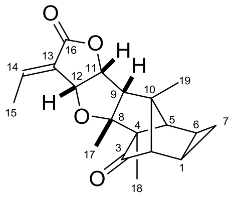

pallambin B (**15**)

Carbon	^{1}H natural[a]	^{1}H synthetic[b]	^{13}C natural[c]	^{13}C synthetic[d]
1	1.40 (m, 1H)	1.44 – 1.34 (m, 2H)	14.2	14.2
2	2.50 (br, 1H)	2.50 (br, 1H)	58.0	58.1
3	-	-	214.4	214.4
4	-	-	66.8	67.0
5	2.42 (br, 1H)	2.42 (br, 1H)	54.9	54.9
6	0.87 (m, 1H)	0.88 (m, 1H)	15.0	15.1
7α	0.56 (dd, *J* = 13.8, 7.5 Hz, 1H)	0.55 (m, 1H)	11.9	12.0
7β	1.42 (m, 1H)	1.44 – 1.34 (m, 2H)		
8	-	-	90.1	90.2
9	2.48 (d, *J* = 7.1 Hz, 1H)	2.48 (d, *J* = 7.0 Hz, 1H)	60.5	60.6
10	-	-	44.6	44.6
11	4.98 (dd, *J* = 7.1, 3.9 Hz, 1H)	5.01 – 4.97 (m, 2H)	85.4	85.4
12	5.00 (d, *J* = 3.9 Hz, 1H)	5.01 – 4.97 (m, 2H)	75.6	75.7
13	-	-	127.5	127.5
14	7.03 (q, *J* = 6.8 Hz, 1H)	7.03 (qd, *J* = 7.2, 1.0 Hz, 1H)	142.0	142.0
15	2.05 (d, *J* = 6.8 Hz, 3H)	2.04 (d, *J* = 7.2 Hz, 3H)	16.0	16.0
16	-	-	170.3	169.5
17	1.13 (s, 3H)	1.13 (s, 3H)	19.4	19.5
18	1.17 (s, 3H)	1.17 (s, 3H)	7.2[e]	7.2
19	1.39 (s, 3H)	1.34 (s, 3H)	21.6	21.6

[a] According to ref. 7, 600 MHz, referenced chloroform to 7.28 ppm; [b] 600 MHz, referenced chloroform to 7.26 ppm; [c] According to ref. 7, 150 MHz, referenced $CDCl_3$ to 77.0 ppm; [d] 150 MHz, referenced $CDCl_3$ to 77.16 ppm; [e] Although Table 1 in ref. 7 states this signal at 7.8 ppm, the reported ^{13}C NMR spectrum clearly shows this signal at 7.2 ppm. Therefore a typing error in the isolation report is assumed.

4 Conclusion

Pallambins A and B are norditerpenoid natural products, isolated in 2012 from the liverwort *Pallavicina ambigua*. These natural products possess an unprecedented and highly congested tetracyclo[4.4.$0^{3,5}$.$0^{2,8}$]decane core, which comprises a cyclopropane in a sterically hindered environment. Furthermore, pallambins A and B are endowed with not less than ten contiguous stereocenters, two of which are quaternary. These challenging structural features prompted us to embark on a total synthesis of these unique norditerpenoids.

The synthetic strategy developed in this thesis is centered around the use of pentafulvene (**79**) as a diene component in a thus far unprecedented Diels–Alder reaction. After extensive experimentation and optimization, it could indeed be established that despite its high reactivity and tendency to polymerize, pentafulvene can be employed in a [4+2] cycloaddition with methyl acrylate under Lewis acid catalysis (Scheme 4.1).

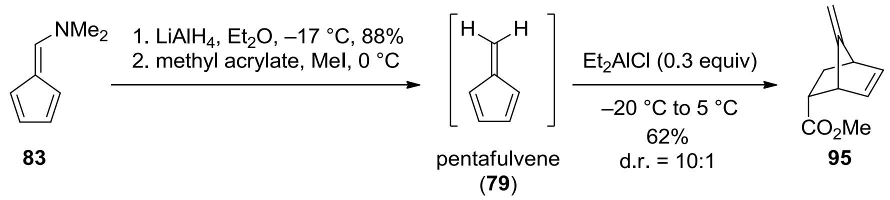

Scheme 4.1: Generation of pentafulvene and subsequent Diels–Alder reaction with methyl acrylate.

Furthermore, it could be shown that the utilization of this particular transformation entails several advantages as compared to substituted cyclopentadienes. Firstly, the often observed isomerizations of substituted cyclopentadienes under Diels–Alder conditions are excluded in the case of pentafulvene. Secondly, the sp^2-hybridized bridge carbon atom enables a wider variety of functionalization methods than sp^3-hybridized adducts of a dienophile with cyclopentadienes. Thirdly, we became intrigued to realize such a Diels–Alder reaction with pentafulvene, since it would constitute the first use of such a transformation in complex natural product synthesis. The synthetic strategy developed in this thesis relies on a number of highly chemo-, regio- and diastereoselective functionalizations, as evidenced by the absence of protecting groups.

After discovering that cyclopropanation is not possible with the C(10) methyl group installed and that a Pd(II)-mediated hydroalkylation reaction with the already introduced cyclopropane failed, the synthetic plan had to be revised. The thereby observed steric shielding of the *Si* face of the *exo* olefin by the cyclopropane opened the possibility for highly diastereoselective *Re* functionalization. Hence, after tedious screening, conditions for an exceedingly chemoselective *endo* cyclopropanation of **95** have been identified to provide **148** in 85% yield (Scheme 4.2). Subsequent completely chemo- and diastereoselective hydrogenolysis of the remaining *exo* olefin with Wilkinson's catalyst gave saturated ester **150** in 96% yield. Next, the C(3) ketone was generated by an efficient sequence of α-hydroxylation, reduction and subsequent diol cleavage to provide **146** in 82% overall yield.

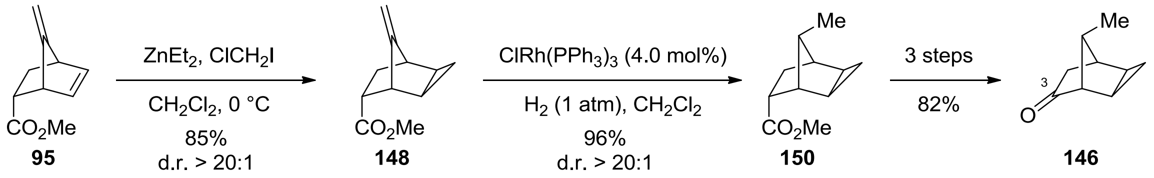
CO2Me
95
ZnEt2, ClCH2I
CH2Cl2, 0 °C
85%
d.r. > 20:1
CO2Me
148
ClRh(PPh3)3 (4.0 mol%)
H2 (1 atm), CH2Cl2
96%
d.r. > 20:1
Me
CO2Me
150
3 steps
82%
Me
3
O
146

Scheme 4.2: Chemo- and diastereoselective cyclopropanation and hydrogenolysis and subsequent C(3) ketone generation.

Methylation and subsequent acylation *via* Mukaiyama aldol reaction followed by *t*BuOH accelerated Dess–Martin oxidation provided diketone **155** in 62% overall yield as an inseparable 5:1 mixture of diastereomers (Scheme 4.3). Diazo transfer under the conditions described by DANHEISER *et al.*[84] followed by exposure of the crude reaction mixture to 1.0 mol% of $Rh_2(OAc)_4$ gave C–H inserted tetracycle **76** in 76% overall yield from **155**.

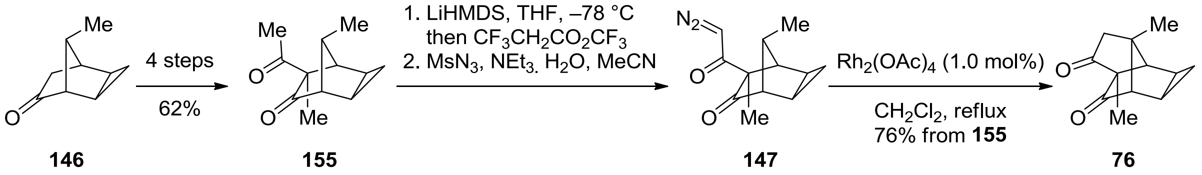
Me
O
146
4 steps
62%
Me
Me
O
O
Me
155
1. LiHMDS, THF, –78 °C
then CF3CH2CO2CF3
2. MsN3, NEt3, H2O, MeCN
N2
Me
O
O
Me
147
Rh2(OAc)4 (1.0 mol%)
CH2Cl2, reflux
76% from 155
Me
O
O
Me
76

Scheme 4.3: α-Functionalization of ketone **146** and subsequent C–H insertion to generate tetracycle **76**.

Since addition of organometallic reagents towards the C(8) ketone was considered futile due to the steric shielding of the norbornane system, a 1,3-dipolar cycloaddition approach was pursued. Such a transformation would not only generate the C(8)- but also the C(9) stereocenter. Thus, diketone **76** was first transformed into the corresponding triflate, which was further reacted under Negishi conditions to produce olefin **172** (Scheme 4.4). To our delight, **172** smoothly underwent completely regio- and diastereoselective 1,3-dipolar cycloaddition in 91% yield with bromonitrile oxide, generated *in situ* from dibromoformaldoxime and $KHCO_3$. Due to the failure of various direct functionalizations of bromoisoxazole **177**, bromide methoxide exchange was pursued with LiOMe to produce **188** in 94% yield.

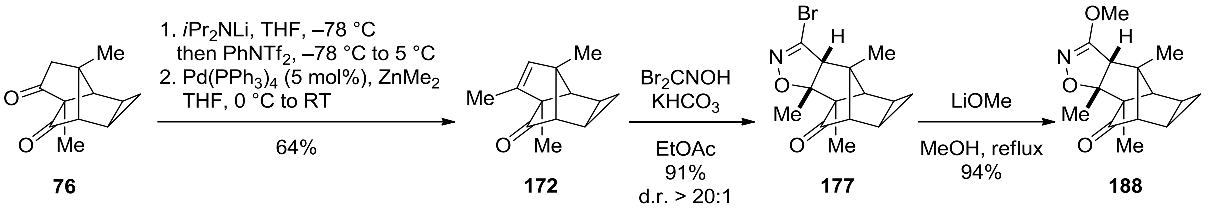
1. *i*Pr2NLi, THF, –78 °C then PhNTf2, –78 °C to 5 °C
2. Pd(PPh3)4 (5 mol%), ZnMe2 THF, 0 °C to RT
64%
76
172
Br2CNOH
KHCO3
EtOAc
91%
d.r. > 20:1
177
LiOMe
MeOH, reflux
94%
188

Scheme 4.4: Stereoselective simultaneous C(8) and C(9) functionalization *via* 1,3-dipolar cycloaddition.

Isoxazoline **188** was converted into an inseparable 60:40 diastereomeric mixture of diol **74** within four steps in 73% overall yield (Scheme 4.5). The remaining tetrahydrofuran *γ*-lactone motif was subsequently generated by Pd(II)-catalyzed alkoxycarbonylation employing the conditions described by YANG and co-workers.[16] Finally, lactone **202** smoothly underwent a two-step aldol condensation providing pallambin A (**14**) in 11% and pallambin B (**15**) in 87% yield respectively.

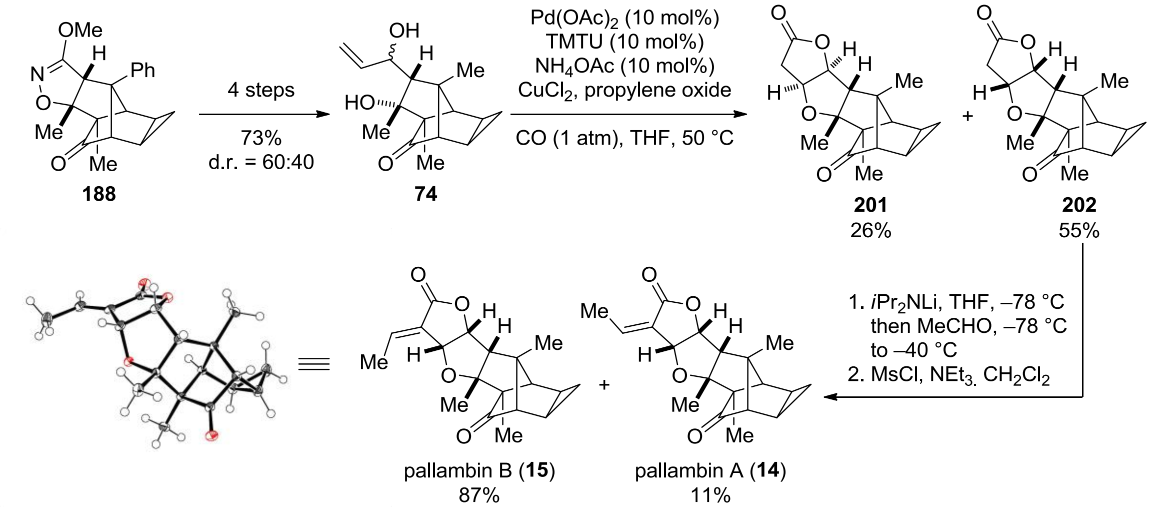
188
4 steps
73%
d.r. = 60:40
74
Pd(OAc)2 (10 mol%)
TMTU (10 mol%)
NH4OAc (10 mol%)
CuCl2, propylene oxide
CO (1 atm), THF, 50 °C
201
26%
202
55%
1. *i*Pr2NLi, THF, –78 °C then MeCHO, –78 °C to –40 °C
2. MsCl, NEt3, CH2Cl2
pallambin B (15)
87%
pallambin A (14)
11%

Scheme 4.5: Completion of the synthesis of pallambins A (**14**) and B (**15**) *via* Pd(II)-catalyzed alkoxycarbonylation. ORTEP representation of pallambin B with thermal ellipsoids at 50% probability.

Part II

Regioselective Ti(III)-Mediated Epoxide Opening

5 Introduction

5.1 Established Methods for Reductive Epoxide Openings

The ease of generation along with reliable methods for their enantioselective introduction rendered epoxides one of the most popular and widely used building blocks in synthetic organic chemistry. Additionally, epoxides can undergo a variety of functional group interconversions and serve thus as valuable intermediates.[108] Due to the extensive number of methods for the stereoselective introduction of epoxides, reductive opening of such species became an expedient tool for the generation of free hydroxy groups (Scheme 5.1). However, controlling the regioselectivity of the hydride transfer has proven to be a considerable challenge.

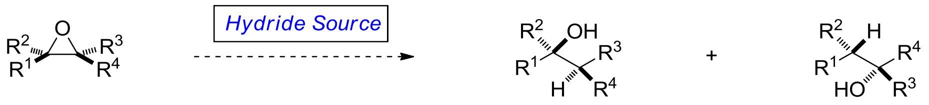

Scheme 5.1: Reductive epoxide opening yielding two different regioisomeric alcohols.

5.1.1 Metal Hydrides

Lithium aluminum hydride has become one of the most prominent reductants for the opening of epoxides.[109] As indicated in Table 5.1, both the reactivity and the regioselectivity are highly dependent on steric factors. Hence, the hydride delivery usually takes place at the more accessible carbon atom.

Table 5.1: Reduction of selected epoxides with lithium aluminum hydride.[110]

Entry	Epoxide	Yield	Products		Ratio
1	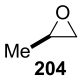 **204**	60%	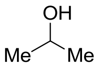 **205**	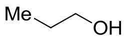 **206**	100:0
2	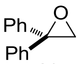 **207**	97%	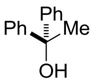 **208**	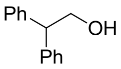 **209**	96:4
3	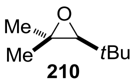 **210**	21%	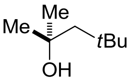 **211**	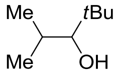 **212**	0:100

---

[108] For an excellent overview of epoxides in complex molecule synthesis, see: P. Crotti, M. Pineschi in *Aziridines and Epoxides in Organic Synthesis* (Ed. A. K. Yudin), Wiley-VCH, Weinheim, **2006**, pp. 271-313.

[109] The collection of methods for the reductive opening of epoxides is mainly taken from: S. Murai, T. Murai, S. Kato in *Comprehensive Organic Synthesis, Vol. 8* (Eds. B. M. Trost, I. Flemming), Pergamon Press, Oxford, **1991**, pp. 871-893.

[110] Taken from ref. 109.

In 1972, HARTMAN and RICKBORN investigated the effect of neighboring alcohol and ether groups in cyclohexene oxides.[111] However, the results presented in Scheme 5.2 combined with the employment of $LiAlD_4$ clearly ruled out any strong directing influence by intramolecular hydride delivery.

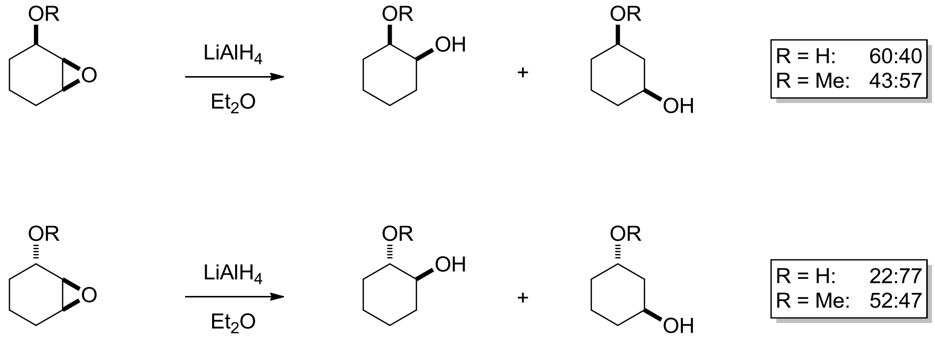

Scheme 5.2: Reduction of *syn*- and *anti*-cyclohexene oxide derivatives with lithium aluminum hydride.

One decade later, FINAN and KISHI reported the controlled reductive ring openings of 2,3-epoxyalcohols.[112] A screening of three aluminum based hydrides, $LiAlH_4$, Red-Al[113] and DIBAL revealed a remarkably different behavior (Scheme 5.3). While exposure of **212** to $LiAlH_4$ provided a 1:1 mixture of alcohols **213** and **214**, Red-Al gave a selectivity of up to 150:1 favoring 1,3-diol **213**. Noteworthy, upon switching to Lewis acidic DIBAL the selectivity was reversed to 1:13 favoring 1,2-diol **214**.

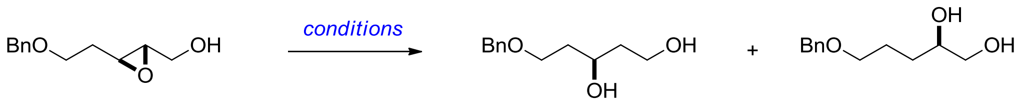

212 **213** **214**

$LiAlH_4$, THF, RT:	1:1
Red-Al, THF, –20 °C:	150:1
DIBAL, C_6H_6, RT:	1:13

Scheme 5.3: Reduction of 2,3-epoxyalcohols with $LiAlH_4$, Red-Al and DIBAL.

The authors surmised that the Red-Al reduction occurs *via* initial complex formation followed by intramolecular hydride delivery. If DIBAL is employed initial complexation with concomitant H_2 formation with the hydroxy group also occurs. However, the vacant coordination site might now act as a Lewis acid coordinating to the epoxide and thereby facilitating intermolecular hydride delivery.

---

[111] B. C. Hartman, B. Rickborn, *J. Org. Chem.* **1972**, *37*, 4246-4249.
[112] J. M. Finan, Y. Kishi, *Tetrahedron. Lett.* **1982**, *23*, 2719-2722.
[113] Red-Al® is used for sodium bis(2-methoxy)aluminum hydride.

Due to the relatively high reactivity of aluminum-based reductants, borohydrides have also been investigated for the opening of epoxides. SOAI and co-workers reported the use of alkali borohydrides in *t*BuOH–MeOH mixtures.[114] However, it should be noted that in order to overcome the relatively low reactivity of the reductants, reflux of the reaction mixture was crucial and high yields were only obtained reliably for styrene derivatives.

A powerful boron based hydride, lithium triethylborohydride (*"superhydride"*) has been introduced by H. C. BROWN and co-workers as a reagent especially suitable for hindered tri- and tetrasubstituted epoxides (Table 5.2).[115]

Table 5.2: Reduction of selected epoxides with $LiEt_3BH$.[110]

Entry	Epoxide	Temperature	Yield	Product
1	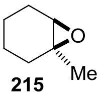 **215**	RT	99%	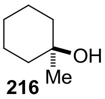 **216**
2	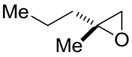 **217**	RT	100%	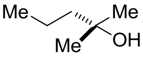 **218**
3	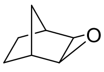 **219**	65 °C	100%	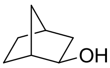 **220**

5.1.2 Dissolving Metals

Alkali metals in combination with amine solvents also possess the ability to reduce epoxides to the corresponding alcohol derivatives. Despite their relatively high reactivity and the thus associated potential side reactions, alkali metals bear some advantages over metal hydrides.

Table 5.3: Reduction of selected epoxides with alkali metals. [110]

Entry	Epoxide	Metal	Yield	Product
1	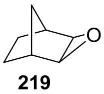 **219**	Li	86%	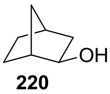 **220**
2	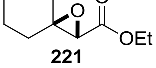 **221**	Na	46%	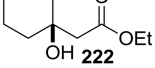 **222**
3	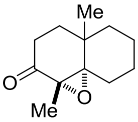 **223**	Li	53%	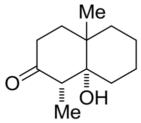 **224**

---

[114] A. Ookawa, H. Hiratsuka, K. Soai, *Bull. Chem. Soc. Jpn.* **1987**, *60*, 1813-1817.

[115] S. Krishnamurthy, R. M. Schubert, H. C. Brown, *J. Am. Chem. Soc.* **1973**, *95*, 8486-8487.

Most importantly, as shown in Table 5.3, functional groups such as ketones and esters can be tolerated. Additionally, in contrast to $LiAlH_4$, lithium in ethylenediamine reduces bicyclic epoxides without skeletal rearrangement. Furthermore, calcium,[116] aluminum[117] and zinc[118] have been used as safer and more economical alternatives.

5.1.3 Hydrogenolysis

Due to the mostly required high pressure, hydrogenolysis of epoxides, is only of major importance for industrial applications rather than on laboratory scale. However, some mild examples have been reported employing Ra–Ni in the presence of 1 atm of hydrogen.[119] Noteworthy, in contrast to metal hydride and dissolving metal reductions, only the less substituted alcohol is formed.

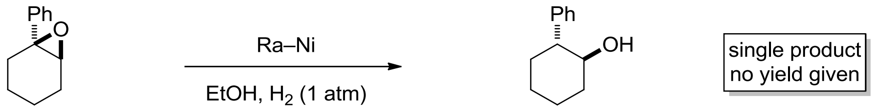

225 **226**

Scheme 5.4: Hydrogenolysis of **225** in the presence of Ra–Ni.

---

[116] R. A. Benkeser, A. Rappa, L. A. Wolsieffer, *J. Org. Chem.* **1986**, *51*, 3391-3393.

[117] a) E. J. Corey, E. J. Trybulski, L. S. Melvin, K. C. Nicolaou, J. A. Secrist, R. Lett, P. W. Sheldrake, J. R. Falck, D. J. Brunelle, M. F. Haslanger, S. Kim, S. E. Yoo, *J. Am. Chem. Soc.* **1978**, *100*, 4618-4620; b) A. E. Greene, M. A. Teixeira, E. Barreiro, A. Cruz, P. Crabbé, *J. Org. Chem.* **1982**, *47*, 2553-2564.

[118] a) D. Bittler, H. Hofmeister, H. Laurent, K. Nickisch, R. Nickolson, K. Petzoldt, R. Wiechert, *Angew. Chem. Int. Ed.* **1982**, *21*, 696-697; b) Y. D. Vankar, P. S. Arya, C. T. Rao, *Synth. Commun.* **1983**, *13*, 869-872.

[119] S. Mitsui, Y. Sugi, M. Fujimoto, K. Yokoō, *Tetrahedron* **1974**, *30*, 31-37.

5.1.4 Low Valent Titanium

In 1994, RAJANBABU and NUGENT reported their investigation of low valent titanium(III) for the generation of radicals from epoxides.[120] As indicated in Table 5.4, the researchers found that when an epoxide substrate is slowly added to an excess of Cp_2TiCl, readily generated by zinc-mediated reduction of Cp_2TiCl_2, the corresponding olefinic product is obtained in high yields.

Table 5.4: Reduction of epoxides to alkenes mediated by Cp_2TiCl.

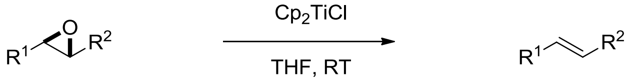

Entry	Epoxide	Product	Yield
1	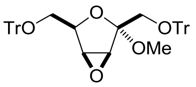 **227**	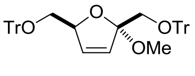 **228**	66%
2	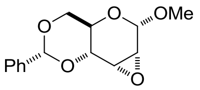 **229**	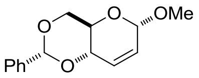 **230**	78%
3	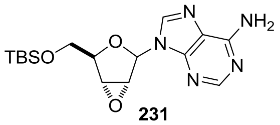 **231**	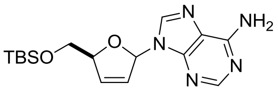 **232**	68%
4	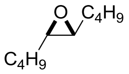 **233** or 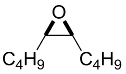 **234**	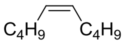 **235** + 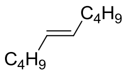 **236** 73:27	not given

The examination of both (*Z*)- and (*E*)-5,6-epoxydecane (**233** and **234**) in separate experiments provided the exact same *Z/E* mixture of 73:27, thus revealing an intriguing mechanistic detail. RAJANBABU and NUGENT suggest a long-living radical intermediate, generated by a single electron transfer mechanism, in order to explain the complete loss of stereochemistry. The thus derived complete mechanistic proposal is illustrated in Scheme 5.5.

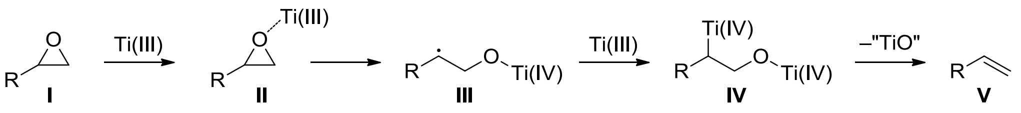

Scheme 5.5: Mechanistic proposal for the Ti(III)-mediated epoxide reduction by RAJANBABU and NUGENT.

A first equivalent of Ti(III) might form a σ-complex with epoxide **I**, entailing a ring strain releasing single electron reduction to provide radical intermediate **III**. A second equivalent of Ti(III) could then perform another single electron reduction to generate **IV**, which undergoes elimination to generate olefin **V**. RAJANBABU and NUGENT deliberated about whether intermediate **III** would be long-living enough to undergo further radical reactions, i.e. if it could be trapped by H· or olefins. Accordingly, for such a scenario to occur, the Ti(III) concentration must be kept marginal in order to allow a certain life time of species **III**. Indeed, in a first experiment, slow addition of a solution of Cp_2TiCl in THF to a mixture of 1,1'-epoxyethylcyclohexane (**237**) and 1,4-cyclohexadiene as an H-atom donor provided 1-cyclohexanol (**238**) in 91% yield. Remarkably, the opposite regioselectivity compared to standard metal hydrides is observed (*cf.* Chapter 5.1.1).

---

[120] T. V. Rajanbabu, W. A. Nugent, *J. Am. Chem. Soc.* **1994**, *116*, 986-997.

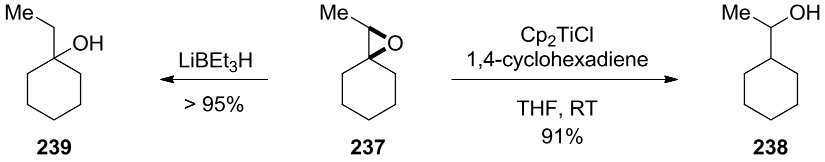

Scheme 5.6: Reductive epoxide opening with Ti(III) and subsequent H-atom transfer compared to conventional metal hydrides.

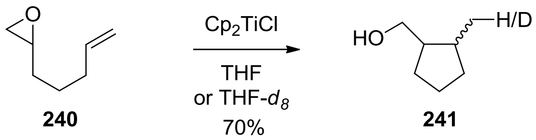

Scheme 5.7: Reductive epoxide opening and subsequent cyclization.

Furthermore, as presented in Scheme 5.7, the authors also investigated the intramolecular trapping of the newly formed radical species by alkenes and alkynes. In the event, slow addition of Ti(III) to 1-epoxy-6-heptenes, such as **240**, provided the corresponding cyclopentanes in good yields. Importantly, the addition of an external hydride source was not necessary, since, as shown by isotope labelling, H-atom abstraction from the solvent occurred.

A few years after the seminal publication of RAJANBABU and NUGENT, GANSÄUER *et al.* developed a catalytic variant of the Ti(III)-mediated reductive epoxide opening, thus setting the cornerstone for asymmetric versions of this intriguing transformation.[121] In order to render this reductive process catalytic, several obstacles had to be overcome. Firstly, a suitable and cheap stoichiometric reductant needed to be found, which does not spontaneously react with the starting material. Secondly, an acid additive needed to be identified, in order to effectively cleave the newly formed titanium alkoxide and thus enable turnover of the catalyst. Zinc and manganese quickly imposed as efficient reductants. However, the quest for a suitable acid proved to be more complicated. Firstly, the acid must not oxidize the metal or any titanium species. Secondly, it must be strong enough to break the titanium-oxygen bond, but weak enough to not protonate and thus open the starting epoxide. Thirdly, the corresponding base must not coordinate to and thence deactivate any catalytically active titanium species. The therefore required pK_a range should be between 5.25-12.5. Out of a laborious screening, 2,4,6-collidine hydrochloride (pK_a = 7.43) emerged as a highly efficient acid additive. Table 5.5 displays some of the results obtained with the developed catalytic system.[122]

---

[121] A. Gansäuer, H. Bluhm, M. Pierobon, *J. Am. Chem. Soc.* **1998**, *120*, 12849-12859.

Table 5.5: Catalytic Ti(III)-mediated reductive epoxide opening developed by GANSÄUER *et al.*

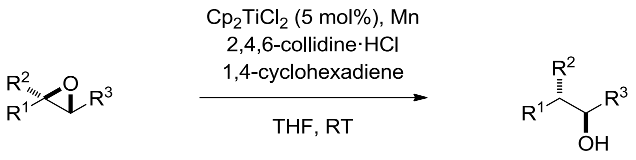
Cp$_2$TiCl$_2$ (5 mol%), Mn
2,4,6-collidine·HCl
1,4-cyclohexadiene
THF, RT
R^1
R^2
R^3
O
OH

Entry	Epoxide	Product	Yield
1	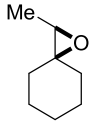 **237**	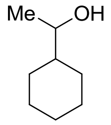 **238**	81%
2	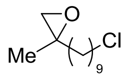 **242**	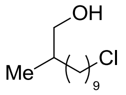 **243**	74%
3	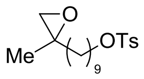 **244**	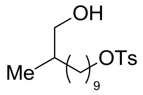 **245**	58%
4	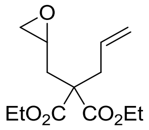 **240**	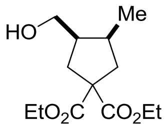 **241**	78% (*syn:anti = 86:14)*

Based on the results presented in Table 5.5, GANSÄUER and co-workers investigated the use of a chiral Ti(III) complex.[123] When epoxide **246** was subjected to 5 mol% of **247**, alcohol **248** was isolated in 65% yield and 93% *ee*, thus demonstrating the utility of this method for the desymmetrization of epoxides (Scheme 5.8).

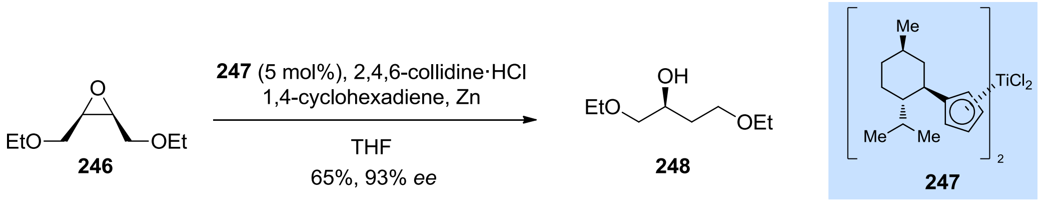
O
EtO
OEt
246
247 (5 mol%), 2,4,6-collidine·HCl
1,4-cyclohexadiene, Zn
THF
65%, 93% ee
OH
EtO
OEt
248
Me
TiCl$_2$
Me
Me
2
247

Scheme 5.8: Desymmetrization of *meso* epoxide **246** with chiral Ti(III) complex **247**.

---

[122] For a recent review of the use of Cp$_2$TiCl in natural product synthesis see: S. P. Morcillo, D. Miguel, A. G. Campana, L. A. de Cienfuegos, J. Justicia, J. M. Cuerva, *Org. Chem. Front.* **2014**, *1*, 15-33.

[123] A. Gansäuer, T. Lauterbach, H. Bluhm, M. Noltemeyer, *Angew. Chem. Int. Ed.* **1999**, *38*, 2909-2910.

6 Aim of the Project

6.1 Total Synthesis of Microcin SF608

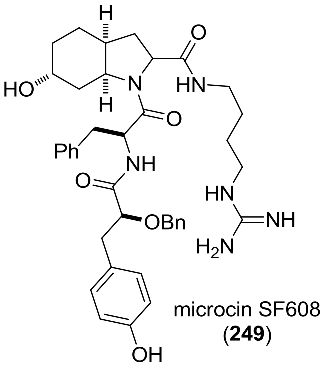

Figure 6.1: Microcin SF608.

The objective of this project grew on an observation made earlier in our group during the total synthesis of microcin SF608 (**249**, Figure 6.1).[124] This Aeruginosin natural product was first isolated in 1999 from the cyanobacterium *Microcystis sp.* and displayed selective inhibition of the serine protease trypsin (IC_{50} = 0.5 µg/mL).[125] Structurally, **249** is characterized by a carboxy hydroxyoctahydroindole (Choi) core, an amino acid and a guanidine side chain.

In 2010, CARREIRA and co-workers reported the total synthesis of microcin SF608, which was centered around a Lewis acid-mediated oxabicycle opening (Scheme 6.1). The oxabicyclic system was smoothly generated by a Diels–Alder reaction of furan. However, the endocyclic olefin needed to undergo a regioselective formal addition of water. While initial hydroboration attempts failed, a reductive epoxide opening of **251** was investigated. Remarkably, upon exposure to the conditions reported by RAJANBABU and NUGENT,[120] alcohol **252** was the sole product observed.

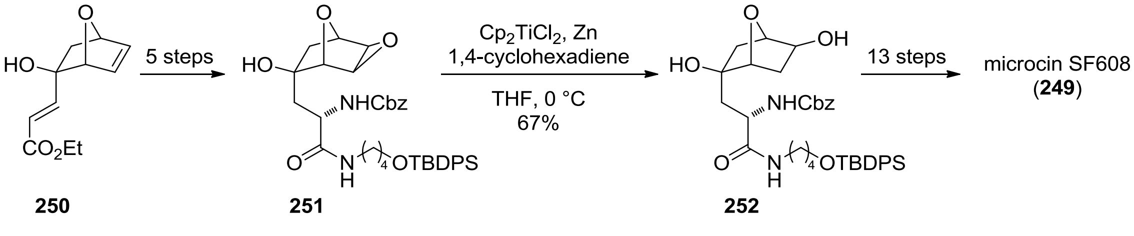

Scheme 6.1: Regioselective reductive epoxide opening of **251** during the total synthesis of microcin SF608 (**249**).

While the reductive epoxide opening event itself is not unexpected based on the results of RAJANBABU and NUGENT, the regioselectivity of the reaction is exciting. Importantly, the proposed mechanism presented in Chapter 5.1.4 cannot account for the exclusive formation of alcohol **252** and consequently a different reaction pathway must be operating.

---

[124] S. Diethelm, C. S. Schindler, E. M. Carreira, *Org. Lett.* **2010**, *12*, 3950-3953.
[125] R. Banker, S. Carmeli, *Tetrahedron* **1999**, *55*, 10835.

6.2 Studies on the Origin of Selectivity[126]

In order to gain further insight into the origin of the observed regioselectivity during the reductive epoxide opening of **251** to **252**, DIETHELM and CARREIRA undertook a detailed mechanistic study.

In accordance with the proposed mechanism of RAJANBABU and NUGENT, an initial Ti(III)-mediated opening of the epoxide to isomeric radicals **253** and **254** should occur (Scheme 6.2). Since there is no obvious reason for the selective formation of **253**, a rapid equilibrium between these two radical species is assumed. Furthermore, a Curtin-Hammett scenario might be operating, in which radical **253** is quenched much faster than its isomer **254**. A potential reason for the more rapid quenching of radical **253** might be an intramolecular H-atom transfer from the N–H amide group or the electron donor substituted C(2)–H. Noteworthy, even though O–H and N–H moieties are known to be poor hydrogen atom donors due to their relatively high bond strength (85-110 kcal/mol for N–H), it has been shown that coordination of a Lewis acid, such as Cp_2TiCl, can convert them into potent donors.[127]

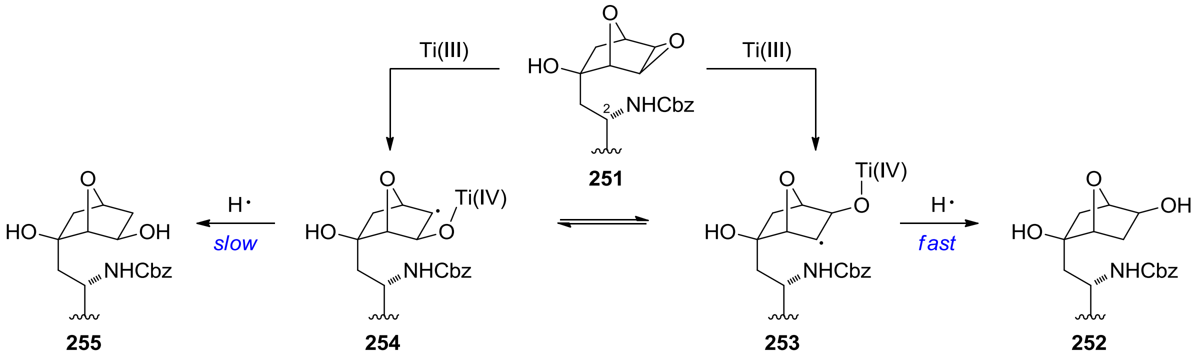

Scheme 6.2: Equilibrium between **253** and **254** proposed by DIETHELM and CARREIRA.

In order to discover the origin of the H-atom, a series of deuteration experiments were performed (Scheme 6.3). When doubly deuterated **256** was employed under the standard reaction conditions, up to 40% deuterium incorporation has been observed. However, in the two other cases shown, in which either deuterated THF or deuterated water were used for the quenching of the reaction mixture, no D-incorporation could be detected. These results suggest that the hydrogen atom is indeed delivered by the carbamate nitrogen.

---

[126] In order to provide a full picture of the investigation of this transformation, the experiments performed and designed by STEFAN DIETHELM during his PhD thesis are shown here. The author of this thesis (C. E.) did not contribute to the results presented in Chapter 6.2. Taken from: S. Diethelm, Diss. ETH No. 21575, pp. 31-47.

[127] a) J. M. Cuerva, A. G. Campana, J. Justicia, A. Rosales, J. L. Oller-Lopez, R. Robles, D. J. Cardenas, E. Bunuel, J. E. Oltra, *Angew. Chem. Int. Ed.* **2006**, *45*, 5522-5526; b) R. E. Estevez, M. Paradas, A. Millan, T. Jimenez, R. Robles, J. M. Cuerva, J. E. Oltra, *J. Org. Chem.* **2008**, *73*, 1616-1619; c) J. Jin, M. Newcomb, *J. Org. Chem.* **2008**, *73*, 7901-7905.

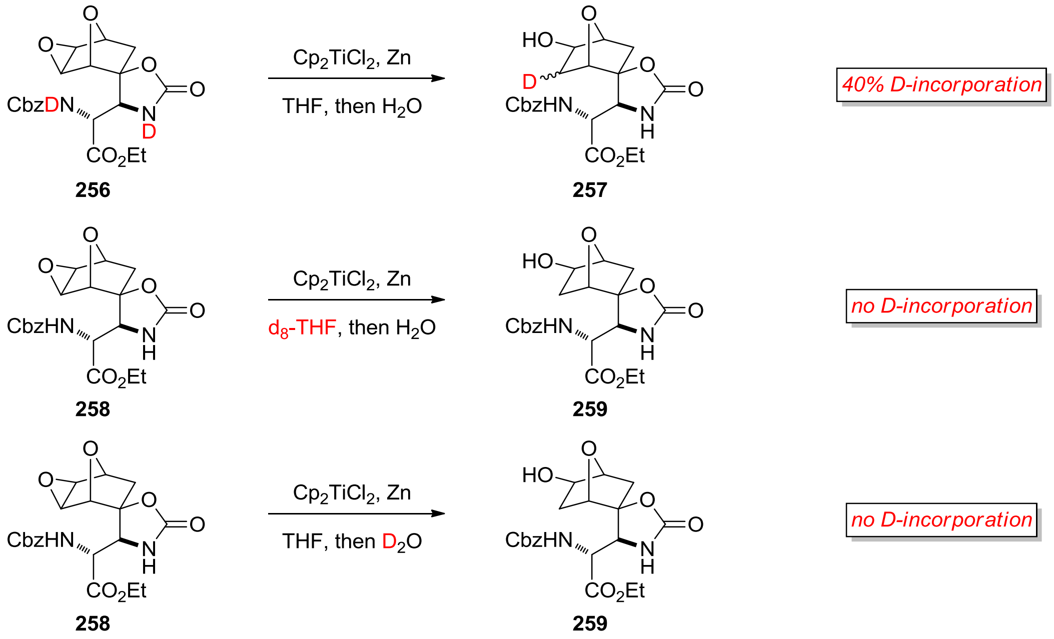
Cp2TiCl2, Zn
THF, then H2O
40% D-incorporation
256
257
Cp2TiCl2, Zn
d8-THF, then H2O
no D-incorporation
258
259
Cp2TiCl2, Zn
THF, then D2O
no D-incorporation
258
259

Scheme 6.3: Deuterium experiments of **256** and **258**.

Interestingly, when epoxide **251** was subjected to Cp_2TiCl without the addition of 1,4-cyclohexadiene, epimerization at C(2) could be observed (Scheme 6.4).

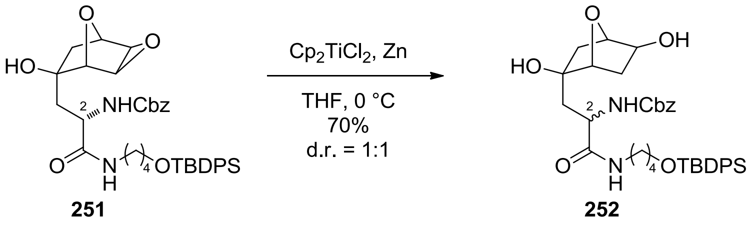
Cp2TiCl2, Zn
THF, 0 °C
70%
d.r. = 1:1
251
252

Scheme 6.4: Epimerization of epoxide **251** at C(2).

In order to test the reason for this epimerization and also exclude the possibility of the C(2)-position to be the origin of the hydrogen atom transferred, another series of deuteration experiments has been performed. At first, N–D deuterated carbamate was employed, without any additives. The observed product displayed a deuterium incorporation of 35% at C(2). When the same epoxide was used in the presence of 100 equivalents of D_2O, 55% D-incorporation was observed. These results indicate that the epimerization event might be a consequence of the H-atom donation from the N–H carbamate. The thus generated N-centered radical might undergo a [1,2]-hydrogen shift to form a radical species at C(2). In addition, this would also explain why the use of an external hydrogen atom donor such as 1,4-cyclohexadiene significantly decreases the epimerization event (d.r. = 12:1, *cf.* Scheme 6.1). Accrodingly, the presence of an excess of hydrogen atom donor quenches the N-centered radical before the hydrogen shift occurs.

Based on the results presented in this chapter, the mechanistic hypothesis shown in Scheme 6.5 is proposed. After Ti(III)-mediated epoxide opening to rapidly equilibrating radicals **253** and **254**, the former suffers from fast intramolecular hydrogen atom transfer from the N–H amide group. If an excess of an external hydrogen atom donor such as 1,4-cyclohexadiene is present, N-centered radical **260** is ultimately quenched to furnish the desired product **252**. However, in the absence of an H-donor, **260** undergoes a [1,2]-hydride shift to C(2)-centered radical **261**, which then leads, after H-donation from THF or a further single electron reduction and proton quench, to epimerization at C(2).

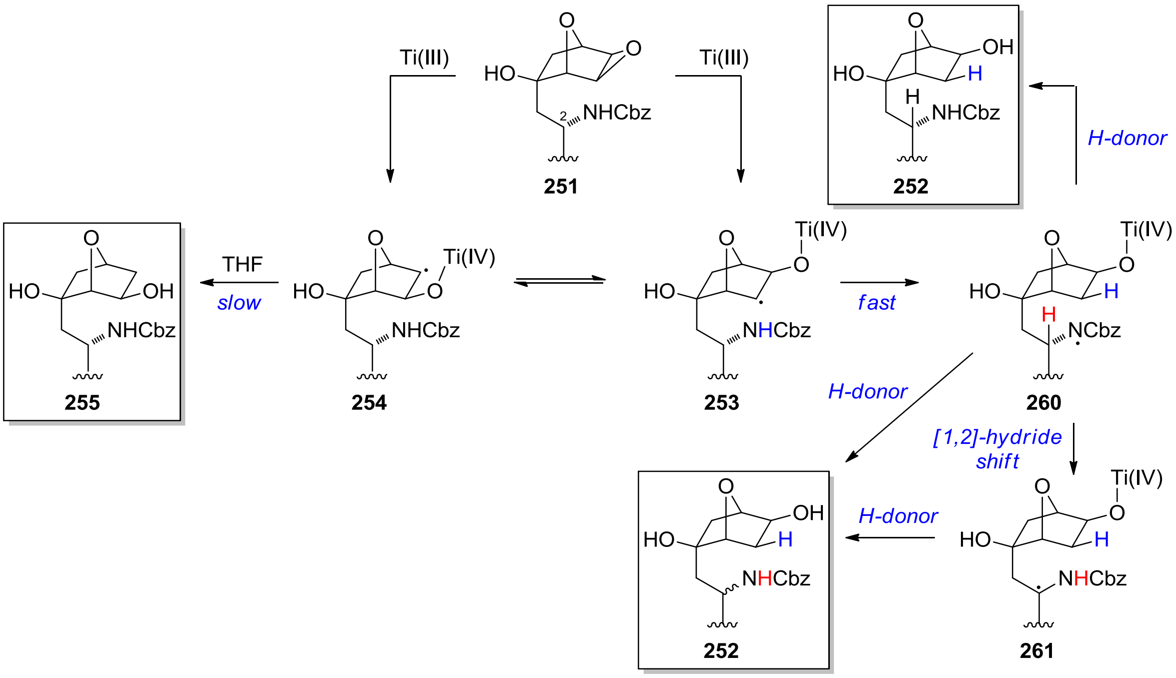

Ti(III)
Ti(III)
HO
O
O
2
NHCbz
251
HO
OH
H
H
NHCbz
252
H-donor
HO
OH
NHCbz
255
THF
slow
HO
Ti(IV)
O
NHCbz
254
HO
Ti(IV)
O
NHCbz
253
fast
HO
Ti(IV)
O
H
H
NCbz
260
H-donor
[1,2]-hydride shift
HO
OH
H
NHCbz
252
H-donor
HO
Ti(IV)
O
H
NHCbz
261

Scheme 6.5: Comprehensive mechanistic hypothesis for the regioselective epoxide opening of **251** by DIETHELM and CARREIRA.

In the light of this mechanistic rationale, this transformation might have a more general applicability for the regioselective opening of 1,2-disubstituted epoxides. As the most commonly employed methods for reductive epoxide openings rely on steric influences (*cf.* Chapter 5.1.1) or on the formation of a more stable radical (*cf.* Chapter 5.1.4), such a transformation would expand the utility of epoxides as precursors for alcohols (Scheme 6.6).

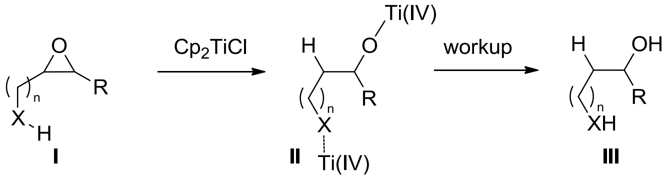

O
n
R
X
H
I
Cp2TiCl
Ti(IV)
H
O
n
R
X
II
Ti(IV)
workup
H
OH
n
R
XH
III

Scheme 6.6: Proposed general regioselective epoxide opening for the generation of alcohols.

7 Results and Discussion

7.1 Substrate Design and Preparation[128]

7.1.1 Acyclic Backbones

In order to design valuable substrates to test the general applicability of this epoxide opening reaction, several requirements needed to be addressed. At first, the X–H donor should be able to efficiently approach the epoxide. Secondly, the two C–O bonds of the epoxide substrates should ideally possess similar electronic and steric environments. The regioselectivity should then be determined by the bias of hydrogen atom transfer to one of the two positions.

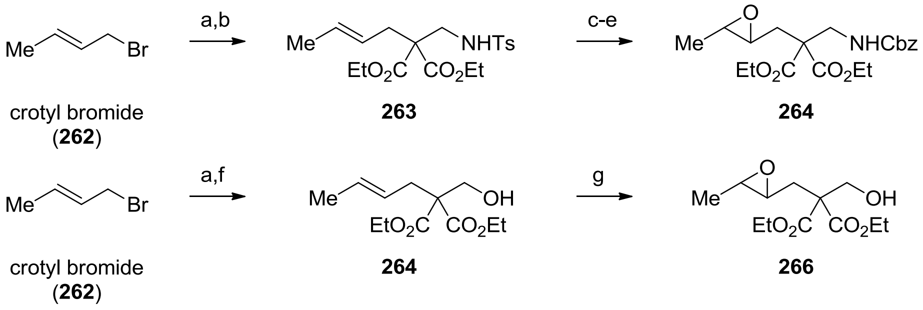

Scheme 7.1: Synthesis of epoxide substrates **264** and **266**. Reagents and conditions: a) diethyl malonate, NaH, THF, 0 °C, 51%; b) $(CH_2O)_n$, $TsNH_2$, DBU, CH_2Cl_2, 61%; c) NaH, CbzCl, THF, 65%; d) Mg, MeOH, ultrasonication, 32%; e) *m*CPBA, CH_2Cl_2, 87%; f) $(CH_2O)_n$, DBU, THF, 61%; g) *m*CPBA, CH_2Cl_2, 22%.

Due to the ease of synthetic access, epoxides with linear backbones were investigated first. We initially prepared *β*-diester **264** in order to later exploit the Thorpe-Ingold effect (Scheme 7.1).[129] Furthermore, to test the hydrogen atom donor ability of hydroxy functionalities, epoxide **266** was synthesized in three steps from crotyl bromide (**262**).

In order to still benefit from the Thorpe-Ingold effect, but also reduce any other functional group interference, *gem*-dimethyl epoxides **271** and **273** were synthesized *via* Horner–Wadsworth–Emmons olefination (Scheme 7.2).

---

[128] Some of the reactions presented in this chapter, were executed by the laboratory-technician trainee ALEXANDRA EBERLE under the supervision of the author of this thesis (C. E.) during her three year apprenticeship.

[129] a) R. M. Beesley, C. K. Ingold, J. F. Thorpe, *J. Chem. Soc.* **1915**, *107*, 1080-1106; b) C. K. Ingold, *J. Chem. Soc.***1921**, *119*, 305-329.

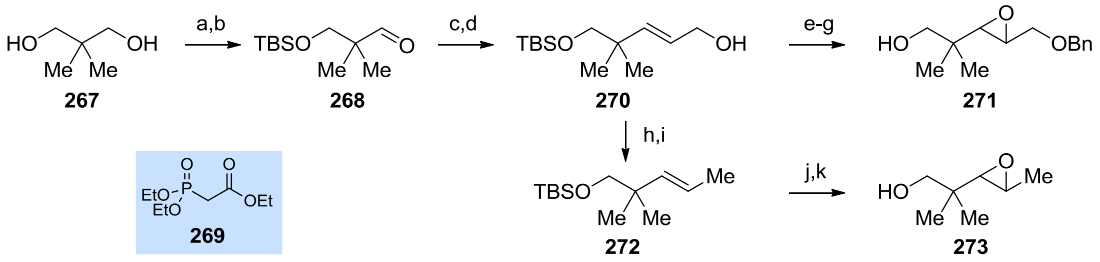

Scheme 7.2: Synthesis of epoxide substrates **271** and **273**. Reagents and conditions: a) TBSCl, imidazole, CH_2Cl_2, 97%; b) SO_3·Py, NEt_3, DMSO, 0 °C, 76%; c) LiCl, **269**, DBU, MeCN, 81%, d) DIBAL, CH_2Cl_2, −78 °C to RT, quant; e) **270**, NaH, THF, then BnBr, reflux, quant; f) *m*CPBA, CH_2Cl_2, 86%; g) TBAF, THF, 91%; h) MsCl, NEt_3, DMAP, CH_2Cl_2, 0 °C, 68%; i) $LiAlH_4$, THF, 87%; j) *m*CPBA, CH_2Cl_2, 71%; k) TBAF, THF, 0 °C, 43%.

7.1.2 Cyclic Backbones

In addition to acyclic substrates, we surmised that a cyclic backbone might entail higher regioselectivities. Not only are these substrates better mimics for epoxide **251**, but also possess a more rigid structure, thus reducing the degrees of freedom of the donating X–H group. Due to the straightforward synthetic accessibility, we anticipated that a cyclohexane backbone might be a good starting point for further investigation. Noteworthy, the envisioned cyclic epoxides bear the advantage of differentiating between *syn*- and *anti*-isomers and testing their potential different behavior in the Ti(III)-mediated reductive epoxide opening.

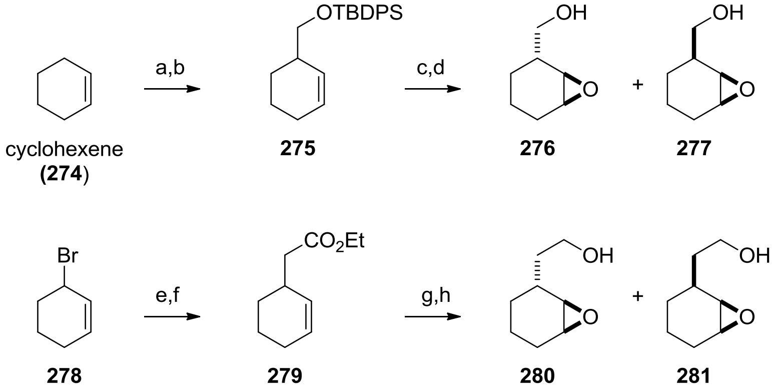

Scheme 7.3: Synthesis of epoxide substrates **276**, **277**, **280** and **281**. Reagents and conditions: a) *n*BuLi, KO*t*Bu, cyclohexene, then $(CH_2O)_n$, 0 °C to 60 °C, 83%; b) TBDPSCl, NEt_3, DMAP, CH_2Cl_2, 94%; c) *m*CPBA, CH_2Cl_2, 21% for the *anti*-isomer, 20% for the *syn*-isomer; d) TBAF, THF, 82% for **276**, 80% for **277**; e) NaH, ethyl malonate, then **278**, 42%; f) LiCl, H_2O, DMSO, 160 °C, 51%; i) $LiAlH_4$, THF, 99%; g) *m*CPBA, CH_2Cl_2, 7% for **280**, 50% for **281**.

Hence, as shown in Scheme 7.3, starting from cyclohexene, *syn*- and *anti*-isomers **276** and **277** could be accessed within four simple steps. Since we also wanted to investigate the influence of the distance of the donating X–H group, *syn*- and *anti*-isomers **280** and **281** were synthesized within four steps from bromocyclohexene **278**.

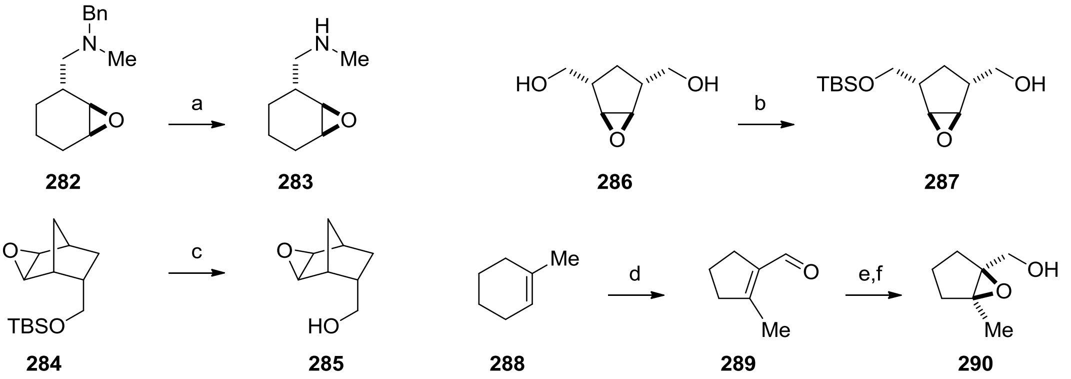

Scheme 7.4: Synthesis of epoxides **283**, **287**, **285** and **290**. Reagents and conditions: a) AcOH, Pd/C (10 mol%), H_2 (1 atm), MeOH, 62%; b) TBSCl, imidazole, DMAP (10 mol%), CH_2Cl_2, 51%; c) TBAF, THF, 0 °C to RT, 71%; d) O_3, CH_2Cl_2, –78 °C, then PPh_3, –78 °C to RT, then F_3CCO_2H, Bn_2NH, CH_2Cl_2, 0 °C to RT, 29%; e) $NaBH_4$, MeOH, 0 °C, 51%; f) *m*CPBA, CH_2Cl_2, 0 °C to RT, 80%.

In order to provide a comparison between O–H and N–H as hydrogen atom donors, epoxyamine **283** was synthesized from literature known amine **282**[130] by hydrogenation (Scheme 7.4). Known silyl ether **284**[131] was deprotected with TBAF to yield hydroxyepoxide **285**. Furthermore, known diol **286**[132] was mono-protected to give **287**. Since it would also be of value to investigate tetrasubstituted epoxides, **290** was synthesized *via* ozonolysis followed by aldol condensation of methyl cyclohexene **288**.

Additionally, as shown in Scheme 7.5 both TBS- and Bn-protected oxabicycles **293** and **295** were prepared within a few steps from diol **291**.[133]

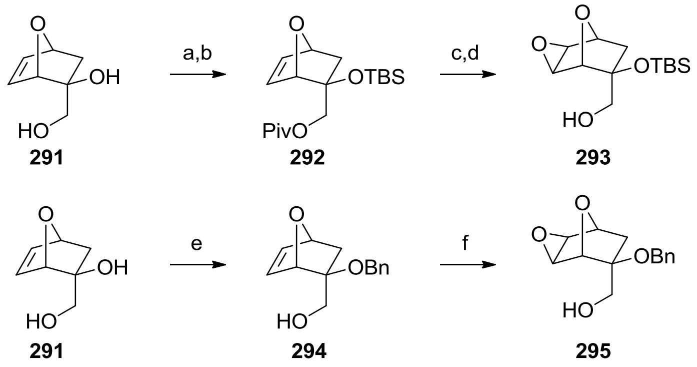

Scheme 7.5: Synthesis of epoxides **293** and **295**. Reagents and conditions: a) PivCl, NEt_3, DMAP (15 mol%), CH_2Cl_2, 93%; b) TBSOTf, 2,6-lutidine, CH_2Cl_2, 0 °C to RT; c) DIBAL, toluene, –78 °C, 74% over two steps; d) *m*CPBA, CH_2Cl_2, yield not determined; e) benzaldehyde dimethyl acetal, CSA (2.5 mol%), CH_2Cl_2, then NEt_3 (3 mol%), then DIBAL, CH_2Cl_2, 0 °C 76%; f) *m*CPBA, CH_2Cl_2, 93%.

---

[130] C. W. Bond, A. J. Cresswell, S. G. Davies, A. M. Fletcher, W. Kurosawa, J. A. Lee, P. M. Roberts, A. J. Russell, A. D. Smith, J. E. Thomson, *J. Org. Chem.* **2009**, *74*, 6735-6748.

[131] P. Mayo, G. Orlova, J. D. Goddard, W. Tam, *J. Org. Chem.* **2001**, *66*, 5182-5191.

[132] M. H. Wu, K. B. Hansen, E. N. Jacobsen, *Angew. Chem. Int. Ed.* **1999**, *38*, 2012-2014.

[133] Substrates **293** and **295** were prepared by HANNES F. ZIPFEL in the course of his PhD thesis. The author of this thesis (C. E.) gratefully acknowledges the generous donation of these samples. For the preparation, see: a) H. F. Zipfel, E. M. Carreira, *Org. Lett.* **2014**, *16*, 2854-2857; b) H. F. Zipfel, E. M. Carreira, *Chem. Eur. J.* **2015**, *21*, 12475-12480; c) H. F. Zipfel, Diss. ETH. No. 23528.

7.2 Exploration of the Substrate Scope

7.2.1 Acyclic Backbones

We commenced the exploration of the scope of the Ti(III)-mediated epoxide opening *via* intramolecular hydrogen atom donation with the testing of linear substrates. The screening was performed using the following standard conditions: syringe pump addition of two equivalents of a 0.2 M solution of freshly prepared Cp_2TiCl solution in THF to a THF solution of the substrate. As shown in Scheme 7.6, subjection of **264** to the standard conditions led to the isolation of alcohols **296** and **297** in a 2:1 ratio and 31% yield.

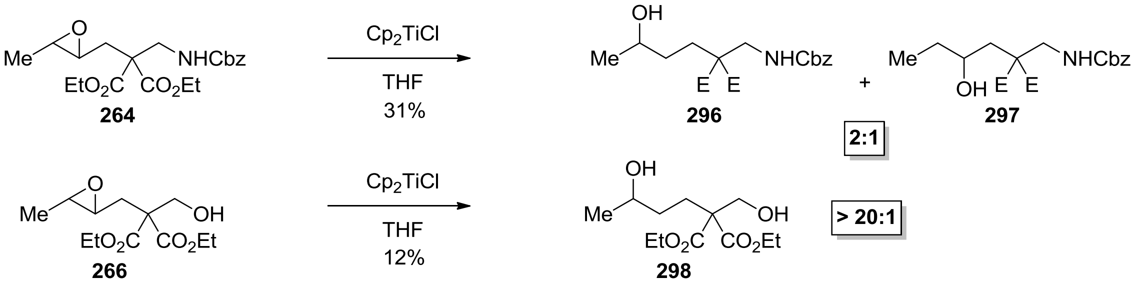

Scheme 7.6: Reductive epoxide opening of **264** and **266**.

In order to compare O–H vs N–H donors, hydroxyepoxide **266** was tested next. Much to our delight, diol **298** was isolated with excellent regioselectivity of >20:1. However, the isolated yield was only 12%. We surmised that a higher degree of preorganization of the substrate might lead to a more efficient H-atom transfer and thus increase the overall yield.

7.2.2 Cyclic Backbones

The first epoxide investigated, equipped with a cyclic backbone, was *anti*-cyclohexene oxide **276**. When exposed to Cp_2TiCl, we were excited to isolate diol **299** in 73% yield along with only 7% of regioisomer **300**. We next elongated the distance of the donating O−H bond by one CH_2 unit. Strikingly, when *syn*-epoxide **281** was used, the regioselectivity dropped drastically to 3:2. Even more peculiar is the full recovery of starting material when *anti*-epoxide **280** or *syn*-epoxide **277** were employed.

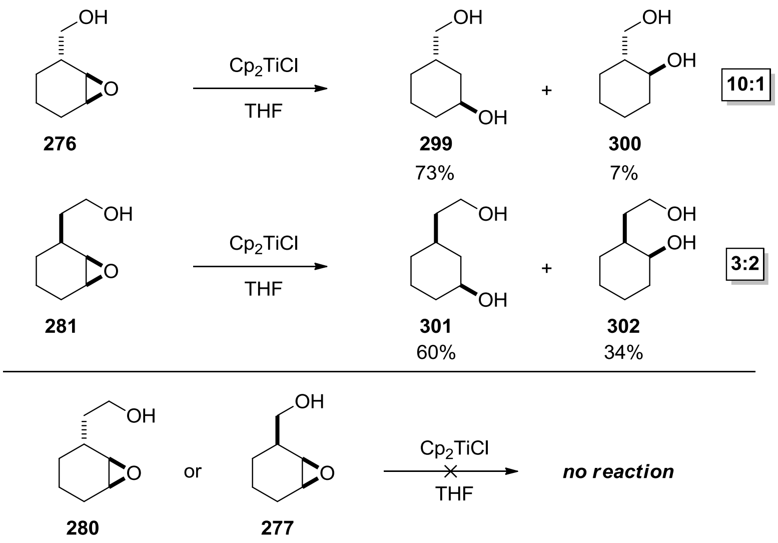

Scheme 7.7: Reductive epoxide opening of **276**, **277**, **280** and **281**.

The complete lack of reactivity of these substrates remains thus far unclear. However, the remarkable selectivity of *anti*-isomer **276** taken together with the absence of selectivity of *syn*-isomer **281** demands for an elaboration of the mechanistic rationale provided in Chapter 6.2 (*cf.* Scheme 6.5).[134] Previous mechanistic investigations of the Ti(III)-mediated epoxide reduction describe the opening as a homolytic substitution at the oxygen atom of the epoxide, in which the incoming titanium reagent displaces a carbon leaving group.[135] Based on the observation above, we speculate that the reductive epoxide opening with intramolecular hydrogen atom donation takes place *via* a S_H2-type mechanism, in which the C–O bond is displaced by an incoming H-atom (Scheme 7.8).[136] Such a mechanistic picture would explain why the reduction of *anti*-epoxide **276** and also microcin SF608 intermediate **251** proceeds with high regioselectivity. If transition state **II** is not adoptable due to geometric constraints, unselective intermolecular H-atom donation by another substrate molecule or THF might occur.

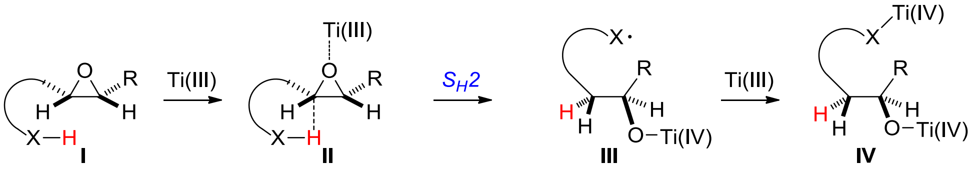

Scheme 7.8: Proposed S_H2 mechanism for the Ti(III)-mediated reductive epoxide opening with intramolecular H-atom donation.

---

[134] Rationalized in collaboration with STEFAN DIETHELM, see also ref. 126.

[135] a) See ref. 126; b) A. Gansäuer, A. Fleckhaus, M. A. Lafont, A. Okkel, K. Kotsis, A. Anoop, F. Neese, *J. Am. Chem. Soc.* **2009**, *131*, 16989-16999.

[136] For reviews, see: a) K. U. Ingold, B. P. Roberts, in *Free Radical Substitution Reactions*, Wiley-Interscience, New York, **1971**; b) C. H. Schiesser, L. M. Wild, *Tetrahedron*, **1996**, *52*, 13265-13314; c) J. C. Walton, *Acc. Chem. Res.* **1998**, *31*, 99-107; For examples of S_H2 reaction at cyclopropanes see: d) J. M. Tedder, J. C. Walton, *Free-Radical Chem.* **1980**, *6*, 155; e) M. Anpo, C. Chatgilialoglu, K. U. Ingold, *J. Org. Chem.* **1983**, *48*, 4104-4106.

After the successful reduction of epoxyalcohol **276**, its methyl amine derivative **283** was employed next. To our delight, the expected amino alcohol **303** was isolated in 89% yield, indicating that amines serve as excellent intramolecular hydrogen atom donors in this reaction (Scheme 7.9). Furthermore, oxabicycle **293** provided diol **304** in 68% isolated yield. Unfortunately, tetrasubstituted epoxide **290** furnished a mixture of various products and the isolation of any of the expected regioisomeric diols was unsuccesful.

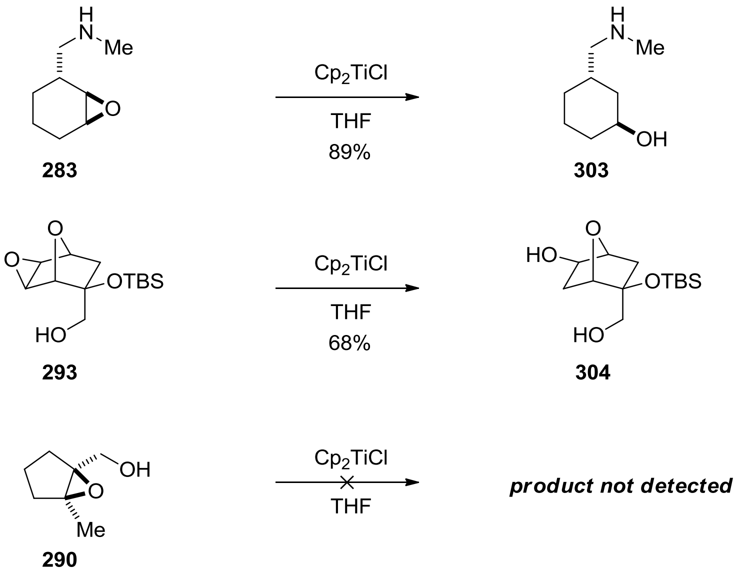

Scheme 7.9: Reductive epoxide opening of **283**, **293** and **290**.

7.2.3 Catalytic Regioselective Reductive Epoxide Opening

Based on the results of GANSÄUER *et al.* presented in Chapter 5.1.4, we surmised that performing this newly developed variant of the Ti(III)-mediated epoxide opening under catalytic conditions would entail several advantages. Not only would the use of 5-10 mol% Cp_2TiCl_2 reduce the overall cost of the reaction, but it would also greatly simplify the reaction setup. Thus far, the air-sensitive Cp_2TiCl solution had to be freshly prepared and added over 6 h *via* syringe pump to the substrate. Instead, a catalytic protocol would only require mixing the substrate, zinc or manganese, the acid additive and titanocene dichloride. Furthermore, we suspected that the presence of two equivalents of Lewis acidic titanium species might trigger side reactions of both substrate and product, which might be minimized by using only catalytic amounts of the titanium complex.

Our screening commenced with the conditions established by GANSÄUER and epoxide **293**, which provided 68% of the desired diol under stoichiometric conditions. In contrast, when using 5 mol% of titanocene dichloride the desired product **304** was isolated in only moderate yield of 41% (Table 7.1, Entry 1). However, increasing the catalyst loading to 15 mol% significantly improved the isolated yield to 83% along with 16% of alkene **305** (Entry 2).

Table 7.1: Catalytic reductive epoxide opening with intramolecular hydrogen atom donation.[a]

Entry	Epoxide	Products	Yield[b]
1[c]	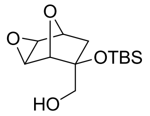 **293**	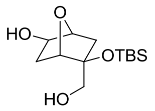 **304**	41%
2	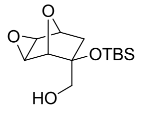 **293**	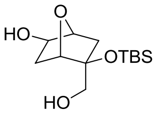 **304** 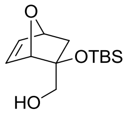 **305**	83% (**304**) 16% (**305**)
3	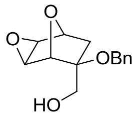 **295**	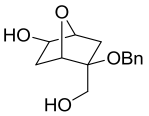 **306** 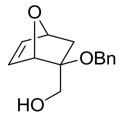 **307**	60% (**306**) 12% (**307**)
4	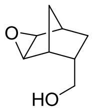 **285**	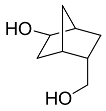 **308**	70%
5	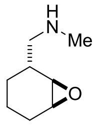 **283**	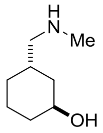 **303**	39%
6	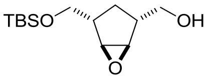 **287**	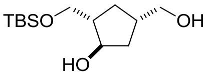 **309** 1:1 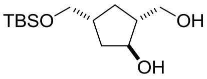 **310**	46%

[a] Standard conditions: Cp_2TiCl_2 (15 mol%), Mn (3 equiv), 2,4,6-collidine·HCl (3 equiv), THF, RT; [b] Isolated yields refer to spectroscopically homogenous material; [c] 5 mol% of Cp_2TiCl_2 were employed.

Next, benzyl protected derivative **295** was tested. As indicated in Entry 3, the desired product **306** could be isolated in 60% yield, along with 10% of its regioisomer and 12% of alkene **307**. We suspect that the benzyl group competes as an intermolecular hydrogen atom donor with the intramolecular donation by the O–H moiety, thus decreasing the selectivity. As displayed in Entry 4, when epoxide **285** was subjected to the catalytic conditions, diol **308** was isolated in 70% yield. Strikingly, amine **283**, which provided 89% of product **303** under stoichiometric conditions, gave only 39% yield under catalytic conditions (Entry 5). It can be hypothesized that coordination of the amino group to any catalytically active titanium species inhibits an efficient catalytic cycle. Silyl ether **287** produced a 1:1 mixture of regioisomeric products **309** and **310**. However, we believe that the complete absence of selectivity originates from migration of the TBS group during the course of the reaction.

8 Conclusion

In summary, our investigation of the Ti(III)-mediated regioselective epoxide opening reaction with intramolecular hydrogen atom transfer provided valuable mechanistic insight. The formation of a single regioisomer of the epoxide opening in microcin SF608 (*cf.* Chapter 6.1) demanded for revision of the mechanistic picture provided by RAJANBABU (Scheme 8.1, A). Employing deuterium labeled epoxide substrates, it could be shown, that an intramolecular hydrogen atom transfer from a neighbouring N–H moiety takes place (Scheme 8.1, B). Furthermore, when *syn*- and *anti*-substrates **276** and **281** were employed, the mechanistic rationale had to be further altered (Scheme 8.1, C). While *anti* **276** provided diol **299** with excellent regioselectivity *syn* **281** showed no significant selectivity. Based on this result, we surmised that the reduction occurs *via* a S_H2 mechanism (Scheme 8.1, D). Thus, the first step is proposed to be a displacement of the C–O epoxide bond by intramolecular hydrogen atom transfer (**XII** → **XIII** Scheme 8.1, D), rather than formation of radicals **VII** and **VIII** (Scheme 8.1, B).

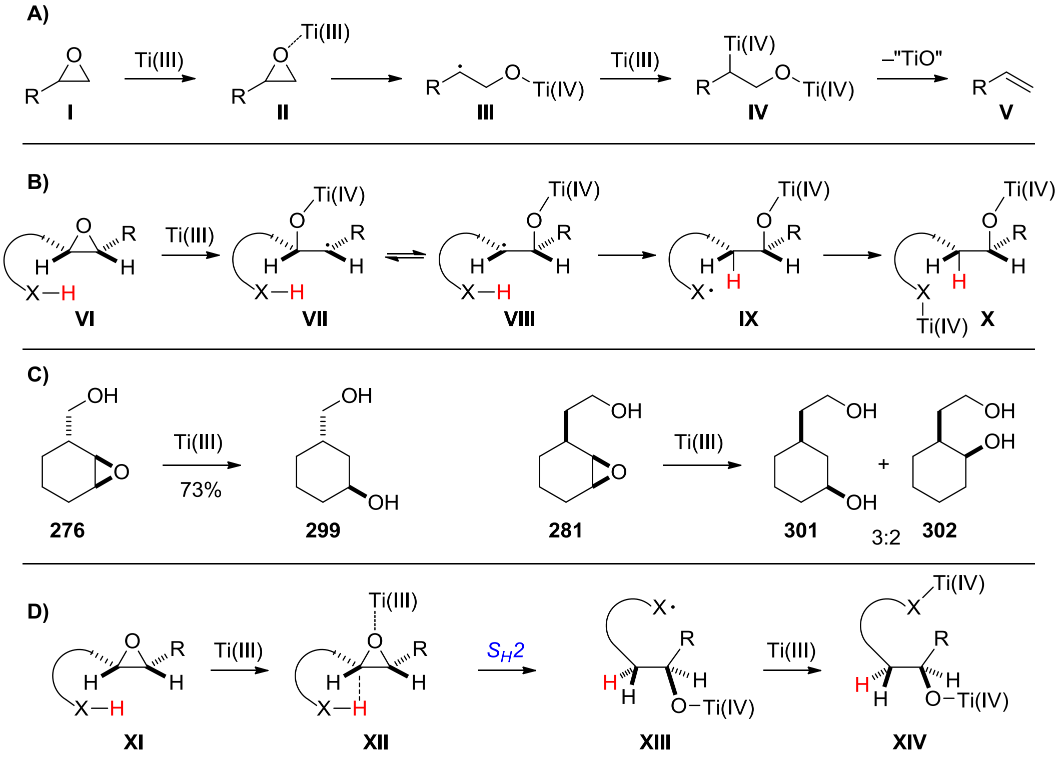

Scheme 8.1: A) Ti(III)-mediated epoxide opening by RAJANBABU and NUGENT; B) Mechanistic rationale for the regioselectivity observed in the Ti(III)-mediated epoxide opening in the total synthesis of microcin SF608; C) Reductive epoxide opening of **276** and **281**; D) S_H2 mechanism to explain the difference of *syn* **276** and *anti* **281**.

Furthermore, we were able to apply GANSÄUER's catalytic conditions to our sytem. However, while alcohols underwent the desired reductive epoxide opening without difficulties, it should be noted that free amines seem to interject the catalytic cycle by coordination to any catalytically active titanium species. When we investigated the general applicability of this reaction, we observed several restrictions. Firstly, the substrate must possess some preorganized backbone to ensure a beneficial reaction pathway. Accordingly, the substrates investigated endowed with linear backbones did not produce the desired products in synthetically useful yields. Furthermore, the geometrical requirement of *anti*-relationship between the epoxide and the donating protic X–H (X = N, O) moiety significantly restricts the substrate selection.

Part III

Synthesis of Raman-Active Epoxyisoprostane Analogs

9 Introduction[137]

9.1 Investigation of the Role of Oxidized Phospholipids in Inflammatory Diseases

Oxidized phospholipids (OxPLs) are important bioactive compounds, which are produced in humans and other organisms upon exposure of biological membranes to reactive oxygen species.[138] However, these intriguing human derived natural products do not simply represent mere byproducts of lipid oxidation, but instead have been recognized as active compounds in inflammation.[139] Intriguingly, while the majority of literature reports suggest pro-inflammatory effects for several oxidized phospholipids,[140] conflicting observations establish anti-inflammatory behavior.[141] A possible explanation for this discrepancy is the experimental design. As it is common practice, a phospholipid precursor is chemically oxidized by various transition metal salts. Cells are then exposed to the thus generated mixture of oxidized phospholipids *in vitro* and *in vivo*. However, the composition of this mixture is highly dependent on the oxidant employed.[142] Hence, a possible circumvention of this problem might be to perform the biological assays with defined pure compounds instead of a composition of oxidized phospholipids. Since the separation and isolation of single compounds from an oxidized mixture of phospholipids is tedious, divergent chemical synthesis might provide an efficient alternative.

9.1.1 Total Syntheses of Epoxyisoprostanes

Recently, our group started a fruitful collaboration with M. KOPF to gain insights into the inflammatory activity of oxidized phospholipids **311-314** (Figure 9.1).[143] Noteworthy, several previous studies associated mixtures of OxPLs with pro-inflammatory activity in rheumatic arthritis,[144] emphysema[145] and atherosclerosis.[146] Hence, in order to perform a reliable biological assay with single compounds, a flexible synthetic strategy was devised.[147]

---

[137] For an excellent introduction into prostaglandins and isoprostanes see J. Egger, Diss. ETH No. 21363.

[138] a) N. Leitinger *et al., J. Immunol.* **2005**, *175*, 501-508; b) U. Jahn, J.-M. Galano, T. Durand, *Angew. Chem. Int. Ed.* **2008**, *47*, 5894-5955.

[139] a) J. A. Berliner, A. D. Watson, *N. Engl. J. Med.* **2005**, *353*, 9-11; b) V. N. Bochkov, A. Kadl, J. Huber, F. Gruber, B. R. Binder, N. Leitinger, *Nature* **2002**, *419*, 77-81; c) S. Lee, K. G. Birukov, C. E. Romanoski, J. R. Springstead, A. J. Lusis, J. A Berliner, *Circ. Res.* **2012**, *111*, 778-799.

[140] a) Y. Imai *et al., Cell* **2008**, *133*, 235-249; b) T. A. Seimon *et al*., *Cell Metab.* **2010**, *12*, 467-482; c) C. R. Stewart *et al., Nat. Immunol.* **2010**, *11*, 155-161.

[141] a) V. N. Bochkov, O. V. Oskolkova, K. G. Birukov, A.-L. Levonen, C. J. Binder, J. Söckl, *Antioxid. Redox Signal.* **2010**, *12*, 1009-1059; b) S. Knapp, U. Matt, N. Leitinger, T. van der Poll, *J. Immunol.* **2007**, *178*, 993-1001.

[142] P. Bretscher, J. Egger, A. Shamshiev, M. Trotzmuller, H. Kofeler, E. M. Carreira, M. Kopf, S. Freigang, *Embo Mol. Med.* **2015**, *7*, 593-607.

[143] a) J. Egger, P. Bretscher, S. Freigang, M. Kopf, E. M. Carreira, *Angew. Chem. Int. Ed.* **2013**, *52*, 5382-5385; b) J. Egger, P. Bretscher, S. Freigang, M. Kopf, E. M. Carreira, *J. Am. Chem. Soc.* **2014**, *136*, 17382-17385; c) J. Egger, S. Fischer, P. Bretscher, S. Freigang, M. Kopf, E. M. Carreira, *Org. Lett.* **2015**, *17*, 4340-4343; d) see also ref. 142.

[144] a) N. Leitinger, *Subcell Biochem.* **2008**, *49*, 325-350; b) I. Levitan, S. Volkov, P. V. Subbaiah, *Antioxid. Redox Signal.* **2010**, *13*, 39-75.

[145] J. C. Ullery, L. J. Marnett, *Biochim. Biophys. Acta Biomembr.* **2012**, *181*, 2424-2435.

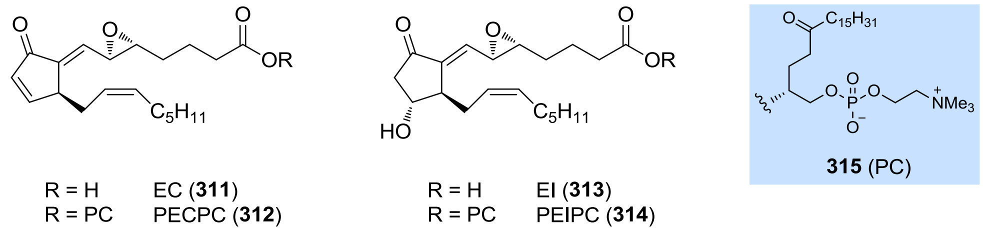

Figure 9.1: Structures of EC (**311**), PECPC (**312**), EI (**313**) and PEIPC (**314**).

As presented in Scheme 9.1, the epoxide side chain was envisioned to be introduced by a late-stage aldol condensation between cyclopentenone **316** and aldehyde **317**. While the latter would be easily accessible in enantiomerically pure form *via* Jørgensen epoxidation from the corresponding enal,[148] the cyclopentenone would arise from homoallylic C–H insertion and subsequent elimination of β-ketoester **318**.

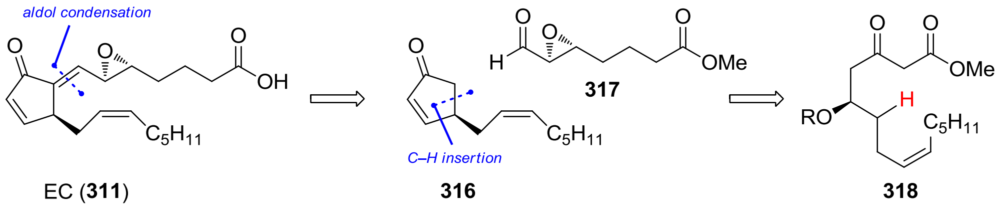

Scheme 9.1: Retrosynthetic analysis of EC (**311**).

According to this plan, the synthesis commenced with the exposure of (*Z*)-decenal **319** to ketene and TMS-protected quinidine **321** under the conditions described by NELSON and co-workers to give β-lactone **320** in 62% yield and 92% *ee* (Scheme 9.2).[149] Opening of the latter with the lithium enolate of methyl acetate, Regitz diazo transfer and subsequent protection provided diazoketoester **322** in 73% overall yield.

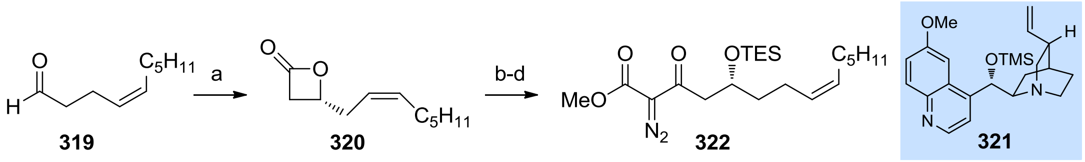

Scheme 9.2: Synthesis of C–H insertion precursor **322**. Reagents and conditions: a) $LiClO_4$, **321** (12 mol%), $i$$Pr_2NEt$, AcCl, CH_2Cl_2–Et_2O (2:1), –78 °C, 62%, 92% *ee*; b) $i$$Pr_2NLi$, MeOAc, THF, –78 °C, then **320**, 77%; c) *p*-ABSA, NEt_3, MeCN, 0 °C to RT 97%; d) TESCl, imidazole, DMF, 0 °C to RT, 98%.

---

[146] a) N. Leitinger, *Mol. Nutr. Food Res.* **2005**, *49*, 1063-1071; b) M. Navab *et al., J. Lipid Res.* **2004**, *45*, 993-1007; c) J. A. Berliner, N. Leitinger, S. Tsimikas, *J. Lipid Res.* **2009**, *50*, 207-212; d) J. A. Berliner, A. D. Watson, *N. Engl. J. Med.* **2005**, *353*, 8-11; e) N. Leitinger *et al., Arterioscler. Thromb. Vasc. Biol.* **2005**, *25*, 633-638; f) A. D. Watson, N. Leitinger, M. Fogelman, J. A. Berliner, *J. Biol. Chem.* **1997**, *272*, 13597-13607; g) A. D. Watson, G. Subbanagounder, D. S. Welsbie, K. F. Faull, N. Navab, M . E. Jung, A. Fogelman, J. A. Berliner, *J. Biol. Chem.* **1999**, *274*, 24787-24798.

[147] For a detailed description and previous total syntheses see ref. 137 and ref. 143a).

[148] M. Marigo, J. Franzén, T. B. Poulsen, W. Zhuang, K. A. Jørgensen, *J. Am. Chem. Soc.* **2005**, *127*, 6964-6965.

[149] C. Zhu, X. Shen, S. G. Nelson, *J. Am. Chem. Soc.* **2004**, *126*, 5352-5253.

The key homoallylic C–H insertion was tackled next. Importantly, several issues needed to be addressed. At the outset of this project it was not clear, whether the desired C–H insertion would have to compete against a potentially possible intramolecular cyclopropanation. Furthermore, the diastereoselectivity of the insertion process needed to be controlled by either the substrate or the catalyst. In an initial attempt, **322** was exposed to $Rh_2(OAc)_4$, providing the cyclization product **324** in 81% yield as a 4:1 mixture favoring the desired *syn* product. The selectivity could be substantially improved by employing bulkier rhodium catalysts. Thus, the use of $Rh_2(esp)_2$ gave a ratio of 6:1, whereas Rh_2(*S*-PTAD)$_4$ (**323**) furnished the desired product in 71% yield with a diastereomeric ratio of 9:1 (Scheme 9.3). Subsequent Krapcho decarboxylation and elimination provided cyclopentenone **316** in 60% yield.

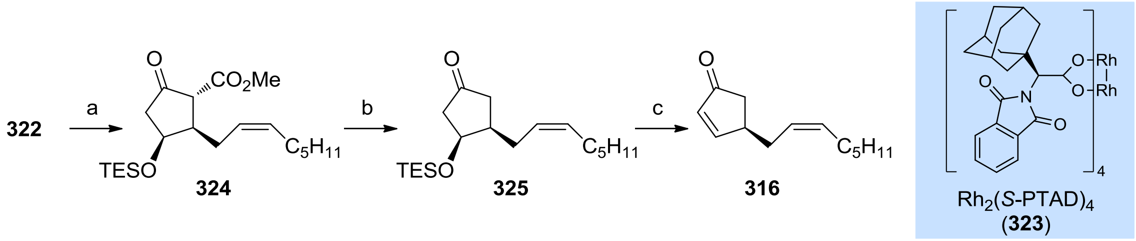

Scheme 9.3: Synthesis of cyclopentenone **316**. Reagents and conditions: a) Rh_2(*S*-PTAD)$_4$ (1.0 mol%), CH_2Cl_2, reflux, 71%, d.r. = 9:1; b) NaCl, DMSO, 140 °C, 65%; c) DBU, CH_2Cl_2, 0 °C, 93%.

As presented in Scheme 9.4 the epoxy-sidechain **317** was smoothly generated from cyclopentene (**326**) *via* ozonolysis, Wittig olefination and Jørgensen epoxidation in 28% yield over three steps and 92% *ee*. The union of the two fragments **316** and **317** by an aldol condensation furnished ester **328** in 64% yield.

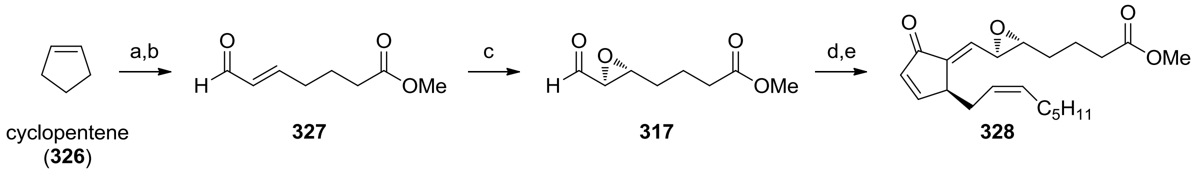

Scheme 9.4: Synthesis of ester **328**. Reagents and conditions: a) O_3, $NaHCO_3$, CH_2Cl_2–MeOH (5:1), –78 °C, then NEt_3, Ac_2O, C_6H_6, 0 °C; b) $Ph_3PCHCHO$, toluene, 70 °C, 55%, d.r. = 5:1, 55% over two steps; c) H_2O_2, (*S*)-2-(diphenyl[(trimethylsilyl)oxy]methyl)pyrrolidine (10 mol%), CH_2Cl_2, 51%, 92% *ee*; d) $LiN(TMS)_2$, **316**, THF, –78 °C, then **317**, THF, –78 °C; e) MsCl, NEt_3, CH_2Cl_2, –78 °C, then Al_2O_3, RT, 64% over two steps.

Finally, ester **328** was enzymatically hydrolyzed to provide EC (**311**) in 70% yield (Scheme 9.5). EC was then coupled with lyso-PC under Yamaguchi's conditions to furnish PECPC (**312**). Furthermore, the missing alcohol functionality in EI (**313**) and PEIPC (**314**) was introduced *via* nucleophilic epoxidation followed by SmI_2-mediated epoxide opening.

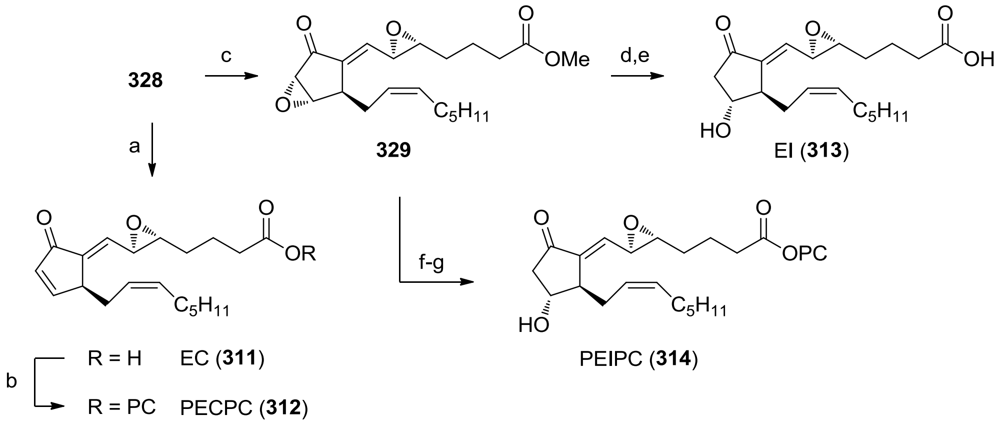

Scheme 9.5: Synthesis of EC, PECPC, EI and PEICP. Reagents and conditions: a) Novozyme, THF–buffer (aqueous, pH 7) (1:4), 70%; b) 2,4,6-$Cl_3C_6H_2COCl$, DMAP, lyso-PC, $CHCl_3$, 69%; c) *t*BuOOH, DBU, THF, 0 °C, 74%; d) SmI_2, THF–MeOH (4:1), –90 °C, 54%; e) Novozyme, THF–buffer (aqueous, pH 7) (1:4), 60%; f) Novozyme, THF–buffer (aqueous, pH 7) (1:4), 74%; g) 2,4,6-$Cl_3C_6H_2COCl$, DMAP, lyso-PC, $CHCl_3$, 69%; h) SmI_2, THF–MeOH (4:1), –90 °C, 43%.

Intriguingly, upon prolonged exposure of EC (**311**) to silica gel varying amounts of a byproduct were observed. Thus, EC was dissolved in $CHCl_3$ and silica gel was added (Scheme 9.6). After 3 hours, the conversion was complete and lactone **330** (CycloEC) could be isolated in 65% yield.[143b)] For the purpose of a complete biological screening (*vide infra*), lactone **330** was further converted into diol **331**.

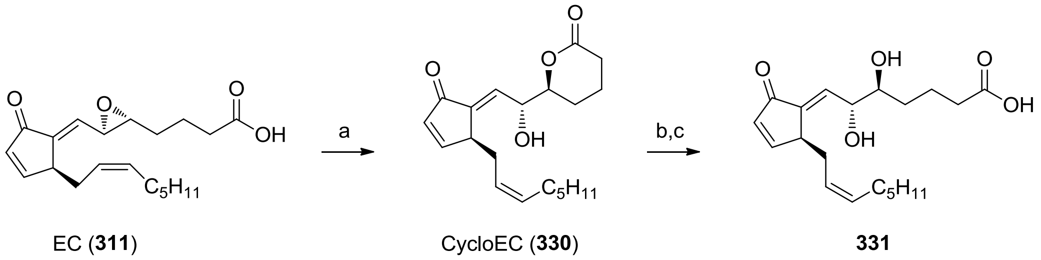

Scheme 9.6: Silica-mediated lactone formation of EC (**311**) to CycloEC (**330**). Reagents and conditions: a) SiO_2, $CHCl_3$, 65%; b) K_2CO_3, MeOH; c) Novozyme, THF–buffer (aqueous, pH 7) (1:4), 30% over two steps.

9.1.2 Biological Testing

Next, the inflammatory effects of isoprostanoids **311** and **313** as well as of their phosphatidylcholine derivatives **312** and **314** were investigated. At first, bone-marrow derived dendritic cells (BMDCs) were exposed to **311-314** in Fetal Bovine Serum (FBS)-supplemented RPMI (Roswell Park Memorial Institute) medium for one hour. After washing, the cells were stimulated for 18 hours with Toll-like receptor ligand R837 (5 µg/mL) in order to induce cytokine secretion. Surprisingly, even though previous studies described these compounds as pro-inflammatory, a dose-dependent decrease in the secretion of pro-inflammatory cytokines IL-6 and IL-12 was observed. In addition, the free acids EC (**311**) and

EI (**313**) showed significantly stronger effects than their phosphatidylcholine counterparts PECPC (**312**) and PEICP (**314**). The comparison between EC (**311**), equipped with an enone functionality, and EI (**313**), possessing a free hydroxy group, indicates a stronger anti-inflammatory effect for the enone.

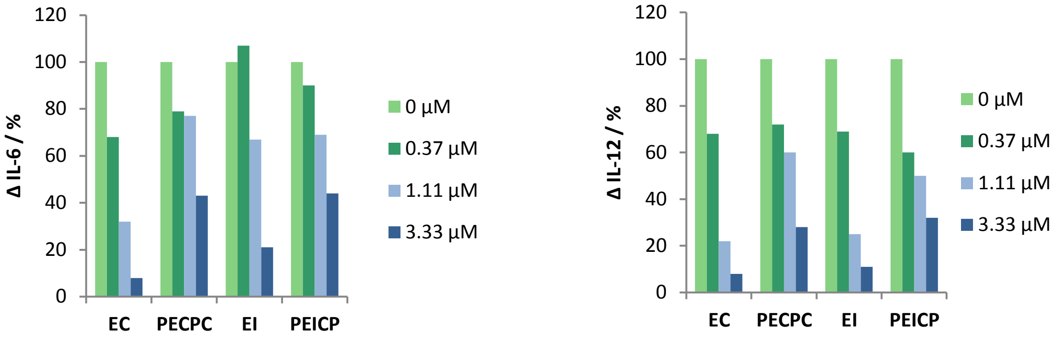

Chart 9.1: IL-6 (left) and IL-12 (right) production by BMDCs exposed to synthetic EC (**311**), PECPC (**312**), EI (**313**) and PEICP (**314**). For PEICP higher concentrations were used: 0, 1.52, 3.04 and 6.07 µM. Data is normalized to the negative control (0 µM). IL-6 and IL-12 levels in the supernatants were determined by ELISA.

Evaluation of lactone **330** (CycloEC) and diol **331** showed a remarkable result. While the diol was considerable less active than EC, **330** exhibits the strongest effect of all compounds investigated to date with regard to inhibition of pro-inflammatory IL-6 and IL-12 secretion (Chart 9.2 and Chart 9.3). Since the large concentration intervals employed in Chart 9.1 only led to three data points until the cytotoxic concentration was reached, a series with smaller intervals was performed.

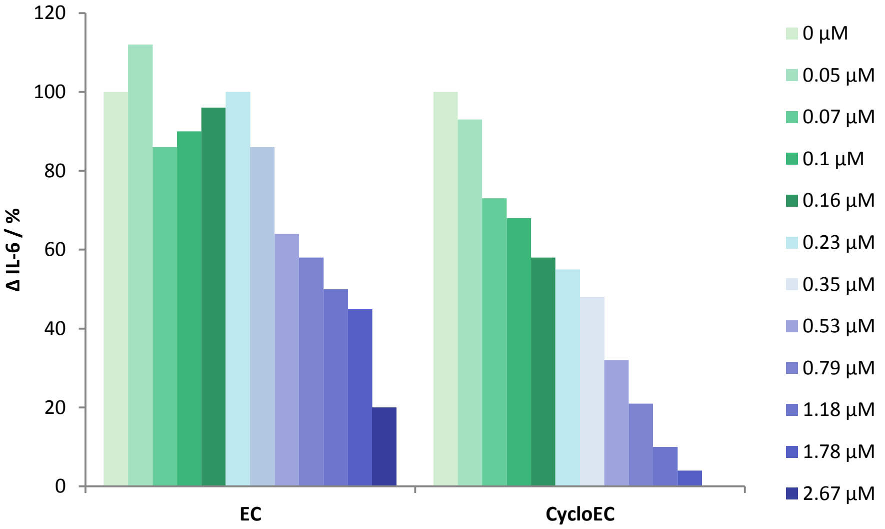

Chart 9.2: IL-6 production by BMDCs exposed to EC (**311**) and CycloEC (**330**).

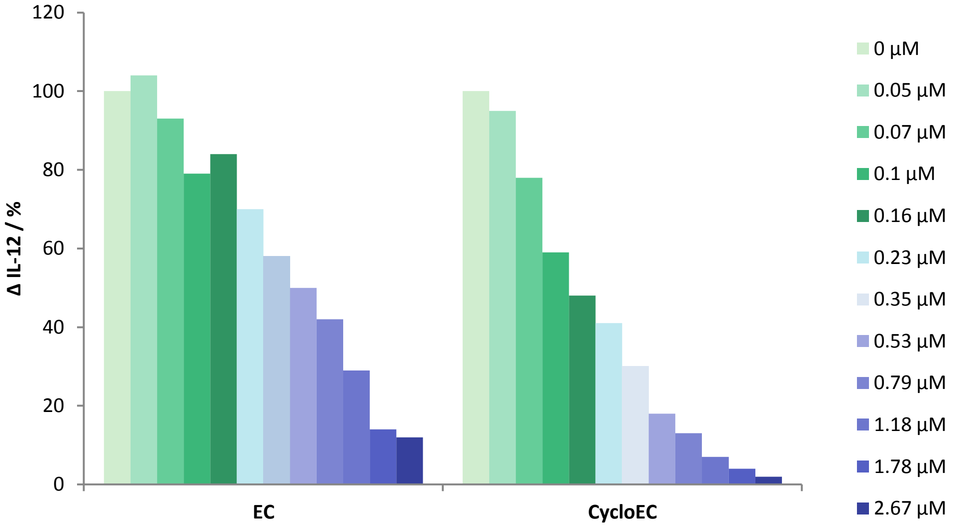

Chart 9.3: IL-12 production by BMDCs exposed to EC (**311**) and CycloEC (**330**).

9.1.3 Conclusion

In summary, a short and divergent total synthesis towards epoxyisoprostanes has been devised. The synthetic strategy relies on an enantioselective formal [2+2] reaction between ketene and aldehyde **319** as well as a chemo- and diastereoselective homoallylic C–H insertion reaction to construct the cyclopentane core of this class of human derived natural products. Furthermore, biological assays revealed that these compounds do not act as pro-inflammatory agents, but possess anti-inflammatory activity with varying efficiency. It could be shown that the free acids EC (**311**) and EI (**313**) are more potent than their phosphatidylcholine derivatives PECPC (**312**) and PEICP (**314**). While EC possesses a higher anti-inflammatory activity than the hydroxylated EI, it could be shown that the coincidentally synthesized CycloEC (**330**) not only displays a remarkably higher activity than EC, but also elicits the strongest effect of all derivatives examined to date.

10 Aim of the Project

10.1 Mode of Action of EC and CycloEC

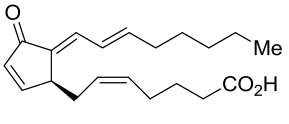

15d-PGJ2 (**332**)

Figure 10.1: Structure of 15d-PGJ2 (**332**).

The recently discovered cyclopentenone prostaglandin 15d-PGJ2 (**332**) has received considerable interest due to its high biological activity in the modulation of inflammatory and apoptotic processes (Figure 10.1).[150] Biological assays identified 15d-PGJ2 as an anti-inflammatory prostaglandin.[151] This effect has been reported to be mediated by interaction with the nuclear hormone receptor peroxisome proliferator-activated receptor-gamma (PPAR-γ) as well as with the transcription factor Nrf2.[152] Due to the structural similarity between 15d-PGJ2 (**332**) and EC (**311**), PRETSCHER *et al.* presumed that both molecules might induce their anti-inflammatory effects by activating similar reaction pathways. Indeed, their detailed study, could not only validate this hypothesis, but also identify Nrf2 as the only mediator of anti-inflammatory response. While removal of PPAR-γ in gene deficient BMDC did not induce any change in the oxidized phospholipid-mediated inhibition of IL-12 production, the bioactivity of EC and 15d-PGJ2 was shut down in the absence of Nrf2.[152] As shown in Figure 10.2, under normal (unstressed) conditions, Nrf2 is kept in the cytoplasm by the protein cluster Kelch-like ECH-associated protein 1 (Keap1). Keap1 anchores Nrf2 and facilitates its ubiquitination and subsequent proteolysis. However under stressed conditions, cysteine alkylation leads to liberation of Nrf2, which then translocates in the nucleus to promote the expression of various antioxidative genes and proteins.[153]

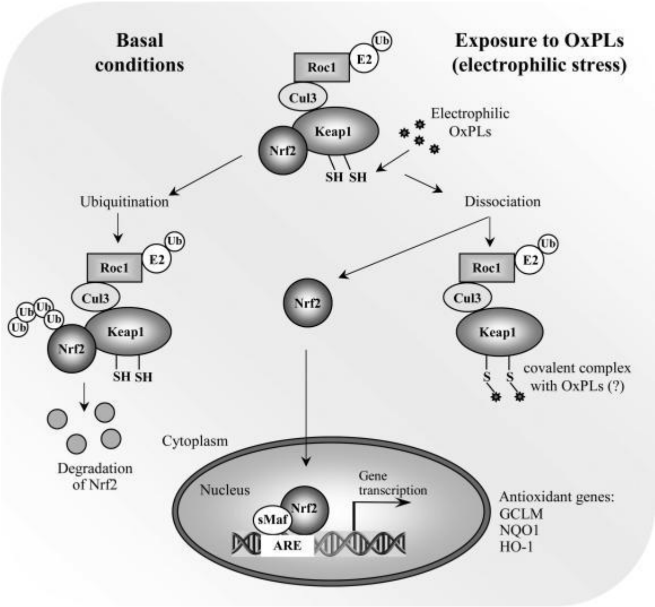
Basal conditions
Exposure to OxPLs (electrophilic stress)
Ub
E2
Roc1
Cul3
Keap1
Nrf2
SH SH
Electrophilic OxPLs
Ubiquitination
Dissociation
Ub
E2
Roc1
Cul3
Ub Ub Ub Ub
Nrf2
Keap1
SH SH
Nrf2
Ub
E2
Roc1
Cul3
Keap1
S S
covalent complex with OxPLs (?)
Degradation of Nrf2
Cytoplasm
Nucleus
Gene transcription
sMaf
Nrf2
ARE
Antioxidant genes:
GCLM
NQO1
HO-1

Figure 10.2: Keap1/Nrf2 pathway induced by OxPLs under oxidative stress (right) and degradation of Nrf2 under unstressed conditions (left). Taken with permission from reference 153 d).

---

[150] a) See J. Egger, Diss. ETH No. 21363, p.7; b) F. A. Fitzpatrick, M. A. Wynalda, *J. Biol. Chem.* **1983**, *258*, 11713-11718.

[151] J. U. Scher, M. H. Pilliger, *Clin. Immunol.* **2005**, *114*, 100-109.

[152] See ref. 142.

[153] a) T. Yamamoto, T. Suzuki, A. Kobayashi, J. Wakabayashi, J. Maher, H. Motohashi, M. Yamamoto, *Mol. Cell. Biol.* **2008**, *28*, 2758-2770; b) K. R. Sekhar, G. Rachakonda, M. L. Freeman, *Toxicol. Appl. Pharmacol.* **2010**, *244*, 21-26; c) K. Itoh, T. Chiba, S. Takahashi, T.

10.2 Imaging of Alkyne-Tagged Biomolecules in Living Cells by Raman Spectroscopy

Raman as well as infrared spectroscopy are two orthogal spectroscopical methods, which are widely used to analyze structural elements of chemical substrates.[154] While IR spectroscopy relies on the detection of a change in the dipole moment caused by irradiation, the Raman scattering process, discovered by C. V. RAMAN in 1928, arises from changes in the polarizability of a vibrating molecule. While the majority of the incident photons do not couple with vibrational excitation, the scattered photons possess the same energy as the incident photons (Raleigh scattering). Nevertheless, if an incoming photon triggers a polarization, which couples with vibrational excitation, inelastic scattering occurs (Raman scattering). The Raman scattering requires a change in polarizability of a chemical bond in such a way that there is a distortion in the electron density around the vibrating nuclei. Hence, molecules containing multiple bonds, e.g. alkynes, nitriles, olefins and carbonyls, are highly suitable substrates for Raman spectroscopy. This so-called spontaneous Raman spectroscopy has already been employed in 1990 by PUPPELS *et al.* for the measurement of living cells and chromosomes.[155] In the following years, alkynes have gained considerable attention as markers for drugs and active agents in the pharmaceutical and agrochemical field due to several notable advantages. Firstly, alkynes possess a very sharp and intense Raman peak at around 2125 cm^{-1} (the intensity of an alkyne Raman peak is about 40 x higher than the popular carbon-deuterium peak). Strikingly, the spectroscopic area of 1800 – 2800 cm^{-1} does not show any contribution of cellular components, thus no overlapping background signals impair the measurement. Secondly, in contrast to commonly employed bulky fluorescent tags, which often alter the biochemical properties of small molecules, alkynes are small and under physiological conditions relatively inert chemical moieties. However, despite these favorable attributes, major challenges are associated with the imaging of living cells *via* spontaneous Raman spectroscopy. The process possesses an extremely small scattering cross section ($\sigma = 10^{-30}\ \mathrm{cm}^2$) compared to fluorescence ($\sigma = 10^{-16}\ \mathrm{cm}^2$) and thus limits the speed of acquisition. Additionally, most of the interesting bioactive small molecules accumulate in intracellular concentrations, which are too low for spontaneous Raman spectroscopy. Thus, recording spectra at physiologically and biologically relevant concentrations is often precluded.

Ishii, K. Igarashi, Y. Katoh, T. Oyake, N. Hayashi, K. Satoh, I. Hatayama, M. Yamamoto, Y. Nabeshima, *Biochem. Biophys. Res. Commun.* **1997**, *236*, 313-322; d) V. N. Bochkov, O. V. Oskolkova, K. G. Birukov, A. L. Levonen, C. J. Binder, J. Stockl, *Antiox. Redox. Signal.* **2010**, *12*, 1009-1059.

[154] For an excellent review of Raman spectroscopy in drug discovery see: W. J. Tipping, M. Lee, A. Serrels, V. G. Brunton, A. N. Hulme, *Chem. Soc. Rev.* **2016**, *45*, 2075-2089.

[155] G. J. Puppels, F. F. M. de Mul, C. Otto, J. Greve, M. Robert-Nicoud, D. J. Arndt-Jovin, T. M. Jovin, *Nature* **1990**, *347*, 301-303.

Fortunately, several strategies and advances have been devised to overcome these problems. One of the major achievements was the development of the stimulated Raman spectroscopy (SRS). This method generates the signals by co-alignment of two beams, the Stokes and the pump beam. These beams differ in the energy Ω, which matches the molecular vibration of the chemical moiety (for an alkyne tag $\Omega = 2125\ \text{cm}^{-1}$), thus accelerating their vibrational excitation. As a consequence, a stimulated Raman excitation of this vibration occurs, which causes an intensity loss of the pump beam and an intensity gain of the Stokes beam. This change can then be measured and used to generate an image. Importantly, SRS increases the vibrational excitation by seven orders of magnitude over spontaneous Raman spectroscopy. Furthermore, when Ω does not match a modular vibration of the sample, no signal is detected. Thus, no non-resonant background signals are observed. In an impressive study, MIN and co-workers employed the stimulated Raman spectroscopy for the live-cell imaging of various small alkyne-tagged biomolecules.[156] The authors could image and locate the metabolic uptake of 5-ethynyl uridine during RNA synthesis, of 5-ethynyl-2'-deoxyuridine (EdU) during DNA synthesis, of L-homopropargylglycine during protein synthesis, of proparglycholine during phospholipid synthesis and of 17-octadecynoic acid during triglyceride synthesis (Figure 10.3).

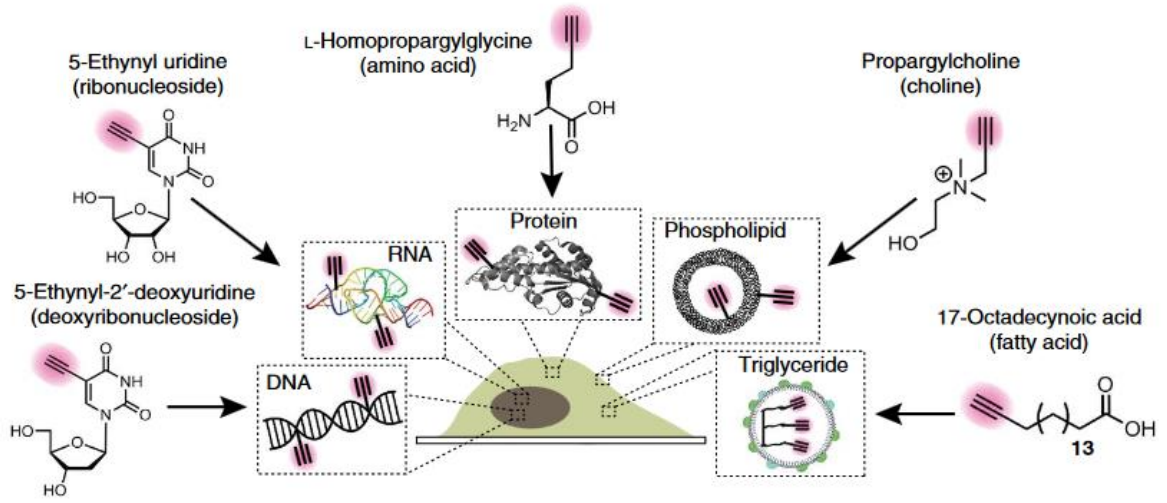
5-Ethynyl uridine
(ribonucleoside)
L-Homopropargylglycine
(amino acid)
Propargylcholine
(choline)
5-Ethynyl-2′-deoxyuridine
(deoxyribonucleoside)
17-Octadecynoic acid
(fatty acid)
RNA
Protein
Phospholipid
DNA
Triglyceride
13

Figure 10.3: Metabolic incorporation of alkyne-tagged small biomolecules. Taken with permission from reference 156.

---

[156] L. Wei, F. Hu, Y. Shen, Z. Chen, Y. Yu, C.-C. Lin, M. C. Wang, W. Min, *Nat. Methods* **2014**, *11*, 410-414.

Figure 10.4 shows the results obtained for the incorporation of EdU in the DNA of living cells. MIN and co-workers were even able to record the cell division by taking time-lapse images.

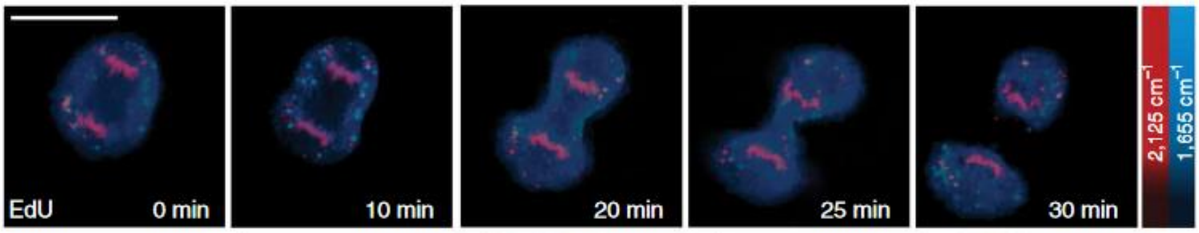

Figure 10.4: Time-lapse images of a dividing cell incubated with 100 μM EdU. Taken with permission from reference 156.

In 2012, SODEOKA and co-workers reported a detailed study of alkyne-tagged Raman imaging of living cells.[157] At first, the authors undertook an in depth investigation of the nature of the alkyne tag by synthesizing and analyzing 89 different alkynes. It could be shown, that an additional conjugated diyne moiety could already increase the intensity of the observed Raman signal by a factor of five (Figure 10.5). Also the conjugation of the alkyne to an aromatic ring resulted in a five times higher Raman intensity. Noteworthy, the combination of these two, a phenyl diyne moiety caused a remarkable intensity increase by a factor of 30.

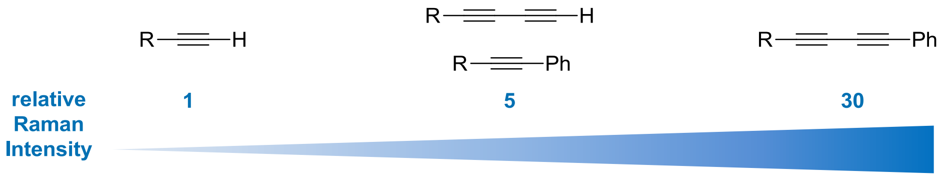

Figure 10.5: Relative Raman intensities of different alkyne moieties studied by SODEOKA and co-workers.

Recently, CHENG and co-workers reported an important finding during the live cell investigation of alkyne-tagged cholesterol.[158] While terminal alkyne groups are chemically relatively inert, the researchers found that terminal alkyne-tagged cholesterol showed cytotoxic effects with an IC_{50} value of 16 μM. Since such a change of biological behavior would lead to falsified results, the alkyne tag was exchanged with a phenyl-diyne moiety. The newly synthesized cholesterol derivative was shown to be biologically inert and did not cause any cytotoxic side effects after 16 hours of incubation.

---

[157] H. Yamakoshi, K. Dodo, A. Palonpon, J. Ando, K. Fujita, S. Kawata, M. Sodeoka, *J. Am. Chem. Soc.* **2012**, *134*, 20681-20689.

[158] H. J. Lee, W. D. Zhang, D. L. Zhang, Y. Yang, B. Liu, E. L. Barker, K. K. Buhman, L. V. Slipchenko, M. J. Dai, J. X. Cheng, *Sci. Rep.* **2015**, *5*, 7930.

10.3 Conclusion

The recent developments and advances in the field of stimulated Raman spectroscopy of alkyne-tagged small biomolecules in living cells prompted us to devise a synthetic route towards an alkyne-tagged analog of CycloEC (**330**). With sufficient material in hand, we might be able to observe and provide further proof for the intracellular interaction between CycloEC and the Keap1 protein cluster. Additionally, it has been discovered that 50% of various cyclopentenone prostaglandins are being transported to the cell nucleus.[159] If such an event does take place in the case of CycloEC could be straightforwardly proven by live cell imaging Raman spectroscopy.

---

[159] S. Narumiya, K. Ohno, M. Fukushima, M. Fujiwara, *J. Pharmacol. Exp. Ther.* **1987**, *242*, 306-311.

11 Synthetic Strategy

Since the general synthetic strategy presented in Chapter 9.1.1 has proven to be both reliable and scalable during the synthesis of various epoxyisoprostanes and analogs thereof, a similar plan was followed for the synthesis of the phenyldiyne derivative of EC (PDEC) and CycloEC (PDCycloEC).[160] Hence, as shown in Scheme 11.1, an aldol condensation between diyne **334** and aldehyde **317** followed by ester hydrolysis would provide PDEC (**333**). Furthermore it was decided to introduce the phenyl diyne motif at a late-stage *via* a C(sp)−C(sp) cross coupling between terminal alkyne **335** and (bromo- or iodoethynyl)-benzene. We surmised that its generation at this stage of the synthesis bears two tactical advantages. Firstly, if an expensive transition metal or ligand was required, performing the coupling reaction at a late-stage would decrease the overall cost. Secondly, we anticipated that the associated removal of the acidic alkyne proton would prove beneficial for the planned subsequent aldol reaction. Cyclopentanone **335** was then envisioned to arise from *β*-ketoester **336** by a C−H insertion, in accordance with the previously presented route (*cf.* Chapter 9.1.1).

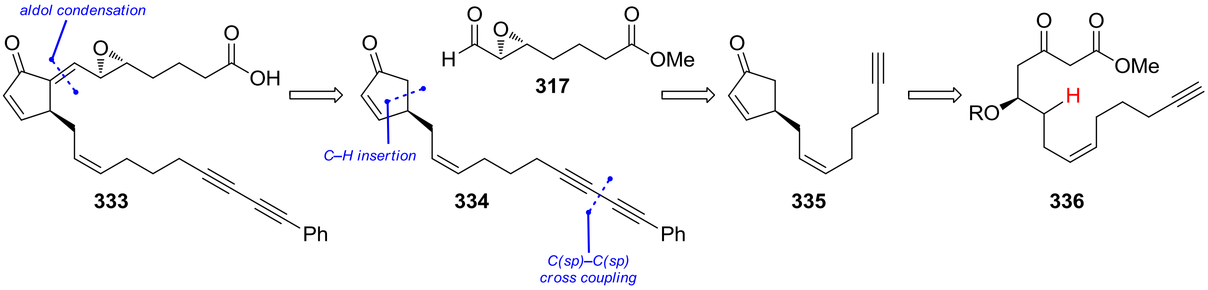

Scheme 11.1: Synthetic strategy for PDEC (**333**).

---

[160] a) See ref. 143.

12 Results and Discussion

12.1 Synthesis of PDEC and PDCycloEC

The synthesis commenced with a Wittig reaction between 5-hexyn-1-al (**338**)[161] and triphenylphosphonium bromide **337**[162] to give (*Z*)-olefin **339** in 76% yield (Scheme 12.1).

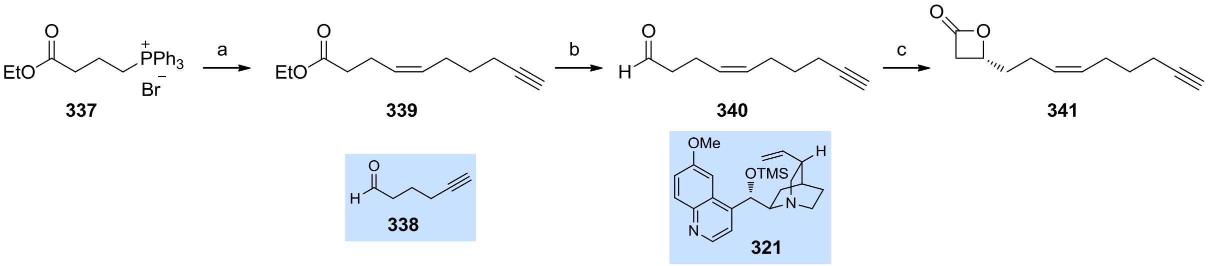
EtO
PPh3
Br
337
a
EtO
339
b
H
340
c
341
H
338
OMe
OTMS
H
N
N
321

Scheme 12.1: Asymmetric synthesis of *β*-lactone **341**. Reagents and conditions: a) KO*t*Bu, THF, –78 °C, then **338**, –78 °C to RT, 76%; b) DIBAL, toluene, –78 °C, 87%; c) $LiClO_4$, **321** (12 mol%), *i*Pr_2NEt, AcCl, CH_2Cl_2–Et_2O (3:1), –78 °C, 75%, *ee* ≥ 94%.

Next, DIBAL reduction to aldehyde **340** proceeded uneventfully in 87% yield. The formal [2+2] cycloaddition between ketene and **340** provided *β*-lactone **341** in 75% yield and ≥ 94% *ee*.[163]

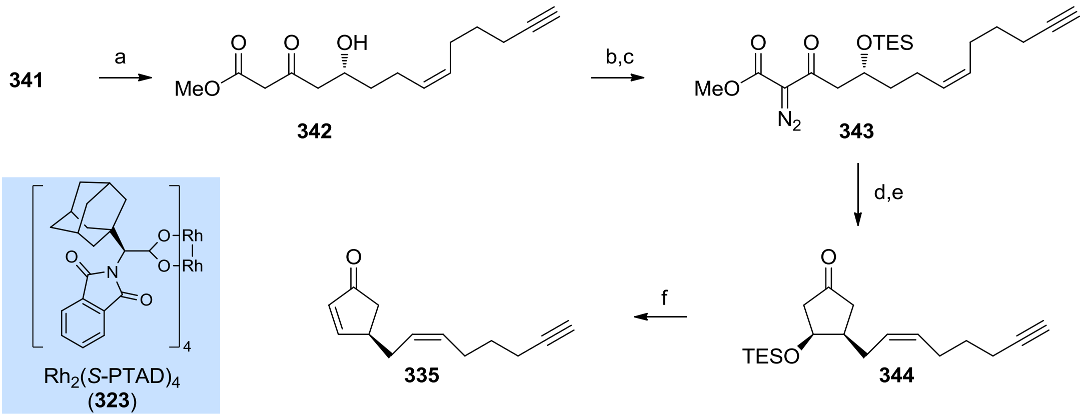
341
a
MeO
OH
342
b,c
MeO
OTES
N2
343
d,e
Rh
Rh
N
Rh2(S-PTAD)4
(323)
335
f
TESO
344

Scheme 12.2: Synthesis of cyclopentenone **335** *via* homoallylic C–H insertion. Reagents and conditions: a) *i*Pr_2NLi, MeOAc, THF, –78 °C, then **341**; b) *p*-ABSA, NEt_3, MeCN; c) TESCl, imidazole, DMF, 56% over three steps; d) Rh_2(*S*-PTAD)$_4$ (**323**) (0.2 mol%), CH_2Cl_2, reflux; e) NaCl, DMSO, 140 °C; f) DBU, CH_2Cl_2, 0 °C, 20% over three steps.

Nucleophilic opening of the *β*-lactone by the lithium enolate of methyl acetate provided alcohol **342**, which smoothly underwent diazo transfer and subsequent TES protection furnishing **343** in 56% overall yield (Scheme 12.2). With sufficient quantities of diazo ester **343** in hand, the stage was set for the Rh(II)-mediated homoallylic C–H insertion reaction. To our delight, the insertion proceeded smoothly and provided, after Krapcho decarboxylation and elimination, cyclopentenone **335** in 19% yield over three steps.

---

[161] Available from 5-hexyn-1-ol *via* Swern oxidation: J. W. Amoroso, L. S. Borketey, G. Prasad, N. A. Schnarr, *Org. Lett.* **2010**, *12*, 2330-2333.

[162] Available from 4-bromobutyricacid ethyl ester in one step: D. C. Braddock, G. Cansell, S. A. Hermitage, *Chem. Commun.* **2006**, 2483-2485.

[163] The enantiomeric excess of **341** was determined later by measuring the *ee* of UV-active intermediate **343** by chiral SFC.

Having a reliable and scalable synthesis of cyclopentenone **335** established, the introduction of the phenyl diyne motif was explored next. Conjugated diynes are most often generated by copper-catalyzed Glaser or Cadiot-Chodkiewicz couplings.[164] However, since both reactions suffer from significant homocoupling, palladium-catalyzed reactions have been developed to overcome this selectivity problem.[165] In 2008, LEI and co-workers published a detailed study for the Pd-catalyzed C(sp)–C(sp) coupling reaction between a bromoalkyne and a terminal alkyne.[165] This study was aiming not only for the improvement of the overall yield but also for a more general applicability. The optimal conditions found required 4 mol% $Pd(dba)_2$, 4 mol% of a phosphine ligand (*vide infra*) and 2 mol% of CuI in the presence of triethylamine in DMF. Under these conditions, a wide range of alkynes underwent the desired coupling reaction in generally high yields (77-99%). Importantly, only a slight excess of the terminal alkyne was necessary (1.2 equiv).

When cyclopentenone **335** was subjected to slightly modified conditions, phenyl diyne **334** was isolated in 42% yield (Scheme 12.3).[166] The yield could be improved to 52% by substituting (bromoethynyl)benzene by (iodoethynyl)benzene (**345**).

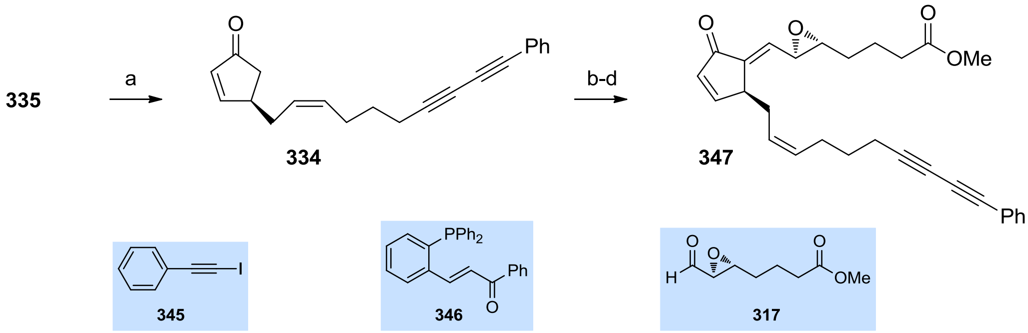

Scheme 12.3: Preparation of phenyl diyne substituted cyclopentenone **347**. Reagents and conditions: a) **345**, CuI (2 mol%), **346** (4 mol%), $Pd(dba)_2$ (4 mol%), NEt_3, DMF, 52%; b) LiHMDS, THF, –78 °C, then **317**; c) MsCl, NEt_3, CH_2Cl_2, –78 °C; d) Al_2O_3, CH_2Cl_2, 49% over three steps.

The following aldol condensation reaction proved to be highly delicate. Although the aldol addition of the lithium anion of cyclopentenone **334** and aldehyde **317** proceeded without difficulties, the elimination and handling of the mesylated derivatives was highly cumbersome. Since no spontaneous elimination during the mesylation could be achieved, we attempted to isolate the mesylated derivatives. However, while purification *via* flash column chromatography was indeed possible, the subsequent evaporation of the solvent led to rapid decomposition of the material.[167] Gratifyingly, after extensive experimentation it was found that an aqueoues workup, followed by concentration of the reaction mixture to 1/5 of the volume and subsequent addition of an excess of neutral and freshly activated Al_2O_3 provided dienone **347** in 49% overall yield.

---

[164] a) F. Diederich, P. J. Stang, R.R. Tykwinski, *Acetylene Chemistry: Chemistry, Biology and Material Science*, Wiley-VCH Verlag GmbH & Co KGaA, Weinheim, Germany, **2005**; b) A. L. K. S. Shun, R. R. Tykwinski, *Angew. Chem. Int. Ed.* **2006**, *45*, 1034-1057; c) E.-I. Negishi, L. Anastasia, *Chem. Rev.* **2003**, *102*, 1979-2017.

[165] For an overview see: W. Shi, Y. Luo, X. Luo, L. Chao, H. Zhang, J. Wang, A. Lei, *J. Am. Chem. Soc.* **2008**, *130*, 14713-14720.

[166] 2.0 equivalents of the haloalkyne were used. The yield refers to cyclopentenone **335**.

Finally, as indicated in Scheme 12.4 ester **347** was hydrolyzed to the corresponding PDEC (**333**). The obtained material was then dissolved in $CHCl_3$ and stirred in the presence of an excess of silica gel. After five days, the targeted PDCycloEC (**348**) was obtained in 50% yield over two steps.

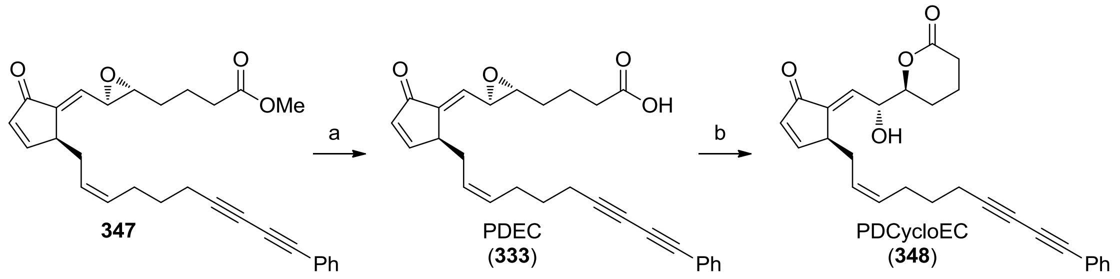

Scheme 12.4: Synthesis of PDCycloEC (**348**) from ester **347**. Reagents and conditions: a) Novozyme, THF–buffer (aqueous, pH 7) (1:4); b) SiO_2, $CHCl_3$, 50% over two steps.

12.2 Conclusion and Outlook

In Part III of this thesis, an efficient and scalable synthesis of the phenyl diyne-tagged derivative of CycloEC has been developed. The synthetic strategy is mostly based on the results reported by EGGER and CARREIRA in their total syntheses of various epoxyisoprostanes and analogs thereof. While the terminal alkyne component could be carried through the whole synthetic sequence to cyclopentenone **344**, we decided to strategically introduce the (ethynyl)benzene motif at a late-stage, prior to the aldol condensation step, by a Pd-catalyzed C(sp)–C(sp) cross coupling.

Targeted PDCycloEC has been submitted to our collaborators for stimulated Raman spectroscopy imaging in order to study its behavior in a living cell. The results of this study will be reported in due course.

---

[167] A column or an aqueous workup was neccesary, since the formed ammonium salts seem to hamper the elimination process mediated by Al_2O_3.

Part IV
Experimental Section

13 Experimental Procedures

13.1 General Methods

All non-aqueous reactions were performed under an inert atmosphere of dry nitrogen or argon in flame dried glassware sealed with a rubber septum unless otherwise noted. The protecting gas was passed over a column of $CaCl_2$ and supplied through a glass manifold. Reactions were stirred magnetically and monitored by thin layer chromatography (TLC). Analytical thin layer chromatography was performed using MERCK SILICA GEL F^{254} TLC glass plates and visualized by ultraviolet light (UV). Additionally, TLC plates were stained with aqueous potassium permanganate ($KMnO_4$) [1.5 g $KMnO_4$, 200 mL H_2O, 10 g K_2CO_3, 2.5 mL 1 M NaOH aq.], cerium ammonium molybdate (CAM) [0.5 g $Ce(NH_4)_2(NO_3)_6$, 12 g $(NH_4)_6Mo_7O_{24}\cdot 4H_2O$, 235 mL H_2O, 15 mL conc. H_2SO_4] or ethanolic *p*-anisaldehyde [3.7 mL *p*-anisaldehyde, 135 mL EtOH, 5 mL conc. H_2SO_4, 1.5 mL AcOH]. Concentration under reduced pressure (= *in vacuo*) was performed by rotator evaporation at 40 °C at the appropriate pressure. Chromatographic purification was performed as flash chromatography[168] on FLUKA silica gel 60 Å (230-400 mesh) at 0.3 – 0.5 bar over-pressure. Yields refer to the purified compound.

13.2 Chemicals

All chemicals and solvents were purchased from ABCR, ACROS, ALDRICH, COMBI-BLOCKS, FLUOROCHEM, J. T. BAKER, FLUKA, MERCK, FISHER-SCIENTIFIC, TCI, STREM or LANCASTER and were used as received from the commercial supplier without further purification unless mentioned otherwise. THF, Et_2O, CH_2Cl_2, MeCN and toluene were dried on a LC TECHNOLOGY SOLUTIONS *SP-1* solvent purification system under N_2. (H_2O content < 30 ppm, *Karl–Fischer* titration).[169] Deuterated solvents were obtained from ARMAR CHEMICALS, Döttingen, Switzerland. MeOH was distilled from magnesium turnings under an atmosphere of dry nitrogen. Diisoproylamine and pyridine were distilled from KOH, DMPU, NEt_3, 2,2,2-trifluoroethyl 2,2,2-trifluoroacetate and TMS–Cl were distilled from calcium hydride under an atmosphere of dry nitrogen or high vacuum. $BF_3\cdot OEt_2$ was purified by a quick, heat gun promoted "bulb-to-bulb" distillation under an atmosphere of nitrogen prior to use. 6-(dimethylamino)fulvene[170], DESS–MARTIN periodinane (DMP)[171] and MsN_3[172] were prepared according to literature procedures. Aqueous buffer solutions were prepared according to the Sørensen's phosphate buffer table from 0.067 M aqueous solutions of Na_2HPO_4 and KH_2PO_4.

---

[168] W. C. Still, M. Kahn, A. J. Mitra, *J. Org. Chem.* **1978**, *43*, 2923-2925.
[169] A. B. Pangborn, M. A. Giardello, R. H. Grubbs, R. K. Rosen, F. J. Timmers, *Organometallics* **1996**, *15*, 1518-1520.
[170] K. Hafner, K. H. Vöpel, G. Ploss, C. König, *Org. Syn. Coll. Vol. 5*, **1973**, 431.
[171] M. Frigerio, M. Santagostino, S. Sputore, *J. Org. Chem.* **1999**, *64*, 4537-4538.
[172] J. Waser, B. Gaspar, H. Nambu, E. M. Carreira, *J. Am. Chem. Soc.* **2006**, *128*, 11693-11712.

13.3 Analytics

Nuclear Magnetic Resonance (NMR) spectra were recorded on VARIAN MERCURY (300 MHz), BRUKER AV and DRX (400 MHz), BRUKER DRX and DRXII (500 MHz) or BRUKER AVIII (600 MHz with cryoprobe) spectrometers. Measurements were carried out at ambient temperature (*ca.* 22 °C). Chemical shifts (δ) are reported in ppm with the residual solvent signal as internal standard (chloroform at 7.26 and 77.16 ppm for ^{1}H- and ^{13}C NMR spectroscopy, respectively), unless otherwise noted. The data is reported as (s = singlet, d = doublet, t = triplet, q = quartet, m = multiplet or unresolved, b = broad signal, app = apparent, coupling constant(s) in Hz, integration). ^{13}C NMR spectra were recorded with broadband ^{1}H-decoupling. Service measurements were performed by the NMR service team of the *Laboratorium für Organische Chemie* at *ETH Zürich* by Mr. *René Arnold,* Mr. *Rainer Frankenstein* and Mr. *Philipp Zumbrunnen* under direction of Dr. *Marc-Olivier Ebert*.

Infrared (IR) spectra were recorded on a PERKIN ELMER TWO-FT-IR (UATR) as thin films. Absorptions are given in wavenumbers (cm^{-1}).

Mass spectrometry (MS) analyses were performed as high resolution EI measurements on a WATERS MICROMASS AUTOSPEC ULTIMA at 70 eV, as high resolution ESI measurements on a BRUKER DALTONICS MAXIS (UHR-TOF) instrument or as MALDI on a BRUKER SOLARIX – MALDI-FTICR-MS instrument by the mass spectrometry service of the *Laboratorium für Organische Chemie* at *ETH Zürich* by Mr. *Louis Bertschi*, Mr. *Oswald Greter* and Mr. *Rolf Häfliger* under direction of Dr. *Xiangyang Zhang*.

X-ray diffraction experiments have been carried out by *Dr. Niels Trapp* and *Mr. Michael Solar* on a BRUKER NONIUS APEX-II system equipped with a graphite monochromator at the *Laboratorium für Organische Chemie* at *ETH Zürich*. The data obtained was deposited at the Cambridge Crystallographic Data Centre.

13.4 Experimental Procedures

13.4.1 Total Syntheses of Pallambins A and B

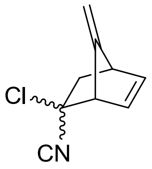

(1*SR*,4*RS*)-2-chloro-7-methylenebicyclo[2.2.1]hept-5-ene-2-carbonitrile (349) and (1*SR*,4*RS*)-2-chloro-7-methylenebicyclo[2.2.1]hept-5-ene-2-carbonitrile (350).[173] A suspension of dimethylaminofulvene (3.97 g, 32.8 mmol) in 150 mL Et_2O was added dropwise with a dropping funnel to a –15 °C cold suspension of $LiAlH_4$ (1.37 g, 36.0 mmol) in 50 mL Et_2O over 40 min.[174] When the addition was over, the wall of the flask was rinsed down with additional ether to bring all material into the suspension. The reaction was stirred at this temperature for 1.5 h and then quenched at –35 °C by the addition of 1.4 mL water, NaOH (10% aqueous, 1.4 mL) and 3.5 mL water. When no gas evolution was visible anymore, the reaction was directly dried by the addition of sufficient $MgSO_4$. After warming to RT, the dark brown slurry was filtered over filter paper. The filter cake was rinsed with 100 mL of ether, to give a bright yellow to orange solution. Careful evaporation of the solvent, gave crude amine (3.14 g, 25.5 mmol, 78%) as an orange oil and as a mixture of two isomers. To a solution of 0.80 g (6.49 mmol) of the two isomeric amine products in 5 mL Et_2O was added MeI (0.41 mL, 6.49 mmol) at 0 °C. After 1 h, the ammonium salt was filtered over celite (rinsed with 5 mL ether) and 2-chloroacrylonitrile (0.78 mL, 9.73 mmol) was added. The reaction was refluxed overnight and additional 2-chloroacrylonitrile (1.56 mL, 19.5 mmol) was added. After 24 h, the reaction was poured into a separation funnel containing 25 mL water and 20 mL ether. The phases were separated and the aqueous phase was extracted with ether (3 x 20 mL). The combined organic phases were dried over $MgSO_4$ and concentrated. Purification using flash column chromatography (hexane/EtOAc 3:1) provided a mixture of **349** and **350** (0.29 g, 1.77 mmol, 27%).

R_f = 0.37 (hexane/toluene 1:1, $KMnO_4$); ^1H NMR (300 MHz, $CDCl_3$) δ *for the major isomer* ^1H NMR (300 MHz, $CDCl_3$) δ 6.58 (dd, J = 6.0, 3.1 Hz, 1H), 6.27 (dd, J = 6.0, 3.1 Hz, 1H), 4.67 (bs, 1H), 4.60 (bs, 1H), 3.68 (d, J = 3.1 Hz, 1H), 3.32 (app. t, J = 3.6 Hz, 1H), 2.76

---

[173] Fulvene was generated according to a modified literature procedure: B. M. Trost, R. M. Cory, *J. Org. Chem.* **1972**, *37*, 1106-1110.

[174] The dimethylaminofulvene does not completely dissolve, therefore a Chemglass™ addition funnel with threaded valve (Chemglass™ catalog number: CG-1714-16) was used for the addition. The valve sometimes clocks, is then opened more to release the solids and closed again.

(dd, *J* = 13.1, 3.9 Hz, 1H), 1.79 (d, J = 13.1 Hz, 1H) ppm; HRMS (ESI) calcd for $C_9H_8ClN^+$ [*M*+H^+] 164.0262, found 164.0261.

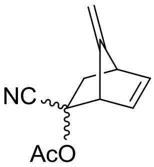

(1*SR*,2*RS*,4*RS*)-2-cyano-7-methylenebicyclo[2.2.1]hept-5-en-2-yl acetate (351) and (1*SR*,2*SR*,4*RS*)-2-cyano-7-methylenebicyclo[2.2.1]hept-5-en-2-yl acetate (352).[173] A suspension of dimethylaminofulvene (3.97 g, 32.8 mmol) in 150 mL Et_2O was added dropwise with a dropping funnel to a –15 °C cold suspension of $LiAlH_4$ (1.37 g, 36.0 mmol) in 50 mL Et_2O over 40 min.[174] When the addition was over, the wall of the flask was rinsed down with additional ether to bring all material into the suspension. The reaction was stirred at this temperature for 1.5 h and then quenched at –35 °C by the addition of 1.4 mL water, NaOH (10% aqueous, 1.4 mL) and 3.5 mL water. When no gas evolution was visible anymore, the reaction was directly dried by the addition of sufficient $MgSO_4$. After warming to RT, the dark brown slurry was filtered over filter paper. The filter cake was rinsed with 100 mL of ether, to give a bright yellow to orange solution. Careful evaporation of the solvent, gave crude amine (3.14 g, 25.5 mmol, 78%) as an orange oil and as a mixture of two isomers. To a solution of 1.45 g (11.8 mmol) of this amine in 6 mL ether was added MeI (0.73 mL, 11.8 mmol) dropwise at 0 °C. After 1 h, the ammonium salt was filtered over celite (rinsed with 6 mL ether). ZnI_2 (1.13 g, 3.54 mmol), 2-acetoxyacrylonitrile (1.24 mL, 11.8 mmol) and a crystal of BHT were added. After four days, the reaction was poured into a separation funnel containing 25 mL water and 20 mL ether. The phases were separated and the aqueous phase was extracted with ether (3 x 20 mL). The combined organic phases were dried over $MgSO_4$ and concentrated. The unreacted 2-acetoxyacrylonitrile was distilled of at 45 °C (high vacuum). The crude product was purified by flash column chromatography (hexane/Et_2O 2:1) to yield **351** and **352** (0.402 g, 2.124 mmol, 18%) as a 6:1 mixture.

R_f = 0.47 (hexane/Et_2O 1:1, $KMnO_4$); ^1H NMR (300 MHz, $CDCl_3$) *δ for the major isomer* 6.56 (dd, *J* = 5.8, 3.1 Hz, 1H), 6.07 (dd, *J* = 5.8, 3.1 Hz), 4.65 (app. s, 1H) 4.58 (app. s, 1H), 3.95 (app. d, *J* = 3.1 Hz, 1H), 3.26 (app. t, *J* = 3.7 Hz, 1H), 2.64 (dd, *J* = 13.2, 3.9 Hz, 1H), 2.05 (s, 3H), 1.65 (d, *J* = 13.2 Hz, 1H) ppm.

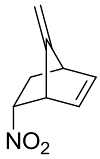

(1*RS*,4*SR*,5*RS*)-7-methylene-5-nitrobicyclo[2.2.1]hept-2-ene (353).[173] A suspension of dimethylaminofulvene (3.97 g, 32.8 mmol) in 150 mL Et_2O was added dropwise with a dropping funnel to a –15 °C cold suspension of $LiAlH_4$ (1.37 g, 36.0 mmol) in 50 mL Et_2O over 40 min.[174] When the addition was over, the wall of the flask was rinsed down with additional ether to bring all material into the suspension. The reaction was stirred at this temperature for 1.5 h and then quenched at –35 °C by the addition of 1.4 mL water, NaOH (10% aqueous, 1.4 mL) and 3.5 mL water. When no gas evolution was visible anymore, the reaction was directly dried by the addition of sufficient $MgSO_4$. After warming to RT, the dark brown slurry was filtered over filter paper. The filter cake was rinsed with 100 mL of ether, to give a bright yellow to orange solution. Careful evaporation of the solvent, gave crude amine (3.14 g, 25.5 mmol, 78%) as an orange oil and as a mixture of two isomers. To a solution of 0.50 g (4.06 mmol) of this amine in 5 mL ether was added MeI (0.25 mL, 4.06 mmol) dropwise at 0 °C. After 1 h, the ammonium salt was filtered over celite (rinsed with 5 mL ether), nitroethene (10% solution in benzene, 14.8 g, 20.3 mmol) was added and the reaction refluxed for 48 h. Then additional nitroethene solution (14.8 g, 20.3 mmol) was added. After another 40 h, the solvents were evaporated and the crude product purified by flash column chromatography (hexane:Et_2O 20:1) to give **353** and **354** (16.1 mg, 0.11 mmol, 3%).

R_f = 0.66 (hexane:Et_2O 9:1, $KMnO_4$); ^1H NMR (400 MHz, $CDCl_3$) δ 6.55 (dd, J = 6.2, 3.2 Hz, 1H), 6.11 (dd, J = 6.2, 3.2 Hz, 1H), 4.98 (app. dt, J = 8.7, 3.8 Hz, 1H), 4.42 (bs, 1H), 4.41 (bs, 1H), 3.81 (app. t, J = 3.6 Hz, 1H), 3.24 (app. t, J = 3.7 Hz, 1H), 2.28 (ddd, J = 12.9, 8.7, 3.8 Hz, 1H), 1.98 (dd, J = 12.9, 3.2 Hz) ppm.

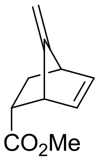

(1*RS*,2*RS*,4*RS*)-methyl-7-methylenebicyclo[2.2.1]hept-5-ene-2-carboxylate (95).[174] A suspension of dimethylaminofulvene (36.80 g, 303.7 mmol) in 720 mL Et_2O was added dropwise with a dropping funnel to a –15 °C cold suspension of $LiAlH_4$ (11.53 g, 303.8 mmol) in 200 mL Et_2O over 40 min.[175] When the addition was over, the wall of the flask was rinsed down with additional ether to bring all material into the suspension. The reaction was stirred at this temperature for 1.5 h and then quenched at –35 °C by the addition of 10 mL water, NaOH (10% aqueous, 10 mL) and 20 mL water. When no gas evolution was visible anymore, the reaction was directly dried by the addition of sufficient $MgSO_4$. After warming to RT, the dark brown slurry was filtered over filter paper. The filter cake was rinsed with 300 mL of ether, to give a bright yellow to orange solution. Careful evaporation of the solvent, gave crude amine (32.93 g, 267.3 mmol, 88%) as an orange oil and as a mixture of two isomers.

The crude amine was then dissolved in 200 mL methylacrylate, cooled to 0 °C and MeI (16.64 mL, 267.0 mmol) was added dropwise. The formation of the ammonium salt became visible after 5 min. In the meantime, diethylaluminium chloride (1.0 M in hexanes, 90 mL, 90 mmol) was added in a separate flask slowly at –15 °C to 90 mL methyl acrylate. After 1.5 h, the ammonium salt was filtered over a frit of celite into a 1 L flask. The frit was rinsed with 250 mL methylacrylate until the rinsing solvent did not look bright yellow anymore. The receiving flask was precooled to 0 °C. This mixture was then cannulated to the methylacrylate/Et_2AlCl solution and stirred for 17 h at –20 °C and then at 5 °C for further 44 h.

The reaction was then cannulated into a 0 °C mixture of 150 mL Et_2O and 300 mL HCl (1.0 M, aqueous). The flask and the cannula were rinsed with additional 50 mL Et_2O. The suspension was transferred into a 2 L separation funnel and shaken, upon which most of the formed precipitate dissolved. The phases were separated and the aqueous phase extracted with Et_2O (4 x 300 mL). The combined organic layers were dried over $MgSO_4$ and concentrated *in vacuo* to give the crude material as a red oil, which was purified by column chromatography (hexane/Et_2O 10:1 to 6:1) to give **95** as a yellow oil with characteristic smell (27.06 g, 164.8 mmol, 62%, d.r = 10:1).

R$_f$ = 0.33 (hexane/Et$_2$O 10:1, KMnO$_4$); ^{1}H NMR (400 MHz, CDCl$_3$) δ *for the major diastereomer* 6.34 (dd, *J* = 5.9, 3.2 Hz, 1H), 6.09 (dd, *J* = 5.9, 3.2 Hz, 1H), 4.25 (d, *J* = 7.6 Hz, 2H), 3.62 (s, 3H), 3.39 (bt, 1H), 3.09 (bt, 1H), 2.96 (dt, *J* = 9.4, 4.3 Hz, 1H), 1.99 (ddd, *J* = 11.6, 9.4, 3.9 Hz, 1H), 1.53 (dd, *J* = 11.6, 4.3 Hz, 1H) ppm; ^{13}C NMR (101 MHz, CDCl$_3$) δ *for the major diastereomer* 174.4, 162.4, 137.8, 132.7, 91.8, 51.7, 48.6, 45.6, 42.4, 29.7 ppm; FT-IR (neat) ν_{max} = 2992, 2951, 1737, 1435, 1326, 1203, 1040, 881, 733, 632 cm^{-1}; HRMS (ESI) calcd for $C_{10}H_{13}O_2^+$ [*M*+H$^+$] 165.0910, found 165.0915.

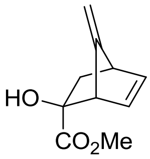

(1*SR*,2*SR*,4*RS*)-methyl 2-hydroxy-7-methylenebicyclo[2.2.1]hept-5-ene-2-carboxylate (102). *n*BuLi (1.6 M in hexane, 1.14 mL, 1.8 mmol) was added at 0 °C to *i*Pr$_2$NH (0.30 mL, 2.11 mmol) in 3 mL THF and stirred for 20 min. The solution was cooled to –78 °C and **95** (231 mg, 1.41 mmol) in 2 mL THF was added dropwise. After 15 min the reaction was warmed to –40 °C, then slowly warmed to 0 °C over 1.5 h, before being recooled to −78 °C. P(OEt)$_3$ (0.24 mL, 1.41 mmol) was added and oxygen was bubbled through the solution for 1 h 15 min. The reaction was quenched by the addition of 8 mL NH$_4$Cl (saturated, aqueous) and 10 mL water. 50 mL ether were added and the phases separated. The aqueous phase was extracted with ether (3 x 20 mL), dried over Na$_2$SO$_4$ and concentrated. The crude product was purified by flash column chromatography (hexane/EtOAc 5:1) to give **102** as a 3:1 mixture of diastereomers a yellow oil (149 mg, 0.83 mmol, 59%).

R$_f$ = 0.18 (hexane/EtOAc 5:1, KMnO$_4$); ^{1}H NMR (300 MHz, CDCl$_3$) δ 6.45 (dd, *J* = 6.0, 3.0 Hz, 1H), 6.10 (dd, *J* = 6.0, 3.0 Hz, 1H), 4.55 (bs, 1H), 4.53 (bs, 1H), 3.74 (s, 3H), 3.20 (bs, 1H), 3.08 (bs, 1H), 2.79 (s, 1H), 2.14 (d, *J* = 12.4 Hz, 1H), 1.78 (dd, *J* = 12.4, 3.8 Hz, 1H) ppm; ^{13}C NMR (101 MHz, CDCl$_3$) δ 174.4, 161.9, 140.1, 132.3, 95.4, 80.0, 57.5, 52.6, 45.2, 41.6 ppm; HRMS (ESI) calcd for $C_{10}H_{12}NaO_3^+$ [*M*+Na$^+$] 203.0679, found 203.0673.

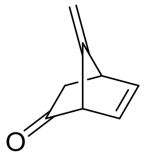

(1*SR*,4*RS*)-7-methylenebicyclo[2.2.1]hept-5-en-2-one (88). To a solution of alcohol **102** (2.470 g, 13.71 mmol) in 90 mL Et_2O was added $LiAlH_4$ (4.0 M in Et_2O, 5.14 mL, 20.6 mmol) dropwise at 0 °C. After 10 min, the reaction mixture was allowed to warm to RT and stirred for another 50 min before being quenched by the addition of 0.8 mL water, then 0.8 mL NaOH (10%, aqueous), followed by 2.4 mL water. Na_2SO_4 was added and the suspension filtered. Evaporation of the solvent provided diol **103** (1.868 g, 12.27 mmol, 90%), which was used for the next step without further purification. Diol **103** was then dissolved in 120 mL THF–H_2O (1:1) and $NaIO_4$ (3.94 g, 18.41 mmol) was added in one portion. After 30 min, the reaction was quenched by the addition of 80 mL $Na_2S_2O_3$ (aqueous, saturated) and diluted with 100 mL Et_2O. The phases were separated and the aqueous phase extracted with ether (3 x 200 mL). The combined organic phases were washed with 100 mL brine, dried over $MgSO_4$ and concentrated *in vacuo*.[175] The crude product was purified by flash column chromatography (pentane/Et_2O 10:1) to give ketone **88** (0.933 g, 7.765 mmol, 63%) as a faint yellow liquid.

R_f = 0.63 (hexane/Et_2O 1:1, $KMnO_4$); ^{1}H NMR (300 MHz, $CDCl_3$) δ 6.70 (dd, J = 5.9, 2.8 Hz, 1H), 6.27 (dd, J = 5.9, 3.2 Hz, 1H), 4.70 (bs, 1H), 4.57 (bs, 1H), 3.49 (bs, 1H), 3.38 (app. d, J = 3.0 Hz, 1H), 2.21 (dd, J = 16.5, 3.4 Hz, 1H), 2.09 (d, J = 16.5 Hz, 1H) ppm; ^{13}C NMR (101 MHz, $CDCl_3$) δ 209.9, 161.8, 142.8, 130.8, 97.6, 60.9, 45.6, 40.8 ppm; FT-IR (neat) ν_{max} = 3068, 2993, 2921, 1754, 1414, 1312, 1267, 1113, 1056, 889, 868, 740 cm^{-1}; No satisfying HRMS could be obtained.

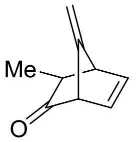

(1*SR*,3*SR*,4*SR*)-3-methyl-7-methylenebicyclo[2.2.1]hept-5-en-2-one (104). To a solution of *i*Pr_2NLi in 1.0 mL THF was added a solution of **88** (25.0 mg, 0.21 mmol) in 0.28 mL THF at –78 °C. After 45 min, MeI (59.0 mg, 0.42 mmol) in 0.28 mL THF was added. The cooling bath was removed and the reaction was quenched after 1 h by the addition of 2 mL NH_4Cl (aqueous, saturated) and 5 mL water. Dilution with 10 mL Et_2O, phase separation and extraction of the aqueous phase with Et_2O (3 x 10 mL), drying over $MgSO_4$

---

[175] Ketone **88** proved to be highly volatile. Therefore care should be taken during distillation of the solvents.

and concentration *in vacuo* furnished crude **104**. Purification *via* flash column chromatography (pentane/Et_2O 3:1) provided 24.2 mg (0.18 mmol, 86%) of a yellow liquid.

R_f = 0.57 (hexane/Et_2O 1:1, $KMnO_4$); ^1H NMR (300 MHz, $CDCl_3$) δ 6.72 (dd, *J* = 5.9, 2.9 Hz, 1H), 6.28 (ddd, *J* = 5.9, 3.3, 1.1 Hz), 4.75 (bs, 1H), 4.68 (bs, 1H), 3.34 – 3.32 (m, 1H), 3.10 (bs, 1H), 2.24 (q, *J* = 7.4 Hz, 1H), 1.10 (d, *J* = 7.4 Hz, 3H) ppm; ^{13}C NMR (101 MHz, $CDCl_3$) δ 212.6, 160.4, 143.1, 131.3, 100.0, 60.8, 52.0, 44.2, 16.4 ppm.

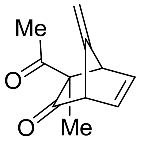

(1*SR*,3*SR*,4*RS*)-3-acetyl-3-methyl-7-methylenebicyclo[2.2.1]hept-5-en-2-one (78). To a solution of **104** (25 mg, 0.21 mmol) in 1.5 mL CH_2Cl_2 was added NEt_3 (0.10 mL, 0.72 mmol) and TMSOTf (0.10 mL, 0.55 mmol) at 0 °C. After 30 min, the cooling bath was removed and the reaction allowed to warm to RT. After 6 h, the reaction mixture was quenched by the addition of 5 mL pH7 phosphate buffer. The phases were separated and the aqueous phase was extracted with pentane (3 x 10 mL). The combined organic phases were dried over K_2CO_3 and concentrated. A suspension of $ZnCl_2$ (29.1 mg, 0.21 mmol) in 0.5 mL CH_2Cl_2 and 30 μL Et_2O was cooled to 0 °C. Acetyl chloride (15 μL, 0.2 mmol) was added, followed by dropwise addition of the crude silyl enol ether (44.0 mg, 0.21 mmol) in 0.5 mL CH_2Cl_2. After 1.5 h, the reaction was quenched by the addition of 3 mL water and diluted with 4 mL CH_2Cl_2. The phases were separated and the aqueous phase was extracted with CH_2Cl_2 (3 x 10 mL). The combined organic phases were dried over $MgSO_4$ and concentrated. The crude product was purified by flash column chromatography providing **78** (22.0 mg, 0.13 mmol, 59%) along with recovered **104** (12.0 mg, 0.09 mmol, 42%).[176]

R_f = 0.61 (hexane/Et_2O 1:1, $KMnO_4$); ^1H NMR (300 MHz, $CDCl_3$) δ 6.64 (dd, 5.8, 2.9 Hz, 1H), 6.31 (ddd, *J* = 5.8, 3.3, 1.3 Hz, 1H), 4.76 (bs, 1H), 4.63 (bs, 1H), 3.75 – 3.74 (m, 1H), 3.46 – 3.44 (m, 1H), 2.18 (s, 3H), 1.31 (s, 3H) ppm.

---

[176] The starting ketone **104** was recovered as its α methyl epimer

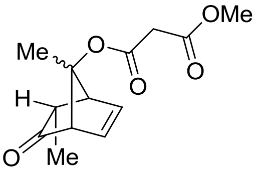

(1*SR*,4*SR*,5*SR*)-5,7-dimethyl-6-oxobicyclo[2.2.1]hept-2-en-7-yl methyl malonate (107).[177] To a solution of **104** (64 mg, 0.48 mmol) in 1.5 mL CH_2Cl_2 was added NEt_3 (0.10 mL, 0.72 mmol) and TMSOTf (0.10 mL, 0.55 mmol) at 0 °C. After 30 min, the cooling bath was removed and the reaction allowed to warm to RT. After 6 h, the reaction mixture was quenched by the addition of 5 mL pH7 phosphate buffer. The phases were separated and the aqueous phase was extracted with pentane (3 x 10 mL). The combined organic phases were dried over K_2CO_3 and concentrated. To a –78 °C cold solution of the crude silyl enol ether (33.0 mg, 0.16 mmol) in 1.8 mL toluene was added TMSOTf (0.50 M in toluene, 0.12 mL, 0.06 mmol) and methoxymalonyl chloride (24.0 μL, 0.21 mmol). After 15 min, the reaction was warmed to 0 °C, stirred for 1 h and then allowed to warm to RT. After stirring overnight, 5 mL water and 10 mL EtOAc were added, the phases separated and the aqueous phase extracted with EtOAc (3 x 20 mL). The combined organic phases were dried over $MgSO_4$ and concentrated. The crude product was purified by flash column chromatography (hexane/Et_2O 5:1 → 2:1 → 1:1) yielding 23 mg (0.09 mmol, 57%) of **107**.

R_f = 0.09 (hexane/Et_2O 2:1, $KMnO_4$); ^1H NMR (400 MHz, $CDCl_3$) δ 6.48 (dd, J = 6.0, 3.1 Hz, 1H), 6.01 – 5.98 (m, 1H), 3.73 (s, 3H), 3.39 (bs, 1H), 3.33 (s, 2H), 3.22 (bs, 1H), 2.49 (qd, J = 7.0, 3.5 Hz, 1H), 1.65 (s, 3H), 1.07 (d, J = 7.0 Hz, 3H) ppm; ^{13}C NMR (101 MHz, $CDCl_3$) δ 213.9, 166.8, 165.3, 140.7, 127.9, 99.5, 63.9, 52.7, 52.3, 42.1, 39.5, 15.93, 15.88 ppm; HRMS (ESI) calcd for $C_{13}H_{16}NaO_5^+$ [M+Na^+] 275.0890 found 275.0889.

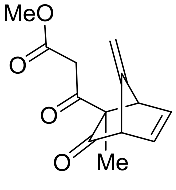

Methyl-3-((1*RS*,2*SR*,4*SR*)-2-methyl-7-methylene-3-oxobicyclo[2.2.1]hept-5-en-2-yl)-3-oxopropanoate (106). A solution of **78** (44.0 mg, 0.25 mmol) in 2 mL THF was added dropwise to a –78 °C cold solution of iPr_2NLi (1.0 M in THF, 0.30 mmol). After 30 min, methyl cyanoformate (30 μL, 0.4 mmol) was added in one portion. The mixture was stirred for 45 min, then warmed to 0 °C and quenched after an additional hour by the addition of

---

[177] The stereochemistry at the bridge position was not established.

5 mL $NaHCO_3$ (aqueous, saturated). The biphasic mixture was diluted with 5 mL EtOAc and the phases separated. The aqueous phase was extracted with EtOAc (3 x 15 mL), the combined organic phases were dried over $MgSO_4$ and concentrated. The crude material was purified by flash column chromatography (hexane/Et_2O 2:1) to provide 7.10 mg (0.03 mmol, 12%) of ketoester **106**.

R_f = 0.37 (hexane/Et_2O 2:1, $KMnO_4$); ^1H NMR (400 MHz, $CDCl_3$) δ 6.65 (dd, *J* = 5.9, 2.9 Hz, 1H), 6.33 (ddd, *J* = 5.9, 3.4, 1.3 Hz, 1H), 4.81 (bs, 1H), 4.67 (bs, 1H), 3.82 (bs, 1H), 3.72 (d, *J* = 9.6 Hz, 1H), 3.70 (s, 3H), 3.53 (d, *J* = 16.3 Hz, 1H), 3.48 (bs, 1H), 1.35 (s, 3H) ppm; ^{13}C NMR (101 MHz, $CDCl_3$) δ 207.0, 200.1, 167.5, 158.6, 140.6, 132.5, 101.2, 64.8, 60.7, 52.5, 51.9, 45.2, 22.4 ppm.

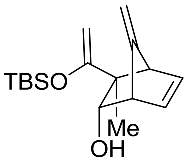

(1*SR*,2*SR*,3*RS*,4*RS*)-3-(1-((*tert*-butyldimethylsilyl)oxy)vinyl)-3-methyl-7-methylene-bicyclo[2.2.1]hept-5-en-2-ol (354). To a solution of **78** (83.0 mg, 0.47 mmol) in 2.3 mL CH_2Cl_2 was added NEt_3 (0.1 mL, 0.7 mmol) and TBSOTf (0.12 mL, 0.54 mmol) at 0 °C. After 1 h, the reaction was warmed to RT and stirred for additional 3 h. The reaction was quenched by the addition of 8 mL water. The phases were separated and the aqueous phase extracted with pentane (3 x 30 mL). The combined organic phases were dried over $MgSO_4$ and concentrated. The resulting crude silyl enol ether (113 mg, 0.39 mmol) was directly dissolved in 3 mL THF and cooled to –40 °C. $LiAlH_4$ (4.0 M in Et_2O, 0.10 mL, 0.39 mmol) was added dropwise. After 10 min, the reaction was quenched by the addition of 10 mL potassium sodium tartrate (aqueous, saturated). The mixture was diluted with 10 mL ether and stirred vigorously for 30 min. The phases were separated, the aqueous phase was extracted with Et_2O (3 x 30 mL) and the combined organic phases were dried over Na_2SO_4. Concentration afforded crude **354** which was purified by flash column chromatography (hexane/Et_2O 5:1 → 2:1) to give 55.4 mg (0.19 mmol, 39% over two steps) of alcohol **354**.

R_f = 0.17 (hexane/Et_2O 2:1, $KMnO_4$); ^1H NMR (300 MHz, $CDCl_3$) δ 6.54 (ddd, *J* = 6.2, 3.5, 0.9 Hz, 1H), 6.35 (dd, *J* = 6.2, 3.0 Hz, 1H), 4.40 – 4.35 (m, 2H), 4.30 (bs, 1H), 4.14 (d, *J* = 2.1 Hz, 1H), 4.03 (d, *J* = 2.1 Hz, 1H), 3.25 (bs, 1H), 3.17 (bs, 1H), 1.19 (d, *J* = 8.4 Hz, 1H), 0.99 (s, 3H), 0.95 (s, 9 H), 0.19 (s, 3H), 0.18 (s, 3H) ppm.

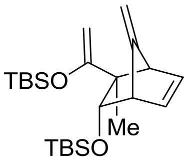

***tert*-Butyl((1-((1*RS*,2*RS*,3*SR*,4*SR*)-3-((*tert*-butyldimethylsilyl)oxy)-2-methyl-7-methylenebicyclo[2.2.1]hept-5-en-2-yl)vinyl)oxy)dimethylsilane (123).** To a solution of **354** (33.0 mg, 0.11 mmol) in 2 mL CH_2Cl_2 was added NEt_3 (24 µL, 0.2 mmol) and TBSOTf (30 µL, 0.1 mmol) at 0 °C. After 30 min, the reaction was quenched by the addition of 10 mL water. The phases were separated and the aqueous phase was extracted with pentane (2 x 20 mL) and once with CH_2Cl_2 (1 x 40 mL). The combined organic phases were washed once with 40 mL brine, dried over $MgSO_4$ and concentrated to yield **123** (36.3 mg, 0.09 mmol, 79%), which did not require further purification.

R_f = 0.89 (hexane/EtOAc 5:1, $KMnO_4$); ^{1}H NMR (300 MHz, $CDCl_3$) δ 6.37 (ddd, *J* = 6.0, 3.2, 0.9 Hz, 1H), 6.22 (dd, *J* = 6.0, 2.9 Hz, 1H), 4.40 (d, *J* = 4.1 Hz, 1H), 4.32 (bs, 1H), 4.27 (bs, 1H), 4.11 (d, *J* = 2.1 Hz, 1H), 4.05 (d, *J* = 2.1 Hz, 1H), 3.18 (app. d, *J* = 2.9 Hz, 1H), 3.11 (app. t, *J* = 3.5 Hz, 1H), 0.96 (s, 9H), 0.93 (s, 3H), 0.86 (s, 9H), 0.19 (s, 3H), 0.17 (s, 3H), 0.09 (s, 3H), 0.06 (s, 3H) ppm.

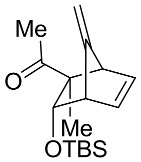

1-((1*RS*,2*RS*,3*SR*,4*SR*)-3-((tert-butyldimethylsilyl)oxy)-2-methyl-7-methylene-bicyclo[2.2.1]hept-5-en-2-yl)ethanone (124). To a solution of silyl enol ether **123** (123.1 mg, 0.303 mmol) in 3 mL CH_2Cl_2 was added AcOH (0.02 mL, 0.36 mmol). After 1 h, additional AcOH (0.06 mL, 1.08 mmol) was added. The reaction was quenched after a total of 4 h by the addition of 5 mL $NaHCO_3$ (aqueous, saturated). The phases were separated and the aqueous phase was extracted with CH_2Cl_2 (2 x 10 mL) and pentane (2 x 10 mL). The combined organic phases were dried over $MgSO_4$ and concentrated. Purification *via* flash column chromatography (hexane/Et_2O 10:1) provided 89.0 mg (0.30 mmol, quant) of ketone **124**.

R_f = 0.43 (hexane/Et_2O 10:1, $KMnO_4$); ^{1}H NMR (300 MHz, $CDCl_3$) δ 6.38 (ddd, *J* = 6.0, 3.2, 0.9 Hz, 1H), 6.28 (dd, *J* = 6.1, 2.9 Hz, 1H), 4.72 (d, *J* = 4.2 Hz, 1H), 4.31 (bs, 2H), 3.26 (app. d, *J* = 2.9 Hz, 1H), 3.10 (app. t, *J* = 3.6 Hz, 1H), 2.18 (s, 3H), 0.97 (s, 3H), 0.87 (s, 9H), 0.11 (s, 3H), 0.07 (s, 3H) ppm.

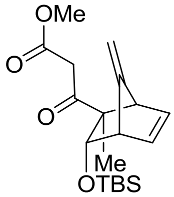

Methyl-3-((1*RS*,2*RS*,3*SR*,4*SR*)-3-((tert-butyldimethylsilyl)oxy)-2-methyl-7-methylenebicyclo[2.2.1]hept-5-en-2-yl)-3-oxopropanoate (125). To a solution of *i*Pr_2NLi (0.39 mmol) in 1.5 mL Et_2O was added **124** (94.0 mg, 0.32 mmol) in 2 mL Et_2O dropwise at –78 °C and the solution was stirred for 1 h 10 min before methyl cyanoformate (51 µL, 0.6 mmol) was added dropwise. After 1 h the reaction was warmed to –40 °C then after 30 min to 0 °C. Another portion of methyl cyanoformate (51 µL, 0.6 mmol) was added. After 3 h, the reaction was quenched by the addition of 5 mL $NaHCO_3$ (aqueous, saturated) and the phases separated. The aqueous phase was extracted with Et_2O (3 x 10 mL), the combined organic phases dried over $MgSO_4$ and concentrated *in vacuo*. Purification was achieved by flash column chromatography (hexane/Et_2O 10:1 → 5:1) to give 11.4 mg (0.03 mmol, 10%) of **125**.

R_f = 0.19 (hexane/Et_2O 5:1, $KMnO_4$); ^1H NMR (300 MHz, $CDCl_3$) δ 6.30 (ddd, *J* = 6.2, 3.2, 0.9 Hz, 1H), 6.23 (dd, *J* = 6.2, 2.6 Hz, 1H), 4.64 (d, *J* = 4.1 Hz, 1H), 4.281 (bs, 1H), 4.284 (bs, 1H), 3.66 (s, 3H), 3.50 (app. d, *J* = 1.3 Hz, 2H), 3.19 (app d, *J* = 2.8 Hz, 1H), 3.05 (app. t, *J* = 3.5 Hz, 1H), 0.92 (s, 3H), 0.80 (s, 9H), 0.04 (s, 3H), 0.00 (s, 3H) ppm.

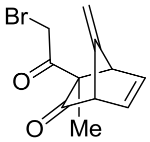

(1*SR*,3*RS*,4*RS*)-3-(2-bromoacetyl)-3-methyl-7-methylenebicyclo[2.2.1]hept-5-en-2-one (128). To a solution of *i*Pr_2NLi (1.0 M in THF, 0.06 mL, 0.1 mmol) was added a solution of **78** (13.1 mg, 0.07 mmol) in 0.5 mL THF at –78 °C. After 30 min, a solution of recrystallized NBS (26.5 mg, 0.15 mmol) in 1 mL THF was added in one portion. After 5 min, 4 mL NH_4Cl (aqueous, saturated), 10 mL water and 20 mL Et_2O were added and the phases separated. The aqueous phase was extracted with Et_2O (3x 40 mL), dried over $MgSO_4$ and concentrated. The crude product was purified by column chromatography (hexane/CH_2Cl_2 1:1) to give bromide **128** (4.1 mg, 0.02 mmol) in 22% yield.

R_f = 0.50 (hexane:Et_2O 2:1, $KMnO_4$); ^1H NMR (300 MHz, $CDCl_3$) δ 6.66 (dd, *J* = 5.8, 2.9 Hz, 1H), 6.35 – 6.33 (m, 1H), 4.82 (s, 1H), 4.68 (s, 1H), 4.27 (d, *J* = 14.4 Hz, 1H), 4.10

(d, *J* = 14.3 Hz, 1H), 3.86 (bs, 1H), 3.50 (bs, 1H), 1.38 (s, 3H) ppm; ^{13}C NMR (101 MHz, $CDCl_3$) δ 207.2, 198.4, 158.5, 140.5, 132.5, 101.6, 64.3, 60.7, 52.5, 32.5, 23.0 ppm.

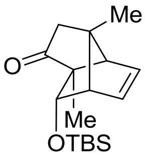

7-((*tert*-butyldimethylsilyl)oxy)-1,3a-dimethyl-1,3a,4,6a-tetrahydro-1,4-methanopentalen-2(3*H*)-one (140). TMSOTf (0.02 mL, 0.10 mmol) was added dropwise to a solution of **124** (26.3 mg, 0.09 mmol) and NEt_3 (0.02 mL, 0.14 mmol) in 1 mL CH_2Cl_2 at 0 °C. After 1 h the reaction was warmed to RT and stirred for further 2.5 h before being quenched by the addition of 5 mL aqueous pH7 buffer. The phases were separated and the aqueous phase extracted with pentane. The combined organic phases were dried over K_2CO_3 and evaporated *in vacuo* to furnish 32.0 mg (0.09 mmol, 98%) of the corresponding silyl enol ether. 11.0 mg (0.03 mmol) of this material were dissolved in 1 mL DMSO, $Pd(OAc)_2$ (7.1 mg, 0.03 mmol) was added and the reaction was heated to 50 °C. After 9 h, 4 drops of formic acid were added, causing immediate precipitation of Pd(0). The suspension was filtered over celite and the excess acid was quenched by the addition of 5 mL $NaHCO_3$ (aqueous, saturated). The phases were separated and the aqueous phase was extracted with EtOAc (3 x 30 mL). The combined organic phases were washed once with 50 mL brine, dried over $MgSO_4$ and concentrated under reduced pressure. Purification *via* flash column chromatography gave **140** (6.0 mg, 0.02 mmol, 68%).

R_f = 0.40 (hexane/Et_2O 5:1, CAM); ^{1}H NMR (300 MHz, $CDCl_3$) δ 6.07 (bs, 2H), 4.01 (d, *J* = 4.6 Hz, 1H), 2.83 (bs, 1H), 2.36 (d, *J* = 18.8 Hz, 1H), 2.34 (bs, 1H), 1.89 (d, *J* = 18.8 Hz, 1H), 1.04 (s, 3H), 0.90 (s, 3H), 0.83 (s, 9H), 0.01 (s, 3H), -0.02 (s, 3H) ppm; ^{13}C NMR (101 MHz, $CDCl_3$) δ 214.6, 136.4, 129.6, 75.7, 61.9, 60.8, 58.6, 44.0, 25.8, 18.3, 16.6, 9.8, −4.8, –5.0 ppm; FT-IR (neat) ν_{max} = 2954, 2929, 2858, 1746, 1472, 1252, 1143, 1130, 1105, 1080, 890, 836, 775 cm^{-1}; HRMS (ESI) calcd for $C_{17}H_{29}O_2Si^+$ [M+H^+] 293.1931, found 293.1930.

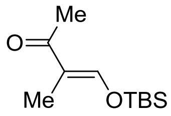

&116

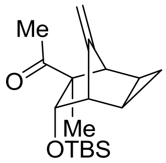

&117

(*E*)-4-((*tert*-butyldimethylsilyl)oxy)-3-methylbut-3-en-2-one (142) and 1-((1*SR*,2*RS*,5*RS*,6*RS*,7*SR*)-7-((tert-butyldimethylsilyl)oxy)-6-methyl-8-methylenetricyclo[3.2.1.0^{2,4}]octan-6-yl)ethanone (143). $ZnEt_2$ (1.0 M in hexane, 0.23 mL, 0.2 mmol) was added to 0.2 mL CH_2Cl_2 at 0 °C. Then TFA (2.0 M in CH_2Cl_2, 0.16 mL, 0.2 mmol) was added dropwise. After 20 min of stirring, the formed white precipitate was dissolved by warming the reaction in a 30 °C water bath. Then the reaction was recooled to 0 °C, upon which a fine white suspension forms, CH_2I_2 (2.0 M in CH_2Cl_2, 0.16 mL, 0.2 mmol) was added and the mixture was stirred again for 20 min. Then **124** (34.0 mg, 0.12 mmol) in 0.4 mL CH_2Cl_2 was added dropwise. The ice bath was removed and after 30 min TLC analysis showed complete conversion. 5 mL NH_4Cl (aqueous, saturated) were added. The biphasic mixture was poured into a separation funnel additional 15 mL of brine were added, followed by 20 mL CH_2Cl_2. Phase separation, extraction of the aqueous phase (CH_2Cl_2, 3 x 30 mL), subsequent drying over $MgSO_4$ and concentration afforded crude **143**. Purification by column chromatography (hexane/Et_2O 20:1 → 5:1 → 2:1) provided 9.2 mg (0.03 mmol, 26%) of **143** along with 18.1 mg (0.08 mmol, 73%) of enol ether **142**.

142:

R_f = 0.13 (hexane:Et_2O, 5:1); ^{1}H NMR (300 MHz, $CDCl_3$) δ 7.46 (q, *J* = 1.4 Hz, 1H), 2.21 (s, 3H), 1.72 (d, *J* = 1.4 Hz, 3H), 0.95 (s, 9H), 0.24 (s, 6H) ppm.

143:

R_f = 0.59 (hexane/Et_2O 5:1, $KMnO_4$); ^{1}H NMR (300 MHz, $CDCl_3$) δ 4.63 (app. d, *J* = 3.6 Hz, 2H), 4.51 (d, *J* = 4.3 Hz, 1H), 2.73 (bs, 1H), 2.53 (app. d, *J* = 4.5 Hz, 1H), 2.11 (s, 3H), 1.31 – 1.26 (m, 1H), 1.19 (s, 3H), 1.12 – 1.06 (m, 1H), 0.92 (s, 9H), 0.11 (s, 3H), 0.08 (s, 3H) ppm; ^{13}C NMR (101 MHz, $CDCl_3$) δ 211.6, 145.6, 106.0, 73.2, 60.1, 50.3, 49.0, 26.0, 25.8, 18.4, 15.1, 9.2, 7.9, 4.1, –4.5, –5.0 ppm.

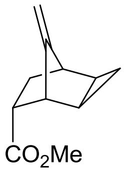

(1*RS*,4*RS*,5*RS*,6*RS*)-methyl-8-methylenetricyclo[3.2.1.0^{2,4}]octane-6-carboxylate (148).[178] $ZnEt_2$ (1.0 M in hexanes, 185 mL, 185 mmol) was added to a 0 °C cold solution of diene **95** (15.17 g, 92.39 mmol) in 450 mL CH_2Cl_2. After 3 min, $ClCH_2I$ (27.6 mL, 370 mmol) was added slowly to the clear solution. The reaction was stirred for 2 h 45 min at this temperature until TLC showed complete conversion of the starting material.

The reaction was quenched with 300 mL saturated sodium potassium tartrate and stirred vigorously for 60 min. The precipitated zinc salts were removed by filtration over a pad of celite, which was rinsed with 400 mL CH_2Cl_2 and 200 mL water. The phases were separated and the aqueous layer was extracted with CH_2Cl_2 (4 x 150 mL). The combined organic layers were washed with brine (200 mL), then dried over $MgSO_4$ and concentrated. The crude product was purified by flash column chromatography (hexane/Et_2O 20:1) to give 13.93 g (78.16 mmol, 85%) of a colorless oil.[179]

R_f = 0.49 (hexane/Et_2O 10:1, anisaldehyde, green spot); ^{1}H NMR (500 MHz, $CDCl_3$) δ 4.65 (d, J = 8.1 Hz, 2H), 3.71 (s, 3H), 2.82 – 2.76 (m, 2H), 2.49 (d, J = 4.0 Hz, 1H), 1.94 (dd, J = 12.0, 4.5 Hz, 1H), 1.76 (ddd, J = 12.0, 10.1, 4.0 Hz, 1H), 0.93 – 0.90 (m, 1H), 0.82 – 0.80 (m, 1H), 0.19 – 0.16 (m, 1H), 0.13 – 0.09 (m, 1H) ppm; ^{13}C NMR (101 MHz, $CDCl_3$) δ 174.8, 150.0, 103.1, 51.8, 45.5, 45.3, 42.2, 31.5, 13.7, 9.7, 3.1 ppm; FT-IR (neat) ν_{max} = 3071, 2951, 2844, 1736, 1435, 1342, 1196, 1168, 1048, 887, 811, 765, 718 cm^{-1}; HRMS (ESI) calcd for $C_{11}H_{15}O_2^+$ [M+H$^+$] 179.1067, found 179.1069.

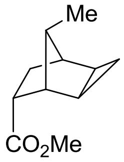

(1*SR*,4*RS*,5*RS*,6*RS*,8*SR*)-methyl-8-methyltricyclo[3.2.1.0^{2,4}]octane-6-carboxylate (150). To a solution of **148** (13.93 g, 78.16 mmol) in 430 mL CH_2Cl_2 was added WILKINSON's catalyst (2.89 g, 3.13 mmol) in one portion. The volume of a standard balloon of H_2 was bubbled through the deep red solution, then it was stirred for 8 h under positive H_2 pressure (1 atm) until reaction ^{1}H NMR displayed full conversion.

---

[178] S. E. Denmark, J. P. Edwards, *J. Org. Chem.* **1991**, *56*, 6974-6981.

[179] Dicyclopropananted byproduct almost coeluates with the desired product **148**. Using anisaldehyde as TLC stain, a color difference is visible (byproduct appears blue, **148** green). **148** is slightly less polar. The mixed fraction was resubjected to flash column chromatography, until separation was complete.

The solvent was evaporated and the residue was purified by flash column chromatography (hexane/Et_2O 10:1) to yield 13.50 g (74.90 mmol, 96%) of **150** as a colorless oil with a characteristic smell.

R_f = 0.40 (hexane/Et_2O 10:1, anisaldehyde, blue spot); ^{1}H NMR (400 MHz, $CDCl_3$) δ 3.66 (s, 3H), 2.72 (ddd, J = 10.0, 4.8, 3.7 Hz, 1H), 2.51 (d, J = 3.4 Hz, 1H), 2.21 (d, J = 3.7 Hz, 1H), 1.76 – 1.60 (m, 2H), 1.47 (q, J = 7.4 Hz, 1H), 0.93 (d, J = 7.4 Hz, 3H), 0.88 – 0.83 (m, 1H), 0.78 – 0.71 (m, 2H), 0.00 – –0.05 (m, 1H) ppm; ^{13}C NMR (75 MHz, $CDCl_3$) δ 175.3, 51.5, 48.1, 45.1, 41.9, 39.1, 33.7, 16.6, 16.2, 12.7, 5.3 ppm; FT-IR (neat) ν_{max} = 3020, 2951, 2886, 1737, 1435, 1333, 1282, 1197, 1169, 1108, 1036, 811, 764, 720 cm^{-1}; HRMS (ESI) calcd for $C_{11}H_{17}O_2^+$ [M+H$^+$] 181.1223, found 181.1223.

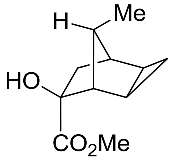

(1*SR*,4*RS*,5*RS*,6*SR*,8*SR*)-methyl-6-hydroxy-8-methyltricyclo[3.2.1.0^{2,4}]octane-6-carboxylate (152).[180] To a solution of 22.4 mL *i*-Pr_2NH (157 mmol) in 240 mL THF was added *n*-BuLi (1.65 M in hexanes, 91 mL, 150 mmol) at 0 °C. After 15 min, the reaction was cooled to –78 °C and **150** (13.50 g, 74.90 mmol) in 60 mL THF was added dropwise *via* cannula. After stirring for 1.5 h, $P(OEt)_3$ (13.1 mL, 74.9 mmol) was added, followed by DMPU (9.0 mL, 74.9 mmol). Then the reaction was cooled to –90 °C and oxygen was bubbled through for 1.5 h.

The reaction was quenched by the addition of 300 mL NH_4Cl (aqueous, saturated) followed by 100 mL water. The phases were separated and the aqueous phase was extracted with EtOAc (4 x 200 mL). The combined organic phases were dried over Na_2SO_4 and concentrated. The crude product was purified by column chromatography (hexane/EtOAc 4:1 → 3:1) to yield 12.44 g (63.39 mmol, 85%) of **152** as a yellow viscous oil and a 10:1 mixture of diastereomers.

R_f = 0.31 (hexane/EtOAc 5:1, anisaldehyde, blue spot); ^{1}H NMR (400 MHz, $CDCl_3$) δ *for the major diastereomer* 3.75 (s, 3H), 2.69 (s, 1H), 2.26 – 2.18 (m, 3H), 2.08 (q, J = 7.4 Hz, 1H), 1.50 (dd, J = 12.6, 3.8 Hz, 1H), 1.02 – 0.88 (m, 5H, methyl group doublet: J = 7.4 Hz),

---

[180] G. Helmchen, A. Krotz, H. P. Neumann, M. L. Ziegler, *Liebigs Ann. Chem.* **1993**, 1313-1317.

0.58 – 0.51 (m, 1H), 0.24 – 0.17 (m, 1H) ppm; ^{13}C NMR (101 MHz, $CDCl_3$) δ 175.1, 83.7, 53.4, 52.4, 43.6, 41.4, 34.9, 17.8, 15.7, 12.3, 9.1 ppm; FT-IR (neat) ν_{max} = 3465, 2951, 3884, 1723, 1500, 1436, 1331, 1272, 1259, 1195, 1164, 1105, 1081, 1040, 989, 969, 911, 868, 857, 814, 799, 754, 667 cm^{-1}; HRMS (MALDI) calcd for $C_{11}H_{16}NaO_3^+$ [*M*+Na$^+$] 219.0992, found 219.0992.

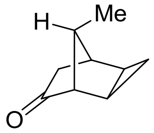

(1*SR*,4*RS*,5*RS*,8*SR*)-8-methyltricyclo[3.2.1.0^{2,4}]octan-6-one (146). To a solution of **152** (6.200 g, 31.59 mmol) in 300 mL Et_2O was added $LiAlH_4$ (4.0 M in Et_2O, 5.53 mL, 22 mmol) dropwise at 0 °C.

After 30 min the reaction was quenched by the addition of 30 mL EtOAc, then 150 mL sodium potassium tartrate (aqueous, saturated) and 50 mL additional water. The mixture was stirred vigorously for 1 h. The phases were separated and the aqueous phase was extracted with EtOAc (10 x 100 mL), dried over Na_2SO_4 and concentrated to give the crude diol as a yellow wax.

This crude material was directly used for the next step without further purification. To a 0 °C solution of the diol in 300 mL of a mixture THF:phosphate-buffer (pH 7) (1:1) was added $NaIO_4$ (9.95 g, 46.5 mmol) in one portion. The reaction was stirred for 1 h and kept between 0 °C and 4 °C.

The excess $NaIO_4$ was quenched by the addition of 100 mL $Na_2S_2O_3$ (aqueous, saturated). After 5 min, the biphasic mixture was diluted with 50 mL water, 100 mL Et_2O were added and the phases separated. The aqueous layer was extracted with Et_2O (3 x 150 mL). The combined organic phases were dried over $MgSO_4$ and concentrated *in vacuo*. Purification by flash column chromatography (pentane/Et_2O 5:1) gave 4.220 g (30.8 mmol, 97% from **S2**) of **146** as a faint yellow oil.[181]

R_f = 0.37 (hexane/Et_2O 5:1, anisaldehyde, green-blue spot); ^{1}H NMR (400 MHz, $CDCl_3$) δ 2.59 (s, 1H), 2.52 (d, *J* = 3.4 Hz, 1H), 2.12 (dd, *J* = 16.9, 3.4 Hz, 1H), 2.03 (d, *J* = 16.9 Hz, 1H), 1.72 (q, *J* = 7.4 Hz, 1H), 1.29 – 1.22 (m, 2H), 1.10 (d, *J* = 7.4 Hz, 3H), 1.03 – 0.97 (m, 1H), 0.53 (app. q, *J* = 7.3 Hz, 1H) ppm; ^{13}C NMR (101 MHz, $CDCl_3$) δ 214.1, 53.8, 47.9, 40.8, 36.1, 19.6, 16.4, 11.7, 11.2 ppm; FT-IR (neat) ν_{max} = 3116, 3029, 2965, 2929, 2875,

---

[181] **146** proved to be highly volatile, therefore extreme care has to be taken during the distillation of the solvents.

1740, 1452, 1439, 1380, 1206, 1038, 949, 890, 804, 714 cm^{-1}; HRMS (EI) calcd for $C_9H_{12}O^+$ [M^+] 136.0888, found 136.0885.

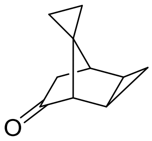

(1'*RS*,4'*RS*,5'*SR*)-spiro[cyclopropane-1,8'-tricyclo[3.2.1.0^{2,4}]octan]-6'-one (355). This compound was obtained as a byproduct, when a mixture of **148** and **149** was taken through the following sequence: Wilkinson reduction, α-hydroxylation, ester reduction and diol cleavage.

R_f = 0.29 (hexane:Et_2O 6:1, $KMnO_4$); ^{1}H NMR (400 MHz, $CDCl_3$) δ 2.30 (dd, J = 16.6, 3.5 Hz, 1H), 2.10 (d, J = 16.6 Hz, 1H), 2.08 (bs, 1H), 1.91 (d, J = 3.5 Hz, 1H), 1.44 – 1.42 (m, 1H), 1.33 – 1.28 (m, 1H), 1.11 – 1.07 (m, 1H), 0.72 – 0.66 (m, 1H), 0.64 – 0.58 (m, 1H), 0.54 – 0.48 (m, 1H), 0.29 – 0.20 (m, 1H) ppm; ^{13}C NMR (101 MHz, $CDCl_3$) δ 213.9, 54.6, 45.8, 41.8, 24.6, 19.1, 11.8, 10.3, 7.7, –0.1 ppm; FT-IR (neat) ν_{max} = 2954, 2918, 1746, 1413, 1310, 1267, 1131, 1043, 1019, 962, 920, 806, 758 cm^{-1}; HRMS (EI) calcd for $C_{10}H_{12}O^+$ [M^+] 148.0883, found 148.0883.

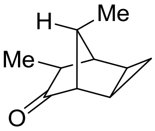

(1*SR*,4*RS*,5*RS*,7*SR*,8*SR*)-7,8-dimethyltricyclo[3.2.1.0^{2,4}]octan-6-one (154).[182] To *i*-Pr_2NH (5.16 mL, 36.2 mmol) in 130 mL THF was added *n*-BuLi (1.66 M in hexanes, 20.3 mL, 33.8 mmol) at 0 °C. After 20 min, the reaction was cooled to –78 °C and **146** (1.85 g, 13.6 mmol) in 2.5 mL THF was added dropwise. The reaction was stirred for 1 h 15 min at this temperature and then 30 min at –40 °C. The mixture was then warmed to 0 °C and stirred for 5 min, before MeI (15.1 mL, 241 mmol) was added rapidly in one shot (t ≈ 1 s).

NEt_3 (33.6 mL, 241 mmol) was added after 5 min and stirring was continued for 15 min. Then 80 mL water were added to dissolve the formed ammonium salt, followed by 100 mL

---

[182] The conditions described here where found best after excessive experimentation. The formation of a byproduct was observed when the reaction was not first quenched with NEt_3 but directly with aqueous solutions. Lower temperature during the alkylation step led to poor and irreproducible conversions.

NH_4Cl (aqueous, saturated). The phases were separated and the aqueous phase was extracted with Et_2O (3 x 200 mL). The combined organic phases were washed with 200 mL NH_4Cl (aqueous, saturated), dried over $MgSO_4$ and concentrated. The crude oil was purified by flash column chromatography (pentane/Et_2O 15:1) to give **154** (1.81g, 12.1 mmol) in 89% yield as a 5:1 mixture of diastereomers.[183]

$R_f = 0.57$ (hexane/Et_2O 4:1, anisaldehyde, green-blue spot); ^1H NMR (400 MHz, $CDCl_3$) δ *for the major diastereomer* 2.54 (s, 1H), 2.22 (s, 1H), 2.12 (q, J = 7.4 Hz, 1H), 1.86 (q, J = 7.3 Hz, 1H), 1.27 – 1.17 (m, 2H), 1.11 (d, J = 7.4 Hz, 3H), 1.09 (d, J = 7.4 Hz, 3H), 1.06 – 1.01 (m, 1H), 0.57 – 0.49 (m, 1H) ppm; ^{13}C NMR (101 MHz, $CDCl_3$) δ *for the major diastereomer* 217.3, 54.1, 51.4, 46.7, 32.4, 20.2, 16.3, 14.7, 11.8, 11.6 ppm; FT-IR (neat) ν_{max} = 2968, 2936, 1743, 1457, 1372, 1323, 1147, 1039, 939, 816, 804, 725 cm^{-1}; HRMS (EI) calcd for $C_{10}H_{14}O^+$ [M^+] 150.1040, found 150.1037.

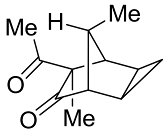

(1*SR*,4*RS*,5*RS*,7*SR*,8*SR*)-7-acetyl-7,8-dimethyltricyclo[3.2.1.0^{2,4}]octan-6-one (155). To a solution of ketone **154** (1.60 g, 10.65 mmol) in 53 mL CH_2Cl_2 was added triethylamine (2.2 mL, 16 mmol). The solution was cooled to 0 °C and TBSOTf (2.6 mL, 11 mmol) was added dropwise. The reaction was stirred at this temperature for 6 h and then quenched by the addition of 20 mL pH 7 buffer. 50 mL pentane were added and the phases separated. The aqueous phase was extracted with pentane (3 x 30 mL), dried over K_2CO_3 and concentrated *in vacuo* to yield the crude silyl enol ether.

This crude material was dissolved in 35 mL CH_2Cl_2 and cooled to –90 °C. Freshly distilled acetaldehyde (6.0 mL, 110 mmol) was added, followed by $BF_3{\cdot}OEt_2$ (2.7 mL, 21 mmol). After 45 min, the reaction was quenched by the addition of pH 7 buffer (30 mL). The phases were separated and the aqueous phase was extracted with CH_2Cl_2 (3 x 80 mL), dried over Na_2SO_4 and concentrated. The crude material was purified by column chromatography (hexane/Et_2O 15:1 to eluate **154**, then hexane/EtOAc 3:1 to eluate the aldol diastereomers). The recovered starting material was recycled. After three cycles, 1.44 g (7.42 mmol) of the aldol products were obtained.

---

[183] **154** proved to be volatile. Therefore care should be taken during the distillation of solvents.

To a suspension of DESS-MARTIN periodinane (6.30 g, 14.9 mmol) and $NaHCO_3$ (2.49 g, 29.7 mmol) in 65 mL CH_2Cl_2 was added *t*BuOH (1.4 mL, 15 mmol) at 0 °C.[184] After 5 min, the aldol products were added (1.44 g, 7.42 mmol) as a solution in 8.5 mL CH_2Cl_2. After 35 min, the reaction was quenched by careful addition of sodium thiosulfate (aqueous, saturated, 70 mL) followed by $NaHCO_3$ (aqueous, saturated, 50 mL). After the mixture was stirred vigorously for 10 min, the phases were separated and the aqueous phase was extracted with CH_2Cl_2 then poured in a separation funnel containing 50 mL CH_2Cl_2 and 50 mL $NaHCO_3$ (aqueous, saturated). The phases were separated and the aqueous phase was extracted with CH_2Cl_2 (3 x 80 mL). The combined organic phases were washed with $NaHCO_3$ (aqueous, saturated, 2 x 100 mL), dried over Na_2SO_4 and concentrated *in vacuo*. The crude material was purified by flash column chromatography (hexane/Et_2O 5:1) to yield diketone **155** (1.424 g, 7.41 mmol, 70% from **S3**) as a 5:1 mixture of diastereomers.

R_f = 0.37 (hexane/EtOAc 4:1, anisaldehyde, yellow spot); ^1H NMR (300 MHz, $CDCl_3$) *δ for the major diastereomer* 2.88 (s, 1H), 2.60 (s, 1H), 2.19 (s, 3H), 1.58 (q, *J* = 7.1 Hz, 1H), 1.38 –1.25 (m, 2H), 1.08 (d, *J* = 7.1 Hz, 3H), 1.09 – 1.02 (m, 4H), 0.55 – 0.47 (m, 1H) ppm; ^{13}C NMR (101 MHz, $CDCl_3$) *δ for the major diastereomer* 212.2, 207.0, 70.9, 54.2, 46.8, 35.2, 26.8, 18.7, 16.5, 14.1, 13.5, 11.3 ppm; FT-IR (neat) ν_{max} = 2973, 2935, 1743, 1700, 1450, 1356, 1215, 1142, 1097, 1039, 814, 773, 723, 669, 554 cm^{-1}; HRMS (EI) calcd for $C_{12}H_{16}O^+$ [M^+] 192.1145, found 192.1147.

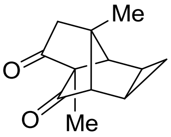

2,4a-dimethylhexahydro-1*H*-2,5-methanocyclopropa[*a*]pentalene-3,6(1a*H*)-dione (76).[185] LiHMDS (0.282 g, 1.685 mmol) was dissolved in 3.4 mL THF and cooled to –78 °C, before a solution of **155** (0.282 g, 1.467 mmol) in 3.4 mL THF was added dropwise. After 45 min, 2,2,2-trifluoroethyl 2,2,2-trifluoroacetate (0.26 mL, 1.94 mmol) was added rapidly in one portion. After 15 min, the reaction was poured into a separation funnel containing 5 mL HCl (5%, aqueous) and 10 mL ether. The aqueous phase was extracted with ether (2 x 20 mL), the combined organic phases were washed with 15 mL brine and concentrated.

The yellow residue was dissolved in 3 mL MeCN, then water (26 μL, 1.5 mmol), followed by triethylamine (0.31 mL, 2.24 mmol) was added. After 2 min, methanesulfonyl azide

---

[184] See ref. 80 a) and b).

[185] R. L. Danheiser, R. F. Miller, R. G. Brisbois, S. Z. Park, *J. Org. Chem.* **1990**, *55*, 1959-1964.

(1.0 M in MeCN, 2.2 mL, 2.2 mmol) was added dropwise. The reaction was stirred for 3.5 h and then concentrated to a volume of circa 2 mL. The reaction mixture was poured in a separation funnel containing 20 mL Et_2O and 10 mL NaOH (10%, aqueous). The organic phase was washed two additional times with NaOH (10%, aqueous), then once with brine (10 mL). The solvent was evaporated and the crude yellow oil directly used in the next step, since attempted column chromatography resulted in decomposition of the material.

A solution of the crude diazo compound dissolved in 8 mL CH_2Cl_2 was added dropwise to a refluxing solution of $Rh_2(OAc)_4$ (6.5 mg, 1.5 mol%) in 10 mL CH_2Cl_2. After 35 min, TLC analysis showed complete consumption of the diazo compound. The reaction was cooled to RT and the solvent evaporated. The crude residue was purified by flash column chromatography to yield **76** as a yellow oil (0.214 g, 1.126 mmol, 76%).

R_f = 0.37 (hexane/EtOAc 4:1, $KMnO_4$); ^{1}H NMR (400 MHz, $CDCl_3$) δ 2.76 (s, 1H), 2.44 (d, J = 19.3 Hz, 1H), 2.40 (s, 1H), 2.16 (d, J = 19.3 Hz, 1H), 1.62 – 1.54 (m, 1H), 1.49 (app. dt, J = 6.8, 3.4 Hz, 1H), 1.34 (s, 3H), 1.23 (s, 3H), 1.15 – 1.08 (m, 1H), 0.69 (app. q, J = 7.5 Hz, 1H) ppm; ^{13}C NMR (101 MHz, $CDCl_3$) δ 207.1, 205.7, 77.3, 58.3, 56.6, 48.4, 39.4, 21.5, 16.4, 15.3, 12.1, 6.9 ppm; FT-IR (neat) ν_{max} = 2931, 1762, 1729, 1450, 1319, 1229, 1174, 1077, 1056, 903, 881, 767, 719, 585 cm^{-1}; HRMS (EI) calcd for $C_{12}H_{14}O_2^+$ [M^+] 190.0989, found 190.0987.

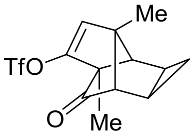

2,4a-dimethyl-6-oxo-1a,1b,2,4a,5,5a-hexahydro-1*H*-2,5-methanocyclopropa[*a*]-pentalen-3-yl trifluoromethanesulfonate (367). To *i*Pr_2NH (0.22 mL, 1.6 mmol) in 6 mL THF was added *n*-BuLi (1.6 M in hexanes, 0.96 mL, 1.5 mmol) at 0 °C. After 10 min, this solution was cooled to –78 °C and a solution of **76** (0.193 g, 1.015 mmol) in 2 mL THF was added dropwise. After 45 min, a solution of $PhNTf_2$ (0.725 g, 2.029 mmol) in 2 mL THF was added dropwise. The dry ice pieces were removed and the bath was warmed to –30 °C by the addition of acetone and then warmed to 0 °C by itself. After 7.5 h reaction was quenched by the addition of 5 mL $NaHCO_3$ (aqueous, saturated). The biphasic mixture was poured in a separation funnel containing 20 mL water and 20 mL ether. The phases were separated and the aqueous phase was extracted with ether (3 x 20 mL). The combined organic phases were dried over Na_2SO_4 and concentrated. Purification using flash column chromatography (hexane/Et_2O 25:1 →15:1) provided **367** as a yellow oil (0.208 g, 0.645 mmol, 64%).

R_f = 0.34 (hexane/EtOAc 15:1, $KMnO_4$); ^1H NMR (300 MHz, CD_2Cl_2) δ 5.55 (s, 1H), 2.81 (s, 1H), 2.47 (s, 1H), 1.33 (s, 3H), 1.30 – 1.20 (m, 6H), 0.59 – 0.50 (m, 1H) ppm; ^{13}C NMR (101 MHz, CD_2Cl_2) δ 206.8, 147.6, 126.2, 118.7 (q, J = 321.0 Hz), 72.6, 64.4, 47.2, 45.0, 21.0, 17.4, 10.9, 10.1, 6.1 ppm; ^{19}F-NMR (282 MHz, CD_2Cl_2) δ 73.6 ppm; FT-IR (neat) ν_{max} = 3032, 2977, 2936, 2881, 1754, 1630, 1425, 1210, 1137, 1059, 1045, 868, 849, 834, 760, 612 cm^{-1}; HRMS (MALDI) calcd for $C_{13}H_{14}F_3O_4S^+$ [M+H^+] 323.0559, found 323.0560.

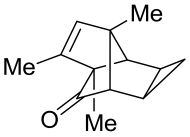

2,3,4a-trimethyl-1a,1b,2,4a,5,5a-hexahydro-1*H*-2,5-methanocyclopropa[*a*]pentalen-6-one (172).

To a solution of **367** (0.209 g, 0.648 mmol) in 2.0 mL of degassed THF was added $Pd(PPh_3)_4$ (0.037 g, 0.032 mmol) dissolved in 1.0 mL of degassed THF at 0 °C. After 5 min, $ZnMe_2$ (1.2 M in toluene, 2.70 ml, 3.2 mmol) was added dropwise and after 5 more min, the cooling bath was removed. The mixture was stirred overnight until TLC showed the complete disappearance of the starting material. The reaction was quenched by careful addition of pH 7 buffer (3 mL) at 0 °C. The cooling bath was removed, 20 mL water were added, followed by

50 mL ether. The phases were separated and the aqueous phase was extracted with ether (3 x 50 mL), dried over Na_2SO_4 and concentrated. The crude material was purified by flash column chromatography (hexane/Et_2O 8:1, buffered with 1% NEt_3) to yield 0.122 g (0.648 mmol, quant) of **172**.[186]

R_f = 0.56 (hexane/EtOAc 10:1, $KMnO_4$); ^{1}H NMR (300 MHz, CD_2Cl_2) δ 5.40 (d, J = 1.7 Hz, 1H), 2.55 (s, 1H), 2.28 (s, 1H), 1.57 (d, J = 1.7 Hz, 3H), 1.26 – 1.11 (m, 9H), 0.48 –0.41 (m, 1H) ppm; ^{13}C NMR (101 MHz, CD_2Cl_2) δ 210.9, 140.1, 139.0, 73.2, 67.5, 49.8, 46.8, 21.4, 17.0, 12.9, 12.3, 10.7, 8.4 ppm; FT-IR (neat) ν_{max} = 3028, 2964, 2929, 2875, 1740, 1452, 1439, 1380, 1248, 1206, 1038, 949, 890, 804, 782, 714 cm^{-1}; HRMS (ESI) calcd for $C_{13}H_{17}O^+$ [M+H$^+$] 189.1274, found 189.1281.

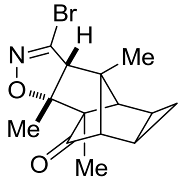

(3a*RS*,6a*RS*)-3-bromo-3b,6,6a-trimethyl-3b,4,4a,5,5a,5b,6,6a-octahydro-3a*H*-4,6-methanocyclopropa[4,5]pentaleno[1,2-*d*]isoxazol-7-one (177).

To a solution of **172** (0.110 g, 0.584 mmol) in 6 mL EtOAc was added potassium bicarbonate (0.292 g, 2.917 mmol), followed by dibromoformaldoxime (0.296 g, 1.459 mmol). After 1 h 15 min, the reaction was diluted with 5 mL CH_2Cl_2 and quenched by careful addition of 3 mL NH_4Cl (aqueous, saturated). The phases were separated and the aqueous phase extracted with CH_2Cl_2 (3 x 25 mL). The combined organic phases were dried over Na_2SO_4 and concentrated *in vacuo*. Purification *via* flash column chromatography yielded **177** as a white amorphous solid (0.165 g, 0.532 mmol, 91%). This material could be crystallized *via* vapor diffusion from hexane → CH_2Cl_2.

R_f = 0.20 (hexane/EtOAc 5:1, CAM); ^{1}H NMR (400 MHz, $CDCl_3$) δ 2.78 (s, 1H), 2.59 (s, 1H), 2.43 (s, 1H), 1.51 – 1.42 (m, 2H), 1.37 (s, 3H), 1.25 (s, 3H), 1.20 (s, 3H), 0.94 – 0.90 (m, 1H), 0.62 – 0.57 (m, 1H) ppm; ^{13}C NMR (101 MHz, $CDCl_3$) δ 211.7, 138.2, 93.9, 67.3, 65.8, 56.5, 54.4, 49.1, 19.2, 18.5, 14.7, 14.0, 12.3, 7.5 ppm; FT-IR (neat) ν_{max} = 2972, 2934, 1748, 1600, 1505, 1450, 1384, 1277, 1207, 1095, 906, 837, 814, 805, 758 cm^{-1}; HRMS (ESI) calcd for $C_{14}H_{17}BrNO_2^+$ [M+H$^+$] 310.0437, found 310.0442.

---

[186] Olefin **172** proved to be unstable upon prolonged exposure to silica gel.

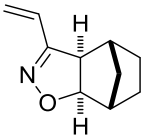

(3a*RS*,4*RS*,7*SR*,7a*RS*)-3-vinyl-3a,4,5,6,7,7a-hexahydro-4,7-methanobenzo[*d*]isoxazole 181. $CeCl_3$ (171 mg, 0.69 mmol) was heated to 140 °C for 2 h, then cooled to RT and suspended in 1 mL THF for 2 h. The suspension was cooled to –78 °C and vinylmagnesium bromide (0.57 M in THF, 1.21 mL, 0.69 mmol) was added dropwise. After 30 min, a solution of **180** (50.0 mg, 0.23 mmol) in 0.5 mL THF was added dropwise at –40 °C. The reaction was then warmed to 5 °C by itself and quenched after 2 h with water. EtOAc (10 mL) was added, the phases separated and the aqueous phase extracted with EtOAc (3x 10 mL). The combined organic phases were washed with brine, dried over Na_2SO_4 and concentrated. The crude material was purified by flash column chromatography to provide **181** (20.0 mg, 0.12 mmol, 53%) as a colorless oil. The spectral data were in accordance to the literature.[187]

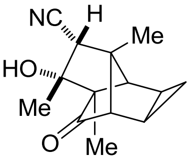

(3*RS*,4*SR*)-3-hydroxy-2,3,4a-trimethyl-6-oxooctahydro-1*H*-2,5-methanocyclopropa-[*a*]pentalene-4-carbonitrile (186). To a 0 °C solution of **177** (35.0 mg, 0.11 mmol) in 1 mL MeCN was added NaI (101 mg, 0.68 mmol) followed by the dropwise addition of TMSCl (87 µL, 0.7 mmol). After 5 min, the cooling bath was removed, after 3.5 h, additional NaI (101 mg, 0.68 mmol) and TMS-Cl (87 µL, 0.7 mmol) were added. After 4.5 h, the reaction was diluted with 5 mL EtOAc and poured in a separation funnel, containing 10 mL $NaHCO_3$ (aqueous, saturated). Phase separation and extraction of the aqueous phase (EtOAc 3 x 10 mL), followed by washing the combined organic phases 50 mL with $Na_2S_2O_3$ (aqueous, saturated), drying over Na_2SO_4 and concentration afforded crude nitrile **186**. Purification *via* flash column chromatography (hexane/EtOAc 4:1) furnished 25.8 mg (0.11 mmol, 99%).

R_f = 0.32 (hexane:EtOAc 3:1, CAM); ^{1}H-NMR (400 MHz, $CDCl_3$) δ 2.82 – 2.78 (m, 2H), 2.54 (s, 1H), 1.98 (bs, 1H), 1.51 – 1.42 (m, 2H), 1.39 (s, 3H), 1.23 (s, 3H), 1.18 (s, 3H), 0.95 – 0.88 (m, 1H), 0.66 – 0.58 (m, 1H) ppm; ^{13}C-NMR (101 MHz, $CDCl_3$) δ 213.2, 117.2, 67.7, 58.9, 54.9, 52.3, 44.7, 22.8, 20.0, 14.3, 14.0, 12.0, 7.3 ppm; FT-IR (neat) ν_{max} = 3458,

---

[187] P. W. Ambler, R. M. Paton, J. M. Tout, *Chem. Commun.* **1994**, 2661-2662.

3032, 2972, 2928, 2243, 1746, 1453, 1386, 1157, 1071, 915, 730 cm^{-1}; HRMS (ESI) calcd for $C_{14}H_{21}N_2O_2^+$ [*M*+NH_4^+] 249.1598, found 249.1597.

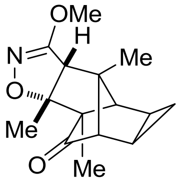

(3a*RS*,6a*RS*)-3-methoxy-3b,6,6a-trimethyl-3b,4,4a,5,5a,5b,6,6a-octahydro-3a*H*-4,6-methanocyclopropa[4,5]pentaleno[1,2-*d*]isoxazol-7-one (188).

To **177** (0.356 g, 1.148 mmol) was added lithium methanolate (1.5 M in MeOH, 15 mL) and the reaction was refluxed for 7 d. The reaction was cooled to RT, concentrated to ca. 5 mL and poured in a separation funnel containing 50 mL water and 50 mL EtOAc. The phases were separated and the aqueous phase was extracted with EtOAc (3 x 10 mL). The combined organic phases were dried over Na_2SO_4 and concentrated to give crude **188** (0.282 g, 1.08 mmol, 94%) which did not require any further purification.

R_f = 0.46 (hexane/EtOAc 2:1, CAM); ^{1}H NMR (400 MHz, $CDCl_3$) δ 3.83 (s, 3H), 2.55 (s, 1H), 2.53 (s, 1H), 2.51 (s, 1H), 1.48 – 1.41 (m, 2H), 1.21 (s, 3H), 1.20 (s, 3H), 1.17 (s, 3H), 0.94 – 0.89 (m, 1H), 0.59 – 0.54 (m, 1H) ppm; ^{13}C NMR (101 MHz, $CDCl_3$) δ 213.0, 167.5, 92.2, 67.9, 60.0, 57.3, 56.8, 54.4, 47.6, 18.5, 18.2, 14.8, 13.9, 12.0, 7.2 ppm; FT-IR (neat) ν_{max} = 3030, 2973, 2934, 2876, 1747, 1622, 1449, 1365, 1204, 1010, 940, 904, 851, 693 cm^{-1}; HRMS (ESI) calcd for $C_{15}H_{20}NO_3^+$ [*M*+H^+] 262.1438, found 262.1437.

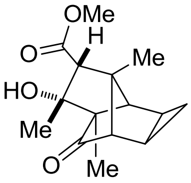

(3*RS*,4*RS*)-methyl-3-hydroxy-2,3,4a-trimethyl-6-oxooctahydro-1*H*-2,5-methanocyclopropa[*a*]pentalene-4-carboxylate (189).

To a solution of **188** (57.0 mg, 0.22 mmol) and $B(OH)_3$ (81 mg, 1.3 mmol) in MeOH/water (5:1, 0.2 mL) was added Raney-Nickel (50% slurry in water) (25.6 mg, 0.22 mmol). The atmosphere was replaced with H_2 (balloon). After 72 h, the catalyst was filtered off over a pad of celite, which was rinsed with 20 mL EtOAc and 10 mL water. The phases were separated and the aqueous phase was extracted with EtOAc (3 x 20 mL). The combined organic phases were dried over Na_2SO_4 and concentrated. The crude product was purified by flash column chromatography (hexane/EtOAc 3:1 to 2:1) to give **189** (52.0 mg, 0.20 mmol, 91%) as a white crystalline solid.

R_f = 0.47 (hexane/EtOAc 2:1, CAM); ^{1}H NMR (300 MHz, CD_2Cl_2) δ 3.70 (s, 3H), 2.78 (s, 1H), 2.67 (s, 1H), 2.48 (s, 1H), 1.48 – 1.42 (m, 1H), 1.39 – 1.35 (m, 1H), 1.11 (bs, 6H), 1.09 (s, 3H), 0.87 – 0.80 (m, 1H), 0.60 – 0.53 (m, 1H) ppm. ^{13}C NMR (101 MHz, CD_2Cl_2) δ 214.5, 173.2, 77.8, 68.8, 63.1, 59.5, 55.3, 52.3, 45.2, 22.9, 19.7, 14.7, 14.4, 12.3, 7.4 ppm; FT-IR (neat) ν_{max} = 3484, 3033, 2964, 2932, 2852, 1741, 1437, 1352, 1286, 1261, 1203, 1159, 1104, 1025, 915 cm^{-1}; HRMS (ESI) calcd for $C_{15}H_{20}NaO_4^+$ [M+Na$^+$] 287.1254, found 287.1257.

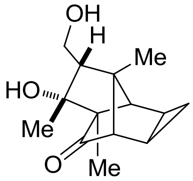

(3*RS*,4*SR*)-3-hydroxy-4-(hydroxymethyl)-2,3,4a-trimethyloctahydro-1*H*-2,5-methanocyclopropa[*a*]pentalen-6-one (190).

To a solution of **189** (86.4 mg, 0.327 mmol) in 3.3 mL THF was added freshly prepared Li(*i*Bu)$_2$(*n*Bu)AlH (0.50 M in hexanes–THF, 1.96 mL, 0.981 mmol) dropwise at –60 °C.[188] The reaction was warmed by itself to 0 °C and kept there. After 3 h in total, the reaction was quenched with 10 mL EtOAc. The solution was poured in a bigger flask containing 40 mL sodium potassium tartrate (aqueous, saturated) and 50 mL EtOAc. After vigorous stirring for 30 min, the phases were separated and the aqueous phase was extracted with EtOAc (4 x 50 mL). The combined organic phases were dried over Na_2SO_4 and concentrated. Purification *via* column chromatography (hexane/EtOAc 1:1) gave **190** as a white amorphous solid (69.1 mg, 0.29 mmol, 89%).

R_f = 0.41 (hexane/EtOAc 1:1, CAM); ^{1}H NMR (300 MHz, $CDCl_3$) δ 4.01 (dd, J = 11.8, 2.6 Hz, 1H), 3.84 (dd, J = 11.8, 5.6 Hz 1H), 2.61 (s, 1H), 2.44 (s, 1H), 1.61 (dd, J = 5.6, 2.6 Hz, 1H), 1.51 – 1.41 (m, 2H), 1.22 (s, 3H), 1.16 (s, 3H), 1.13 (s, 3H), 0.86 – 0.79 (m, 1H), 0.59 – 0.52 (m, 1H) ppm; ^{13}C NMR (101 MHz, $CDCl_3$) δ 216.1, 80.5, 67.3, 60.7, 60.1, 55.6, 54.9, 44.3, 23.8, 17.7, 15.0, 13.7, 12.4, 7.2 ppm; FT-IR (neat) ν_{max} = 3409, 3026, 2964, 2933,

---

[188] Li(*i*Bu)$_2$(*n*Bu)AlH was prepared by the addition of *n*-BuLi (1.58 M in hexanes, 2.53 mL, 4.00 mmol) to a solution of DIBAL (1.0 M in hexanes, 4.0 mL, 4.0 mmol) diluted with 1.45 mL THF at 0 °C. See also S. Kim, K. H. Ahn, *J. Org. Chem.* **1984**, *49*, 1717-1724.

2880, 2849, 1740, 1452, 1381, 1143, 1105, 1060, 969, 916, 819, 720 cm^{-1}; HRMS (Low-Mass-MALDI) calcd for $C_{14}H_{20}NaO_3^+$ [*M*+Na$^+$] 259.1305, found 259.1305.

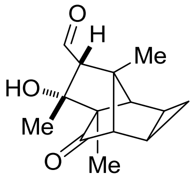

(3*RS*,4*RS*)-3-hydroxy-2,3,4a-trimethyl-6-oxooctahydro-1*H*-2,5-methanocyclopropa[*a*]pentalene-4-carbaldehyde (179).

To a solution of $(COCl)_2$ (40 µL, 0.5 mmol) in 1.0 mL CH_2Cl_2 was added DMSO (56 µL, 0.8 mmol) dropwise at –78 °C. After 15 min, a solution of **190** (69.1 mg, 0.29 mmol) in 1.9 mL CH_2Cl_2 was added dropwise over 4 min. After 1 h, NEt_3 (0.20 mL, 1.46 mmol) was added. The dry ice was removed and the reaction was slowly allowed to warm to RT over 50 min. The reaction was quenched by the addition of 5 mL NH_4Cl (aqueous, saturated) and poured in a separation funnel containing 20 mL water and 30 mL CH_2Cl_2. The phases were separated and the aqueous phase was extracted with CH_2Cl_2 (3 x 40 mL). The combined organic phases were dried over Na_2SO_4 and concentrated. The crude material was purified by flash column chromatography (hexane/EtOAc 2:1) to yield **179** (68.3 mg, 0.29 mmol, quant.) as a faint yellow oil.

R_f = 0.50 (hexane/EtOAc 3:2, CAM); ^{1}H NMR (400 MHz, $CDCl_3$) δ 9.65 (d, *J* = 4.8 Hz, 1H), 2.96 (s, 1H), 2.50 (s, 1H), 2.31 (d, *J* = 4.8 Hz, 1H), 1.95 (bs, 1H), 1.52 – 1.47 (m, 1H), 1.41 – 1.38 (m , 1H), 1.20 (s, 3H), 1.16 (s, 3H), 1.13 (s, 3H), 0.92 – 0.87 (m, 1H), 0.62 – 0.56 (m, 1H) ppm; ^{13}C NMR (101 MHz, $CDCl_3$) δ 214.5, 203.4, 80.2, 67.9, 66.7, 59.1, 55.3, 43.5, 23.9, 19.1, 14.6, 13.8, 12.0, 6.8 ppm; FT-IR (neat) ν_{max} = 3460, 3118, 3030, 2967, 2935, 2876, 2749, 1734, 1715, 1488, 1451, 1383, 1153, 1078, 1043, 952, 930, 915, 810, 717 cm^{-1}; HRMS (ESI) calcd for $C_{14}H_{22}NO_3$ [*M*+NH_4^+] 252.1594, found 252.1593.

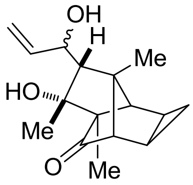

(3*RS*,4*SR*)-3-hydroxy-4-((*SR*)-1-hydroxyallyl)-2,3,4a-trimethyloctahydro-1*H*-2,5-methanocyclopropa[*a*]pentalen-6-one (74).

Anhydrous $CeCl_3$ (215 mg, 0.87 mmol) was suspended in 1.3 mL THF for 2 h. The suspension was cooled to –78 °C and vinylmagnesium bromide (1.01 M in THF, 0.86 mL, 0.87 mmol) was added. After 30 min, **179** (68.3 mg, 0.29 mmol) in 1.6 mL THF was added dropwise. The reaction was stirred at this temperature for 45 min. Then the dry ice was removed and the reaction warmed to RT by itself.[189] The reaction was then quenched with 5 mL NH_4Cl (saturated, aqueous). 10 mL water and 10 mL EtOAc were added. The mixture was filtered over a short plug of celite (rinsed with additional 50 mL EtOAc) and poured in a separation funnel. The phases were separated and the aqueous phase was extracted with EtOAc (3 x 40 mL), dried over Na_2SO_4 and concentrated. The crude diol was purified by flash column chromatography (hexane/EtOAc 3:1 → 2:1) to give **74** (68 mg, 0.26 mmol) as a faint yellow oil in 90% yield as an inseparable 60:40 mixture of diastereomers.

R_f = 0.40 (hexane/EtOAc 2:1, $KMnO_4$); ^{1}H NMR (300 MHz, $CDCl_3$)[190, 191] δ 6.19 (ddd, J = 17.3, 10.8, 5.1 Hz, 1H), 6.03* (ddd, J = 17.3, 10.8, 3.9 Hz, 1H), 5.34 – 5.11 (m, 2H) ‡, 4.69 (bs, 1H), 4.49 (bs, 1H), 2.63 (s, 1H), 2.61* (s, 1H), 2.45 (s, 1H), 2.42* (s, 1H), 1.74 (bs, 1H), 1.66* (d, J = 3.1 Hz, 1H), 1.57 – 1.40 (m, 2H)‡, 1.30 (s, 3H), 1.27* (s, 3H), 1.18 (s, 3H), 1.12* (app. s, 6H, *2 x Me from minor*), 1.08 (s, 3H), 0.81 – 0.76 (m, 1H) ‡, 0.60 – 0.47 (m, 1H)‡ ppm; ^{13}C NMR (101 MHz, $CDCl_3$)[191] δ 216.10, 216.08*, 142.0*, 141.5, 114.4, 113.9*, 81.6, 80.5*, 73.4, 71.1*, 67.7, 66.8*, 61.4*, 60.1, 58.3*, 57.4, 55.6*, 55.3, 45.7*, 45.1, 24.4, 22.6*, 18.9*, 18.0, 15.2, 15.1*, 13.7, 13.3*, 12.7, 12.6*, 7.3*, 7.0 ppm; FT-IR (neat) ν_{max} *for the diastereomeric mixture* = 3373, 3027, 2965, 2935, 2877, 1739, 1729, 1451, 1425, 1381, 1314, 1256, 1145, 1098, 1024, 910, 808, 730 cm^{-1}; HRMS (ESI) calcd for $C_{16}H_{22}NaO_3^+$ [M+Na^+] 285.1461, found 285.1467.

---

[189] The product **74** and the starting material **179** coeluate and are not separable on TLC. However, reaction monitoring is performed best using anisaldehyde as TLC stain. **74** appears bright green, **179** blue.

[190] Overlapping signals are labeled with ‡

[191] The minor diastereomeric peaks are labeled with *.

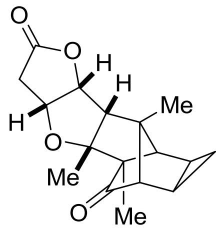

202

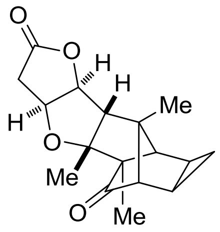

201

(3a*RS*,4a*RS*,7b*SR*,7c*RS*)-4a,5,7a-trimethyldecahydro-2*H*-5,7-methanocyclopropa-[4,5]pentaleno[2,1-*b*]furo[2,3-*d*]furan-2,8(4a*H*,5b*H*)-dione (202)

and (3a*SR*,4a*RS*,7b*SR*,7c*SR*)-4a,5,7a-trimethyldecahydro-2*H*-5,7-methanocyclopropa[4,5]pentaleno[2,1-*b*]furo[2,3-*d*]furan-2,8(4a*H*,5b*H*)-dione (201).

To a suspension of tetramethylthiourea (1.00 mg, 7.62 µmol), $CuCl_2$ (26.1 mg, 0.19 mmol), NH_4OAc (0.6 mg, 8 µmol) and $Pd(OAc)_2$ (1.7 mg, 7.6 µmol) in 0.3 mL THF was added propylene oxide (27 µL, 0.4 mmol). The flask was purged with CO (3 cycles) and **74** (20.0 mg, 0.076 mmol) was added as a 3:2 mixture of diastereomers in 0.5 mL THF. Then the mixture was heated to 50 °C. After 20 h, the CO was removed and replaced by N_2 (3 cycles). The reaction mixture was filtered over a pad of celite, which was rinsed with 50 mL EtOAc. 20 mL NH_4Cl (aqueous, saturated) were added, the phases were separated and the aqueous phase extracted with EtOAc (3 x 30 mL). The combined organic phases were dried over Na_2SO_4 and concentrated. The crude material was purified by flash column chromatography (hexane/EtOAc 2:1 → 1:1) to give **202** (12 mg, 0.042 mmol, 55%, 83% based on the desired diastereomer) along with undesired diastereomer **201** (6 mg, 0.019 mmol, 26%).

202:

R_f = 0.20 (hexane/EtOAc 1:1, CAM); ^{1}H NMR (400 MHz, $CDCl_3$) δ 5.03 (dd, J = 6.9, 3.2 Hz, 1H), 4.60 – 4.58 (m, 1H), 2.68 – 2.67 (m, 2H), 2.48 – 2.47 (m, 1H), 2.42 – 2.40 (m, 2H), 1.43 – 1.34 (m, 2H), 1.29 (s, 3H) 1.16 (s, 3H), 1.07 (s, 3H), 0.89 – 0.84 (m, 1H), 0.57 – 0.51 (m, 1H) ppm; ^{13}C NMR (101 MHz, $CDCl_3$) δ 214.3, 175.3, 89.6, 87.3, 77.4, 67.0, 60.9, 58.1, 55.0, 44.7, 34.8, 21.6, 19.3, 15.2, 14.4, 12.1, 7.3 ppm; FT-IR (neat) ν_{max} = 3032, 2967, 2934, 2875, 1765, 1739, 1453, 1384, 1264, 1203, 1155, 1101, 1051, 989, 947, 922, 888, 863, 816, 799, 743 cm^{-1}; HRMS (ESI) calcd for $C_{17}H_{24}NO_4^+$ [M+NH_4^+] 306.1700, found 106.1697.

201:

R$_f$ = 0.22 (hexane/EtOAc 1:1, CAM); ^{1}H NMR (400 MHz, CDCl$_3$) δ 5.05 (app. d, J = 3.9 Hz, 1H), 4.68 (app. dt, J = 3.9, 1.7 Hz, 1H), 2.73 – 2.72 (m, 2H), 2.57 (s, 1H), 2.46 (s, 1H), 2.21 (s, 1H), 1.48 – 1.43 (m, 1H), 1.36 – 1.33 (m, 1H), 1.22 (s, 3H), 1.17 (s, 3H), 1.15 (s, 3H), 0.93 – 0.89 (m, 1H), 0.62 – 0.57 (m, 1H) ppm; ^{13}C NMR (101 MHz, CDCl$_3$) δ 213.3, 174.7, 91.1, 88.0, 80.0, 68.7, 60.4, 57.9, 55.0, 42.6, 38.4, 21.1, 19.4, 14.2, 14.0, 12.0, 7.3 ppm; FT-IR (neat) ν_{max} = 3034, 2972, 2934, 2878, 1780, 1740, 1452, 1383, 1264, 1188, 1152, 1095, 1063 1039, 996, 959, 890, 861, 740 cm^{-1}; HRMS (ESI) calcd for $C_{17}H_{24}NO_4^+$ [M+NH$_4^+$] 306.1700, found 306.1698.

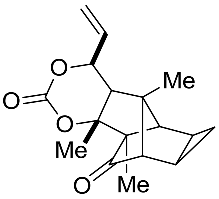

(4*SR*,7a*RS*)-4b,7,7a-trimethyl-4-vinyldecahydro-5,7-methanocyclopropa[4,5]pentaleno[2,1-*d*][1,3]dioxine-2,8-dione (203). This compound was obtained as a side product when diol **74** was subjected to stoichiometric alkoxycarbonylation conditions. Pd(OAc)$_2$ (29.1 mg, 0.13 mmol) was suspended in 0.2 mL THF. The nitrogen atmosphere was replaced by 1 atm of CO and a solution of **74** (20.0 mg, 0.08 mmol) in 0.6 mL THF was added. After 48 h, the CO was replaced by nitrogen, the reaction mixture filtered over a pad of celite and the solvent evaporated. The crude residue was purified by flash column chromatography yielding **201**, **202** and **203** (1.6 mg, 5.6 μmol, 7%).

R$_f$ = 0.40 (hexane/EtOAc 2:1, KMnO$_4$); ^{1}H NMR (400 MHz, CDCl$_3$) δ 5.90 (ddd, J = 17.2, 10.8, 4.6 Hz, 1H), 5.42 –5.36 (m, 2H), 5.07 – 5.04 (m, 1H), 2.58 (bs, 1H), 2.41 (bs, 1H), 1.96 (d, J = 2.6 Hz, 1H), 1.53 – 1.46 (m, 2H), 1.34 (s, 3H), 1.26 (s, 3H), 1.23 (s, 3H), 0.91 – 0.86 (m, 1H), 0.66 – 0.60 (m, 1H) ppm; ^{13}C NMR (101 MHz, CDCl$_3$) δ 212.0, 149.6, 134.7, 118.3, 89.6, 77.0, 68.4, 59.0, 54.3, 51.4, 44.8, 21.4, 17.9, 14.6, 13.4, 12.2, 6.8 ppm; FT-IR (neat) ν_{max} = 3462, 3031, 2932, 1729, 1454, 1374, 1321, 1235, 1191, 1042, 998, 803, 759 cm^{-1}; HRMS (ESI) calcd for $C_{17}H_{24}NO_4^+$ [M+NH$_4^+$] 306.1700, found 306.1704.

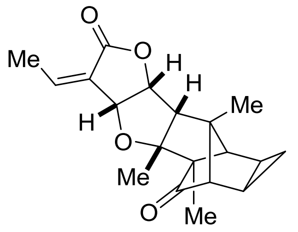

pallambin A (**14**)

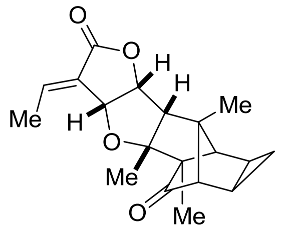

pallambin B (**15**)

Pallambin A (14) and Pallambin B (15).

To a solution of **202** (4.0 mg, 0.014 mmol) in 0.2 mL THF was added freshly prepared $i\mathrm{Pr_2NLi}$ (0.5 M in THF, 50 µL, 0.02 mmol) at –78 °C. After 55 min, MeCHO (2.0 M in THF, 42 µL, 0.08 mmol) was added dropwise. After 1 h, the dry ice was removed and the reaction was warmed to –40 °C and quenched after further 10 min by the addition of 3 mL NH_4Cl (aqueous, saturated). The mixture was poured in a separation funnel containing 5 mL EtOAc and 2 mL water. The phases were separated and the aqueous phase was extracted with EtOAc (5 x 10 mL). The combined organic phases were dried over Na_2SO_4 and concentrated. The crude aldol products were dissolved in 0.14 mL CH_2Cl_2 and NEt_3 (30 µL, 0.21 mmol) and one crystal of DMAP were added. Then MsCl (1.0 M in CH_2Cl_2, 69 µL, 0.1 mmol) was added dropwise. After 20 h, the reaction was diluted with 1 mL CH_2Cl_2 and then quenched by the addition of 2 mL NH_4Cl (aqueous, saturated). The biphasic mixture was poured in a separation funnel containing 5 mL CH_2Cl_2 and 5 mL water. The phases were separated and the aqueous phase extracted with CH_2Cl_2 (3 x 10 mL), dried over Na_2SO_4 and concentrated. The crude product was purified by flash column chromatography (hexane/EtOAc 3:1 → 1:1) to give pallambin A (**1**) and B (**2**) (1:5, 4.6 mg). The natural products were then separated from each other by preparative thin layer chromatography (hexane/EtOAc 3:1, developed 5 times) to yield 3.8 mg of pallambin B (**15**) (0.012 mmol, 87%) and 0.5 mg pallambin A (**14**) (2 µmol, 11%) as white solids.

Pallambin A (**14**):

R_f = 0.51 (hexane/EtOAc 1:1, CAM), ^{1}H NMR (600 MHz, $CDCl_3$)[192] δ 6.67 (qd, J = 7.3, 0.6 Hz, 1H), 4.93 (dd, J = 7.1, 3.5 Hz, 1H), 4.73 (dt, J = 3.5, 0.6 Hz, 1H), 2.47 – 2.46 (m, 2H), 2.43 (d, J = 7.1 Hz, 1H)[193], 2.25 (d, J = 7.3Hz, 3H), 1.42 – 1.37 (m, 2H), 1.32 (s, 3H), 1.16 (s, 3H), 1.09 (s, 3H), 0.89 – 0.85 (m, 1H), 0.55 – 0.52 (m, 1H) ppm; ^{13}C NMR (151 MHz, $CDCl_3$)[194] δ 214.6, 168.5, 145.0, 126.1, 90.0, 84.9, 80.3, 67.1[195], 61.0, 58.2, 55.1, 44.8, 21.7,

---

[192] As it is common practice, the ^{1}H NMR is referenced to 7.26 ppm. Therefore a shift difference of 0.02 ppm between the isolation report and this communication arises (isolation referenced to 7.28 ppm).

[193] Although table 1 in the isolation report states this signal at 2.27 ppm, the reported spectra (^{1}H NMR and HSCQ) clearly show this signal at 2.44 ppm, as observed by us. Therefore a typing error in the isolation report is assumed.

[194] As for all ^{13}C NMR in this communication, also this spectrum is referenced to $CDCl_3$ as 77.16 ppm. Since the isolation report is referenced to 77.00 ppm, a shift difference of 0.2 ppm arises.

19.6, 15.2, 14.6, 14.4, 12.1, 7.4 ppm; FT-IR (neat) ν_{max} = 2963, 2923, 2851, 1742, 1685, 1444, 1382, 1362, 1260, 1217, 1127, 1103, 1046, 1021, 986, 965, 923, 862, 796, 736 cm^{-1}; HRMS (ESI) calcd for $C_{19}H_{23}O_4^+$ [*M*+H$^+$] 315.1591, found 315.1590.

Pallambin B (**15**):

R$_f$ = 0.51 (hexane/EtOAc 1:1, CAM), ^{1}H NMR (400 MHz, CDCl$_3$)[192] δ 7.01 (qd, *J* = 7,2, 1.0 Hz, 1H), 4.99 – 4.95 (m, 2H), 2.48 – 2.45 (m, 2H), 2.40 (s, 1H), 2.02 (d, *J* = 7.2 Hz, 3H), 1.42 –, 1.35 (m, 2H), 1.32 (s, 3H), 1.15 (s, 3H), 1.11 (s, 3H), 0.88 – 0.84 (m, 1H), 0.56 – 0.50 (m, 1H) ppm; ^{13}C NMR (101 MHz, CDCl$_3$)[194] δ 214.6, 169.6, 142.1, 127.7, 90.3, 85.6, 75.8, 67.2, 60.8, 58.3, 55.1, 44.8, 21.8, 19.6, 16.1, 15.2, 14.4, 12.2, 7.4 ppm; FT-IR (neat) ν_{max} = 3031, 2967, 2934, 2872, 1745, 1690, 1447, 1384, 1302, 1259, 1216, 1106, 1047, 978, 922, 862, 812, 735, 616 cm^{-1}; HRMS (ESI) calcd for $C_{19}H_{23}O_4^+$ [*M*+H$^+$] 315.1591, found 315.1592.

---

[195] Although table 1 in the isolation report states this signal at 70.0 ppm, the reported spectrum (^{13}C NMR) clearly shows this signal at 67.0 ppm, as observed by us. Therefore a typing error in the isolation report is assumed.

13.4.2 Ti(III)-Mediated Epoxide Opening

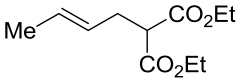

(*E*)-diethyl 2-(but-2-en-1-yl)malonate (356). Diethyl malonate (15.06 g, 94.03 mmol) was added to a suspension of NaH (0.544 g, 22.67 mmol, 60% dispersion in mineral oil) in 150 mL THF and stirred for 15 min. Then the mixture was cooled to 0 °C and 1-bromobut-2-ene (70:30 *trans*/*cis*, 3.00 g, 18.9 mmol) was added. After 30 min the reaction was quenched by the addition of 50 mL water and 50 mL $NaHCO_3$ (aqueous, saturated). The organic phase was separated and the aqueous phase was extracted with EtOAc (3 x 100 mL). The combined organic layers were dried over $MgSO_4$ and concentrated. The colorless oil was purified by flash column chromatography (hexane/EtOAc 80:1 → 40:1) to yield **356** (2.06 g, 9.63 mmol, 51%). The spectra were in agreement with the literature.[196]

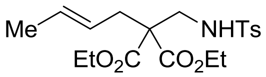

(*E*)-diethyl-2-(but-2-en-1-yl)-2-((4-methylphenylsulfonamido)methyl)malonate (263). Paraformaldehyde (3.31 g, 110 mmol) and tosylamide (22.6 g, 131 mmol) were dissolved in 120 mL CH_2Cl_2 and stirred for 10 min. In a separate flask **356** (4.72 g, 22.0 mmol) and DBU (16.6 mL, 111 mmol) were dissolved in 120 mL CH_2Cl_2. The sulfonimine solution was added and the mixture was stirred overnight. After quenching of the reaction with 50 mL water and 50 mL $NaHCO_3$ (aqueous, saturated) the phases were separated and the aqueous phase was extracted with CH_2Cl_2 (3 x 80 mL). The combined organic layers were dried over $MgSO_4$, concentrated and the crude material purified by flash column chromatography (hexane/EtOAc 10:1 → 0:1) to furnish tosylamide **263** (2.34 g, 13.4 mmol, 61%).

R_f = 0.61 (hexane/EtOAc 3:2, $KMnO_4$); ^{1}H NMR (300 MHz, $CDCl_3$) δ 7.64 (d, J = 8.2 Hz, 2H), 7.20 (d, J = 8.2 Hz, 2H), 5.51 – 5.37 (m, 2H), 5.20 – 5.06 (m, 1H), 4.05 (q, J = 7.2 Hz, 4H), 3.22 (d, J = 6.3 Hz, 2H), 2.54 (d, J = 7.2 Hz, 3H), 2.30 (s, 3H), 1.47 (d, J = 6.3 Hz, 3H), 1.12 (t, J = 7.2 Hz, 6H) ppm; ^{13}C NMR (75 MHz, $CDCl_3$) δ 169.3, 143.1, 136.5, 130.3, 129.4, 126.7, 123.4, 61.5, 57.8, 44.9, 34.8, 21.3, 17.8, 13.9 ppm; FT-IR (neat) ν_{max} = 3282, 2983, 2938, 2360, 1732, 1599, 1446, 1369, 1334, 1304, 1221, 1164, 1093, 1041 cm^{-1}; HRMS (ESI) calcd for $C_{19}H_{28}NO_6S$ [M^+] 398.1632, 398.1620 found.

---

[196] R. Takeuchi, M. Kashio, *J. Am. Chem. Soc.* **1998**, *120*, 8647-8655.

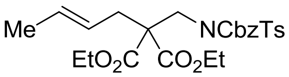

(*E*)-diethyl 2-((*N*-((benzyloxy)carbonyl)-4-methylphenylsulfonamido)methyl)-2-(but-2-en-1-yl)malonate (357). A solution of **263** (2.13 g, 5.36 mmol) in 30 mL THF was added to a suspension of sodium hydride (0.32 g, 13.4 mmol, 60% dispersion in mineral oil) in 20 mL THF. The mixture was stirred for 30 min and CbzCl (2.29 g, 13.4 mmol) was added. The suspension was stirred overnight and quenched with 30 mL NH_4Cl (aqueous, saturated). The phases were separated and the aqueous phase was extracted with EtOAc (3 x 50 mL). The combined organic phases were dried over $MgSO_4$ and concentrated. Purification was achieved by flash column chromatography (hexane/EtOAc 10:1 → 2:1) in order to yield **357** (1.86 g, 3.50 mmol, 65%).

R_f = 0.69 (hexane/EtOAc 3:2, $KMnO_4$); ^{1}H NMR (300 MHz, $CDCl_3$) δ 7.64 (d, J = 8.4 Hz, 2H) 7.22 –7.19 (m, 2H), 5.51 – 5.39 (m, 2H), 5.17– 5.08 (m, 1H), 4.17 – 4.01 (m, 4H), 3.25 – 3.21 (m, 2H) 2.63 –2.55 (m, 2H), 2.30 (s, 3H), 1.48 – 1.46 (m, 3H), 1.12 (t, J = 7.1 Hz, 6H) ppm; ^{13}C NMR (75 MHz, $CDCl_3$) δ 169.3, 143.1, 136.5, 130.3, 129.4, 126.7, 123.4, 61.5, 57.8, 44.9, 34.8, 21.3, 17.8, 13.9 ppm; FT-IR (neat) ν_{max} = 2982, 1732, 1597, 1446, 1359, 1275, 1173, 1088, 1031 cm^{-1}; HRMS (ESI) calcd for $C_{27}H_{34}NO_8S$ $[M+H]^+$ 532.2000, 532.1997 found.

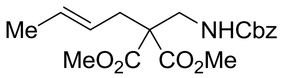

(*E*)-dimethyl-2-((((benzyloxy)carbonyl)amino)methyl)-2-(but-2-en-1-yl)malonate (358). A suspension of **263** (1.00 g, 1.88 mmol) and Mg (0.46 g, 18.8 mmol) in 80 mL methanol was sonicated in an ultrasound bath for 16 h. The solvent was evaporated and the crude product was purified by flash column chromatography (hexane/EtOAc 20:1) to yield **358** (0.21 g, 0.60 mmol, 32%).

^{1}H NMR (300 MHz, $CDCl_3$) δ 7.36 – 7.31 (m, 5H), 5.61 – 5.49 (m, 1H), 5.31 – 5.22 (m, 2H), 5.07 (s, 2H), 3.69 – 3.63 (m, 8H), 2.70 – 2.59 (m, 2H), 1.64 (d, J = 6.1 Hz, 3H) ppm.

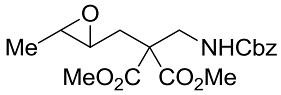

Dimethyl-2-((((benzyloxy)carbonyl)amino)methyl)-2-((3-methyloxiran-2-yl)methyl)-malonate (264). *m*CPBA (693 mg, 3.09 mmol,77%) was added to a solution of **358** (360 mg, 1.03 mmol) in 10 mL CH_2Cl_2 and stirred for 5.5 h. The reaction mixture was quenched with 3 mL $Na_2S_2O_3$ (aqueous, saturated) and 3 mL $NaHCO_3$ (aqueous, saturated). The organic phase was separated and the aqueous phase was extracted with CH_2Cl_2 (3 x 20 ml). The combined organic layers were dried over $MgSO_4$, evaporated and purified via flash column chromatography (hexane/EtOAc 10:1) to yield **264** (327 mg, 0.90 mmol, 87%) as a white crystalline solid.

R_f = 0.29 (hexane/EtOAc 2:1); ^{1}H NMR (400 MHz, $CDCl_3$) δ 7.36 – 7.32 (m, 5H), 5.36 – 5.31 (m, 1H), 5.07 (s, 2H), 3.97 – 3.90 (m, 1H), 3.75 – 3.67 (m, 7H), 2.77 – 2.68 (m, 2H), 2.31 (dd, J = 14.8, 3.6 Hz, 1H), 1.97 – 1.90 (m, 1H), 1.28 (d, J = 5.2 Hz, 3H) ppm; ^{13}C NMR (100 MHz, $CDCl_3$) δ 170.1, 156.2, 136.3, 128.3, 128.0, 66.8, 57.2, 55.4, 54.7, 52.9, 43.9, 34.9, 17.4, ppm; FT-IR (neat) ν_{max} = 3383, 2955, 1733, 1538, 1520, 1456, 1436, 1382, 1227, 1144, 1117, 1011 cm^{-1}; HRMS (ESI) calcd for $C_{18}H_{24}NO_7$ $[M+H]^+$ 366.1547, 366,1548 found.

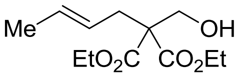

(*E*)-diethyl 2-(but-2-en-1-yl)-2-(hydroxymethyl)malonate (265). DBU (4.90 mL, 32.2 mmol) and paraformaldehyde (0.97 g, 32.3 mmol) were added to a solution of **356** (1.39 g, 6.46 mmol) in 40 mL THF and stirred for 30 min. The solvent was removed *in vacuo* and the crude product was purified by flash column chromatography (hexane/EtOAc 10:1 → 3:2) to give **265** (0.96 g, 3.93 mmol, 61%).

R_f = 0.26 (hexane/EtOAc 4:1, $KMnO_4$); ^{1}H NMR (300 MHz, $CDCl_3$) δ 5.62 – 5.51 (m, 1H), 5.38 – 5.28 (m, 1H), 4.23 (q, J = 7.1 Hz, 4H), 3.94 – 3.91 (m, 2H), 2.71 – 2.56 (m, 3H), 1.65 (d, J = 6.3 Hz, 3H), 1.27 (t, J = 7.1 Hz, 6H) ppm; ^{13}C NMR (75 MHz, $CDCl_3$) δ 170.3, 129.8, 124.4, 64.0, 61.3, 59.5, 34.5, 17.9, 14.0 ppm; FT-IR (neat) ν_{max} = 3522, 2983, 2940, 1732, 1465, 1446, 1368, 1300, 1215, 1095, 1036 cm^{-1}; HRMS (ESI) calcd for $C_{12}H_{20}NaO_5$ $[M+Na]^+$ 267.1203, 267.1204 found.

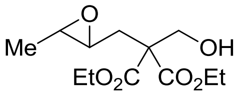

Diethyl 2-(hydroxymethyl)-2-((3-methyloxiran-2-yl)methyl)malonate (266). *m*CPBA (1.32 g, 5.89 mmol, 77%) was added to a solution of **265** (0.96 g, 3.93 mmol) in 30 mL CH_2Cl_2 and stirred for 3 h. The reaction mixture was quenched with 12 mL $Na_2S_2O_3$ (aqueous, saturated) and 15 mL $NaHCO_3$ (aqueous, saturated). The organic phase was separated and the aqueous phase was extracted with CH_2Cl_2 (3 x 50 mL). The combined organic layers were dried over $MgSO_4$, concentrated and the crude product purified *via* flash column chromatography (hexane/EtOAc 5:1 → 0:1) to yield **18** (0.22 g, 0.86 mmol, 22%).

^{1}H NMR (400 MHz, $CDCl_3$) δ 4.24 – 4.16 (m, 4H), 4.11 – 4.03 (m, 2H), 2.86 – 2.74 (m, 3H), 2.31 – 2.30 (m, 1H), 2.00 – 1.96 (m, 2H), 1.26 – 1.21 (m, 9H) ppm; ^{13}C NMR (100 MHz, $CDCl_3$) δ 170.2, 64.5, 61.8, 58.6, 55.9, 55.1, 34.3, 17.4, 14.1 ppm; FT-IR (neat) ν_{max} = 3516, 2986, 1732, 1467, 1447, 1368, 1300, 1221, 1097, 1034 cm^{-1}; HRMS (ESI) calcd for $C_{12}H_{21}O_6$ $[M+H]^+$ 261.1333, 261.1327 found.

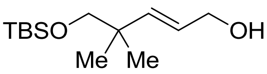

(*E*)-5-((*tert*-butyldimethylsilyl)oxy)-4,4-dimethylpent-2-en-1-ol (270). To a –78 °C solution of (*E*)-ethyl 5-((tert-butyldimethylsilyl)oxy)-4,4-dimethylpent-2-enoate (3.88 g, 13.6 mmol)[197] in 70 mL CH_2Cl_2 was added DIBAL (1.0 M in CH_2Cl_2, 27.1 mL, 27.1 mmol) dropwise. After 2.5 h, additional DIBAL (1.0 M in CH_2Cl_2, 13.6 mL, 13.6 mmol) was added and after additional 1.5 h, the cooling bath was removed. The reaction was quenched by the addition of 10 mL EtOAc and 10 mL potassium sodium tartrate (aqueous, saturated) were added. After vigorous stirring for 30 min, the phases were separated and the aqueous phase extracted with CH_2Cl_2 (3 x 50 mL). The combined organic phases were washed with 100 mL brine, dried over Na_2SO_4 and the solvent evaporated. The crude product was purified by flash column chromatography (hexane/EtOAc 10:1) to furnish **270** (3.30 g, 13.5 mmol, quant).

R_f = 0.22 (hexane/EtOAc 10:1, $KMnO_4$); ^{1}H NMR (400 MHz, $CDCl_3$) δ 5.70 (dt, J = 15.8, 1.1 Hz, 1H), 5.60 (dt, J = 15.8, 5.7 Hz, 1H), 4.11 (td, J = 5.8, 1.0 Hz, 1H), 3.29 (s, 2H), 0.98 (s, 6H), 0.89 (s, 9H), 0.02 (s, 6H) ppm; ^{13}C NMR (101 MHz, $CDCl_3$) δ 140.6, 126.2, 71.9, 64.4, 38.3, 26.1, 24.0, 18.5, –5.3 ppm; FT-IR (neat) ν_{max} = 3315, 2956, 2939, 2857, 1472,

---

[197] P. Mohan, K. Koushik, M. J. Fuertes, *Tetrahedron Lett.* **2015**, *56*, 61-65.

1390, 1361, 1252, 1091, 973, 834, 773 cm^{-1}; HRMS (ESI) calcd for $C_{13}H_{28}NaO_2Si$ [*M*+Na]$^+$ 267.1751, 267.1755 found.

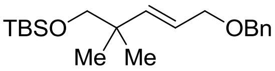

(*E*)-((5-(benzyloxy)-2,2-dimethylpent-3-en-1-yl)oxy)(*tert*-butyl)dimethylsilane (359). To a supsenison of NaH (0.27 g, 6.75 mmol, 60% dispersion in mineral oil) in 15 mL THF was added a solution of **270** (1.50 g, 6.14 mmol) in 10 mL THF dropwise. After 20 min, BnBr (0.84 mL, 7.1 mmol) was added and the reaction heated to reflux overnight. After cooling to RT, 25 mL of water were added and the phases separated. The aqueous phase was extracted with EtOAc (3 x 30 mL) and the combined organic phases washed with 100 mL brine and dried over $MgSO_4$. Evaporation of the solvents gave the crude product which was purified by flash column chromatography (hexane/EtOAc 30:1) to give **359** (2.05 g, 6.14 mmol, quant) as a faint yellow oil.

R$_f$ = 0.71 (hexane/EtOAc 10:1, $KMnO_4$, UV); ^{1}H NMR (400 MHz, $CDCl_3$) δ 7.35 –7.28 (m, 5H), 5.72 (dt, *J* = 15.8, 1.2 Hz, 1H), 5.55 (dt, *J* = 15.8, 6.1 Hz, 1H), 4.50 (s, 2H), 3.99 (dd, *J* = 6.1, 1.2 Hz, 2H), 3.30 (s, 3H), 0.99 (s, 6H), 0.89 (s, 9H), 0.01 (s, 6H) ppm; ^{13}C NMR (101 MHz, $CDCl_3$) δ 142.0, 138.7, 128.5, 128.0, 127.7, 123.5, 71.94, 71.93, 71.5, 38.4, 26.1, 24.0, 18.5, –5.3 ppm; FT-IR (neat) ν_{max} = 2956, 2929, 2856, 1472, 1361, 1253, 1100, 1006, 837, 775, 734, 697 cm^{-1}; HRMS (ESI) calcd for $C_{20}H_{34}NaO_2Si$ [*M*+Na]$^+$ 357.2220, 357.2219 found.

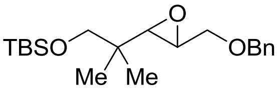

(2-(3-((benzyloxy)methyl)oxiran-2-yl)-2-methylpropoxy)(*tert*-butyl)dimethylsilane (360). To a solution of **359** (0.515 g, 1.539 mmol) in 6 mL CH_2Cl_2 was added *m*CPBA (0.569 g, 2.308 mmol, 70%) in one portion. After 1.5 h, the reaction was quenched carefully with 15 mL $Na_2S_2O_3$ (aqueous, saturated) and then with 15 mL $NaHCO_3$ (aqueous, saturated). The phases were separated and the aqueous phase extracted with CH_2Cl_2 (3 x 30 mL). The combined organic phases were washed with 50 mL $NaHCO_3$ (aqueous, saturated) and dried over $MgSO_4$. Evaporation of the solvent provided the crude epoxide, which was purified by column chromatography (hexane/EtOAc 20:1) to furnish **360** (0.465 g, 1.326 mmol, 86%).

R$_f$ = 0.45 (hexane/EtOAc 10:1, KMnO$_4$, UV); ^{1}H NMR (400 MHz, CDCl$_3$) δ 7.35 – 7.27 (m, 5H), 4.61 (d, J = 11.9 Hz, 1H), 4.55 (d, J = 11.9 Hz, 1H), 3.77 (dd, J = 11.6, 1.9 Hz, 1H), 3.43 – 3.32 (m, 2H), 3.13 (app. dt, J = 6.0, 2.6 Hz, 1H), 2.77 (d, J = 2.4 Hz, 1H), 0.89 (s, 9H), 0.86 (s, 3H), 0.85 (s, 3H), 0.03 (s, 6H) ppm; ^{13}C NMR (101 MHz, CDCl$_3$) δ 138.2, 128.5, 127.9, 127.8, 73.3, 71.0, 69.8, 60.9, 54.2, 36.0, 26.0, 20., 20.2, 18.4, –5.40, –5.45 ppm; FT-IR (neat) ν_{max} = 2955, 2929, 2856, 1472, 1455, 1362, 1252, 1216, 1096, 901, 836, 775, 734, 697 cm^{-1}; HRMS (ESI) calcd for $C_{20}H_{38}NO_3Si$ [M+NH$_4$]$^+$ 368.2615, 268.2608 found.

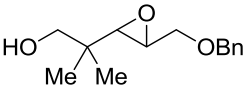

2-(3-((benzyloxy)methyl)oxiran-2-yl)-2-methylpropan-1-ol (271). To a 0 °C cold solution of **360** (0.317 g, 0.904 mmol) in 4.3 mL THF was added TBAF (1.0 M in THF, 1.8 mL, 1.8 mmol). After 1.5 h, 10 mL hexane were added and the resulting suspension filtered over a pad of silica (rinsed with 20 mL hexane–EtOAc 1:1). The solvents were evaporated and the crude product azeotropically dried by evaporation with benzene (5 x 1.5 mL). The crude product was purified by column chromatography (hexane/EtOAc 1:1) to furnish **271** in 91% (0.194 g, 0.821 mmol) yield.

R$_f$ = 0.35 (hexane/EtOAc 1:1, KMnO$_4$, UV); ^{1}H NMR (400 MHz, C$_6$D$_6$) δ 7.30 – 7.27 (m, 2H), 7.19 – 7.15 (m, 2H), 7.11 – 7.09 (m, 1H), 4.39 (d, J = 12.3 Hz, 1H), 4.35 (d, J = 12.3 Hz, 1H), 3.42 (dd, J = 11.3, 3.4 Hz, 1H), 3.24 (dd, J = 11.3, 5.6 Hz, 1H), 3.18 (dd, J = 10.7, 4.5 Hz, 1H), 3.10 (dd, J = 10.7, 5.9 Hz, 1H), 3.02 (ddd, J = 5.6, 3.4, 2.3 Hz, 1H), 2.59 (d, J = 2.3 Hz, 1H), 1.25 (t, J = 5.6 Hz, 1H), 0.81 (s, 3H), 0.68 (s, 3H) ppm; ^{13}C NMR (101 MHz, C$_6$D$_6$)[198] δ 138.9, 128.6, 127.9, 73.2, 71.0, 69.8, 61.6, 53.7, 35.4, 21.0, 20.6 ppm; FT-IR (neat) ν_{max} = 3458, 2871, 1455, 1364, 1200, 1051, 896, 739, 699 cm^{-1}; HRMS (ESI) calcd for $C_{14}H_{20}O_3$ [M]$^+$ 236.1407, 236.1413 found.

---

[198] One aromatic peak lies underneath the solvent signal (C$_6$D$_6$).

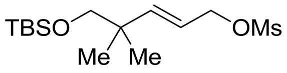

(*E*)-5-((*tert*-butyldimethylsilyl)oxy)-4,4-dimethylpent-2-en-1-yl-methanesulfonate (361). To a solution of **270** (1.00 g, 4.09 mmol) in 20 mL CH_2Cl_2 was added NEt_3 (1.4 mL, 10.2 mmol), DMAP (50 mg, 0.4 mmol) and MsCl (0.78 mL, 10.2 mmol) at 0 °C. After 1 h, the reaction was quenched by the addition of 10 mL NH_4Cl (aqueous, saturated) and 10 mL water. The phases were separated and the aqueous phase was extracted with CH_2Cl_2 (3 x 50 mL). The combined organoc phases were washed with 50 mL brine, dried over $MgSO_4$ and the solvents evaporated. Purification *via* flash column chromatography yielded **361** (0.894 g, 2.77 mmol, 68%) along with minor amounts of chlorination side product.

R_f = 0.72 (hexane/EtOAc 2:1, $KMnO_4$); ^{1}H NMR (300 MHz, $CDCl_3$) δ 5.95 – 5.89 (m, 1H), 5.57 (dt, J = 15.7, 6.8 Hz, 1H), 4.69 (dd, J = 6.8, 1.0 Hz, 2H), 3.31 (s, 2H), 3.00 (s, 3H), 1.00 (s, 6H), 0.88 (s, 9H), 0.02 (s, 6H) ppm; ^{13}C NMR (101 MHz, $CDCl_3$) δ 146.8, 119.6, 71.6, 71.4, 38.8, 38.5, 26.0, 23.8, 18.5, –5.3 ppm; FT-IR (neat) ν_{max} = 2956, 2930, 2857, 1473, 1355, 1252, 1174, 1096, 973, 929, 836, 775, 528 cm^{-1}; HRMS (ESI) calcd for $C_{14}H_{30}O_4SSi$ $[M+Na]^+$ 345.1526, 345.1528 found.

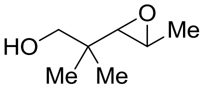

2-methyl-2-(3-methyloxiran-2-yl)propan-1-ol (273). To a solution of **361** (1.272 g, 3.944 mmol) in 40 mL THF was added $LiAlH_4$ (4.0 M in Et_2O, 1.5 mL, 5.9 mmol) dropwise. After 1 h, the reaction was quenched by the addition of 4 mL EtOAc, followed by 30 mL water and 50 mL potassium sodium tartrate (aqueous, saturated). The reaction was stirred vigorously for 20 min, the phases were separated and the aqueous phase extracted with EtOAc (3 x 100 mL). The combined organic phases were washed with 150 mL brine and dried over $MgSO_4$. Evaporation of the solvents provided 0.787 g (3.445 mmol, 87%) of the crude demesylated product, which was directly dissolved in 14 mL CH_2Cl_2 and *m*CPBA (1.27 g, 5.17 mmol, 77%) was added. After 1 h 15 min, the reaction was quenched by the addition of 20 mL $Na_2S_2O_3$ (saturated, aqueous) and 20 mL $NaHCO_3$ (saturated, aqueous). The phases were separated and the aqueous phase was extracted with CH_2Cl_2 (3 x 50 mL). The combined organic phases were washed with 100 mL $NaHCO_3$ (saturated, aqueous), dried over $MgSO_4$ and concentrated *in vacuo*. Purification by flash column chromatography provided the corresponding alcohol (0.600 g, 2.546 mmol), which was dissolved in 12 mL THF and cooled to 0 °C. TBAF (1.0 M in THF, 7.4 mL, 7.4 mmol) was added. After 1 h, additional TBAF (1.0 M in THF, 2.5 mL, 2.5 mmol) was added and after 40 additional minutes, 10 mL hexane were added. The resulting suspension was filtered over a pad of silica (rinsed with 50 mL hexane–EtOAc 1:1). The solvents were evaporated and the crude residue purified by column chromatography (hexane/EtOAc 2:1) to yield **273** (0.137 g, 1.052 mmol, 27% over three steps).

R_f = 0.36 (hexane/EtOAc 2:1, CAM); ^{1}H NMR (400 MHz, $CDCl_3$) δ 3.45 (d, J = 11.0 Hz, 1H), 3.34 (d, J = 11.0 Hz, 1H), 3.05 (qd, J = 5.2, 2.4 Hz, 1H), 2.61 (d, J = 2.4 Hz, 1H), 2.08 (bs, 1H), 1.31 (d, J = 5.2 Hz, 3H), 1.03 (s, 3H), 0.86 (s, 3H) ppm; ^{13}C NMR (101 MHz, $CDCl_3$) δ 70.3, 66.5, 51.3, 35.4, 21.9, 20.7, 17.9 ppm; FT-IR (neat) ν_{max} = 3433, 3964, 1466, 1381, 1047, 902, 854 cm^{-1}; HRMS (ESI) calcd for $C_7H_{14}O_2$ $[M+Na]^+$ 153.0886, 153.0883 found.

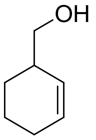

Cyclohex-2-en-1-ylmethanol (362). *n*BuLi (1.6 M in hexanes, 2.7 mL, 4.3 mmol) was added to a degassed suspension of KO*t*Bu (0.46 g, 4.08 mmol) in 10 mL cyclohexene. The reaction mixture was stirred overnight, then cooled to 0 °C and paraformaldehyde (0.14 g, 4.49 mmol) was added carefully. The mixture was heated to 60 °C for 3 h, then cooled to 0 °C, quenched with $NaHCO_3$ (aqueous, saturated) and the organic phase was separated. The aqueous phase was extracted with CH_2Cl_2 (3 x 50 mL). The combined organic layers were dried over $MgSO_4$ and evaporated. Purification was performed by flash column chromatography (hexane/EtOAc 10:1 → 1:10) to give **362** as a yellow oil (0.42 g, 3.73 mmol, 83%), whose spectra were in accordance to the literature.[199]

^{1}H NMR (300 MHz, $CDCl_3$) δ 5.86 – 5.79 (m, 1H), 5.62 – 5.56 (m, 1H), 3.55 (t, J = 4.9 Hz, 2H), 2.34 – 2.28 (m, 1H), 2.01 – 1.97 (m, 2H), 1.83 – 1.71 (m, 2H), 1.63 – 1.49 (m, 2H), 1.46 – 1.34 (m, 2H) ppm.

---

[199] M. B. Brennan, T. D. W. Claridge, R. G. Compton, S. G. Davies, A. M. Fletcher, M. C. Henstridge, D. S. Hewings, W. Kurosawa, J. A. Lee, P. M. Roberts, A. K. Schoonen, J. E. Thomson, *J. Org. Chem.* **2012**, *77*, 7241-7261.

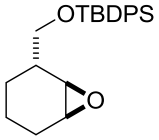

((1*RS*,2*RS*,6*SR*)-7-oxabicyclo[4.1.0]heptan-2-ylmethoxy)(*tert*-butyl)diphenylsilane (363). Triethylamine (5.1 mL, 36 mmol) was added to a solution of **362** (2.70 g, 24.1 mmol) in 30 mL of CH_2Cl_2. Then TBDPSCl (7.42 mL, 28.9 mmol) and a one crystal of DMAP were added after 5 min. After stirring overnight, the reaction mixture was concentrated *in vacuo* and purified by flash column chromatography (hexane/CH_2Cl_2 20:1 → 10:1) yielding **275** (7.93 g, 22.6 mmol, 94%). This material was dissolved in 70 mL CH_2Cl_2 and *m*CPBA (4.75 g, 21.2 mmol, 77%) was added. After 3 h. The reaction mixture was quenched with 10 mL $Na_2S_2O_3$ (aqueous, saturated) and 15 mL $NaHCO_3$ (aqueous, saturated). The organic phase was separated and the aqueous phase was extracted with CH_2Cl_2 (3 x 80 mL). The combined organic layers were dried over $MgSO_4$ and evaporated to yield the crude product which was purified by flash column chromatography (toluene/hexane 2:1 → 1:0). *Anti* diastereoisomer **363** (0.83 g, 2.27 mmol) was obtained in 21% yield.

R_f = 0.68 (toluene, $KMnO_4$, UV); ^{1}H NMR (400 MHz, $CDCl_3$) δ 7.76 – 7.71 (m, 5H), 7.49 – 7.39 (m, 7H), 3.77 – 3.67 (m, 2H), 3.21 – 3.18 (m, 2H), 2.17 – 2.09 (m, 1H), 1.72 – 1.66 (m, 1H), 1.57 – 1.52 (m, 1H), 1.44 – 1.38 (m, 2H), 1.14 (s, 9H), 1.13 – 1.09 (m, 1H) ppm; ^{13}C NMR (100 MHz, $CDCl_3$) δ 135.69, 135.67, 133.72, 133.67, 129.78, 129.76, 127.8, 66.2, 54.5, 52.7, 37.4, 27.0, 25.0, 24.0, 19.4, 17.2 ppm; HRMS (EI) calcd for $C_{19}H_{21}O_2Si$ $[M{-}C_4H_9]^+$ 309.1306, 309.1309 found.

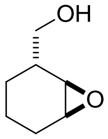

(1*RS*,2*RS*,6*SR*)-7-oxabicyclo[4.1.0]heptan-2-ylmethanol (276). 363 (0.83 g, 2.27 mmol) was dissolved in 15 mL of THF. Then TBAF (1.0 M in THF, 2.7 mL, 2.7 mmol) was added and the mixture was stirred overnight. The solvent was removed *in vacuo* and the crude product was purified by flash column chromatography (hexane/EtOAc 2:1) to give **22** (239 mg, 1.87 mmol, 82%).

R_f = 0.41 (hexane/EtOAc 1:3, $KMnO_4$); ^{1}H NMR (300 MHz, $CDCl_3$) δ 3.75 – 3.60 (m, 2H), 3.19 – 3.18 (m, 1H), 3.10 (d, J = 3.9 Hz, 1H), 2.12 – 2.01 (m, 2H), 1.88 – 1.50 (m, 4H), 1.43 – 1.34 (m, 2H), 1.02 – 0.92 (m, 1H) ppm; ^{13}C NMR (75 MHz, $CDCl_3$) δ 64.8, 54.2, 52.9, 37.4, 24.7, 23.8, 17.1 ppm; FT-IR (neat) ν_{max} = 3409, 2937, 1652, 1445, 1353, 1269, 1126, 1087, 1069, 1049, 1022, 995 cm^{-1}; HRMS (EI) calcd for $C_7H_{11}O_2$ $[M–H]^+$ 127.0754, 127.0754 found.

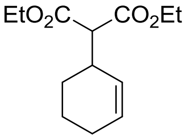

Diethyl 2-(cyclohex-2-en-1-yl)malonate (364). Sodium hydride (0.82 g, 20.6 mmol, 60% dispersion in mineral oil) was suspended in 75 mL THF. Ethyl malonate (4.74 mL, 31.2 mmol) was slowly added and the mixture was stirred for 10 min. Then 3-bromocyclohexene (3.64 mL, 31.2 mmol) was added and the solution was stirred overnight. The reaction mixture was quenched with 50 mL NH_4Cl (aqueous, saturated) and extracted with Et_2O (2 x 50 mL). The combined organic layers were washed with 50 mL brine and dried over $MgSO_4$. Purification *via* flash column chromatography (hexane/EtOAc 20:1) provided **364** (4.96 g, 20.7 mmol, 42%), whose spectra were in accordance to the literature.[200]

^{1}H NMR (300 MHz, $CDCl_3$) δ 5.80 – 5.73 (m, 1H), 5.54 (dd, J = 10.2, 2.4 Hz, 1H), 3.24 (d, J = 9.4 Hz, 1H), 2.94 – 2.85 (m, 1H), 2.02 – 1.95 (m, 2H), 1.84 – 1.67 (m, 2H), 1.62 – 1.50 (m, 1H), 1.44 – 1.33 (m, 1H) ppm.

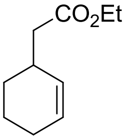

Ethyl 2-(cyclohex-2-en-1-yl)acetate (279). 364 (4.964 g, 20.66 mmol) was dissolved in 150 mL DMSO. Water (1.5 mL, 83 mmol) and LiCl (1.93 g, 45.4 mmol) were added, the mixture was heated to 140 °C and stirred overnight. After one day no conversion was observed. Hence water (1.5 mL, 83 mmol) and LiCl (1.93 g, 45.4 mmol) were added, the mixture was heated to 160 °C and stirred for further 24 h. 50 mL of water and 50 mL EtOAc were added, the organic phase was separated and the aqueous phase was extracted with EtOAc (3 x 50 mL). The combined organic layers were dried over $MgSO_4$ and concentrated *in vacuo*. Flash column chromatography (hexane/EtOAc 10:1) provided **279** (1.78 g, 10.6 mmol, 51%).

---

[200] F. A. Hicks, N. M. Kablaoui, S. L. Buchwald, *J. Am. Chem. Soc.* **1999**, *121*, 5881-5898.

R$_f$ = 0.44 (hexane/EtOAc 10:1, $KMnO_4$); ^{1}H NMR (300 MHz, $CDCl_3$) *δ* 5.75 – 5.68 (m, 1H), 5.56 – 5.52 (m, 1H), 4.14 (q, *J* = 7.1 Hz, 2H), 2.66 – 2.54 (m, 1H), 2.35 – 2.20 (m, 2H), 2.01 – 1.94 (m, 2H), 1.87 – 1.65 (m, 2H), 1.62 – 1.49 (m, 1H), 1.26 (t, *J* = 7.1 Hz, 3H) ppm; ^{13}C NMR (75 MHz, $CDCl_3$) *δ* 172.9, 130.3, 128.2, 60.3, 41.0, 32.4, 28.9, 25.2, 21.1, 14.4 ppm; FT-IR (neat) ν_{max} = 3020, 2982, 2931, 2863, 1738, 1448, 1371, 1336, 1279, 1255, 1209, 1161, 1134, 1096; HRMS (ESI) calcd for $C_{10}H_{16}O_2Na$ [*M*+Na]$^+$ 191.1043, 191,1042 found.

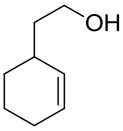

2-(cyclohex-2-en-1-yl)ethanol (365). A solution of **279** (1.78 g, 10.6 mmol) in 20 mL THF was added dropwise to a solution of $LiAlH_4$ (4.0 M in Et_2O, 5.3 mL, 84.8 mmol) in 40 mL THF at room temperature. After 20 min water was carefully added until gas evolution ceased. Then 50 mL HCl (aqueous, 1.0 M) was added. The aqueous phase was extracted with Et_2O (3 x 50 mL). The combined organic layers were dried over $MgSO_4$ and concentrated *in vacuo*. Purification *via* flash column chromatography (hexane/EtOAc 5:1 → 3:1) provided alcohol **279** (1.32 g, 10.5 mmol, 99%).

R$_f$ = 0.31 (hexane/EtOAc 3:1, $KMnO_4$); ^{1}H NMR (300 MHz, $CDCl_3$) *δ* 5.71 – 5.66 (m, 1H), 5.60 – 5.56 (m, 1H), 3.73, (t, *J* = 5.9 Hz, 2H), 2.27 – 2.21 (m, 1H), 2.01 – 1.94 (m, 2H), 1.83 – 1.49 (m, 5H), 1,31 – 1.21 (m, 2H) ppm; ^{13}C NMR (75 MHz, $CDCl_3$) *δ* 131.4, 126.9, 60.3, 39.0, 31.8, 29.0, 25.3, 21.4 ppm; FT-IR (neat) ν_{max} = 3326, 3017, 2928, 2859, 2360, 1648, 1447, 1139, 1067, 1050, 1010 cm^{-1}; HRMS (EI) calcd for $C_8H_{14}O$ [*M*]$^+$ 126.1039, 126.1038 found.

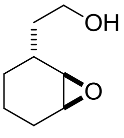

280

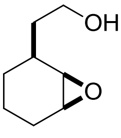

281

2-((1*RS*,2*RS*,6*SR*)-7-oxabicyclo[4.1.0]heptan-2-yl)ethanol (280) and 2-((1*RS*,2*SR*, 6*SR*)-7-oxabicyclo[4.1.0]heptan-2-yl)ethanol (281). *m*CPBA (5.10 g, 22.8 mmol, 77%) was added to a solution of **365** (1.44 g, 11.4 mmol) in 30 mL CH_2Cl_2 and stirred for 3 h. The reaction mixture was quenched with 5 mL $Na_2S_2O_3$ (aqueous, saturated) and 10 mL $NaHCO_3$

(aqueous, saturated). The organic phase was separated and the aqueous phase was extracted with CH_2Cl_2 (3 x 80 mL). The combined organic layers were dried over $MgSO_4$ and evaporated to yield the crude products which were purified by flash column chromatography (CH_2Cl_2/EtOAc 4:1 → 2:1) to yield **280** (116 mg, 0.82 mmol 7%) and **281** (803 mg, 5.65 mmol, 50%).

280:

R_f = 0.18 (CH_2Cl_2/EtOAc 1:1, $KMnO_4$); ^{1}H NMR (300 MHz, $CDCl_3$) δ 4.02 – 3.83 (m, 2H), 3.69 – 3.62 (m, 2H), 2.40 (m, 1H), 1.95 – 1.32 (m, 8H) ppm; ^{13}C NMR (75 MHz, $CDCl_3$) δ 83.3, 69.3, 66.2, 37.2, 30.2, 29.8, 25.6, 19.0 ppm; FT-IR (neat) ν_{max} = 3418, 2933, 2876, 1721, 1455, 1260, 1144, 1084, 1034 cm^{-1}; HRMS (EI) calcd for $C_8H_{14}O_2$ $[M]^+$ 142.0989, 142.0988 found.

281:

R_f = 0.25 (CH_2Cl_2/EtOAc 1:1); ^{1}H NMR (300 MHz, $CDCl_3$) δ 3.84 – 3.74 (m, 2H), 3.23 – 3.20 (m, 1H), 3.13 – 3.11 (m, 1H), 1.89 – 1.63 (m, 3H), 1.54 – 1.47 (m, 1H), 1.41 – 1.33 (m, 1H), 1.20 – 1.13 (m, 1H) ppm; HRMS (EI) calcd for $C_8H_{14}O_2$ $[M]^+$ 142.0989, 142.0991 found.

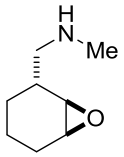

1-((1*RS*,2*RS*,6*SR*)-7-oxabicyclo[4.1.0]heptan-2-yl)-*N*-methylmethanamine (283). To a solution of *N*-((1*RS*,2*RS*,6*SR*)-7-oxabicyclo[4.1.0]heptan-2-ylmethyl)-*N*-methyl-1-phenyl-methanamine (**282**)[201] (0.556 g, 2.403 mmol) and AcOH (0.41 mL, 7.21 mmol) in 12 mL MeOH was added Pd/C (0.256 g, 46 wt. %. The atmosphere was replaced by hydrogen (1 atm) and the reaction stirred for 3 h. Filtration over celite and evaporation of the solvent provided the crude product, which was purified by column chromatography (CH_2Cl_2/MeOH/NH_4OH 10:1:0.1) to give **283** (0.325 g, 2.302 mmol, 96%).

R_f = 0.35 (CH_2Cl_2/MeOH/NH_4OH 10:1:0.2, $KMnO_4$); ^{1}H NMR (400 MHz, $CDCl_3$) δ 3.16 (dt, *J* = 3.9, 2.1 Hz, 1H), 3.00 (app. d, *J* = 3.9 Hz, 1H), 2.70 – 2.58 (m, 2H), 2.46 (s, 3H), 2.13 – 1.95 (m, 2H), 1.73 – 1.55 (m, 2H), 1.44 – 1.30 (m, 3H), 0.95 – 0.81 (m, 1H) ppm; ^{13}C NMR (101 MHz, $CDCl_3$) δ 55.8, 55.2, 52.9, 36.9, 34.9, 25.8, 25.1, 17.3 ppm; FT-IR (neat)

---

[201] For the preparation of **282**, see: ref. 199.

ν_{max} = 3319, 2932, 2851, 2796, 1689, 1447, 1253, 1150, 823, 769 cm^{-1}; HRMS (ESI) calcd for $C_8H_{15}NO$ [*M*+H]$^+$ 142.1226, 142.1230 found.

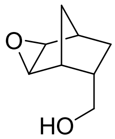

(1*RS*,2*SR*,4*RS*,5*RS*,6*SR*)-3-oxatricyclo[3.2.1.02,4]octan-6-ylmethanol (285). To a solution of ((1*RS*,2*SR*,4*RS*,5*RS*,6*SR*)-3-oxatricyclo[3.2.1.02,4]octan-6-ylmethoxy)(*tert*-butyl)dimethylsilane (**284**) (0.170 g, 0.668 mmol) in 4.5 mL THF was added TBAF (1.0 M in THF, 1.0 mL, 1.0 mmol) at 0 °C. After 10 min, the cooling bath was removed and the reaction allowed to warm to RT. After 2.5 h, the reaction was quenched by the addition of 2 mL $NaHCO_3$ (saturated, aqueous) and 2 mL water. The phases were separated an the aqeuous phase extracted withj EtOAc (3 x 15 mL). The combined organic phases were dried over Na_2SO_4 and the solvents evaporated. Purification by flash column chromatography (hexane/EtOAc 1:1) furnished alcohol **285** (66.4 mg, 0.47 mmol, 71%), which showed 12% contamination of epoxide opening product (5-*exo*-tet cyclization of the primary alcohol).

R_f = 0.16 (hexane:EtOAc 1:1, $KMnO_4$); ^{1}H NMR (400 MHz, $CDCl_3$) δ 3.63 (bs, 1H), 3.61 (bs, 1H), 3.22 (d, *J* = 3.0 Hz, 1H), 3.13 (d, *J* = 3.0 Hz, 1H), 2.58 (dd, *J* = 3.7, 1.8 Hz, 1H), 2.50 (dd, *J* = 4.4, 1.8 Hz, 1H), 2.24 – 2.15 (m, 1H), 1.73 (ddd, *J* = 12.6, 10.0, 4.4 Hz, 1H), 1.40 (dd, *J* = 10.0, 2.3 Hz, 1H), 0.83 – 0.78 (m, 2H) ppm; ^{13}C NMR (101 MHz, $CDCl_3$) δ 63.9, 51.4, 49.6, 43.8, 38.0, 37.3, 28.7, 27.3 ppm.

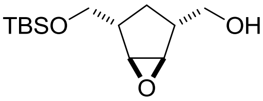

((1*RS*,2*RS*,4*SR*,5*SR*)-4-(((*tert*-butyldimethylsilyl)oxy)methyl)-6-oxabicyclo[3.1.0]-hexan-2-yl)methanol (287). To a solution of (1*RS*,2*RS*,4*SR*,5*SR*)-6-oxabicyclo[3.1.0]hexane-2,4-diyldimethanol (**286**)[202] (0.100 g, 0.694 mmol) in 3.5 mL CH_2Cl_2 was added imidazole (71.0 mg, 1.04 mmol), DMAP (8.5 mg, 0.1 mmol) and TBSCl (0.110 g, 0.728 mmol). After 35 min, the reaction was quenched by the addition of 2 mL NH_4Cl (aqueous, saturated) and 2 mL water. The phases were separated and the aqueous phase extracted with CH_2Cl_2 (3 x 10 mL). The combined organic phases were dried over Na_2SO_4 and the solvent evaporated.

---

[202] Prepared according to: M. H. Wu, E. N. Jacobsen, *Angew. Chem. Int. Ed.* **1999**, *38*, 2012-2014.

Purification *via* flash column chromatography (hexane:EtOAc 3:1) furnished alcohol **287** (0.092 g, 0.36 mmol, 51%).

R_f = 0.42 (hexane/EtOAc 2:1, $KMnO_4$); ^{1}H NMR (400 MHz, $CDCl_3$) δ 3.67 – 3.55 (m, 4H), 3.52 (d, *J* = 2.5 Hz, 1H), 3.49 (d, *J* = 2.5 Hz, 1H), 2.48 – 2.41 (m, 2H), 1.89 – 1.80 (m, 2H), 1.28 (app. dt, *J* = 14.3, 2.3 hz, 1H), 0.91 (s, 9H), 0.07 (s, 6H) ppm; ^{13}C NMR (101 MHz, $CDCl_3$) δ 65.0, 64.8, 61.0, 60.7, 42.4, 42.2, 27.6, 26.1, 18.6, –5.2, –5.3 ppm; FT-IR (neat) ν_{max} = 3426, 2954, 2929, 2885, 2858, 1472, 1391, 1362, 1255, 1095, 1045, 1022, 834, 776 cm^{-1}; HRMS (ESI) calcd for $C_{13}H_{26}O_3Si$ [*M*+H]$^+$ 259.1724, 259.1721 found.

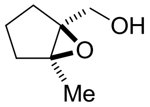

((1*SR*,5*SR*)-5-methyl-6-oxabicyclo[3.1.0]hexan-1-yl)methanol (290). To a solution of (2-methylcyclopent-1-en-1-yl)methanol (**289**)[203] (1.92 g, 17.1 mmol) in 60 mL CH_2Cl_2 was added *m*CPBA (6.33 g, 25.7 mmol) at 0 °C. The ice bath was removed and the reaction stirred for 40 min at RT before being quenched by the addition of 10 mL $Na_2S_2O_3$ (aqueous, saturated) and 10 mL $NaHCO_3$ (aqueous, saturated). The phases were separated and the aqueous phase extracted with CH_2Cl_2 (3 x 100 mL). the combined organic phases were washed with 100 mL brine and dried over Na_2SO_4. Evaporation of the solvent and purification by flash column chromatography (hexane/EtOAc 2:1) provided **290** (1.756 g, 13.70 mmol, 80%).

R_f = 0.39 (hexane/EtOAc 1:1, $KMnO_4$); ^{1}H NMR (400 MHz, $CDCl_3$) δ 3.87 (d, *J* = 12.1 Hz, 1H), 3.7 (d, *J* = 12.1 Hz, 1H), 2.08 (dd, *J* = 13.8, 8.2 Hz, 1H), 1.95 (dd, *J* = 13.8, 8.2 Hz, 1H), 1.75 – 1.62 (m, 2H), 1.57 – 1.49 (m, 1H), 1.42 (s, 3H), 1.40 –1.25 (m, 1H) ppm; ^{13}C NMR (101 MHz, $CDCl_3$) δ 71.0, 69.2, 62.3, 33.3, 28.9, 18.5, 15.6 ppm.

General Procedure A: Stoichiometric Ti(III)-Mediated Reductive Epoxide Opening. An oven dried flask was evacuated and purged with argon. Cp_2TiCl_2 (1.07g, 4.30 mmol) and activated zinc powder (380 mg, 5.81 mmol) were added and the flask was evacuated again. After 5 min the flask was carefully purged with argon. Freshly distilled and degassed THF (20 ml) was added.[204] The mixture was stirred for 1 h resulting in a dark green solution of Cp_2TiCl (c = 0.2 M). Then 2.0 equivalents of this solution were added *via* syringe pump over 6 h to a solution of the epoxide in degassed THF (c = 0.05 M). After completion of the addition, the reaction was stirred overnight, the solvent evaporated and the residue purified by flash column chromatography.

---

[203] Prepared according to: R. P. Short, J. M. Revol, B. C. Ranu, T. Hudlicky, *J. Org. Chem.* **1983**, *48*, 4453-4461.

[204] THF was degassed by three freeze-pump-thaw cycles.

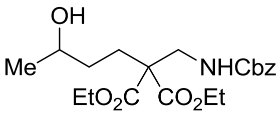

296

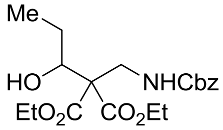

297

Diethyl-2-((((benzyloxy)carbonyl)amino)methyl)-2-(3-hydroxybutyl)malonate (296) and diethyl-2-((((benzyloxy)carbonyl)amino)methyl)-2-(2-hydroxybutyl)malonate (297). Prepared according to genaral procedure A from **264** (100 mg, 0.27 mmol). After flash column chromatography (hexane/EtOAc 10:1 → 0:1) a mixture of **296** (14.0 mg, 0.04 mmol, 15%) and **297** (7.0 mg, 0.02 mmol, 7%) was obtained.

^{1}H NMR (400 MHz, $CDCl_3$) δ 7.37 – 7.32 (m, 13H), 5.40 (bs, 1H), 5.29 (b, 1H), 5.16 – 5.09 (m, 5H), 4.53 (bs, 1H), 4.12 (bs, 1H), 3.83 – 3.71 (m, 19H), 2.52 – 2.47 (m, 2H), 2.36 (bs, 1H), 2.14 – 2.06 (m, 2H), 2.00 – 1.92 (m, 2H), 1.68 – 1.64 (m, 35), 1.48 – 1.40 (m, 3H), 1.30 – 1.19 (m, 7H) ppm; ^{13}C NMR (100 MHz, $CDCl_3$) δ 170.9, 169.7, 157.2, 156.7, 136.5, 136.3, 128.70, 128.66, 128.4, 128.3, 67.8, 67.4, 67.1, 67.0, 58.4, 56.7, 53.6, 52.91, 52.87, 43.5, 43.3, 33.6, 29.5, 27.9, 23.6, 18.0 ppm; FT-IR (neat) ν_{max} = 3390, 3066, 2957, 2360, 1771, 1738, 1538, 1520, 1456, 1436, 1254, 1150, 1013 cm^{-1}; HRMS (ESI) calcd for $C_{18}H_{26}NO_7$ $[M+H]^+$ 368.1704, 368,1705 found.

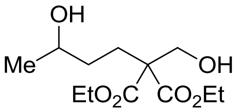

Diethyl-2-(3-hydroxybutyl)-2-(hydroxymethyl)malonate (298). Prepared according to genaral procedure A from **266** (100 mg, 0.38 mmol). After flash column chromatography (hexane/EtOAc 10:1 → 0:1) **298** (12.0 mg, 0.05 mmol, 12%) was obtained.

R_f = 0.18 (hexane/EtOAc 2:3, $KMnO_4$); ^{1}H NMR (400 MHz, $CDCl_3$) δ 4.23 (q, J = 7.1 Hz, 4H), 3.95 (s, 2H), 3.79 – 3.77 (m, 1H), 2.89 (bs, 1H), 2.09 – 2.06 (m, 1H), 1.98 – 1.94 (m, 1H), 1.75 (bs, 1H) 1.48 – 1.43 (m, 2H), 1.27 (t, J = 7.1 Hz, 6H), 1.20 (d, J = 6.2 Hz, 3H) ppm; ^{13}C NMR (151 MHz, $CDCl_3$) δ 171.1, 68.1, 64.4, 61.7, 59.5, 33.8, 27.5, 23.6, 14.2 ppm; FT-IR (neat) ν_{max} = 3392, 2978, 1728, 1448, 1369, 1218, 1096, 1033 cm^{-1}; HRMS (ESI) calcd for $C_{12}H_{23}O_6$ $[M+H]^+$ 263.1489, 263, 1475 found.

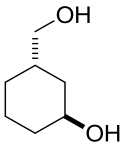

299

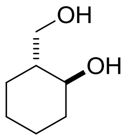

300

(1*SR*,3*SR*)-3-(hydroxymethyl)cyclohexanol (299) and (1*SR*,2*RS*)-2-(hydroxymethyl)-cyclohexanol (300). Prepared according to general procedure A from **276** (239 mg, 1.87 mmol). After flash column chromatography (CH_2Cl_2/MeOH 1:0 → 10:1) **299** (176 mg, 1.35 mmol, 73%) and **300** (18.0 mg, 0.14 mmol, 7%) were obtained.

299:

R_f = 0.40 (CH_2Cl_2/MeOH 10:1, $KMnO_4$); ^{1}H NMR (400 MHz, CD_3OD) δ 3.98 – 3.96 (m, 1H), 3.34 – 3.32 (m, 2H), 1.90 – 1.81 (m, 1H), 1.68 –1.64 (m, 4H), 1.47 – 1.44 (m, 2H), 1.24 (ddd, J = 13.7, 11.0, 2.8 Hz, 1H), 1.06 – 0.96 (m, 1H) ppm; ^{13}C NMR (100 MHz, CD_3OD) δ 68.0, 67.0, 36.6, 35.4, 33.8, 29.6, 20.6 ppm; ; FT-IR (neat) ν_{max} = 3448, 2934, 2360, 1630, 1450, 1400, 1257, 1126, 1086, 1015, 981 cm^{-1}; HRMS (EI) calcd for $C_7H_{12}O$ $[M\text{–}H_2O]^+$ 112.0883, 112.0882 found.

300

^{1}H NMR (400 MHz, CD_3OD) δ 3.74 – 3.70 (m, 1H), 3.56 – 3.52 (m, 1H), 3.37 – 3.33 (m, 1H), 3.39 – 3.36 (m, 2H), 1.95 – 1.90 (m, 1H), 1.82 – 1.66 (m, 4H), 1.45 – 1.38 (m, 2H), 1.29 – 1.22 (m, 3H), 1.09 – 0.99 (m, 1H) ppm; ^{13}C NMR (101 MHz, CD_3OD) δ 73.7, 66.2, 48.1, 36.4, 28.9, 26.4, 25.8 ppm; FT-IR (neat) ν_{max} = 3340, 2937, 2864, 1448, 1347, 1296, 1262, 1144, 1088, 1026, 991 cm^{-1}; HRMS (EI) calcd for $C_7H_{14}O_2$ $[M\text{–}H_2O]^+$ 112.0883, 112,0883 found.

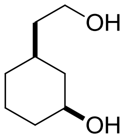

301

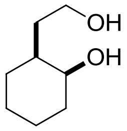

302

(1*SR*,3*SR*)-3-(2-hydroxyethyl)cyclohexanol (301) and (1*SR*,2*SR*)-2-(2-hydroxy-ethyl)cyclohexanol (302). Prepared according to genaral procedure A from **281** (205 mg, 1.44 mmol). After flash column chromatography (hexane/EtOAc 4:1 → 0:1) **301** (124 mg, 0.86 mmol, 60%) and **302** (70.0 mg, 0.49 mmol, 34%) were obtained.

301:

R_f = 0.21 (EtOAc); ^{1}H NMR (400 MHz, CD_3OD) δ 3.57 (t, J = 6.5 Hz, 2H), 3.50 – 3.42 (m, 1H), 1.96 –1.85 (m, 2H), 1.75 – 1.68 (m, 1H), 1.66 – 1.60 (m, 1H), 1.49 – 1.38 (m, 3H), 1.31 – 1.19 (m, 1H), 1.13 –1.03 (m, 1H), 0.98 – 0.73 (m, 2H) ppm; ^{13}C NMR (100 MHz,

CD_3OD) δ 71.3, 60.6, 43.2, 40.7, 36.3, 34.1, 33.2, 25.1 ppm; FT-IR (neat) ν_{max} = 3515, 2935, 2856, 1626, 1464, 1451, 1403, 1367, 1099, 1042, 1008 cm^{-1}.

302:

R_f = 0.32 (EtOAc); ^1H NMR (400 MHz, CD_3OD) δ 3.77 – 3.75 (m, 1H), 3.59 – 3.52 (m, 2H), 1.70 – 1.64 (m, 1H), 1.63 – 1.52 (m, 4H), 1.44 – 1.22 (m, 6H) ppm; ^{13}C NMR (100 MHz, CD_3OD) δ 70.1, 60.9, 39.2, 35.5, 33.8, 27.8, 26.0, 21.8 ppm; FT-IR (neat) ν_{max} = 3501, 2935, 2360, 2340, 1704, 1652, 1634, 1538, 1446, 1398, 1010 cm^{-1}.

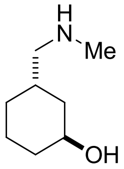

(1*SR*,3*SR*)-3-((methylamino)methyl)cyclohexanol (303). Prepared according to genaral procedure A from **283** (129 mg, 0.91 mmol). After flash column chromatography (CH_2Cl_2/MeOH/NH_4OH 3:1:0.1 → 1:1:0.1) **303** (117 mg, 0.82 mmol, 89%) was obtained.

^1H NMR (400 MHz, MeOD) δ 7.41 (bs, 1H), 4.06 (bs, 1H), 2.88 (app. d, *J* = 2.0 Hz, 1H), 2.87 (app. d, *J* = 1.4 Hz, 1H), 2.70 (s, 3H), 2.22 – 2.12 (m, 1H), 1.84 – 1.67 (m, 4H), 1.59 – 1.46 (m, 2H), 1.36 – 1.30 (m, 1H), 1.17 – 1.10 (m, 1H) ppm; ^{13}C NMR (101 MHz, MeOD) δ 66.3, 56.0, 37.5, 34.2, 33.3, 30.7, 30.6, 20.4 ppm; FT-IR (neat) ν_{max} = 3117, 3016, 2805, 1392, 1260, 988 cm^{-1}; HRMS (ESI) calcd for $C_8H_{17}NO$ $[M+H]^+$ 144.1383, 144.1385 found.

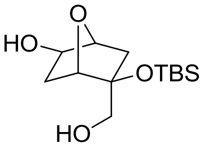

(1*SR*,2*RS*,4*SR*,5*SR*)-5-((*tert*-butyldimethylsilyl)oxy)-5-(hydroxymethyl)-7-oxabicyclo-[2.2.1]heptan-2-ol (304). Prepared according to genaral procedure A from **293** (50.0 mg, 0.18 mmol). After flash column chromatography (CH_2Cl_2/MeOH 50:1) **304** (34.0 mg, 0.12 mmol, 68%) was obtained.

R_f = 0.23 (hexane/EtOAc 1:1, CAM); ^1H NMR (400 MHz, $CDCl_3$) δ 4.39 (d, *J* = 6.5 Hz, 1H), 4.33 (d, *J* = 6.0 Hz, 1H), 3.83 (app. t, *J* = 6.7 Hz, 1H), 3.58 (dd, *J* = 11.2, 4.5 Hz, 1H), 3.46 (dd, *J* = 11.2, 7.9 Hz, 1H), 2.18 – 2.09, 1.99 (d, *J* = 8.4 Hz, 1H), 1.79 (ddd, *J* = 13.9, 6.6, 1.4 Hz, 1H), 1.48 (dddd, *J* = 14.4, 6.0, 2.2, 1.4 Hz, 1H), 1.24 (dd, *J* = 13.8 Hz, 1H), 0.87 (s, 9H), 0.17 (s, 3H), 0.15 (s, 3H) ppm; ^{13}C NMR (101 MHz, $CDCl_3$) δ 84.4, 82.5, 82.0, 73.9, 67.5, 38.7, 37.1, 26.1, 18.4, –2.6, –3.3 ppm; FT-IR (neat) ν_{max} = 3401, 1953, 1928, 2856, 1472, 1389, 1360, 1252, 1120, 1041, 1018, 995, 971, 835, 776 cm^{-1}; HRMS (ESI) calcd for $C_{13}H_{26}O_4Si$ [*M*+Na]$^+$ 297.1493, 297.1488 found.

General Procedure B: Catalytic Ti(III)-Mediated Reductive Epoxide Opening. Cp_2TiCl_2 (15 mol%), manganese powder (3.0 equiv) and 2,4,6-collidine·HCl (3.0 equiv) were weighted into a round bottom flask, which was evacuated for 5 min and subsequently backfilled with argon. Degassed THF[204] (c_{total} = 0.05 M) was added, followed by a solution of the epoxide in THF (approximately 1/3 of the total volume of THF). The reaction was stirred vigorously overnight under argon upon which a metallic blue color was visible. The mixture was filtered over a pad of celite (rinsed with EtOAc), the solvents evaporated and the crude residue purified by flash column chromatography.

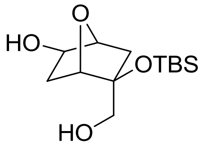

304

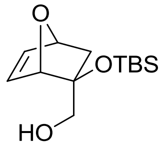

305

(1*SR*,2*RS*,4*SR*,5*SR*)-5-((*tert*-butyldimethylsilyl)oxy)-5-(hydroxymethyl)-7-oxabicyclo-[2.2.1]heptan-2-ol (304) and ((1*SR*,2*SR*,4*SR*)-2-((*tert*-butyldimethylsilyl)oxy)-7-oxabicyclo[2.2.1]hept-5-en-2-yl)methanol (305). Prepared according to general procedure B from **293** (60.0 mg, 0.22 mmol). After flash column chromatography (hexane/EtOAc 3:1 → 1:1) **304** (48.2 mg, 0.18 mmol, 80%) and **305** (11.0 mg, 0.04 mmol, 19%) were obtained.

305:

R_f = 0.73 (hexane/EtOAc 1:1, CAM); ^{1}H NMR (400 MHz, $CDCl_3$) δ 6.40 (bs, 2H), 5.01 (d, *J* = 4.6 Hz, 1H), 4.68 (bs, 1H),3.55 (d, *J* = 11.1 Hz, 1H), 3.25 (d, *J* = 11.1 Hz, 1H), 2.18 (bs, 1H), 1.87 (dd, *J* = 12.3, 4.8 Hz, 1H), 1.26 (d, *J* = 12.3 Hz, 1H), 0.89 (s, 9H), 0.16 (s, 6H) ppm; ^{13}C NMR (101 MHz, $CDCl_3$) δ 138.7, 133.6, 85.1, 84.3, 78.2, 69.6, 37.7, 26.1, 18.4, –2.6, –3.2 ppm; FT-IR (neat) ν_{max} = 3478, 2953, 2929, 2885, 2856, 1472, 1313, 1249, 1097, 1003, 833, 776, 709 cm^{-1}; HRMS (MALDI) calcd for $C_{13}H_{24}O_3Si$ [*M*+H]$^+$ 257.1567, 257.1568 found.

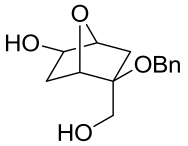

306

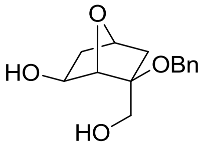

366

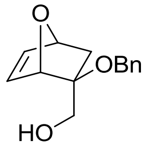

307

(1*SR*,2*RS*,4*SR*,5*SR*)-5-(benzyloxy)-5-(hydroxymethyl)-7-oxabicyclo[2.2.1]heptan-2-ol (306), (1*SR*,2*SR*,4*RS*,6*SR*)-6-(benzyloxy)-6-(hydroxymethyl)-7-oxabicyclo[2.2.1]heptan-2-ol (366) and ((1*SR*,2*SR*,4*SR*)-2-(benzyloxy)-7-oxabicyclo[2.2.1]hept-5-en-2-yl)methanol (307). Prepared according to general procedure B from **295** (30.0 mg, 0.12 mmol). After flash column chromatography (CH_2Cl_2/MeOH 20:1) **306** (18.00 mg, 0.072 mmol, 60%), **366** (3.00 mg, 0.01 mmol, 10%) and **307** (3.30 mg, 0.01 mmol, 10%) were obtained.

306:

R_f = 0.24 (toluene/acetone 1:1, CAM, UV); ^{1}H NMR (400 MHz, MeOD) δ 7.42 – 7.23 (m, 5H), 4.62 – 4.52 (m, 3H), 4.38 (dd, *J* = 6.2, 1.2 Hz, 1H), 3.97 (d, *J* = 12.6 Hz, 1H), 3.91 (dd, *J* = 7.0, 2.8 Hz, 1H), 3.57 (d, *J* = 12.6 Hz, 1H), 2.29 (dd, *J* = 13.5, 7.0 Hz, 1H), 1.89 (ddd, *J* = 13.5, 6.2, 1.2 Hz, 1H), 1.52 (dddd, *J* = 13.5, 6.2, 2.8, 1.2 Hz, 1H) ppm; ^{13}C NMR (101 MHz, MeOD) δ 140.7, 129.2, 129.2, 128.6, 128.2, 88.3, 84.3, 82.5, 74.1, 66.3, 64.2, 37.4, 36.8 ppm; FT-IR (neat) ν_{max} = 3390, 2927, 2872, 1569, 1454, 1312, 1201, 1106, 1039, 973, 922 cm^{-1}.

366:

R_f = 0.24 (toluene/acetone 1:1, CAM, UV); ^{1}H NMR (400 MHz, MeOD) δ 7.42 – 7.23 (m, 5H), 4.69 (app. td, *J* = 5.6, 1.3 Hz, 1H), 4.62 (d, *J* = 11.7 Hz, 1H), 4.54 (d, *J* = 11.7 Hz, 1H), 4.31 (dd, *J* = 6.9, 1.9 Hz, 1H), 4.02 (d, *J* = 12.6 Hz, 1H), 3.51 (d, *J* = 12.6 Hz, 1H), 1.96 – 1.87 (m, 2H), 1.63 – 1.59 (m, 1H), 1.35 (d, *J* = 12.8 Hz, 1H) ppm; ^{13}C NMR (101 MHz, MeOD) δ 140.7, 129.2, 128.6, 128.2, 89.7, 87.1, 77.1, 70.5, 66.0, 64.4, 41.9, 40.8 ppm; FT-IR (neat) ν_{max} = 3392, 2926, 2856, 1454, 1289, 1246, 1201, 1117, 1086, 1049, 975, 738, 698 cm^{-1}.

307:

R_f = 0.67 (toluene/acetone 1:1, CAM, UV); ^{1}H NMR (300 MHz, $CDCl_3$) δ 7.41 – 7.29 (m, 5H), 6.50 (dd, *J* = 5.9, 1.7 Hz, 1H), 6.46 (dd, *J* = 5.9, 1.5 Hz, 1H), 5.09 (app. dt, *J* = 4.8, 1.3 Hz, 1H), 4.95 (bs, 1H), 4.64 – 4.57 (m, 2H), 3.81 (dd, *J* = 11.9, 3.5 Hz, 1H), 3.34 (dd, *J* = 11.9, 8.8 Hz, 1H), 2.12 – 2.07 (m, 2H), 1.23 (d, *J* = 12.1 Hz, 1H), 1.21 ppm; ^{13}C NMR (101 MHz, $CDCl_3$) δ 139.0, 138.7, 134.2, 128.7, 128.6, 127.7, 127.5, 87.5, 83.8, 78.4, 66.9, 66.4, 33.3 ppm; FT-IR (neat) ν_{max} = 3431, 2944, 2874, 1497, 1454, 1383, 1315, 1244, 1209, 1095, 1028, 914, 738 cm^{-1}.

13.4.3 Synthesis of Raman-Active Epoxyisoprostane Analogs

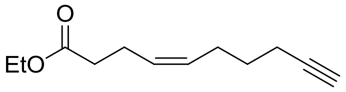

(*Z*)-ethyl dec-4-en-9-ynoate (339). To a solution of ethyl butanoate-4-triphenylphosphonium bromide (31.9 g, 69.7 mmol) in 270 mL THF was added KO*t*Bu (9.39 g, 83.7 mmol) at –78 °C. After 1 h, hex-5-ynal (6.70 g, 52.7 mmol) in 50 mL THF was added dropwise. After 1 h, the cooling bath was removed and the reaction stirred for one additional hour. The orange suspenion was quenched by the addition of 50 mL NH_4Cl (saturated, aqueous) and 30 mL water. The phases were separated and the aqueous phase extraced with Et_2O (3 x 150 mL). The combined organic phases were dried over Na_2SO_4 and concentrated. Purification *via* flash column chromatography (hexane/Et_2O 30:1 → 20:1 → 10:1) gave **339** (10.24 g, 52.71 mmol, 76%) as a colorless liquid.

^{1}H NMR (400 MHz, $CDCl_3$) δ 5.43 – 5.35 (m, 2H), 4.13 (q, J = 7.1 Hz, 2H), 2.41 – 2.32 (m, 4H), 2.22 –2.15 (m, 4H), 1.63 – 1.55 (m, 2H), 1.26 (t, J = 7.1 Hz, 3H) ppm; ^{13}C NMR (101 MHz, $CDCl_3$) δ 173.3, 130.1, 128.8, 84.5, 68.6, 60.5, 34.5, 28.5, 26.3, 23.0, 18.0, 14.4 ppm; FT-IR (neat) ν_{max} = 2981, 2938, 2865, 1733, 1447, 1372, 1349, 1178, 1153, 1096, 1040 cm^{-1}; HRMS (EI) calcd for $C_{10}H_{13}O_2$ $[M–C_2H_5]^+$ 165.0910, 165.0910 found.

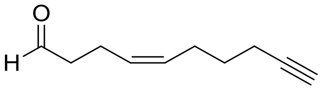

(*Z*)-dec-4-en-9-ynal (340). To a solution of **339** (10.24 g, 52.71 mmol) in 100 mL toluene was added DIBAL (1.0 M in toluene, 52.7 mL, 53 mmol) dropwise over 1 h at −78 °C. After 2 h of stirring at this temperature, the reaction was quenched by the addition of EtOAc (50 mL), then 200 mL potassium sodium tartrate (aqueous, saturated) and 100 mL water. After vigorous stirring for 3 h, the phases were separated and the aqueous phase extracted with EtOAc (3 x 100 mL). The combined organic phases were dried over $MgSO_4$ and concentrated *in vacuo*. The crude product was purified by flash column chromatography (hexane/Et_2O 10:1) to give 87% of **340** (6.87 g, 45.7 mmol).

R_f = 0.18 (hexane/Et_2O 20:1, $KMnO_4$); ^{1}H NMR (400 MHz, $CDCl_3$) δ 9.78 (t, J = 1.6 Hz, 1H), 5.46 – 5.35 (m, 2H), 2.52 – 2.48 (m, 2H), 2.42 – 2.37 (m, 2H), 2.22 – 2.16 (m, 4H), 1.95 (t, J = 2.6 Hz, 1H), 1.63 – 1.55 (m, 2H) ppm; ^{13}C NMR (101 MHz, $CDCl_3$) δ 202.2, 130.3, 128.5, 84.4, 68.6, 43.9, 28.3, 26.2, 20.2, 18.0 ppm; FT-IR (neat) ν_{max} = 3010, 2936, 2863, 2724, 1722, 1433, 1409, 1390, 1348, 1056 cm^{-1}; HRMS (EI) calcd for $C_{10}H_{14}O$ [*M*–H]$^+$ 149.0961, 149.0958 found.

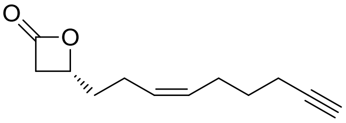

(*R*,*Z*)-4-(non-3-en-8-yn-1-yl)oxetan-2-one (341). $LiClO_4$ (15.1 g, 142 mmol, dried overnight at 180 °C under high vacuum) was suspended in 120 mL Et_2O and TMS-quinidine **321** (2.18 g, 5.49 mmol) was added. The mixture was stirred at RT until all solids dissolved. Then 280 mL CH_2Cl_2 were added and the reaction cooled to –78°C. *i*Pr_2NEt (20.8 mL, 119 mmol) followed by a solution of **340** (6.87 g, 45.7 mmol) in 20 mL CH_2Cl_2 were added. AcCl (8.13 ml, 114 mmol) was dissolved in 30 mL CH_2Cl_2 and added dropwise over 4 h *via* syringe pump. After stirring at –78 °C overnight, 200 mL ether were added and the suspension filtered over a pad of silica (rinsed with 100 mL ether) and concentrated. The crude material was purified by flash column chromatography (hexane/Et_2O 4:1 → 3:1 → 2:1) to yield **341** (6.62 g, 34.4 mmol, 75%).

R_f = 0.44 (hexane/Et_2O 2:1, $KMnO_4$); ^{1}H NMR (400 MHz, $CDCl_3$) δ 5.46 – 5.36 (m, 2H), 4.55 – 4.49 (m, 1H), 3.52 (dd, *J* = 16.3, 5.8 Hz, 1H), 3.09 (dd, *J* = 16.3, 4.3 Hz, 1H), 2.24 – 2.14 (m, 6H), 1.99 – 1.90 (m, 2H), 1.85 – 1.77 (m, 1H), 1.62 – 1.55 (m, 2H) ppm; ^{13}C NMR (101 MHz, $CDCl_3$) δ 168.3, 130.6, 128.5, 84.4, 70.9, 68.7, 43.1, 34.8, 28.3, 26.1, 23.0, 17.9 ppm; FT-IR (neat) ν_{max} = 3009, 2936, 2864, 1823, 1455, 1433, 1280, 1136, 1117, 861, 825 cm^{-1}; HRMS (ESI) calcd for $C_{12}H_{16}NaO_2$ [*M*+Na]$^+$ 215.1043, 215.1041 found; $[\alpha]_D^{23°C}$ = +27.12 (c = 1.0, $CHCl_3$).

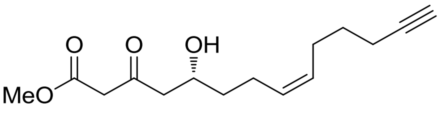

(*R*,*Z*)-methyl 5-hydroxy-3-oxotetradec-8-en-13-ynoate (342). *n*BuLi (1.6 M in hexane, 82 mL, 131 mmol) was added to a solution of *i*Pr_2NH (19 mL, 134 mmol) in 120 mL THF at 0 °C. After 15 min, the solution was cooled to –78 °C and MeOAc (10.4 mL, 131 mmol) in 20 mL THF was added. After 20 min, a solution of **341** (6.62 g, 34.4 mmol) in 16 mL THF was added. After 3 h, the reaction was warmed to RT and then quenched by the addition of 150 mL NH_4Cl (saturated, aqueous). Phase separation, extraction of the aqueous phase with EtOAc (3 x 100 mL) and subsequent drying over Na_2SO_4 furnished after concentration the crude product. Purification *via* flash column chromatography (hexane/EtOAc 3:1 → 2:1 → 1:1) gave **342** (7.01 g, 26.3 mmol, 77%) as a faint yellow oil.

R_f = 0.25 (hexane/EtOAc 2:1, $KMnO_4$); ^1H NMR (400 MHz, $CDCl_3$) *contains 10% enol tautomer* δ 5.43 – 5.33 (m, 2H), 4.12 –4.05 (m, 1H), 3.75 (s, 3H), 3.49 (s, 2H), 2.79 – 2.69 (m, 2H), 2.21 – 2.15 (m, 6H), 1.96 (t, J = 2.6 Hz, 1H), 1.62, – 1.53 (m, 3H), 1.50 – 1.41 (m, 1H) ppm; ^{13}C NMR (101 MHz, $CDCl_3$) *contains 10% enol tautomer* δ 203.6, 167.5, 130.0, 129.6, 84.6, 68.6, 67.2, 52.6, 49.8, 49.8, 36.4, 28.5, 26.2, 23.4, 18.0 ppm; FT-IR (neat) ν_{max} = 3507, 3290, 2006, 2934, 2863, 2116, 1741, 1714, 1434, 1406, 1323, 1267, 1205, 1155, 859 cm^{-1}; HRMS (ESI) calcd for $C_{15}H_{22}NaO_4$ $[M+Na]^+$ 289.1410, 289.1411 found; $[\alpha]_D^{23°C}$ = –21.23 (c = 1.0, $CHCl_3$).

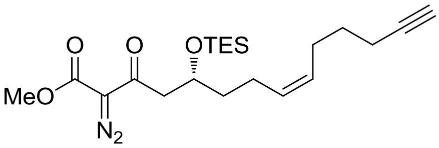

(*R*,*Z*)-methyl 2-diazo-5-hydroxy-3-oxotetradec-8-en-13-ynoate (343). To a solution of **342** (7.01 g, 26.3 mmol) in 230 mL MeCN was added NEt_3 (7.34 mL, 52.7 mmol) and *p*-ABSA (8.22 g, 34.2 mmol). After stirring overnight, the reaction was filtered over a pad of celite and concentrated. Purification by flash column chromatography (hexane/EtOAc 3:1 → 2:1 gave the corresponding diazo alcohol (6.62 g, 22.7 mmol, 86%) as a yellow oil. This material was dissolved in 45 mL DMF and imidazole (3.08 g, 45.2 mmol) and TESCl (5.7 mL, 34 mmol) were added. After 3 h, 150 mL ether were added and the mixture was washed with water (2 x 200 mL). The organic phase was dried over $MgSO_4$ and concentrated. Purification *via* flash column chromatography (hexane/Et_2O 10:1) gave **343** (7.83 g, 19.3 mmol, 85%, 73% over two steps, 94% *ee*[205]).

R_f = 0.30 (hexane/Et_2O 10:1, $KMnO_4$, UV); ^1H NMR (400 MHz, $CDCl_3$) δ 5.44 – 5.30 (m, 2H), 4.31 – 4.25 (m, 1H), 3.83 (s, 3H), 3.16 (dd, J = 15.6, 7.2 Hz, 1H), 2.91 (dd, J = 15.6, 5.3 Hz, 1H), 2.89 – 2.06 (m, 6 H), 1.95 t, J = 2.6 Hz, 1H), 1.62 – 1.52 (m, 4H), 0.94 (t, J = 7.9 Hz, 9H), 0.58 (q, J = 7.9 Hz, 6H) ppm; ^{13}C NMR (101 MHz, $CDCl_3$) δ 191.0, 161.8, 130.5, 129.0, 84.6, 68.8, 68.5, 52.4, 47.4, 38.1, 28.6, 26.2, 23.2, 18.0, 7.0, 5.1 ppm; FT-IR (neat) ν_{max} = 3007, 2954, 2913, 2877, 2134, 1723, 1656, 1437, 1200, 1005, 743 cm^{-1}; HRMS

---

[205] The racemic sample was prepared by mixing equimolar amounts of both enantiomers. The other enantiomer and the mixture were prepared and measured by MICHAEL SCHNEIDER and ANDREJ SHEMET. The author of this thesis (C.E) gratefully acknowledges the supply of the racemic spectra.

(ESI) calcd for $C_{21}H_{34}NaO_4Si$ $[M+Na]^+$ 401.2119, 401.2127 found; $[\alpha]_D^{23°C} = -16.46$ (c = 1.0, $CHCl_3$).

SFC (CO_2–MeOH 98:2, 2.0 mL/min, 25 °C), racemic

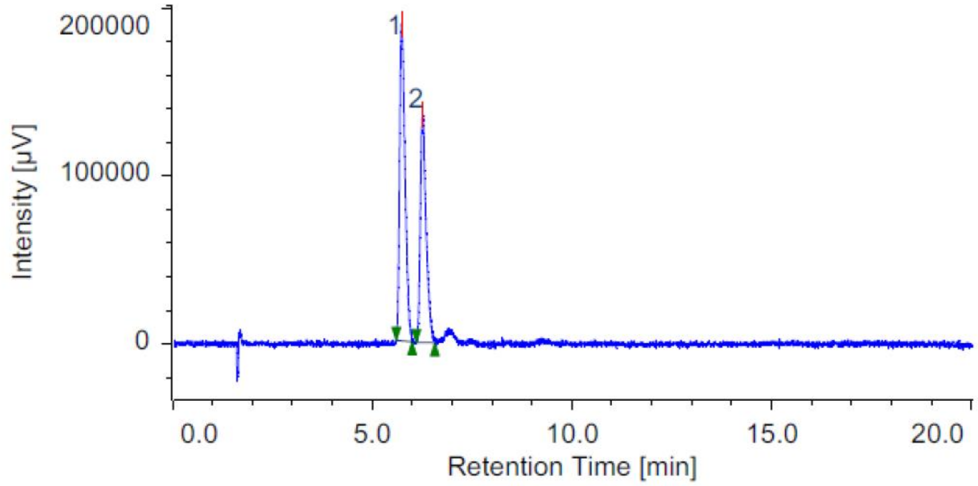

#	Peak Name	CH	tR [min]	Area [µV·sec]	Height [µV]	Area%	Height%	Quantity	NTP	Resolution	Symmetry Factor	Warning
1	Unknown	10	5.733	1788741	188248	56.104	58.130	N/A	8861	2.084	1.531	
2	Unknown	10	6.260	1399540	135593	43.896	41.870	N/A	9048	N/A	1.485	

SFC (CO_2–MeOH 98:2, 2.0 mL/min, 25 °C), enantioenriched

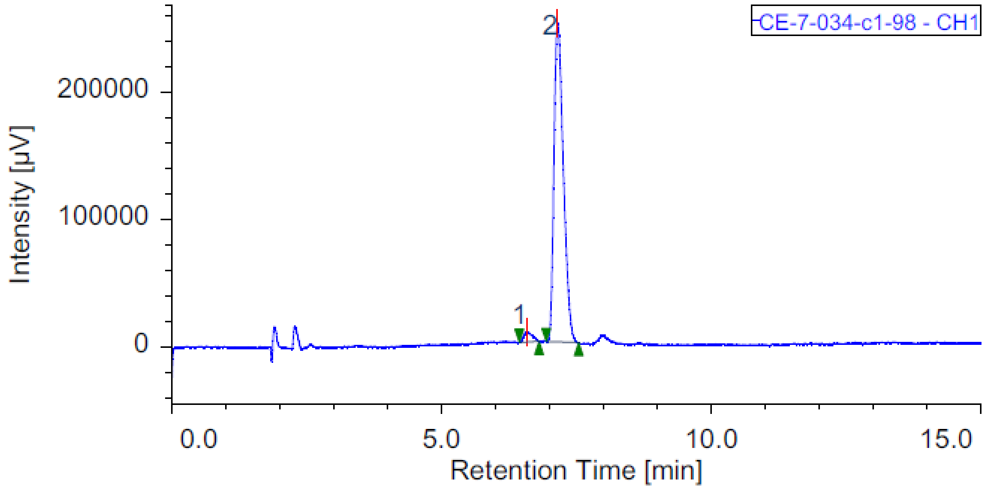

#	Peak Name	CH	tR [min]	Area [µV·sec]	Height [µV]	Area%	Height%	Quantity	NTP	Resolution	Symmetry Factor	Warning
1	Unknown	1	6.583	88842	7972	2.861	3.094	N/A	7354	1.808	1.332	
2	Unknown	1	7.150	3015957	249655	97.139	96.906	N/A	7914	N/A	1.449	

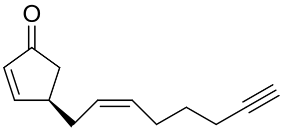

(*R*,*Z*)-4-(oct-2-en-7-yn-1-yl)cyclopent-2-enone (335).

To a refluxing solution of $Rh_2(S\text{-PTAD})_4$ (55.0 mg, 0.04 mmol) in 380 mL CH_2Cl_2 was added a solution of **343** (7.83 g, 19.3 mmol) in 50 mL CH_2Cl_2 dropwise over 30 min. After additional 30 min, the reaction was allowed to cool to RT and the solvent evaporated. The crude material was purified by flash column chromatohgraphy (hexane/Et_2O 4:1) to yield a diastereomeric mixture of the C–H inserted products (6.85 g). This material was then dissolved in 200 mL DMSO and NaCl (33.8 g, 578 mmol) was added. The mixture was degassed and placed in a 140 °C preheated oil bath.[206] After 2.5 h, the reaction was allowed to cool to RT, befor 300 mL of water were added. This solution was then extracted with EtOAc (4 x 200 mL). The combined organic phases were dried over $MgSO_4$ and concentrated. Purification *via* flash column chromatography (hexane/EtOAc 7:1 → 6:1) allowed for the separation of the diastereomers. The obtained 2.20 g (6.86 mmol) of the *syn* isomer were dissolved in 60 mL CH_2Cl_2 and cooled to 0 °C. DBU (10.4 mL, 68.8 mmol) was added and the reaction stirred for 17 h at 4 °C. The solution was quenched by the addition of 150 mL NH_4Cl (aqueous, saturated) and the phases separated. The aqueous phase was extracted with EtOAc (3 x 150 mL) and the combined organic phases dried over $MgSO_4$. The crude material was purified by flash column chromatography providing **335** (0.73 g, 3.88 mol, 20% over three steps) as a yellow oil.

R_f = 0.29 (hexane/EtOAc 4:1, $KMnO_4$, UV); ^1H NMR (400 MHz, $CDCl_3$) δ 7.63 (dd, J = 5.7, 2.5 Hz, 1H), 6.17 (dd, J = 5.7, 2.0 Hz, 1H), 5.52 – 5.37 (m, 2H), 3.04 – 2.98 (m, 1H), 2.52 (dd, J = 18.9, 6.4 Hz, 1H), 2.37 – 2.13 (m, 7H), 2.03 (dd, J = 18.9, 2.2 Hz, 1H), 1.95 (t, J = 2.6 Hz, 1H), 1.63 – 1.55 (m, 2H) ppm; ^{13}C NMR (101 MHz, $CDCl_3$) δ 209.9, 168.0, 134.3, 131.5, 126.8, 84.3, 68.7, 41.5, 40.6, 32.1, 28.3, 26.3, 18.0 ppm; FT-IR (neat) ν_{max} = 3294, 3009, 2934, 1711, 1587, 1435, 1407, 1348, 1184, 835, 784 cm^{-1}; HRMS (EI) calcd for $C_{13}H_{17}O$ $[M+H]^+$ 187.1117, 187.1127 found; $[\alpha]_D^{23°C}$ = +97.73 (c = 0.67, $CHCl_3$).

---

[206] DMSO was degassed by bubbling nitrogen through the solution for 10 min.

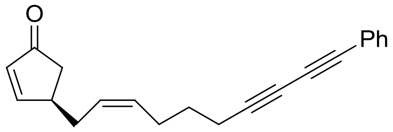

(*R*,*Z*)-4-(10-phenyldeca-2-en-7,9-diyn-1-yl)cyclopent-2-enone (334). **335** (300 mg, 1.59 mmol) and (iodoethynyl)benzene (0.545 g, 2.39 mmol) were dissolved in 4.5 mL DMF. CuI (6.0 mg, 0.03 mmol), Pd(dba)$_2$ (37.0 mg, 0.06 mmol), (*E*)-3-(2-(diphenylphosphino)phenyl)-1-phenylprop-2-en-1-one (**346**) (25.0 mg, 0.06 mmol) and NEt$_3$ (0.44 mL, 3.2 mmol) were added. After 6 h, the 5 mL water and 5 mL EtOAc were added. The phases were separated and the aqueous phase extracted with EtOAc (3 x 10 mL). The combined organic phases were dried over MgSO$_4$ and concentrated. Purification by flash column chromatography (hexane/EtOAc 10:1 → 4:1 → 3:1) provided **334** (240 mg, 0.83 mmol, 52%)

R$_f$ = 0.33 (hexane/EtOAc 3:1, CAM, UV); ^{1}H NMR (400 MHz, CDCl$_3$) δ 7.64 (dd, *J* = 5.7, 2.5 Hz, 1H), 7.48 – 7.46 (m, 2H), 7.36 – 7.28 (m, 3H), 6.18 (dd, *J* = 5.7, 2.0 Hz, 1H), 5.52 – 5.39 (m, 2H), 3.05 – 2.99 (m, 1H), 2.54 (dd, *J* = 18.8, 6.5 Hz, 1H) 2.39 – 2.33 (m, 3H), 2.29 – 2.15 (m, 3H), 2.04 (dd, *J* = 18.8, 2.2 Hz, 1H), 1.68 – 1.57 (m, 2H) ppm; ^{13}C NMR (101 MHz, CDCl$_3$) δ 209.9, 167.9, 134.3, 132.6, 131.2, 129.0, 128.5, 127.1, 122.1, 84.3, 75.1, 74.4, 65.7, 41.6, 40.7, 32.1, 28.0, 26.4, 19.1 ppm; FT-IR (neat) ν_{max} = 3009, 2929, 2862, 2243, 1711, 1587, 1490, 1407, 1348, 1183, 756 cm^{-1}; HRMS (MALDI) calcd for $C_{21}H_{24}NO$ $[M+NH_4]^+$ 306.1852, 306.1854 found; $[\alpha]_D^{23°C}$ = +120.90 (c = 0.47, CHCl$_3$).

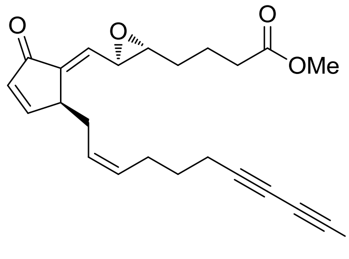

Methyl-4-((2*R*,3*R*)-3-((*E*)-((*S*)-2-oxo-5-((*Z*)-10-phenyldeca-2-en-7,9-diyn-1-yl)cyclopent-3-en-1-ylidene)methyl)oxiran-2-yl)butanoate (347). To a solution of LiHMDS (26.4 mg, 0.16 mmol) in 0.6 mL THF was added **334** (35.0 mg, 0.12 mmol) in 0.4 mL THF at –78 °C. The reaction was stirred for 30 min, before **317** (52.2 mg, 0.30 mmol) in 0.3 mL THF was added dropwise at –78 °C. After 2 h, the reaction was quenched by the addition of 5 mL NH$_4$Cl (aqueous, saturated) and 3 mL water. Then, 5 mL EtOAc were added, the phases were separated and the aqueous phase extracted with EtOAc (3 x 5 mL). The combined organic phases were dried over Na_2SO_4 and concentrated. Flash column chromatography (hexane/EtOAc 2:1 → 1:1) separated the aldol products from residual aldehyde **317**. The crude material was disolved in 0.6 mL CH_2Cl_2 and cooled to –78 °C. NEt_3 (0.17 mL, 1.21 mmol) and MsCl (57 µL, 0.7 mmol) were added. After stirring at this temperature for 1 h, the cooling bath was removed and the reaction allowed to warm to RT. The reaction was quenched by the addition of 2 mL $NaHCO_3$ (aqueous, saturated) and the phases separated. The aqueous phase was extracted with CH_2Cl_2 (3 x 5 mL) and the combined organic phases were dried over Na_2SO_4 and filtered over a short pad of silica. The pad was rinsed with 15 mL EtOAc and the residue carefully concentrated to 0.5 mL (concentrated at RT since decomposition was observed at 40 °C). Additional 0.5 mL CH_2Cl_2 were added, followed by Al_2O_3 (124 mg, 1.21 mmol).[207] After 12 h, additional 100 mg of Al_2O_3 was added. If the reaction was not done, additional 100 mg were added (this process was repeated until full conversion was achieved). The material was directly loaded on a column and purified (hexane/EtOAc 3:1 → 2:1 → 1:1) to give **347** (25.0 mg, 0.06 mmol, 49%)

R_f = 0.76 (hexane/EtOAc 1:1, $KMnO_4$, UV); ^{1}H NMR (300 MHz, $CDCl_3$) δ 7.55 (dd, *J* = 5.9, 2.8 Hz, 1H), 7.49 – 7.45 (m, 2H), 7.34 – 7.30 (m, 3H), 6.38 – 6.34 (m, 1H), 6.22 – 6.19 (m, 1H), 5.53 – 5.37 (m, 2H), 3.68 – 3.67 (m, 4H), 3.40 (dd, *J* = 8.1, 2.1 Hz, 1H), 3.00 – 2.95 (m, 1H), 2.67 – 2.54 (m, 1H), 2.42 – 2.34 (m, 5H), 2.21 – 2.11 (m, 2H), 1.85 – 1.76 (m, 3H), 1.70 – 1.55 (m, 3H) ppm; ^{13}C NMR (101 MHz, $CDCl_3$) δ 195.8, 173.6, 161.8, 141.0, 134.8, 132.7, 131.7, 131.1, 129.1, 128.5, 126.1, 122.0, 84.2, 75.2, 74.3, 68.9, 60.1, 55.1, 51.8, 43.3, 33.6, 31.9, 31.4, 28.0, 26.4, 21.5, 19.1 ppm; FT-IR (neat) ν_{max} = 3009, 2936, 2861, 2244, 1736, 1703, 1656, 1490, 1438, 1204, 1171, 758, 692 cm^{-1}; HRMS (ESI) calcd for $C_{29}H_{31}O_4$ $[M+H]^+$ 443.2217, 443.2216 found; $[\alpha]_D^{23°C}$ = +91.87 (c = 1.0, $CHCl_3$).

---

[207] The Al_2O_3 was activated by heating to 180 °C under high vacuum for 3 h.

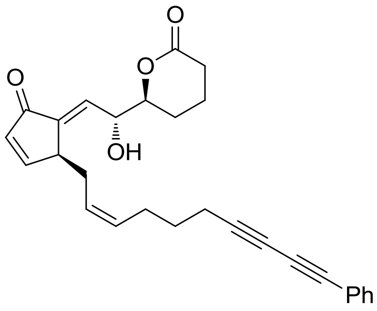

(*S*)-6-((*R*,*E*)-1-hydroxy-2-((*S*)-2-oxo-5-((*Z*)-10-phenyldeca-2-en-7,9-diyn-1-yl)cyclopent-3-en-1-ylidene)ethyl)tetrahydro-2*H*-pyran-2-one (PDCycloEC, 348). To a solution of ester **347** (35.0 mg, 0.08 mmol) in 2.6 mL pH 7 buffer–THF (4:1) was added Novozyme (30 mg). After 1 h, the reaction was filtered over cotton and concentrated. The crude material was purified by flash column chromatography (CH_2Cl_2/MeOH 20:1). The obtained carboxylic acid was then dissolved in 2 mL $CHCl_3$ and 300 mg of silica was added. After 5 d, the reaction was filtered over celite and purified by flash column chromatography (CH_2Cl_2/MeOH 40:1) to yield PDCycloEC (**348**) (17.0 mg, 0.04 mmol, 50% over two steps).

R_f = 0.31 (CH_2Cl_2/MeOH 20:1, $KMnO_4$, UV); ^1H NMR (400 MHz, $CDCl_3$) δ 7.59 (dd, J = 6.3, 2.7 Hz, 1H), 7.48 – 7.46 (m, 2H), 7.36 – 7.28 (m, 3H), 6.48 – 6.35 (m, 2H), 5.50 – 5.44 (m, 1H), 5.40 – 5.34 (m, 1H), 4.82 – 4.80 (m, 1H), 4.44 – 4.40 (m, 1H), 3.82 – 3.78 (m, 1H), 2.76 – 2.68 (m, 1H), 2.62 – 2.56 (m, 1H), 2.48 – 2.43 (m, 1H), 2.37 – 2.34 (m, 3H), 2.19 – 2.14 (m, 2H), 1.97 – 1.92 (m, 1H), 1.86 – 1.79 (m, 3H), 1.64 – 1.60 (m, 2H) ppm; ^{13}C NMR (101 MHz, $CDCl_3$) δ 196.7, 171.3, 163.2, 140.8, 134.4, 132.7, 131.6, 129.1, 128.7, 128.5, 126.2, 122.0, 84.4, 82.6, 75.1, 74.4, 70.8, 65.7, 43.6, 31.3, 29.8, 27.9, 26.4, 21.6, 19.1, 18.5 ppm; FT-IR (neat) ν_{max} = 3406, 3010, 2927, 2244, 1732, 1704, 1656, 1580, 1490, 1443, 1350, 1240, 1208, 1186, 1051, 975, 933, 842, 809, 758 cm^{-1}; HRMS (ESI) calcd for $C_{28}H_{33}NO_4$ $[M+NH_4]^+$ 446.2326, 446.2319 found; $[\alpha]_D^{22°C}$ = +69.12 (c = 1.0, $CHCl_3$).

13.5 X-Ray Chrystallographic Data

13.5.1 Compound 177

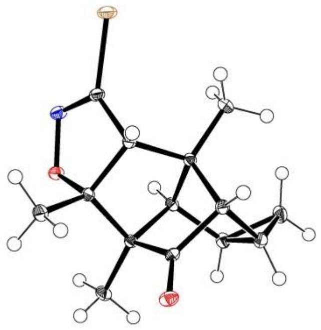

Table 13.1: Crystal data and structure refinement for **177**.

Identification code	mo_ca260814_0ma
Empirical formula	$C_{14}H_{16}BrNO_2$
Formula weight	310.19
Temperature/K	100.0(2)
Crystal system	triclinic
Space group	P-1
a/Å	7.5003(9)
b/Å	8.1284(14)
c/Å	10.6703(12)
α/°	99.451(4)
β/°	95.875(3)
γ/°	100.128(2)
Volume/Å^3	625.89(15)
Z	2
ρ_{calc}g/cm^3	1.646
μ/mm^{-1}	3.277
F(000)	316.0
Crystal size/mm^3	0.3 × 0.21 × 0.19
Radiation	MoKα (λ = 0.71073)
2Θ range for data collection/°	3.906 to 61.05
Index ranges	$-10 \leq h \leq 8$, $-11 \leq k \leq 11$, $-15 \leq l \leq 14$
Reflections collected	26831
Independent reflections	3738 [R_{int} = 0.0195, R_{sigma} = 0.0116]
Data/restraints/parameters	3738/0/166
Goodness-of-fit on F^2	1.057
Final R indexes [I>=2σ (I)]	R_1 = 0.0167, wR_2 = 0.0432
Final R indexes [all data]	R_1 = 0.0176, wR_2 = 0.0436
Largest diff. peak/hole / e Å^{-3}	0.48/-0.21

Table 13.2: Fractional Atomic Coordinates (×10^4) and Equivalent Isotropic Displacement Parameters (Å^2×10^3) for **177**. U_{eq} is defined as 1/3 of of the trace of the orthogonalised U_{IJ} tensor.

Atom	*x*	*y*	*z*	U(eq)
Br1	13698.4(2)	11082.2(2)	3816.8(2)	16.59(4)
O1	10342.6(10)	7093.4(9)	4530.9(7)	12.40(13)
O2	8116.3(10)	4104.4(9)	464.9(7)	14.47(14)
N1	11599.8(12)	8663.0(11)	4823.0(8)	13.53(16)
C1	11929.2(14)	9120.0(12)	3765.1(9)	11.82(17)
C2	10942.9(13)	7946.2(11)	2560.6(9)	9.53(16)
C3	9193.9(13)	8463.7(11)	1942.0(9)	9.58(16)
C4	8432.6(13)	7212.1(12)	664.3(9)	10.60(16)
C5	6383.0(14)	7248.2(13)	458.5(9)	12.79(17)
C6	5537.8(15)	8733.5(13)	1013.3(10)	15.47(18)
C7	10227.1(13)	6388.1(11)	3149.7(9)	9.56(16)
C8	9581.3(15)	10347.2(12)	1839(1)	14.59(18)
C9	7644.7(13)	7691.2(12)	2682.2(9)	10.11(16)
C10	8197.6(13)	5912.0(12)	2579.2(9)	9.62(16)
C11	7038.0(14)	4528.6(13)	3108(1)	14.60(18)
C12	8269.0(13)	5505.8(12)	1117.4(9)	10.12(16)
C13	5839.3(14)	7436.6(12)	1818(1)	12.49(17)
C14	11333.8(14)	4991.1(12)	3044.4(10)	13.68(18)

Table 15.3: Anisotropic Displacement Parameters (Å^2×10^3) for **177**. The Anisotropic displacement factor exponent takes the form: $-2\pi^2[h^2a^{*2}U_{11}+2hka^*b^*U_{12}+\ldots]$.

Atom	U_{11}	U_{22}	U_{33}	U_{23}	U_{13}	U_{12}
Br1	15.49(6)	13.30(5)	17.23(5)	1.10(3)	0.37(4)	-4.55(3)
O1	14.7(3)	12.4(3)	8.5(3)	1.7(2)	1.2(3)	-1.3(3)
O2	13.5(3)	12.0(3)	15.7(3)	-2.2(3)	0.8(3)	1.8(3)
N1	13.0(4)	12.5(4)	12.8(4)	-0.1(3)	0.0(3)	-0.4(3)
C1	10.9(4)	10.0(4)	13.0(4)	0.4(3)	0.1(3)	0.3(3)
C2	9.9(4)	8.9(4)	9.2(4)	1.5(3)	1.4(3)	0.5(3)
C3	10.8(4)	9.2(4)	8.8(4)	2.2(3)	1.6(3)	1.3(3)
C4	11.4(4)	11.5(4)	8.7(4)	2.2(3)	1.4(3)	1.5(3)
C5	12.2(4)	14.2(4)	12.0(4)	3.5(3)	0.2(3)	2.3(3)
C6	14.4(5)	16.6(4)	17.7(5)	7.0(4)	1.7(4)	5.7(4)
C7	10.9(4)	9.3(4)	8.1(4)	1.5(3)	1.0(3)	1.3(3)
C8	17.0(5)	9.8(4)	17.1(4)	4.9(3)	1.5(4)	1.3(3)
C9	11.5(4)	10.0(4)	9.6(4)	2.5(3)	3.1(3)	2.5(3)
C10	10.1(4)	9.2(4)	9.6(4)	2.3(3)	1.8(3)	1.3(3)

C11	13.3(5)	13.4(4)	17.6(4)	7.1(3)	3.0(4)	-0.2(3)
C12	7.4(4)	11.4(4)	11.0(4)	1.5(3)	0.6(3)	1.1(3)
C13	11.1(4)	13.8(4)	13.9(4)	4.5(3)	2.9(3)	3.6(3)
C14	13.8(5)	12.0(4)	16.0(4)	3.6(3)	1.2(4)	4.3(3)

Table 13.4: Bond Lengths for **177**.

Atom	**Atom**	**Length/Å**	**Atom**	**Atom**	**Length/Å**
Br1	C1	1.8760(10)	C4	C5	1.5366(14)
O1	N1	1.4143(11)	C4	C12	1.5313(13)
O1	C7	1.4789(11)	C5	C6	1.5235(14)
O2	C12	1.2136(12)	C5	C13	1.5376(14)
N1	C1	1.2789(13)	C6	C13	1.4971(14)
C1	C2	1.5046(13)	C7	C10	1.5373(14)
C2	C3	1.5625(14)	C7	C14	1.5165(13)
C2	C7	1.5423(13)	C9	C10	1.5632(13)
C3	C4	1.5494(13)	C9	C13	1.5198(14)
C3	C8	1.5316(13)	C10	C11	1.5180(13)
C3	C9	1.5692(13)	C10	C12	1.5489(13)

Table 13.5: Bond Angles for **177**.

Atom	**Atom**	**Atom**	**Angle/°**	**Atom**	**Atom**	**Atom**	**Angle/°**
N1	O1	C7	108.82(7)	O1	C7	C2	103.95(7)
C1	N1	O1	107.92(8)	O1	C7	C10	108.08(7)
N1	C1	Br1	118.53(8)	O1	C7	C14	106.84(8)
N1	C1	C2	116.28(9)	C10	C7	C2	102.84(7)
C2	C1	Br1	125.03(7)	C14	C7	C2	116.23(8)
C1	C2	C3	115.58(8)	C14	C7	C10	117.86(8)
C1	C2	C7	98.70(7)	C10	C9	C3	95.13(7)
C7	C2	C3	105.12(8)	C13	C9	C3	107.44(8)
C2	C3	C9	103.80(7)	C13	C9	C10	106.86(8)
C4	C3	C2	109.07(7)	C7	C10	C9	102.17(7)
C4	C3	C9	94.01(7)	C7	C10	C12	103.09(7)
C8	C3	C2	110.69(8)	C11	C10	C7	115.72(8)
C8	C3	C4	115.18(8)	C11	C10	C9	118.84(8)
C8	C3	C9	122.39(8)	C11	C10	C12	115.03(8)
C5	C4	C3	105.04(7)	C12	C10	C9	99.49(7)

C12	C4	C3	100.74(7)	O2	C12	C4	127.58(9)
C12	C4	C5	97.61(7)	O2	C12	C10	126.43(9)
C4	C5	C13	104.06(8)	C4	C12	C10	105.86(7)
C6	C5	C4	124.60(9)	C6	C13	C5	60.25(7)
C6	C5	C13	58.56(6)	C6	C13	C9	119.28(9)
C13	C6	C5	61.19(6)	C9	C13	C5	103.88(8)

Table 13.6: Torsion Angles for **177**.

A	**B**	**C**	**D**	**Angle/°**	**A**	**B**	**C**	**D**	**Angle/°**
Br1	C1	C2	C3	-85.87(10)	C3	C9	C13	C6	-38.00(11)
Br1	C1	C2	C7	162.68(7)	C4	C3	C9	C10	64.45(7)
O1	N1	C1	Br1	-175.28(6)	C4	C3	C9	C13	-45.02(8)
O1	N1	C1	C2	0.40(12)	C4	C5	C6	C13	-85.65(10)
O1	C7	C10	C9	67.35(8)	C4	C5	C13	C6	122.20(9)
O1	C7	C10	C11	-63.30(10)	C4	C5	C13	C9	6.16(9)
O1	C7	C10	C12	170.26(7)	C5	C4	C12	O2	90.44(11)
N1	O1	C7	C2	-20.58(9)	C5	C4	C12	C10	-85.60(8)
N1	O1	C7	C10	-129.37(8)	C5	C6	C13	C9	89.79(9)
N1	O1	C7	C14	102.86(8)	C6	C5	C13	C9	-116.04(9)
N1	C1	C2	C3	98.76(10)	C7	O1	N1	C1	13.19(10)
N1	C1	C2	C7	-12.69(11)	C7	C2	C3	C4	-76.69(9)
C1	C2	C3	C4	175.67(8)	C7	C2	C3	C8	155.60(8)
C1	C2	C3	C8	47.96(11)	C7	C2	C3	C9	22.58(9)
C1	C2	C3	C9	-85.07(9)	C7	C10	C12	O2	97.93(11)
C1	C2	C7	O1	18.66(9)	C7	C10	C12	C4	-85.97(8)
C1	C2	C7	C10	131.28(7)	C8	C3	C4	C5	-80.50(10)
C1	C2	C7	C14	-98.42(9)	C8	C3	C4	C12	178.52(8)
C2	C3	C4	C5	154.36(7)	C8	C3	C9	C10	-172.22(9)
C2	C3	C4	C12	53.38(9)	C8	C3	C9	C13	78.31(11)
C2	C3	C9	C10	-46.31(8)	C9	C3	C4	C5	48.27(8)
C2	C3	C9	C13	-155.78(7)	C9	C3	C4	C12	-52.71(8)
C2	C7	C10	C9	-42.19(8)	C9	C10	C12	O2	-157.10(10)
C2	C7	C10	C11	-172.85(8)	C9	C10	C12	C4	19.00(9)
C2	C7	C10	C12	60.71(8)	C10	C9	C13	C5	-75.72(9)
C3	C2	C7	O1	-100.92(8)	C10	C9	C13	C6	-139.14(9)
C3	C2	C7	C10	11.70(9)	C11	C10	C12	O2	-28.95(14)
C3	C2	C7	C14	141.99(8)	C11	C10	C12	C4	147.15(8)
C3	C4	C5	C6	25.21(12)	C12	C4	C5	C6	128.53(9)
C3	C4	C5	C13	-36.07(9)	C12	C4	C5	C13	67.25(8)
C3	C4	C12	O2	-162.60(10)	C13	C9	C10	C7	164.37(7)

C3	C4	C12	C10	21.36(9)	C13	C9	C10	C11	-66.91(11)
C3	C9	C10	C7	54.39(8)	C13	C9	C10	C12	58.66(9)
C3	C9	C10	C11	-176.89(8)	C14	C7	C10	C9	-171.49(8)
C3	C9	C10	C12	-51.32(8)	C14	C7	C10	C11	57.85(11)
C3	C9	C13	C5	25.42(9)	C14	C7	C10	C12	-68.59(10)

Table 13.7: Hydrogen Atom Coordinates (Å×10^4) and Isotropic Displacement Parameters (Å^2×10^3) for **177**

Atom	***x***	***y***	***z***	**U(eq)**
H2	11789	7689	1921	11
H4	9120	7343	-80	13
H5	5593	6339	-217	15
H6A	6343	9871	1254	19
H6B	4264	8737	665	19
H8A	9432	11039	2650	22
H8B	8724	10538	1146	22
H8C	10836	10670	1655	22
H9	7669	8312	3576	12
H11A	7484	3465	2907	22
H11C	5763	4360	2719	22
H11B	7119	4868	4040	22
H13	4758	6632	1987	15
H14A	12610	5475	3403	21
H14B	11272	4472	2141	21
H14C	10834	4123	3521	21

Experimental

Single crystals of $C_{14}H_{16}BrNO_2$ **177** were obtained by vapor diffusion from hexane → CH_2Cl_2. A suitable crystal was selected and measured on a 'ETH_LOC_ApexIID8_Mo' diffractometer. The crystal was kept at 100.0(2) K during data collection. Using Olex2 [I], the structure was solved with the XS[II] structure solution program using Direct Methods and refined with the XL[III] refinement package using Least Squares minimisation.

I: Dolomanov, O.V., Bourhis, L.J., Gildea, R.J, Howard, J.A.K. & Puschmann, H. (2009), J. Appl. Cryst. 42, 339-341.

II: Sheldrick, G.M. (2008). Acta Cryst. A64, 112-122.

III: Sheldrick, G.M. (2008). Acta Cryst. A64, 112-122.

Crystal Data for $C_{14}H_{16}BrNO_2$ (M =310.19 g/mol): triclinic, space group P-1 (no. 2), a = 7.5003(9) Å, b = 8.1284(14) Å, c = 10.6703(12) Å, α = 99.451(4)°, β = 95.875(3)°, γ =

100.128(2)°, $V = 625.89(15)$ Å^3, $Z = 2$, $T = 100.0(2)$ K, μ(MoKα) = 3.277 mm^{-1}, $Dcalc$ = 1.646 g/cm^3, 26831 reflections measured ($3.906° \leq 2\Theta \leq 61.05°$), 3738 unique ($R_{int} = 0.0195$, $R_{sigma} = 0.0116$) which were used in all calculations. The final R_1 was 0.0167 ($I > 2\sigma(I)$) and wR_2 was 0.0436 (all data).

13.5.2 Compound 201

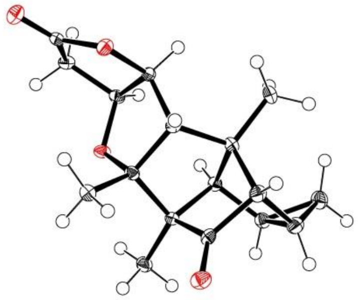

Table 13.8: Crystal data and structure refinement for **201**.

Identification code	mo_ca180415_1_1_0m
Empirical formula	$C_{17}H_{20}O_4$
Formula weight	288.33
Temperature/K	100.0(2)
Crystal system	triclinic
Space group	P-1
a/Å	8.6729(13)
b/Å	8.7400(12)
c/Å	10.0843(16)
α/°	96.793(4)
β/°	100.510(4)
γ/°	109.424(5)
Volume/Å^3	695.48(18)
Z	2
ρ_{calc}g/cm^3	1.377
μ/mm^{-1}	0.097
F(000)	308.0
Crystal size/mm^3	0.08 × 0.04 × 0.02
Radiation	MoKα (λ = 0.71073)
2Θ range for data collection/°	4.186 to 55.05
Index ranges	$-11 \leq h \leq 11, -11 \leq k \leq 9, -13 \leq l \leq 13$
Reflections collected	4884
Independent reflections	3186 [R_{int} = 0.0530, R_{sigma} = 0.1269]
Data/restraints/parameters	3186/0/193
Goodness-of-fit on F^2	1.008
Final R indexes [I>=2σ (I)]	R_1 = 0.0613, wR_2 = 0.1001
Final R indexes [all data]	R_1 = 0.1401, wR_2 = 0.1233
Largest diff. peak/hole / e Å^{-3}	0.28/-0.31

Table 13.9: Fractional Atomic Coordinates ($\times 10^4$) and Equivalent Isotropic Displacement Parameters (Å$^2\times 10^3$) for **201**. U_{eq} is defined as 1/3 of of the trace of the orthogonalised U_{IJ} tensor.

Atom	*x*	*y*	*z*	U(eq)
O1	11093(2)	1275(2)	7565.1(18)	19.4(5)
O2	6171(2)	4363(2)	11954.2(18)	19.4(5)
O0AA	6209(2)	1018(2)	8764.9(18)	14.3(4)
O4	7207(2)	4598(2)	10084.6(17)	15.3(4)
C5	6026(3)	3846(3)	10768(3)	13.9(6)
C6	6705(3)	3803(3)	8632(3)	12.7(6)
C7	8085(3)	3140(3)	6659(3)	13.5(6)
C8	8158(3)	3412(3)	8232(3)	12.0(6)
C9	9869(3)	1629(3)	7184(3)	12.8(6)
C10	7064(3)	1249(3)	6134(2)	12.4(6)
C11	8070(3)	697(3)	7308(3)	11.4(6)
C12	7527(3)	735(3)	4818(3)	14.9(6)
C13	4631(3)	2410(3)	9796(3)	14.5(6)
C14	7925(3)	1703(3)	8621(3)	12.1(6)
C15	9082(3)	1718(3)	9950(3)	15.8(6)
C16	5339(3)	2147(3)	8568(3)	13.2(6)
C17	7594(3)	-1150(3)	7274(3)	17.0(6)
C1	9751(3)	3008(3)	6420(3)	15.8(6)
C2	9303(3)	1990(3)	4959(3)	17.0(6)
C3	7831(3)	1868(3)	3814(3)	19.8(6)
C0AA	7604(4)	4467(3)	6014(3)	19.5(6)

Table 13.10: Anisotropic Displacement Parameters (Å$^2\times 10^3$) for **201**. The Anisotropic displacement factor exponent takes the form: $-2\pi^2[h^2a^{*2}U_{11}+2hka^*b^*U_{12}+\ldots]$.

Atom	U_{11}	U_{22}	U_{33}	U_{23}	U_{13}	U_{12}
O1	15.9(10)	23.7(11)	18.0(11)	0.7(8)	1.1(8)	9.1(8)
O2	20.7(11)	22.6(10)	14.4(11)	1.1(9)	5.1(8)	7.7(8)
O0AA	11.4(9)	11.7(9)	23.0(11)	5.5(8)	8.0(8)	5.3(7)
O4	15.6(10)	13.1(9)	15.8(10)	1.0(8)	6.0(8)	2.9(8)
C5	16.5(15)	13.1(13)	15.5(15)	5.5(11)	4.4(12)	8.6(11)
C6	17.5(14)	12.5(13)	8.6(14)	1.0(11)	1.8(11)	6.9(11)
C7	14.8(14)	12.6(13)	13.7(14)	4.7(11)	2.5(11)	5.6(11)
C8	9.1(13)	11.4(12)	14.4(14)	1.3(11)	2.9(11)	2.6(10)
C9	13.0(14)	15.9(13)	6.8(13)	-1.8(11)	0.0(11)	4.4(11)
C10	11.3(13)	14.3(13)	11.5(14)	2.7(11)	1.9(11)	4.9(10)
C11	11.6(13)	10.9(12)	12.6(14)	2.9(11)	2.3(11)	5(1)

C12	13.4(14)	16.1(13)	15.4(15)	4.4(11)	2.3(11)	5.8(11)
C13	13.7(14)	12.5(12)	17.3(15)	1.6(11)	3.9(11)	5(1)
C14	11.1(13)	13.3(12)	12.7(14)	3.5(10)	2.2(11)	5.6(10)
C15	17.0(14)	16.5(14)	15.5(15)	4.7(12)	4.2(12)	7.2(11)
C16	12.0(13)	13.8(13)	14.0(14)	2.9(11)	0.6(11)	6.4(10)
C17	22.4(15)	15.0(13)	15.1(15)	3.2(11)	3.9(12)	8.9(12)
C1	13.4(14)	13.6(13)	18.7(15)	2.3(11)	5.0(11)	2.5(11)
C2	18.1(15)	17.8(13)	15.9(15)	2.0(12)	4.7(12)	7.6(11)
C3	23.5(16)	22.6(15)	13.7(15)	4.1(12)	2.6(12)	9.7(12)
C0AA	26.6(16)	19.3(14)	17.6(15)	9.9(12)	8.8(13)	10.8(12)

Table 13.11: Bond Lengths for **201**.

Atom	Atom	Length/Å	Atom	Atom	Length/Å
O1	C9	1.212(3)	C8	C14	1.547(3)
O2	C5	1.195(3)	C9	C11	1.537(3)
O0AA	C14	1.449(3)	C9	C1	1.526(4)
O0AA	C16	1.439(3)	C10	C11	1.560(3)
O4	C5	1.369(3)	C10	C12	1.516(4)
O4	C6	1.464(3)	C11	C14	1.550(3)
C5	C13	1.506(3)	C11	C17	1.522(3)
C6	C8	1.519(3)	C12	C2	1.534(3)
C6	C16	1.521(3)	C12	C3	1.495(4)
C7	C8	1.562(4)	C13	C16	1.505(4)
C7	C10	1.564(3)	C14	C15	1.516(3)
C7	C1	1.547(4)	C1	C2	1.538(4)
C7	C0AA	1.530(3)	C2	C3	1.523(4)

Table 13.12: Bond Angles for **201**.

Atom	Atom	Atom	Angle/°	Atom	Atom	Atom	Angle/°
C16	O0AA	C14	111.86(18)	C14	C11	C10	102.58(19)
C5	O4	C6	110.92(19)	C17	C11	C9	116.0(2)
O2	C5	O4	121.0(2)	C17	C11	C10	117.6(2)
O2	C5	C13	129.4(3)	C17	C11	C14	115.2(2)
O4	C5	C13	109.6(2)	C10	C12	C2	104.0(2)
O4	C6	C8	109.23(19)	C3	C12	C10	120.5(2)
O4	C6	C16	104.4(2)	C3	C12	C2	60.32(17)
C8	C6	C16	106.2(2)	C16	C13	C5	104.0(2)
C8	C7	C10	104.12(19)	O0AA	C14	C8	106.56(19)

C1	C7	C8	109.7(2)	O0AA	C14	C11	108.26(19)
C1	C7	C10	93.7(2)	O0AA	C14	C15	107.7(2)
C0AA	C7	C8	110.7(2)	C8	C14	C11	102.5(2)
C0AA	C7	C10	122.7(2)	C15	C14	C8	115.7(2)
C0AA	C7	C1	114.4(2)	C15	C14	C11	115.6(2)
C6	C8	C7	115.4(2)	O0AA	C16	C6	105.2(2)
C6	C8	C14	103.3(2)	O0AA	C16	C13	109.2(2)
C14	C8	C7	105.01(19)	C13	C16	C6	104.8(2)
O1	C9	C11	126.3(2)	C9	C1	C7	101.3(2)
O1	C9	C1	128.0(2)	C9	C1	C2	96.7(2)
C1	C9	C11	105.6(2)	C2	C1	C7	105.4(2)
C11	C10	C7	95.01(18)	C12	C2	C1	103.7(2)
C12	C10	C7	107.5(2)	C3	C2	C12	58.57(16)
C12	C10	C11	107.1(2)	C3	C2	C1	124.8(2)
C9	C11	C10	99.5(2)	C12	C3	C2	61.11(17)
C9	C11	C14	103.63(19)				

Table 13.13: Torsion Angles for **201**.

A	B	C	D	Angle/°	A	B	C	D	Angle/°
O1	C9	C11	C10	-156.7(2)	C10	C7	C8	C14	24.0(2)
O1	C9	C11	C14	97.7(3)	C10	C7	C1	C9	-52.1(2)
O1	C9	C11	C17	-29.5(4)	C10	C7	C1	C2	48.2(2)
O1	C9	C1	C7	-162.9(2)	C10	C11	C14	O0AA	71.4(2)
O1	C9	C1	C2	89.8(3)	C10	C11	C14	C8	-40.9(2)
O2	C5	C13	C16	-167.7(3)	C10	C11	C14	C15	-167.7(2)
O4	C5	C13	C16	13.8(3)	C10	C12	C2	C1	5.3(3)
O4	C6	C8	C7	-159.71(19)	C10	C12	C2	C3	-117.4(2)
O4	C6	C8	C14	86.3(2)	C10	C12	C3	C2	89.3(3)
O4	C6	C16	O0AA	-90.7(2)	C11	C9	C1	C7	20.2(2)
O4	C6	C16	C13	24.5(2)	C11	C9	C1	C2	-87.0(2)
C5	O4	C6	C8	-130.0(2)	C11	C10	C12	C2	-74.8(2)
C5	O4	C6	C16	-16.8(3)	C11	C10	C12	C3	-138.3(2)
C5	C13	C16	O0AA	89.1(2)	C12	C10	C11	C9	57.7(2)
C5	C13	C16	C6	-23.2(3)	C12	C10	C11	C14	164.1(2)
C6	O4	C5	O2	-176.7(2)	C12	C10	C11	C17	-68.4(3)
C6	O4	C5	C13	2.0(3)	C14	O0AA	C16	C6	-13.6(3)
C6	C8	C14	O0AA	17.7(2)	C14	O0AA	C16	C13	-125.7(2)
C6	C8	C14	C11	131.3(2)	C16	O0AA	C14	C8	-2.6(3)
C6	C8	C14	C15	-102.0(2)	C16	O0AA	C14	C11	-112.3(2)
C7	C8	C14	O0AA	-103.6(2)	C16	O0AA	C14	C15	122.1(2)

C7	C8	C14	C11	10.0(2)	C16	C6	C8	C7	88.2(3)
C7	C8	C14	C15	136.7(2)	C16	C6	C8	C14	-25.7(2)
C7	C10	C11	C9	-52.4(2)	C17	C11	C14	O0AA	-57.6(3)
C7	C10	C11	C14	54.0(2)	C17	C11	C14	C8	-170.0(2)
C7	C10	C11	C17	-178.4(2)	C17	C11	C14	C15	63.3(3)
C7	C10	C12	C2	26.4(3)	C1	C7	C8	C6	171.8(2)
C7	C10	C12	C3	-37.2(3)	C1	C7	C8	C14	-75.2(2)
C7	C1	C2	C12	-35.5(3)	C1	C7	C10	C11	64.3(2)
C7	C1	C2	C3	25.5(3)	C1	C7	C10	C12	-45.5(2)
C8	C6	C16	O0AA	24.7(3)	C1	C9	C11	C10	20.2(2)
C8	C6	C16	C13	139.9(2)	C1	C9	C11	C14	-85.3(2)
C8	C7	C10	C11	-47.1(2)	C1	C9	C11	C17	147.4(2)
C8	C7	C10	C12	-156.9(2)	C1	C2	C3	C12	-85.0(3)
C8	C7	C1	C9	54.3(2)	C3	C12	C2	C1	122.7(2)
C8	C7	C1	C2	154.7(2)	C0AA	C7	C8	C6	44.7(3)
C9	C11	C14	O0AA	174.67(19)	C0AA	C7	C8	C14	157.7(2)
C9	C11	C14	C8	62.3(2)	C0AA	C7	C10	C11	-173.6(2)
C9	C11	C14	C15	-64.5(3)	C0AA	C7	C10	C12	76.7(3)
C9	C1	C2	C12	68.2(2)	C0AA	C7	C1	C9	179.4(2)
C9	C1	C2	C3	129.2(3)	C0AA	C7	C1	C2	-80.3(3)
C10	C7	C8	C6	-89.0(2)					

Table 13.14: Hydrogen Atom Coordinates (Å×10^4) and Isotropic Displacement Parameters (Å^2×10^3) for **201**.

Atom	***x***	***y***	***z***	**U(eq)**
H6	6296	4483	8024	15
H8	9263	4259	8763	14
H10	5828	900	6076	15
H12	7300	-463	4498	18
H13A	4349	1414	10215	17
H13B	3607	2678	9535	17
H15A	8943	2432	10709	24
H15B	10252	2141	9870	24
H15C	8798	592	10129	24
H16	4460	1776	7685	16
H17A	7537	-1708	6354	26
H17B	6496	-1592	7495	26
H17C	8445	-1338	7951	26
H1	10759	4056	6657	19
H2	10152	1547	4695	20
H3A	7385	2774	3878	24

H3B	7803	1383	2867	24
H0AA	6378	4087	5693	29
H0AB	8122	4673	5234	29
H0AC	8005	5491	6701	29

Experimental

Single crystals of $C_{17}H_{20}O_4$ **201** were obtained by vapor diffusion from hexane → CH_2Cl_2. A suitable crystal was selected and measured on a 'ETH_LOC_ApexIID8_Mo' diffractometer. The crystal was kept at 100.0(2) K during data collection. Using Olex2 [I], the structure was solved with the XS[II] structure solution program using Direct Methods and refined with the XL[III] refinement package using Least Squares minimisation.

I: Dolomanov, O.V., Bourhis, L.J., Gildea, R.J, Howard, J.A.K. & Puschmann, H. (2009), J. Appl. Cryst. 42, 339-341.

II: Sheldrick, G.M. (2008). Acta Cryst. A64, 112-122.

III: Sheldrick, G.M. (2008). Acta Cryst. A64, 112-122.

Crystal Data for $C_{17}H_{20}O_4$ (M =288.33 g/mol): triclinic, space group P-1 (no. 2), a = 8.6729(13) Å, b = 8.7400(12) Å, c = 10.0843(16) Å, α = 96.793(4)°, β = 100.510(4)°, γ = 109.424(5)°, V = 695.48(18) Å^3, Z = 2, T = 100.0(2) K, μ(MoKα) = 0.097 mm^{-1}, $Dcalc$ = 1.377 g/cm^3, 4884 reflections measured (4.186° ≤ 2Θ ≤ 55.05°), 3186 unique (R_{int} = 0.0530, R_{sigma} = 0.1269) which were used in all calculations. The final R_1 was 0.0613 (I > 2σ(I)) and wR_2 was 0.1233 (all data).

13.5.3 Compound 203

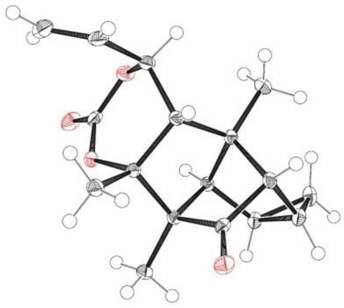

Table 13.15: Crystal data and structure refinement for **203**.

Identification code	mo_ca180315_1_1_0m
Empirical formula	$C_{17}H_{20}O_4$
Formula weight	288.33
Temperature/K	100.0(2)
Crystal system	monoclinic
Space group	$P2_1/c$
a/Å	7.9776(3)
b/Å	17.3871(7)
c/Å	12.3045(4)
α/°	90
β/°	123.970(2)
γ/°	90
Volume/Å^3	1415.44(9)
Z	4
ρ_{calc}g/cm^3	1.353
μ/mm^{-1}	0.096
F(000)	616.0
Crystal size/mm^3	0.2 × 0.16 × 0.12
Radiation	MoKα (λ = 0.71073)
2Θ range for data collection/°	4.628 to 55.006
Index ranges	$-9 \leq h \leq 10, -22 \leq k \leq 22, -15 \leq l \leq 13$
Reflections collected	12636
Independent reflections	3254 [R_{int} = 0.0239, R_{sigma} = 0.0221]
Data/restraints/parameters	3254/0/193
Goodness-of-fit on F^2	1.052
Final R indexes [I>=2σ (I)]	R_1 = 0.0361, wR_2 = 0.0898
Final R indexes [all data]	R_1 = 0.0447, wR_2 = 0.0944
Largest diff. peak/hole / e Å^{-3}	0.38/-0.23

Table 13.16: Fractional Atomic Coordinates ($\times10^4$) and Equivalent Isotropic Displacement Parameters ($Å^2\times10^3$) for **203**. U_{eq} is defined as 1/3 of of the trace of the orthogonalised U_{IJ} tensor.

Atom	***x***	***y***	***z***	**U(eq)**
O1	2558.0(13)	3598.7(5)	6516.6(8)	14.57(19)
O2	1023.7(15)	3290.3(5)	4432.7(9)	22.3(2)
O3	281.7(13)	2599.7(5)	5617.3(8)	17.2(2)
O4	2607.0(13)	4734.7(5)	9844.1(8)	19.5(2)
C5	959.5(18)	2366.4(7)	6939.3(12)	15.3(2)
C6	2550.0(17)	3667.7(6)	7714.0(11)	11.6(2)
C7	1448.3(17)	4427.9(6)	7573.0(11)	11.2(2)
C8	-533.6(17)	4004.3(7)	8431.0(11)	13.4(2)
C9	-1984.2(18)	4689.9(7)	7814.7(12)	15.5(2)
C10	4766.0(17)	3637.6(7)	8826.5(12)	15.8(2)
C11	1272.3(18)	3173.0(7)	5476.9(12)	15.2(2)
C12	1391.8(17)	4428.8(6)	8812.7(11)	12.7(2)
C13	-861.0(17)	3510.5(7)	7272.1(11)	12.3(2)
C14	1155.5(17)	3069.1(7)	7740.4(11)	12.2(2)
C15	2347.1(18)	5147.0(7)	7400.6(12)	15.9(2)
C16	2863(2)	1894.4(7)	7572.0(13)	19.0(3)
C17	-3962.3(18)	4666.7(8)	6482.1(12)	18.5(3)
C18	-809.1(17)	4225.7(6)	6515.5(11)	11.7(2)
C19	-2067.4(18)	4861.7(7)	6564.3(12)	14.7(2)
C20	3859(2)	1704.4(7)	7043.0(14)	23.8(3)
C21	-2663.5(18)	2964.6(7)	6683.9(13)	18.6(3)

Table 13.17: Anisotropic Displacement Parameters ($Å^2\times10^3$) for **203**. The Anisotropic displacement factor exponent takes the form: $-2\pi^2[h^2a^{*2}U_{11}+2hka^*b^*U_{12}+\ldots]$.

Atom	**U_{11}**	**U_{22}**	**U_{33}**	**U_{23}**	**U_{13}**	**U_{12}**
O1	18.2(4)	15.8(4)	15.7(4)	-1.9(3)	13.1(4)	-1.9(3)
O2	35.1(5)	20.4(5)	17.8(5)	0.1(4)	18.7(4)	3.2(4)
O3	22.6(4)	15.3(4)	14.9(4)	-3.6(3)	11.3(4)	-3.3(3)
O4	20.3(4)	22.3(5)	14.8(4)	-7.2(4)	9.1(4)	-3.7(4)
C5	20.6(6)	11.9(5)	16.8(6)	-1.3(5)	12.7(5)	-2.8(5)
C6	14.6(5)	11.6(5)	11.3(5)	-0.4(4)	8.9(5)	-0.7(4)
C7	11.8(5)	11.1(5)	11.8(5)	0.7(4)	7.3(5)	-0.2(4)
C8	14.9(5)	15.5(5)	13.2(5)	-0.2(4)	9.9(5)	-1.0(4)
C9	16.5(6)	17.5(6)	16.3(6)	0.6(5)	11.5(5)	2.1(5)
C10	13.1(5)	15.1(6)	17.9(6)	-0.3(5)	7.8(5)	-0.4(4)

C11	19.8(6)	12.4(5)	16.9(6)	-0.6(4)	12.4(5)	3.3(4)
C12	14.3(5)	11.2(5)	13.3(6)	0.2(4)	8.1(5)	2.1(4)
C13	13.6(5)	12.9(5)	12.4(5)	-0.2(4)	8.5(5)	-0.7(4)
C14	14.0(5)	11.5(5)	12.6(5)	0.2(4)	8.3(5)	-1.0(4)
C15	17.6(6)	12.0(5)	20.6(6)	1.1(5)	12.1(5)	-0.9(4)
C16	25.9(6)	10.2(5)	23.2(6)	1.0(5)	15.1(6)	0.2(5)
C17	14.7(6)	23.5(6)	19.9(6)	3.4(5)	11.3(5)	3.4(5)
C18	12.6(5)	13.4(5)	10.4(5)	-0.1(4)	7.2(5)	-0.7(4)
C19	15.2(5)	16.1(6)	15.0(6)	2.0(5)	9.7(5)	2.4(4)
C20	29.3(7)	15.9(6)	30.7(8)	0.3(5)	19.5(6)	3.4(5)
C21	16.3(6)	17.8(6)	23.0(6)	-3.1(5)	11.6(5)	-4.8(5)

Table 13.18: Bond Lengths **203**.

Atom	**Atom**	**Length/Å**	**Atom**	**Atom**	**Length/Å**
O1	C6	1.4817(13)	C7	C18	1.5624(16)
O1	C11	1.3305(15)	C8	C9	1.5345(16)
O2	C11	1.2029(15)	C8	C12	1.5226(16)
O3	C5	1.4561(14)	C8	C13	1.5564(16)
O3	C11	1.3419(15)	C9	C17	1.5129(17)
O4	C12	1.2076(15)	C9	C19	1.5318(16)
C5	C14	1.5219(16)	C13	C14	1.5727(16)
C5	C16	1.5051(17)	C13	C18	1.5676(15)
C6	C7	1.5425(15)	C13	C21	1.5262(16)
C6	C10	1.5157(16)	C16	C20	1.3193(18)
C6	C14	1.5370(15)	C17	C19	1.4964(16)
C7	C12	1.5511(15)	C18	C19	1.5170(16)
C7	C15	1.5140(15)			

Table 13.19: Bond Angles for **203**.

Atom	**Atom**	**Atom**	**Angle/°**	**Atom**	**Atom**	**Atom**	**Angle/°**
C11	O1	C6	124.88(9)	O1	C11	O3	118.85(10)
C11	O3	C5	118.23(9)	O2	C11	O1	120.74(11)
O3	C5	C14	109.85(9)	O2	C11	O3	120.39(11)
O3	C5	C16	111.55(10)	O4	C12	C7	125.91(11)
C16	C5	C14	113.20(10)	O4	C12	C8	128.08(10)
O1	C6	C7	106.04(9)	C8	C12	C7	105.95(9)
O1	C6	C10	104.14(9)	C8	C13	C14	108.66(9)
O1	C6	C14	111.80(9)	C8	C13	C18	93.44(8)

C10	C6	C7	115.78(10)	C18	C13	C14	104.11(8)
C10	C6	C14	116.76(10)	C21	C13	C8	114.13(9)
C14	C6	C7	102.07(9)	C21	C13	C14	111.72(9)
C6	C7	C12	102.60(9)	C21	C13	C18	122.83(10)
C6	C7	C18	102.71(9)	C5	C14	C6	110.10(9)
C12	C7	C18	99.55(8)	C5	C14	C13	116.14(10)
C15	C7	C6	116.02(9)	C6	C14	C13	105.43(9)
C15	C7	C12	114.41(10)	C20	C16	C5	126.36(13)
C15	C7	C18	119.00(10)	C19	C17	C9	61.20(8)
C9	C8	C13	106.36(9)	C7	C18	C13	94.85(8)
C12	C8	C9	97.36(9)	C19	C18	C7	106.46(9)
C12	C8	C13	100.02(8)	C19	C18	C13	108.48(9)
C17	C9	C8	123.84(11)	C17	C19	C9	59.93(8)
C17	C9	C19	58.87(8)	C17	C19	C18	119.87(10)
C19	C9	C8	104.20(9)	C18	C19	C9	103.85(9)

Table 13.20: Torsion Angles for **203**.

A	B	C	D	Angle/°	A	B	C	D	Angle/°
O1	C6	C7	C12	176.64(8)	C11	O1	C6	C10	138.18(11)
O1	C6	C7	C15	-57.89(12)	C11	O1	C6	C14	11.25(14)
O1	C6	C7	C18	73.66(10)	C11	O3	C5	C14	50.39(13)
O1	C6	C14	C5	26.46(13)	C11	O3	C5	C16	-75.96(12)
O1	C6	C14	C13	-99.53(10)	C12	C7	C18	C13	-50.72(9)
O3	C5	C14	C6	-54.93(12)	C12	C7	C18	C19	60.19(10)
O3	C5	C14	C13	64.75(12)	C12	C8	C9	C17	130.72(11)
O3	C5	C16	C20	0.44(18)	C12	C8	C9	C19	68.91(10)
C5	O3	C11	O1	-12.64(15)	C12	C8	C13	C14	51.48(11)
C5	O3	C11	O2	166.15(11)	C12	C8	C13	C18	-54.66(9)
C6	O1	C11	O2	160.90(11)	C12	C8	C13	C21	176.87(10)
C6	O1	C11	O3	-20.32(16)	C13	C8	C9	C17	27.97(14)
C6	C7	C12	O4	94.27(13)	C13	C8	C9	C19	-33.84(11)
C6	C7	C12	C8	-88.32(10)	C13	C8	C12	O4	-159.00(12)
C6	C7	C18	C13	54.63(9)	C13	C8	C12	C7	23.67(11)
C6	C7	C18	C19	165.54(9)	C13	C18	C19	C9	26.20(12)
C7	C6	C14	C5	139.40(10)	C13	C18	C19	C17	-36.83(14)
C7	C6	C14	C13	13.41(11)	C14	C5	C16	C20	-124.06(14)
C7	C18	C19	C9	-74.85(11)	C14	C6	C7	C12	59.47(10)
C7	C18	C19	C17	-137.89(11)	C14	C6	C7	C15	-175.06(10)
C8	C9	C17	C19	-86.57(12)	C14	C6	C7	C18	-43.51(10)
C8	C9	C19	C17	121.21(11)	C14	C13	C18	C7	-45.03(10)

C8	C9	C19	C18	4.47(12)	C14	C13	C18	C19	-154.19(9)
C8	C13	C14	C5	159.97(9)	C15	C7	C12	O4	-32.24(16)
C8	C13	C14	C6	-77.85(11)	C15	C7	C12	C8	145.16(10)
C8	C13	C18	C7	65.18(9)	C15	C7	C18	C13	-175.64(10)
C8	C13	C18	C19	-43.97(10)	C15	C7	C18	C19	-64.73(12)
C9	C8	C12	O4	92.87(14)	C16	C5	C14	C6	70.49(12)
C9	C8	C12	C7	-84.46(10)	C16	C5	C14	C13	-169.84(10)
C9	C8	C13	C14	152.28(9)	C17	C9	C19	C18	-116.74(11)
C9	C8	C13	C18	46.14(10)	C18	C7	C12	O4	-160.29(12)
C9	C8	C13	C21	-82.33(12)	C18	C7	C12	C8	17.11(11)
C9	C17	C19	C18	89.22(11)	C18	C13	C14	C5	-101.40(11)
C10	C6	C7	C12	-68.45(11)	C18	C13	C14	C6	20.78(11)
C10	C6	C7	C15	57.02(14)	C21	C13	C14	C5	33.18(13)
C10	C6	C7	C18	-171.43(9)	C21	C13	C14	C6	155.36(10)
C10	C6	C14	C5	-93.30(12)	C21	C13	C18	C7	-173.07(10)
C10	C6	C14	C13	140.70(10)	C21	C13	C18	C19	77.77(13)
C11	O1	C6	C7	-99.19(12)					

Table 13.21: Hydrogen Atom Coordinates (Å×10^4) and Isotropic Displacement Parameters (Å^2×10^3) for **203**.

Atom	***x***	***y***	***z***	**U(eq)**
H5	-97	2038	6868	18
H8	-517	3729	9132	16
H9	-1761	5125	8388	19
H10A	5490	4030	8702	24
H10B	5309	3143	8838	24
H10C	4903	3721	9644	24
H14	1768	2907	8650	15
H15A	2398	5091	6643	24
H15B	3689	5223	8163	24
H15C	1523	5583	7286	24
H16	3390	1720	8419	23
H17A	-4566	4167	6131	22
H17B	-4923	5078	6265	22
H18	-1115	4115	5641	14
H19	-1863	5392	6391	18
H20A	3391	1866	6198	29
H20B	5027	1409	7515	29
H21A	-3725	3201	6714	28
H21B	-2256	2495	7177	28
H21C	-3143	2855	5790	28

Experimental

Single crystals of $C_{17}H_{20}O_4$ **203** were obtained by vapor diffusion from hexane → CH_2Cl_2. A suitable crystal was selected and measured on a 'ETH_LOC_ApexIID8_Mo' diffractometer. The crystal was kept at 100.0(2) K during data collection. Using Olex2 [**I**], the structure was solved with the XS[**II**] structure solution program using Direct Methods and refined with the XL[**III**] refinement package using Least Squares minimisation.

I: Dolomanov, O.V., Bourhis, L.J., Gildea, R.J, Howard, J.A.K. & Puschmann, H. (2009), J. Appl. Cryst. 42, 339-341.

II: Sheldrick, G.M. (2008). Acta Cryst. A64, 112-122.

III: Sheldrick, G.M. (2008). Acta Cryst. A64, 112-122.

Crystal Data for $C_{17}H_{20}O_4$ (M =288.33 g/mol): monoclinic, space group $P2_1/c$ (no. 14), a = 7.9776(3) Å, b = 17.3871(7) Å, c = 12.3045(4) Å, β = 123.970(2)°, V = 1415.44(9) Å^3, Z = 4, T = 100.0(2) K, μ(MoKα) = 0.096 mm^{-1}, $Dcalc$ = 1.353 g/cm^3, 12636 reflections measured ($4.628° \leq 2\Theta \leq 55.006°$), 3254 unique ($R_{\text{int}}$ = 0.0239, R_{sigma} = 0.0221) which were used in all calculations. The final R_1 was 0.0361 ($I > 2\sigma(I)$) and wR_2 was 0.0944 (all data).

13.5.4 Pallambin B (15)

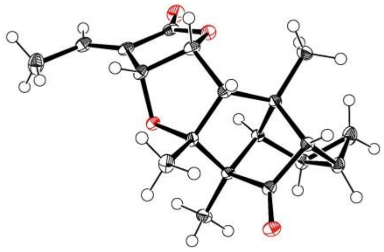

Table 13.22: Crystal data and structure refinement for pallambin B (**15**).

Identification code	ca170415_1_1_0m
Empirical formula	$C_{19}H_{22}O_4$
Formula weight	314.36
Temperature/K	100.0(2)
Crystal system	triclinic
Space group	P-1
a/Å	6.0847(11)
b/Å	10.6892(19)
c/Å	12.022(2)
α/°	95.308(5)
β/°	91.245(5)
γ/°	91.125(5)
Volume/Å^3	778.2(2)
Z	2
ρ_{calc}g/cm^3	1.342
μ/mm^{-1}	0.093
F(000)	336.0
Crystal size/mm^3	0.22 × 0.18 × 0.04
Radiation	MoKα (λ = 0.71073)
2Θ range for data collection/°	3.404 to 55.076
Index ranges	$-7 \le h \le 7$, $-13 \le k \le 13$, $-15 \le l \le 15$
Reflections collected	13280
Independent reflections	3536 [R_{int} = 0.0386, R_{sigma} = 0.0351]
Data/restraints/parameters	3536/0/212
Goodness-of-fit on F^2	1.035
Final R indexes [I>=2σ (I)]	R_1 = 0.0454, wR_2 = 0.1206
Final R indexes [all data]	R_1 = 0.0559, wR_2 = 0.1301
Largest diff. peak/hole / e Å^{-3}	0.44/-0.31

Table 13.23: Fractional Atomic Coordinates ($\times10^4$) and Equivalent Isotropic Displacement Parameters ($\text{Å}^2\times10^3$) for pallambin B (**15**). U_{eq} is defined as 1/3 of of the trace of the orthogonalised U_{IJ} tensor.

Atom	*x*	*y*	*z*	U(eq)
O1	-301.5(15)	5903.7(9)	1830.1(8)	13.7(2)
O2	591.6(16)	6752.6(10)	4240.2(8)	16.6(2)
O3	3598.7(17)	8626.7(10)	-47.7(9)	18.6(2)
O4	-2617.2(18)	6414.0(11)	5054.2(9)	22.6(3)
C5	4006(2)	9120.1(13)	1997.2(12)	13.7(3)
C6	803(2)	7915.5(13)	1216.2(11)	11.7(3)
C7	1593(2)	6613.4(13)	1498.7(11)	12.4(3)
C8	2958(2)	8554.3(13)	896.0(12)	13.2(3)
C9	425(2)	5184.0(13)	2717.2(12)	14.7(3)
C10	467(2)	8647.8(13)	2391.3(11)	11.8(3)
C11	-1314(2)	6091.9(14)	4339.2(12)	16.4(3)
C12	2811(2)	8371.6(13)	2866.8(11)	12.6(3)
C13	3003(2)	6934.1(13)	2584.2(11)	12.8(3)
C14	-1450(2)	5015.3(13)	3474.8(12)	14.9(3)
C15	1634(3)	10959.6(14)	3051.6(14)	21.2(3)
C16	2754(2)	5826.4(14)	574.3(13)	18.0(3)
C17	2008(2)	6086.1(14)	3421.1(12)	15.1(3)
C18	-1034(2)	7893.1(14)	343.9(12)	16.8(3)
C19	-2985(2)	4110.5(14)	3454.5(13)	17.4(3)
C20	2835(2)	10386.7(14)	2039.2(13)	16.8(3)
C21	3596(3)	8770.1(15)	4076.0(12)	19.5(3)
C22	-3240(3)	3010.6(15)	2604.5(15)	25.2(4)
C23	420(2)	10044.1(13)	2223.1(12)	15.7(3)

Table 13.24: Anisotropic Displacement Parameters ($\text{Å}^2\times10^3$) for pallambin B (**15**). The Anisotropic displacement factor exponent takes the form: $-2\pi^2[h^2a^{*2}U_{11}+2hka^*b^*U_{12}+\ldots]$.

Atom	U_{11}	U_{22}	U_{33}	U_{23}	U_{13}	U_{12}
O1	12.9(5)	16.5(5)	12.1(5)	3.1(4)	4.3(4)	-3.8(4)
O2	17.2(5)	20.5(5)	12.3(5)	2.1(4)	6.6(4)	-2.6(4)
O3	19.4(5)	24.5(6)	12.5(5)	3.0(4)	8.1(4)	-2.6(4)
O4	25.0(6)	25.9(6)	17.4(6)	1.7(5)	12.6(4)	-0.2(4)
C5	11.6(6)	16.9(7)	12.8(7)	1.7(5)	2.7(5)	-3.0(5)
C6	10.9(6)	15.5(7)	9.0(6)	1.3(5)	4.1(5)	-1.5(5)
C7	11.3(6)	14.0(7)	12.0(7)	0.5(5)	5.2(5)	-2.9(5)
C8	12.4(6)	14.0(7)	13.5(7)	2.2(5)	3.7(5)	0.3(5)

C9	14.7(6)	14.1(7)	15.9(7)	3.7(5)	5.6(5)	1.0(5)
C10	11.8(6)	13.7(7)	9.9(6)	-0.2(5)	3.8(5)	-0.5(5)
C11	17.7(7)	19.0(7)	13.6(7)	6.9(6)	3.8(5)	0.2(5)
C12	12.7(6)	14.9(7)	10.1(7)	0.8(5)	2.4(5)	-1.8(5)
C13	10.8(6)	14.8(7)	13.3(7)	2.3(5)	3.5(5)	0.3(5)
C14	15.1(7)	16.9(7)	14.0(7)	5.9(5)	6.2(5)	3.1(5)
C15	25.1(8)	14.9(7)	23.1(8)	-2.5(6)	5.5(6)	-0.4(6)
C16	19.0(7)	17.4(7)	17.3(7)	-2.1(6)	9.5(6)	-1.0(5)
C17	13.5(6)	17.7(7)	14.8(7)	4.1(6)	4.6(5)	2.5(5)
C18	14.6(7)	22.5(8)	13.2(7)	1.8(6)	0.1(5)	-2.0(5)
C19	16.1(7)	18.9(7)	18.2(7)	5.9(6)	6.2(5)	1.7(5)
C20	16.3(7)	16.0(7)	18.2(7)	2.1(6)	3.2(5)	-3.0(5)
C21	22.4(7)	22.8(8)	13.1(7)	1.5(6)	-1.1(6)	-4.1(6)
C22	24.5(8)	20.1(8)	30.7(9)	-0.3(7)	9.0(7)	-4.7(6)
C23	15.4(7)	14.6(7)	17.3(7)	1.4(6)	5.0(5)	0.7(5)

Table 13.25: Bond Lengths for pallambin B (**15**).

Atom	**Atom**	**Length/Å**	**Atom**	**Atom**	**Length/Å**
O1	C7	1.4506(15)	C7	C16	1.5254(19)
O1	C9	1.4385(17)	C9	C14	1.4936(19)
O2	C11	1.3589(17)	C9	C17	1.533(2)
O2	C17	1.4666(16)	C10	C12	1.5684(19)
O3	C8	1.2162(17)	C10	C23	1.525(2)
O4	C11	1.2133(18)	C11	C14	1.477(2)
C5	C8	1.5248(19)	C12	C13	1.5499(19)
C5	C12	1.5579(19)	C12	C21	1.540(2)
C5	C20	1.540(2)	C13	C17	1.5409(19)
C6	C7	1.5460(19)	C14	C19	1.330(2)
C6	C8	1.5393(18)	C15	C20	1.519(2)
C6	C10	1.5698(18)	C15	C23	1.501(2)
C6	C18	1.5146(19)	C19	C22	1.488(2)
C7	C13	1.5539(19)	C20	C23	1.5333(19)

Table 13.26: Bond Angles for pallambin B (**15**).

Atom	**Atom**	**Atom**	**Angle/°**	**Atom**	**Atom**	**Atom**	**Angle/°**
C9	O1	C7	107.12(10)	O2	C11	C14	109.70(12)
C11	O2	C17	110.59(11)	O4	C11	O2	121.10(14)
C8	C5	C12	102.17(11)	O4	C11	C14	129.21(14)

C8	C5	C20	96.70(11)	C5	C12	C10	93.23(10)
C20	C5	C12	104.83(11)	C13	C12	C5	111.48(11)
C7	C6	C10	103.75(11)	C13	C12	C10	103.11(11)
C8	C6	C7	102.09(10)	C21	C12	C5	112.64(12)
C8	C6	C10	99.49(10)	C21	C12	C10	123.82(11)
C18	C6	C7	115.43(12)	C21	C12	C13	111.09(12)
C18	C6	C8	114.78(11)	C12	C13	C7	105.53(11)
C18	C6	C10	118.81(11)	C17	C13	C7	103.96(11)
O1	C7	C6	107.99(10)	C17	C13	C12	116.65(11)
O1	C7	C13	105.56(10)	C11	C14	C9	106.19(12)
O1	C7	C16	108.68(11)	C19	C14	C9	130.58(14)
C6	C7	C13	102.89(11)	C19	C14	C11	123.23(13)
C16	C7	C6	116.44(12)	C23	C15	C20	61.00(9)
C16	C7	C13	114.56(11)	O2	C17	C9	104.02(11)
O3	C8	C5	128.47(13)	O2	C17	C13	113.69(11)
O3	C8	C6	126.11(13)	C9	C17	C13	104.87(11)
C5	C8	C6	105.34(11)	C14	C19	C22	126.16(14)
O1	C9	C14	108.75(11)	C15	C20	C5	123.87(13)
O1	C9	C17	103.83(11)	C15	C20	C23	58.92(9)
C14	C9	C17	103.69(12)	C23	C20	C5	104.12(11)
C12	C10	C6	95.07(10)	C10	C23	C20	103.59(11)
C23	C10	C6	107.36(11)	C15	C23	C10	118.75(13)
C23	C10	C12	107.44(11)	C15	C23	C20	60.08(9)

Table 13.27: Torsion Angles for pallambin B (**15**).

A	B	C	D	Angle/°	A	B	C	D	Angle/°
O1	C7	C13	C12	-110.30(11)	C10	C6	C7	C16	-161.07(11)
O1	C7	C13	C17	12.99(13)	C10	C6	C8	O3	-155.74(14)
O1	C9	C14	C11	-90.26(13)	C10	C6	C8	C5	21.29(13)
O1	C9	C14	C19	90.62(18)	C10	C12	C13	C7	30.09(12)
O1	C9	C17	O2	89.72(11)	C10	C12	C13	C17	-84.73(14)
O1	C9	C17	C13	-29.94(13)	C11	O2	C17	C9	20.21(14)
O2	C11	C14	C9	-8.18(16)	C11	O2	C17	C13	133.69(12)
O2	C11	C14	C19	171.01(13)	C11	C14	C19	C22	179.16(15)
O4	C11	C14	C9	171.42(15)	C12	C5	C8	O3	-163.99(14)
O4	C11	C14	C19	-9.4(3)	C12	C5	C8	C6	19.08(13)
C5	C12	C13	C7	-68.77(13)	C12	C5	C20	C15	25.43(17)
C5	C12	C13	C17	176.42(11)	C12	C5	C20	C23	-36.39(14)
C5	C20	C23	C10	5.72(14)	C12	C10	C23	C15	-36.39(16)
C5	C20	C23	C15	121.29(13)	C12	C10	C23	C20	26.70(14)

C6	C7	C13	C12	2.82(12)	C12	C13	C17	O2	12.81(17)
C6	C7	C13	C17	126.11(11)	C12	C13	C17	C9	125.78(12)
C6	C10	C12	C5	63.76(11)	C14	C9	C17	O2	-23.90(14)
C6	C10	C12	C13	-49.18(12)	C14	C9	C17	C13	-143.56(11)
C6	C10	C12	C21	-176.11(13)	C15	C20	C23	C10	-115.58(13)
C6	C10	C23	C15	-137.65(12)	C16	C7	C13	C12	130.18(12)
C6	C10	C23	C20	-74.57(13)	C16	C7	C13	C17	-106.53(13)
C7	O1	C9	C14	149.62(11)	C17	O2	C11	O4	172.43(13)
C7	O1	C9	C17	39.69(12)	C17	O2	C11	C14	-7.93(15)
C7	C6	C8	O3	97.86(16)	C17	C9	C14	C11	19.77(14)
C7	C6	C8	C5	-85.11(12)	C17	C9	C14	C19	-159.35(15)
C7	C6	C10	C12	51.85(12)	C18	C6	C7	O1	-55.32(15)
C7	C6	C10	C23	161.91(10)	C18	C6	C7	C13	-166.64(11)
C7	C13	C17	O2	-102.88(13)	C18	C6	C7	C16	67.20(15)
C7	C13	C17	C9	10.09(13)	C18	C6	C8	O3	-27.8(2)
C8	C5	C12	C10	-51.34(11)	C18	C6	C8	C5	149.26(12)
C8	C5	C12	C13	54.11(14)	C18	C6	C10	C12	-178.43(12)
C8	C5	C12	C21	179.79(11)	C18	C6	C10	C23	-68.37(15)
C8	C5	C20	C15	129.95(14)	C20	C5	C8	O3	89.21(16)
C8	C5	C20	C23	68.13(12)	C20	C5	C8	C6	-87.72(12)
C8	C6	C7	O1	179.48(10)	C20	C5	C12	C10	49.07(12)
C8	C6	C7	C13	68.15(12)	C20	C5	C12	C13	154.52(11)
C8	C6	C7	C16	-58.01(15)	C20	C5	C12	C21	-79.81(14)
C8	C6	C10	C12	-53.19(11)	C20	C15	C23	C10	89.64(13)
C8	C6	C10	C23	56.87(13)	C21	C12	C13	C7	164.71(11)
C9	O1	C7	C6	-142.77(11)	C21	C12	C13	C17	49.89(16)
C9	O1	C7	C13	-33.27(13)	C23	C10	C12	C5	-46.24(12)
C9	O1	C7	C16	90.08(13)	C23	C10	C12	C13	-159.18(11)
C9	C14	C19	C22	-1.9(3)	C23	C10	C12	C21	73.89(16)
C10	C6	C7	O1	76.42(12)	C23	C15	C20	C5	-86.47(15)
C10	C6	C7	C13	-34.91(12)					

Table 13.28: Hydrogen Atom Coordinates ($\text{Å}\times10^{4}$) and Isotropic Displacement Parameters ($\text{Å}^{2}\times10^{3}$) for pallambin B (**15**).

Atom	***x***	***y***	***z***	**U(eq)**
H5	5649	9155	2045	16
H9	1113	4375	2443	18
H10	-786	8332	2820	14
H13	4572	6715	2449	15
H15A	2032	10674	3788	25

H15B	1247	11856	3069	25
H16A	1776	5689	-86	27
H16B	3135	5014	835	27
H16C	4097	6270	381	27
H17	3175	5618	3797	18
H18A	-2253	7360	558	25
H18B	-489	7556	-382	25
H18C	-1549	8749	291	25
H19	-4017	4172	4038	21
H20	3154	10942	1434	20
H21A	4480	9549	4095	29
H21B	4490	8106	4351	29
H21C	2319	8909	4551	29
H22A	-3156	2233	2974	38
H22B	-2063	3035	2063	38
H22C	-4669	3040	2217	38
H23	-747	10357	1726	19

Experimental

Single crystals of $C_{19}H_{22}O_4$ pallambin B (**15**) were obtained by vapor diffusion from hexane → CH_2Cl_2. A suitable crystal was selected and measured on a 'ETH_LOC_ApexIID8_Mo' diffractometer. The crystal was kept at 100.0(2) K during data collection. Using Olex2 [I], the structure was solved with the XS[II] structure solution program using Direct Methods and refined with the XL[III] refinement package using Least Squares minimisation.

I: Dolomanov, O.V., Bourhis, L.J., Gildea, R.J, Howard, J.A.K. & Puschmann, H. (2009), J. Appl. Cryst. 42, 339-341.

II: Sheldrick, G.M. (2008). Acta Cryst. A64, 112-122.

III: Sheldrick, G.M. (2008). Acta Cryst. A64, 112-122.

Crystal Data for $C_{19}H_{22}O_4$ (M =314.36 g/mol): triclinic, space group P-1 (no. 2), a = 6.0847(11) Å, b = 10.6892(19) Å, c = 12.022(2) Å, α = 95.308(5)°, β = 91.245(5)°, γ = 91.125(5)°, V = 778.2(2) $Å^3$, Z = 2, T = 100.0(2) K, $\mu(MoK\alpha) = 0.093\ mm^{-1}$, $Dcalc$ = 1.342 g/cm^3, 13280 reflections measured ($3.404° \leq 2\Theta \leq 55.076°$), 3536 unique ($R_{int}$ = 0.0386, R_{sigma} = 0.0351) which were used in all calculations. The final R_1 was 0.0454 ($I > 2\sigma(I)$) and wR_2 was 0.1301 (all data).

13.6 NMR Spectra

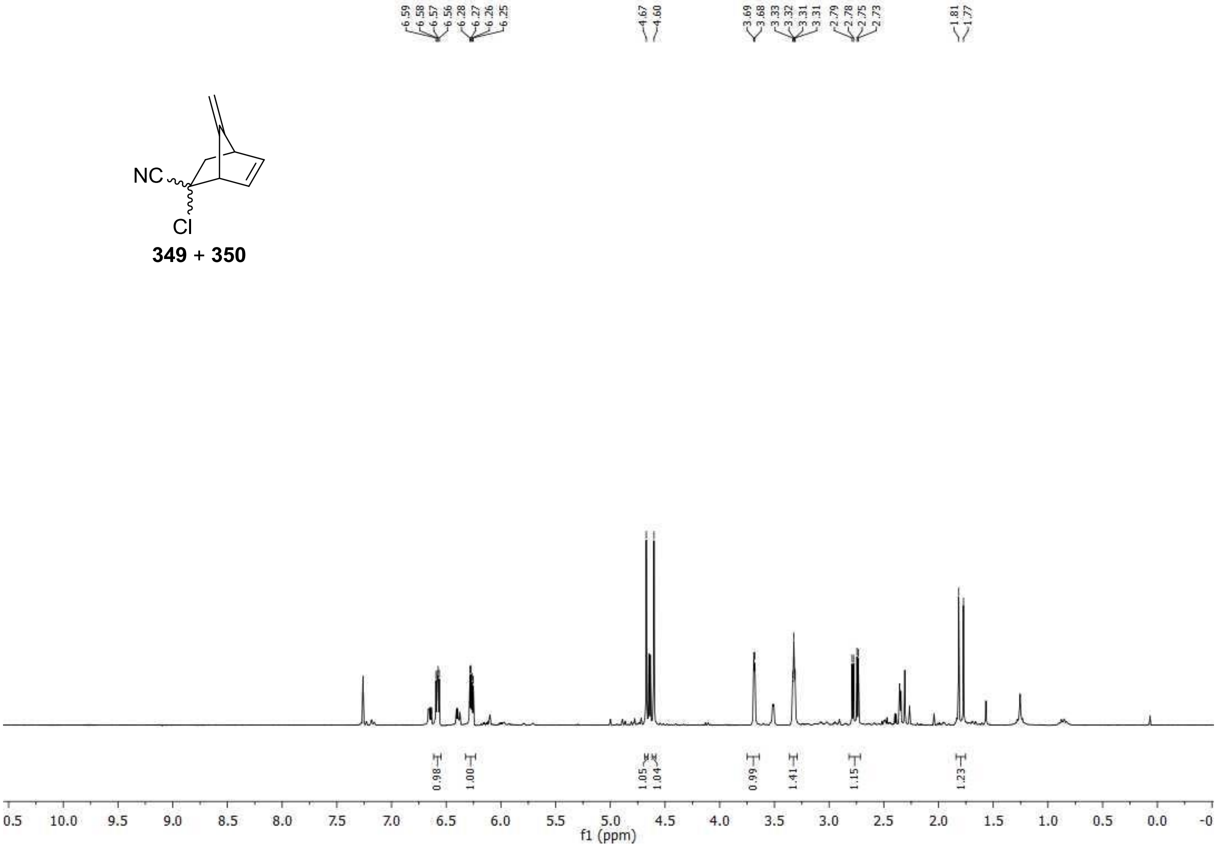

349 + 350

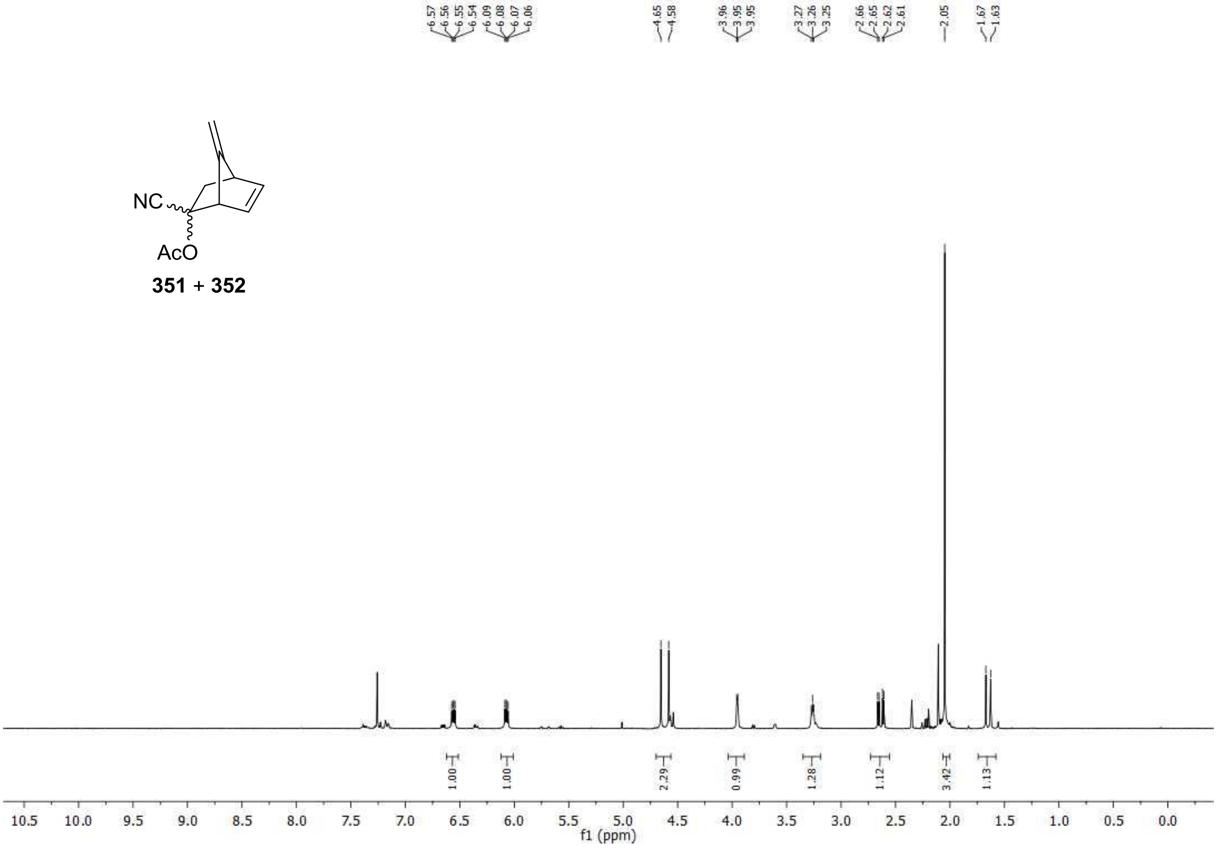

351 + 352

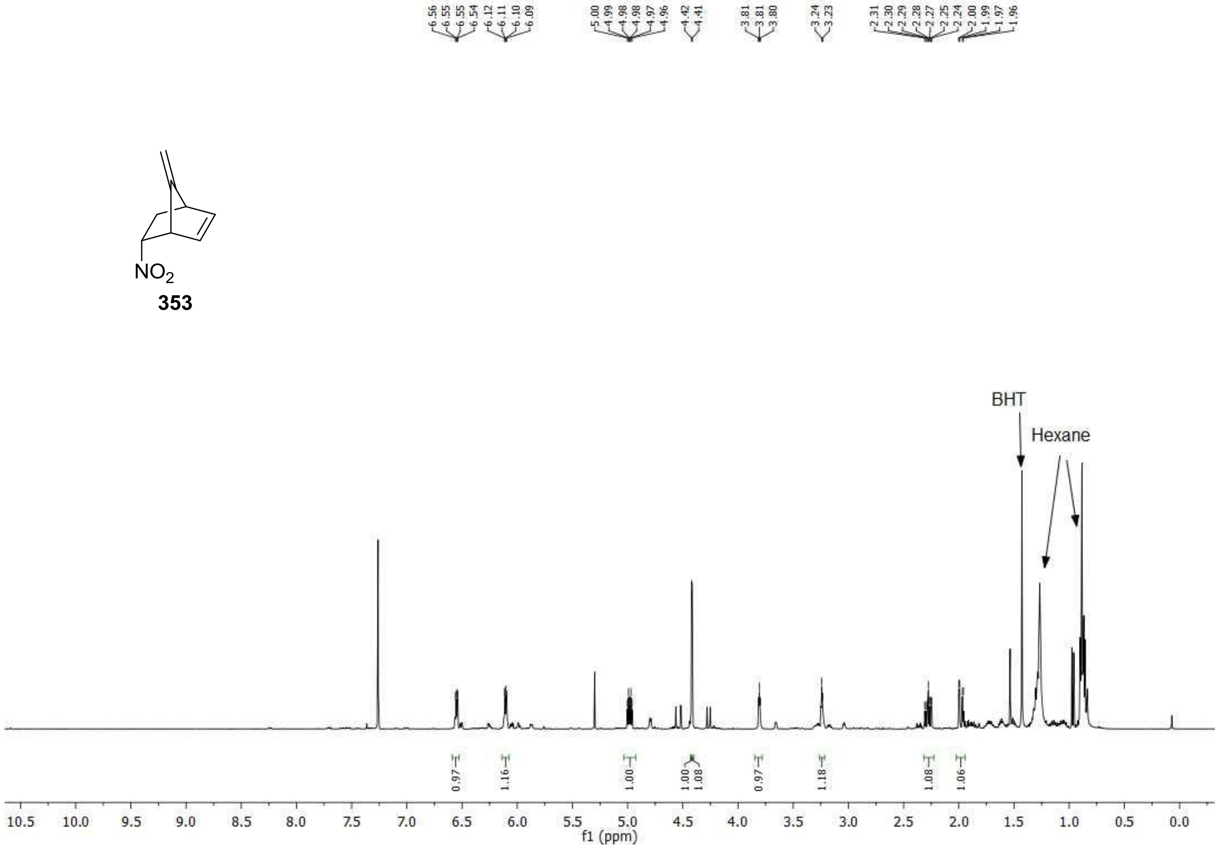

353
6.56
6.55
6.55
6.54
6.12
6.11
6.10
6.09
5.00
4.99
4.98
4.98
4.97
4.96
4.42
4.41
3.81
3.81
3.80
3.24
3.23
2.31
2.30
2.29
2.28
2.27
2.25
2.24
2.00
1.99
1.97
1.96
BHT
Hexane
0.97
1.16
1.00
1.00
1.08
0.97
1.18
1.08
1.06
10.5
10.0
9.5
9.0
8.5
8.0
7.5
7.0
6.5
6.0
5.5
5.0
4.5
4.0
3.5
3.0
2.5
2.0
1.5
1.0
0.5
0.0
f1 (ppm)

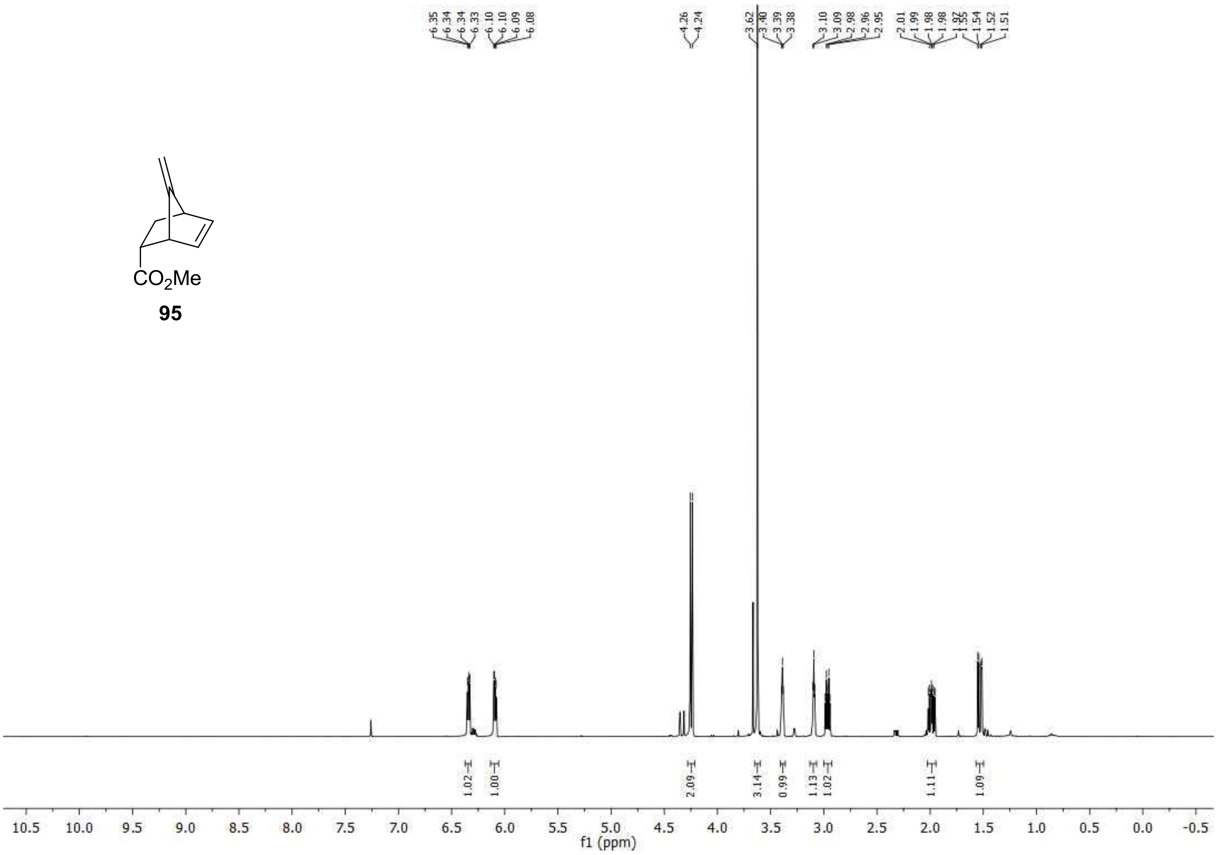
CO$_2$Me
6.35
6.34
6.34
6.33
6.10
6.10
6.09
6.08
4.26
4.24
3.62
3.40
3.39
3.38
3.10
3.09
2.98
2.96
2.95
2.01
1.99
1.98
1.98
1.97
1.55
1.54
1.52
1.51
1.02
1.00
2.09
3.14
0.99
1.13
1.02
1.11
1.09
10.5
10.0
9.5
9.0
8.5
8.0
7.5
7.0
6.5
6.0
5.5
5.0
4.5
4.0
3.5
3.0
2.5
2.0
1.5
1.0
0.5
0.0
-0.5
f1 (ppm)

95

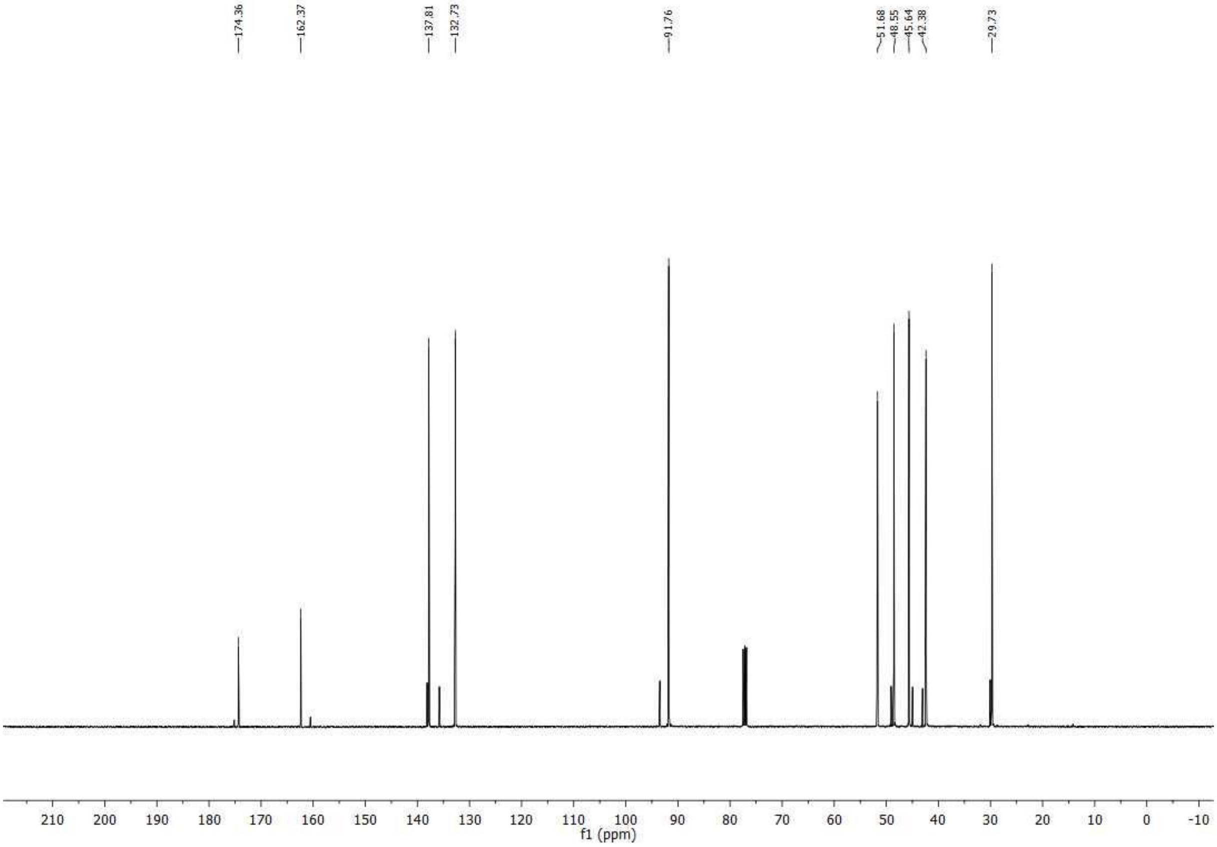
174.36
162.37
137.81
132.73
91.76
51.68
48.55
45.64
42.38
29.73
210
200
190
180
170
160
150
140
130
120
110
100
90
80
70
60
50
40
30
20
10
0
-10
f1 (ppm)

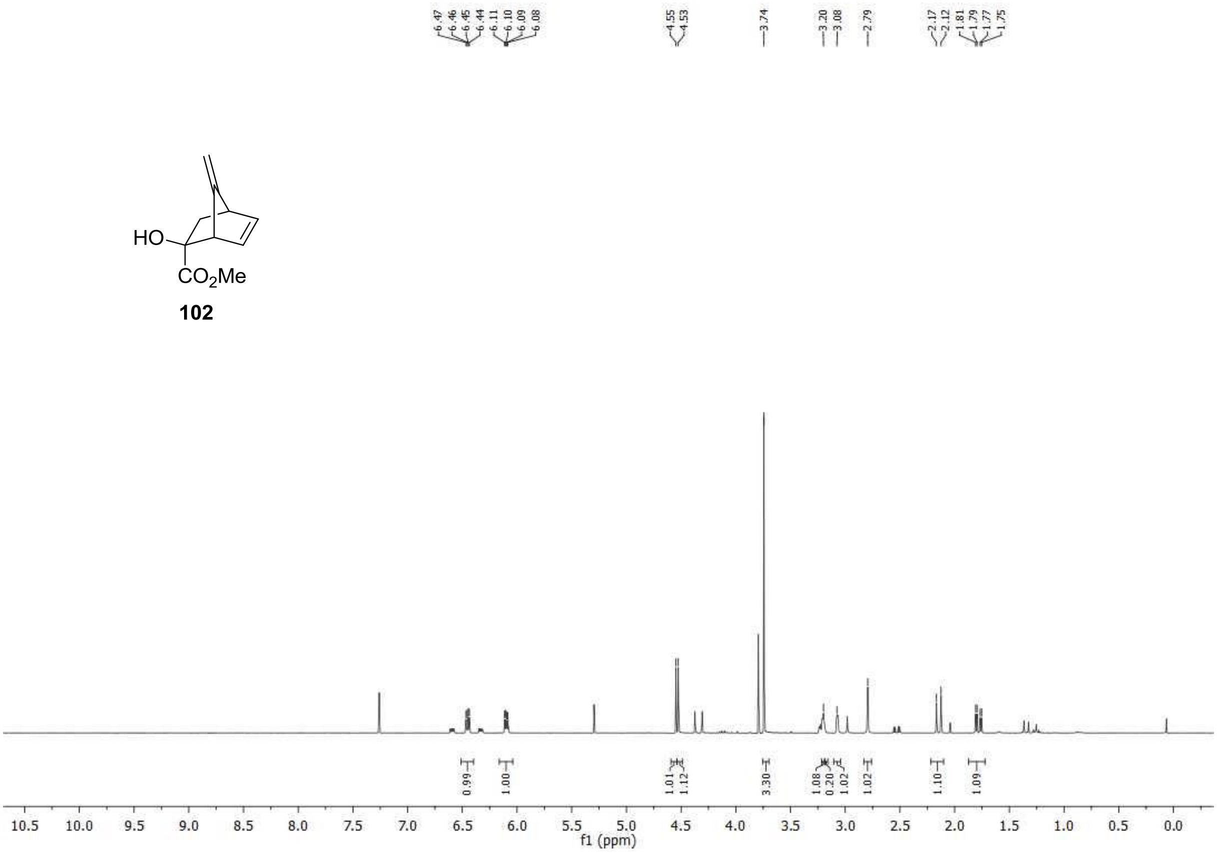
6.47
6.46
6.45
6.44
6.11
6.10
6.09
6.08
4.55
4.53
3.74
3.20
3.08
2.79
2.17
2.12
1.81
1.79
1.77
1.75
HO
CO2Me
102
0.99
1.00
1.01
1.12
3.30
1.08
0.20
1.02
1.02
1.10
1.09
10.5
10.0
9.5
9.0
8.5
8.0
7.5
7.0
6.5
6.0
5.5
5.0
4.5
4.0
3.5
3.0
2.5
2.0
1.5
1.0
0.5
0.0
f1 (ppm)

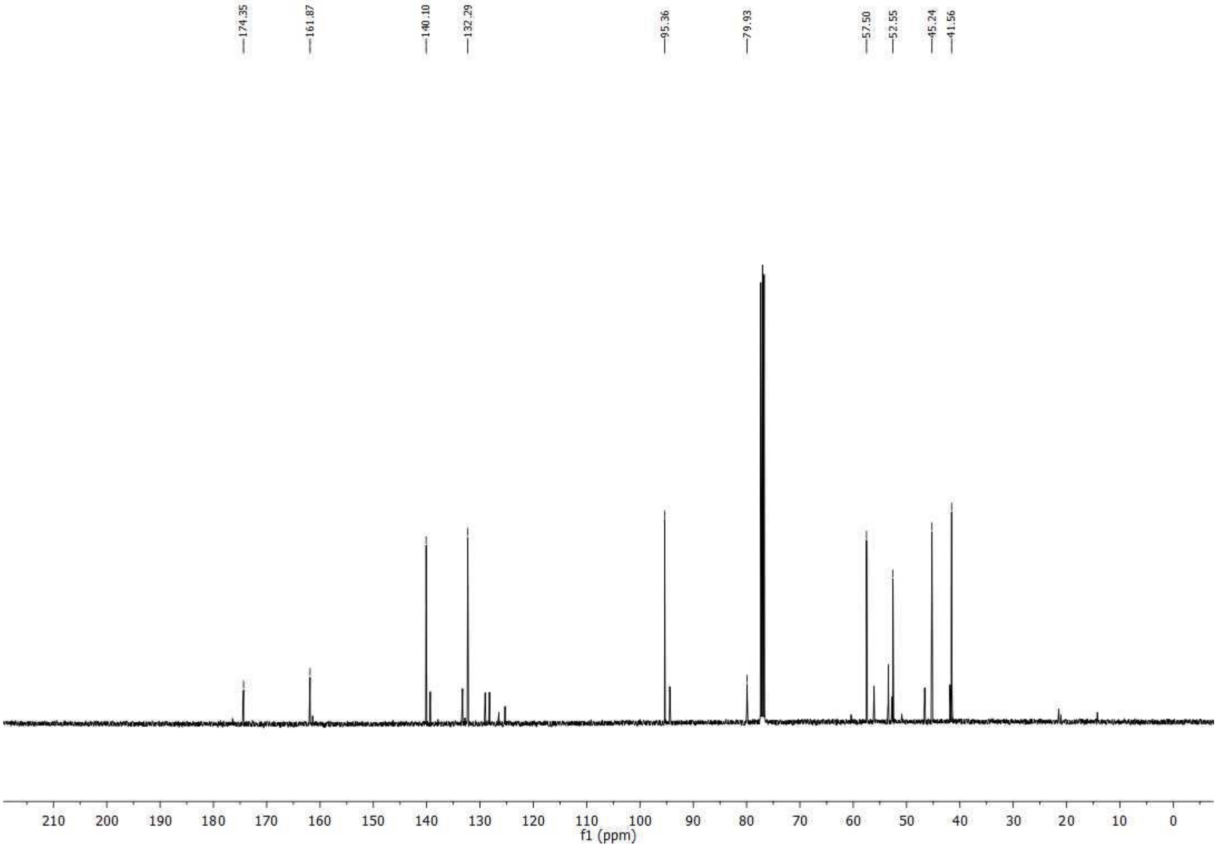
174.35
161.87
140.10
132.29
95.36
79.93
57.50
52.55
45.24
41.56
210
200
190
180
170
160
150
140
130
120
110
100
90
80
70
60
50
40
30
20
10
0
f1 (ppm)

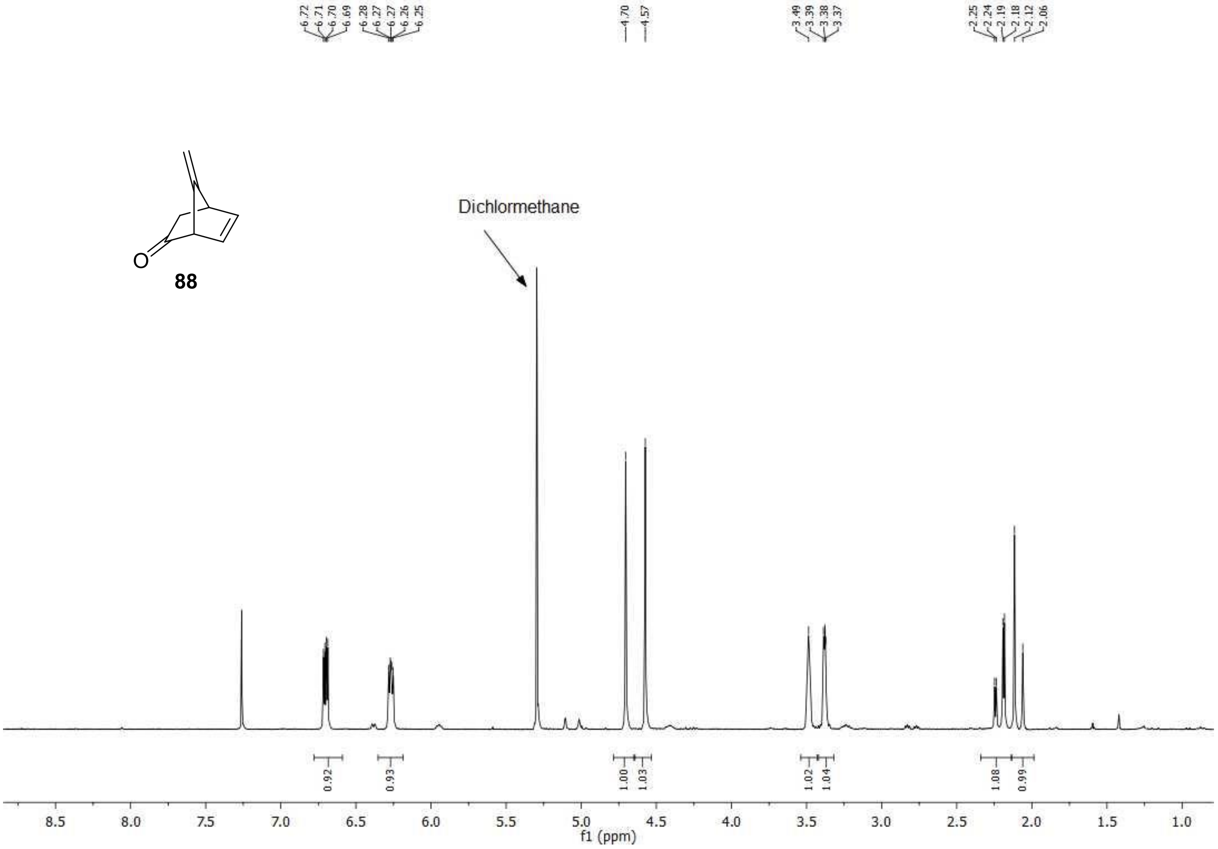
6.72
6.71
6.70
6.69
6.28
6.27
6.27
6.26
6.25
4.70
4.57
3.49
3.39
3.38
3.37
2.25
2.24
2.19
2.18
2.12
2.06
O
88
Dichlormethane
0.92
0.93
1.00
1.03
1.02
1.04
1.08
0.99
8.5
8.0
7.5
7.0
6.5
6.0
5.5
5.0
4.5
4.0
3.5
3.0
2.5
2.0
1.5
1.0
f1 (ppm)

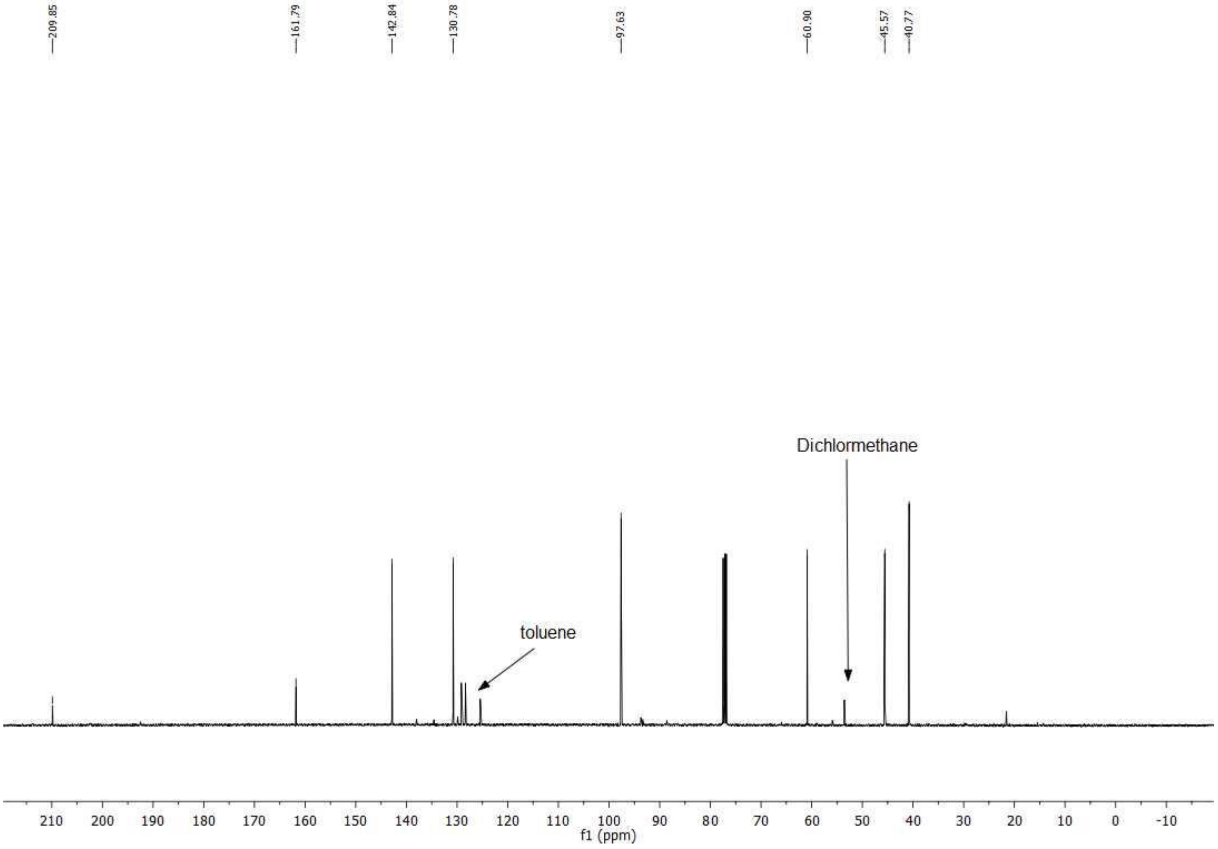
209.85
161.79
142.84
130.78
97.63
60.90
45.57
40.77
Dichlormethane
toluene
210
200
190
180
170
160
150
140
130
120
110
100
90
80
70
60
50
40
30
20
10
0
-10
f1 (ppm)

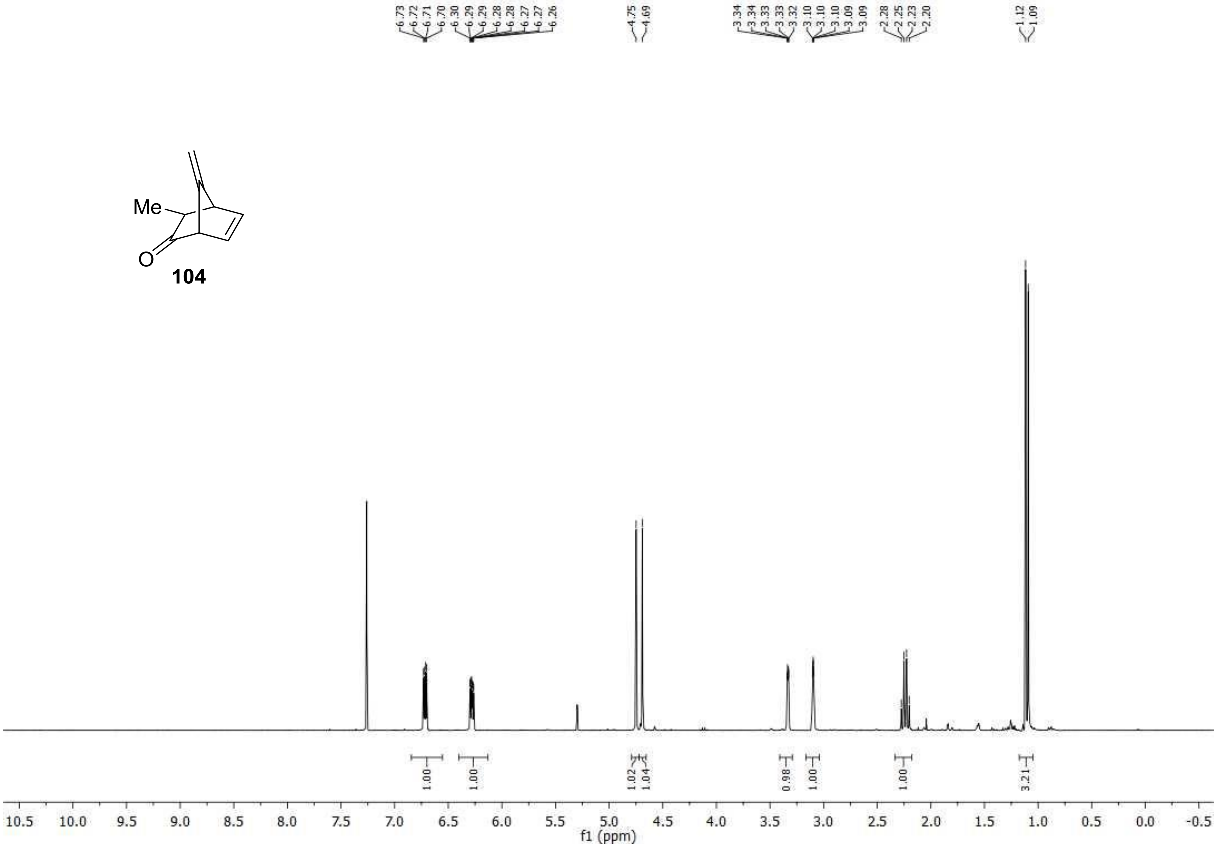
Me
O
6.73
6.72
6.71
6.70
6.30
6.29
6.29
6.28
6.28
6.27
6.27
6.26
4.75
4.69
3.34
3.34
3.33
3.33
3.32
3.10
3.10
3.10
3.09
3.09
2.28
2.25
2.23
2.20
1.12
1.09
1.00
1.00
1.02
1.04
0.98
1.00
1.00
3.21
f1 (ppm)

104

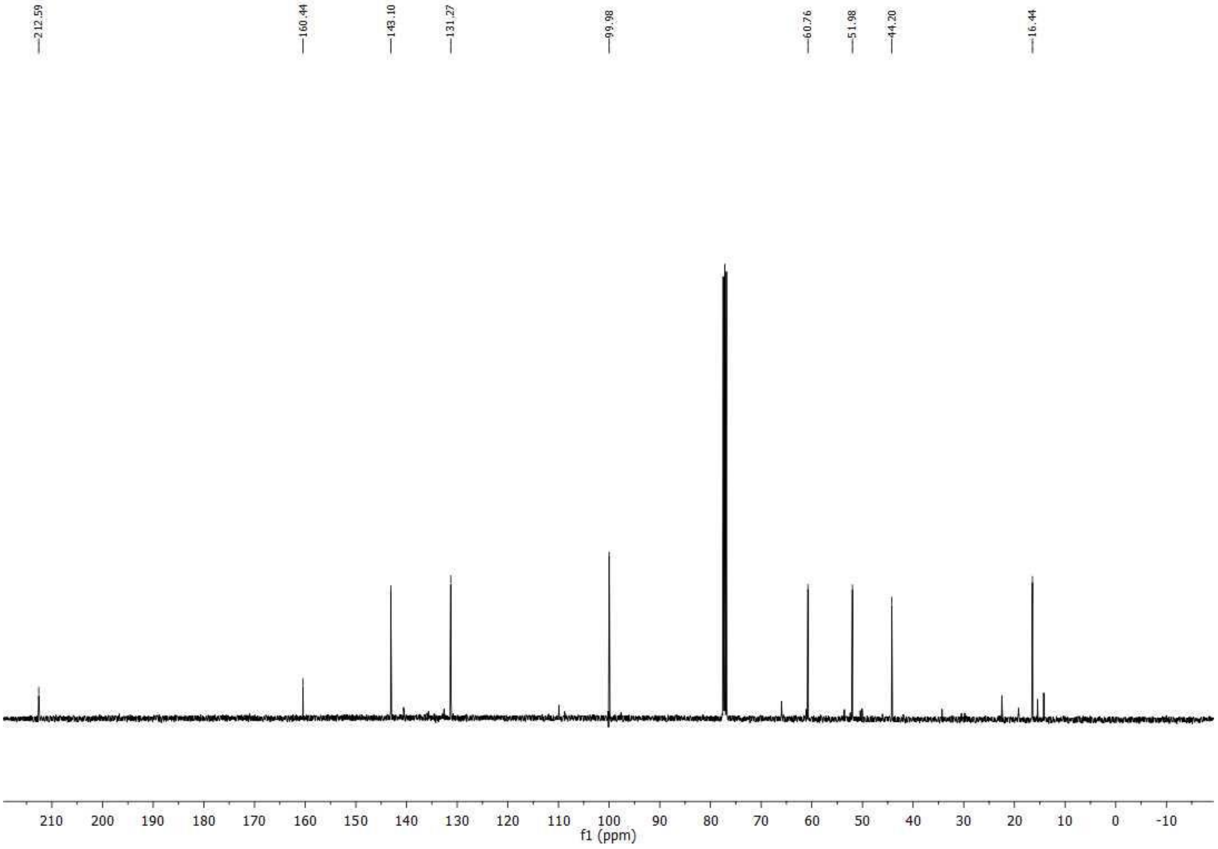
212.59
160.44
143.10
131.27
99.98
60.76
51.98
44.20
16.44
f1 (ppm)

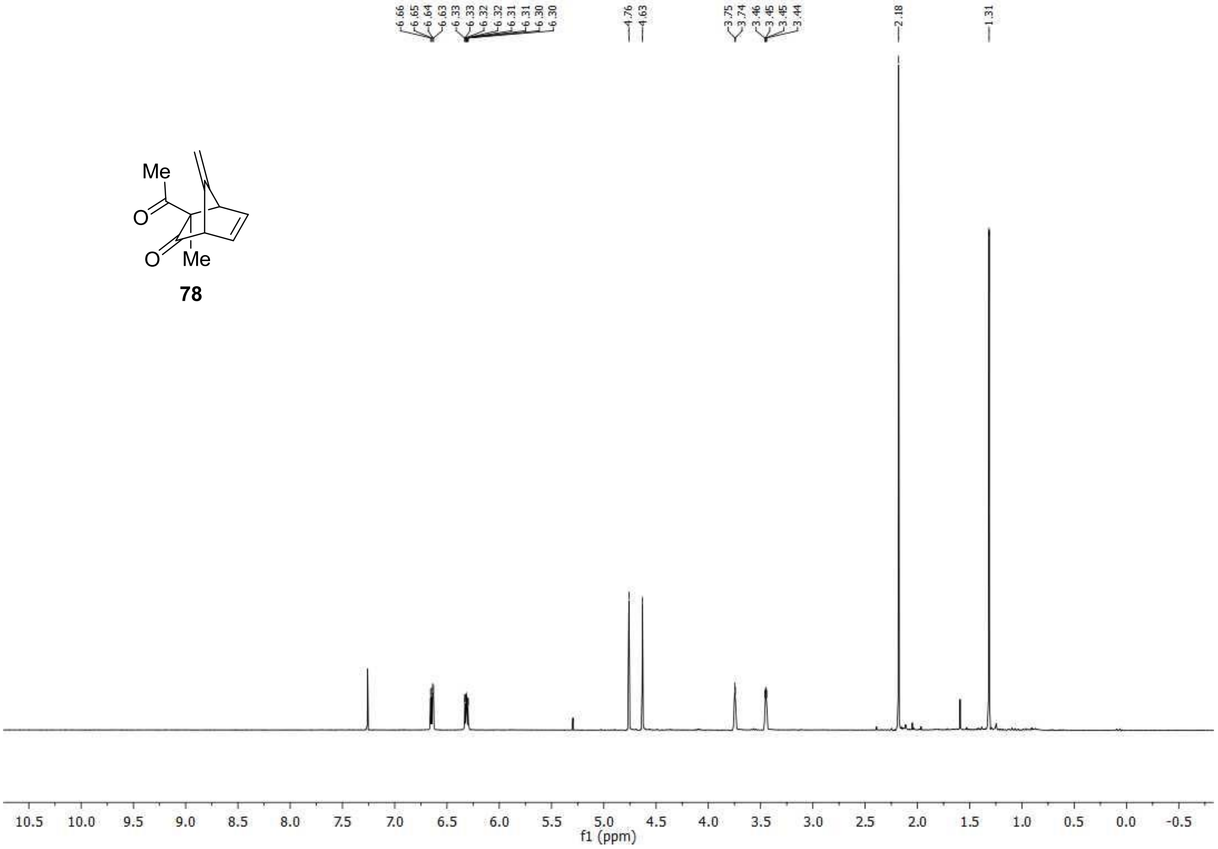
6.66
6.65
6.64
6.63
6.33
6.33
6.32
6.32
6.31
6.31
6.30
6.30
4.76
4.63
3.75
3.74
3.46
3.45
3.45
3.44
2.18
1.31
Me
O
O
Me
78
10.5
10.0
9.5
9.0
8.5
8.0
7.5
7.0
6.5
6.0
5.5
5.0
4.5
4.0
3.5
3.0
2.5
2.0
1.5
1.0
0.5
0.0
-0.5
f1 (ppm)

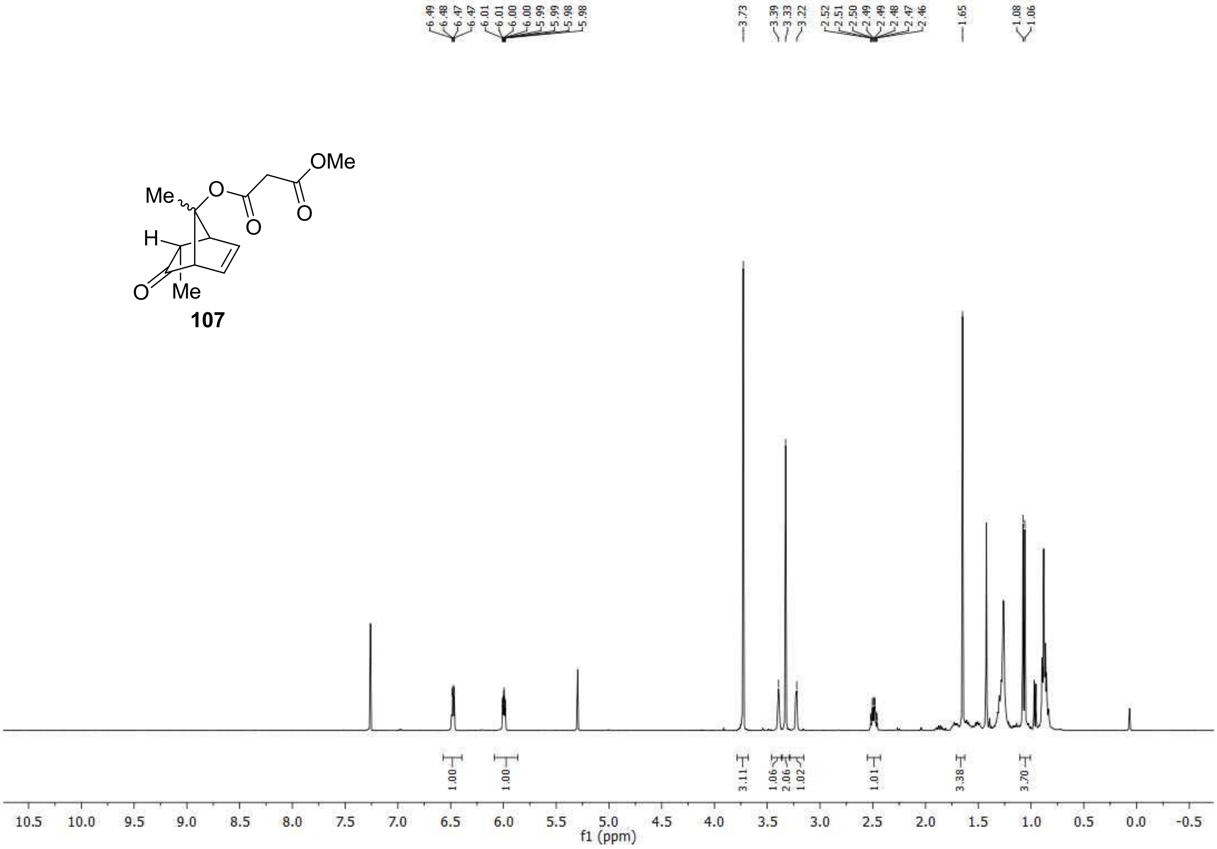
6.49
6.48
6.47
6.47
6.01
6.01
6.00
6.00
5.99
5.99
5.98
5.98
3.73
3.39
3.33
3.22
2.52
2.51
2.50
2.49
2.49
2.48
2.47
2.46
1.65
1.08
1.06
OMe
Me
O
O
O
H
O
Me
107
1.00
1.00
3.11
1.06
2.06
1.02
1.01
3.38
3.70
10.5
10.0
9.5
9.0
8.5
8.0
7.5
7.0
6.5
6.0
5.5
5.0
4.5
4.0
3.5
3.0
2.5
2.0
1.5
1.0
0.5
0.0
-0.5
f1 (ppm)

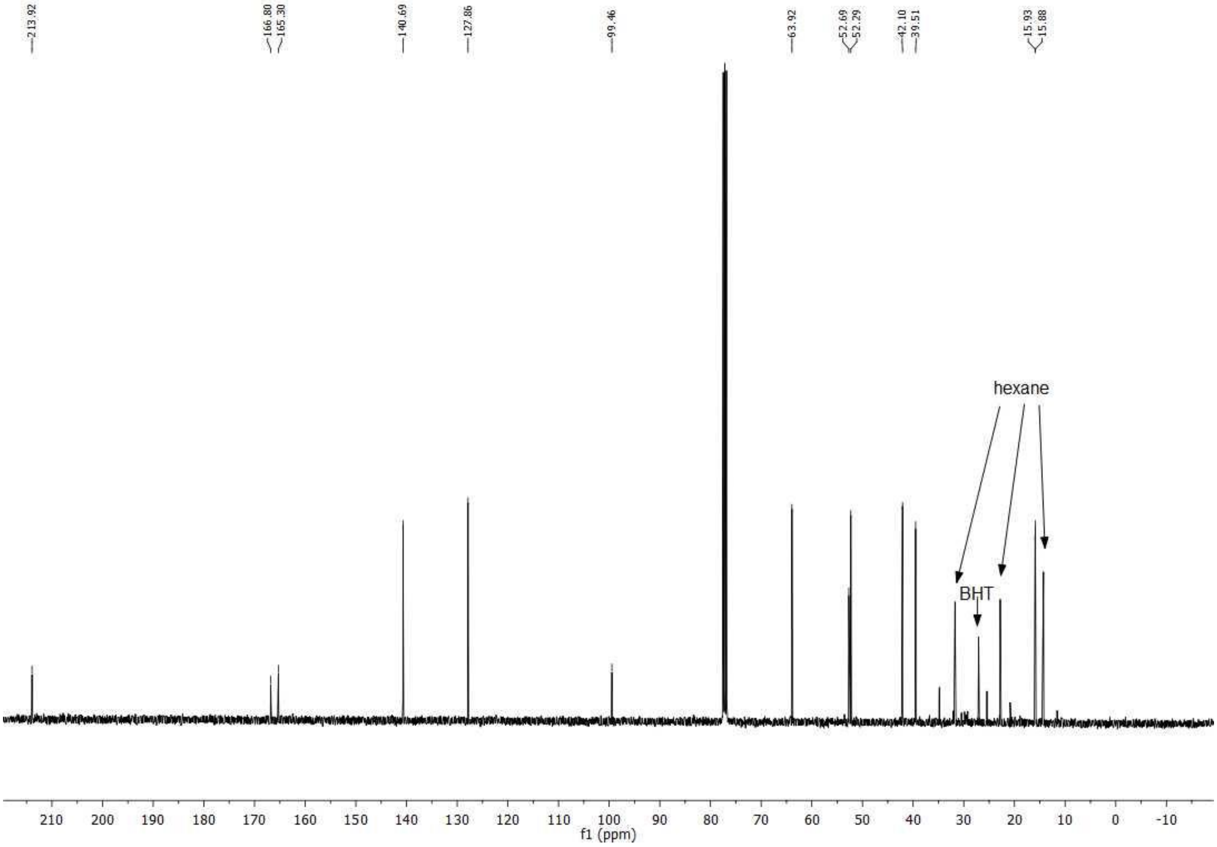
213.92
166.80
165.30
140.69
127.86
99.46
63.92
52.69
52.29
42.10
39.51
15.93
15.88
hexane
BHT
210
200
190
180
170
160
150
140
130
120
110
100
90
80
70
60
50
40
30
20
10
0
-10
f1 (ppm)

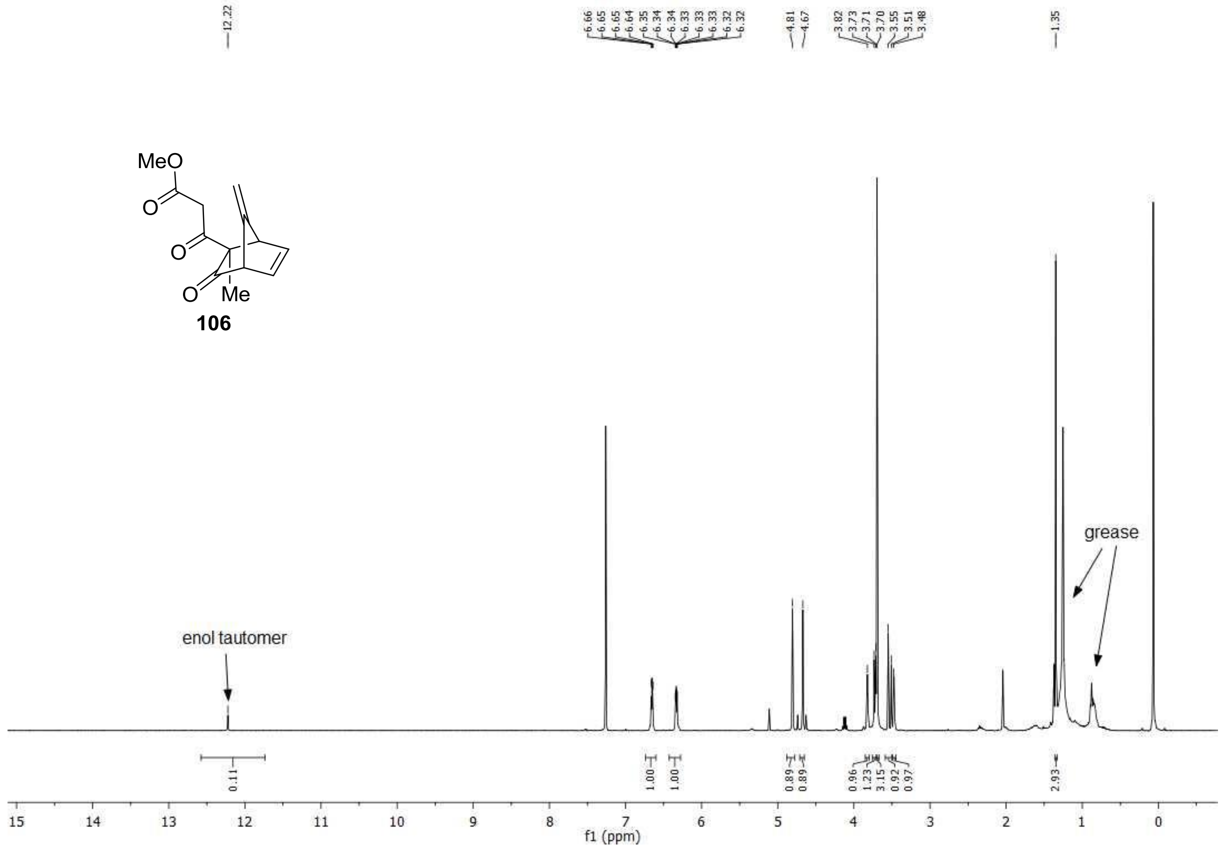
12.22
6.66
6.65
6.65
6.64
6.35
6.34
6.34
6.33
6.33
6.33
6.33
6.32
6.32
4.81
4.67
3.82
3.73
3.71
3.70
3.55
3.51
3.48
1.35
MeO
O
O
O
Me
106
enol tautomer
grease
0.11
1.00
1.00
0.89
0.89
0.96
1.23
3.15
0.92
0.97
2.93
15
14
13
12
11
10
9
8
7
6
5
4
3
2
1
0
f1 (ppm)

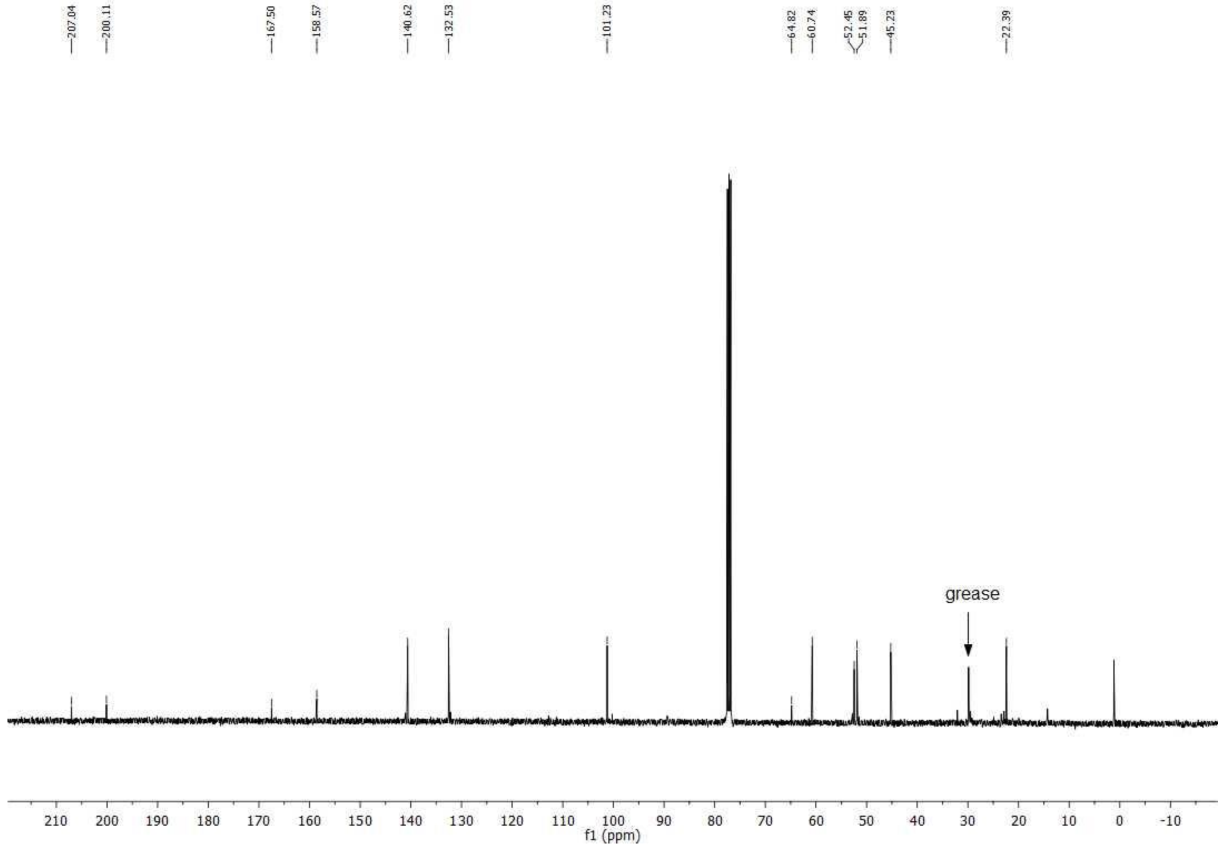
207.04
200.11
167.50
158.57
140.62
132.53
101.23
64.82
60.74
52.45
51.89
45.23
22.39
grease
210
200
190
180
170
160
150
140
130
120
110
100
90
80
70
60
50
40
30
20
10
0
-10
f1 (ppm)

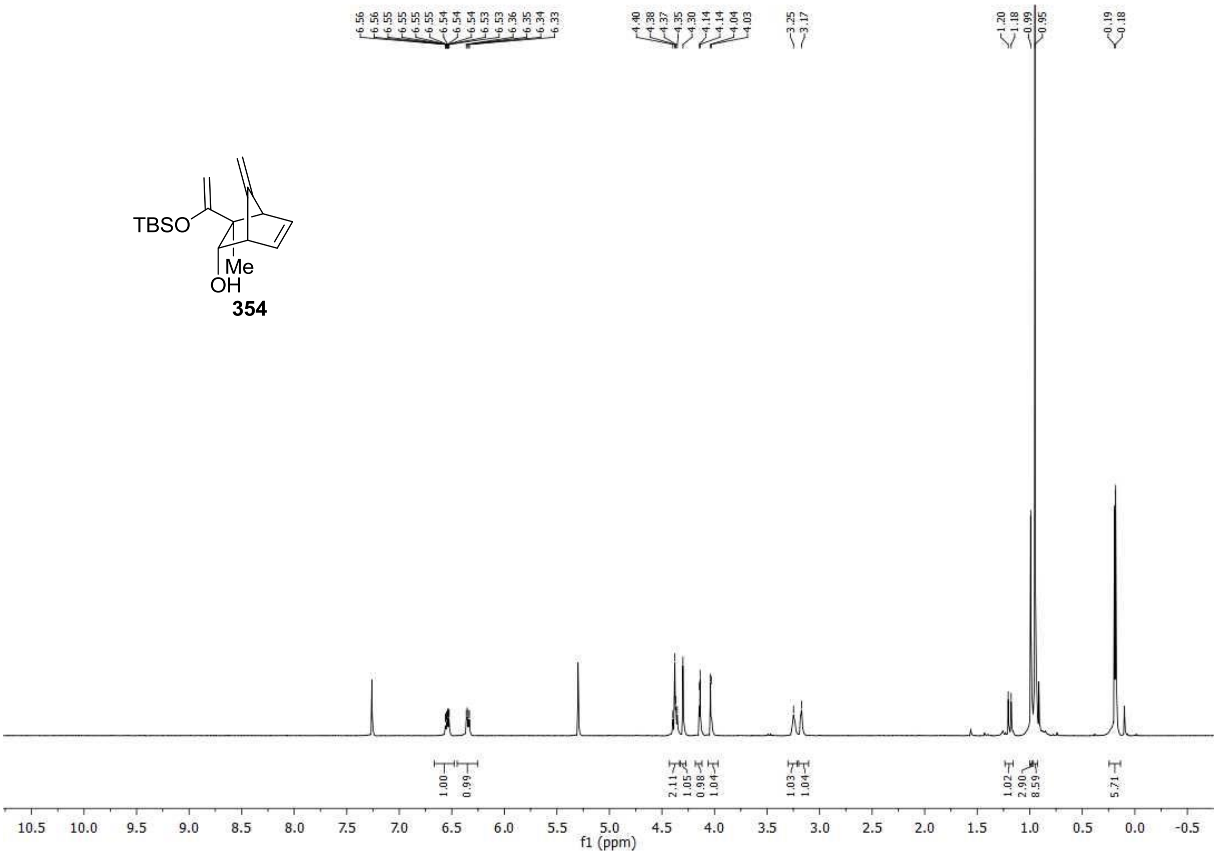
6.56 6.56 6.55 6.55 6.55 6.55 6.54 6.54 6.54 6.53 6.53 6.36 6.35 6.34 6.33
4.40 4.38 4.37 4.35 4.30 4.14 4.14 4.04 4.03
3.25 3.17
1.20 1.18 0.99 0.95
0.19 0.18
TBSO
Me
OH
1.00 0.99 2.11 1.05 0.98 1.04 1.03 1.04 1.02 2.90 8.59 5.71
10.5 10.0 9.5 9.0 8.5 8.0 7.5 7.0 6.5 6.0 5.5 5.0 4.5 4.0 3.5 3.0 2.5 2.0 1.5 1.0 0.5 0.0 -0.5
f1 (ppm)

354

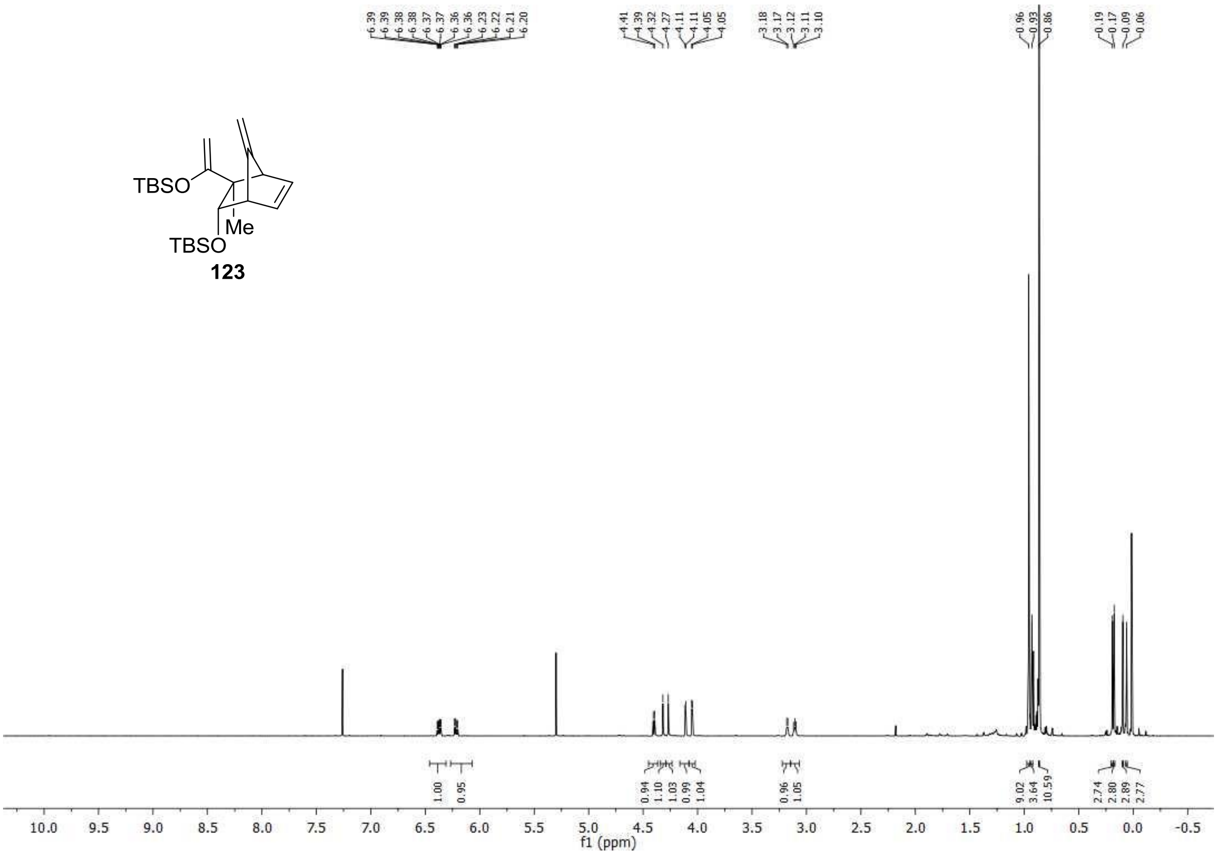
6.39 6.39 6.38 6.37 6.37 6.36 6.36 6.23 6.22 6.21 6.20
4.41 4.39 4.32 4.27 4.11 4.11 4.05 4.05
3.18 3.17 3.12 3.11 3.10
0.96 0.93 0.86
0.19 0.17 0.09 0.06
TBSO
Me
TBSO
1.00 0.95 0.94 1.10 1.03 0.99 1.04 0.96 1.05 9.02 3.64 10.59 2.74 2.80 2.89 2.77
10.0 9.5 9.0 8.5 8.0 7.5 7.0 6.5 6.0 5.5 5.0 4.5 4.0 3.5 3.0 2.5 2.0 1.5 1.0 0.5 0.0 -0.5
f1 (ppm)

123

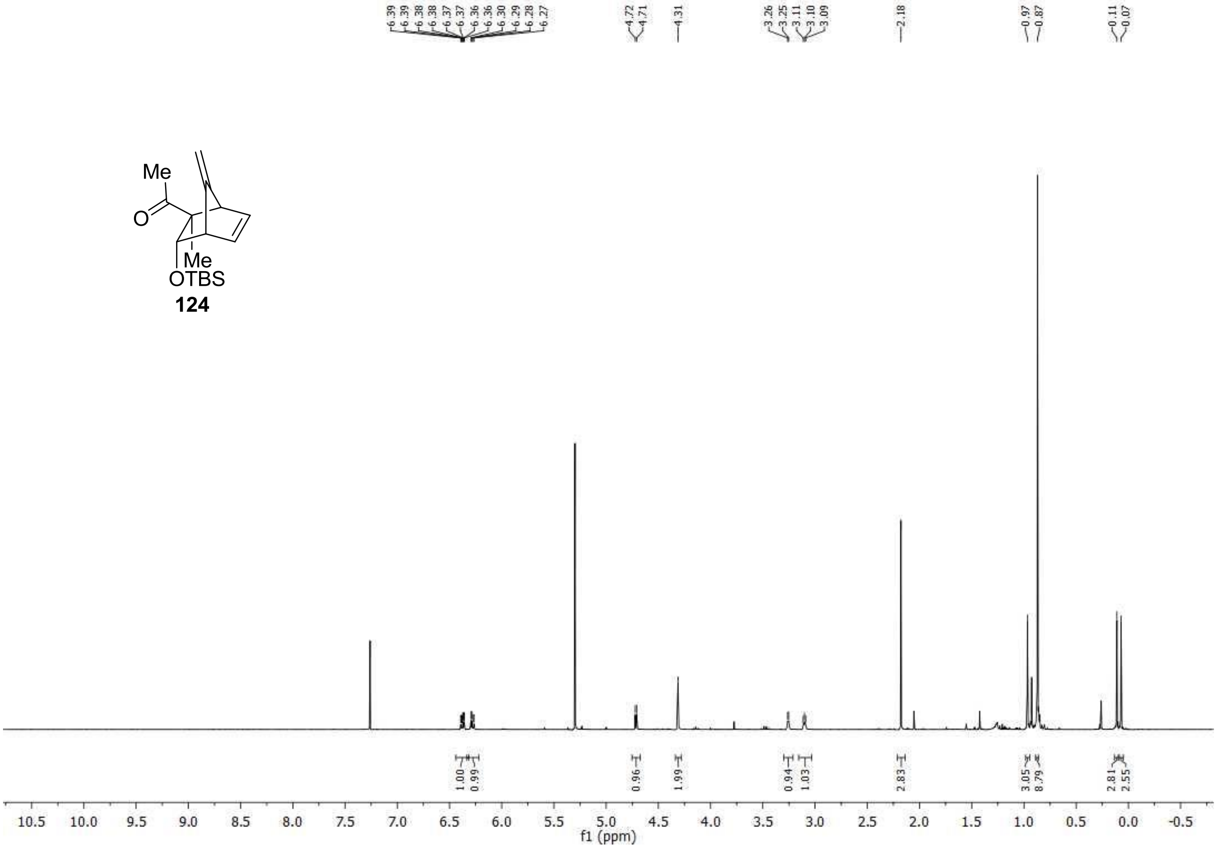
6.39
6.39
6.38
6.38
6.37
6.37
6.36
6.36
6.30
6.29
6.29
6.28
6.27
4.72
4.71
4.31
3.26
3.25
3.11
3.10
3.09
2.18
0.97
0.87
0.11
0.07
Me
O
Me
OTBS
1.00
0.99
0.96
1.99
0.94
1.03
2.83
3.05
8.79
2.81
2.55
10.5 10.0 9.5 9.0 8.5 8.0 7.5 7.0 6.5 6.0 5.5 5.0 4.5 4.0 3.5 3.0 2.5 2.0 1.5 1.0 0.5 0.0 -0.5
f1 (ppm)

124

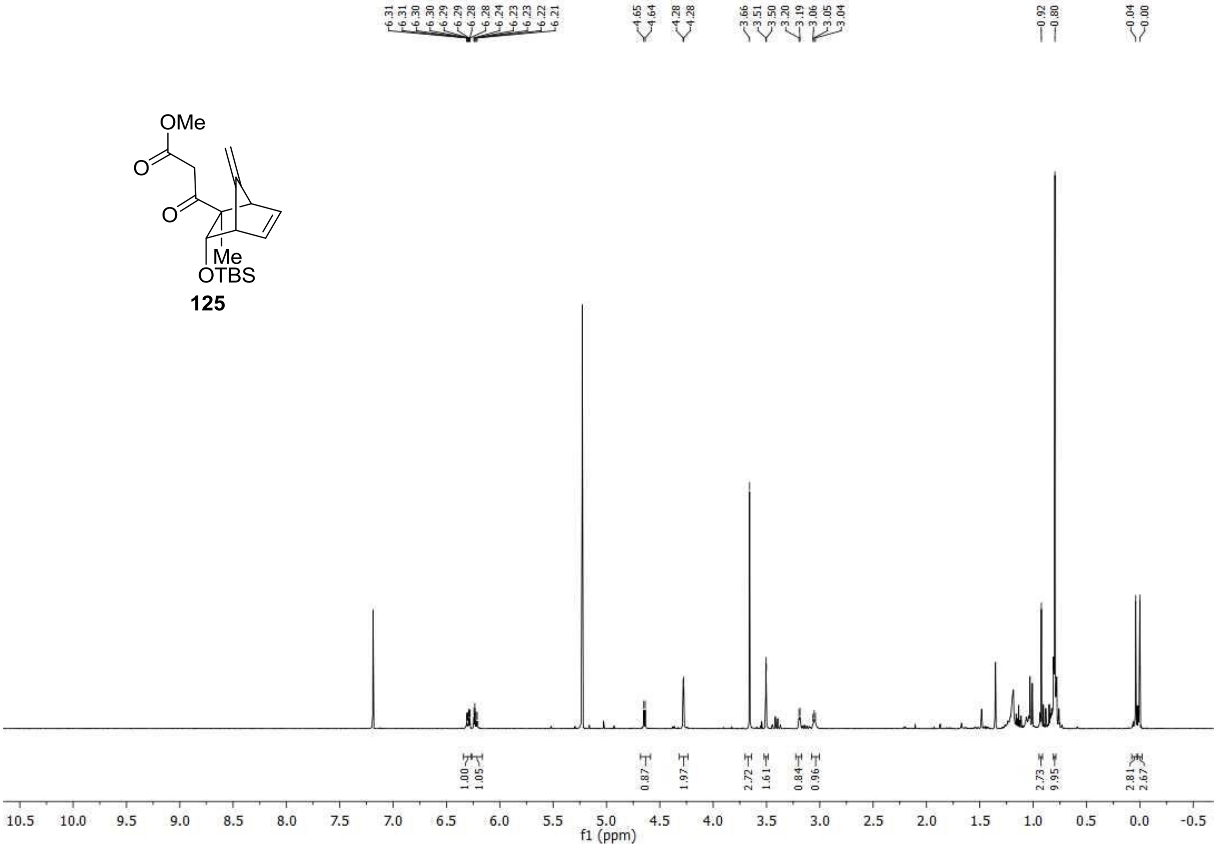
6.31
6.31
6.30
6.30
6.29
6.29
6.28
6.28
6.24
6.24
6.23
6.23
6.22
6.21
4.65
4.64
4.28
4.28
3.66
3.51
3.50
3.20
3.19
3.06
3.05
3.04
0.92
0.80
0.04
0.00
OMe
O
O
Me
OTBS
1.00
1.05
0.87
1.97
2.72
1.61
0.84
0.96
2.73
9.95
2.81
2.67
10.5 10.0 9.5 9.0 8.5 8.0 7.5 7.0 6.5 6.0 5.5 5.0 4.5 4.0 3.5 3.0 2.5 2.0 1.5 1.0 0.5 0.0 -0.5
f1 (ppm)

125

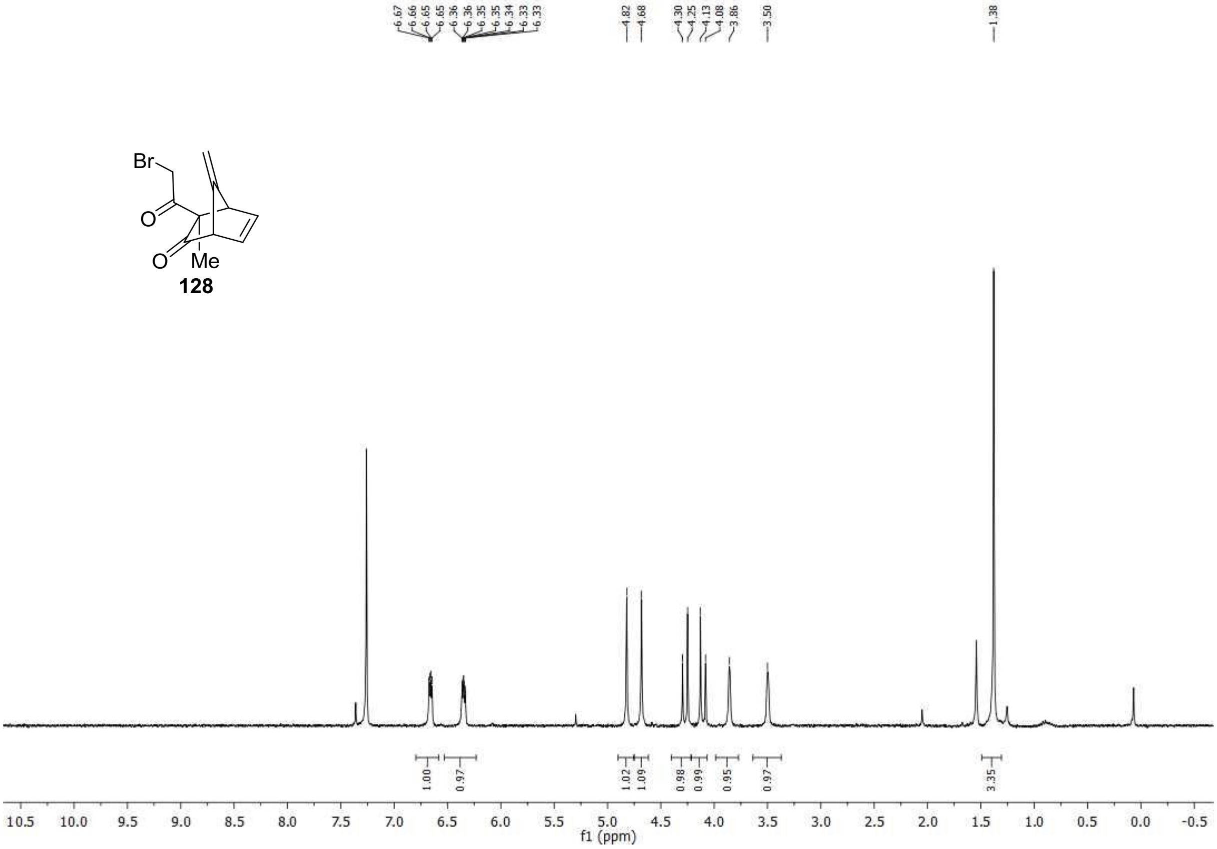
6.67
6.66
6.65
6.65
6.36
6.36
6.35
6.35
6.34
6.33
6.33
4.82
4.68
4.30
4.25
4.13
4.08
3.86
3.50
1.38
Br
O
O
Me
128
1.00
0.97
1.02
1.09
0.98
0.99
0.95
0.97
3.35
10.5
10.0
9.5
9.0
8.5
8.0
7.5
7.0
6.5
6.0
5.5
5.0
4.5
4.0
3.5
3.0
2.5
2.0
1.5
1.0
0.5
0.0
-0.5
f1 (ppm)

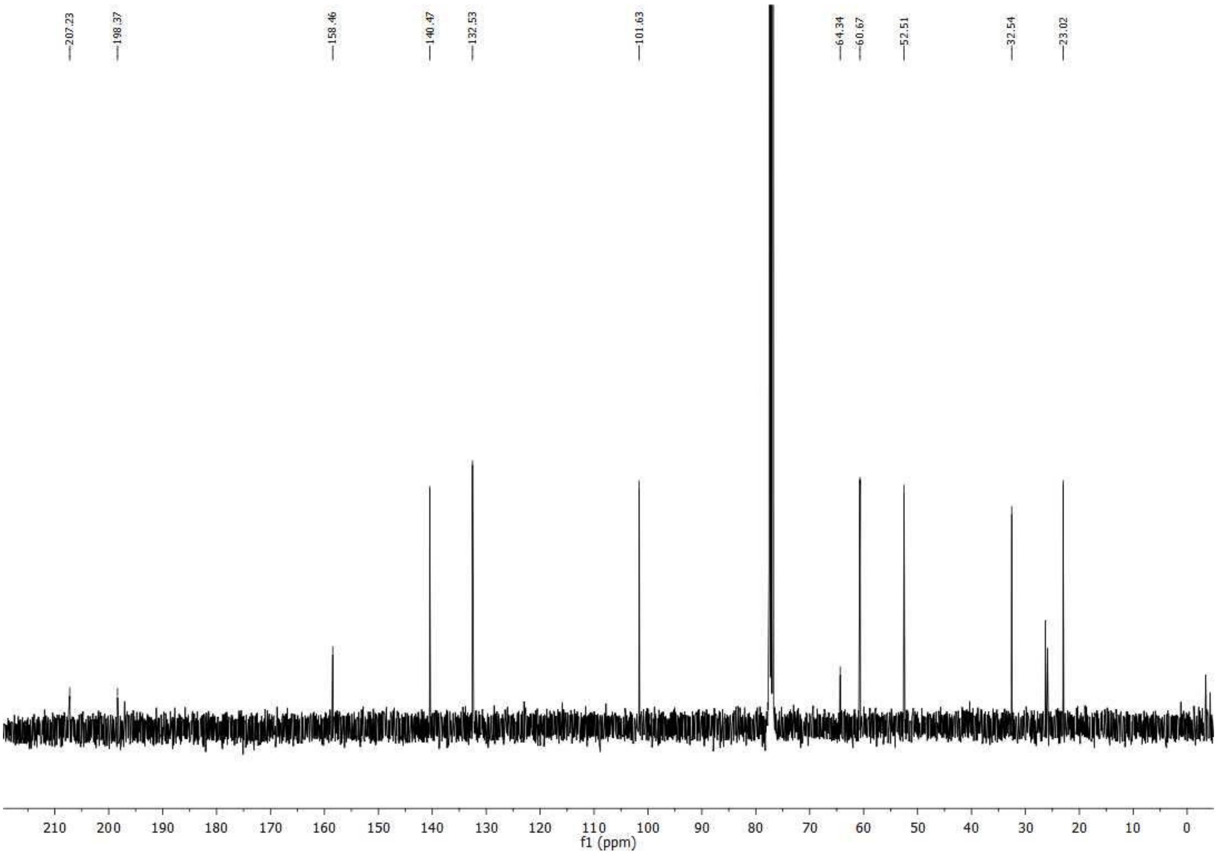
207.23
198.37
158.46
140.47
132.53
101.63
64.34
60.67
52.51
32.54
23.02
210
200
190
180
170
160
150
140
130
120
110
100
90
80
70
60
50
40
30
20
10
0
f1 (ppm)

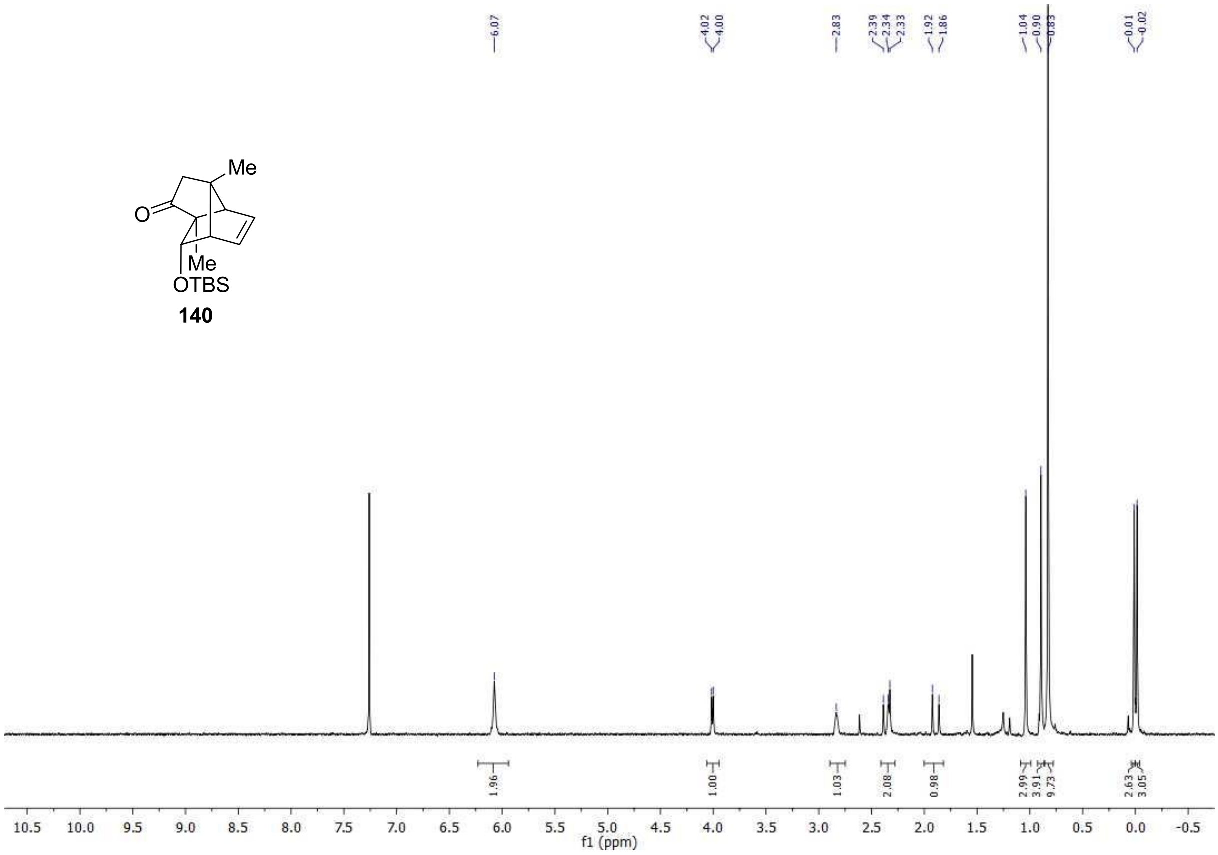
Me
O
Me
OTBS
6.07
4.02
4.00
2.83
2.39
2.34
2.33
1.92
1.86
1.04
0.90
0.83
0.01
-0.02
1.96
1.00
1.03
2.08
0.98
2.99
3.91
9.73
2.63
3.05
10.5 10.0 9.5 9.0 8.5 8.0 7.5 7.0 6.5 6.0 5.5 5.0 4.5 4.0 3.5 3.0 2.5 2.0 1.5 1.0 0.5 0.0 -0.5
f1 (ppm)

140

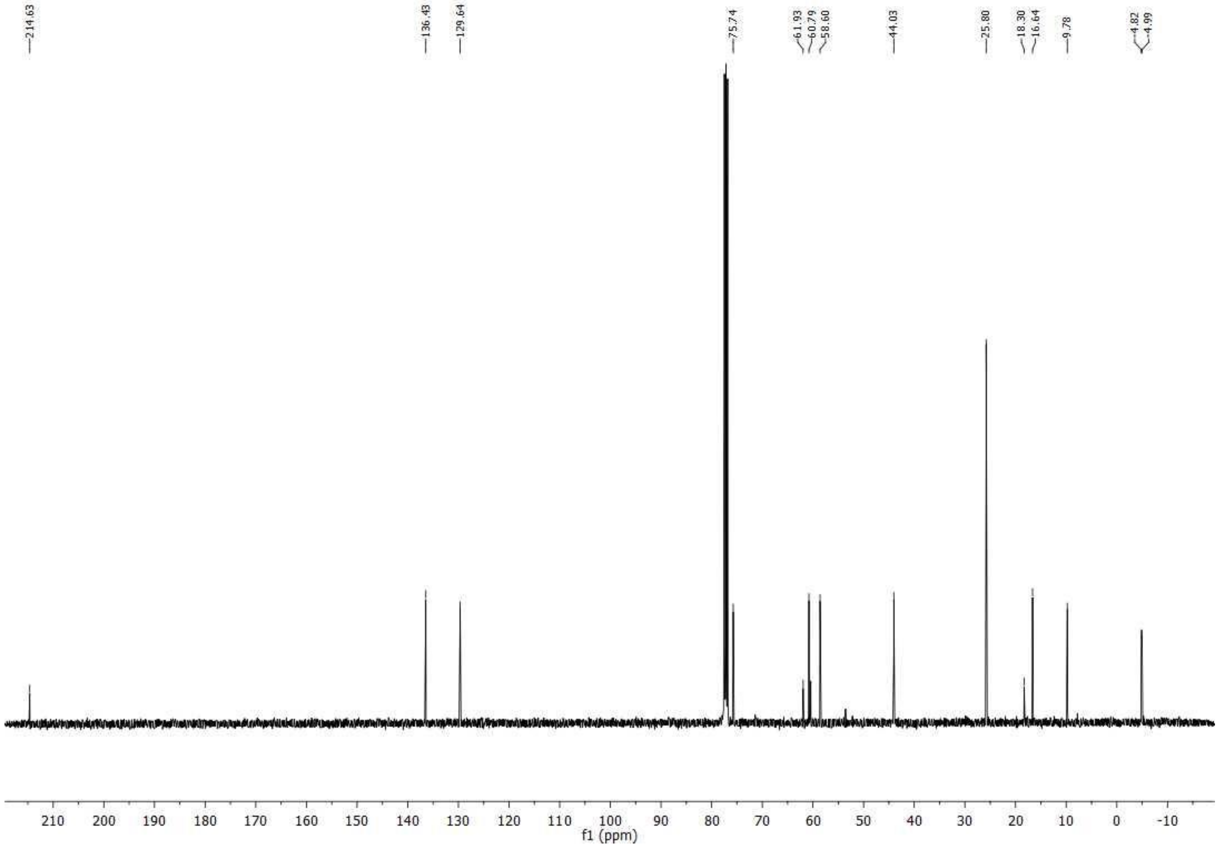
214.63
136.43
129.64
75.74
61.93
60.79
58.60
44.03
25.80
18.30
16.64
9.78
-4.82
-4.99
210 200 190 180 170 160 150 140 130 120 110 100 90 80 70 60 50 40 30 20 10 0 -10
f1 (ppm)

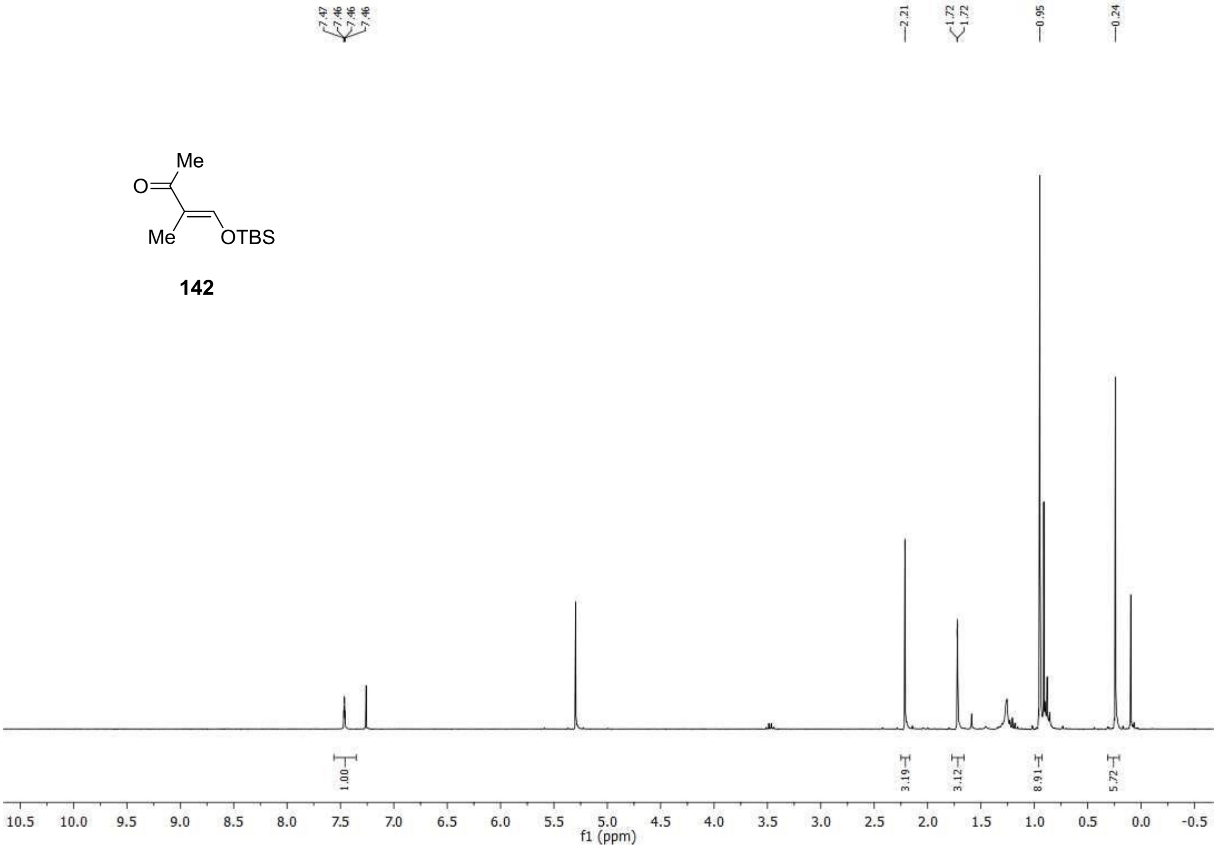
7.47
7.46
7.46
7.46
2.21
1.72
1.72
0.95
0.24
Me
O
Me
OTBS
1.00
3.19
3.12
8.91
5.72
10.5 10.0 9.5 9.0 8.5 8.0 7.5 7.0 6.5 6.0 5.5 5.0 4.5 4.0 3.5 3.0 2.5 2.0 1.5 1.0 0.5 0.0 -0.5
f1 (ppm)

142

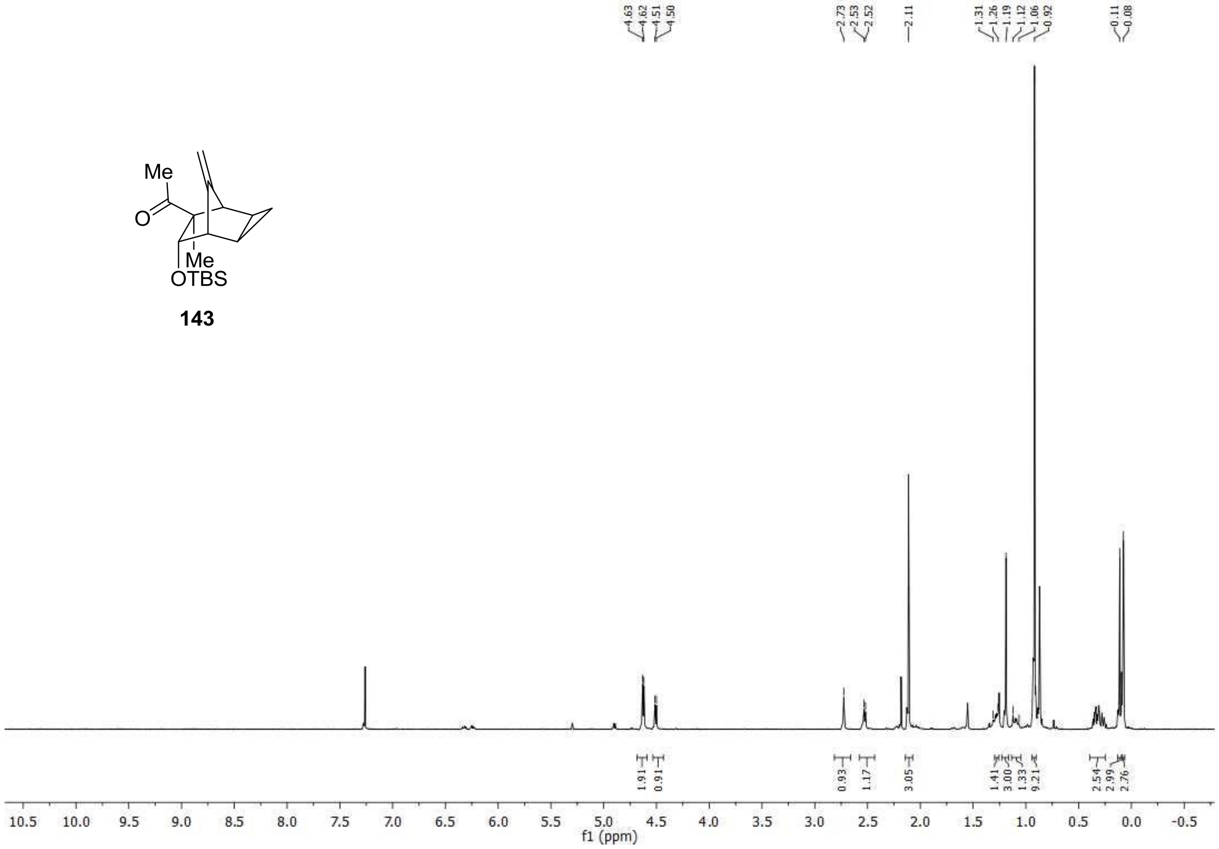
Me
O
Me
OTBS

143

4.63
4.62
4.51
4.50
2.73
2.53
2.52
2.11
1.31
1.26
1.19
1.12
1.06
0.92
0.11
0.08
1.91
0.91
0.93
1.17
3.05
1.41
3.00
1.33
9.21
2.54
2.99
2.76
10.5
10.0
9.5
9.0
8.5
8.0
7.5
7.0
6.5
6.0
5.5
5.0
4.5
4.0
3.5
3.0
2.5
2.0
1.5
1.0
0.5
0.0
-0.5
f1 (ppm)

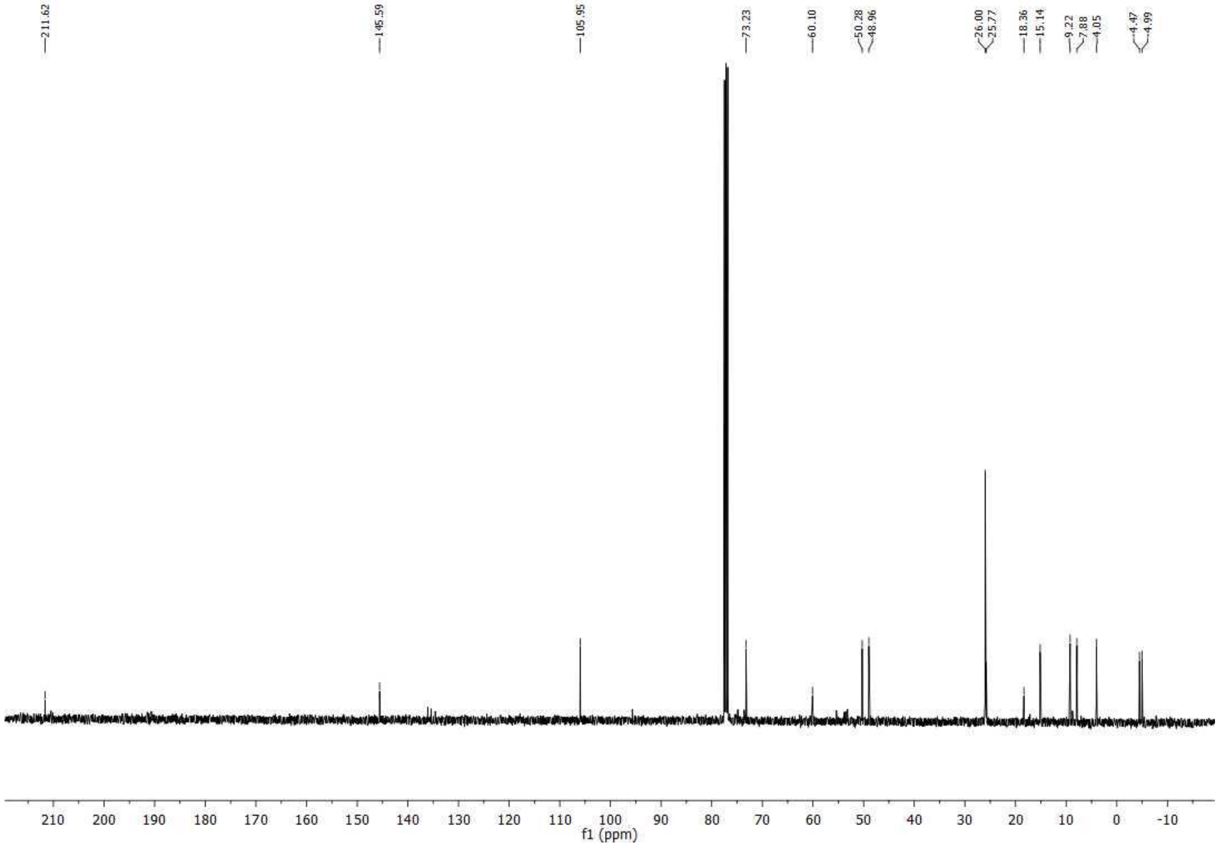
211.62
145.59
105.95
73.23
60.10
50.28
48.96
26.00
25.77
18.36
15.14
9.22
7.88
4.05
-4.47
-4.99
210
200
190
180
170
160
150
140
130
120
110
100
90
80
70
60
50
40
30
20
10
0
-10
f1 (ppm)

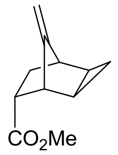
CO$_2$Me

148

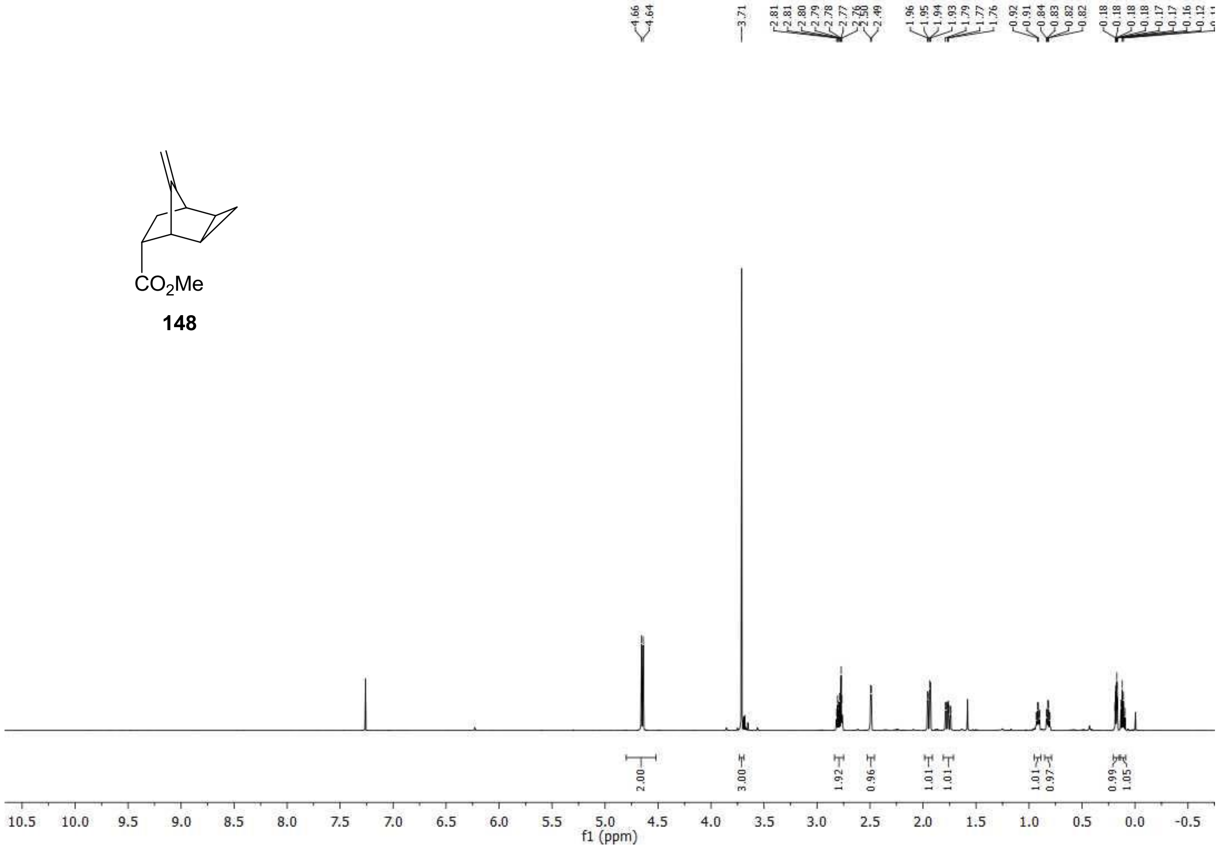
4.66
4.64
3.71
2.81
2.81
2.80
2.79
2.78
2.77
2.76
2.50
2.49
1.96
1.95
1.94
1.93
1.79
1.77
1.76
0.92
0.91
0.84
0.83
0.82
0.82
0.18
0.18
0.18
0.18
0.17
0.17
0.16
0.12
2.00
3.00
1.92
0.96
1.01
1.01
1.01
0.97
0.99
1.05
10.5
10.0
9.5
9.0
8.5
8.0
7.5
7.0
6.5
6.0
5.5
5.0
4.5
4.0
3.5
3.0
2.5
2.0
1.5
1.0
0.5
0.0
-0.5
f1 (ppm)

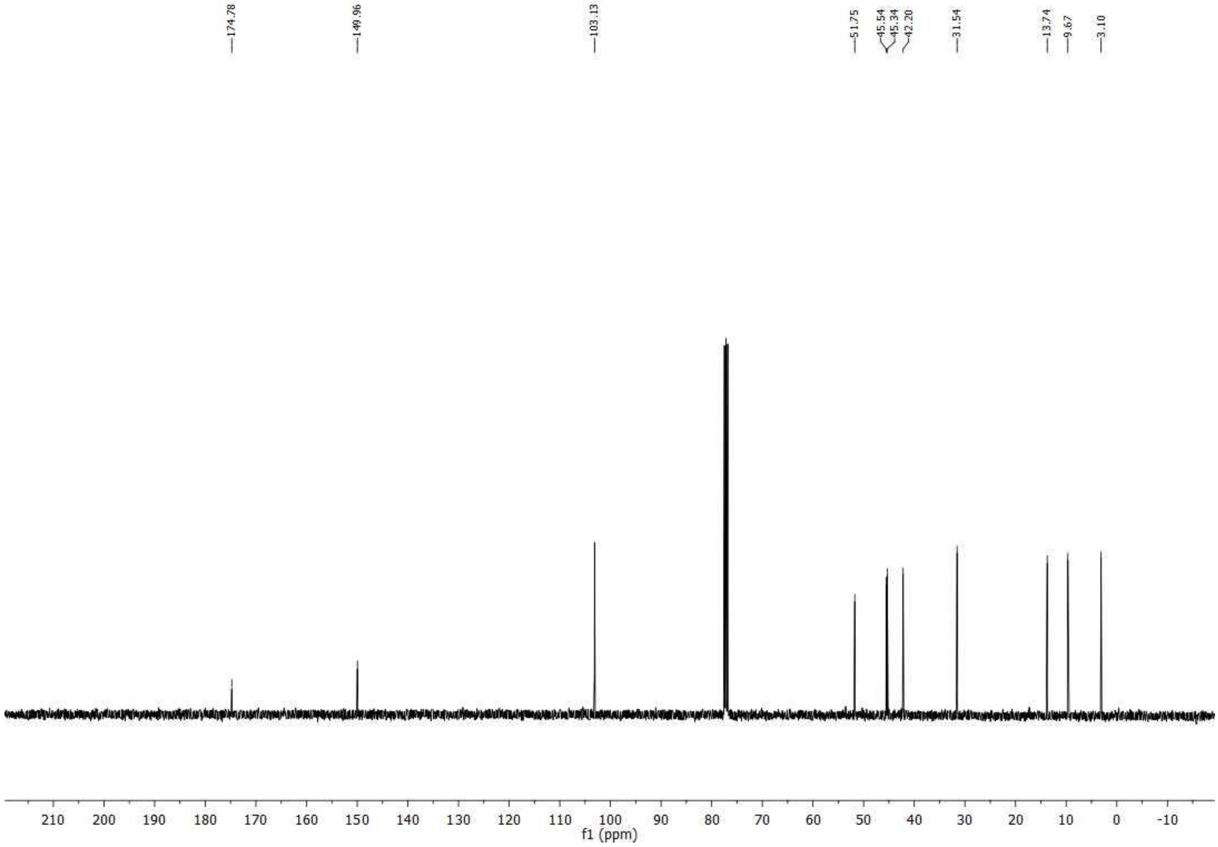
174.78
149.96
103.13
51.75
45.54
45.34
42.20
31.54
13.74
9.67
3.10
210
200
190
180
170
160
150
140
130
120
110
100
90
80
70
60
50
40
30
20
10
0
-10
f1 (ppm)

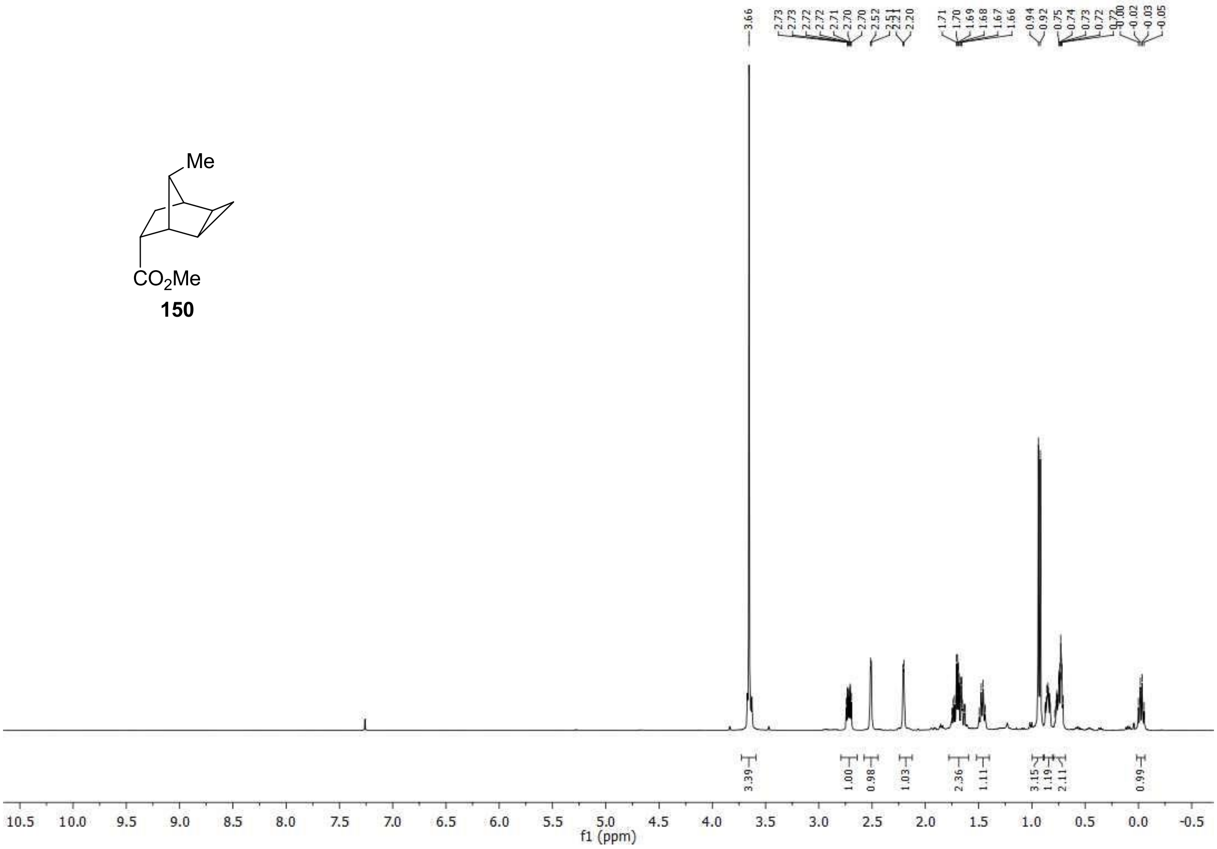

Me
CO$_2$Me

150

3.66
2.73
2.73
2.72
2.72
2.71
2.70
2.70
2.52
2.51
2.21
2.20
1.71
1.70
1.69
1.68
1.67
1.66
0.94
0.92
0.75
0.74
0.73
0.72
0.72
0.00
-0.02
-0.03
-0.05
3.39
1.00
0.98
1.03
2.36
1.11
3.15
1.19
2.11
0.99
10.5
10.0
9.5
9.0
8.5
8.0
7.5
7.0
6.5
6.0
5.5
5.0
4.5
4.0
3.5
3.0
2.5
2.0
1.5
1.0
0.5
0.0
-0.5
f1 (ppm)

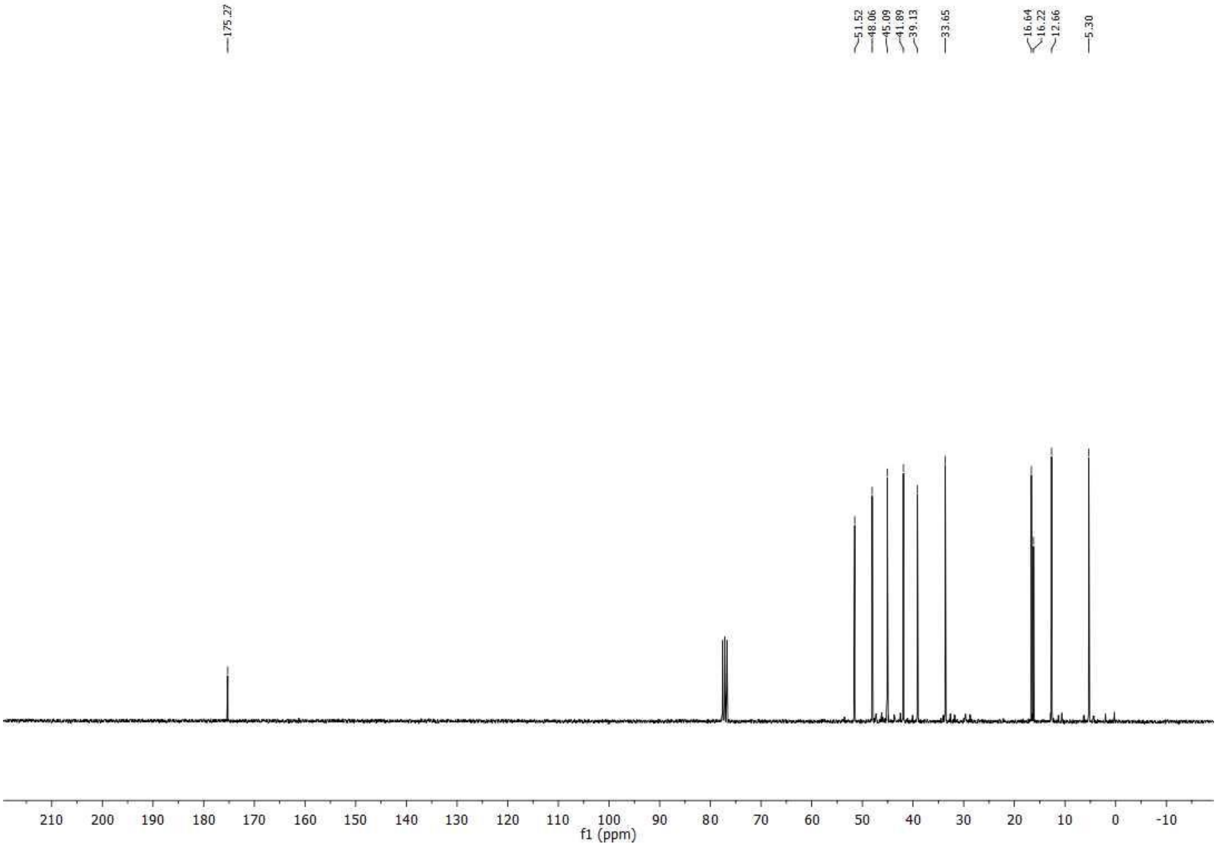

175.27
51.52
48.06
45.09
41.89
39.13
33.65
16.64
16.22
12.66
5.30
210
200
190
180
170
160
150
140
130
120
110
100
90
80
70
60
50
40
30
20
10
0
-10
f1 (ppm)

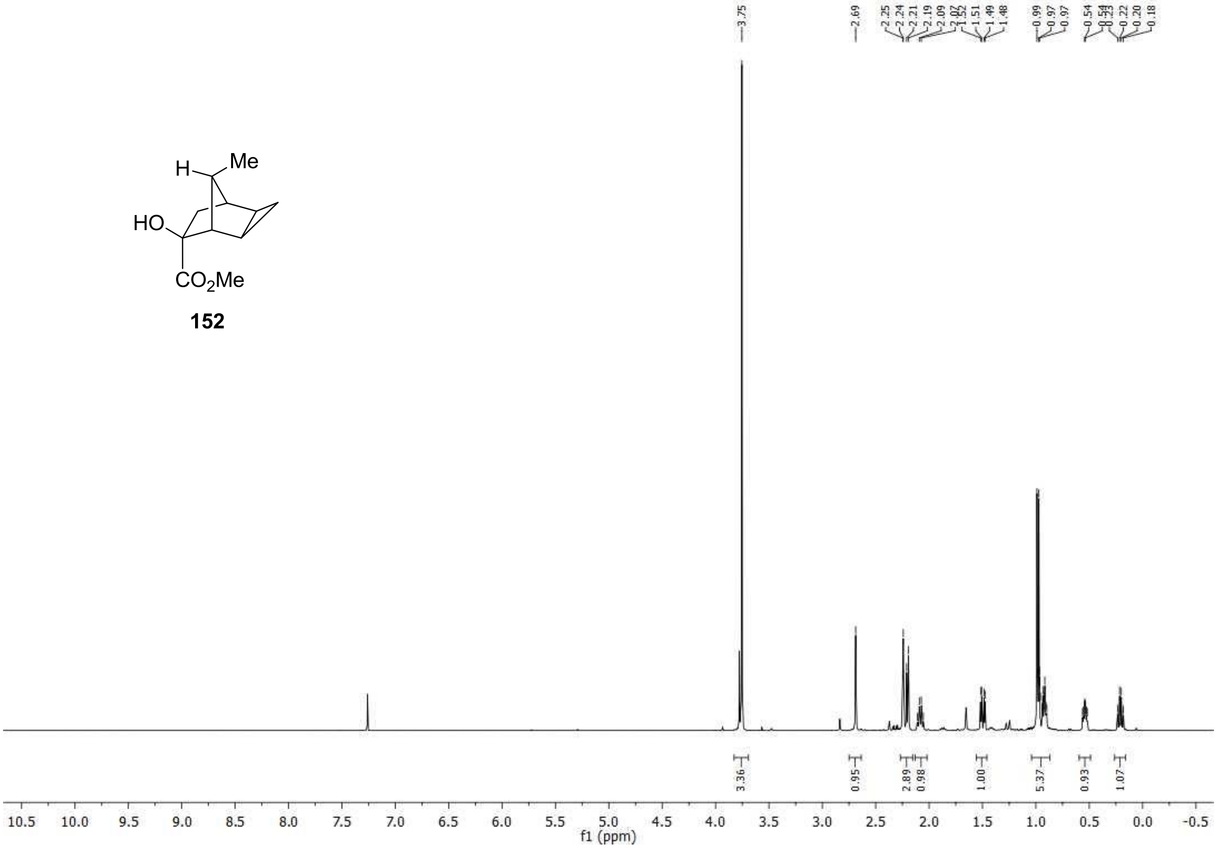

152

H
Me
HO
CO2Me
3.75
2.69
2.25
2.24
2.21
2.19
2.09
2.07
1.52
1.51
1.49
1.48
0.99
0.97
0.97
0.54
0.54
0.23
0.22
0.20
0.18
3.36
0.95
2.89
0.98
1.00
5.37
0.93
1.07
10.5
10.0
9.5
9.0
8.5
8.0
7.5
7.0
6.5
6.0
5.5
5.0
4.5
4.0
3.5
3.0
2.5
2.0
1.5
1.0
0.5
0.0
-0.5
f1 (ppm)

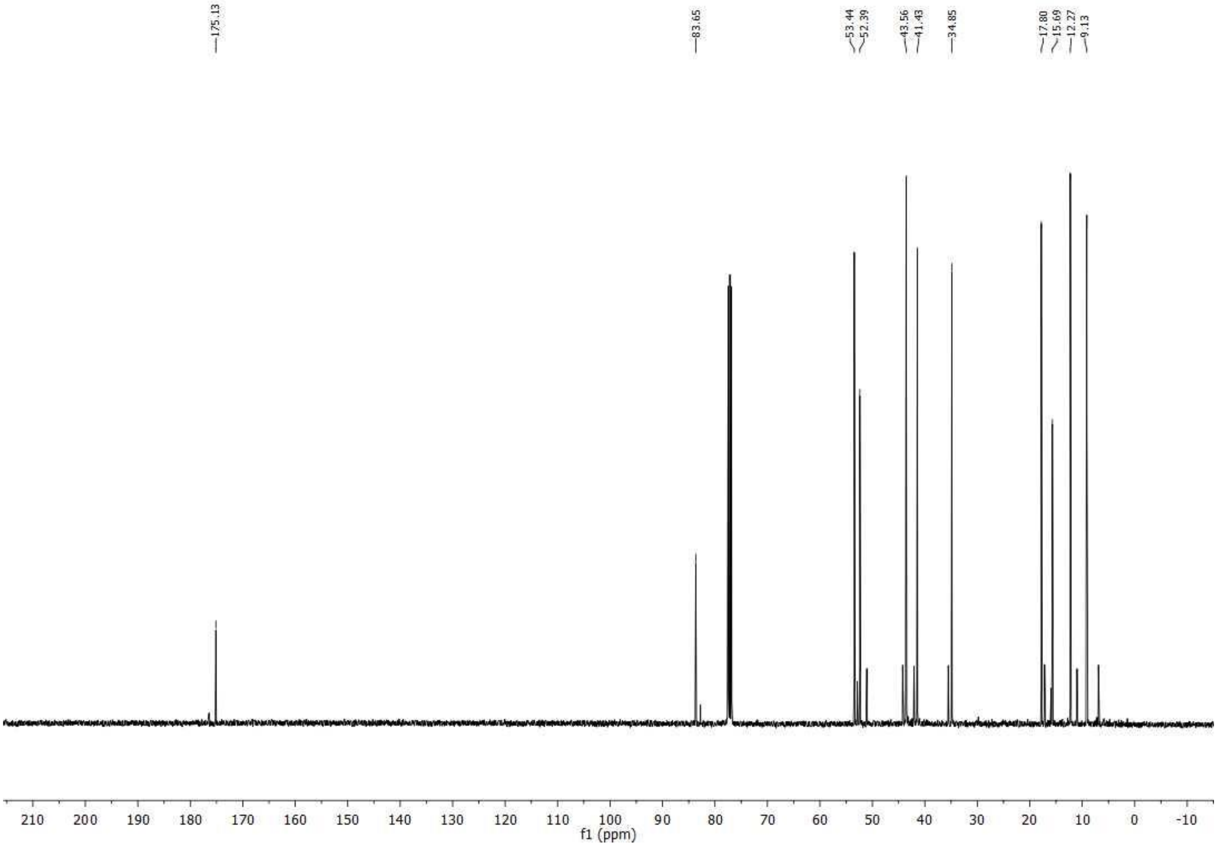

175.13
83.65
53.44
52.39
43.56
41.43
34.85
17.80
15.69
12.27
9.13
210
200
190
180
170
160
150
140
130
120
110
100
90
80
70
60
50
40
30
20
10
0
-10
f1 (ppm)

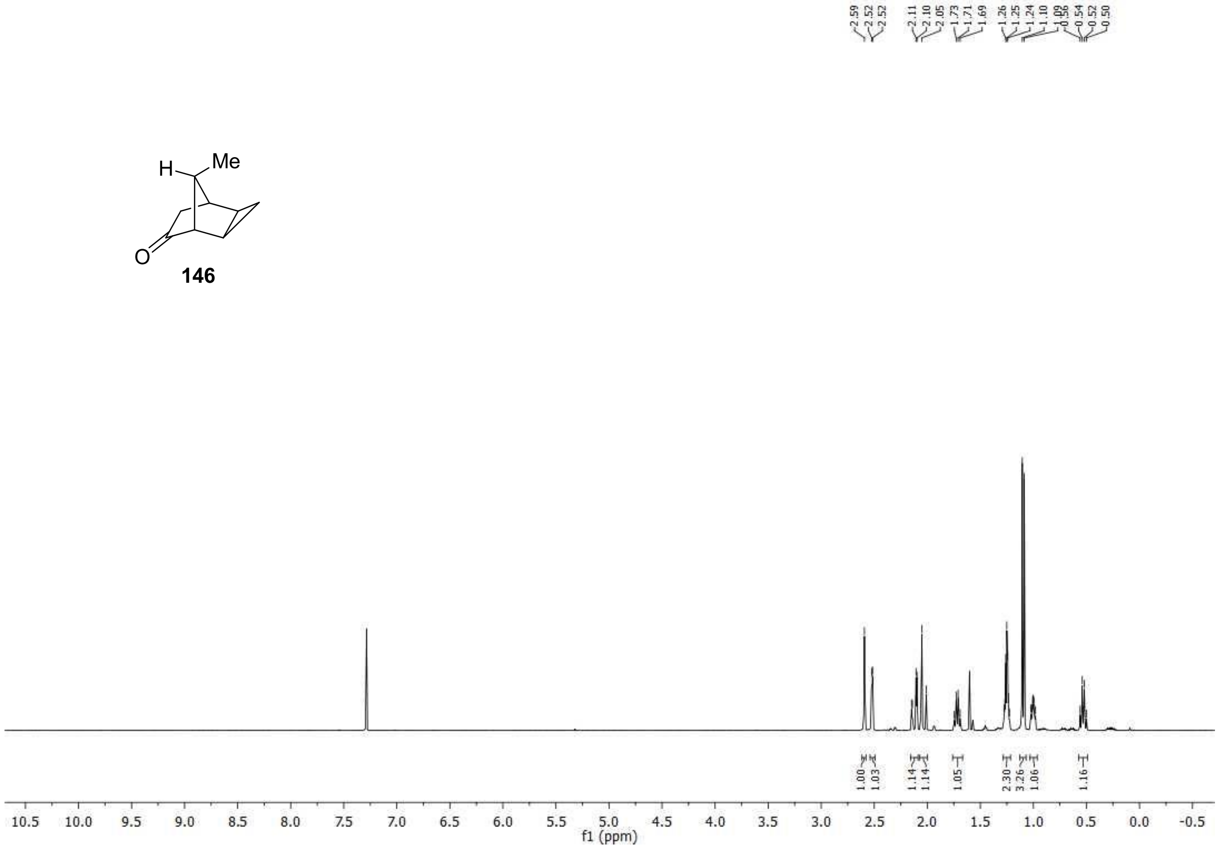
H
Me
O

146

2.59
2.52
2.52
2.11
2.10
2.05
1.73
1.71
1.69
1.26
1.25
1.24
1.10
1.09
0.56
0.54
0.52
0.50
1.00
1.03
1.14
1.14
1.05
2.30
3.26
1.06
1.16
10.5
10.0
9.5
9.0
8.5
8.0
7.5
7.0
6.5
6.0
5.5
5.0
4.5
4.0
3.5
3.0
2.5
2.0
1.5
1.0
0.5
0.0
-0.5
f1 (ppm)

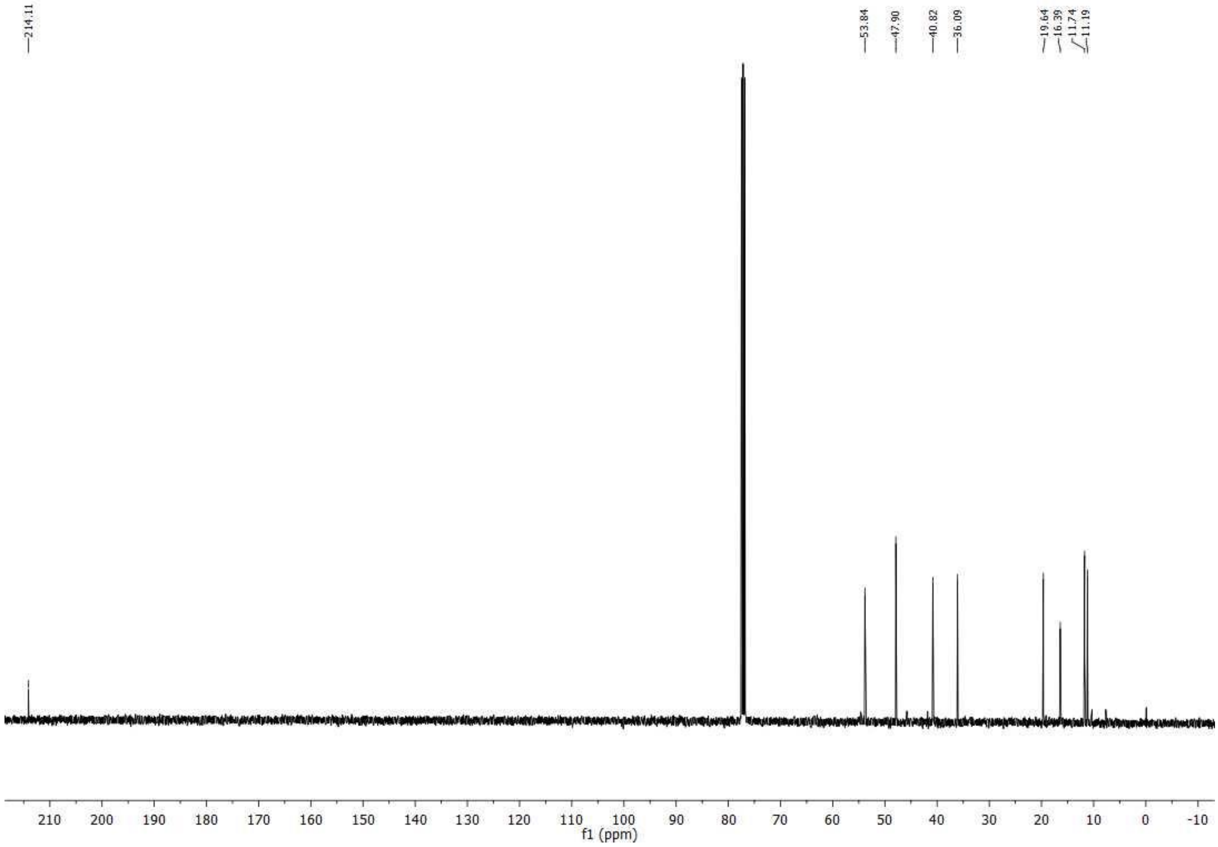
214.11
53.84
47.90
40.82
36.09
19.64
16.39
11.74
11.19
210
200
190
180
170
160
150
140
130
120
110
100
90
80
70
60
50
40
30
20
10
0
-10
f1 (ppm)

O

355

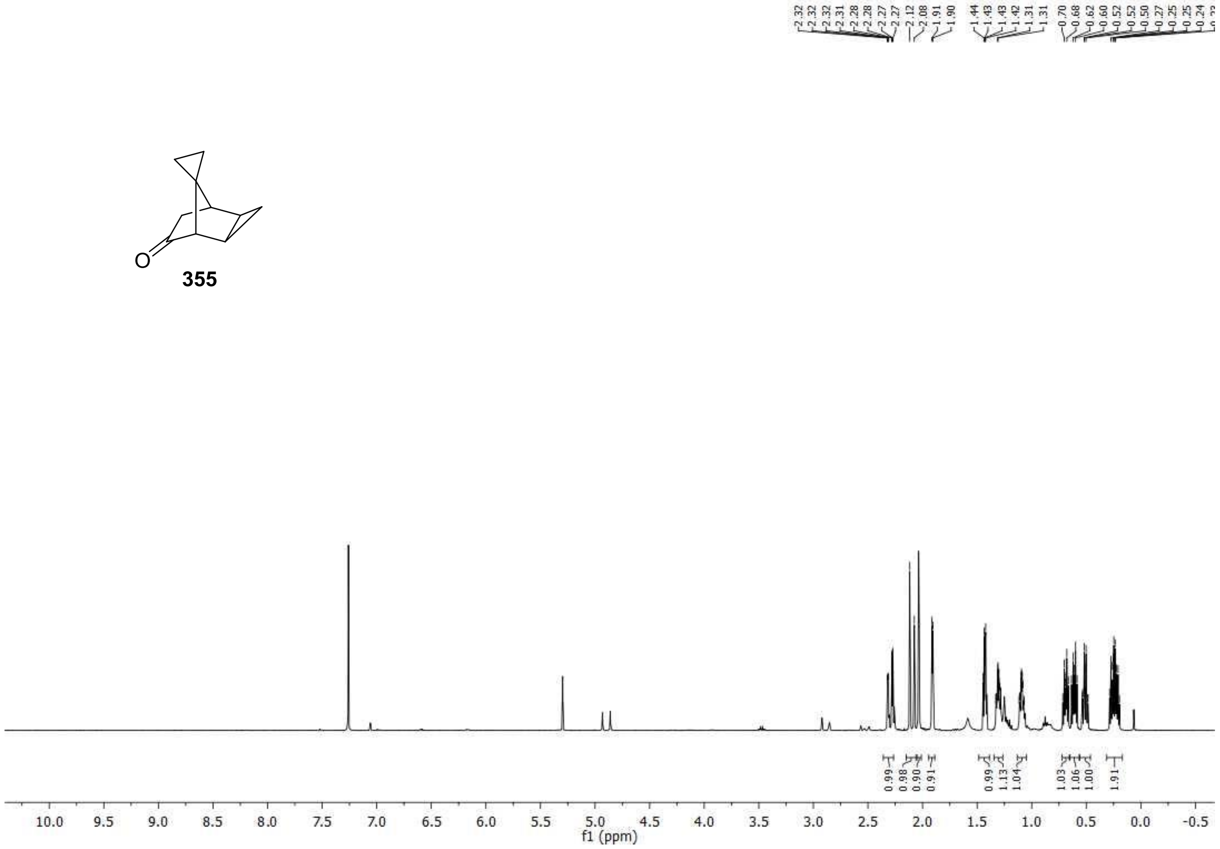
2.32
2.32
2.32
2.31
2.28
2.28
2.27
2.27
2.12
2.08
1.91
1.90
1.44
1.43
1.43
1.42
1.31
1.31
0.70
0.68
0.62
0.60
0.52
0.52
0.50
0.27
0.25
0.25
0.24
0.99
0.98
0.90
0.91
0.99
1.13
1.04
1.03
1.06
1.00
1.91
10.0
9.5
9.0
8.5
8.0
7.5
7.0
6.5
6.0
5.5
5.0
4.5
4.0
3.5
3.0
2.5
2.0
1.5
1.0
0.5
0.0
-0.5
f1 (ppm)

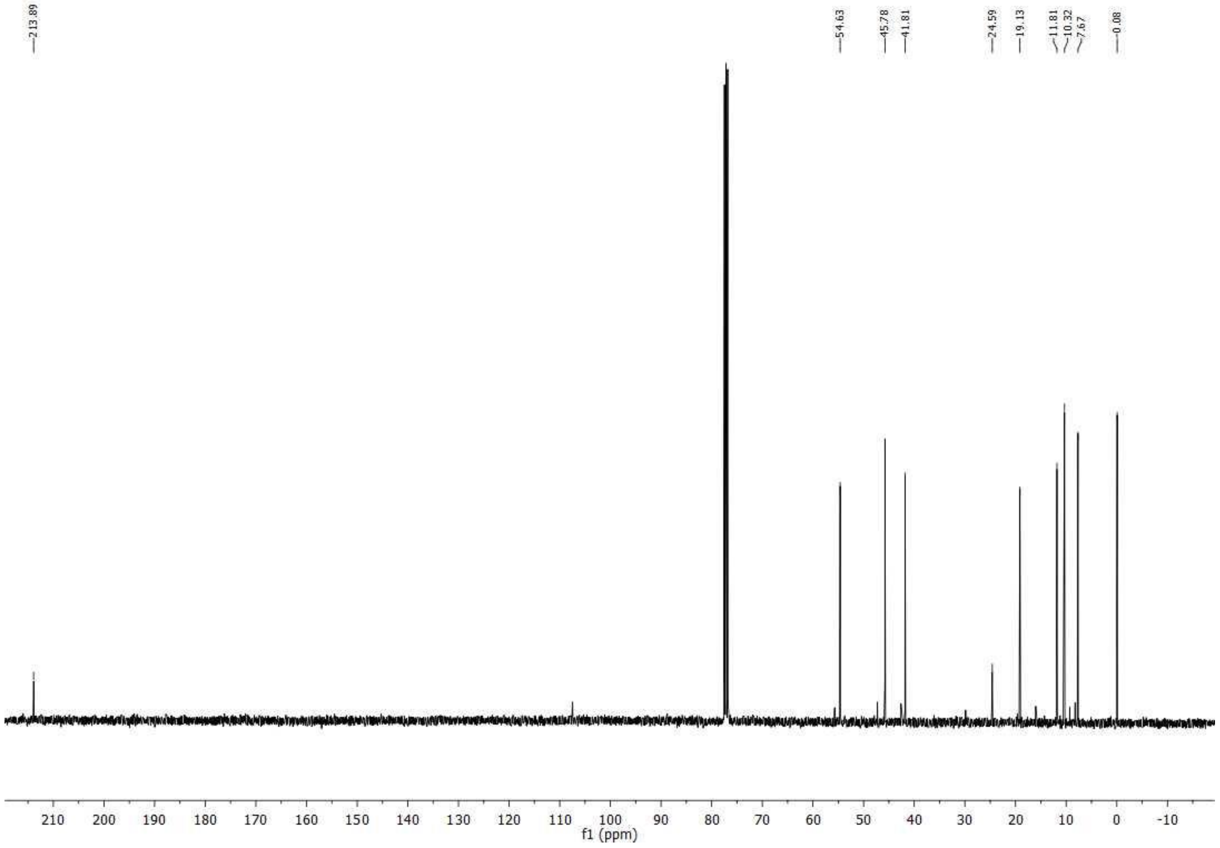
213.89
54.63
45.78
41.81
24.59
19.13
11.81
10.32
7.67
0.08
210
200
190
180
170
160
150
140
130
120
110
100
90
80
70
60
50
40
30
20
10
0
-10
f1 (ppm)

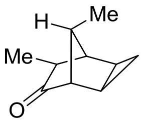
H
Me
Me
O

154

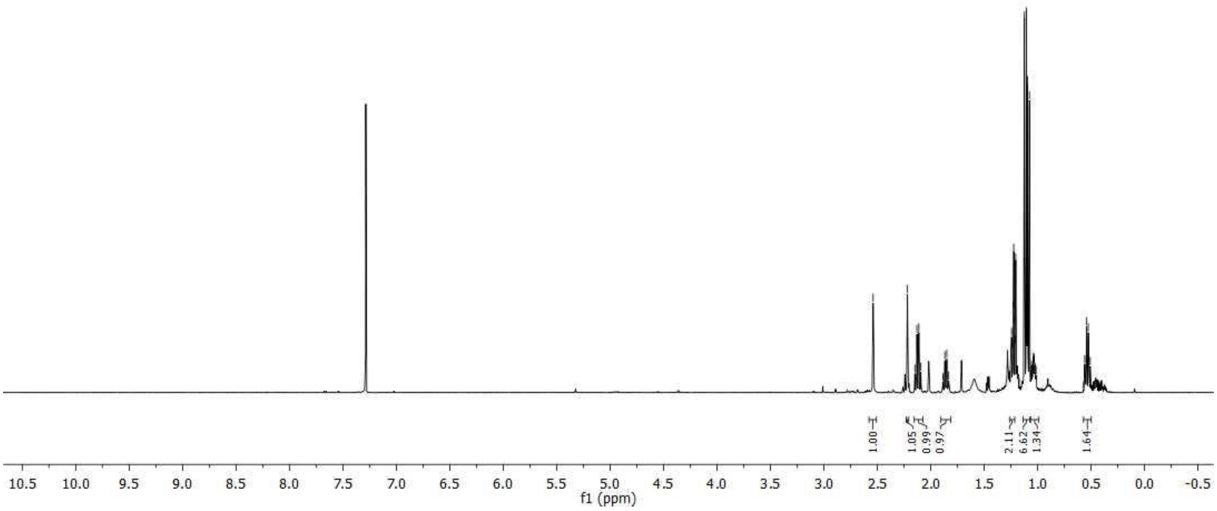
2.54
2.22
2.15
2.13
2.11
2.09
1.87
1.85
1.22
1.12
1.10
1.09
1.08
0.57
0.56
0.54
0.53
0.51
1.00
1.05
0.99
0.97
2.11
6.62
1.34
1.64
10.5
10.0
9.5
9.0
8.5
8.0
7.5
7.0
6.5
6.0
5.5
5.0
4.5
4.0
3.5
3.0
2.5
2.0
1.5
1.0
0.5
0.0
-0.5
f1 (ppm)

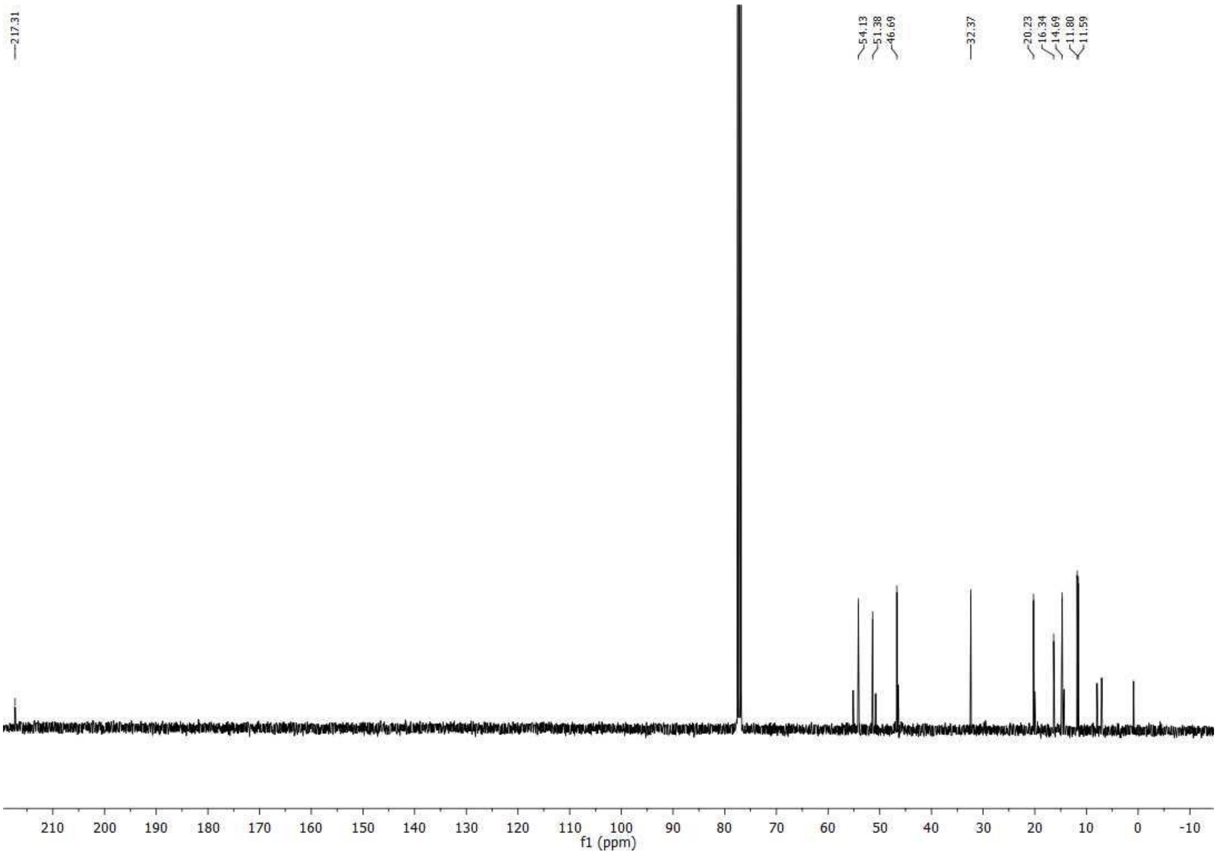
217.31
54.13
51.38
46.69
32.37
20.23
16.34
14.69
11.80
11.59
210
200
190
180
170
160
150
140
130
120
110
100
90
80
70
60
50
40
30
20
10
0
-10
f1 (ppm)

Me
H
Me
O
O
Me

155

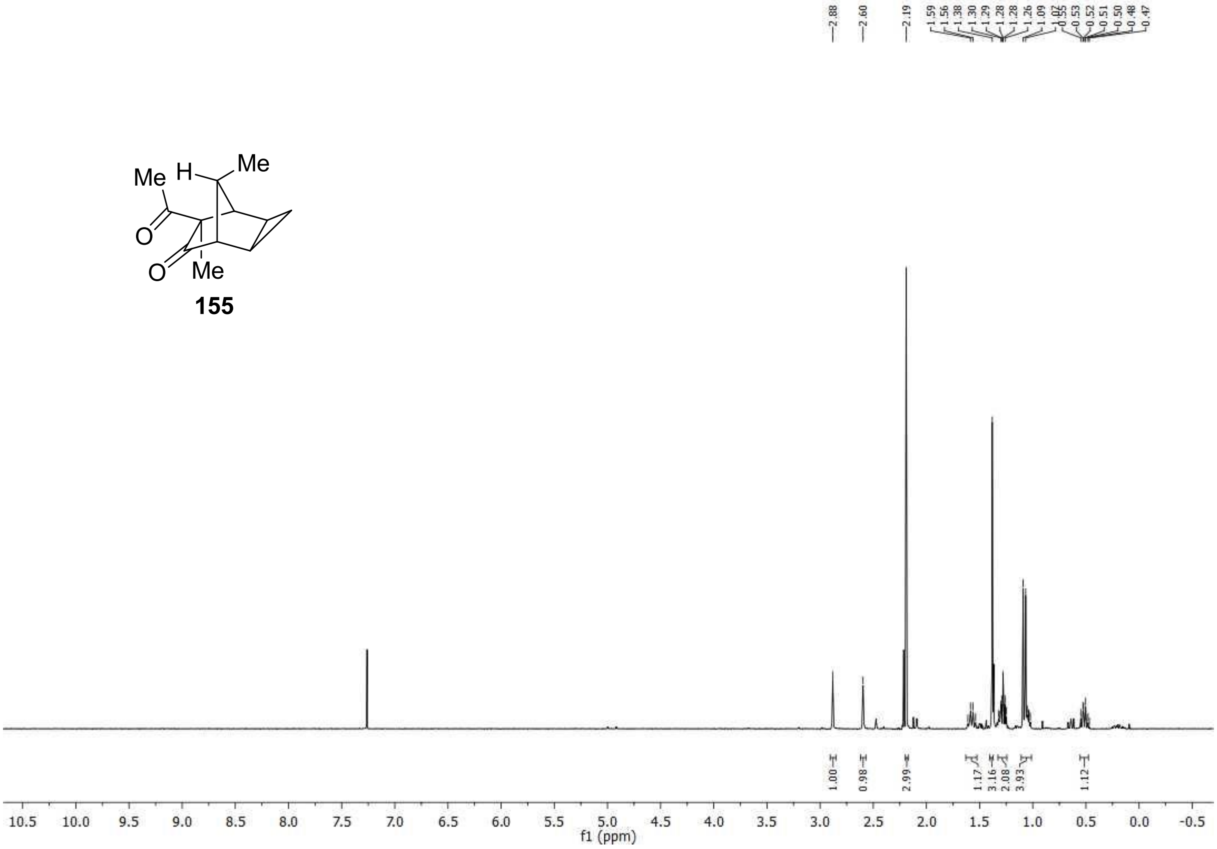
2.88
2.60
2.19
1.59
1.56
1.38
1.30
1.29
1.28
1.28
1.26
1.09
1.07
0.55
0.53
0.52
0.51
0.50
0.48
0.47
1.00
0.98
2.99
1.17
3.16
2.08
3.93
1.12
10.5 10.0 9.5 9.0 8.5 8.0 7.5 7.0 6.5 6.0 5.5 5.0 4.5 4.0 3.5 3.0 2.5 2.0 1.5 1.0 0.5 0.0 -0.5
f1 (ppm)

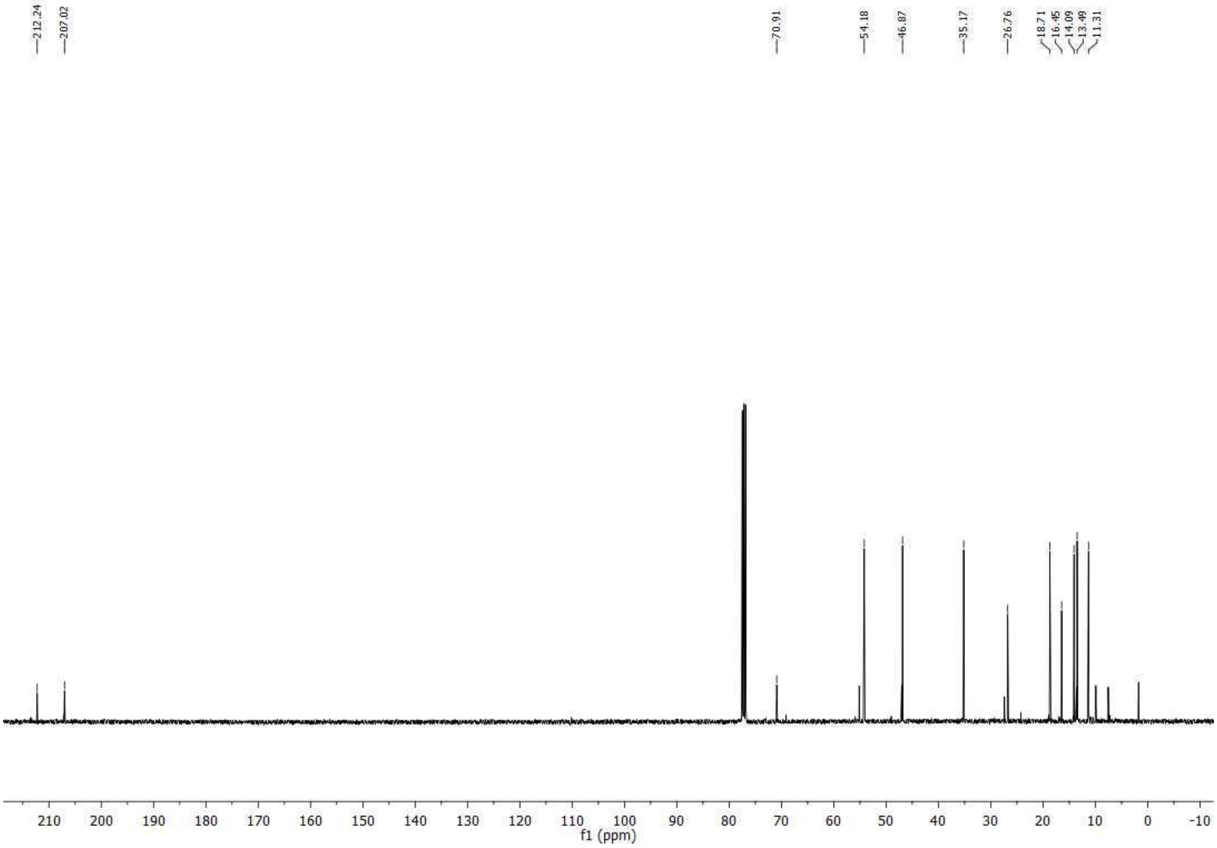
212.24
207.02
70.91
54.18
46.87
35.17
26.76
18.71
16.45
14.09
13.49
11.31
210 200 190 180 170 160 150 140 130 120 110 100 90 80 70 60 50 40 30 20 10 0 -10
f1 (ppm)

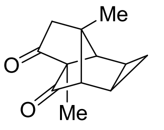
Me
O
O
Me

76

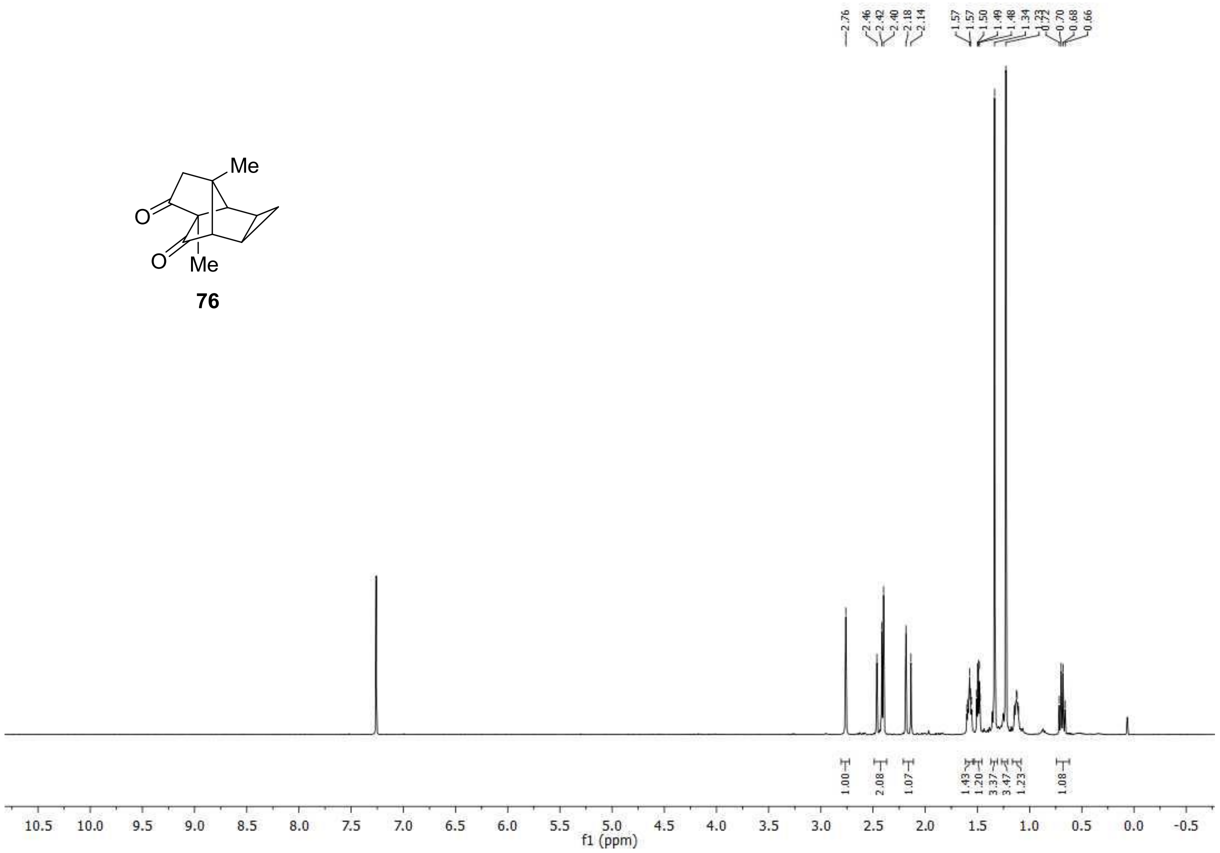
2.76
2.46
2.42
2.40
2.18
2.14
1.57
1.57
1.50
1.49
1.48
1.34
1.23
0.72
0.70
0.68
0.66
1.00
2.08
1.07
1.43
1.20
3.37
3.47
1.23
1.08
10.5
10.0
9.5
9.0
8.5
8.0
7.5
7.0
6.5
6.0
5.5
5.0
4.5
4.0
3.5
3.0
2.5
2.0
1.5
1.0
0.5
0.0
-0.5
f1 (ppm)

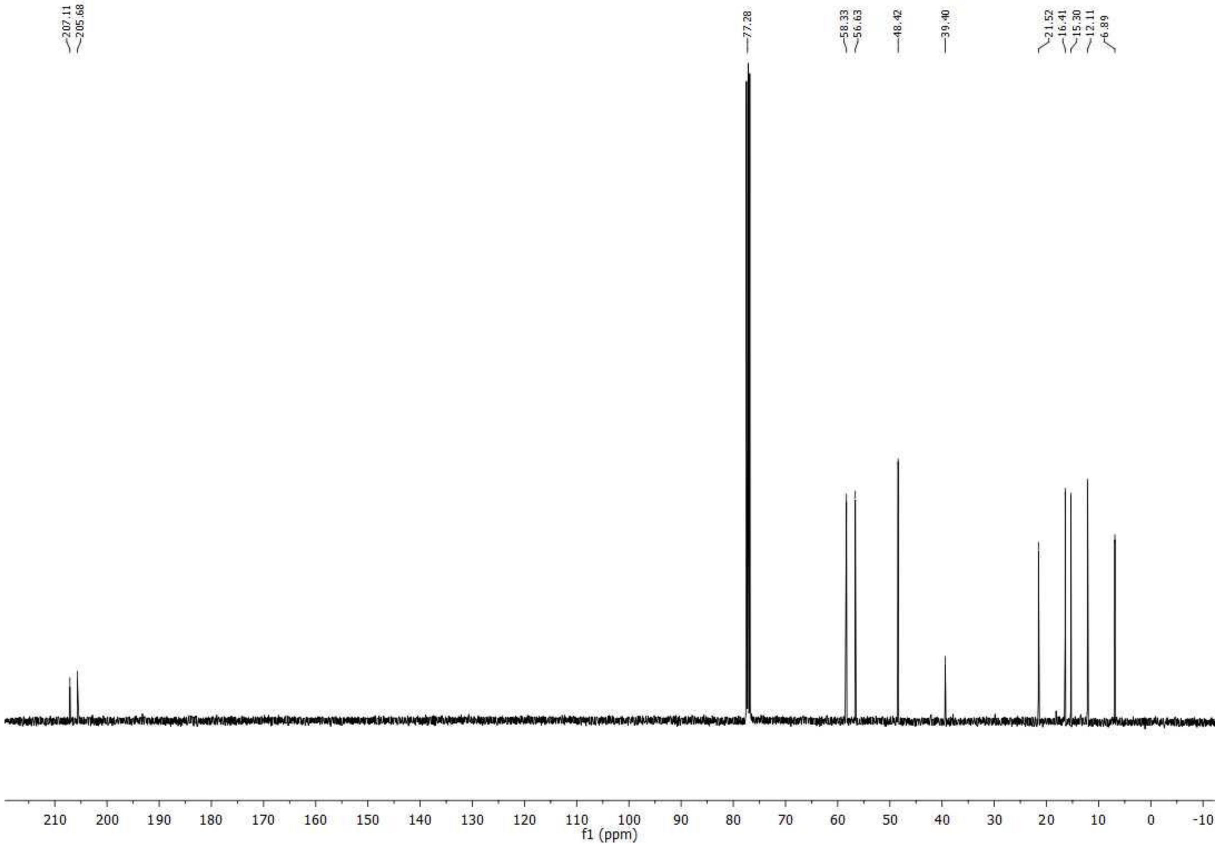
207.11
205.68
77.28
58.33
56.63
48.42
39.40
21.52
16.41
15.30
12.11
6.89
210
200
190
180
170
160
150
140
130
120
110
100
90
80
70
60
50
40
30
20
10
0
-10
f1 (ppm)

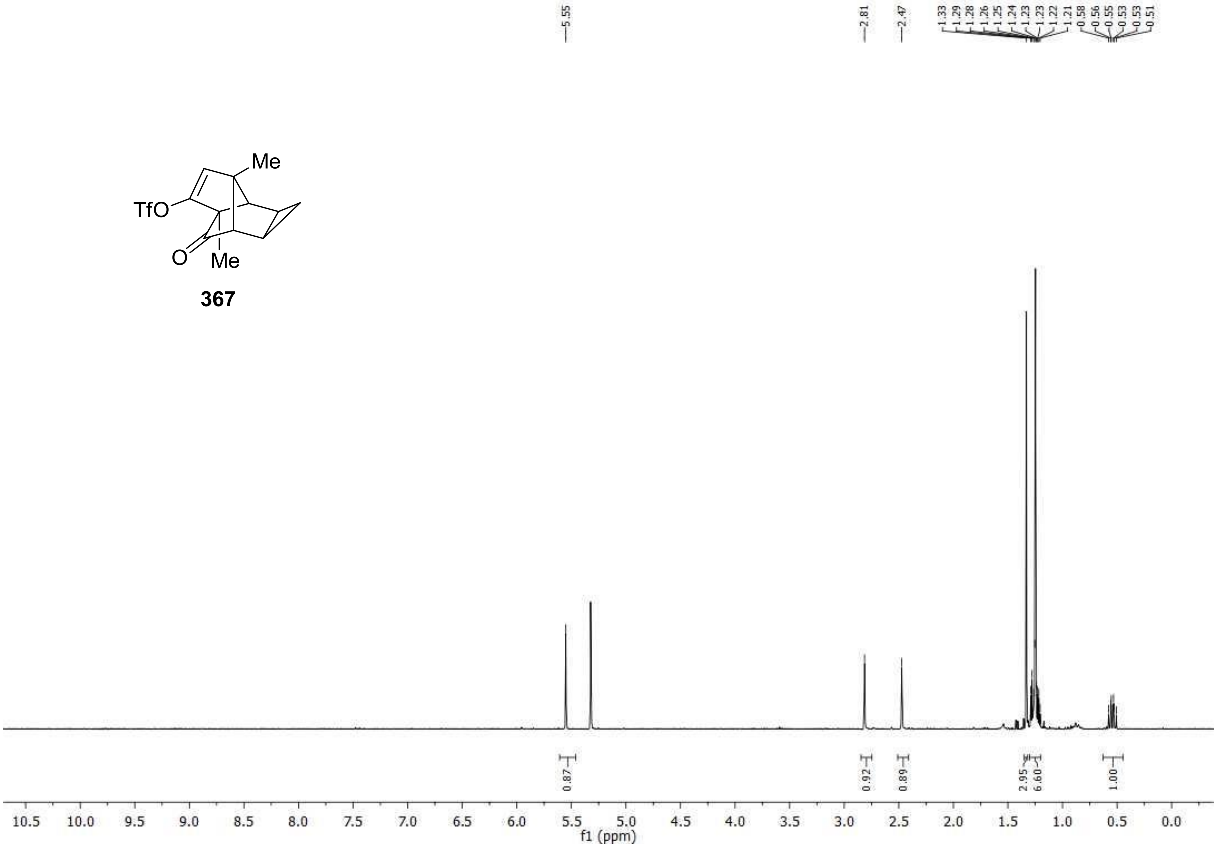
5.55
2.81
2.47
1.33
1.29
1.28
1.26
1.25
1.24
1.23
1.23
1.22
1.21
0.58
0.56
0.55
0.53
0.53
0.51
TfO
Me
O
Me
367
0.87
0.92
0.89
2.95
6.60
1.00
10.5 10.0 9.5 9.0 8.5 8.0 7.5 7.0 6.5 6.0 5.5 5.0 4.5 4.0 3.5 3.0 2.5 2.0 1.5 1.0 0.5 0.0
f1 (ppm)

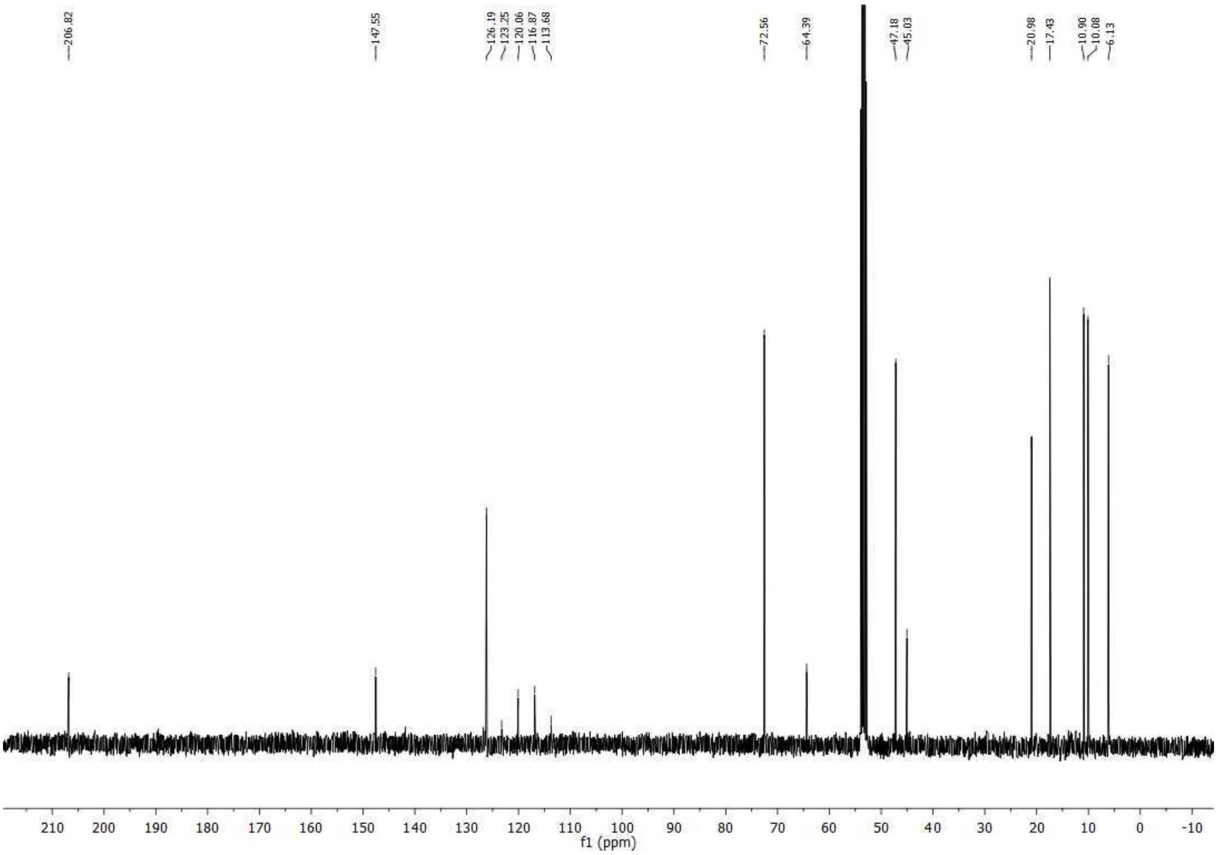
206.82
147.55
126.19
123.25
120.06
116.87
113.68
72.56
64.39
47.18
45.03
20.98
17.43
10.90
10.08
6.13
210 200 190 180 170 160 150 140 130 120 110 100 90 80 70 60 50 40 30 20 10 0 -10
f1 (ppm)

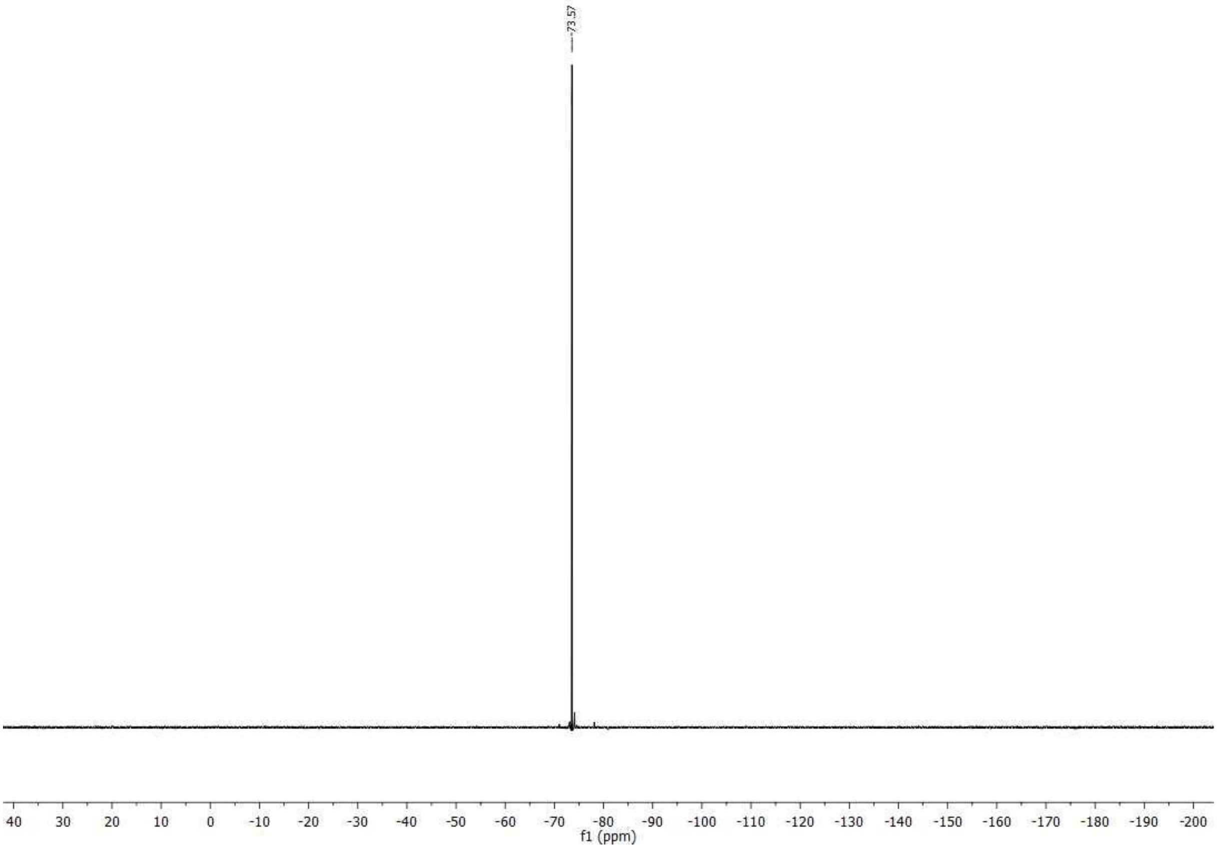
-73.57
40
30
20
10
0
-10
-20
-30
-40
-50
-60
-70
-80
-90
-100
-110
-120
-130
-140
-150
-160
-170
-180
-190
-200
f1 (ppm)

Me
Me
O
Me

172

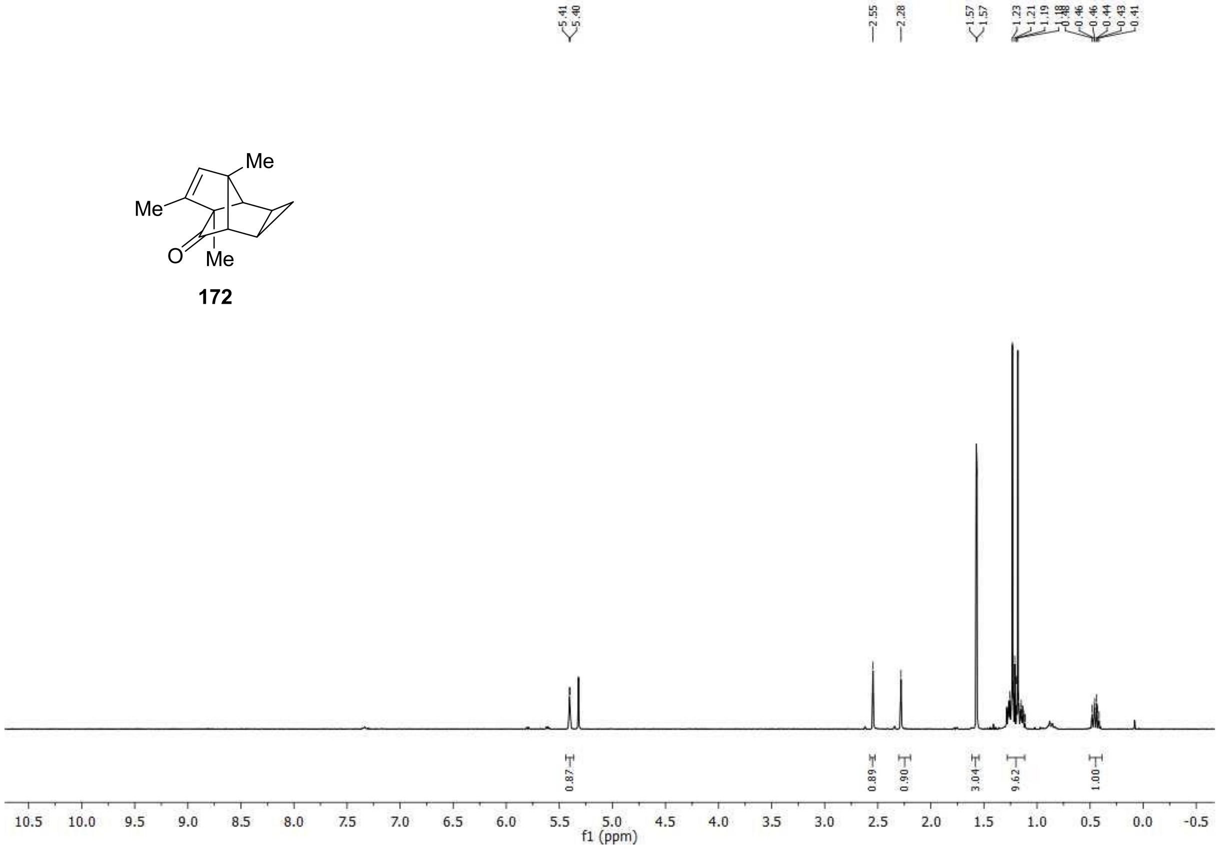
5.41
5.40
2.55
2.28
1.57
1.57
1.23
1.21
1.19
1.18
1.18
0.46
0.46
0.44
0.43
0.41
0.87
0.89
0.90
3.04
9.62
1.00
10.5
10.0
9.5
9.0
8.5
8.0
7.5
7.0
6.5
6.0
5.5
5.0
4.5
4.0
3.5
3.0
2.5
2.0
1.5
1.0
0.5
0.0
-0.5
f1 (ppm)

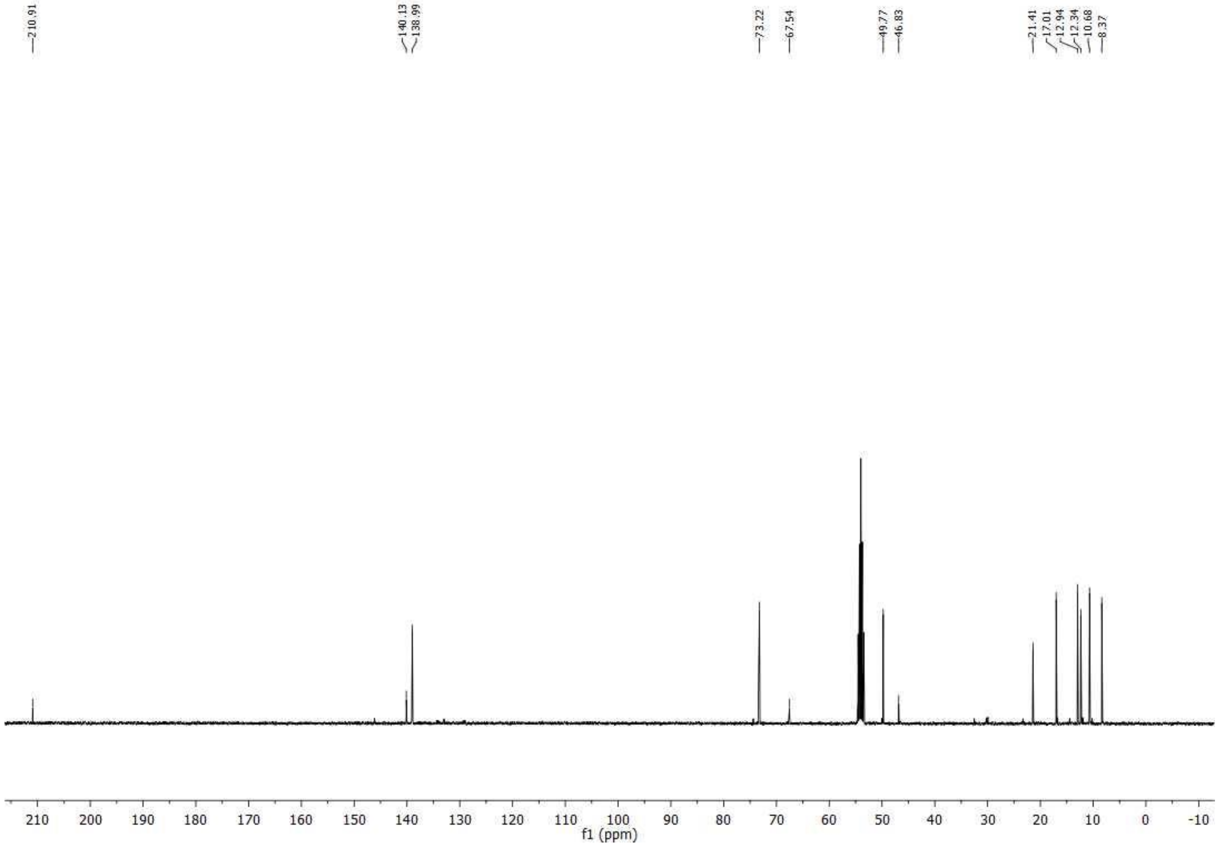
210.91
140.13
138.99
73.22
67.54
49.77
46.83
21.41
17.01
12.94
12.34
10.68
8.37
210
200
190
180
170
160
150
140
130
120
110
100
90
80
70
60
50
40
30
20
10
0
-10
f1 (ppm)

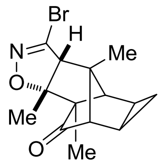
Br
H
N
O
Me
Me
O
Me

177

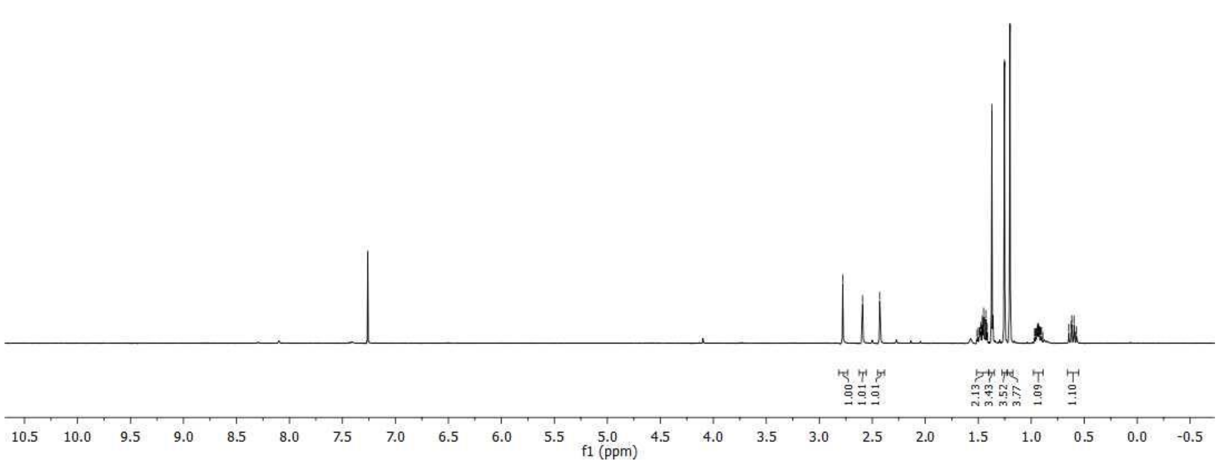
2.78
2.59
2.43
1.49
1.48
1.46
1.45
1.44
1.43
1.42
1.37
1.25
1.20
0.94
0.94
0.93
0.93
0.92
0.92
0.92
0.90
0.64
0.62
0.62
0.60
1.00
1.01
1.01
2.13
3.43
3.52
3.77
1.09
1.10
10.5
10.0
9.5
9.0
8.5
8.0
7.5
7.0
6.5
6.0
5.5
5.0
4.5
4.0
3.5
3.0
2.5
2.0
1.5
1.0
0.5
0.0
-0.5
f1 (ppm)

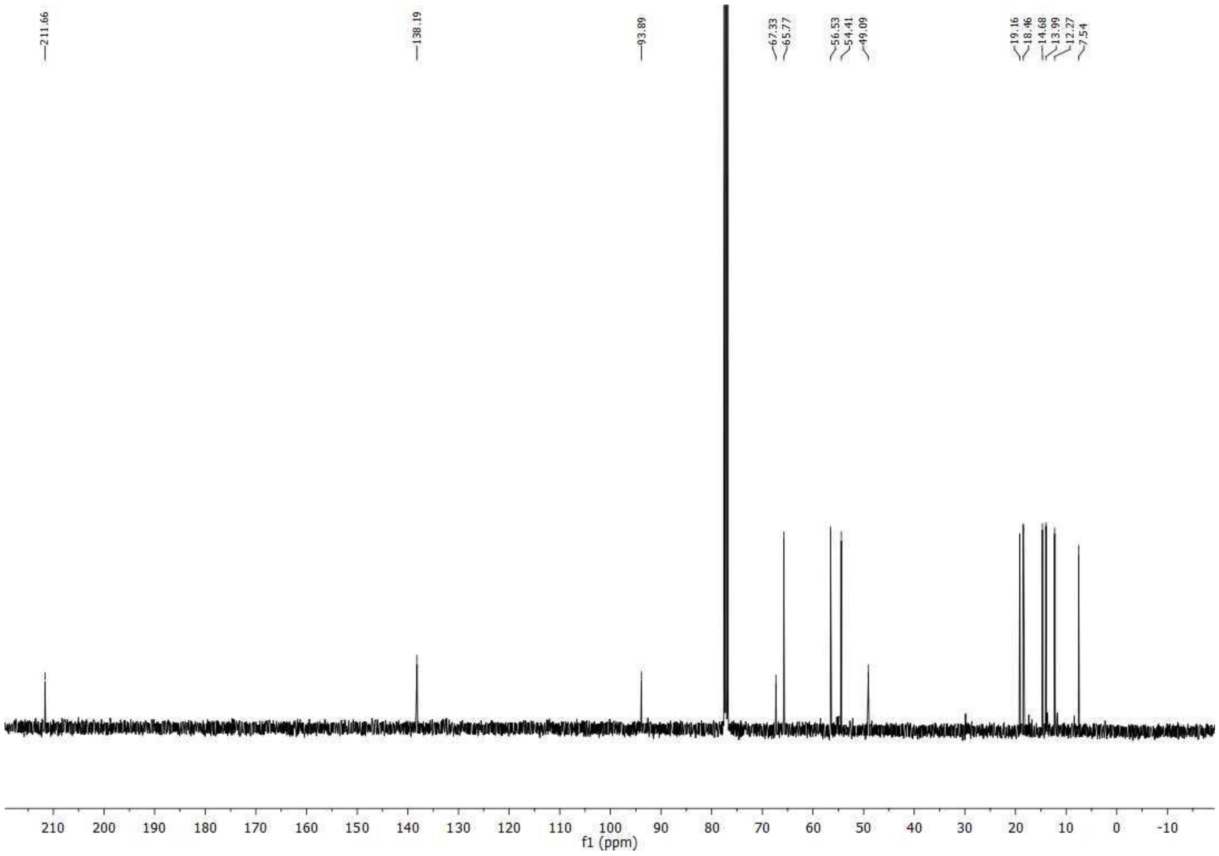
211.66
138.19
93.89
67.33
65.77
56.53
54.41
49.09
19.16
18.46
14.68
13.99
12.27
7.54
210
200
190
180
170
160
150
140
130
120
110
100
90
80
70
60
50
40
30
20
10
0
-10
f1 (ppm)

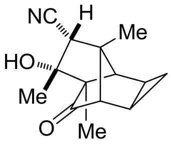
NC
H
Me
HO
Me
O
Me

186

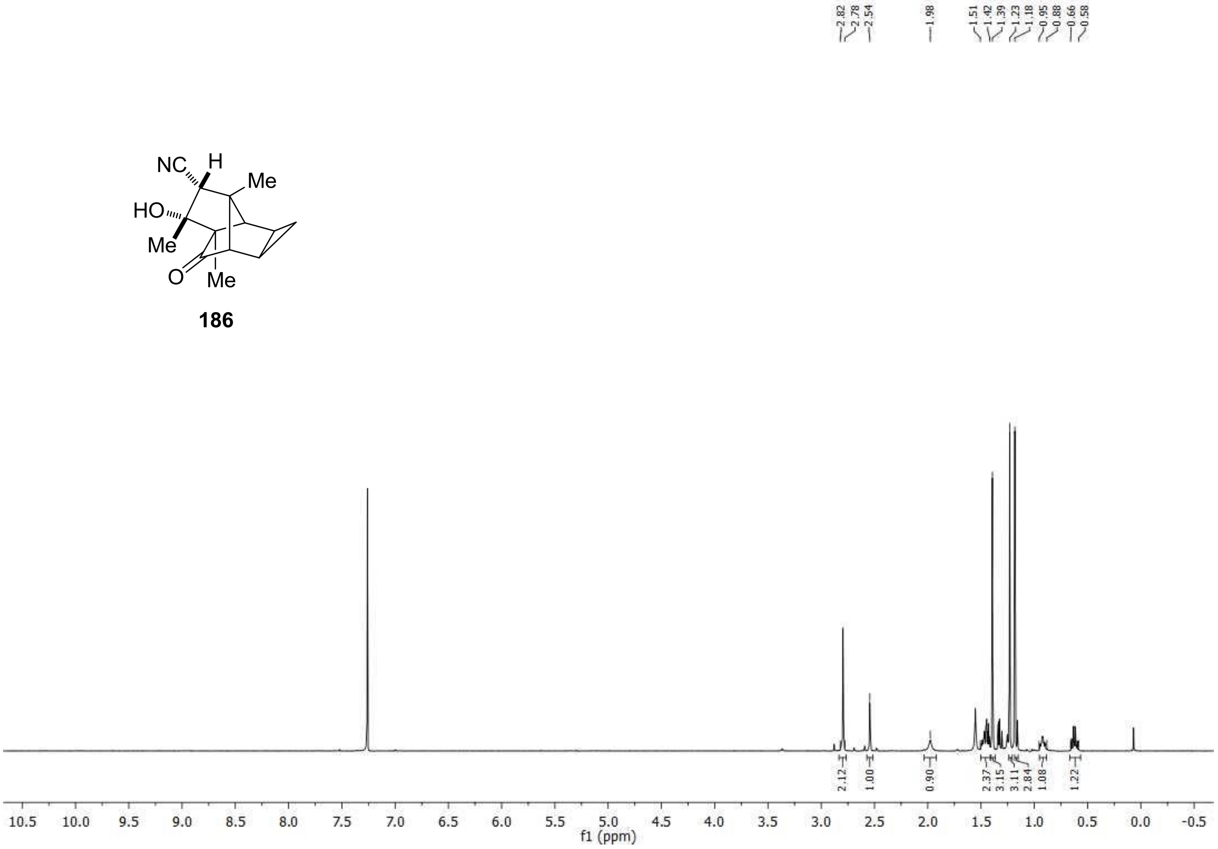
2.82
2.78
2.54
1.98
1.51
1.42
1.39
1.23
1.18
0.95
0.88
0.66
0.58
2.12
1.00
0.90
2.37
3.15
3.11
2.84
1.08
1.22
10.5
10.0
9.5
9.0
8.5
8.0
7.5
7.0
6.5
6.0
5.5
5.0
4.5
4.0
3.5
3.0
2.5
2.0
1.5
1.0
0.5
0.0
-0.5
f1 (ppm)

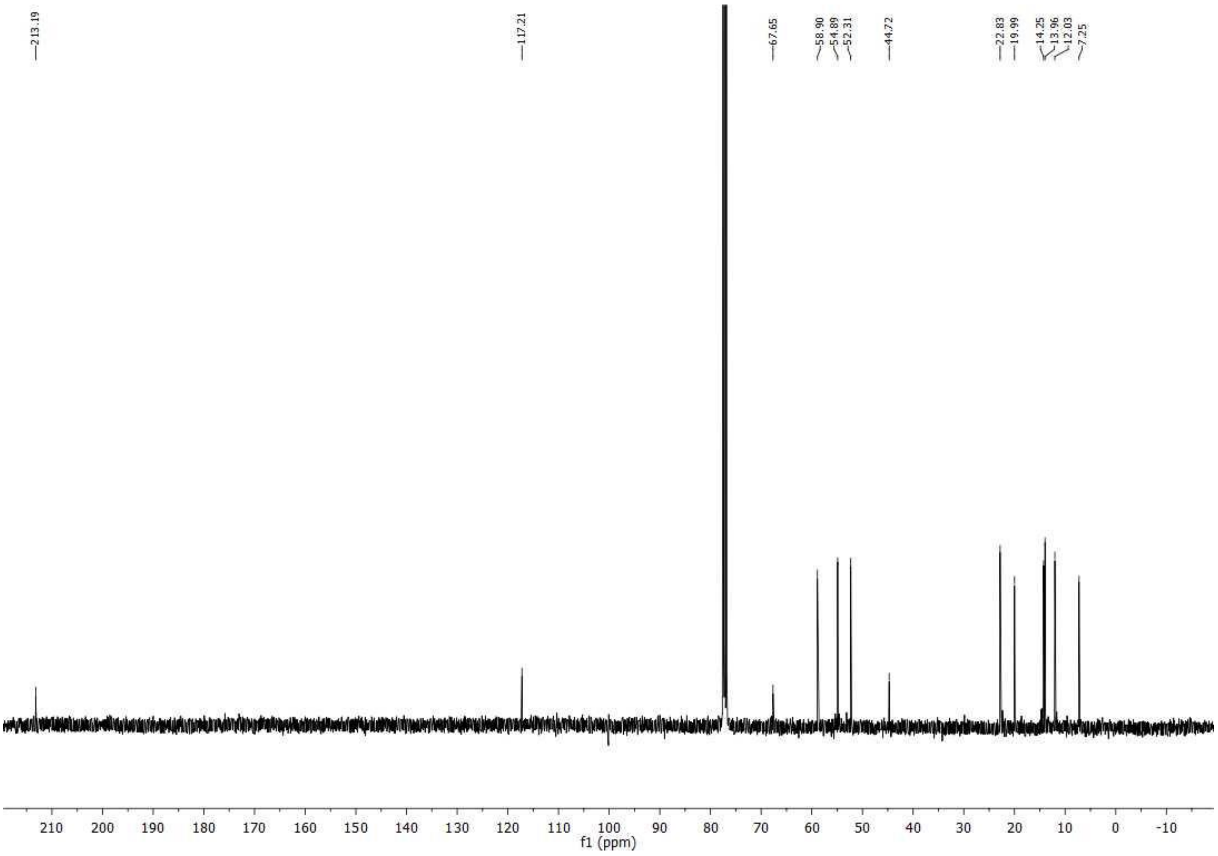
213.19
117.21
67.65
58.90
54.89
52.31
44.72
22.83
19.99
14.25
13.96
12.03
7.25
210
200
190
180
170
160
150
140
130
120
110
100
90
80
70
60
50
40
30
20
10
0
-10
f1 (ppm)

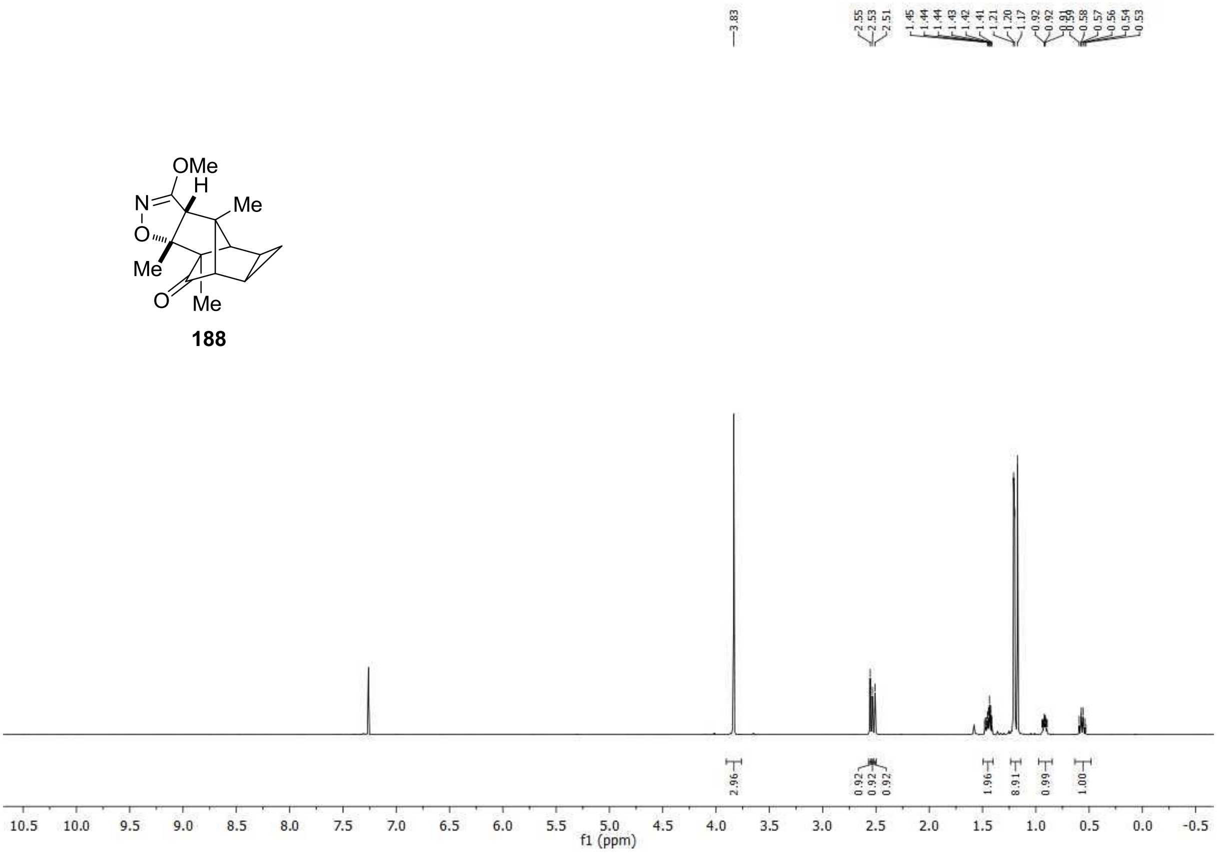
3.83
2.55
2.53
2.51
1.45
1.44
1.44
1.43
1.42
1.41
1.21
1.20
1.17
0.92
0.92
0.91
0.59
0.58
0.57
0.56
0.54
0.53
OMe
H
N
O
Me
Me
O
Me
188
2.96
0.92
0.92
0.92
1.96
8.91
0.99
1.00
10.5
10.0
9.5
9.0
8.5
8.0
7.5
7.0
6.5
6.0
5.5
5.0
4.5
4.0
3.5
3.0
2.5
2.0
1.5
1.0
0.5
0.0
-0.5
f1 (ppm)

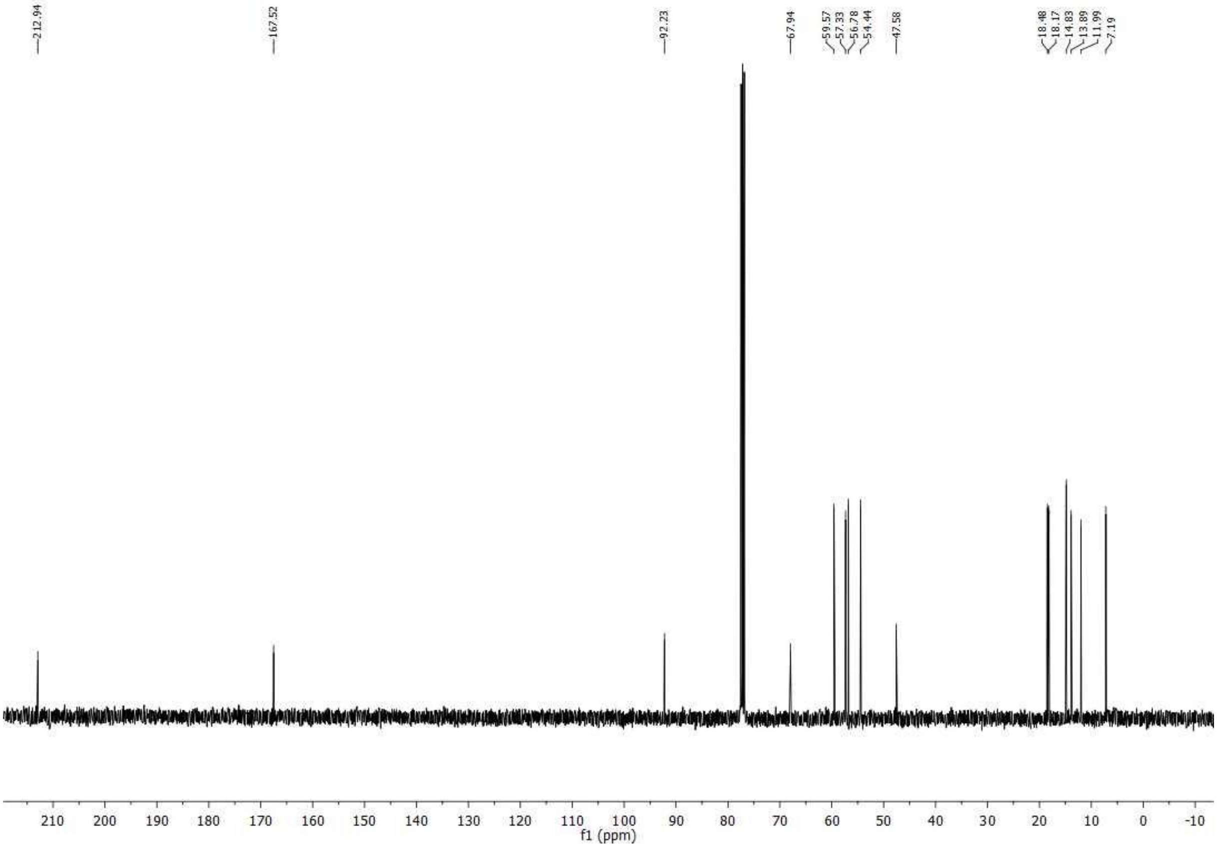
212.94
167.52
92.23
67.94
59.57
57.33
56.78
54.44
47.58
18.48
18.17
14.83
13.89
11.99
7.19
210
200
190
180
170
160
150
140
130
120
110
100
90
80
70
60
50
40
30
20
10
0
-10
f1 (ppm)

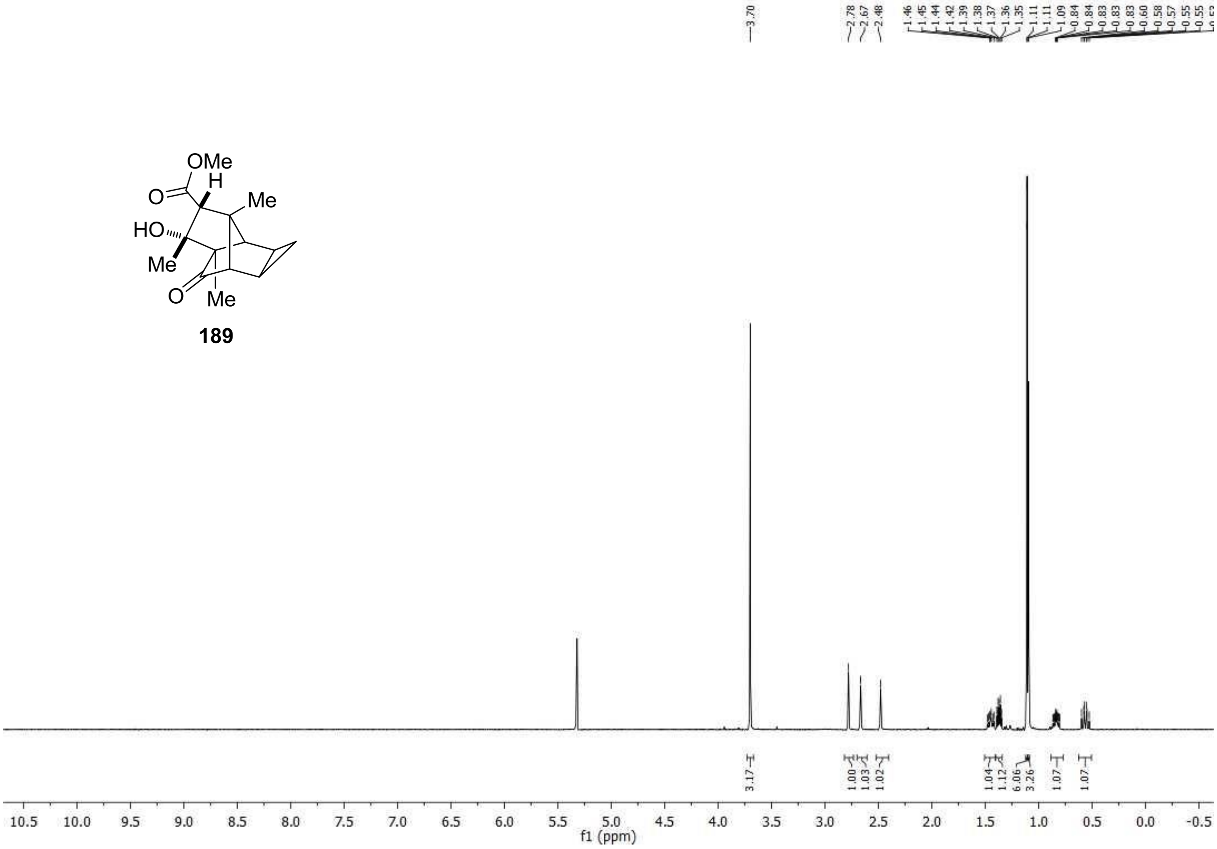
OMe
H
O
Me
HO
Me
O
Me

189

3.70
2.78
2.67
2.48
1.46
1.45
1.44
1.42
1.39
1.38
1.37
1.36
1.35
1.11
1.11
1.09
0.84
0.84
0.83
0.83
0.83
0.60
0.58
0.57
0.55
0.55
3.17
1.00
1.03
1.02
1.04
1.12
6.06
3.26
1.07
1.07
10.5
10.0
9.5
9.0
8.5
8.0
7.5
7.0
6.5
6.0
5.5
5.0
4.5
4.0
3.5
3.0
2.5
2.0
1.5
1.0
0.5
0.0
-0.5
f1 (ppm)

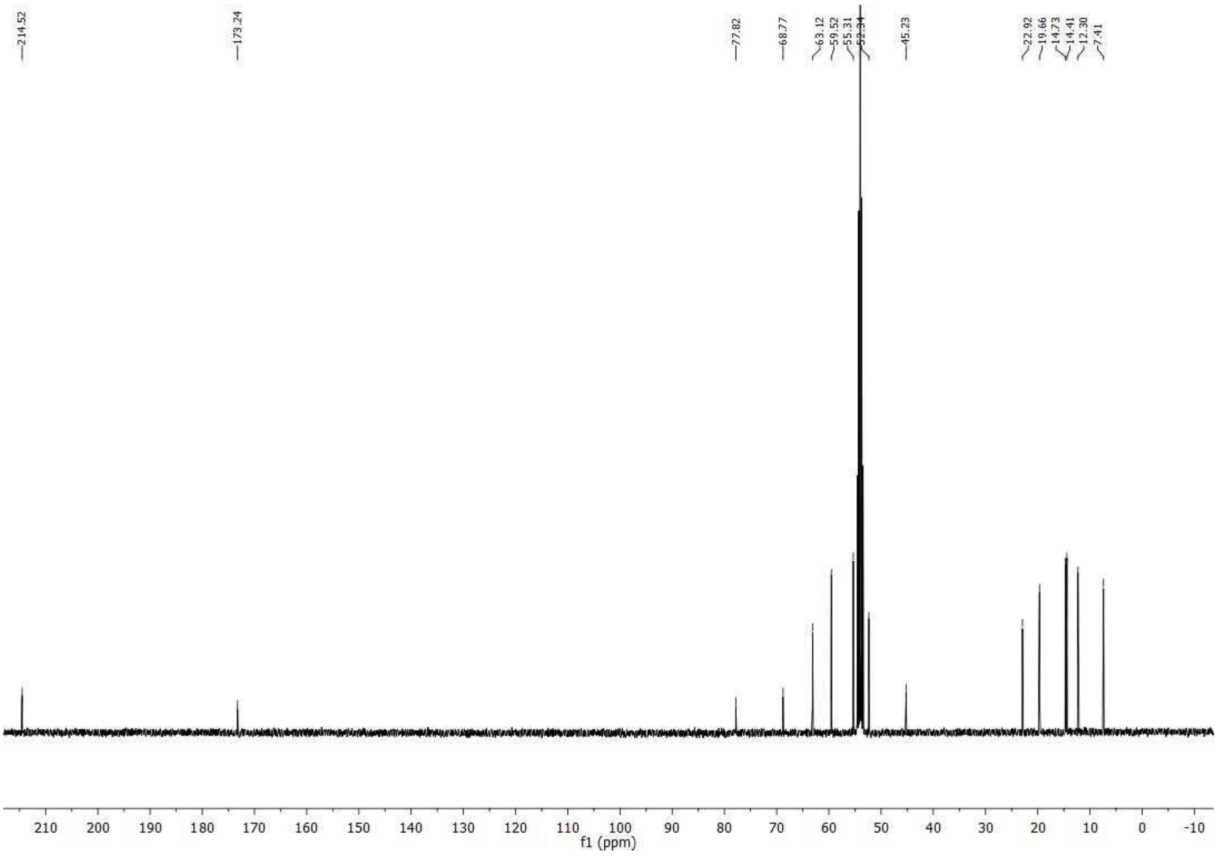
214.52
173.24
77.82
68.77
63.12
59.52
55.31
52.34
45.23
22.92
19.66
14.73
14.41
12.30
7.41
210
200
190
180
170
160
150
140
130
120
110
100
90
80
70
60
50
40
30
20
10
0
-10
f1 (ppm)

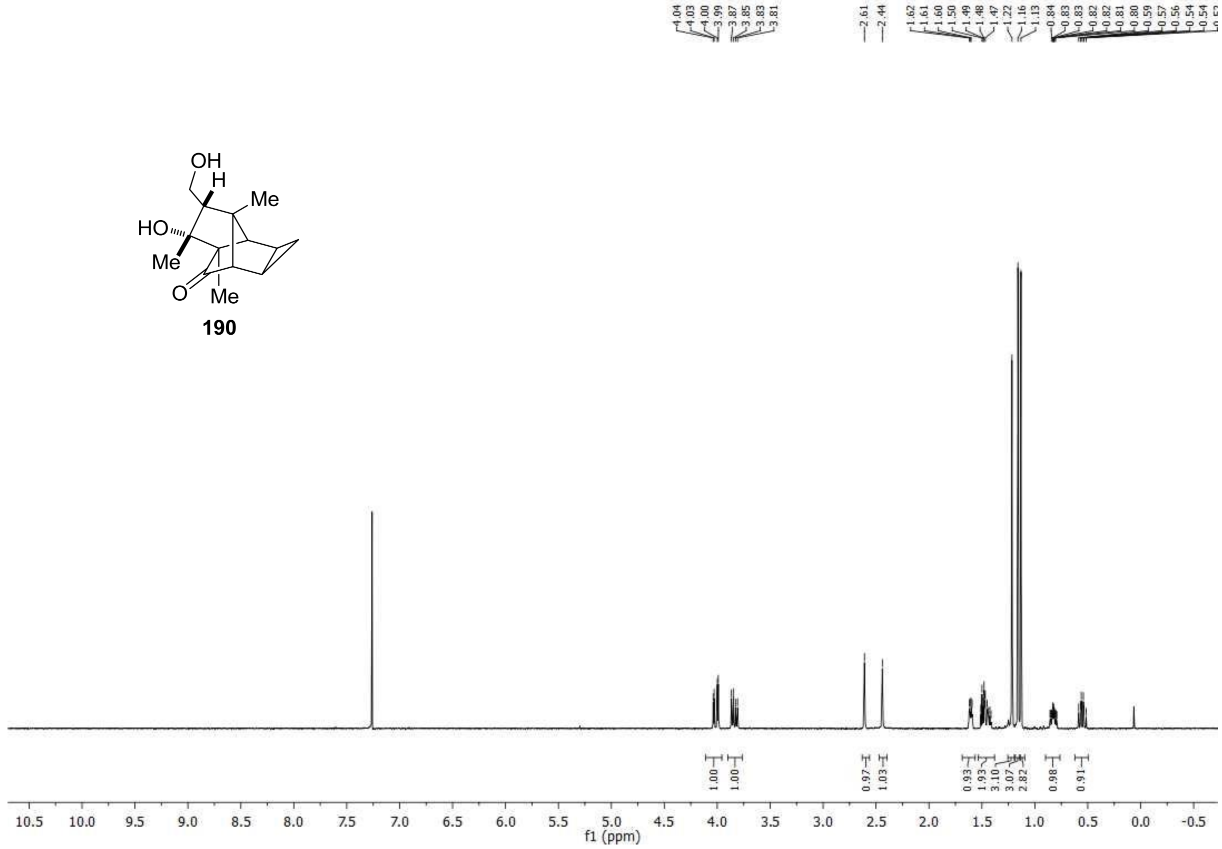

190

4.04
4.03
4.00
3.99
3.87
3.85
3.83
3.81
2.61
2.44
1.62
1.61
1.60
1.50
1.49
1.48
1.47
1.22
1.16
1.13
0.84
0.83
0.83
0.82
0.82
0.81
0.80
0.59
0.57
0.56
0.54
0.54
OH
H
Me
HO
Me
O
Me
1.00
1.00
0.97
1.03
0.93
1.93
3.10
3.07
2.82
0.98
0.91
10.5 10.0 9.5 9.0 8.5 8.0 7.5 7.0 6.5 6.0 5.5 5.0 4.5 4.0 3.5 3.0 2.5 2.0 1.5 1.0 0.5 0.0 -0.5
f1 (ppm)

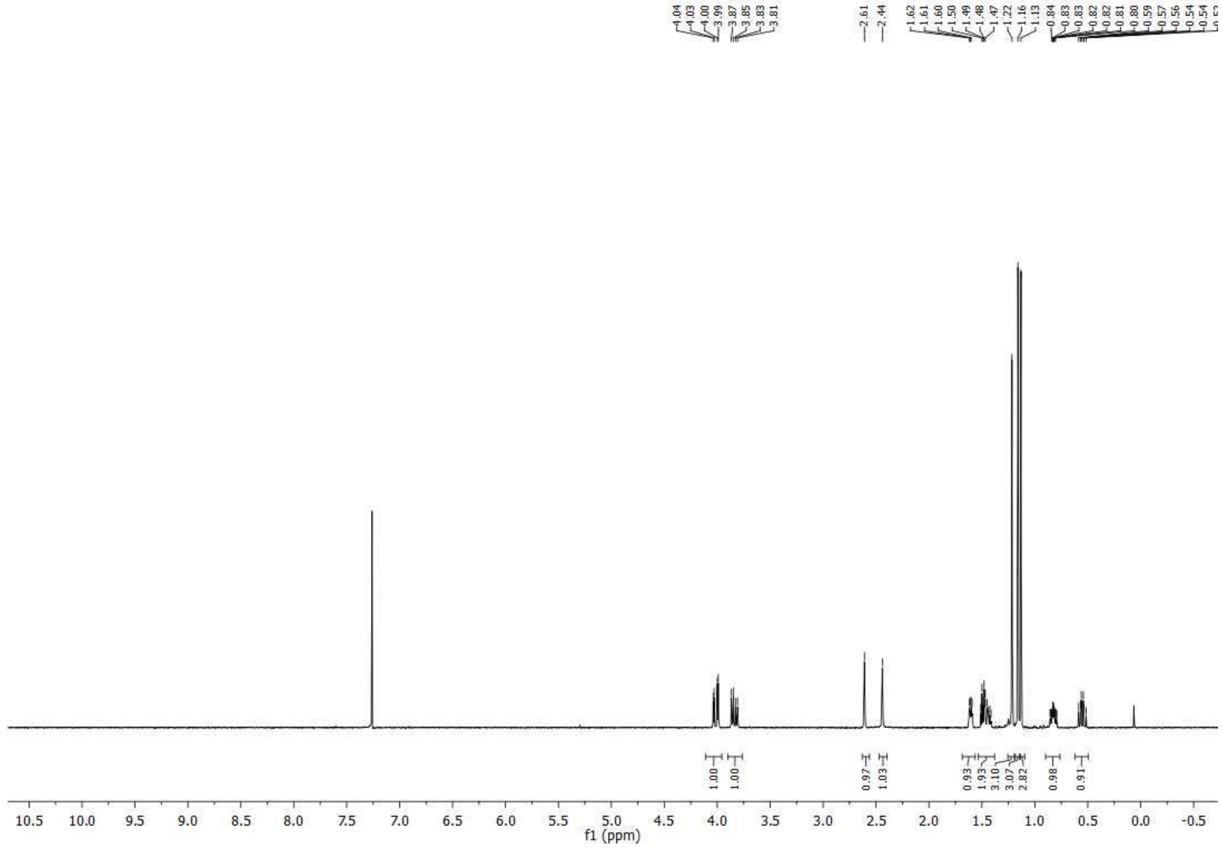

4.04
4.03
4.00
3.99
3.87
3.85
3.83
3.81
2.61
2.44
1.62
1.61
1.60
1.50
1.49
1.48
1.47
1.22
1.16
1.13
0.84
0.83
0.83
0.82
0.82
0.81
0.80
0.59
0.57
0.56
0.54
0.54
1.00
1.00
0.97
1.03
0.93
1.93
3.10
3.07
2.82
0.98
0.91
10.5 10.0 9.5 9.0 8.5 8.0 7.5 7.0 6.5 6.0 5.5 5.0 4.5 4.0 3.5 3.0 2.5 2.0 1.5 1.0 0.5 0.0 -0.5
f1 (ppm)

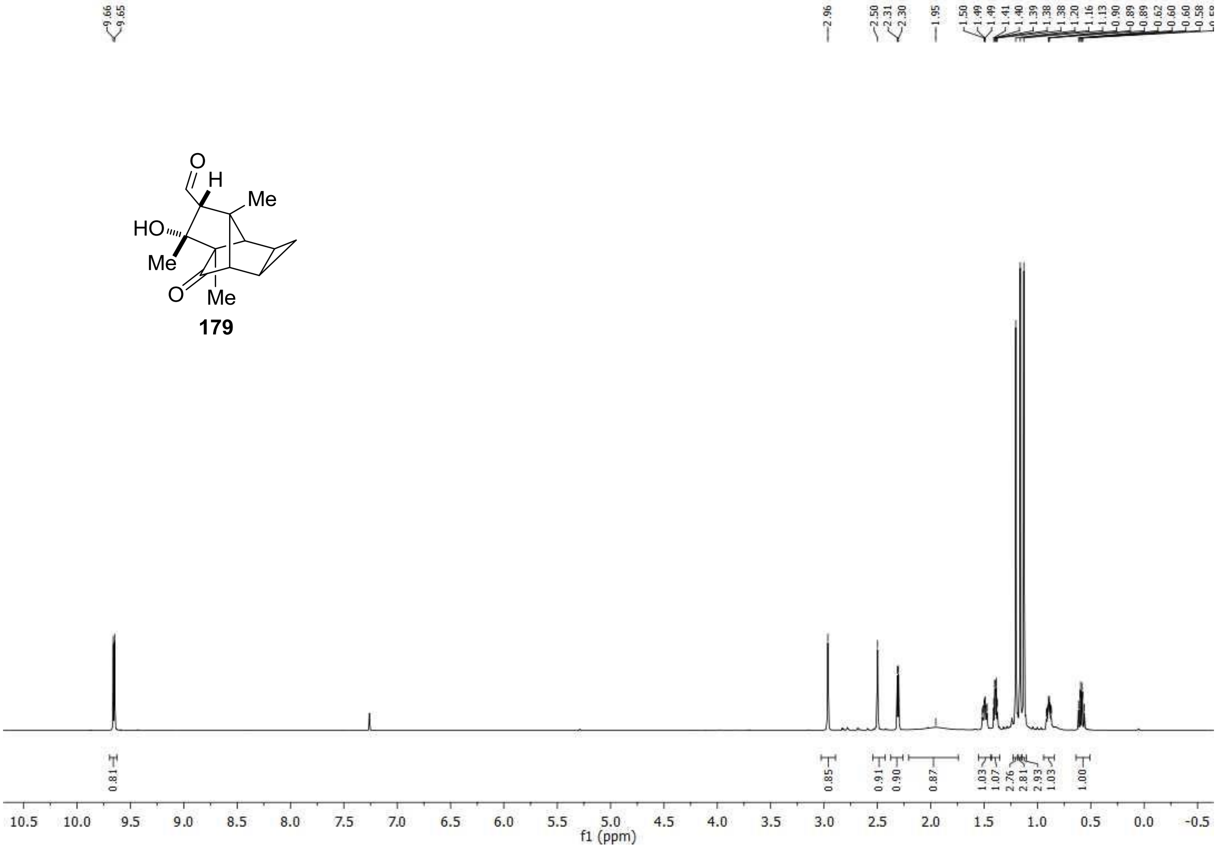
9.66
9.65
2.96
2.50
2.31
2.30
1.95
1.50
1.49
1.49
1.41
1.40
1.39
1.38
1.38
1.20
1.16
1.13
0.90
0.89
0.89
0.62
0.60
0.60
0.58
O
H
Me
HO
Me
O
Me
179
0.81
0.85
0.91
0.90
0.87
1.03
1.07
2.76
2.81
2.93
1.03
1.00
10.5
10.0
9.5
9.0
8.5
8.0
7.5
7.0
6.5
6.0
5.5
5.0
4.5
4.0
3.5
3.0
2.5
2.0
1.5
1.0
0.5
0.0
-0.5
f1 (ppm)

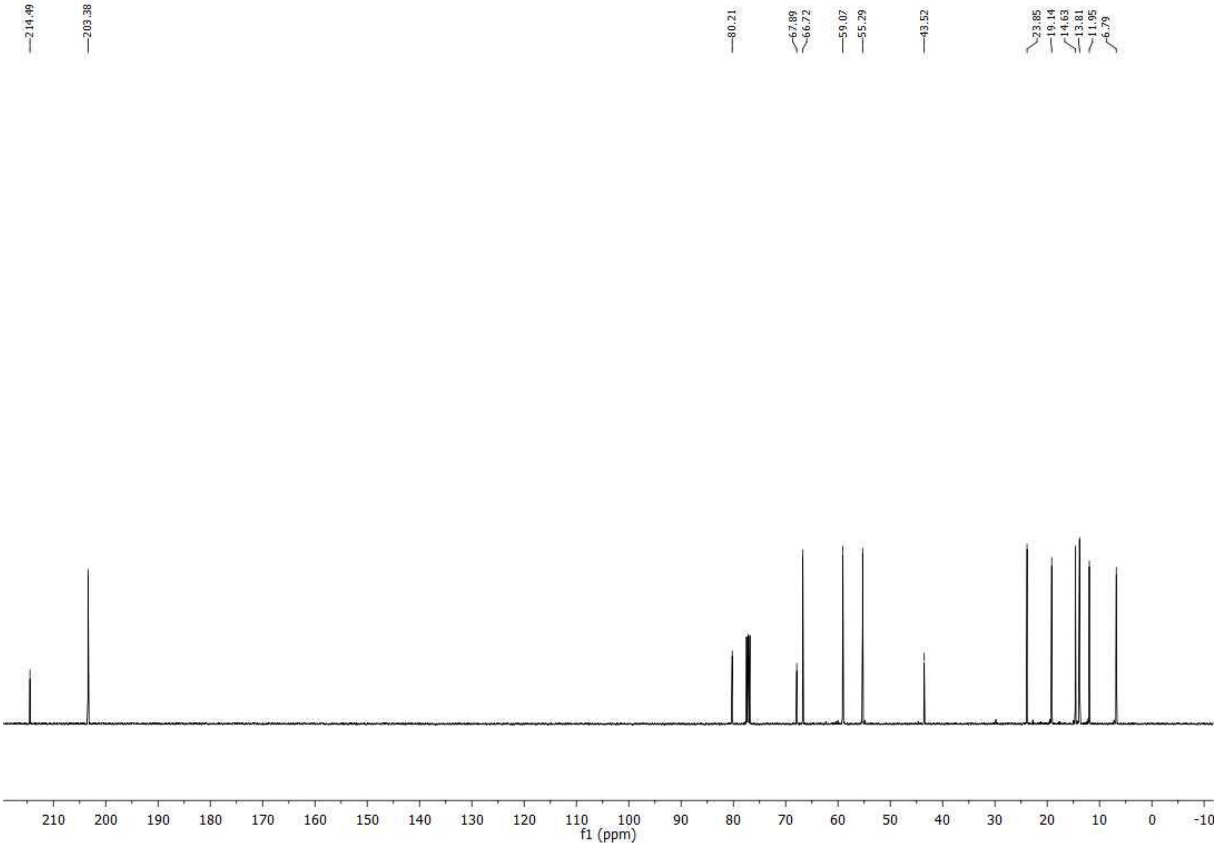
214.49
203.38
80.21
67.89
66.72
59.07
55.29
43.52
23.85
19.14
14.63
13.81
11.95
6.79
210
200
190
180
170
160
150
140
130
120
110
100
90
80
70
60
50
40
30
20
10
0
-10
f1 (ppm)

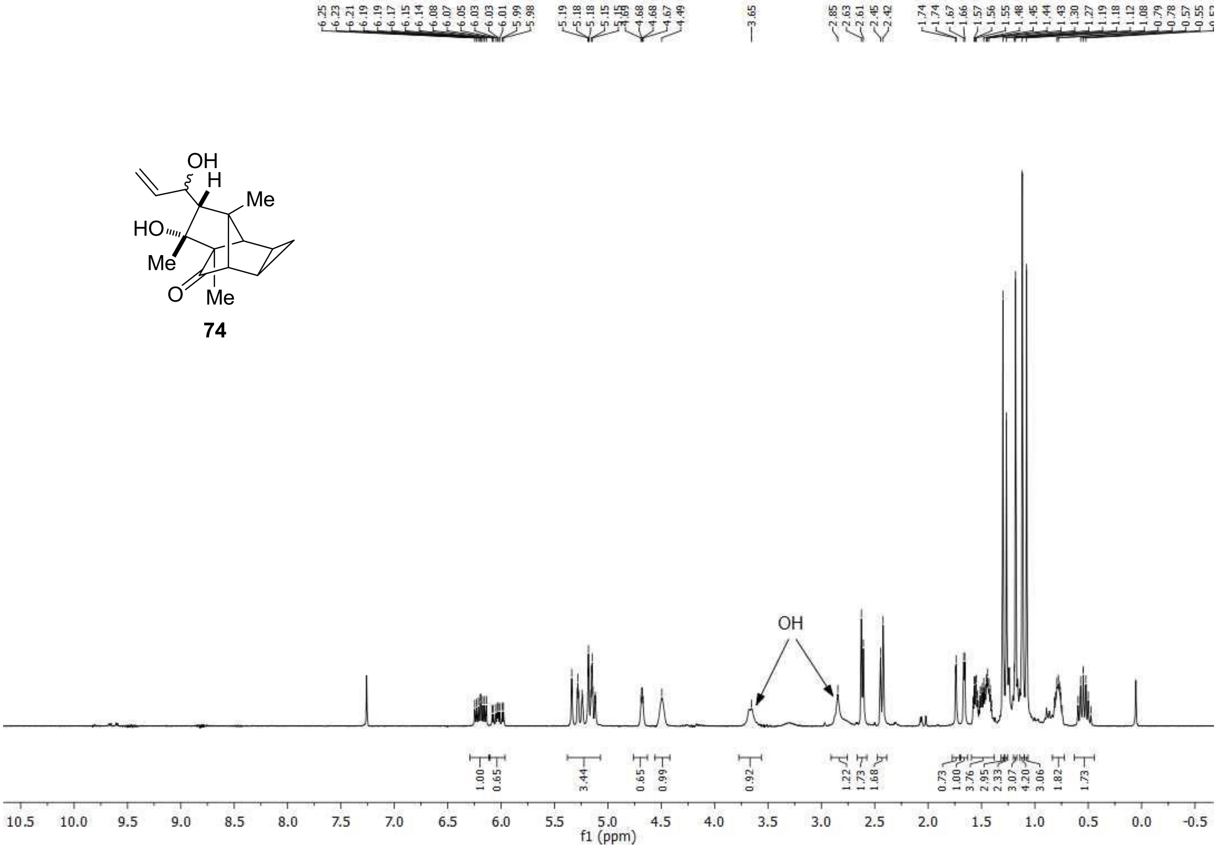

74

OH
H
Me
HO
Me
O
Me
6.25
6.23
6.21
6.19
6.19
6.17
6.15
6.14
6.08
6.07
6.05
6.03
6.03
6.01
5.99
5.98
5.19
5.18
5.18
5.15
5.15
4.69
4.68
4.68
4.67
4.49
3.65
2.85
2.63
2.61
2.45
2.42
1.74
1.74
1.67
1.66
1.57
1.56
1.55
1.48
1.45
1.44
1.43
1.30
1.27
1.19
1.18
1.12
1.08
0.79
0.78
0.57
0.55
OH
1.00
0.65
3.44
0.65
0.99
0.92
1.22
1.73
1.68
0.73
1.00
3.76
2.95
2.33
3.07
4.20
3.06
1.82
1.73
10.5
10.0
9.5
9.0
8.5
8.0
7.5
7.0
6.5
6.0
5.5
5.0
4.5
4.0
3.5
3.0
2.5
2.0
1.5
1.0
0.5
0.0
-0.5
f1 (ppm)

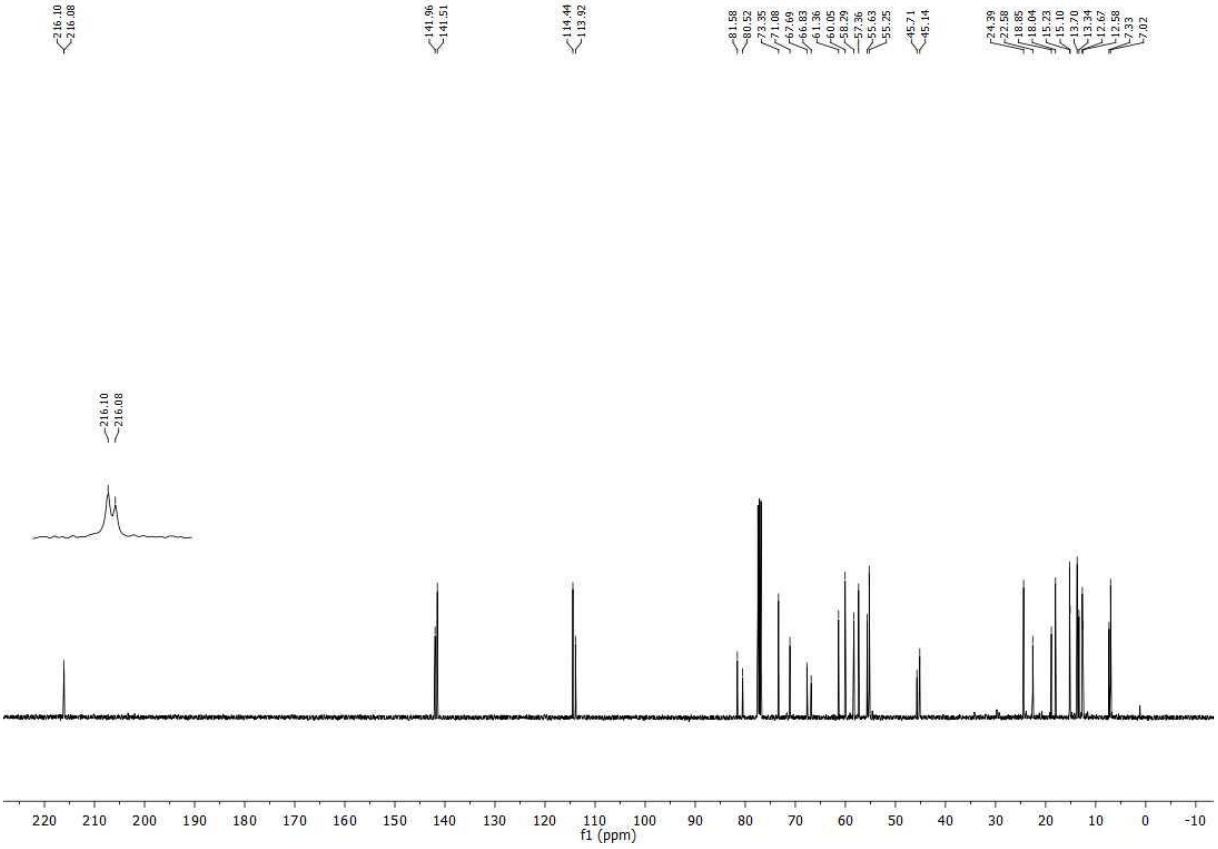

216.10
216.08
141.96
141.51
114.44
113.92
81.58
80.52
73.35
71.08
67.69
66.83
61.36
60.05
58.29
57.36
55.63
55.25
45.71
45.14
24.39
22.58
18.85
18.04
15.23
15.10
13.70
13.34
12.67
12.58
7.33
7.02
216.10
216.08
220
210
200
190
180
170
160
150
140
130
120
110
100
90
80
70
60
50
40
30
20
10
0
-10
f1 (ppm)

O
O
H
H
Me
H
O
Me
O
Me

201

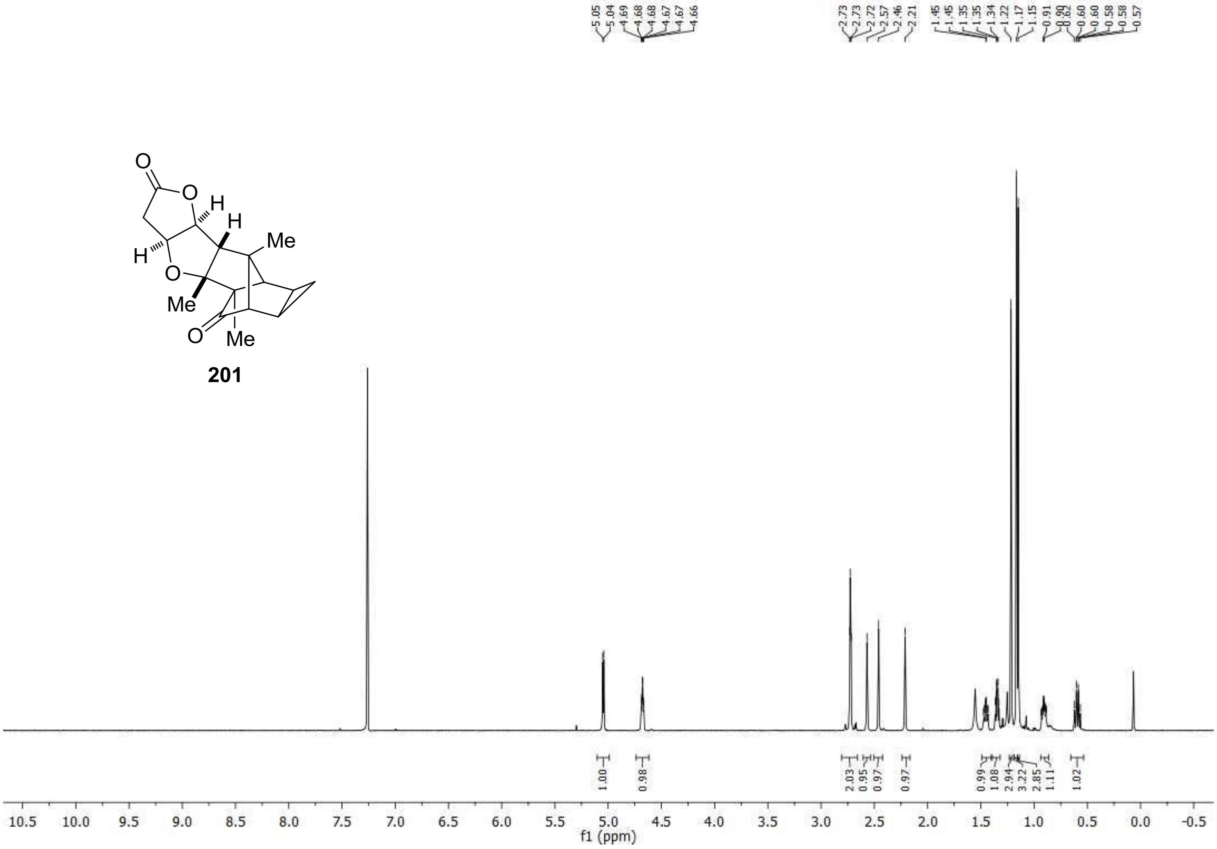
5.05
5.04
4.69
4.68
4.68
4.67
4.67
4.66
2.73
2.73
2.72
2.57
2.46
2.21
1.45
1.45
1.35
1.35
1.34
1.22
1.17
1.15
0.91
0.90
0.89
0.60
0.60
0.58
0.58
0.57
1.00
0.98
2.03
0.95
0.97
0.97
0.99
1.08
2.94
3.22
2.85
1.11
1.02
10.5
10.0
9.5
9.0
8.5
8.0
7.5
7.0
6.5
6.0
5.5
5.0
4.5
4.0
3.5
3.0
2.5
2.0
1.5
1.0
0.5
0.0
-0.5
f1 (ppm)

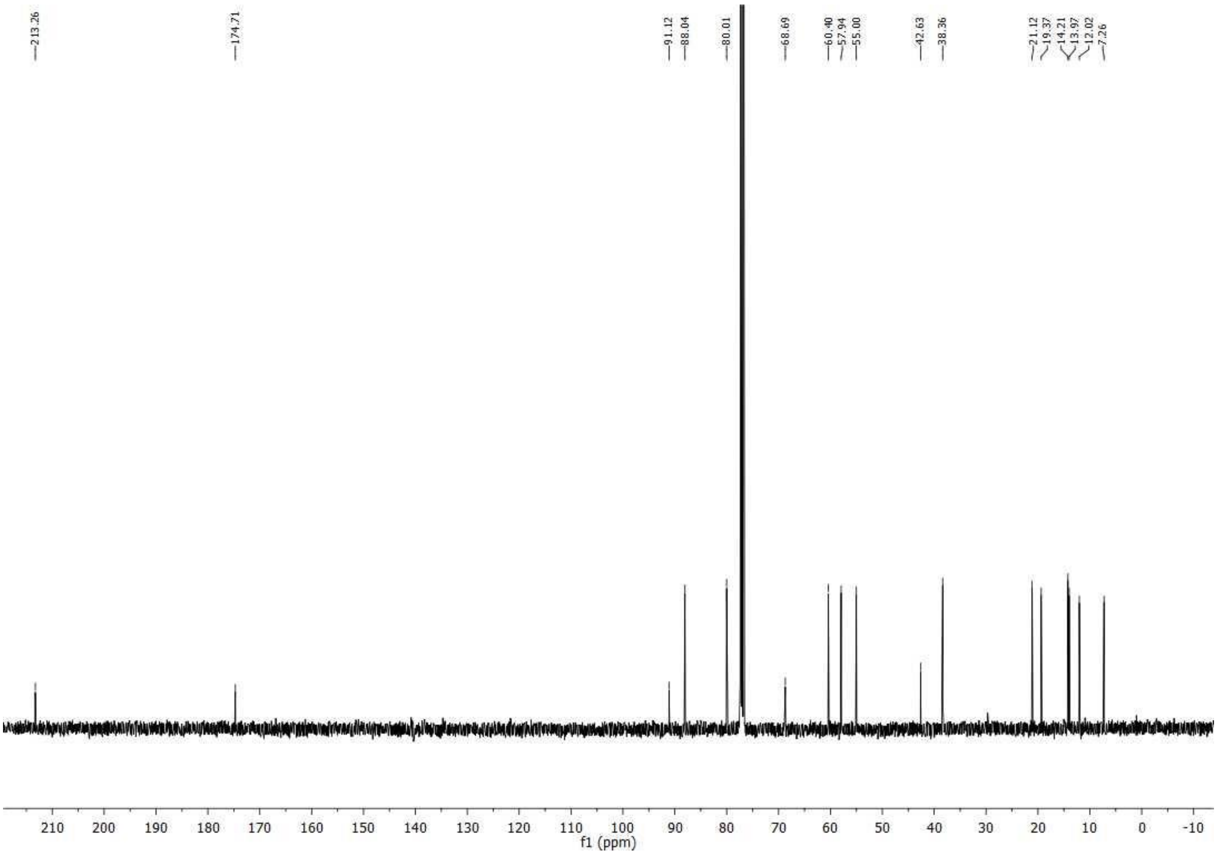
213.26
174.71
91.12
88.04
80.01
68.69
60.40
57.94
55.00
42.63
38.36
21.12
19.37
14.21
13.97
12.02
7.26
210
200
190
180
170
160
150
140
130
120
110
100
90
80
70
60
50
40
30
20
10
0
-10
f1 (ppm)

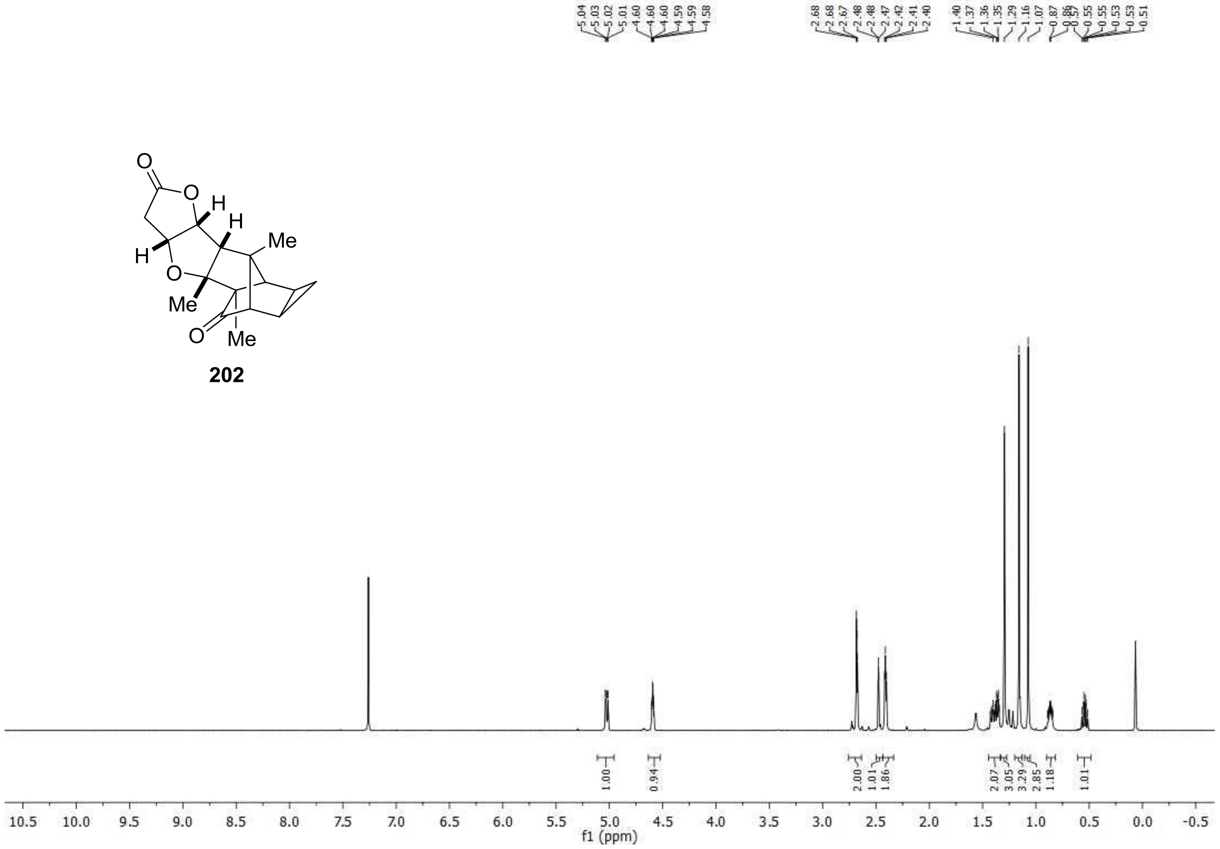
5.04
5.03
5.02
5.01
4.60
4.60
4.60
4.59
4.59
4.58
2.68
2.68
2.67
2.48
2.48
2.47
2.42
2.41
2.40
1.40
1.37
1.36
1.35
1.29
1.16
1.07
0.87
0.86
0.57
0.55
0.55
0.53
0.53
0.51
O
O
H
H
Me
H
O
Me
O
Me
202
1.00
0.94
2.00
1.01
1.86
2.07
3.05
3.29
2.85
1.18
1.01
10.5
10.0
9.5
9.0
8.5
8.0
7.5
7.0
6.5
6.0
5.5
5.0
4.5
4.0
3.5
3.0
2.5
2.0
1.5
1.0
0.5
0.0
-0.5
f1 (ppm)

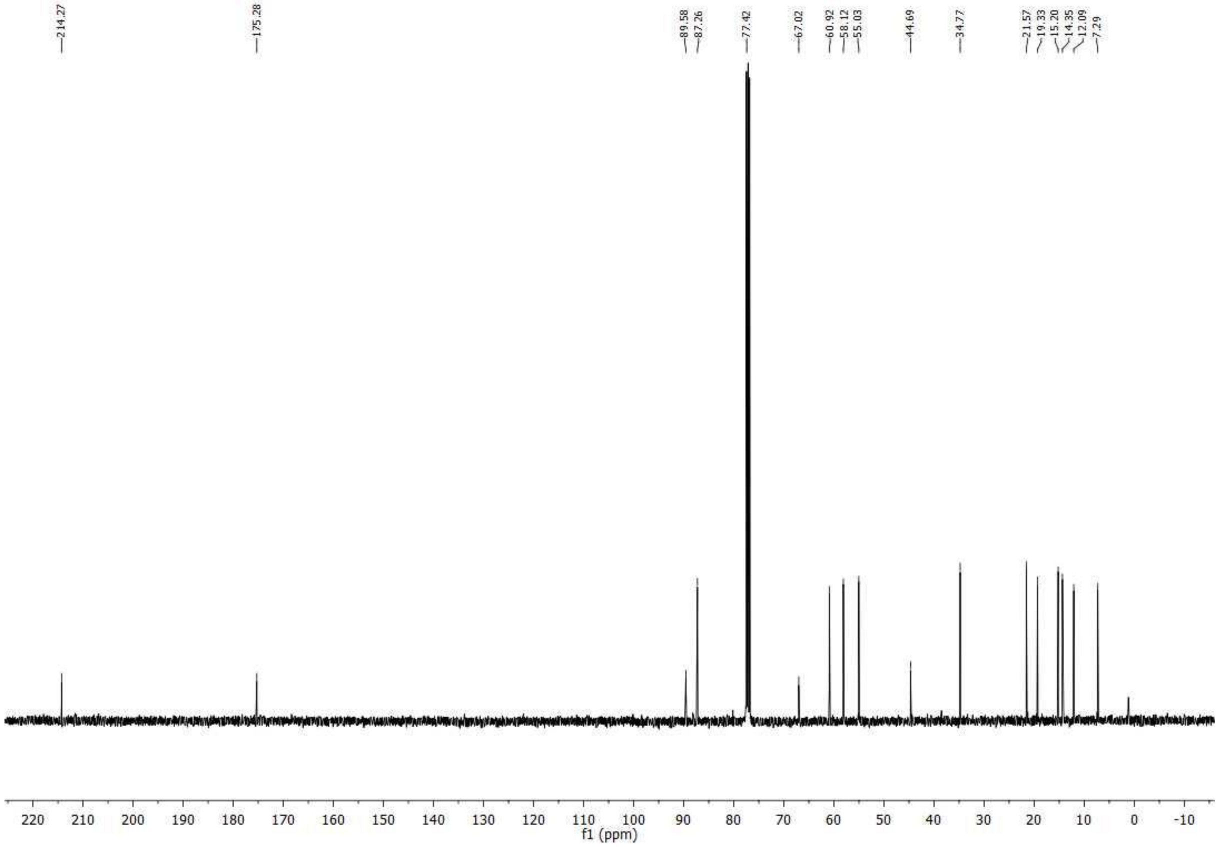
214.27
175.28
89.58
87.26
77.42
67.02
60.92
58.12
55.03
44.69
34.77
21.57
19.33
15.20
14.35
12.09
7.29
220
210
200
190
180
170
160
150
140
130
120
110
100
90
80
70
60
50
40
30
20
10
0
-10
f1 (ppm)

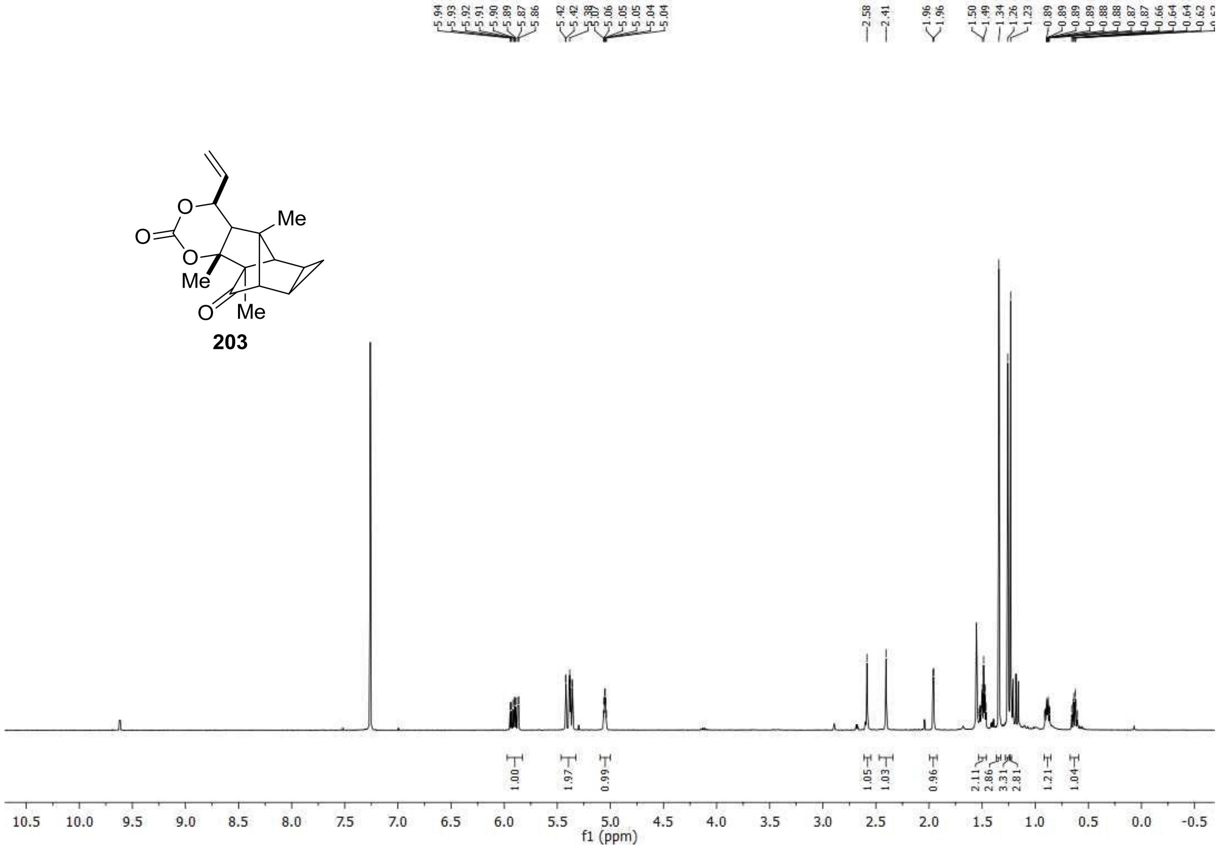
5.94
5.93
5.92
5.91
5.90
5.89
5.87
5.86
5.42
5.42
5.38
5.07
5.06
5.05
5.05
5.04
5.04
2.58
2.41
1.96
1.96
1.50
1.49
1.34
1.26
1.23
0.89
0.89
0.89
0.89
0.88
0.88
0.87
0.87
0.66
0.64
0.64
0.62
O
O
O
Me
Me
O
Me
1.00
1.97
0.99
1.05
1.03
0.96
2.11
2.86
3.31
2.81
1.21
1.04
10.5
10.0
9.5
9.0
8.5
8.0
7.5
7.0
6.5
6.0
5.5
5.0
4.5
4.0
3.5
3.0
2.5
2.0
1.5
1.0
0.5
0.0
-0.5
f1 (ppm)

203

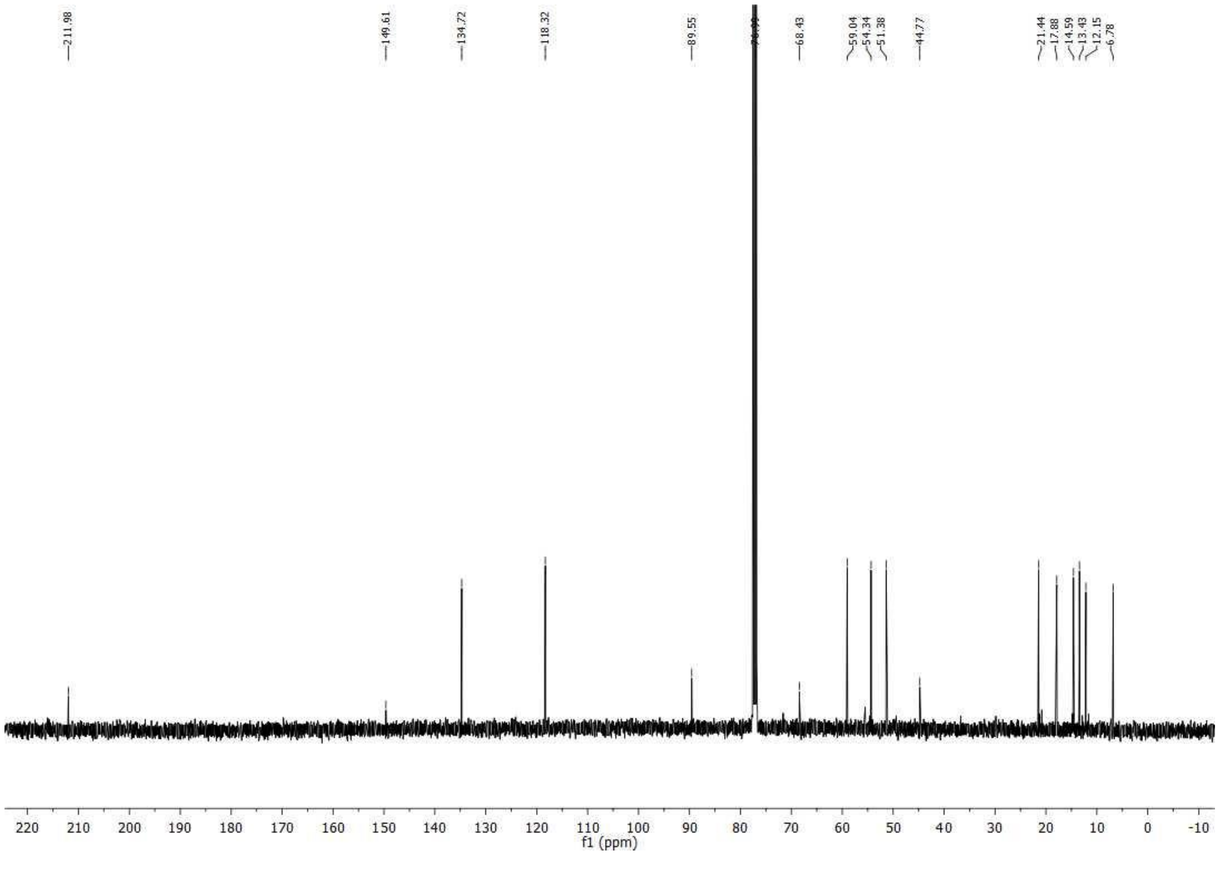
211.98
149.61
134.72
118.32
89.55
68.43
59.04
54.34
51.38
44.77
21.44
17.88
14.59
13.43
12.15
6.78
220
210
200
190
180
170
160
150
140
130
120
110
100
90
80
70
60
50
40
30
20
10
0
-10
f1 (ppm)

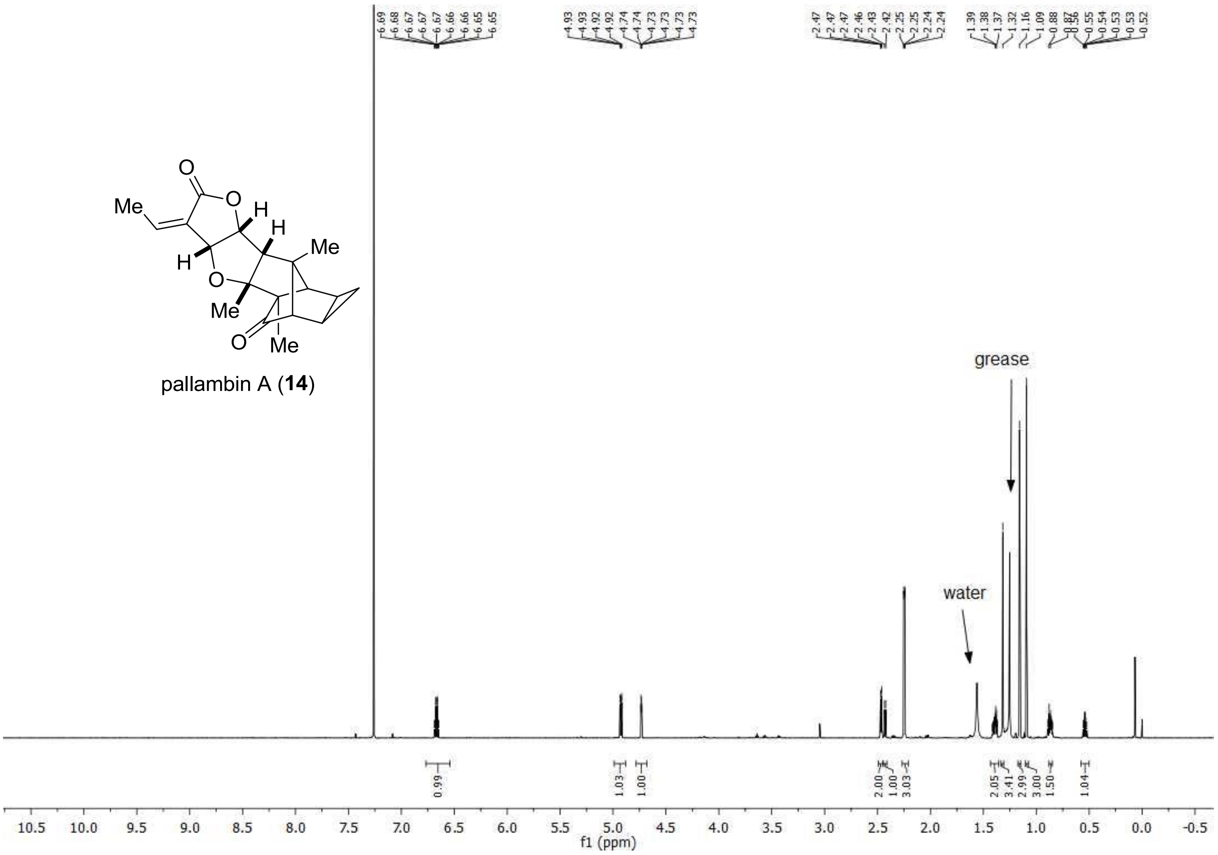
6.69
6.68
6.67
6.67
6.66
6.66
6.65
6.65
4.93
4.93
4.92
4.92
4.74
4.74
4.73
4.73
4.73
4.73
2.47
2.47
2.47
2.46
2.43
2.42
2.25
2.25
2.24
2.24
1.39
1.38
1.37
1.32
1.16
1.09
0.88
0.87
0.86
0.55
0.54
0.53
0.53
0.52
Me
O
O
H
H
Me
H
O
Me
O
Me
pallambin A (**14**)
grease
water
0.99
1.03
1.00
2.00
1.00
3.03
2.05
3.41
2.99
3.00
1.50
1.04
10.5
10.0
9.5
9.0
8.5
8.0
7.5
7.0
6.5
6.0
5.5
5.0
4.5
4.0
3.5
3.0
2.5
2.0
1.5
1.0
0.5
0.0
-0.5
f1 (ppm)

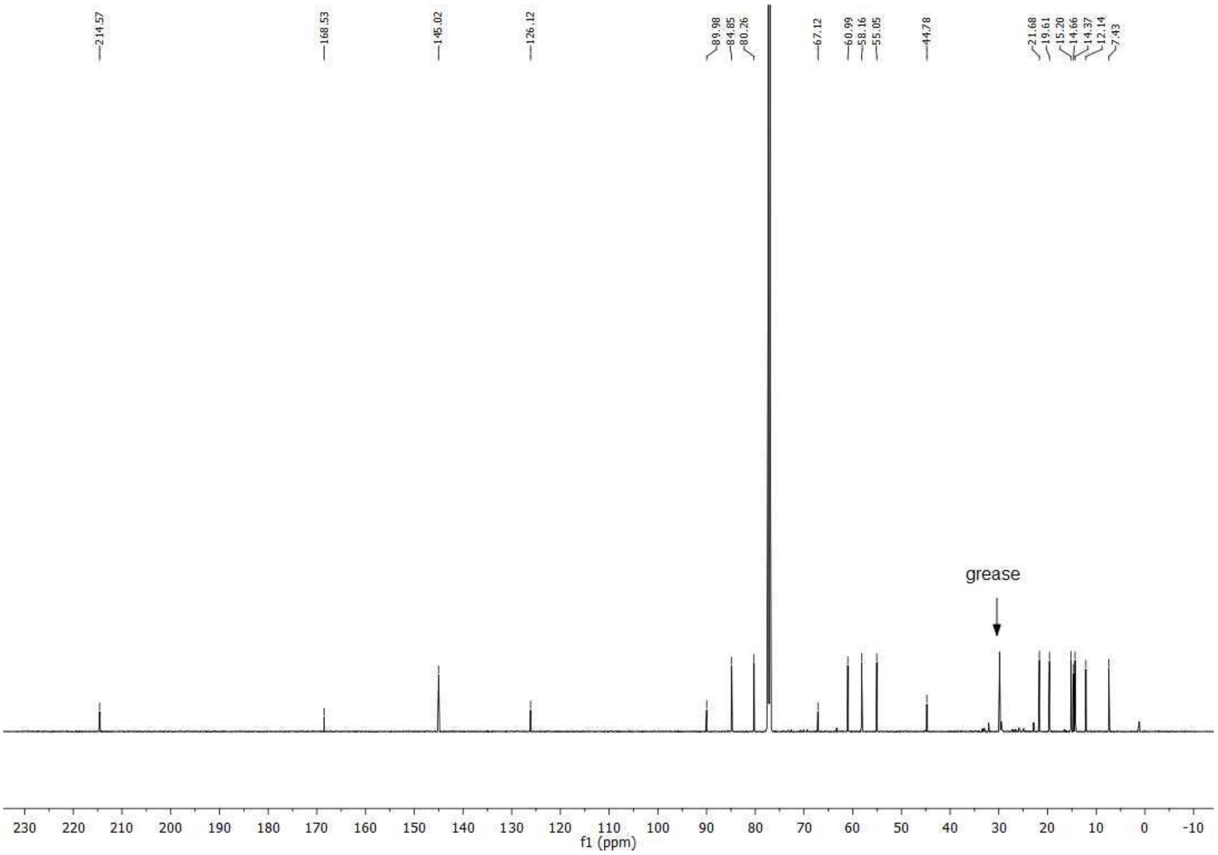
214.57
168.53
145.02
126.12
89.98
84.85
80.26
67.12
60.99
58.16
55.05
44.78
21.68
19.61
15.20
14.66
14.37
12.14
7.43
grease
230
220
210
200
190
180
170
160
150
140
130
120
110
100
90
80
70
60
50
40
30
20
10
0
-10
f1 (ppm)

O
O
H
H
Me
Me
H
O
Me
O
Me

pallambin B (**15**)

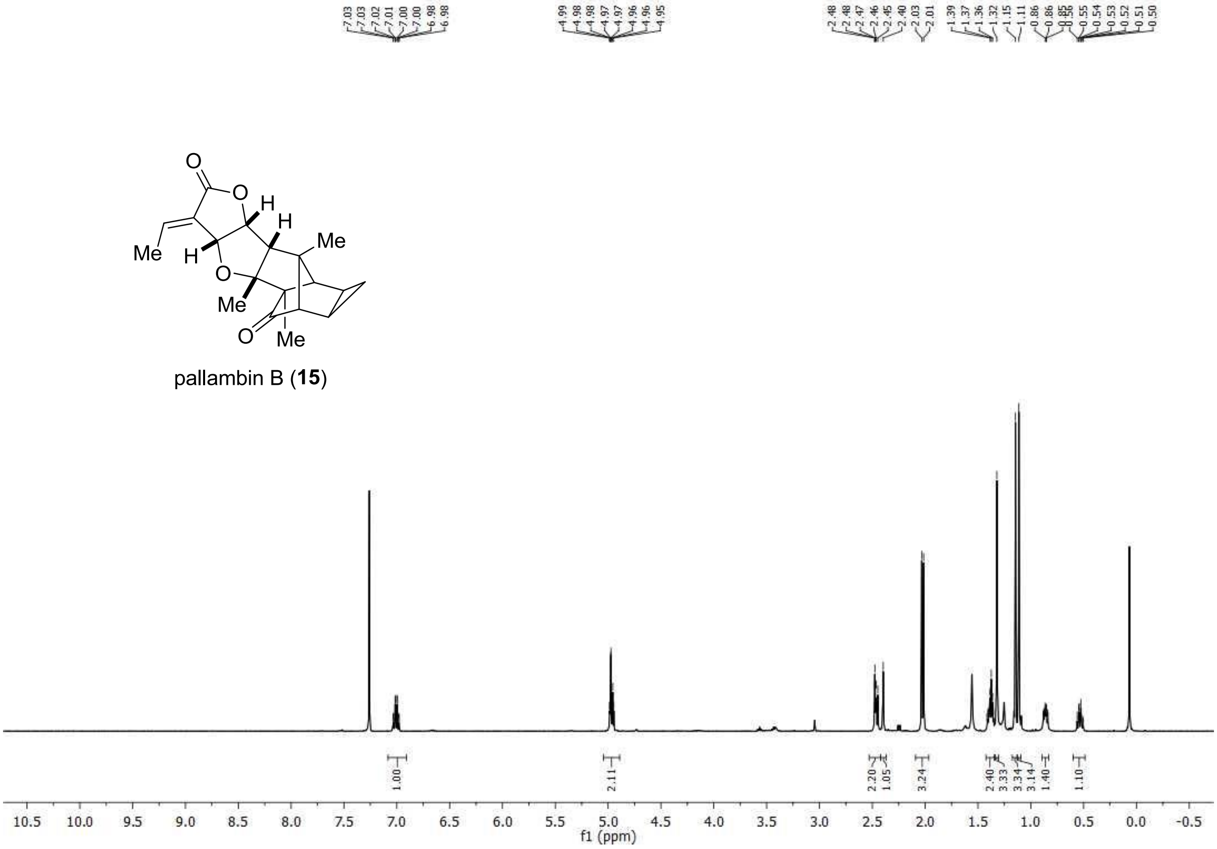

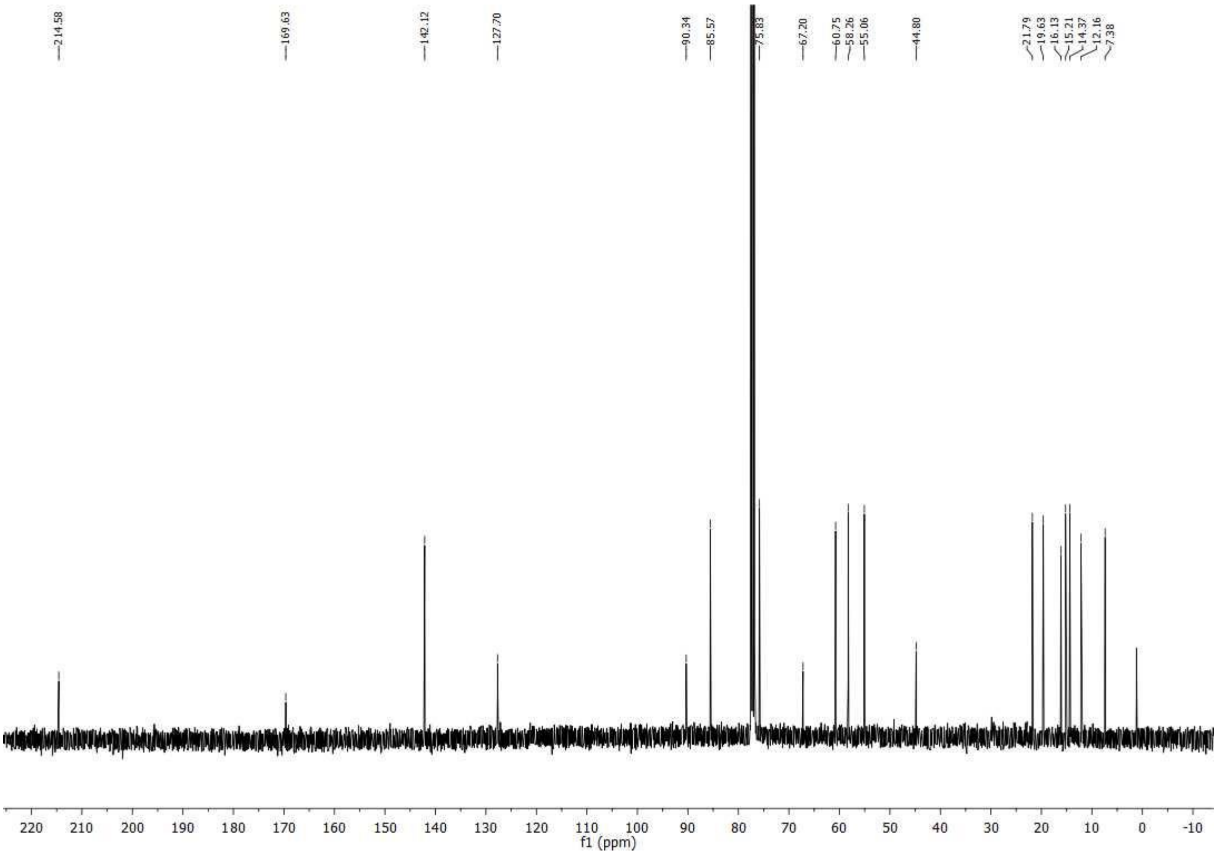

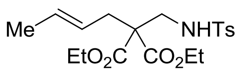
Me
NHTs
EtO$_2$C
CO$_2$Et

263

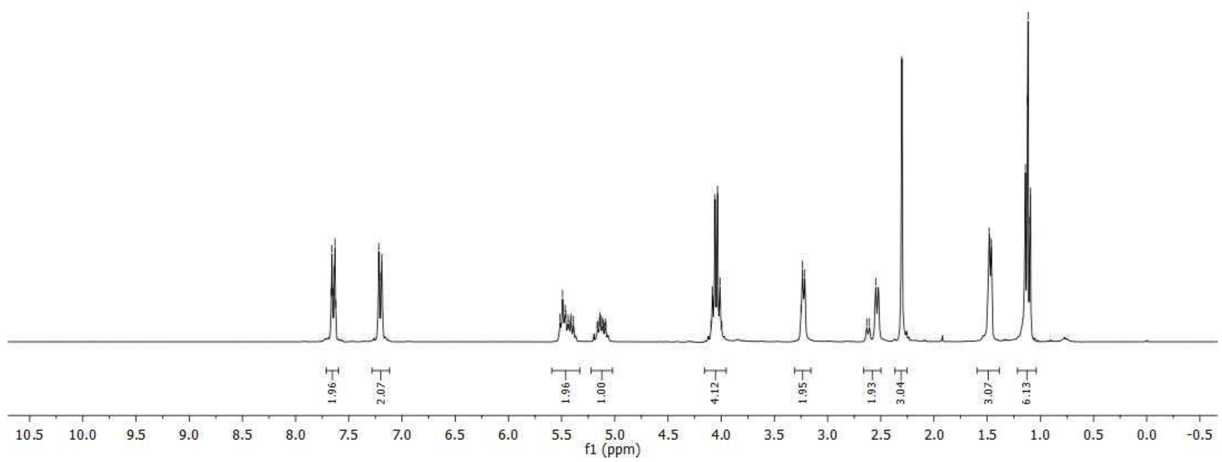
7.66
7.66
7.65
7.64
7.63
7.62
7.22
7.20
7.19
5.51
5.49
5.47
5.46
5.44
5.43
5.41
5.41
5.39
5.17
5.16
5.14
5.14
5.13
5.12
5.11
5.10
5.09
5.08
4.10
4.08
4.06
4.03
4.01
4.00
3.25
3.24
3.21
2.63
2.61
2.55
2.30
1.48
1.48
1.46
1.46
1.15
1.14
1.12
1.12
1.10
1.09
1.96
2.07
1.96
1.00
4.12
1.95
1.93
3.04
3.07
6.13
10.5
10.0
9.5
9.0
8.5
8.0
7.5
7.0
6.5
6.0
5.5
5.0
4.5
4.0
3.5
3.0
2.5
2.0
1.5
1.0
0.5
0.0
-0.5
f1 (ppm)

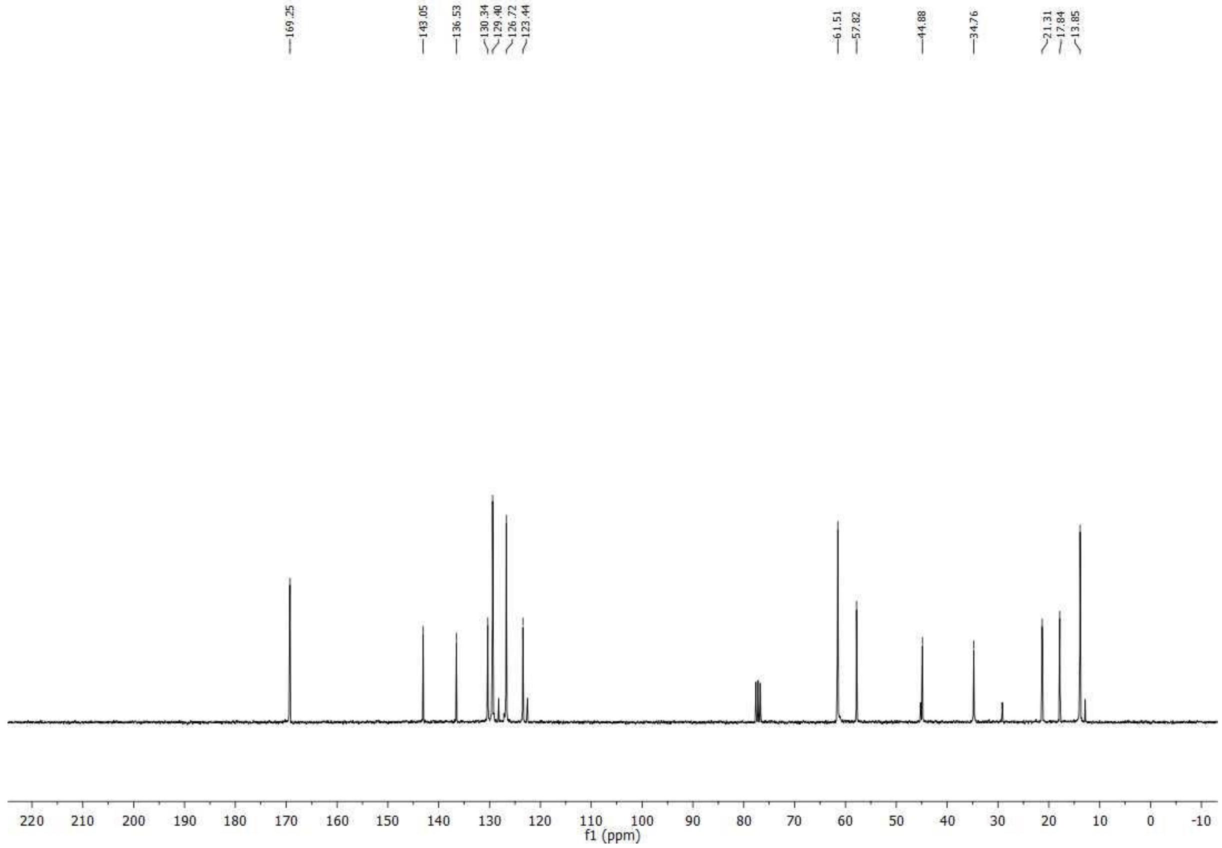
169.25
143.05
136.53
130.34
129.40
126.72
123.44
61.51
57.82
44.88
34.76
21.31
17.84
13.85
220
210
200
190
180
170
160
150
140
130
120
110
100
90
80
70
60
50
40
30
20
10
0
-10
f1 (ppm)

Me
NCbzTs
EtO2C
CO2Et

357

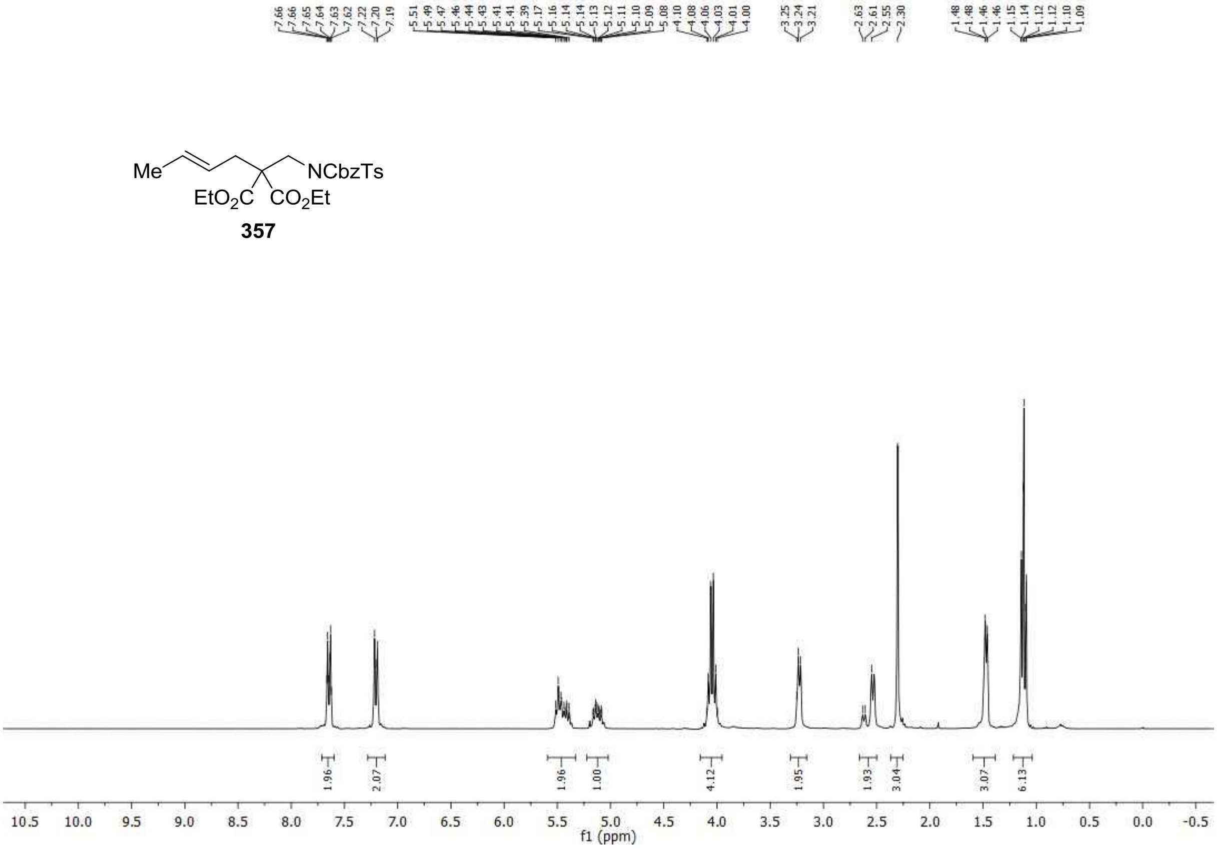
7.66
7.66
7.65
7.64
7.63
7.62
7.22
7.20
7.19
5.51
5.49
5.47
5.46
5.44
5.43
5.41
5.41
5.39
5.17
5.16
5.14
5.14
5.13
5.12
5.11
5.10
5.09
5.08
4.10
4.08
4.06
4.03
4.01
4.00
3.25
3.24
3.21
2.63
2.61
2.55
2.30
1.48
1.48
1.46
1.46
1.15
1.14
1.12
1.12
1.10
1.09
1.96
2.07
1.96
1.00
4.12
1.95
1.93
3.04
3.07
6.13
10.5
10.0
9.5
9.0
8.5
8.0
7.5
7.0
6.5
6.0
5.5
5.0
4.5
4.0
3.5
3.0
2.5
2.0
1.5
1.0
0.5
0.0
-0.5
f1 (ppm)

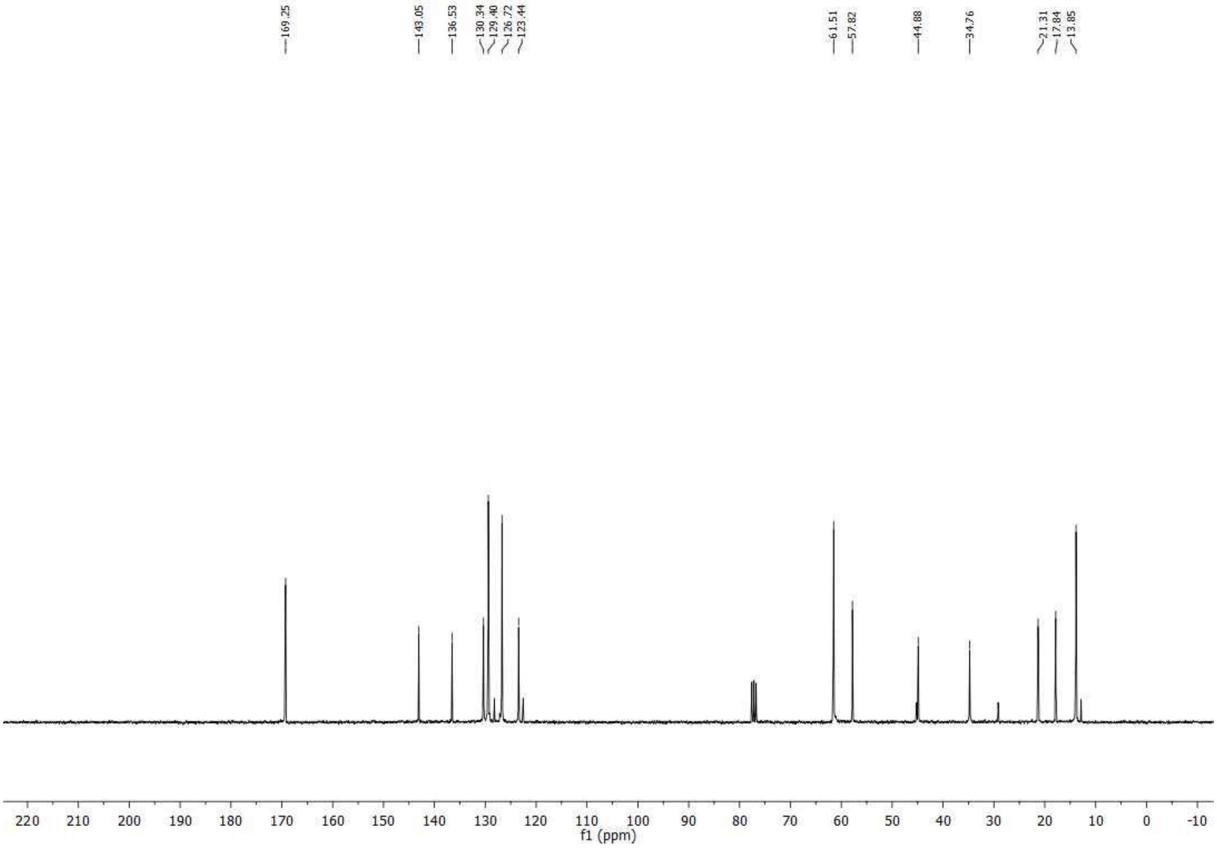
169.25
143.05
136.53
130.34
129.40
126.72
123.44
61.51
57.82
44.88
34.76
21.31
17.84
13.85
220
210
200
190
180
170
160
150
140
130
120
110
100
90
80
70
60
50
40
30
20
10
0
-10
f1 (ppm)

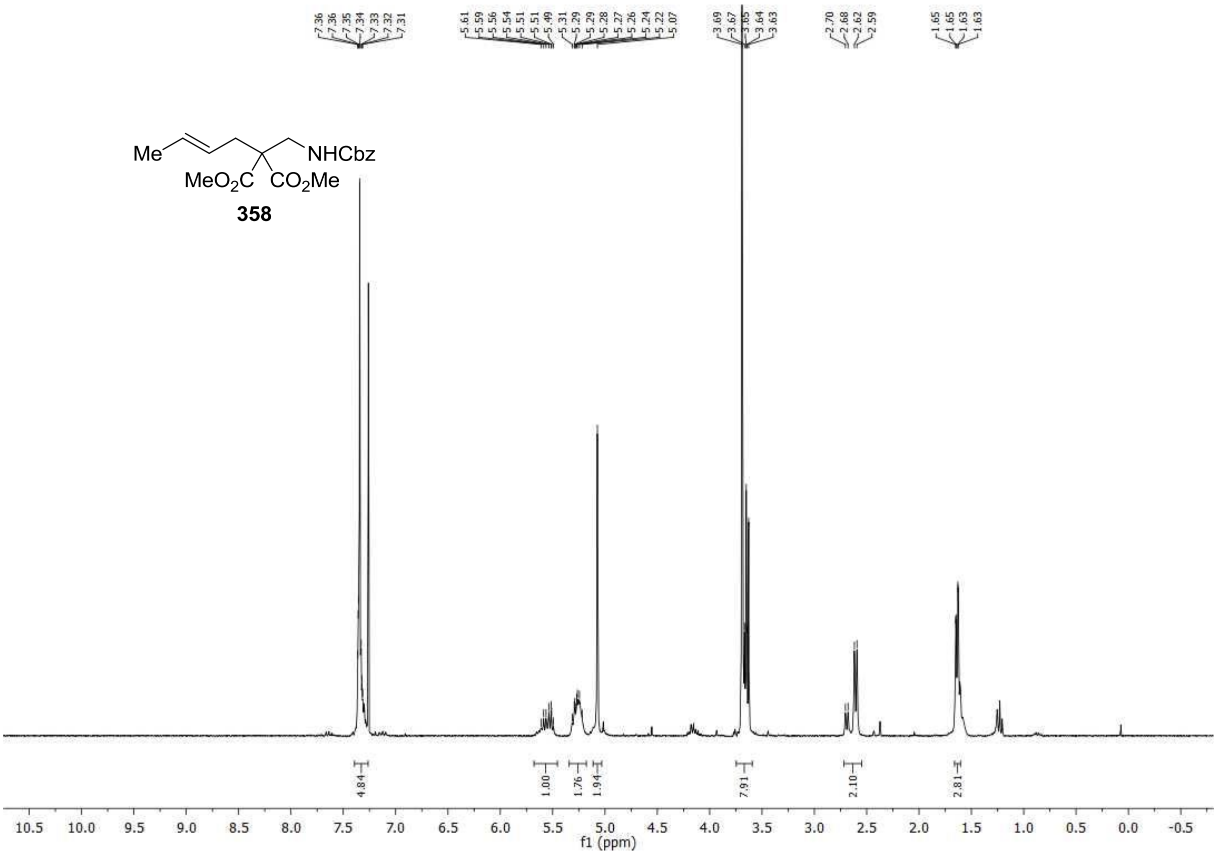
7.36
7.36
7.35
7.34
7.33
7.32
7.31
5.61
5.59
5.56
5.54
5.51
5.51
5.49
5.31
5.29
5.29
5.28
5.27
5.26
5.24
5.22
5.07
3.69
3.67
3.65
3.64
3.63
2.70
2.68
2.62
2.59
1.65
1.65
1.63
1.63
Me
NHCbz
MeO2C
CO2Me
4.84
1.00
1.76
1.94
7.91
2.10
2.81
10.5
10.0
9.5
9.0
8.5
8.0
7.5
7.0
6.5
6.0
5.5
5.0
4.5
4.0
3.5
3.0
2.5
2.0
1.5
1.0
0.5
0.0
-0.5
f1 (ppm)

358

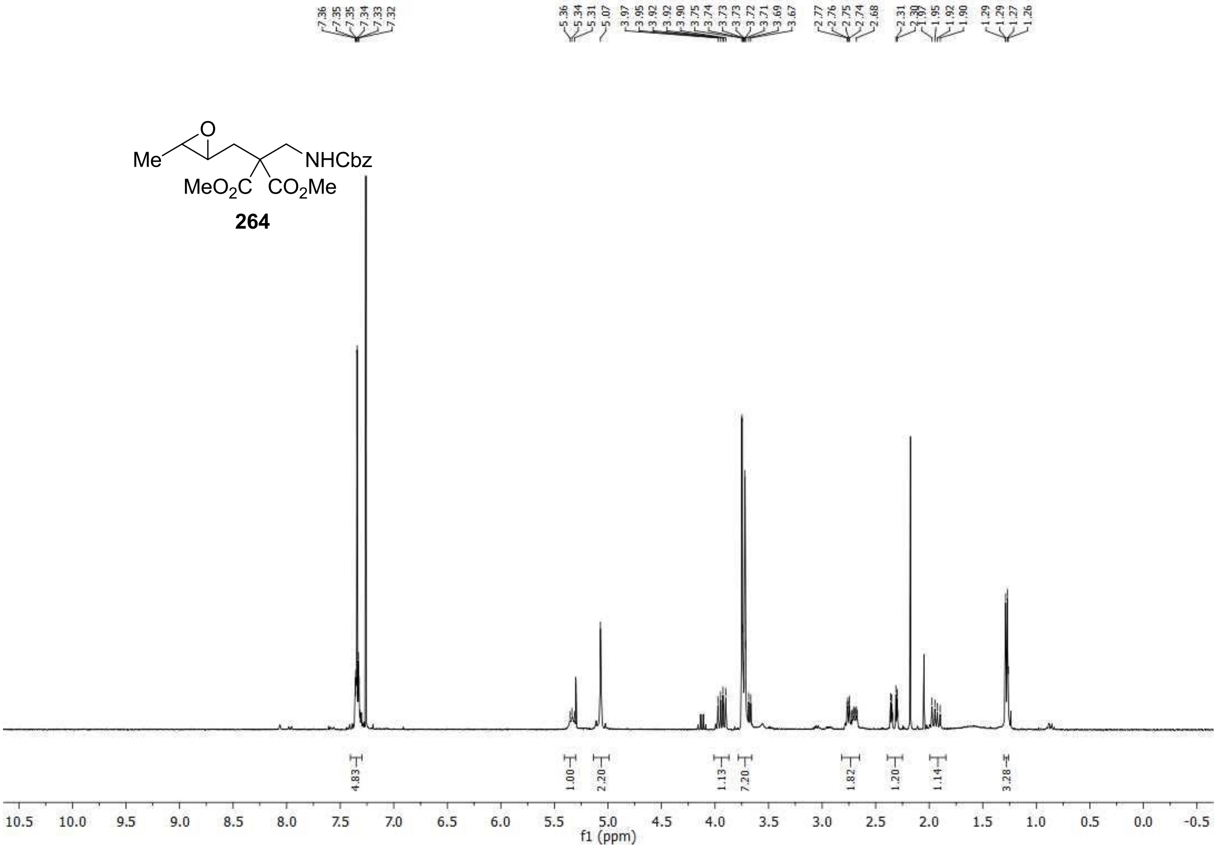

264

Me
O
NHCbz
MeO2C
CO2Me
7.36
7.35
7.35
7.34
7.33
7.32
5.36
5.34
5.31
5.07
3.97
3.95
3.92
3.92
3.90
3.75
3.74
3.73
3.73
3.72
3.71
3.69
3.67
2.77
2.76
2.75
2.74
2.68
2.31
2.30
1.97
1.95
1.92
1.90
1.29
1.29
1.27
1.26
4.83
1.00
2.20
1.13
7.20
1.82
1.20
1.14
3.28
10.5
10.0
9.5
9.0
8.5
8.0
7.5
7.0
6.5
6.0
5.5
5.0
4.5
4.0
3.5
3.0
2.5
2.0
1.5
1.0
0.5
0.0
-0.5
f1 (ppm)

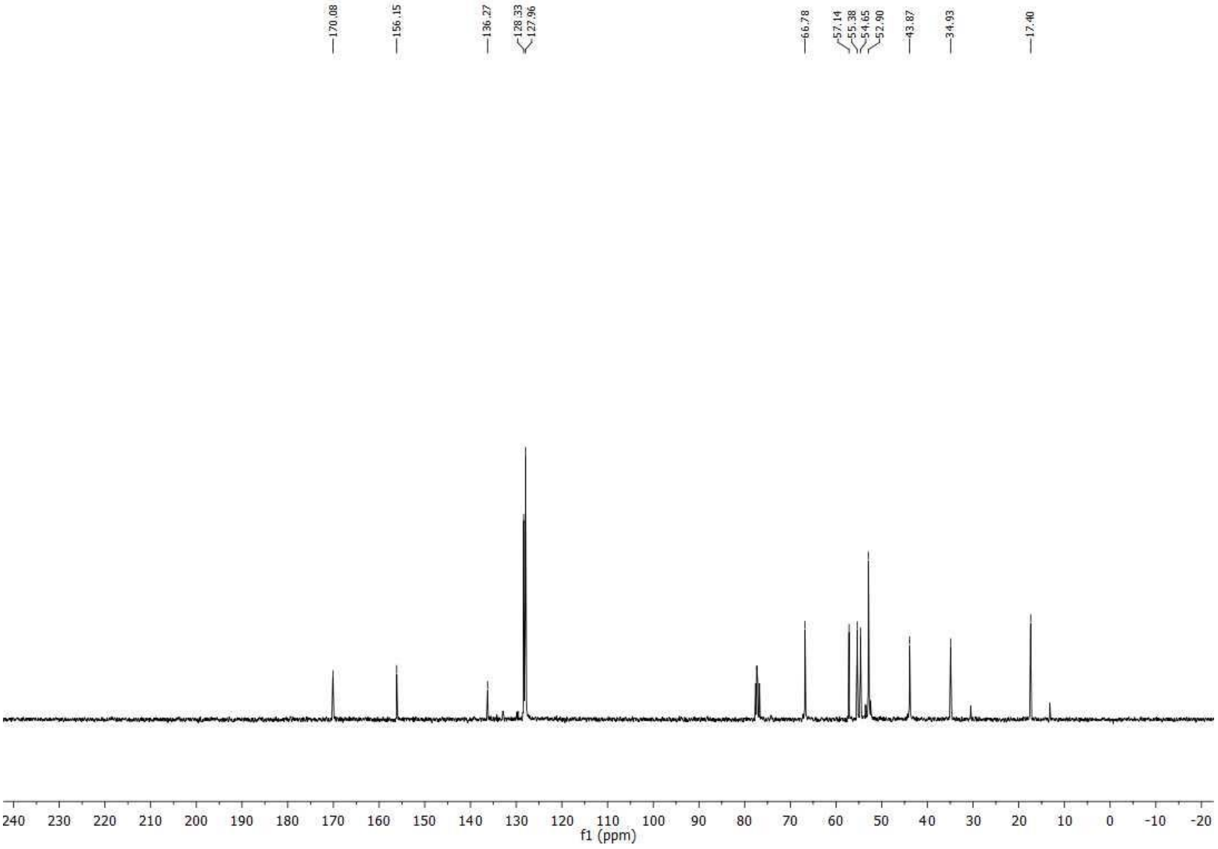

170.08
156.15
136.27
128.33
127.96
66.78
57.14
55.38
54.65
52.90
43.87
34.93
17.40
240
230
220
210
200
190
180
170
160
150
140
130
120
110
100
90
80
70
60
50
40
30
20
10
0
-10
-20
f1 (ppm)

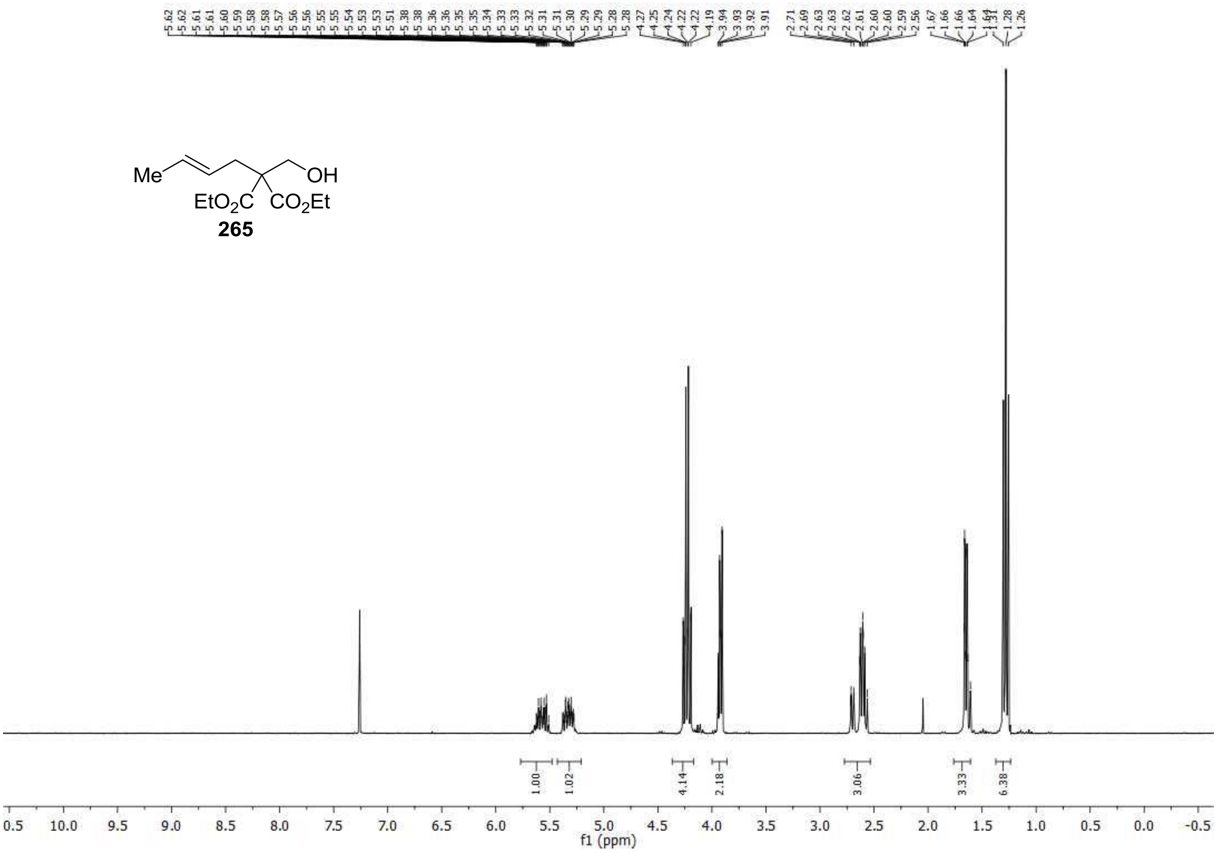
5.62
5.62
5.61
5.61
5.60
5.59
5.58
5.58
5.57
5.56
5.56
5.55
5.55
5.54
5.53
5.53
5.51
5.38
5.38
5.36
5.36
5.35
5.35
5.34
5.33
5.33
5.32
5.31
5.31
5.30
5.29
5.29
5.28
5.28
4.27
4.25
4.24
4.22
4.22
4.19
3.94
3.93
3.92
3.91
2.71
2.69
2.63
2.63
2.62
2.61
2.60
2.60
2.59
2.56
1.67
1.66
1.66
1.64
1.64
1.31
1.28
1.26
Me
OH
EtO2C
CO2Et
1.00
1.02
4.14
2.18
3.06
3.33
6.38
0.5
10.0
9.5
9.0
8.5
8.0
7.5
7.0
6.5
6.0
5.5
5.0
4.5
4.0
3.5
3.0
2.5
2.0
1.5
1.0
0.5
0.0
-0.5
f1 (ppm)

265

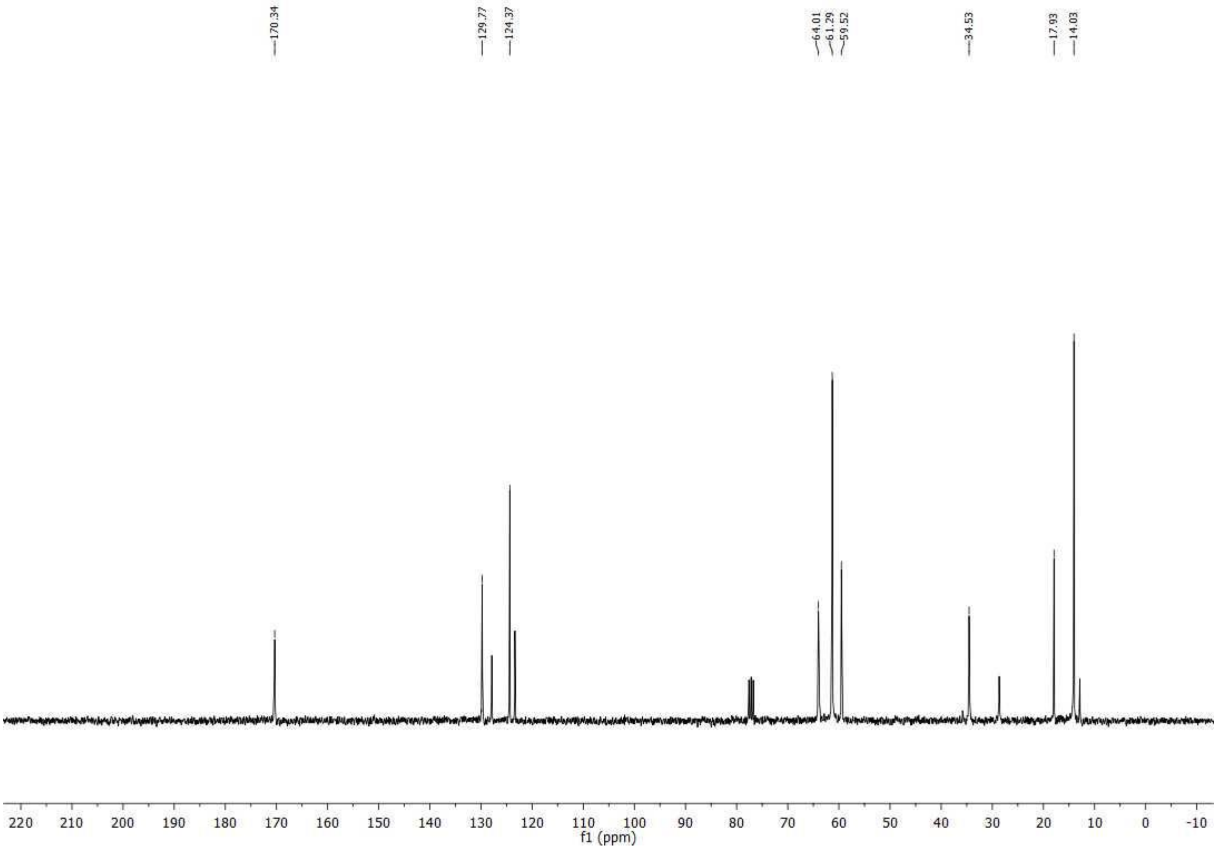
170.34
129.77
124.37
64.01
61.29
59.52
34.53
17.93
14.03
220
210
200
190
180
170
160
150
140
130
120
110
100
90
80
70
60
50
40
30
20
10
0
-10
f1 (ppm)

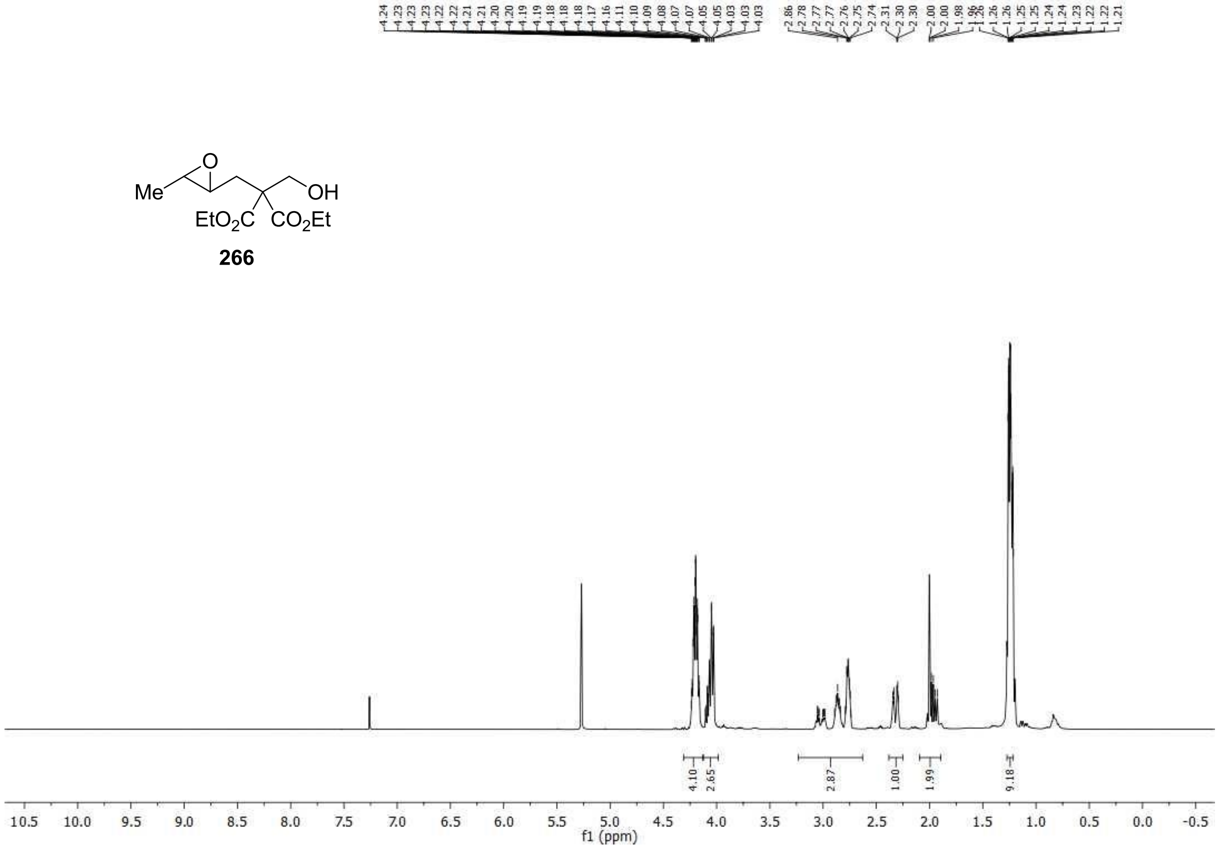
O
Me
OH
EtO2C
CO2Et

266

4.24
4.23
4.23
4.23
4.22
4.22
4.21
4.21
4.20
4.20
4.19
4.19
4.18
4.18
4.18
4.17
4.16
4.11
4.10
4.09
4.08
4.07
4.07
4.05
4.05
4.03
4.03
4.03
2.86
2.78
2.77
2.77
2.76
2.75
2.74
2.31
2.30
2.30
2.00
2.00
1.98
1.96
1.26
1.26
1.26
1.25
1.25
1.24
1.24
1.23
1.22
1.22
1.21
4.10
2.65
2.87
1.00
1.99
9.18
10.5
10.0
9.5
9.0
8.5
8.0
7.5
7.0
6.5
6.0
5.5
5.0
4.5
4.0
3.5
3.0
2.5
2.0
1.5
1.0
0.5
0.0
-0.5
f1 (ppm)

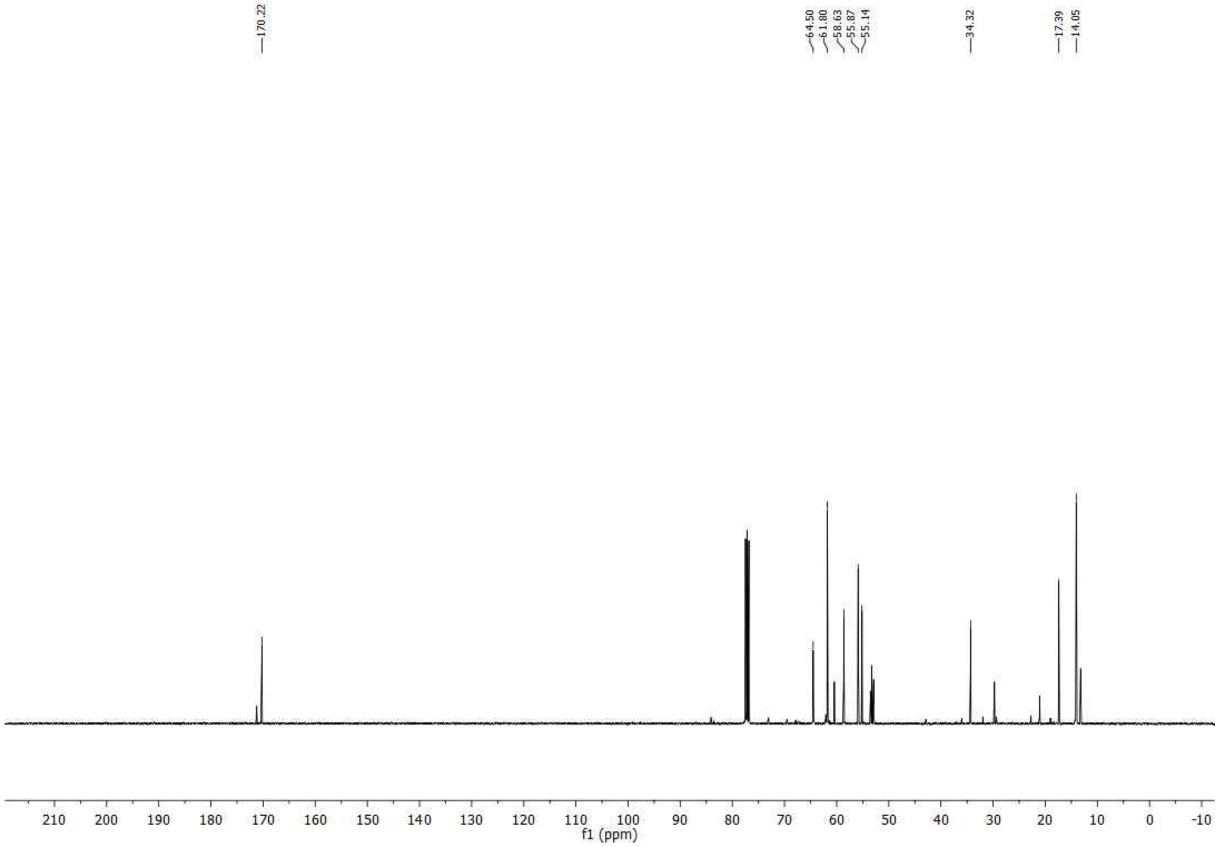
170.22
64.50
61.80
58.63
55.87
55.14
34.32
17.39
14.05
210
200
190
180
170
160
150
140
130
120
110
100
90
80
70
60
50
40
30
20
10
0
-10
f1 (ppm)

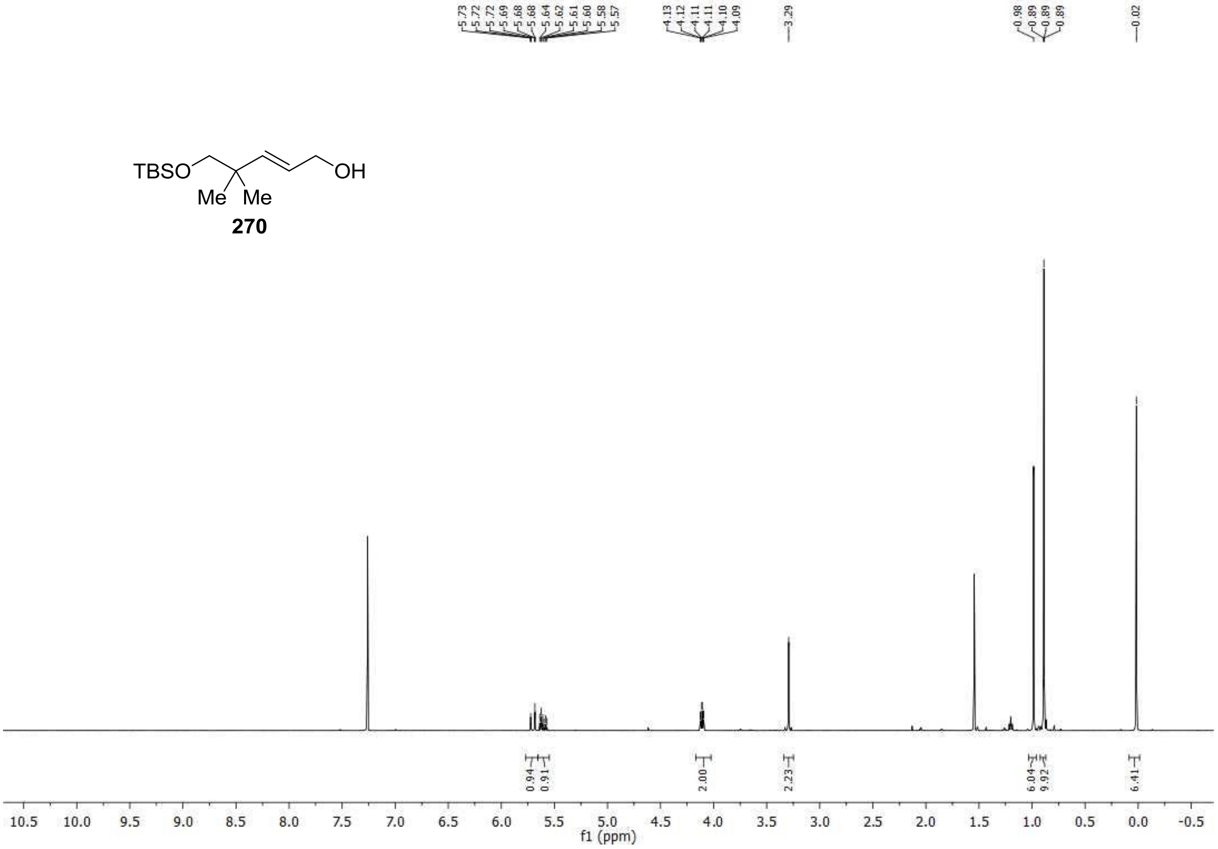
5.73
5.72
5.72
5.69
5.68
5.68
5.64
5.62
5.61
5.60
5.58
5.57
4.13
4.12
4.11
4.11
4.10
4.09
3.29
0.98
0.89
0.89
0.89
0.02
TBSO
OH
Me
Me
270
0.94
0.91
2.00
2.23
6.04
9.92
6.41
10.5
10.0
9.5
9.0
8.5
8.0
7.5
7.0
6.5
6.0
5.5
5.0
4.5
4.0
3.5
3.0
2.5
2.0
1.5
1.0
0.5
0.0
-0.5
f1 (ppm)

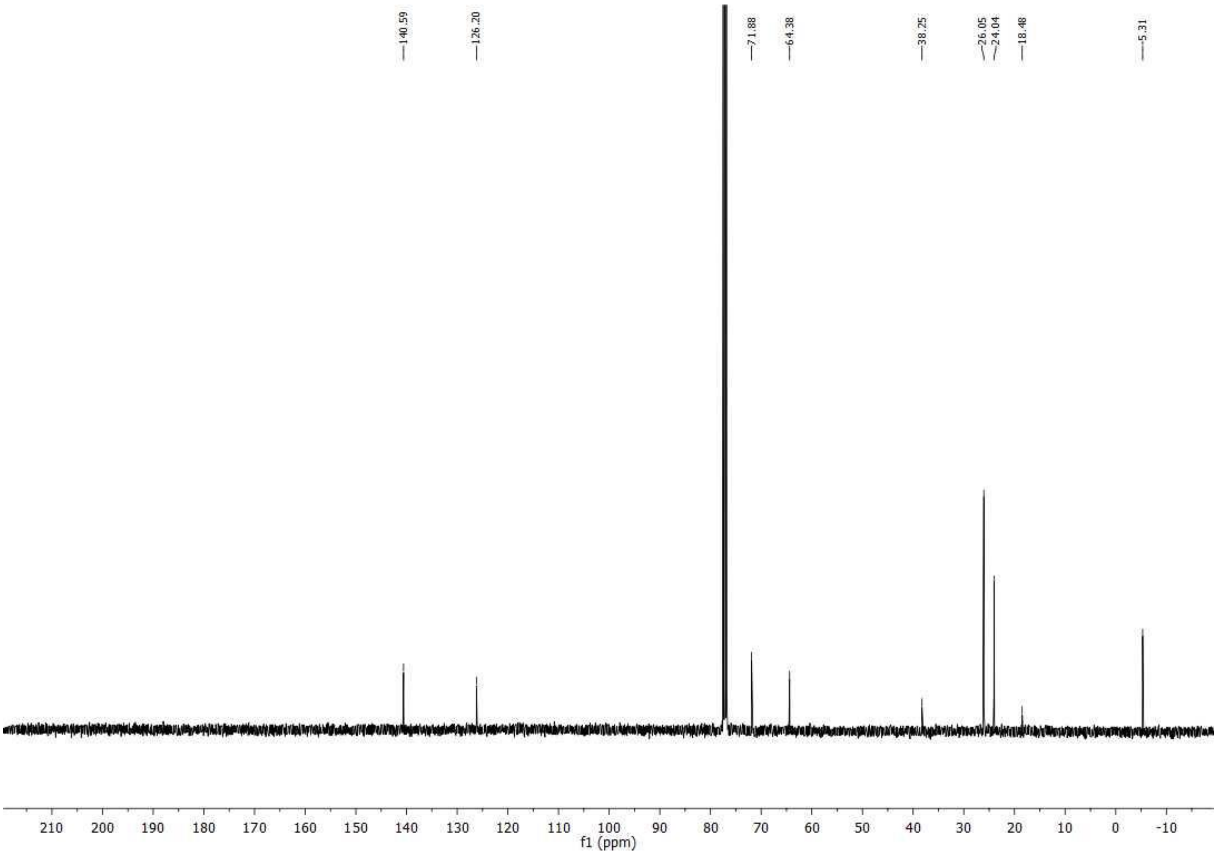
140.59
126.20
71.88
64.38
38.25
26.05
24.04
18.48
-5.31
210
200
190
180
170
160
150
140
130
120
110
100
90
80
70
60
50
40
30
20
10
0
-10
f1 (ppm)

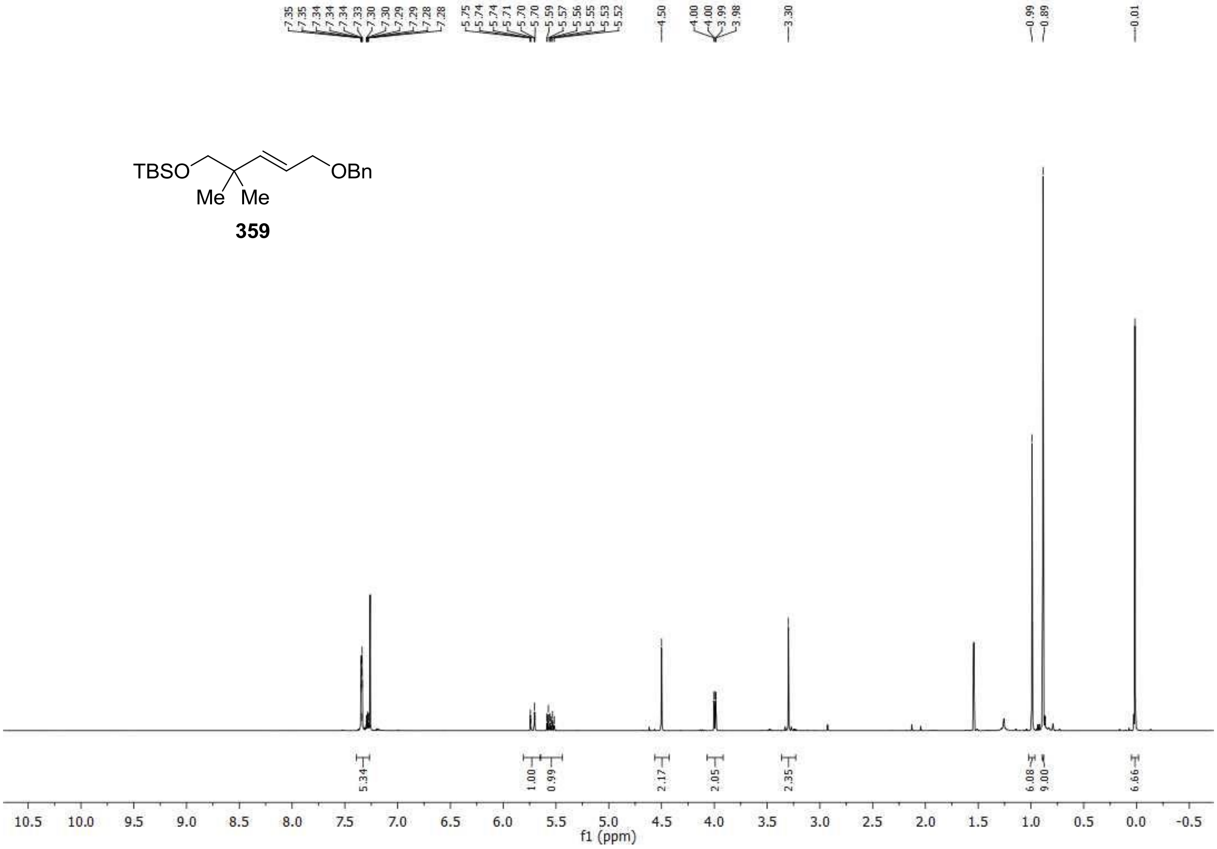
7.35
7.35
7.34
7.34
7.34
7.33
7.30
7.30
7.29
7.29
7.28
7.28
5.75
5.74
5.74
5.71
5.70
5.70
5.59
5.57
5.56
5.55
5.53
5.52
4.50
4.00
4.00
3.99
3.98
3.30
0.99
0.89
0.01
TBSO
OBn
Me
Me
359
5.34
1.00
0.99
2.17
2.05
2.35
6.08
9.00
6.66
10.5
10.0
9.5
9.0
8.5
8.0
7.5
7.0
6.5
6.0
5.5
5.0
4.5
4.0
3.5
3.0
2.5
2.0
1.5
1.0
0.5
0.0
-0.5
f1 (ppm)

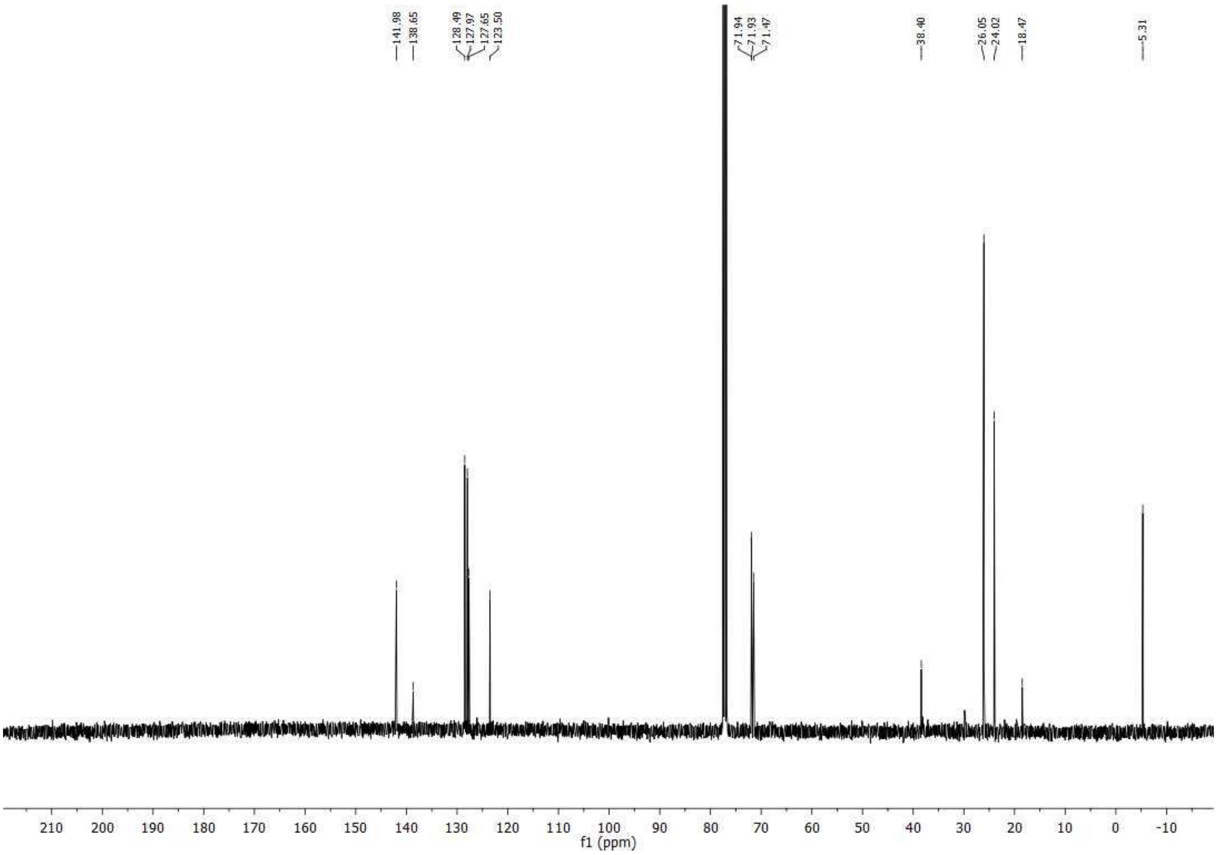
141.98
138.65
128.49
127.97
127.65
123.50
71.94
71.93
71.47
38.40
26.05
24.02
18.47
-5.31
210
200
190
180
170
160
150
140
130
120
110
100
90
80
70
60
50
40
30
20
10
0
-10
f1 (ppm)

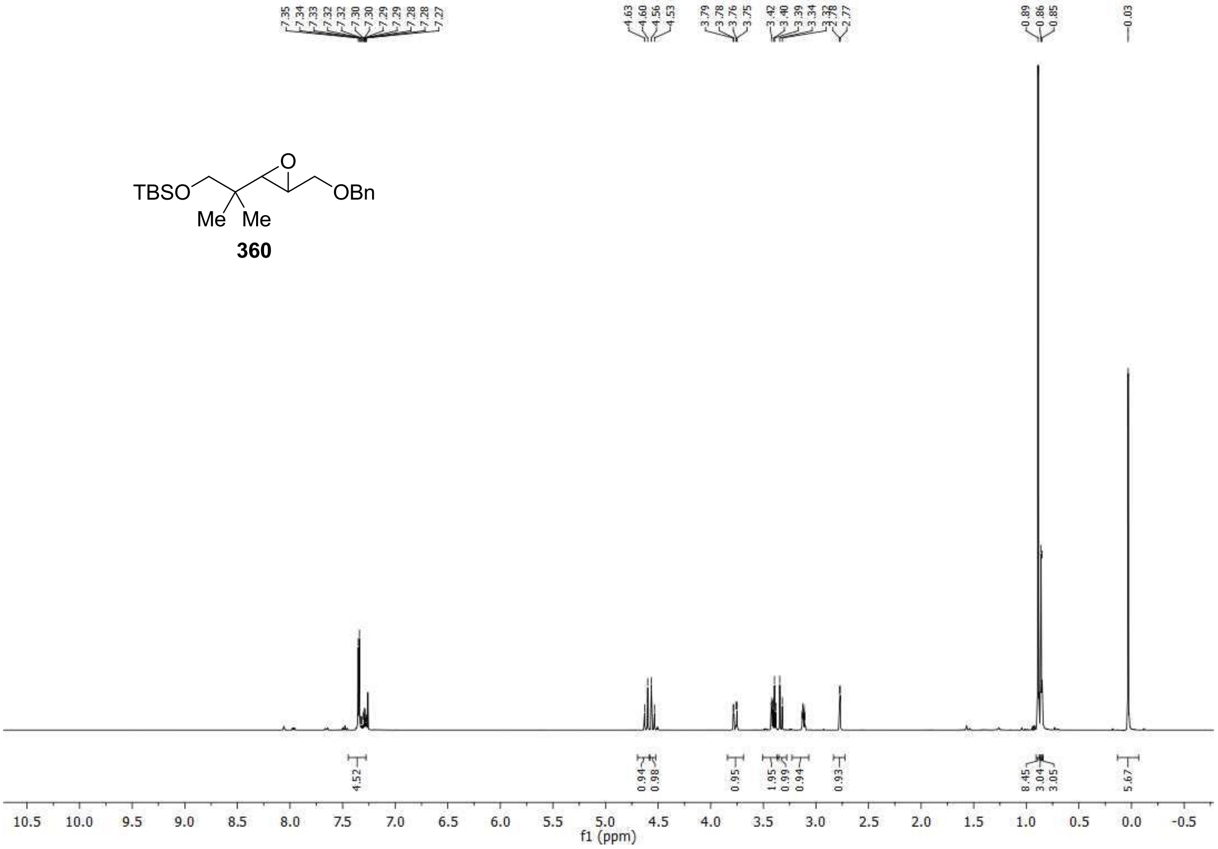
7.35
7.34
7.33
7.32
7.32
7.30
7.30
7.29
7.29
7.28
7.28
7.27
4.63
4.60
4.56
4.53
3.79
3.78
3.76
3.75
3.42
3.40
3.39
3.34
3.32
2.78
2.77
0.89
0.86
0.85
0.03
TBSO
O
OBn
Me
Me
4.52
0.94
0.98
0.95
1.95
0.99
0.94
0.93
8.45
3.04
3.05
5.67
10.5
10.0
9.5
9.0
8.5
8.0
7.5
7.0
6.5
6.0
5.5
5.0
4.5
4.0
3.5
3.0
2.5
2.0
1.5
1.0
0.5
0.0
-0.5
f1 (ppm)

360

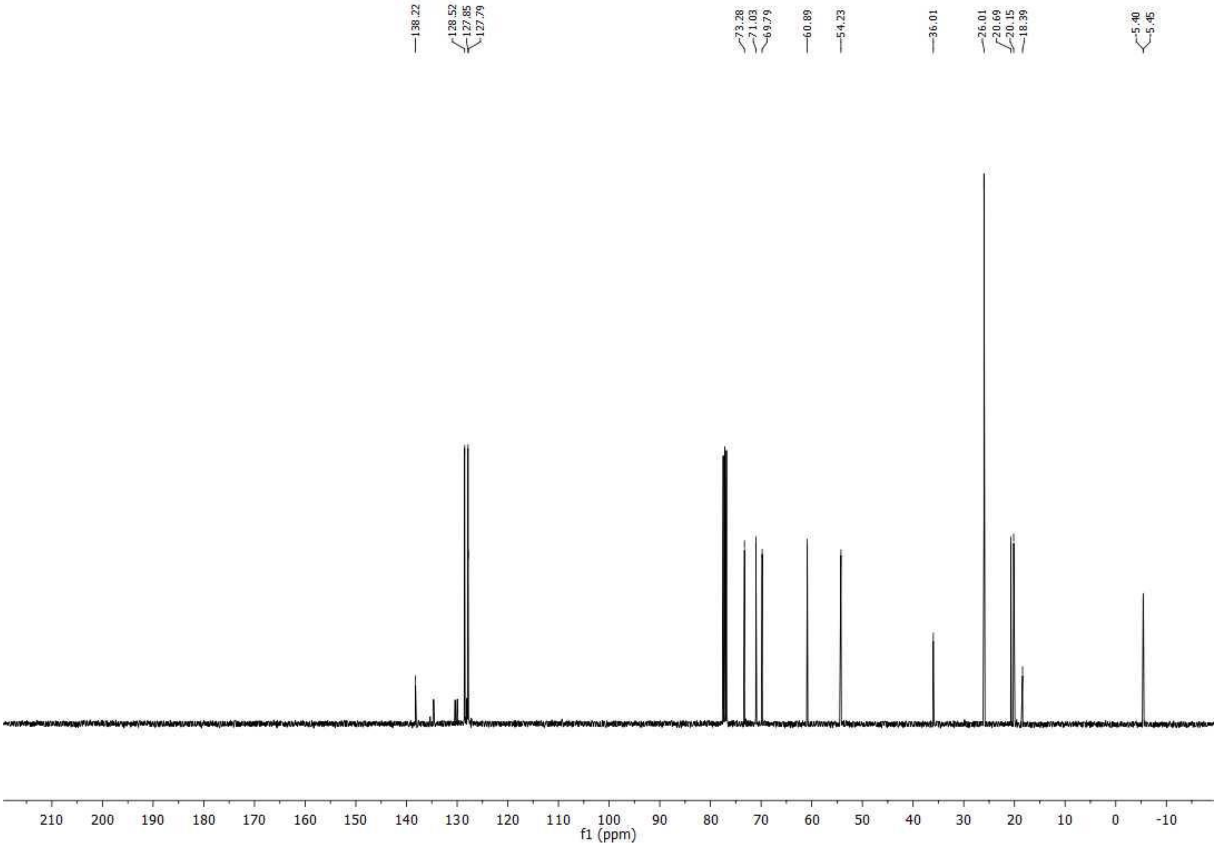
138.22
128.52
127.85
127.79
73.28
71.03
69.79
60.89
54.23
36.01
26.01
20.69
20.15
18.39
-5.40
-5.45
210
200
190
180
170
160
150
140
130
120
110
100
90
80
70
60
50
40
30
20
10
0
-10
f1 (ppm)

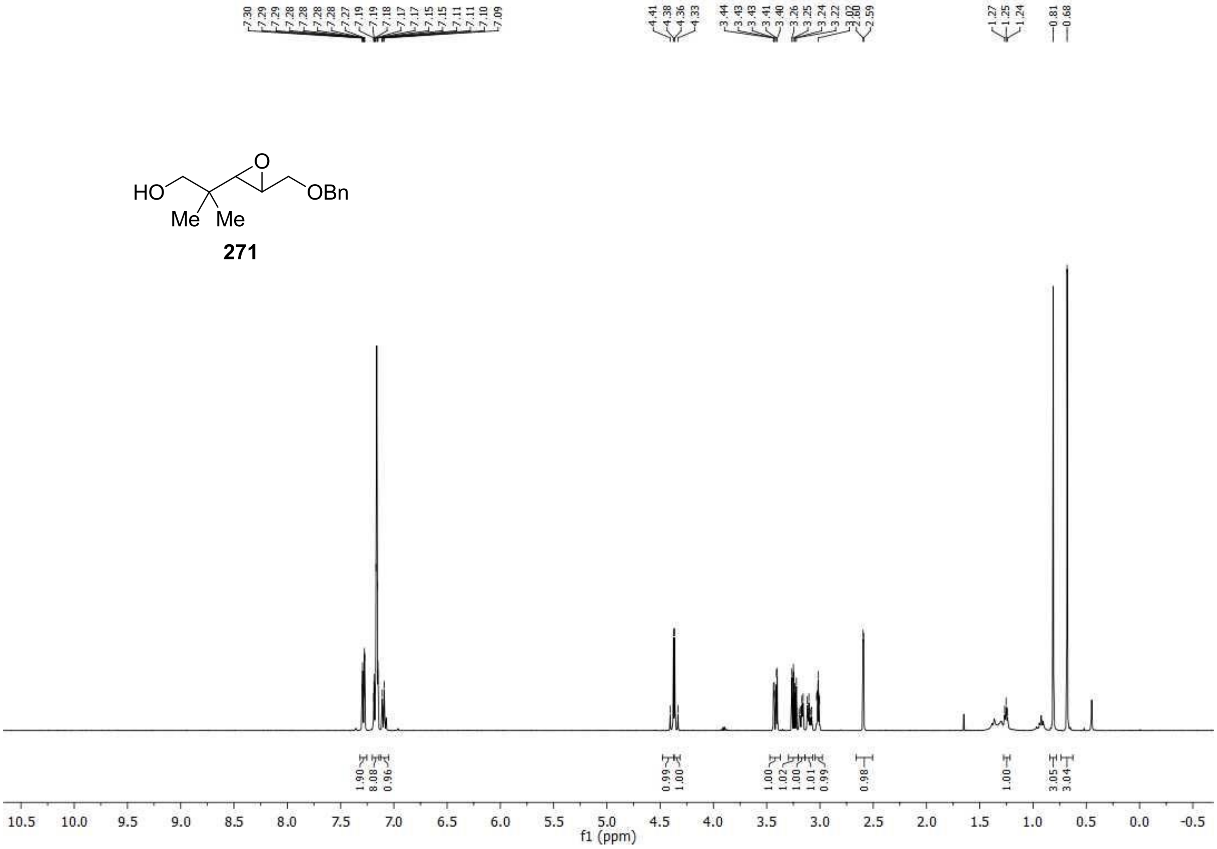
7.30
7.29
7.29
7.28
7.28
7.28
7.28
7.27
7.19
7.19
7.18
7.17
7.17
7.15
7.15
7.11
7.11
7.10
7.09
4.41
4.38
4.36
4.33
3.44
3.43
3.43
3.41
3.40
3.26
3.25
3.24
3.22
3.02
3.00
2.59
1.27
1.25
1.24
0.81
0.68
HO
O
OBn
Me
Me
1.90
8.08
0.96
0.99
1.00
1.00
1.02
1.00
1.01
0.99
0.98
1.00
3.05
3.04
10.5
10.0
9.5
9.0
8.5
8.0
7.5
7.0
6.5
6.0
5.5
5.0
4.5
4.0
3.5
3.0
2.5
2.0
1.5
1.0
0.5
0.0
-0.5
f1 (ppm)

271

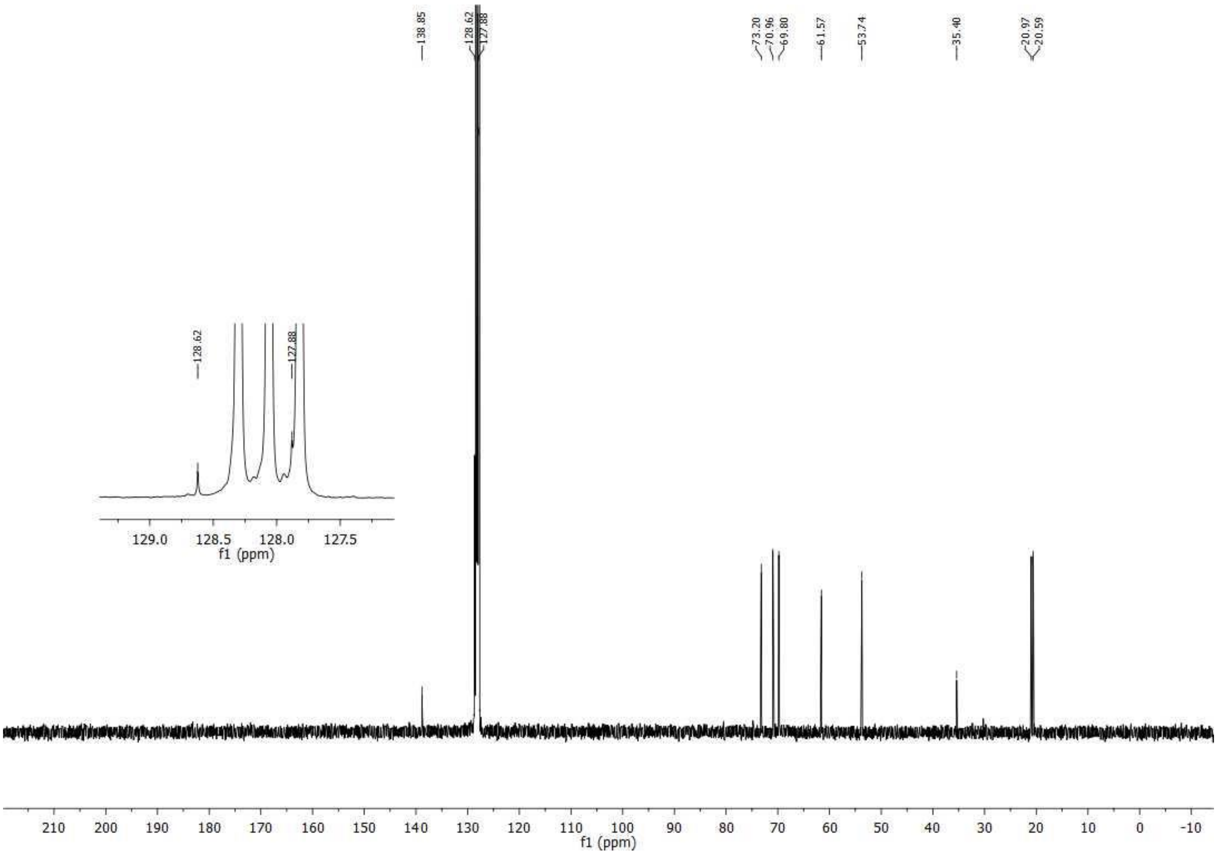
138.85
128.62
127.88
73.20
70.96
69.80
61.57
53.74
35.40
20.97
20.59
128.62
127.88
129.0
128.5
128.0
127.5
f1 (ppm)
210
200
190
180
170
160
150
140
130
120
110
100
90
80
70
60
50
40
30
20
10
0
-10
f1 (ppm)

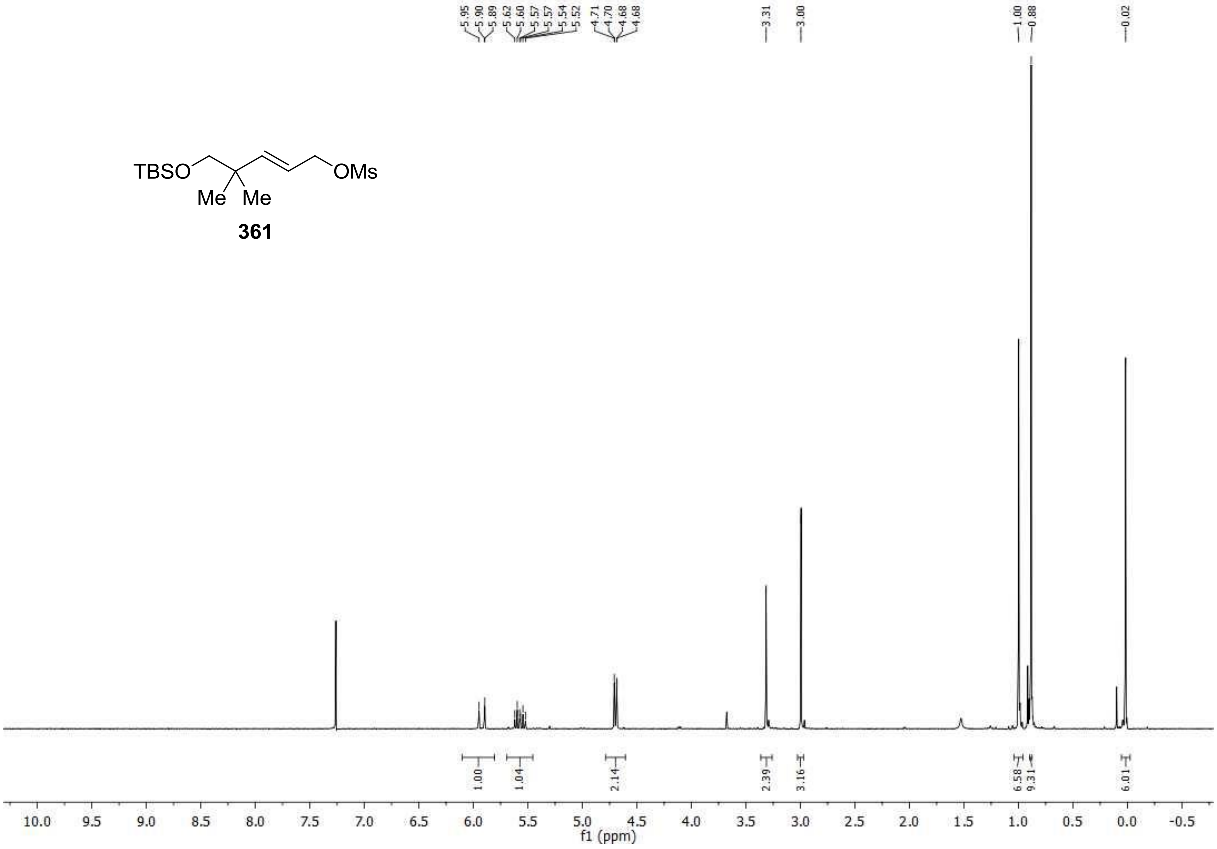

361

TBSO
OMs
Me Me
5.95
5.90
5.89
5.62
5.60
5.57
5.57
5.54
5.52
4.71
4.70
4.68
4.68
3.31
3.00
1.00
0.88
0.02
1.00
1.04
2.14
2.39
3.16
6.58
9.31
6.01
10.0
9.5
9.0
8.5
8.0
7.5
7.0
6.5
6.0
5.5
5.0
4.5
4.0
3.5
3.0
2.5
2.0
1.5
1.0
0.5
0.0
-0.5
f1 (ppm)

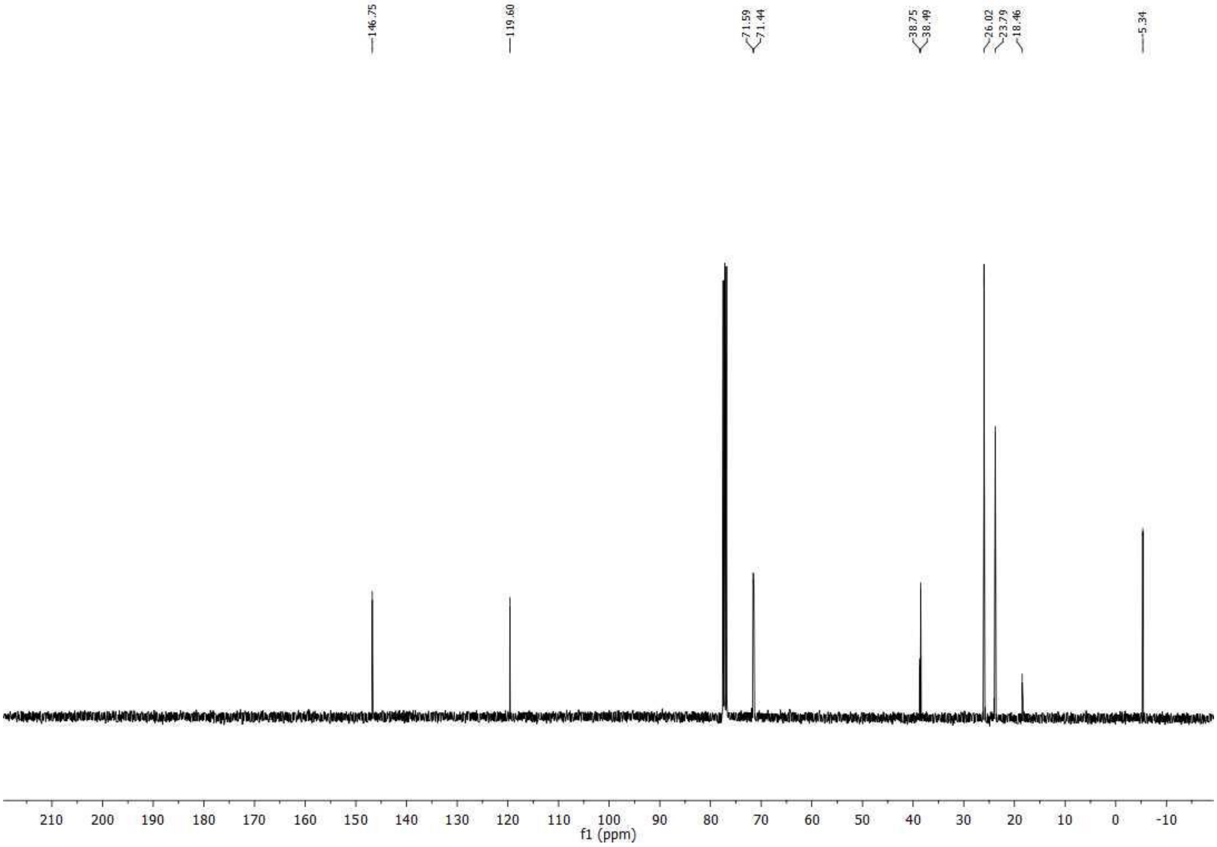

146.75
119.60
71.59
71.44
38.75
38.49
26.02
23.79
18.46
5.34
210
200
190
180
170
160
150
140
130
120
110
100
90
80
70
60
50
40
30
20
10
0
-10
f1 (ppm)

HO
O
Me
Me
Me

273

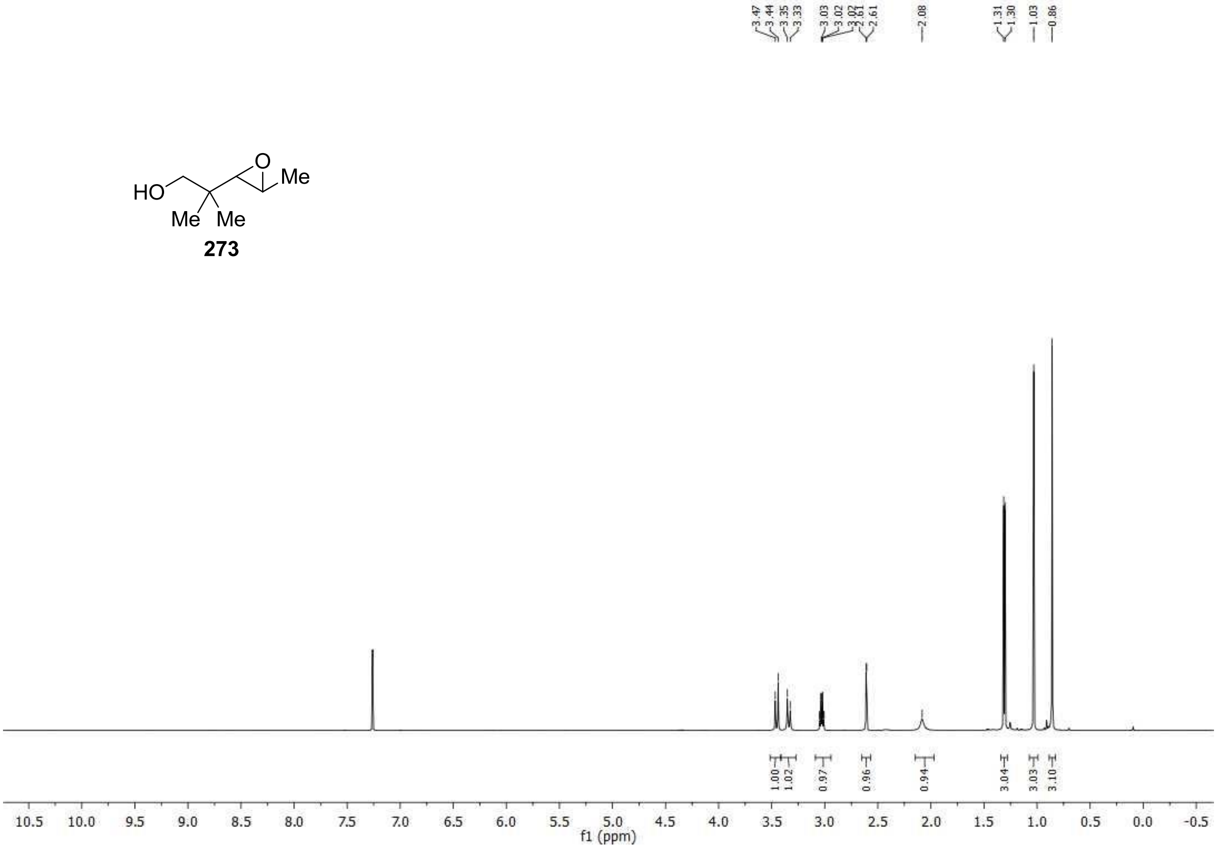
3.47
3.44
3.35
3.33
3.03
3.02
3.02
2.61
2.61
2.08
1.31
1.30
1.03
0.86
1.00
1.02
0.97
0.96
0.94
3.04
3.03
3.10
10.5
10.0
9.5
9.0
8.5
8.0
7.5
7.0
6.5
6.0
5.5
5.0
4.5
4.0
3.5
3.0
2.5
2.0
1.5
1.0
0.5
0.0
-0.5
f1 (ppm)

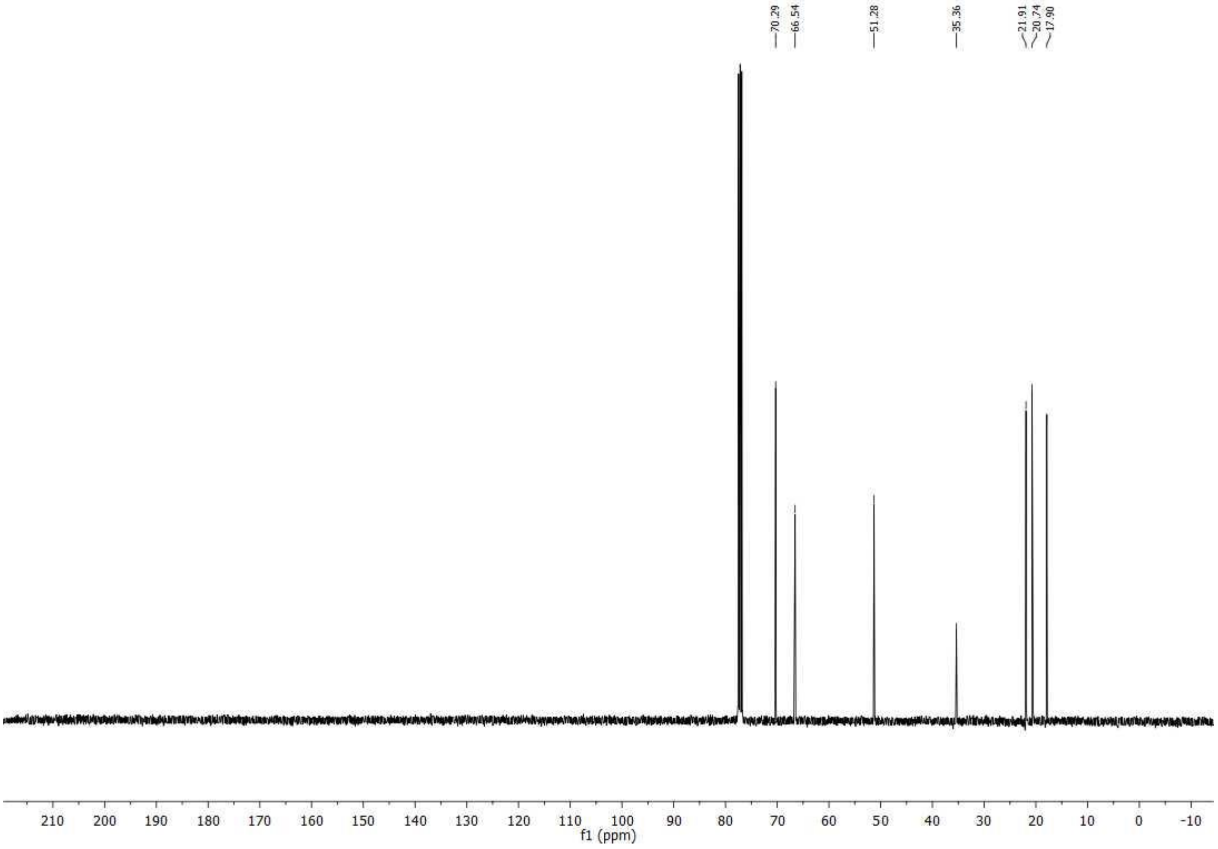
70.29
66.54
51.28
35.36
21.91
20.74
17.90
210
200
190
180
170
160
150
140
130
120
110
100
90
80
70
60
50
40
30
20
10
0
-10
f1 (ppm)

OTBDPS
O

363

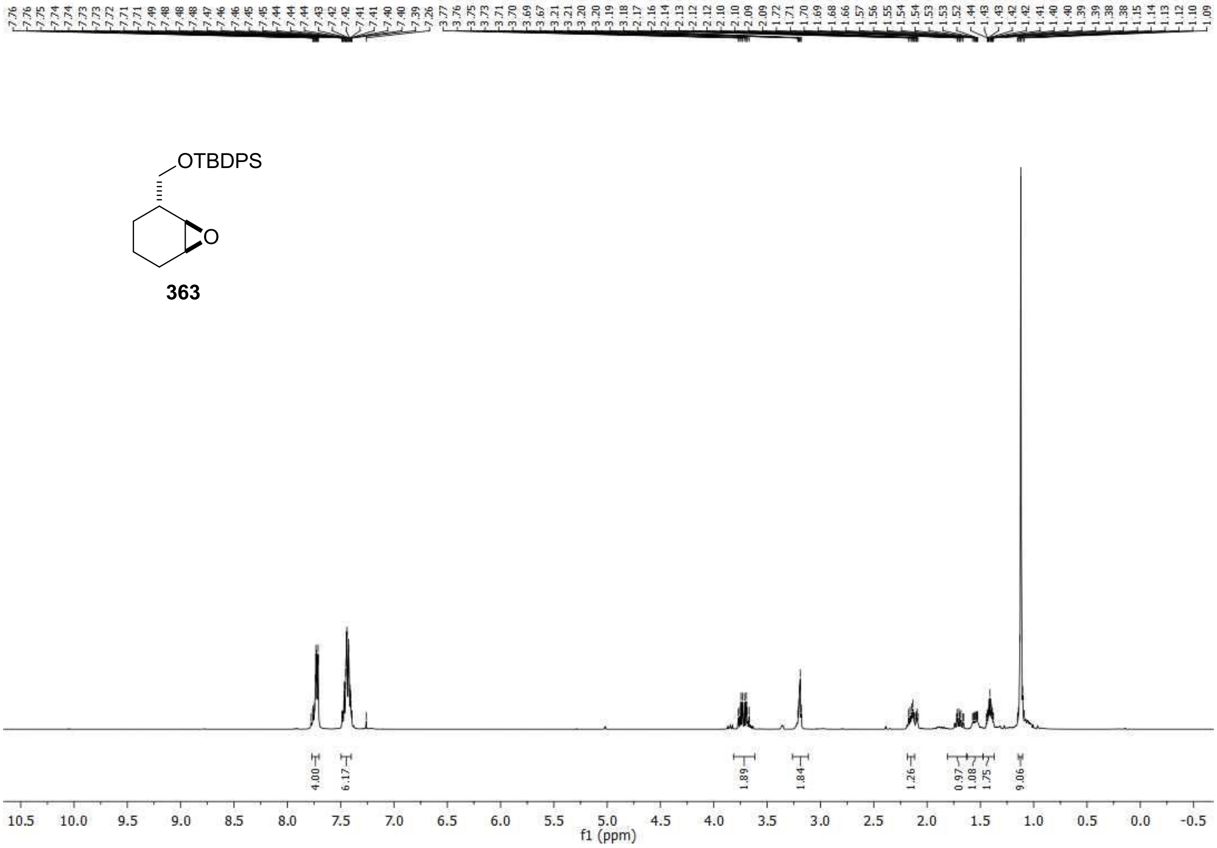
7.76
7.76
7.75
7.74
7.74
7.73
7.73
7.72
7.71
7.71
7.49
7.48
7.48
7.48
7.47
7.46
7.46
7.45
7.45
7.44
7.44
7.43
7.42
7.42
7.41
7.41
7.40
7.40
7.39
7.26
3.77
3.76
3.75
3.73
3.71
3.70
3.69
3.67
3.21
3.21
3.20
3.20
3.19
3.18
2.17
2.16
2.14
2.13
2.12
2.12
2.10
2.10
2.09
2.09
1.72
1.71
1.70
1.69
1.68
1.66
1.57
1.56
1.55
1.55
1.54
1.54
1.53
1.53
1.52
1.44
1.43
1.43
1.42
1.42
1.41
1.40
1.40
1.39
1.39
1.38
1.38
1.15
1.14
1.13
1.12
1.10
1.09
4.00
6.17
1.89
1.84
1.26
0.97
1.08
1.75
9.06
10.5
10.0
9.5
9.0
8.5
8.0
7.5
7.0
6.5
6.0
5.5
5.0
4.5
4.0
3.5
3.0
2.5
2.0
1.5
1.0
0.5
0.0
-0.5
f1 (ppm)

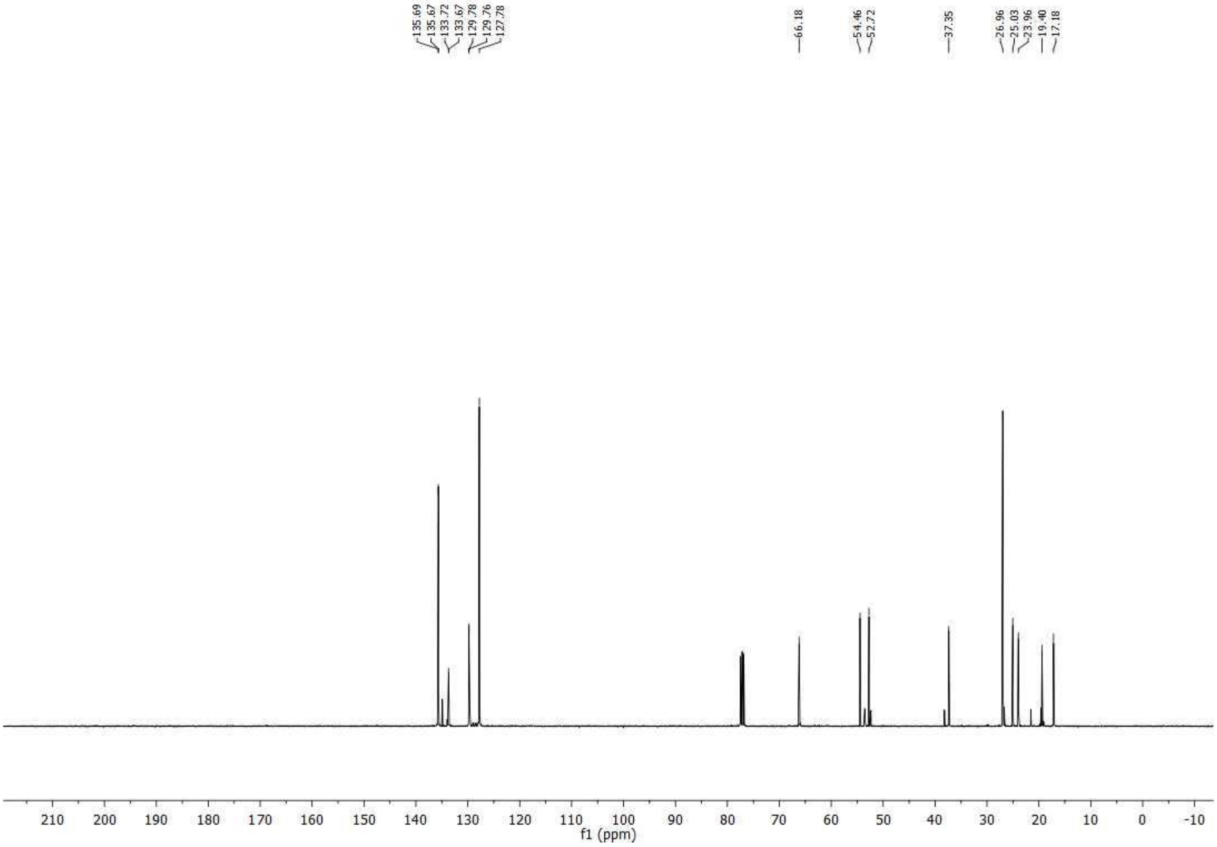
135.69
135.67
133.72
133.67
129.78
129.76
127.78
66.18
54.46
52.72
37.35
26.96
25.03
23.96
19.40
17.18
210
200
190
180
170
160
150
140
130
120
110
100
90
80
70
60
50
40
30
20
10
0
-10
f1 (ppm)

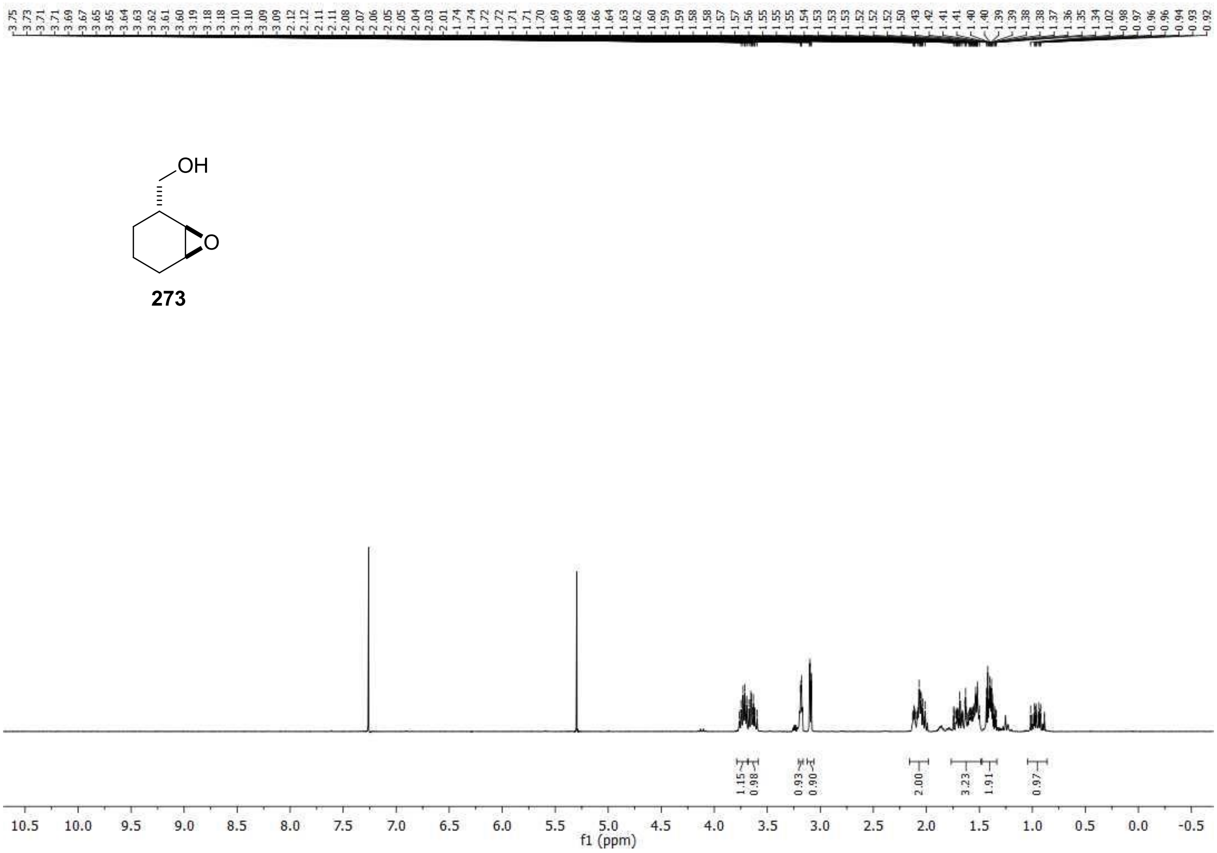
3.75
3.73
3.71
3.71
3.69
3.67
3.65
3.65
3.64
3.63
3.62
3.61
3.60
3.19
3.18
3.18
3.10
3.10
3.09
3.09
2.12
2.12
2.11
2.11
2.08
2.07
2.06
2.05
2.05
2.04
2.03
2.01
1.74
1.74
1.72
1.72
1.71
1.71
1.70
1.69
1.69
1.68
1.66
1.64
1.63
1.62
1.60
1.59
1.59
1.58
1.58
1.57
1.56
1.55
1.55
1.55
1.54
1.53
1.53
1.53
1.52
1.52
1.52
1.50
1.43
1.42
1.41
1.41
1.40
1.40
1.39
1.39
1.38
1.38
1.37
1.36
1.35
1.34
1.02
0.98
0.97
0.96
0.96
0.94
0.93
0.92
OH
O
273
1.15
0.98
0.93
0.90
2.00
3.23
1.91
0.97
10.5
10.0
9.5
9.0
8.5
8.0
7.5
7.0
6.5
6.0
5.5
5.0
4.5
4.0
3.5
3.0
2.5
2.0
1.5
1.0
0.5
0.0
-0.5
f1 (ppm)

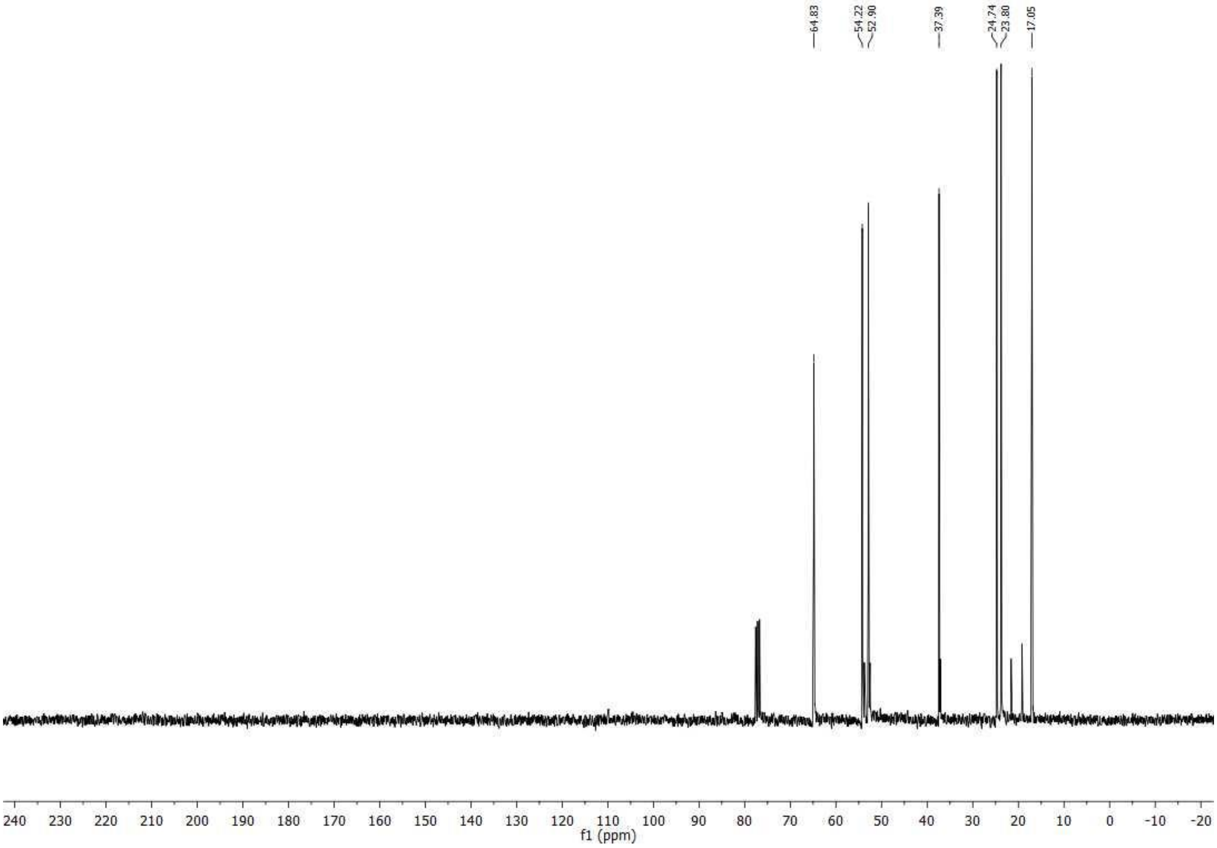
64.83
54.22
52.90
37.39
24.74
23.80
17.05
240
230
220
210
200
190
180
170
160
150
140
130
120
110
100
90
80
70
60
50
40
30
20
10
0
-10
-20
f1 (ppm)

CO$_2$Et

279

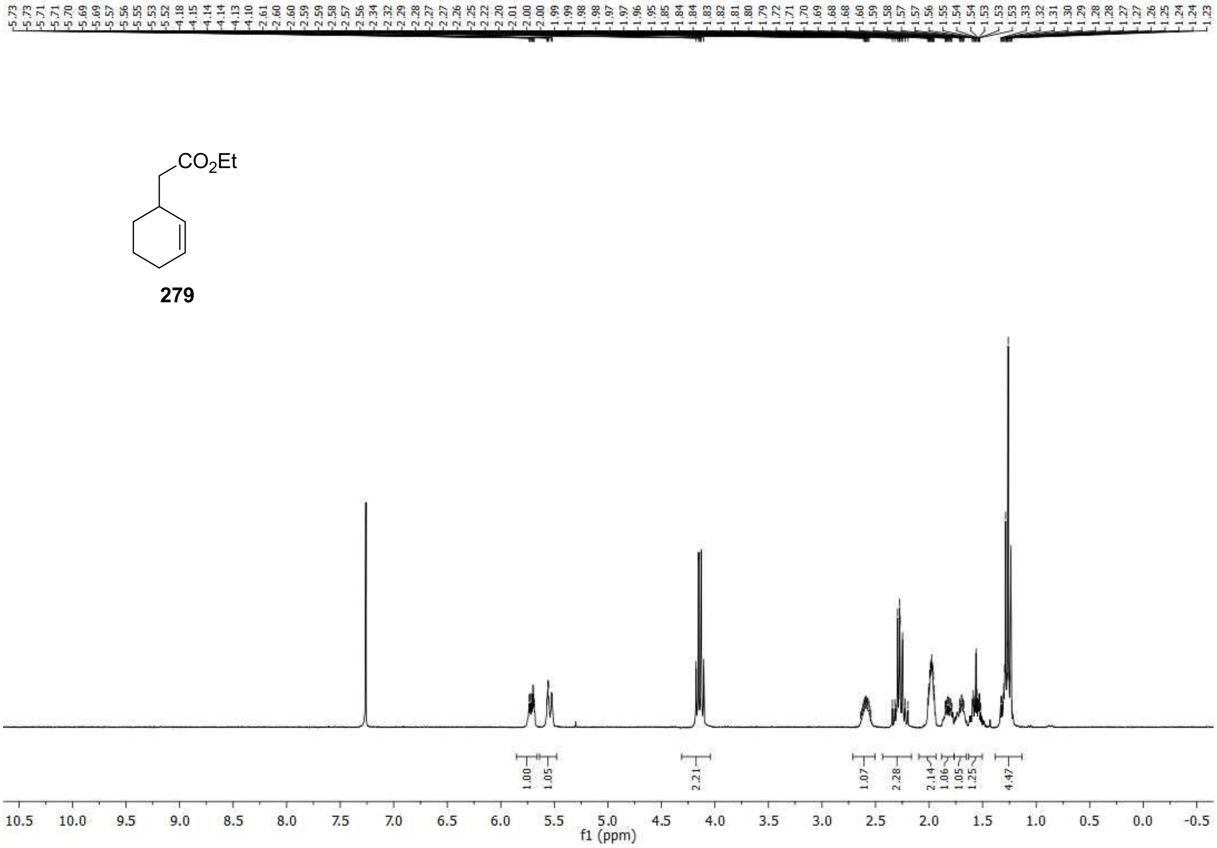
5.73
5.73
5.71
5.70
5.69
5.69
5.57
5.56
5.55
5.53
5.52
4.18
4.15
4.14
4.14
4.13
4.10
2.61
2.60
2.59
2.59
2.58
2.57
2.56
2.34
2.32
2.29
2.28
2.27
2.27
2.26
2.25
2.22
2.20
2.01
2.00
2.00
1.99
1.99
1.98
1.98
1.97
1.97
1.96
1.95
1.85
1.84
1.84
1.83
1.82
1.81
1.80
1.79
1.72
1.71
1.70
1.69
1.68
1.68
1.60
1.59
1.58
1.57
1.57
1.56
1.55
1.54
1.54
1.53
1.53
1.53
1.33
1.32
1.31
1.30
1.29
1.28
1.28
1.27
1.27
1.26
1.25
1.24
1.24
1.23
1.00
1.05
2.21
1.07
2.28
2.14
1.06
1.05
1.25
4.47
10.5
10.0
9.5
9.0
8.5
8.0
7.5
7.0
6.5
6.0
5.5
5.0
4.5
4.0
3.5
3.0
2.5
2.0
1.5
1.0
0.5
0.0
-0.5
f1 (ppm)

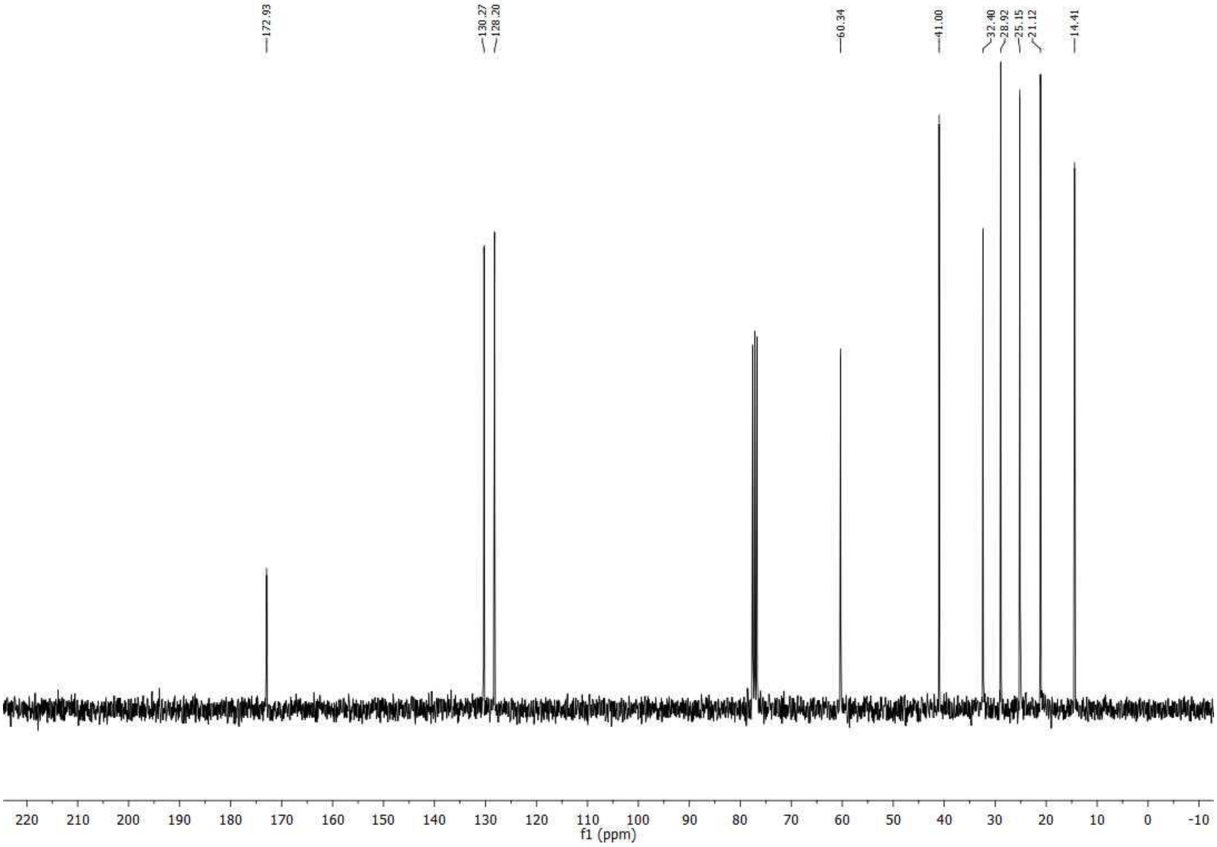
172.93
130.27
128.20
60.34
41.00
32.40
28.92
25.15
21.12
14.41
220
210
200
190
180
170
160
150
140
130
120
110
100
90
80
70
60
50
40
30
20
10
0
-10
f1 (ppm)

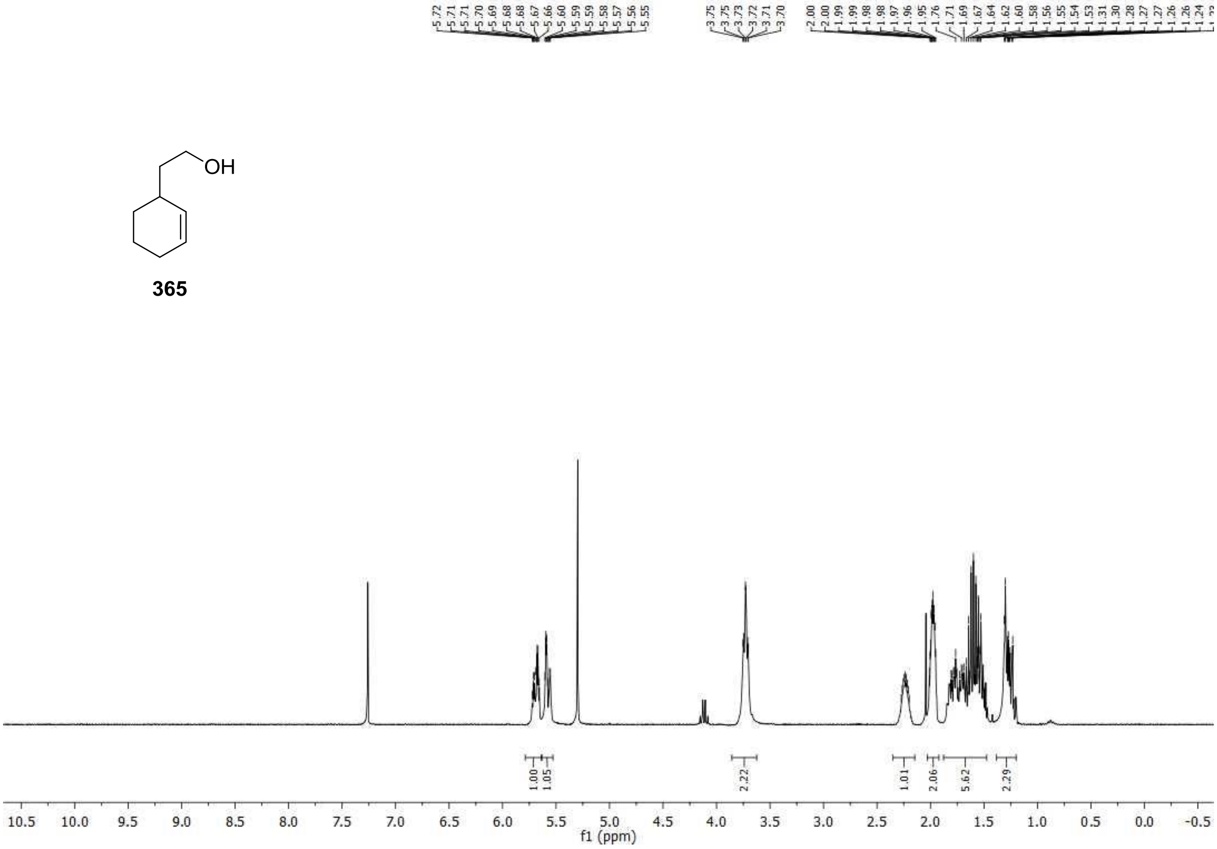
OH

365

5.72
5.71
5.71
5.70
5.69
5.68
5.68
5.67
5.66
5.60
5.59
5.59
5.58
5.57
5.56
5.55
3.75
3.75
3.73
3.72
3.71
3.70
2.00
2.00
1.99
1.99
1.98
1.98
1.97
1.96
1.95
1.76
1.71
1.69
1.67
1.64
1.62
1.60
1.58
1.56
1.55
1.54
1.53
1.31
1.30
1.28
1.27
1.27
1.26
1.26
1.24
1.00
1.05
2.22
1.01
2.06
5.62
2.29
10.5
10.0
9.5
9.0
8.5
8.0
7.5
7.0
6.5
6.0
5.5
5.0
4.5
4.0
3.5
3.0
2.5
2.0
1.5
1.0
0.5
0.0
-0.5
f1 (ppm)

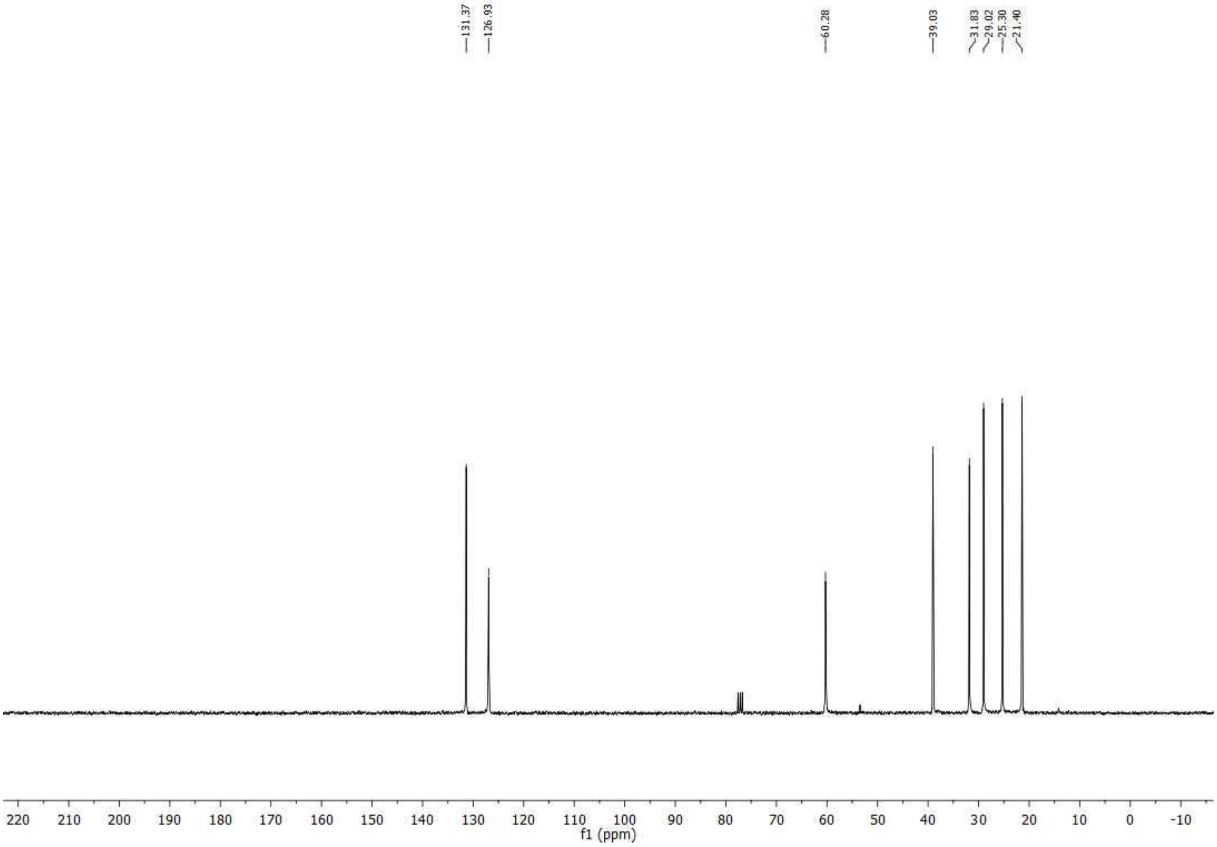
131.37
126.93
60.28
39.03
31.83
29.02
25.30
21.40
220
210
200
190
180
170
160
150
140
130
120
110
100
90
80
70
60
50
40
30
20
10
0
-10
f1 (ppm)

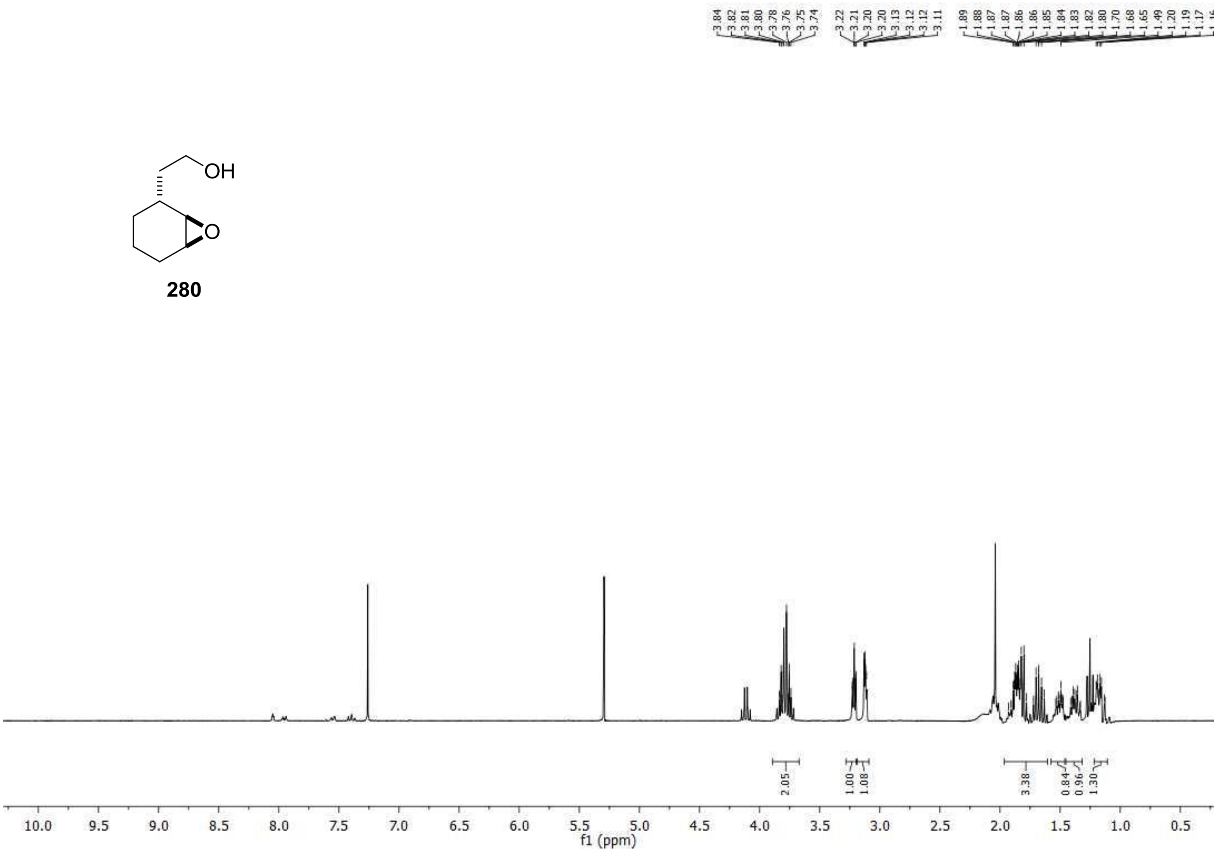
3.84
3.82
3.81
3.80
3.78
3.76
3.75
3.74
3.22
3.21
3.20
3.20
3.13
3.12
3.12
3.11
1.89
1.88
1.87
1.87
1.86
1.86
1.85
1.84
1.83
1.82
1.80
1.70
1.68
1.65
1.49
1.20
1.19
1.17
OH
O
2.05
1.00
1.08
3.38
0.84
0.96
1.30
10.0
9.5
9.0
8.5
8.0
7.5
7.0
6.5
6.0
5.5
5.0
4.5
4.0
3.5
3.0
2.5
2.0
1.5
1.0
0.5
f1 (ppm)

280

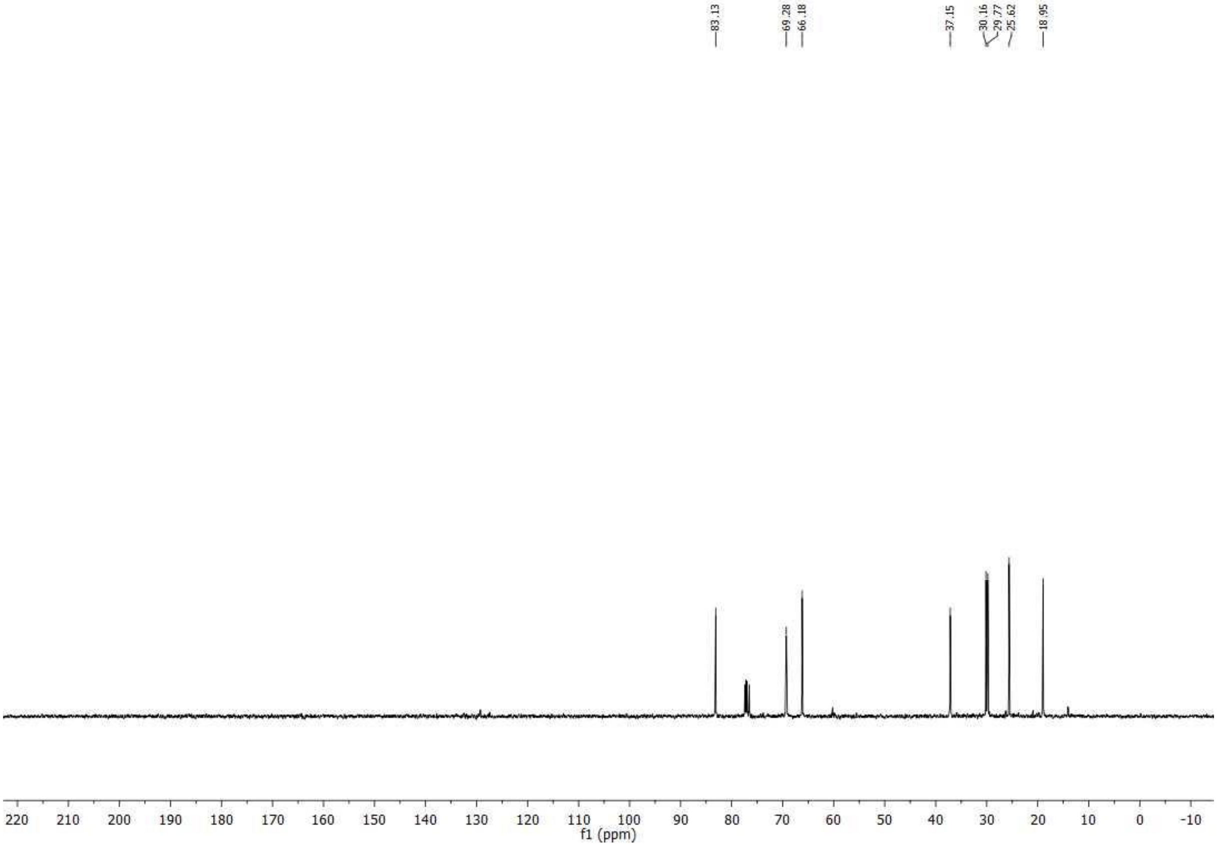
83.13
69.28
66.18
37.15
30.16
29.77
25.62
18.95
220
210
200
190
180
170
160
150
140
130
120
110
100
90
80
70
60
50
40
30
20
10
0
-10
f1 (ppm)

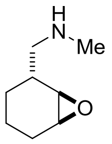
H
N
Me
O

283

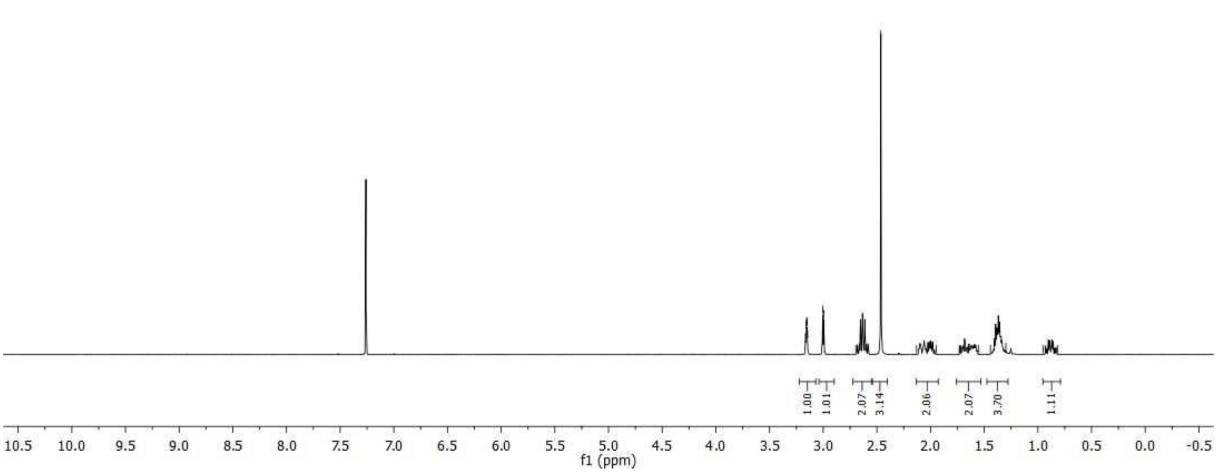
3.17
3.16
3.16
3.15
3.15
3.00
2.99
2.70
2.58
2.46
2.13
1.95
1.73
1.55
1.44
1.30
0.95
0.81
1.00
1.01
2.07
3.14
2.06
2.07
3.70
1.11
10.5
10.0
9.5
9.0
8.5
8.0
7.5
7.0
6.5
6.0
5.5
5.0
4.5
4.0
3.5
3.0
2.5
2.0
1.5
1.0
0.5
0.0
-0.5
f1 (ppm)

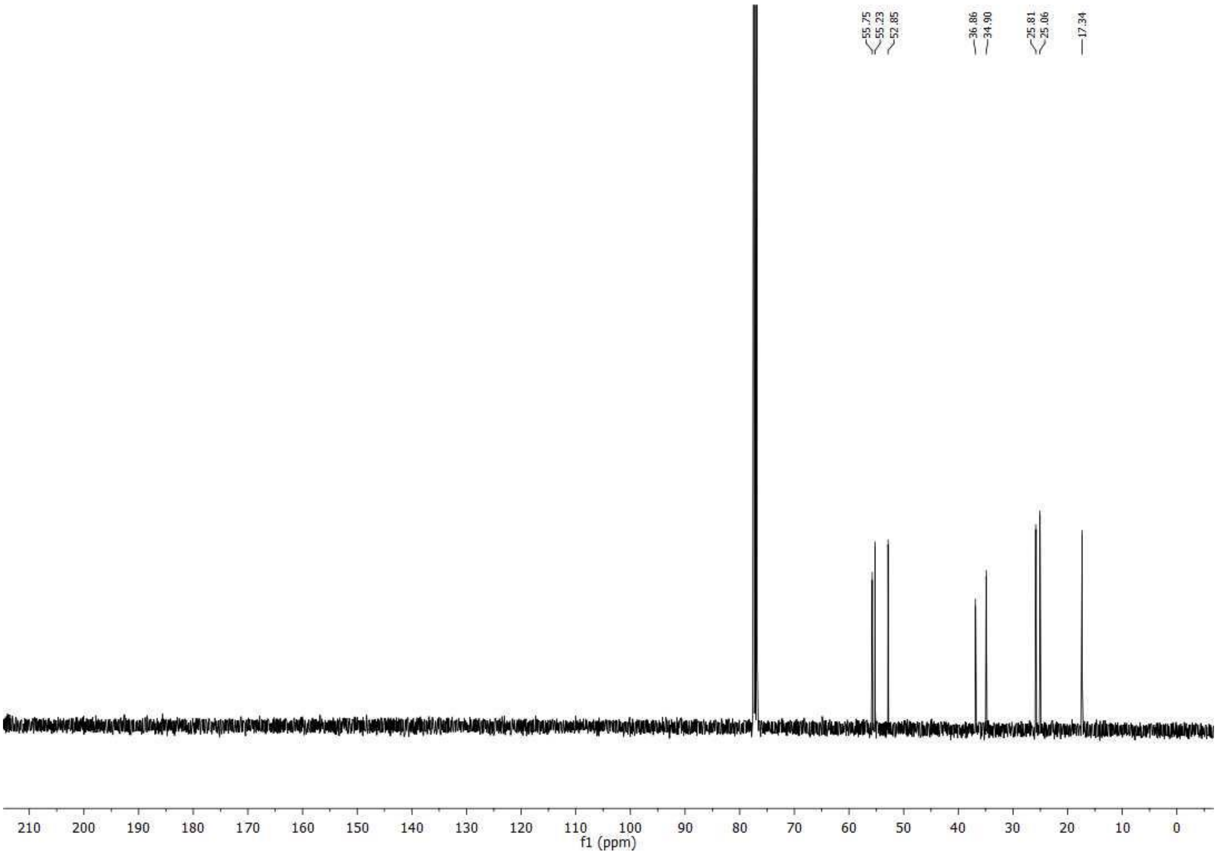
55.75
55.23
52.85
36.86
34.90
25.81
25.06
17.34
210
200
190
180
170
160
150
140
130
120
110
100
90
80
70
60
50
40
30
20
10
0
f1 (ppm)

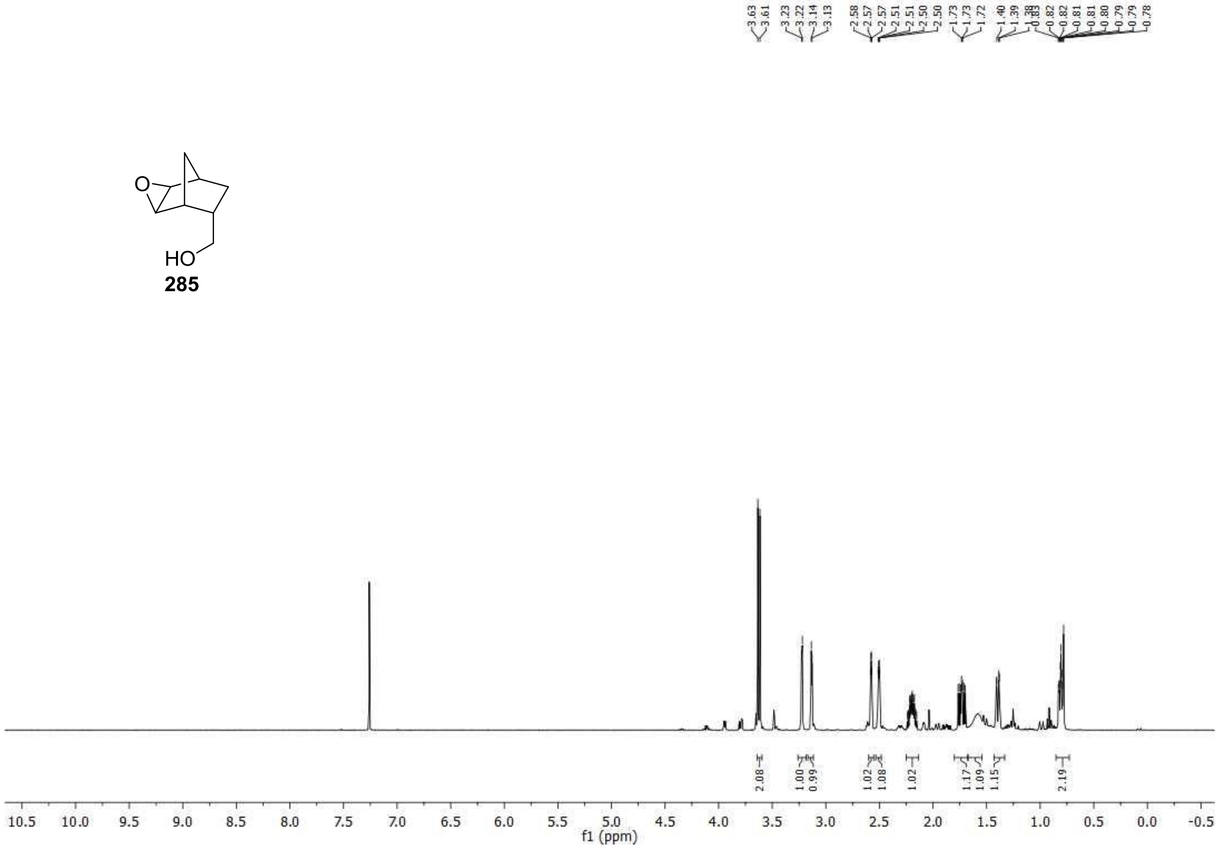
O
HO

285

3.63
3.61
3.23
3.22
3.14
3.13
2.58
2.57
2.57
2.51
2.51
2.50
2.50
1.73
1.73
1.72
1.40
1.39
1.38
0.83
0.82
0.82
0.81
0.81
0.80
0.79
0.79
0.78
2.08
1.00
0.99
1.02
1.08
1.02
1.17
1.09
1.15
2.19
10.5
10.0
9.5
9.0
8.5
8.0
7.5
7.0
6.5
6.0
5.5
5.0
4.5
4.0
3.5
3.0
2.5
2.0
1.5
1.0
0.5
0.0
-0.5
f1 (ppm)

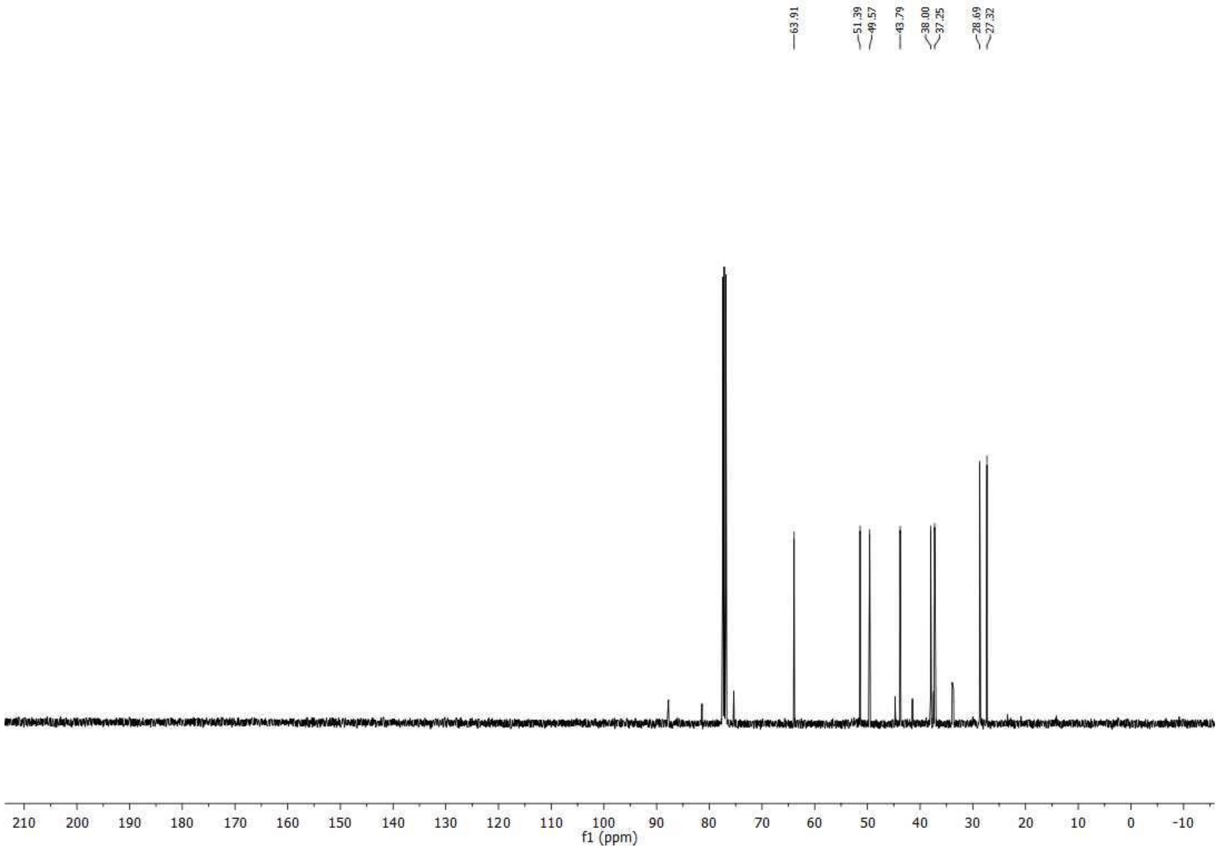
63.91
51.39
49.57
43.79
38.00
37.25
28.69
27.32
210
200
190
180
170
160
150
140
130
120
110
100
90
80
70
60
50
40
30
20
10
0
-10
f1 (ppm)

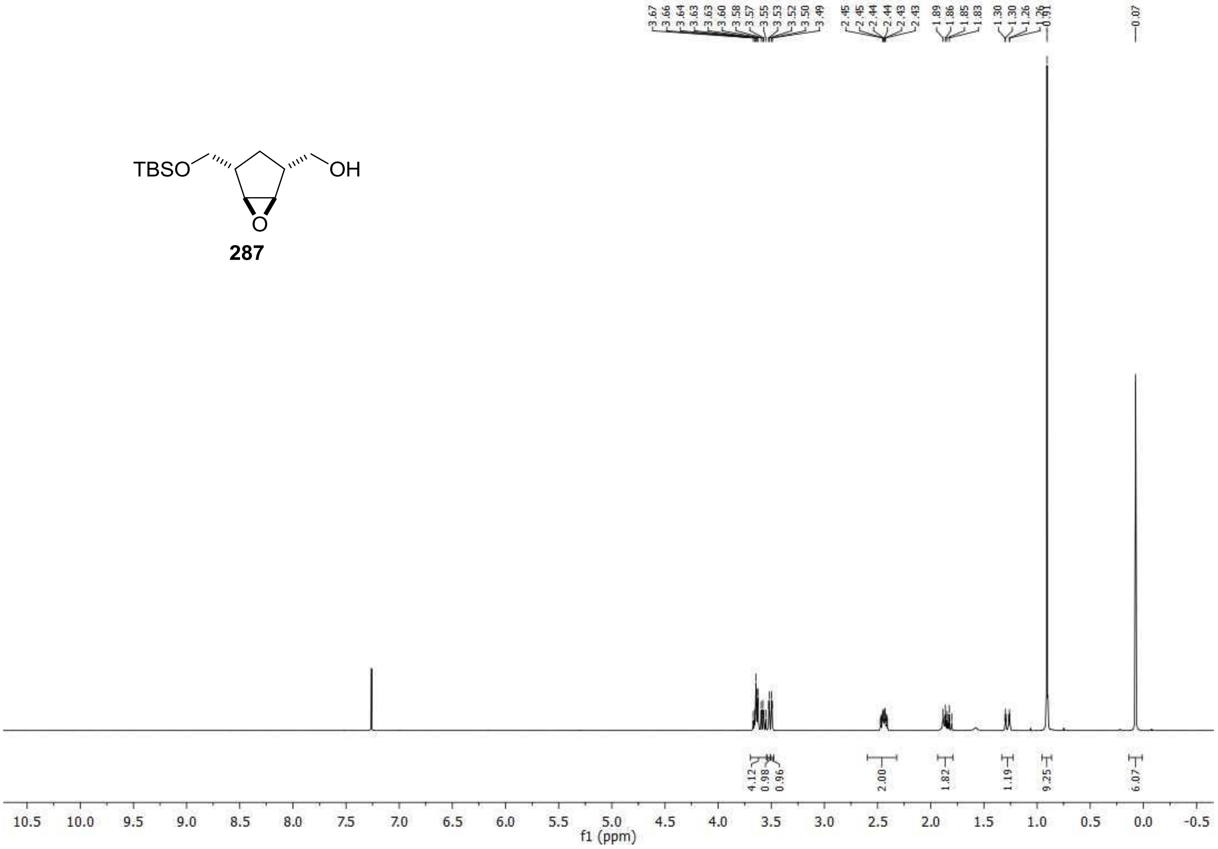
TBSO
OH
O
3.67
3.66
3.64
3.63
3.63
3.60
3.58
3.57
3.55
3.53
3.52
3.50
3.49
2.45
2.45
2.44
2.44
2.43
2.43
1.89
1.86
1.85
1.83
1.30
1.30
1.26
1.26
0.91
0.07
4.12
0.98
0.96
2.00
1.82
1.19
9.25
6.07
10.5
10.0
9.5
9.0
8.5
8.0
7.5
7.0
6.5
6.0
5.5
5.0
4.5
4.0
3.5
3.0
2.5
2.0
1.5
1.0
0.5
0.0
-0.5
f1 (ppm)

287

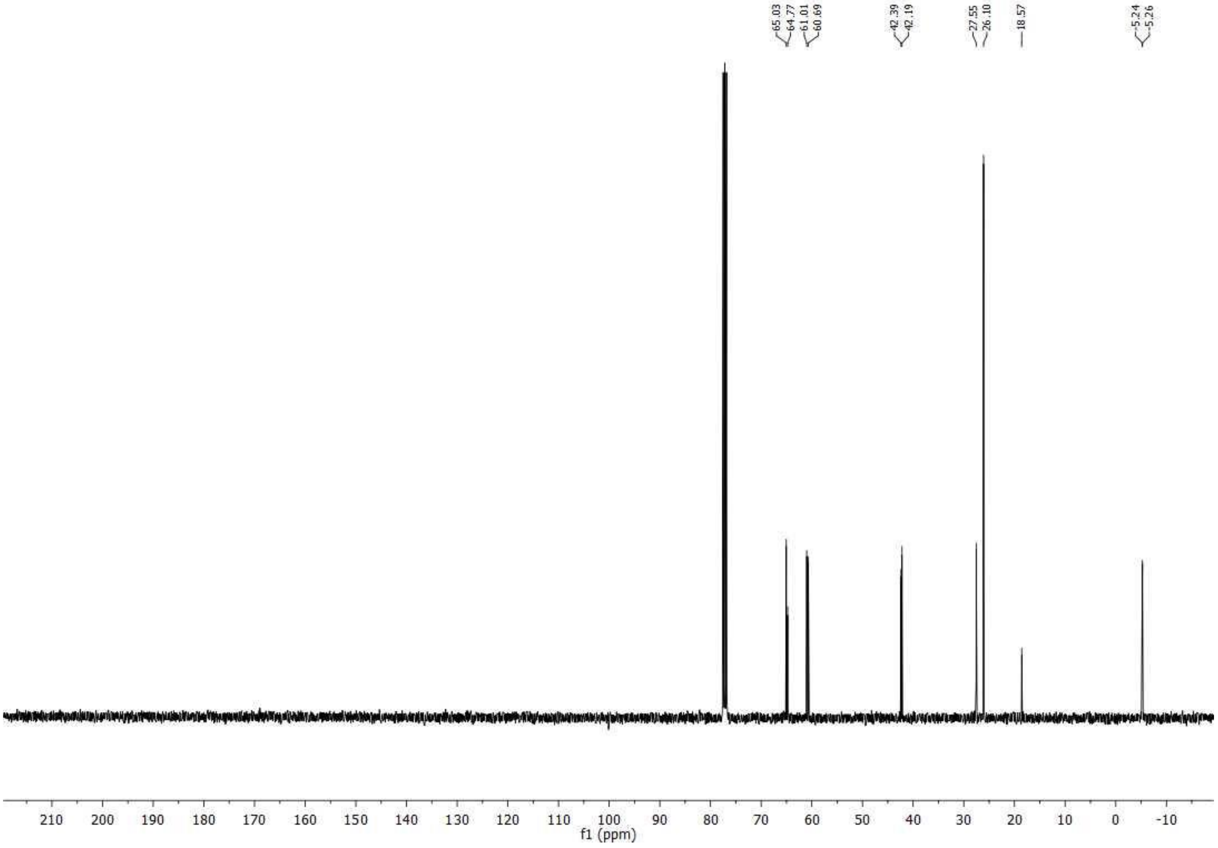
65.03
64.77
61.01
60.69
42.39
42.19
27.55
26.10
18.57
-5.24
-5.26
210
200
190
180
170
160
150
140
130
120
110
100
90
80
70
60
50
40
30
20
10
0
-10
f1 (ppm)

OH
O
Me

290

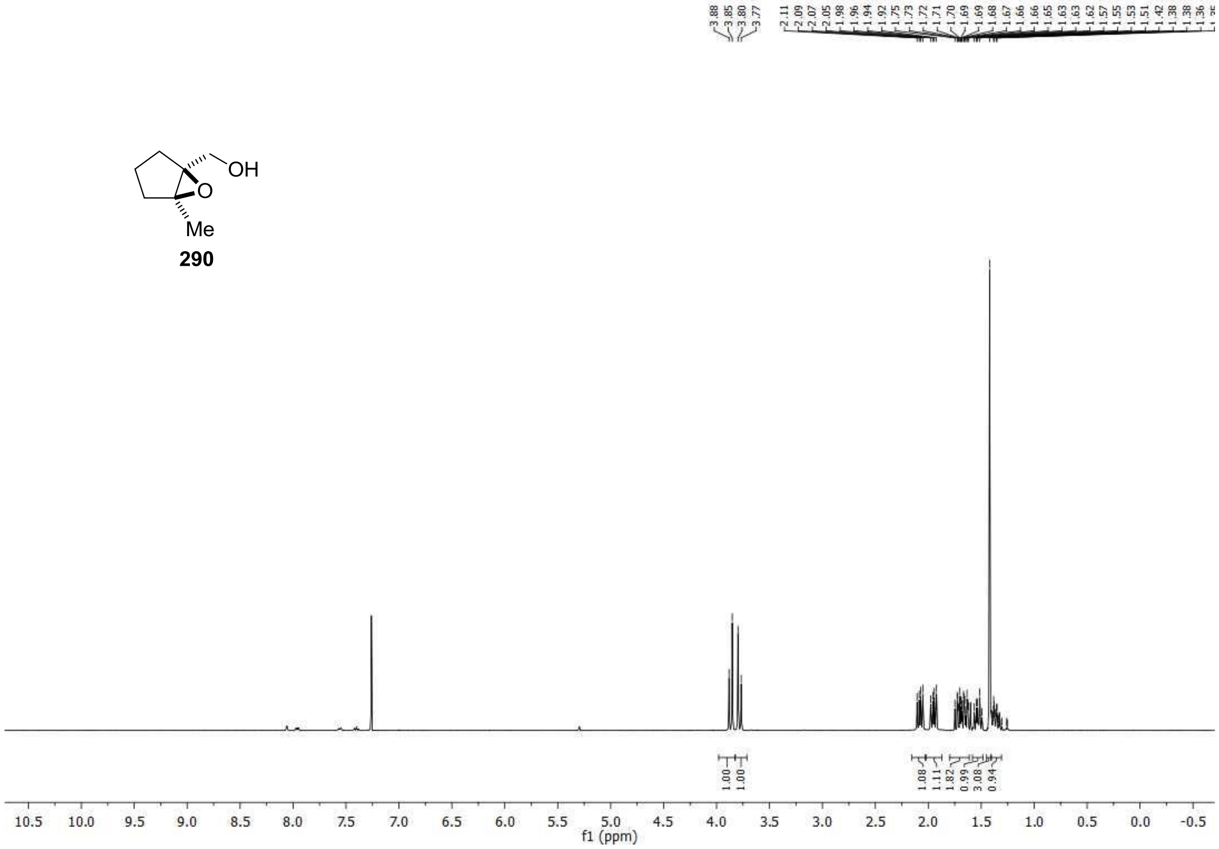
3.88
3.85
3.80
3.77
2.11
2.09
2.07
2.05
1.98
1.96
1.94
1.92
1.75
1.73
1.72
1.71
1.70
1.69
1.69
1.68
1.67
1.66
1.66
1.65
1.63
1.63
1.62
1.57
1.55
1.53
1.51
1.42
1.38
1.38
1.36
1.00
1.00
1.08
1.11
1.82
0.99
3.08
0.94
10.5
10.0
9.5
9.0
8.5
8.0
7.5
7.0
6.5
6.0
5.5
5.0
4.5
4.0
3.5
3.0
2.5
2.0
1.5
1.0
0.5
0.0
-0.5
f1 (ppm)

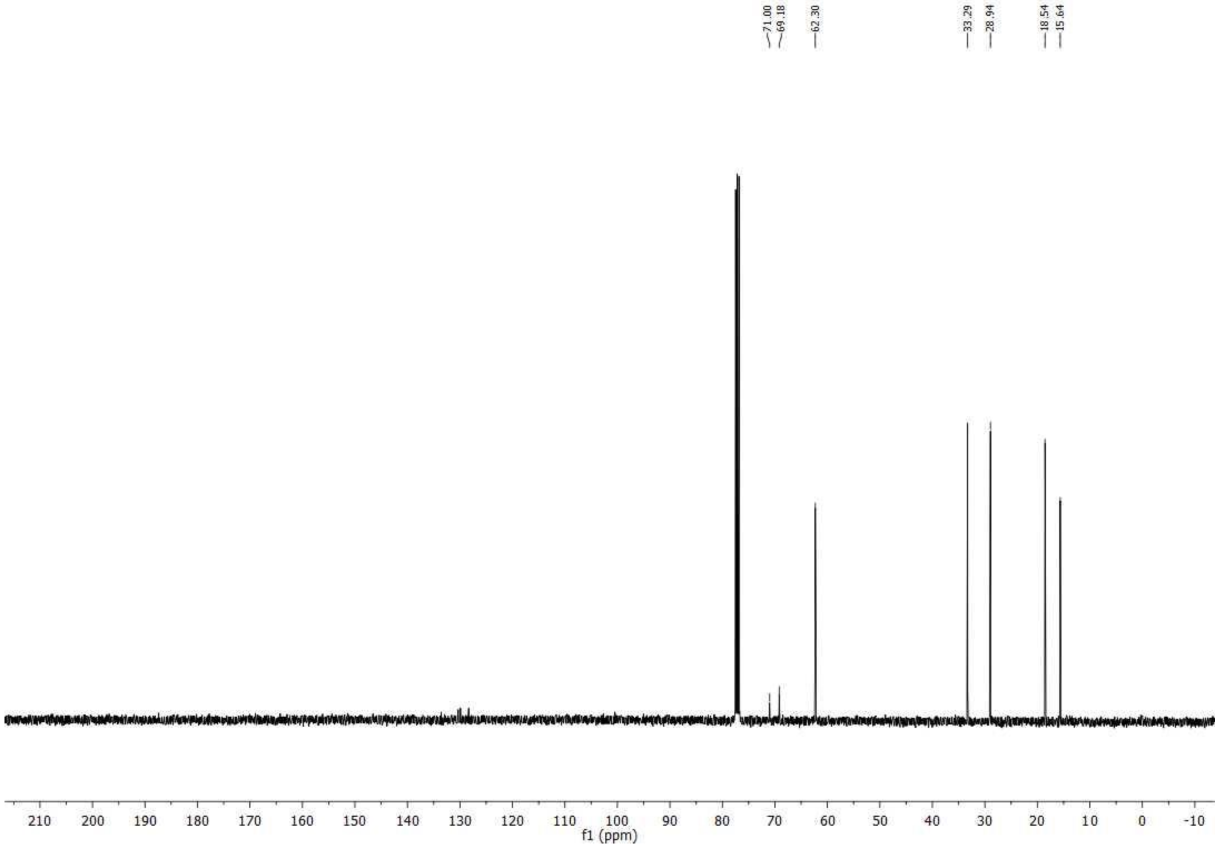
71.00
69.18
62.30
33.29
28.94
18.54
15.64
210
200
190
180
170
160
150
140
130
120
110
100
90
80
70
60
50
40
30
20
10
0
-10
f1 (ppm)

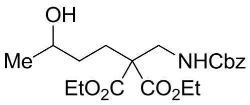
OH
Me
NHCbz
EtO₂C CO₂Et

296

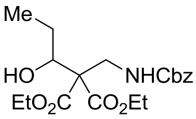
Me
HO
NHCbz
EtO₂C CO₂Et

297

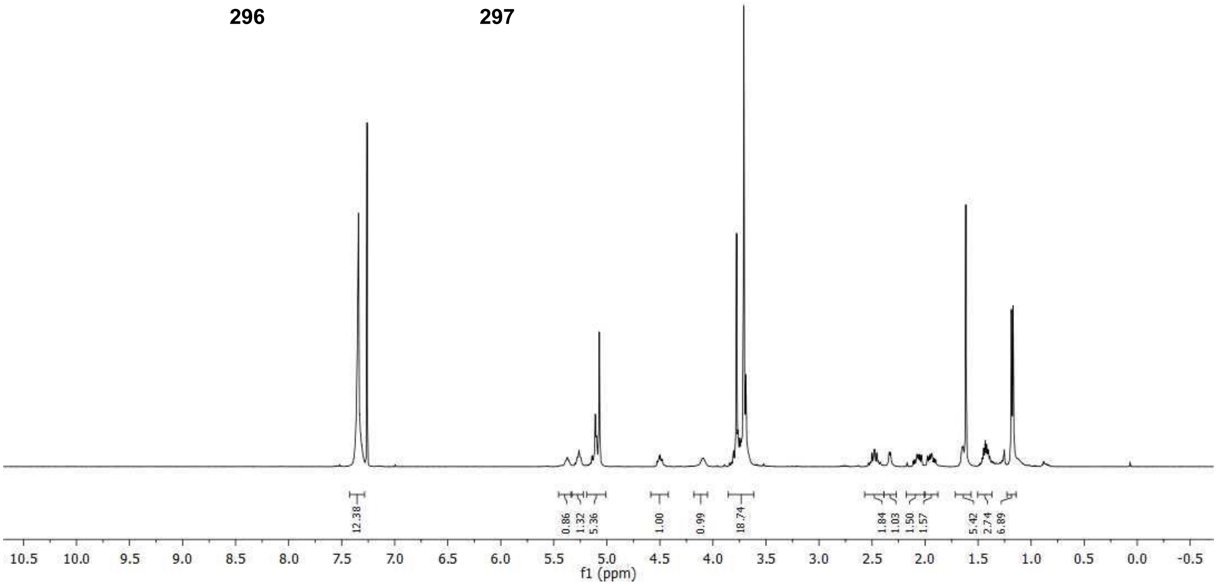
12.38
0.86
1.32
5.36
1.00
0.99
18.74
1.84
1.03
1.50
1.57
5.42
2.74
6.89
10.5
10.0
9.5
9.0
8.5
8.0
7.5
7.0
6.5
6.0
5.5
5.0
4.5
4.0
3.5
3.0
2.5
2.0
1.5
1.0
0.5
0.0
-0.5
f1 (ppm)

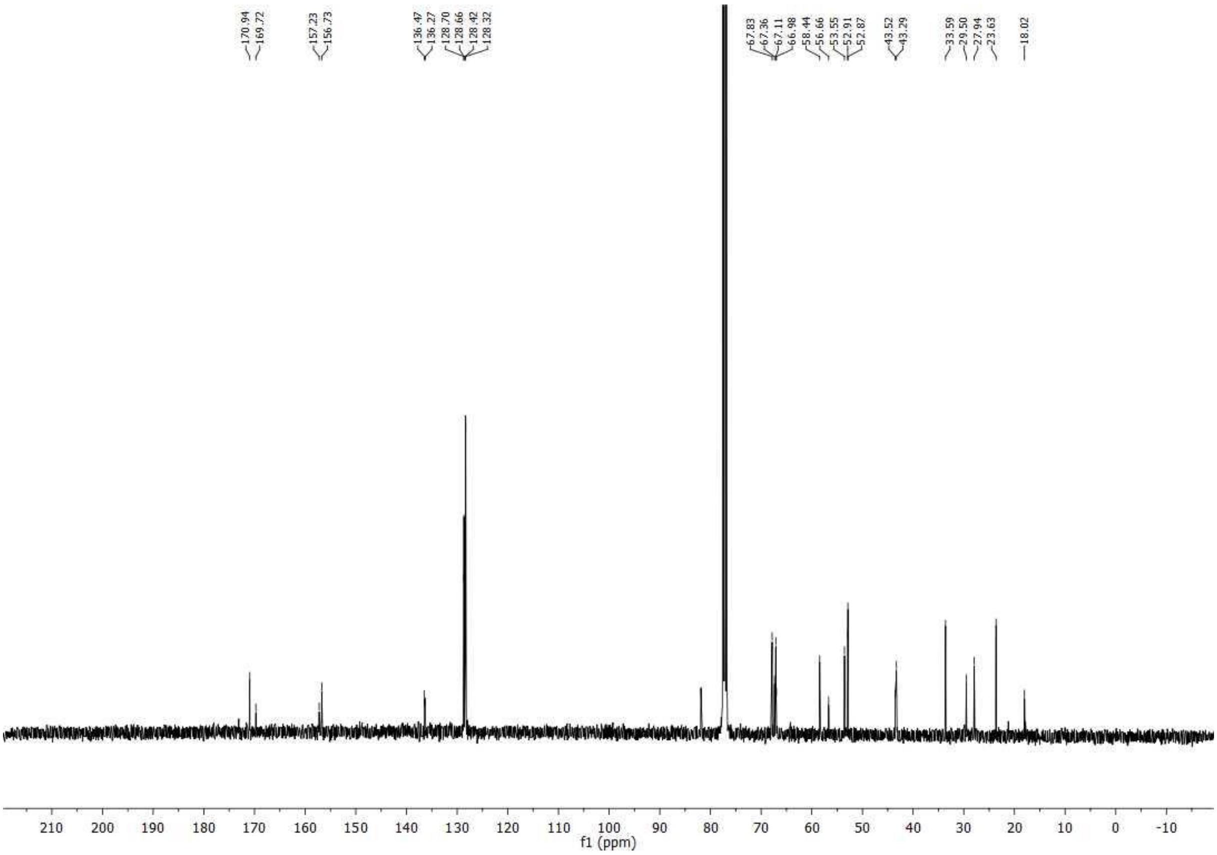
170.94
169.72
157.23
156.73
136.47
136.27
128.70
128.66
128.42
128.32
67.83
67.36
67.11
66.98
58.44
56.66
53.55
52.91
52.87
43.52
43.29
33.59
29.50
27.94
23.63
18.02
210
200
190
180
170
160
150
140
130
120
110
100
90
80
70
60
50
40
30
20
10
0
-10
f1 (ppm)

OH
Me
OH
EtO$_2$C
CO$_2$Et

298

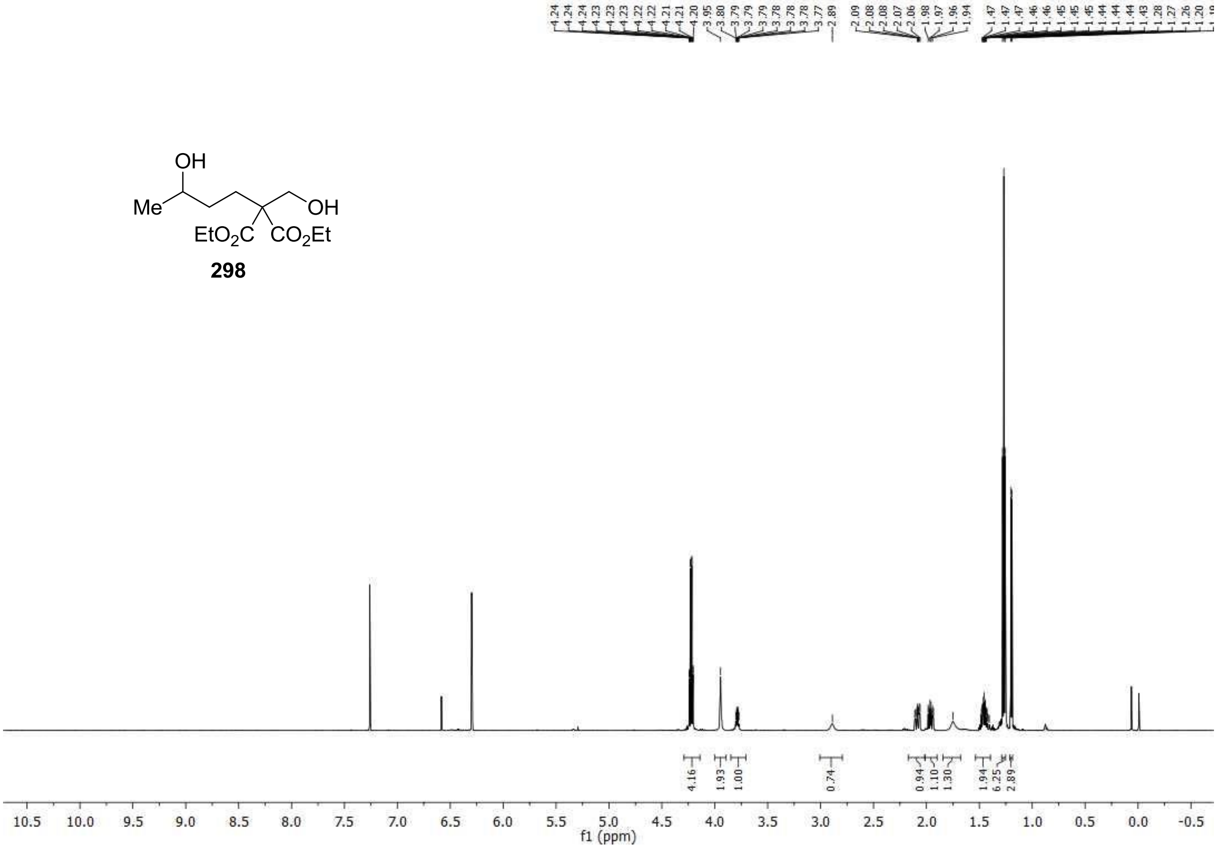
4.24
4.24
4.24
4.23
4.23
4.23
4.22
4.22
4.21
4.21
4.20
3.95
3.80
3.79
3.79
3.79
3.78
3.78
3.78
3.77
2.89
2.09
2.08
2.08
2.07
2.06
1.98
1.97
1.96
1.94
1.47
1.47
1.47
1.46
1.46
1.45
1.45
1.45
1.44
1.44
1.44
1.43
1.28
1.27
1.26
1.20
4.16
1.93
1.00
0.74
0.94
1.10
1.30
1.94
6.25
2.89
10.5
10.0
9.5
9.0
8.5
8.0
7.5
7.0
6.5
6.0
5.5
5.0
4.5
4.0
3.5
3.0
2.5
2.0
1.5
1.0
0.5
0.0
-0.5
f1 (ppm)

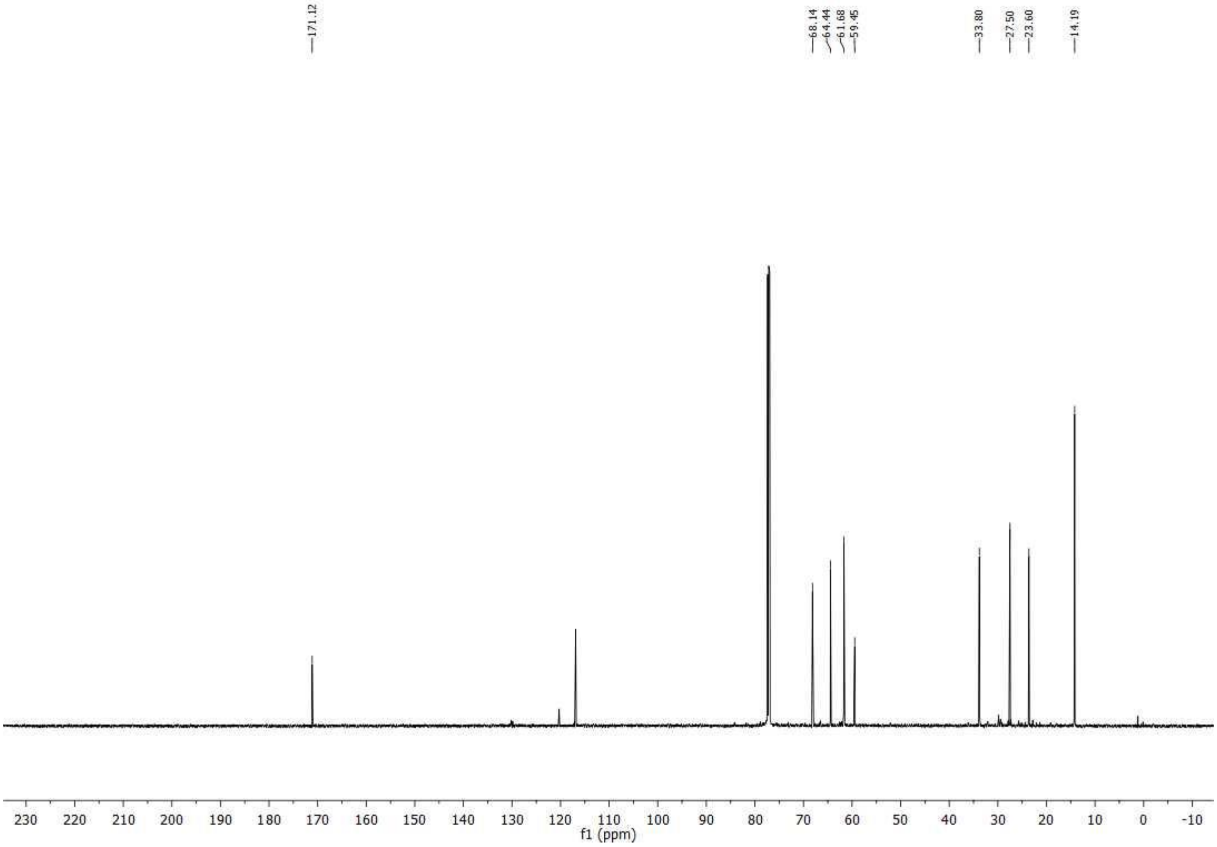
171.12
68.14
64.44
61.68
59.45
33.80
27.50
23.60
14.19
230
220
210
200
190
180
170
160
150
140
130
120
110
100
90
80
70
60
50
40
30
20
10
0
-10
f1 (ppm)

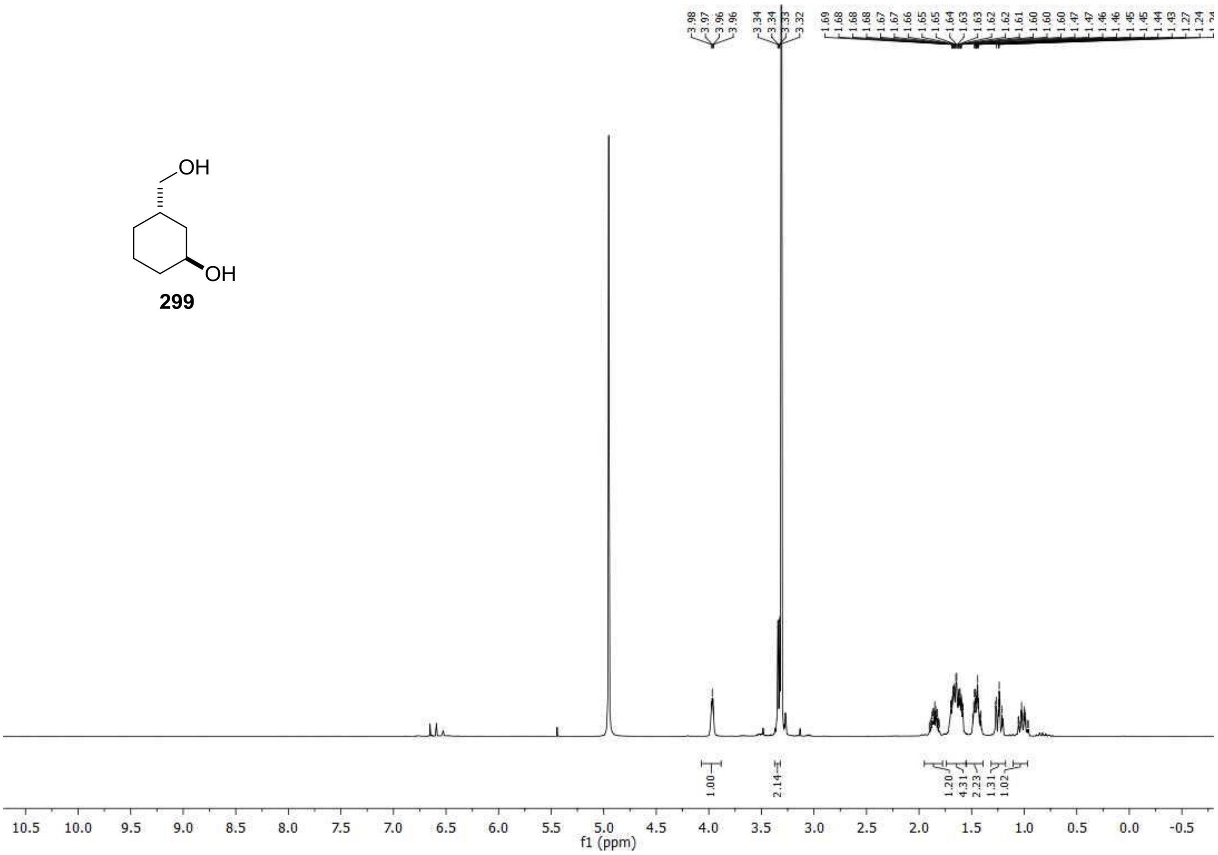
OH
OH

299

3.98
3.97
3.96
3.96
3.34
3.34
3.33
3.32
1.69
1.68
1.68
1.68
1.67
1.67
1.66
1.65
1.65
1.64
1.63
1.63
1.62
1.62
1.61
1.60
1.60
1.60
1.47
1.47
1.46
1.46
1.45
1.45
1.44
1.43
1.27
1.24
1.00
2.14
1.20
4.31
2.23
1.31
1.02
10.5
10.0
9.5
9.0
8.5
8.0
7.5
7.0
6.5
6.0
5.5
5.0
4.5
4.0
3.5
3.0
2.5
2.0
1.5
1.0
0.5
0.0
-0.5
f1 (ppm)

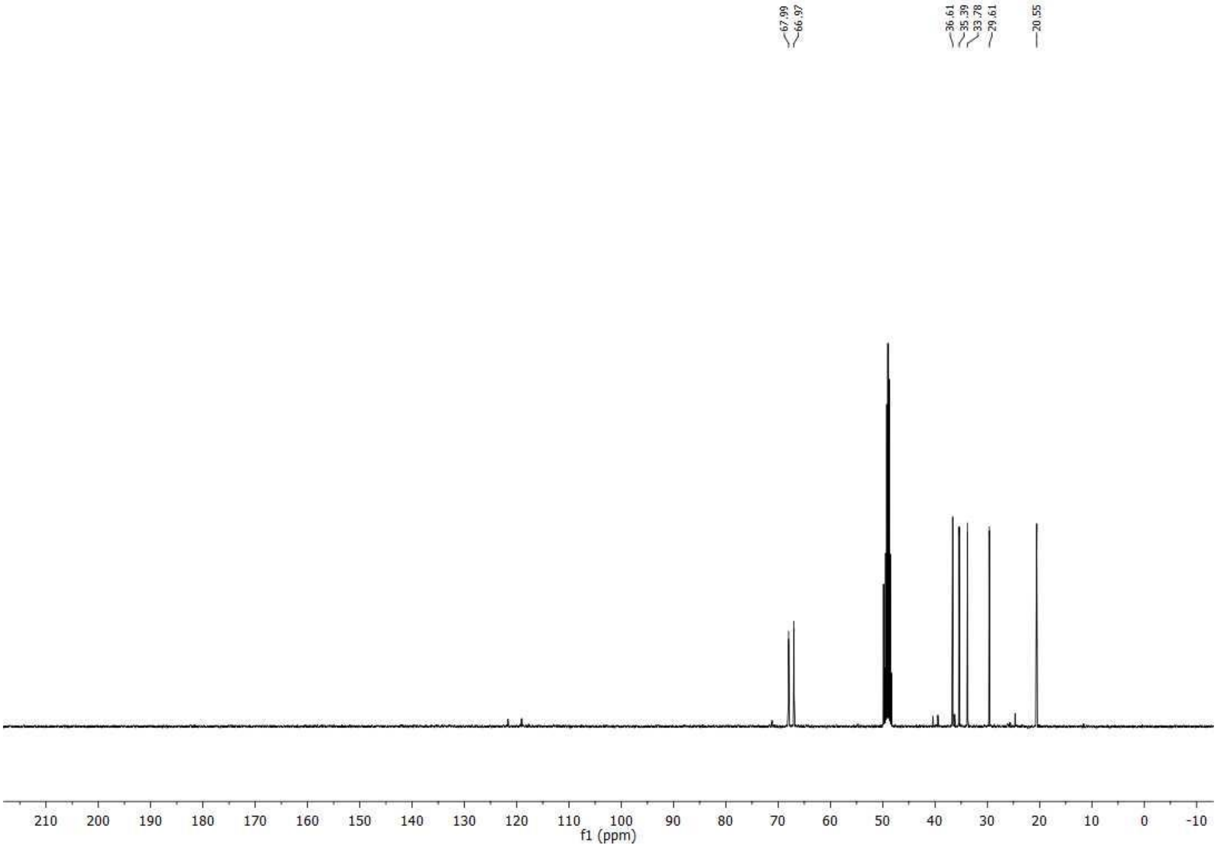
67.99
66.97
36.61
35.39
33.78
29.61
20.55
210
200
190
180
170
160
150
140
130
120
110
100
90
80
70
60
50
40
30
20
10
0
-10
f1 (ppm)

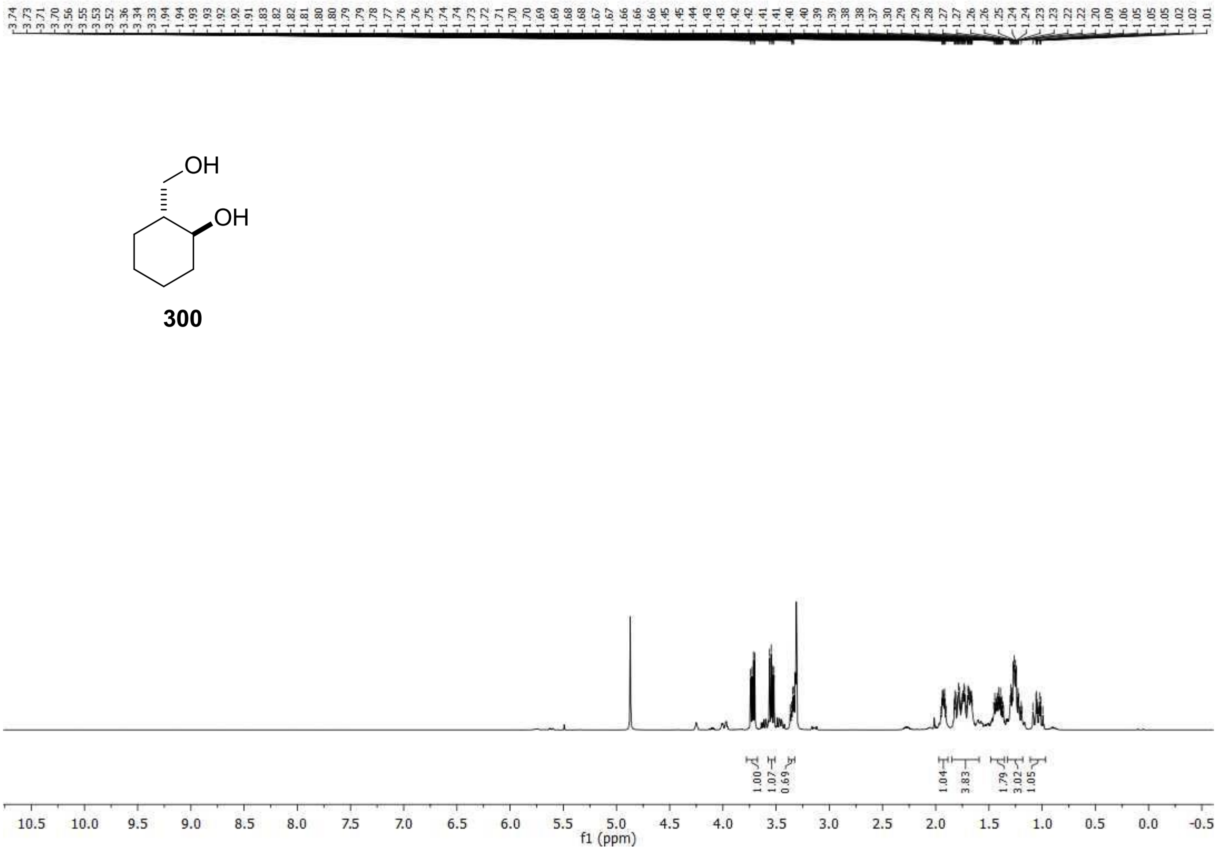
3.74 3.73 3.71 3.70 3.56 3.55 3.53 3.52 3.36 3.34 3.33 1.94 1.93 1.93 1.92 1.92 1.91 1.83 1.82 1.81 1.80 1.79 1.78 1.77 1.76 1.75 1.74 1.74 1.73 1.72 1.71 1.70 1.69 1.68 1.68 1.67 1.67 1.66 1.66 1.66 1.45 1.45 1.44 1.43 1.43 1.42 1.42 1.41 1.41 1.40 1.40 1.39 1.38 1.38 1.37 1.30 1.29 1.29 1.28 1.27 1.27 1.26 1.26 1.25 1.24 1.24 1.23 1.23 1.22 1.22 1.20 1.09 1.06 1.05 1.05 1.05 1.02 1.01
OH
OH
1.00
1.07
0.69
1.04
3.83
1.79
3.02
1.05
10.5 10.0 9.5 9.0 8.5 8.0 7.5 7.0 6.5 6.0 5.5 5.0 4.5 4.0 3.5 3.0 2.5 2.0 1.5 1.0 0.5 0.0 -0.5
f1 (ppm)

300

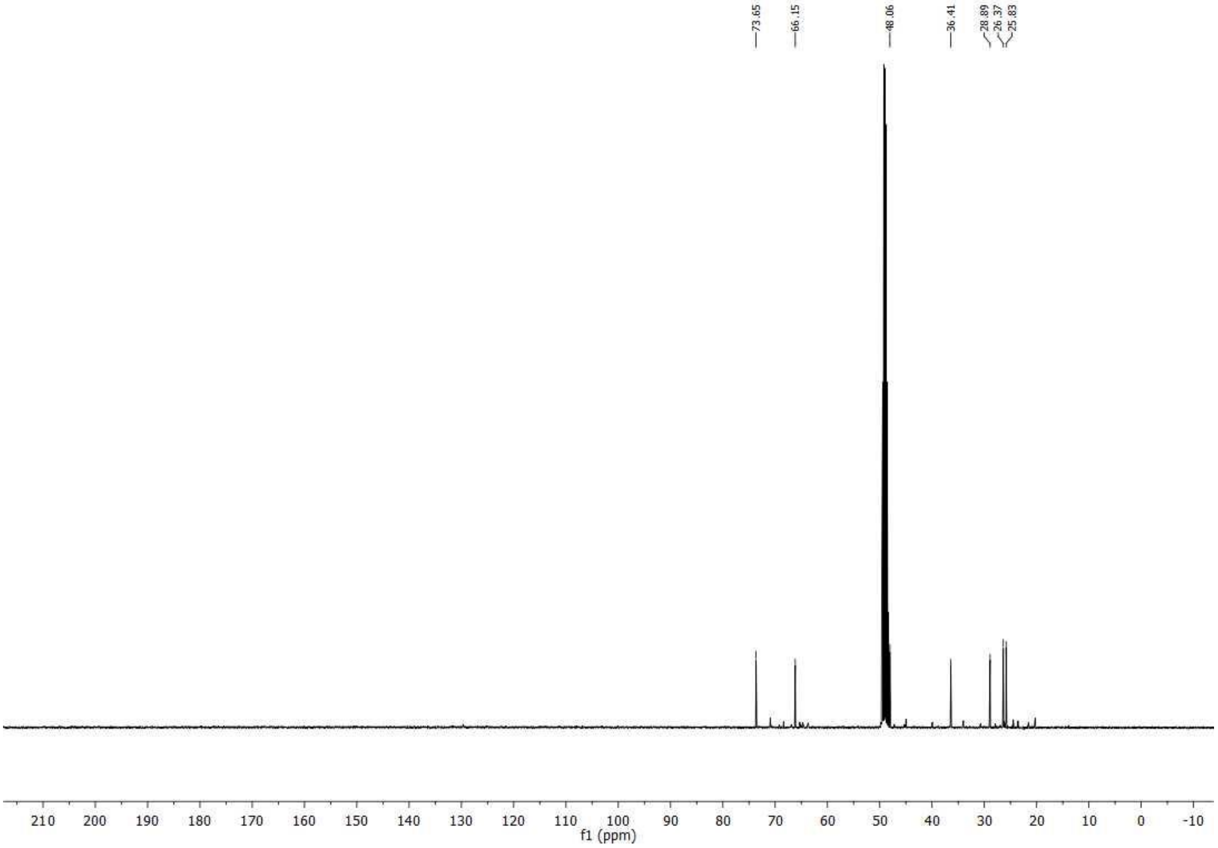
73.65
66.15
48.06
36.41
28.89
26.37
25.83
210 200 190 180 170 160 150 140 130 120 110 100 90 80 70 60 50 40 30 20 10 0 -10
f1 (ppm)

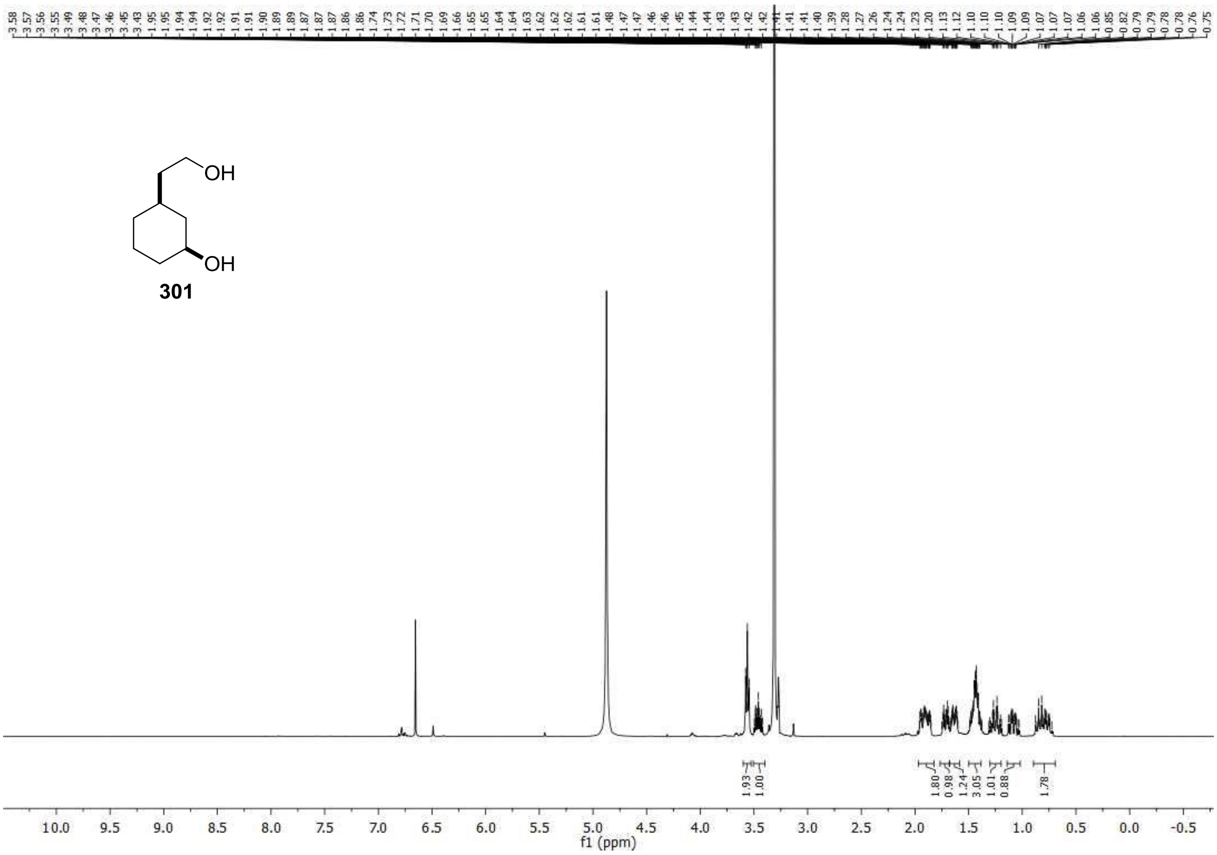

301

3.58 3.57 3.56 3.55 3.49 3.48 3.47 3.46 3.45 3.43 1.95 1.95 1.94 1.94 1.92 1.92 1.91 1.91 1.90 1.89 1.89 1.87 1.87 1.87 1.86 1.86 1.74 1.73 1.72 1.71 1.70 1.69 1.66 1.65 1.65 1.64 1.64 1.63 1.62 1.62 1.62 1.61 1.61 1.48 1.47 1.47 1.46 1.46 1.45 1.44 1.44 1.43 1.43 1.42 1.42 1.41 1.41 1.41 1.40 1.39 1.28 1.27 1.26 1.24 1.24 1.23 1.20 1.13 1.12 1.10 1.10 1.10 1.09 1.09 1.07 1.07 1.07 1.06 1.06 0.85 0.82 0.79 0.79 0.78 0.78 0.76 0.75
OH
OH
1.93
1.00
1.80
0.98
1.24
3.05
1.01
0.88
1.78
10.0 9.5 9.0 8.5 8.0 7.5 7.0 6.5 6.0 5.5 5.0 4.5 4.0 3.5 3.0 2.5 2.0 1.5 1.0 0.5 0.0 -0.5
f1 (ppm)

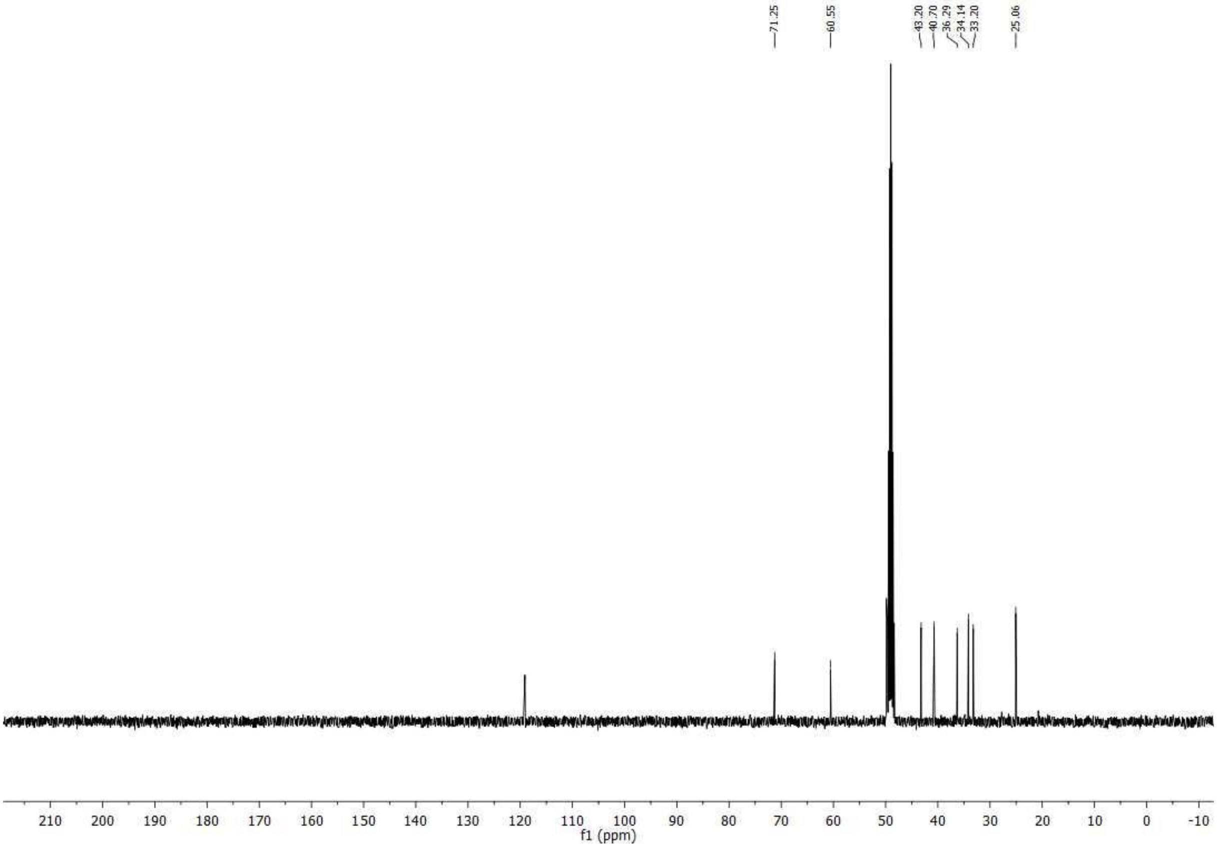

71.25
60.55
43.20
40.70
36.29
34.14
33.20
25.06
210 200 190 180 170 160 150 140 130 120 110 100 90 80 70 60 50 40 30 20 10 0 -10
f1 (ppm)

OH
OH

302

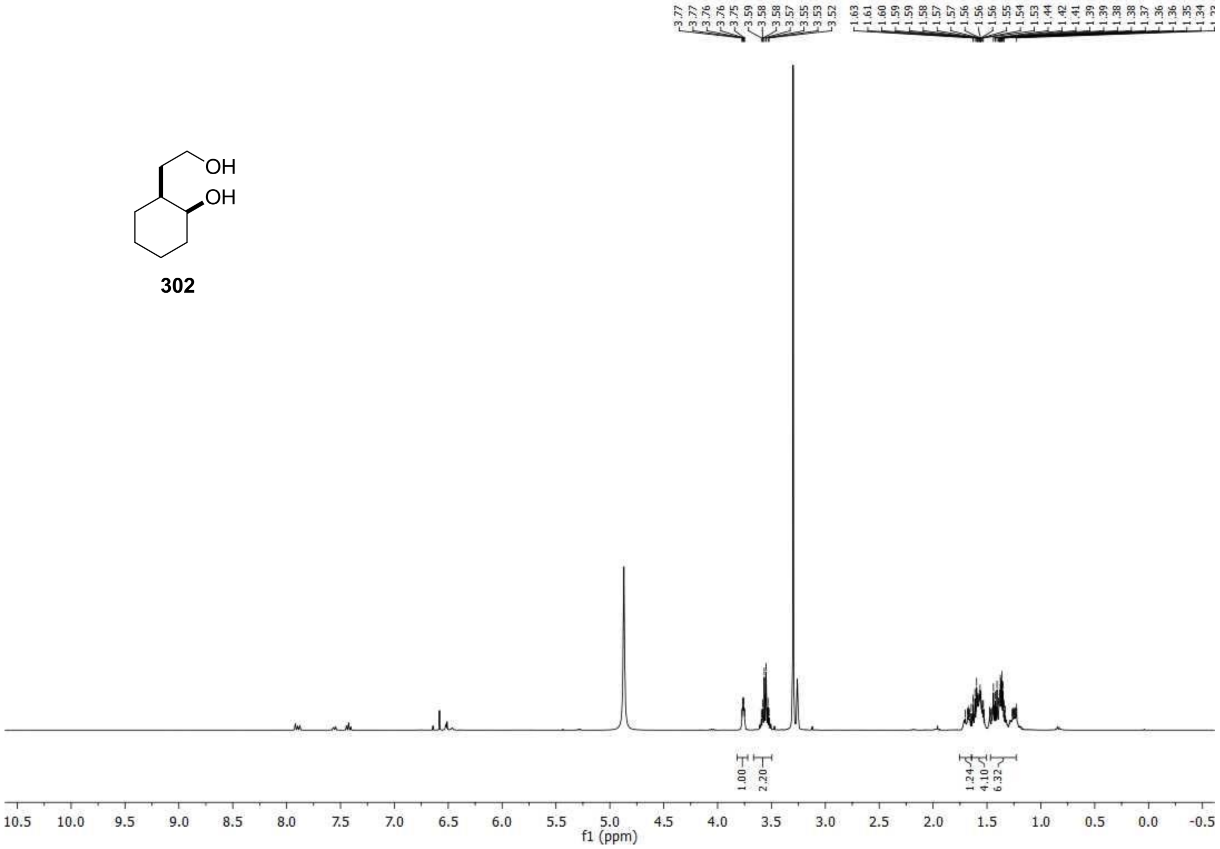
3.77
3.77
3.76
3.75
3.59
3.58
3.58
3.57
3.55
3.53
3.52
1.63
1.61
1.60
1.59
1.59
1.58
1.57
1.57
1.56
1.56
1.56
1.55
1.54
1.53
1.44
1.42
1.41
1.39
1.39
1.38
1.38
1.37
1.36
1.36
1.35
1.34
1.00
2.20
1.24
4.10
6.32
10.5
10.0
9.5
9.0
8.5
8.0
7.5
7.0
6.5
6.0
5.5
5.0
4.5
4.0
3.5
3.0
2.5
2.0
1.5
1.0
0.5
0.0
-0.5
f1 (ppm)

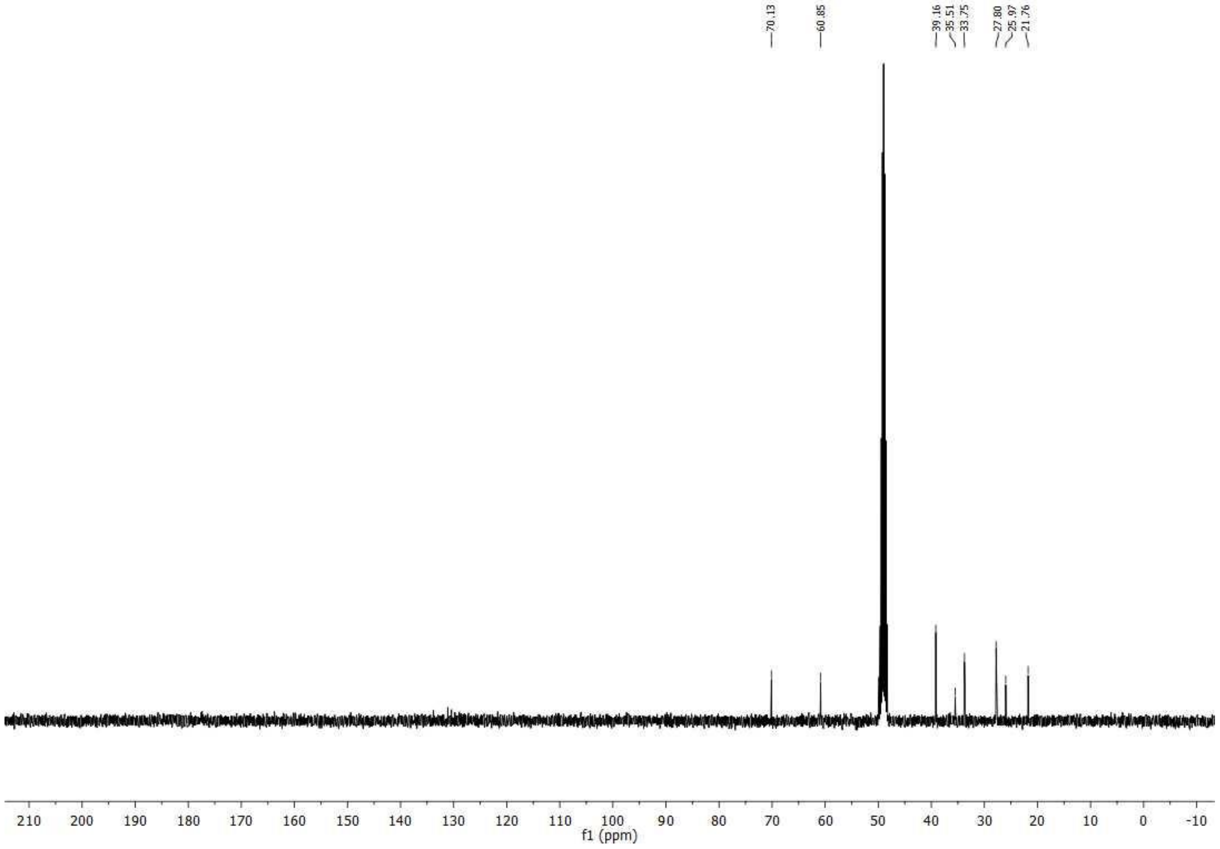
70.13
60.85
39.16
35.51
33.75
27.80
25.97
21.76
210
200
190
180
170
160
150
140
130
120
110
100
90
80
70
60
50
40
30
20
10
0
-10
f1 (ppm)

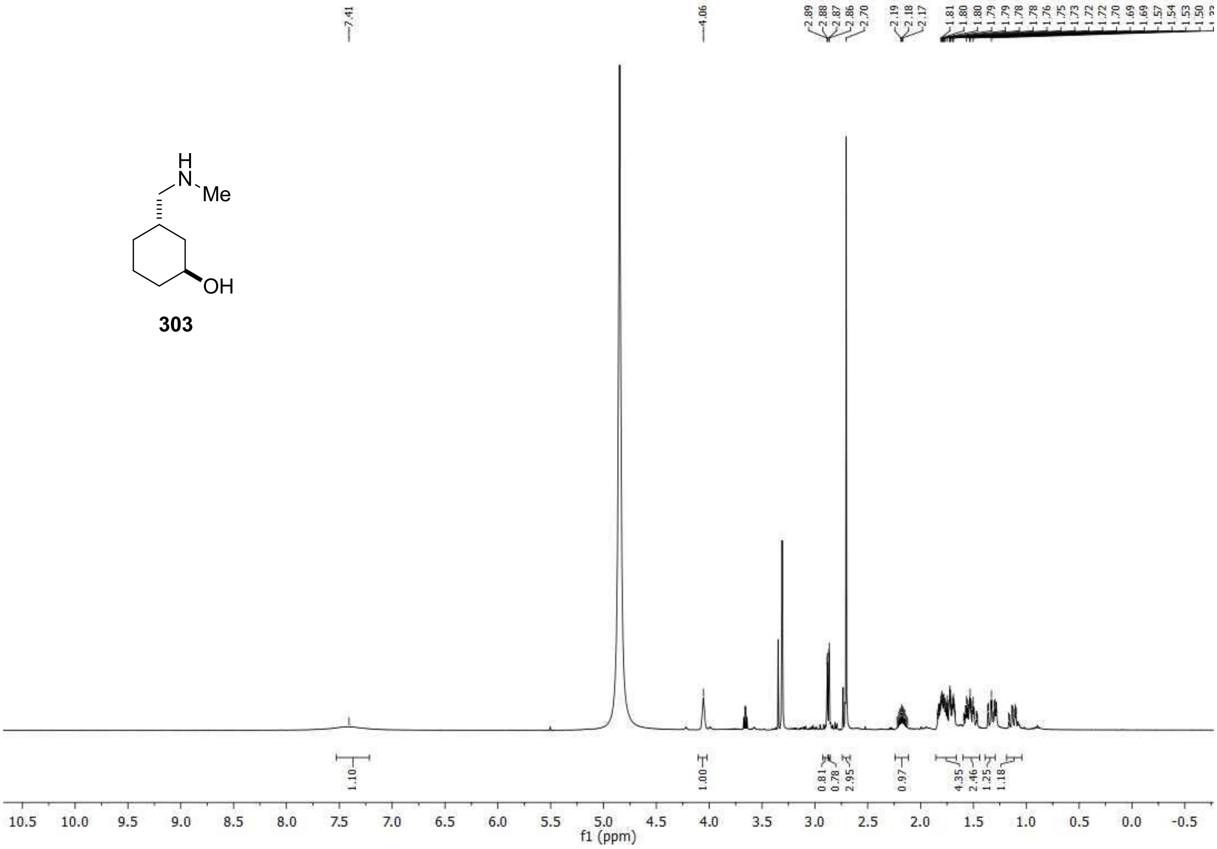
7.41
4.06
2.89
2.88
2.87
2.86
2.70
2.19
2.18
2.17
1.81
1.80
1.80
1.79
1.79
1.78
1.78
1.76
1.75
1.73
1.72
1.72
1.70
1.69
1.69
1.57
1.54
1.53
1.50
H
N
Me
OH
303
1.10
1.00
0.81
0.78
2.95
0.97
4.35
2.46
1.25
1.18
10.5 10.0 9.5 9.0 8.5 8.0 7.5 7.0 6.5 6.0 5.5 5.0 4.5 4.0 3.5 3.0 2.5 2.0 1.5 1.0 0.5 0.0 -0.5
f1 (ppm)

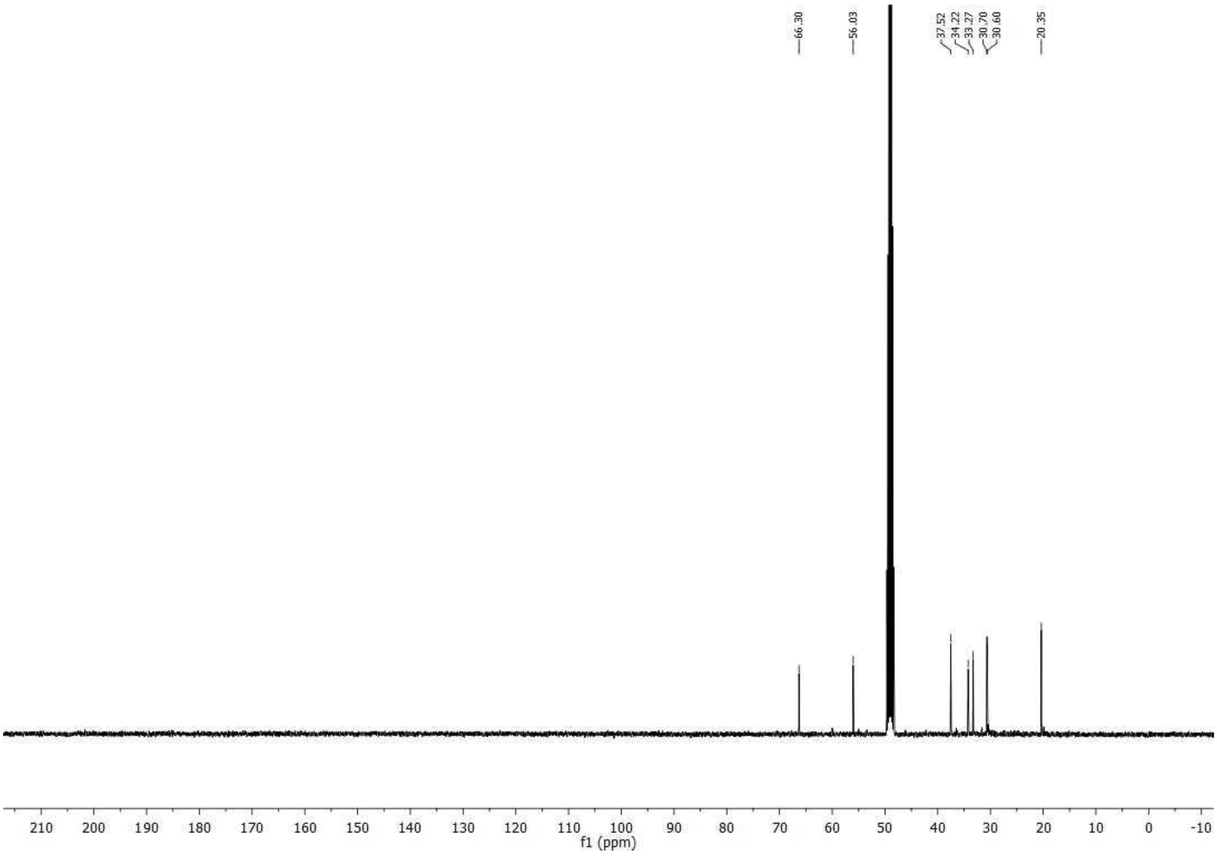
66.30
56.03
37.52
34.22
33.27
30.70
30.60
20.35
210 200 190 180 170 160 150 140 130 120 110 100 90 80 70 60 50 40 30 20 10 0 -10
f1 (ppm)

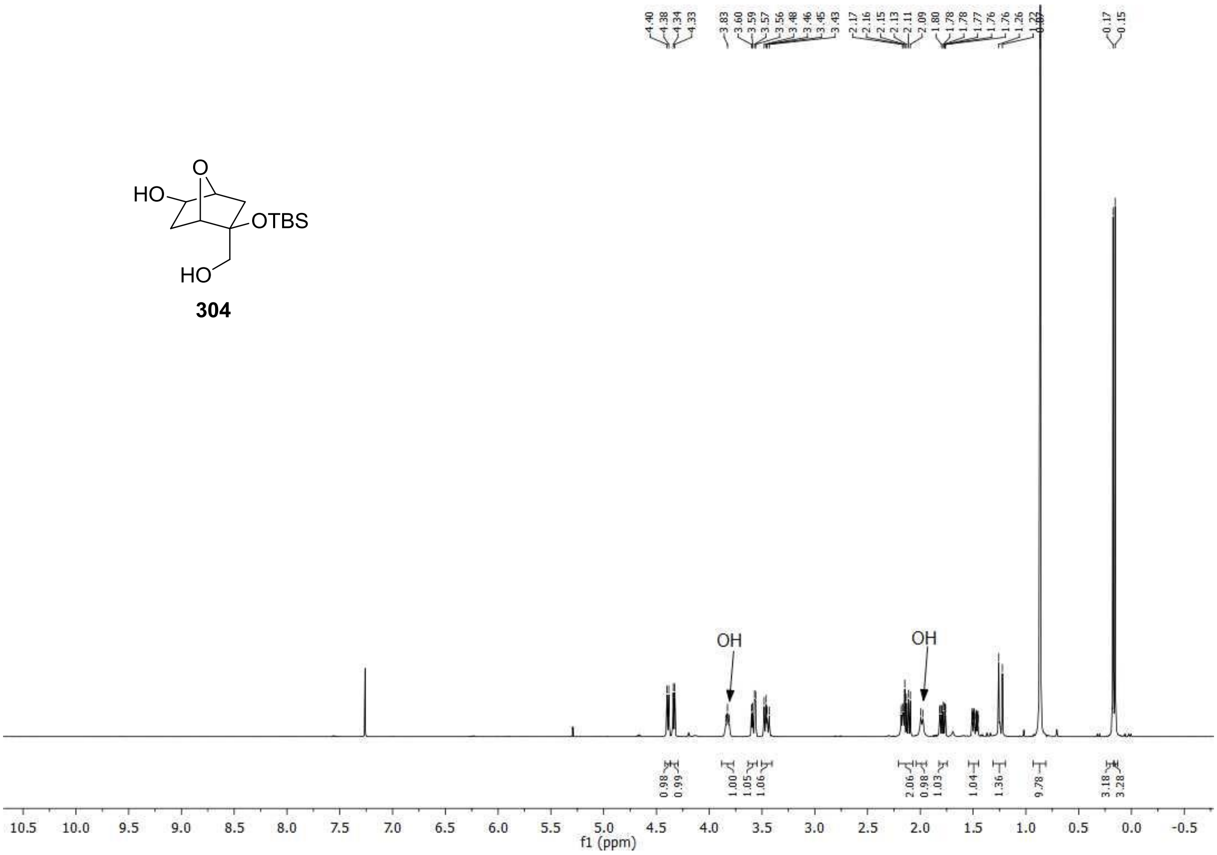
4.40
4.38
4.34
4.33
3.83
3.60
3.59
3.57
3.56
3.48
3.46
3.45
3.43
2.17
2.16
2.15
2.13
2.11
2.09
1.80
1.78
1.78
1.77
1.76
1.76
1.26
1.22
0.87
0.17
0.15
HO
O
OTBS
HO
OH
OH
0.98
0.99
1.00
1.05
1.06
2.06
0.98
1.03
1.04
1.36
9.78
3.18
3.28
10.5
10.0
9.5
9.0
8.5
8.0
7.5
7.0
6.5
6.0
5.5
5.0
4.5
4.0
3.5
3.0
2.5
2.0
1.5
1.0
0.5
0.0
-0.5
f1 (ppm)

304

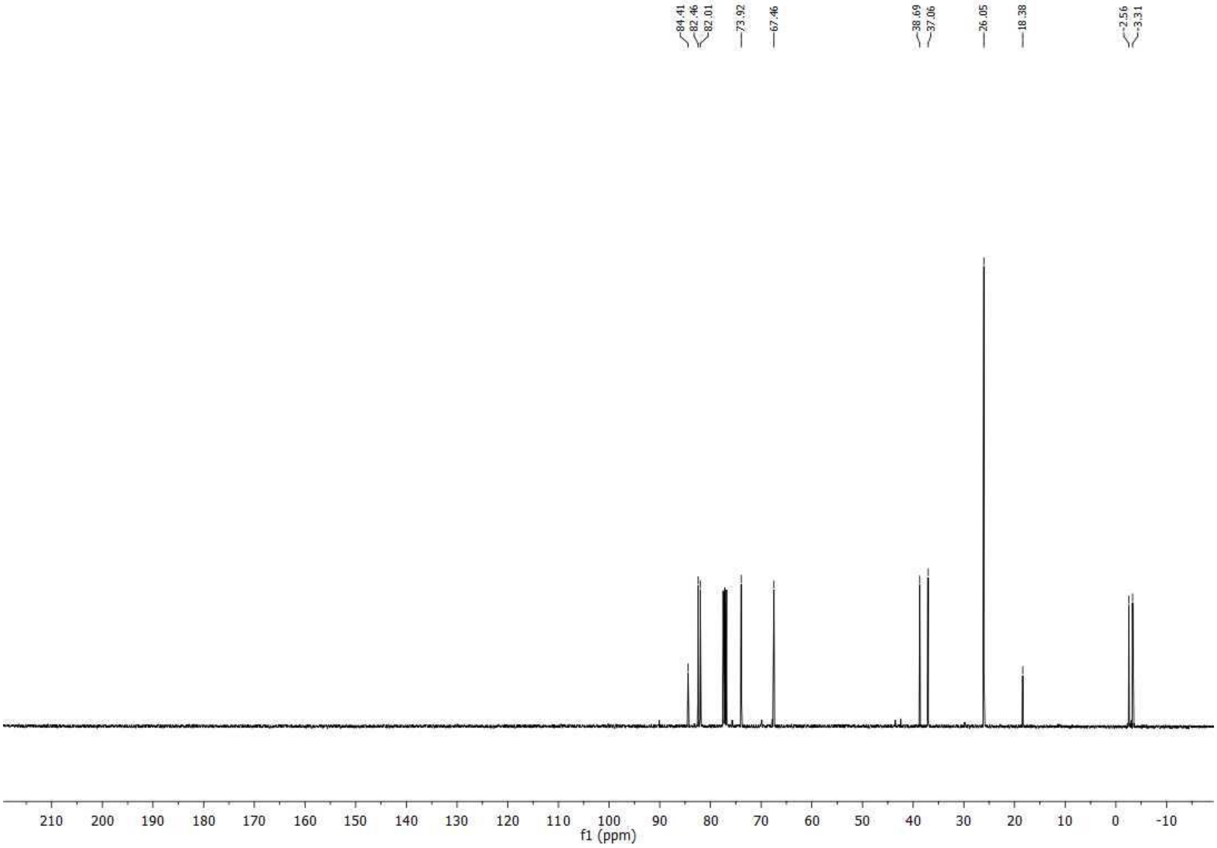
84.41
82.46
82.01
73.92
67.46
38.69
37.06
26.05
18.38
-2.56
-3.31
210
200
190
180
170
160
150
140
130
120
110
100
90
80
70
60
50
40
30
20
10
0
-10
f1 (ppm)

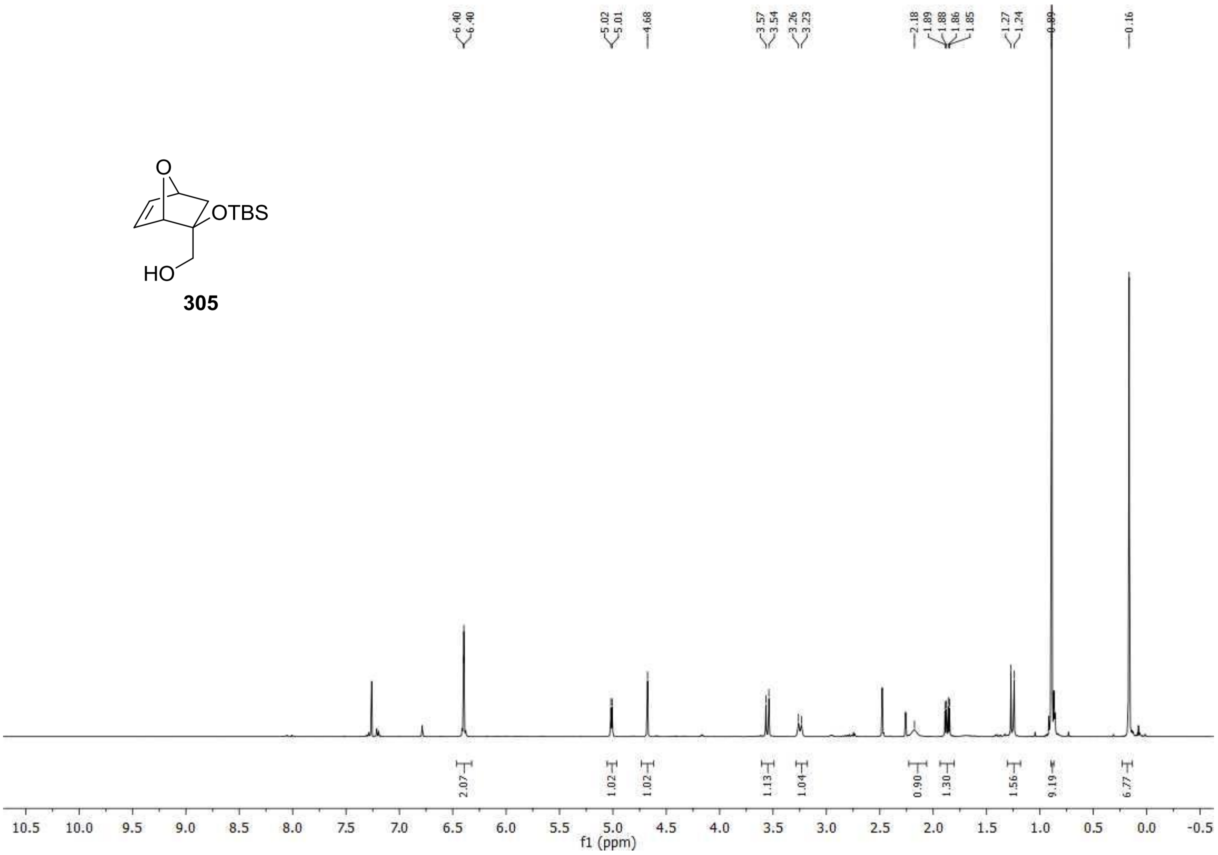
O
OTBS
HO
305
6.40
6.40
5.02
5.01
4.68
3.57
3.54
3.26
3.23
2.18
1.89
1.88
1.86
1.85
1.27
1.24
0.89
0.16
2.07
1.02
1.02
1.13
1.04
0.90
1.30
1.56
9.19
6.77
10.5
10.0
9.5
9.0
8.5
8.0
7.5
7.0
6.5
6.0
5.5
5.0
4.5
4.0
3.5
3.0
2.5
2.0
1.5
1.0
0.5
0.0
-0.5
f1 (ppm)

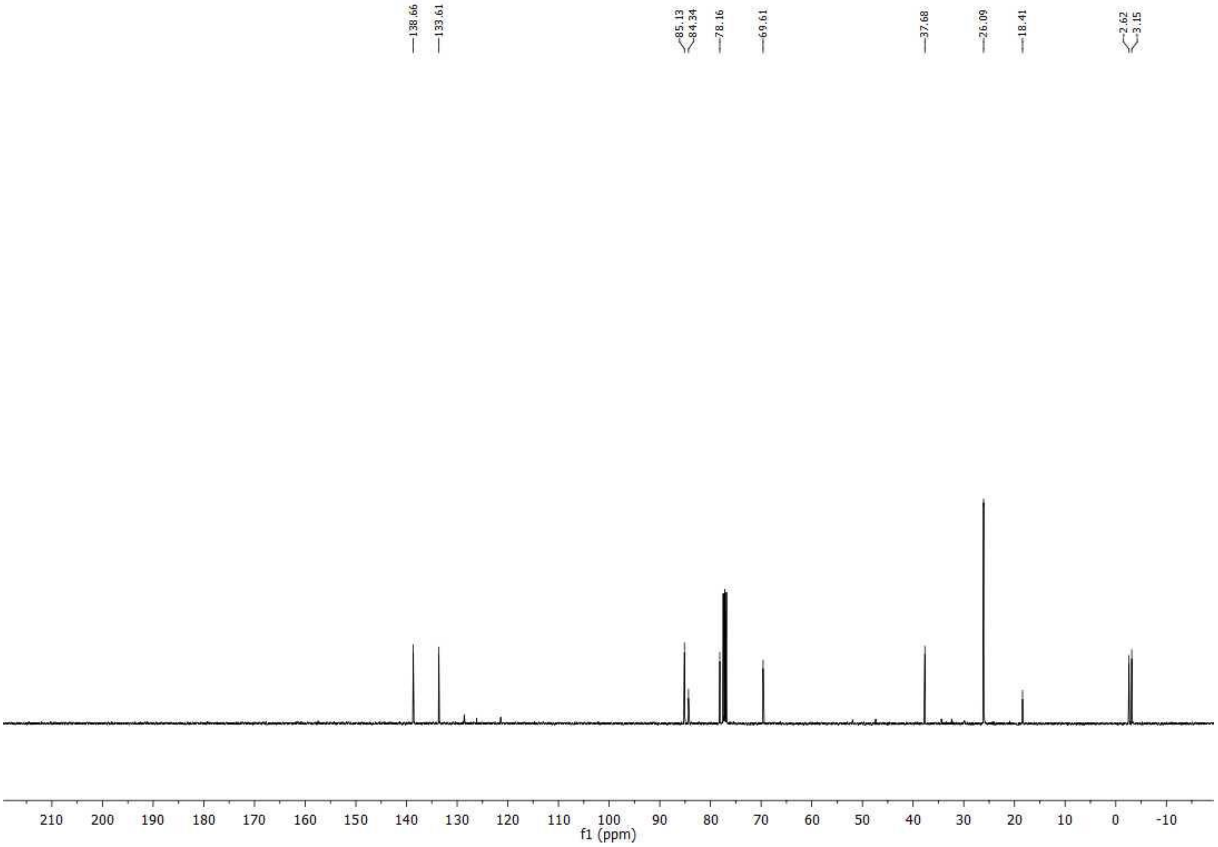
138.66
133.61
85.13
84.34
78.16
69.61
37.68
26.09
18.41
-2.62
-3.15
210
200
190
180
170
160
150
140
130
120
110
100
90
80
70
60
50
40
30
20
10
0
-10
f1 (ppm)

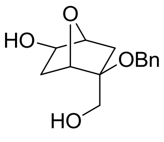
O
HO
OBn
HO

306

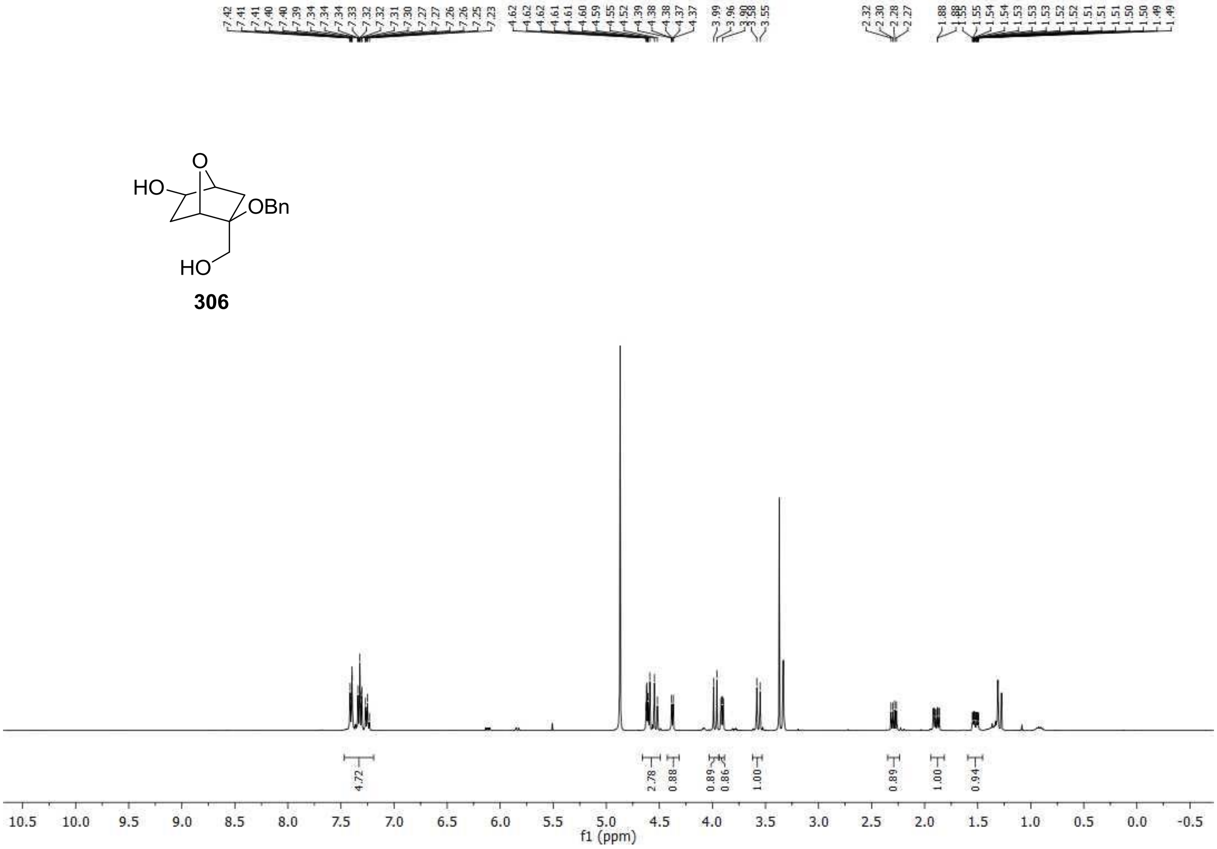
7.42
7.41
7.41
7.40
7.40
7.39
7.34
7.34
7.34
7.34
7.33
7.32
7.32
7.31
7.30
7.27
7.27
7.26
7.26
7.25
7.23
4.62
4.62
4.62
4.61
4.61
4.60
4.59
4.55
4.52
4.39
4.38
4.38
4.37
4.37
3.99
3.96
3.90
3.58
3.55
2.32
2.30
2.28
2.27
1.88
1.88
1.55
1.55
1.54
1.54
1.53
1.53
1.53
1.52
1.52
1.51
1.51
1.51
1.50
1.50
1.49
1.49
4.72
2.78
0.88
0.89
0.86
1.00
0.89
1.00
0.94
10.5
10.0
9.5
9.0
8.5
8.0
7.5
7.0
6.5
6.0
5.5
5.0
4.5
4.0
3.5
3.0
2.5
2.0
1.5
1.0
0.5
0.0
-0.5
f1 (ppm)

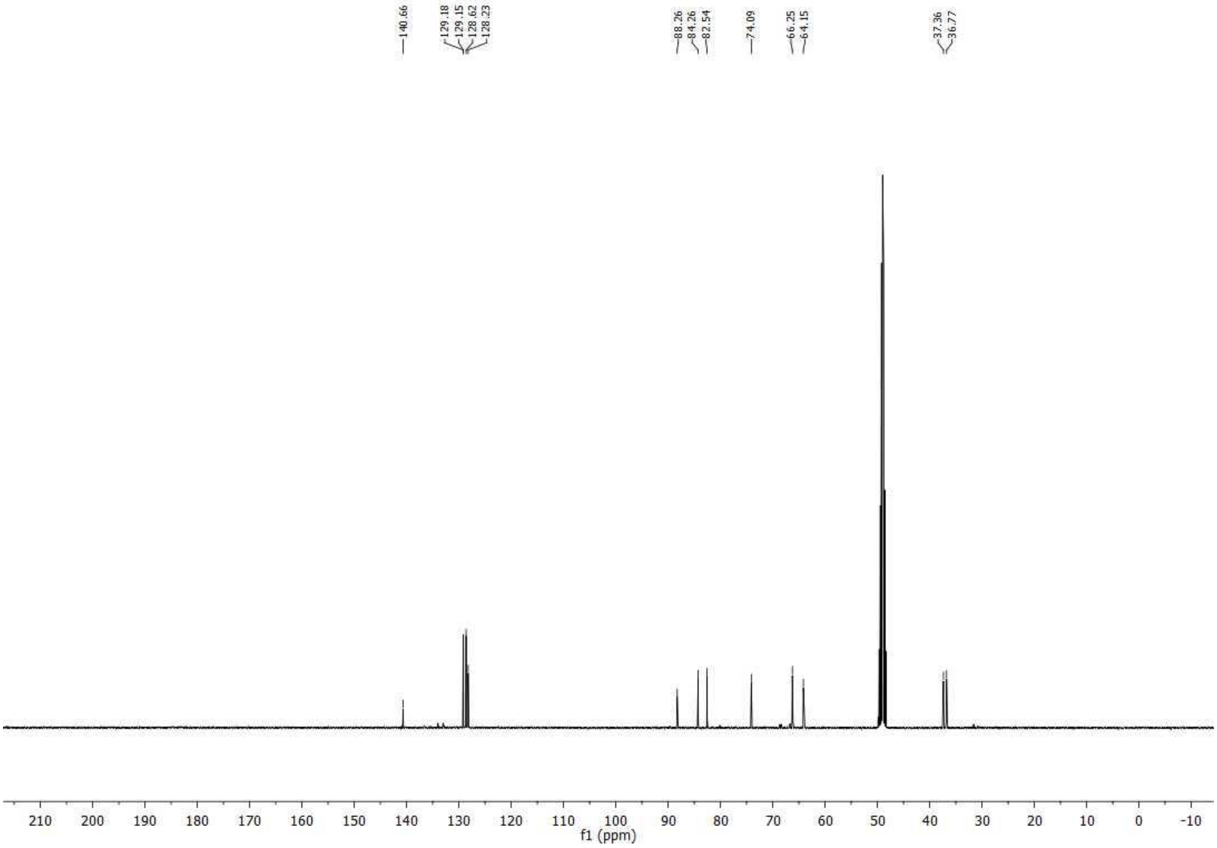
140.66
129.18
129.15
128.62
128.23
88.26
84.26
82.54
74.09
66.25
64.15
37.36
36.77
210
200
190
180
170
160
150
140
130
120
110
100
90
80
70
60
50
40
30
20
10
0
-10
f1 (ppm)

O
HO
OBn
HO

362

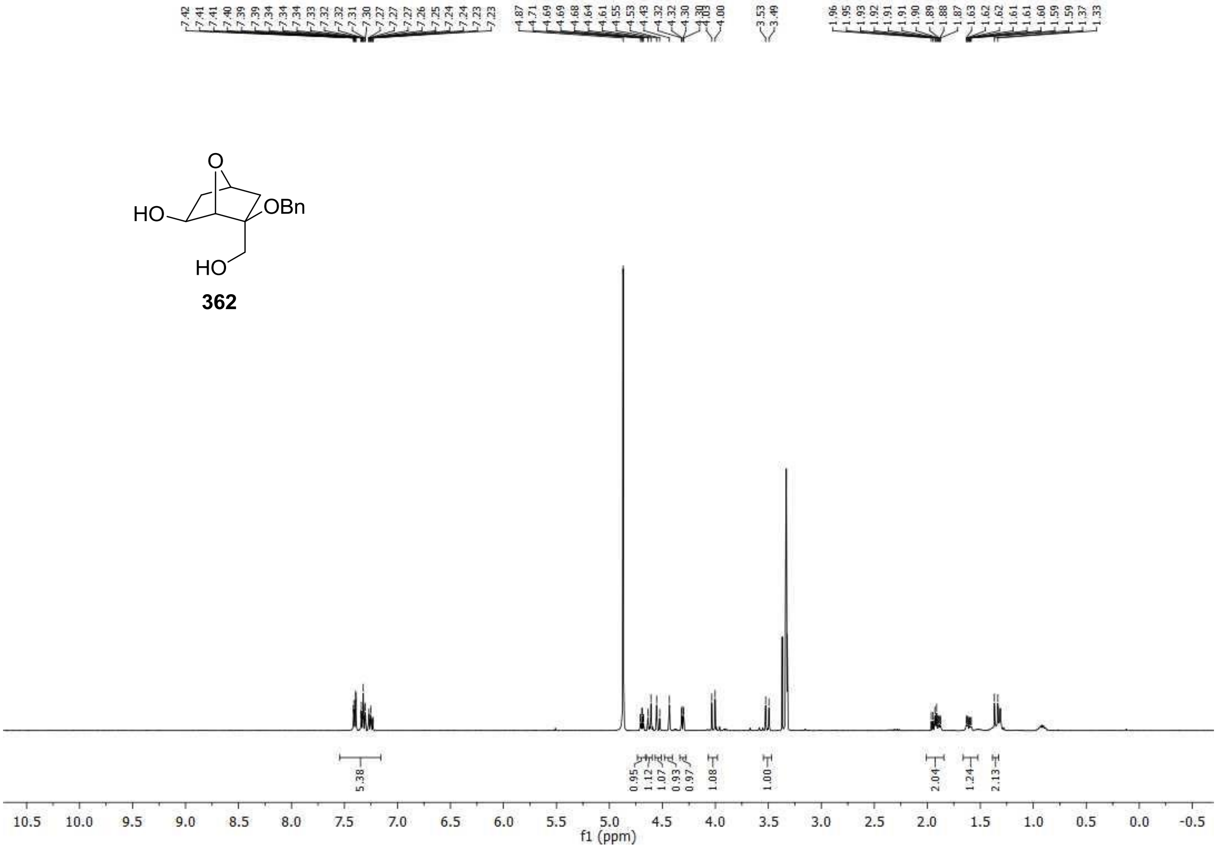
7.42
7.41
7.41
7.40
7.39
7.39
7.34
7.34
7.34
7.33
7.32
7.32
7.31
7.30
7.27
7.27
7.27
7.26
7.25
7.24
7.24
7.23
7.23
4.87
4.71
4.69
4.69
4.68
4.64
4.61
4.55
4.53
4.43
4.32
4.32
4.30
4.30
4.03
4.00
3.53
3.49
1.96
1.95
1.93
1.92
1.91
1.91
1.90
1.89
1.88
1.87
1.63
1.62
1.61
1.61
1.60
1.59
1.59
1.37
1.33
5.38
0.95
1.12
1.07
0.93
0.97
1.08
1.00
2.04
1.24
2.13
10.5
10.0
9.5
9.0
8.5
8.0
7.5
7.0
6.5
6.0
5.5
5.0
4.5
4.0
3.5
3.0
2.5
2.0
1.5
1.0
0.5
0.0
-0.5
f1 (ppm)

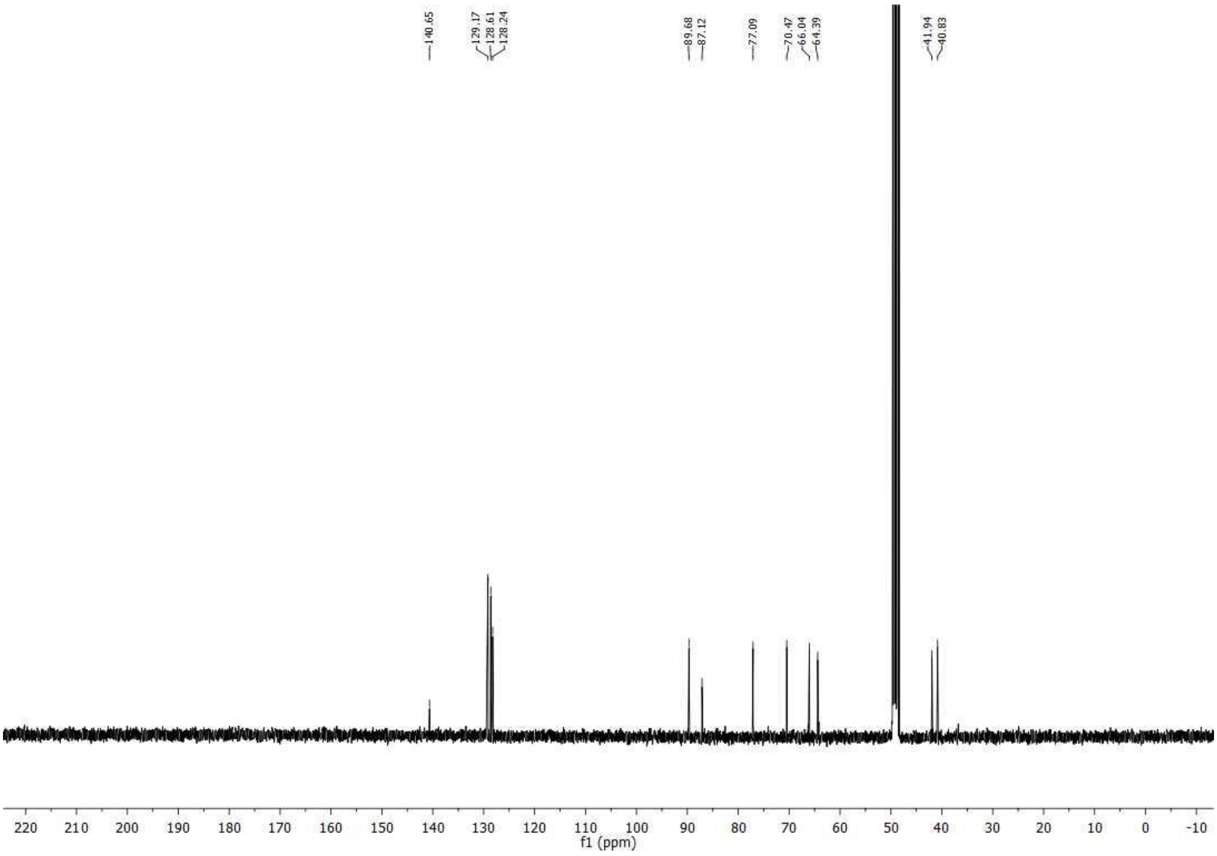
140.65
129.17
128.61
128.24
89.68
87.12
77.09
70.47
66.04
64.39
41.94
40.83
220
210
200
190
180
170
160
150
140
130
120
110
100
90
80
70
60
50
40
30
20
10
0
-10
f1 (ppm)

O
OBn
HO

307

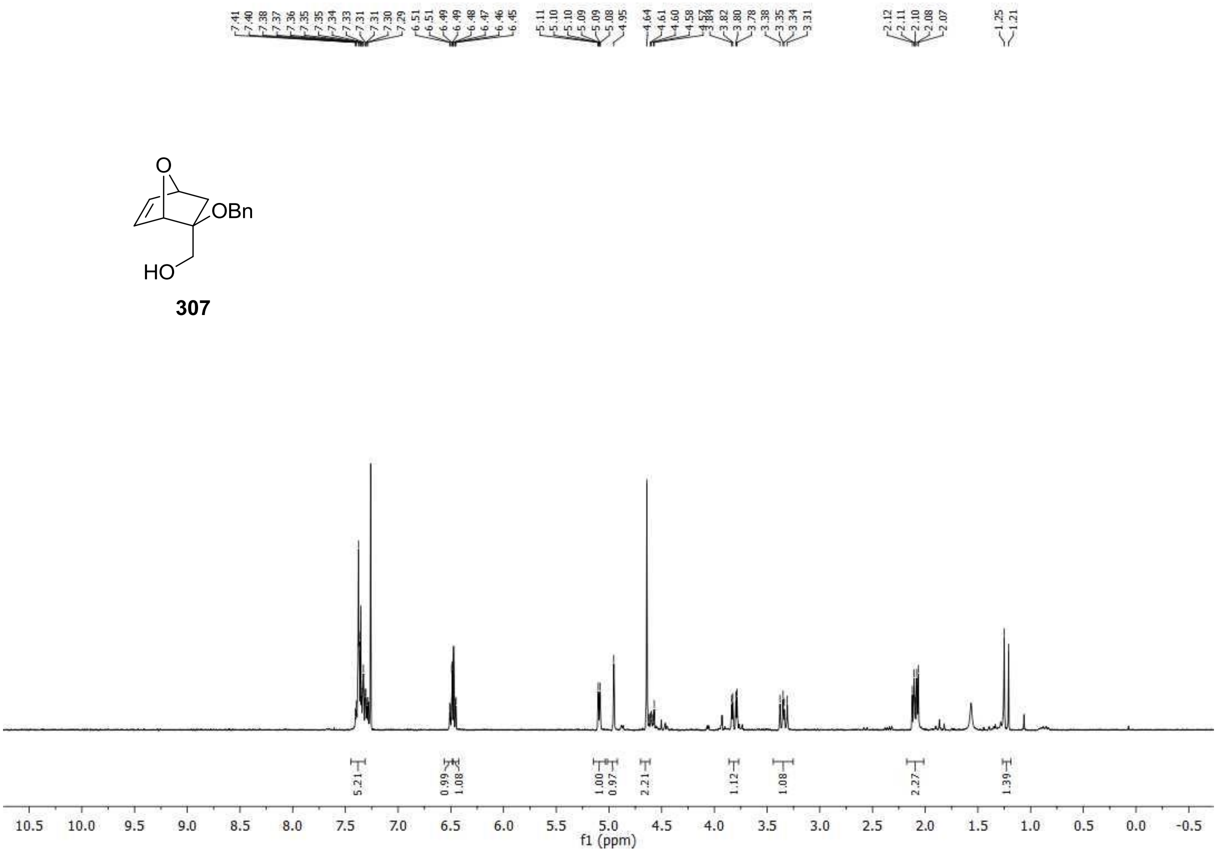
7.41
7.40
7.38
7.37
7.36
7.35
7.35
7.34
7.33
7.31
7.31
7.30
7.29
6.51
6.51
6.49
6.49
6.48
6.47
6.46
6.45
5.11
5.10
5.10
5.09
5.09
5.08
4.95
4.64
4.61
4.60
4.58
4.57
3.84
3.82
3.80
3.78
3.38
3.35
3.34
3.31
2.12
2.11
2.10
2.08
2.07
1.25
1.21
5.21
0.99
1.08
1.00
0.97
2.21
1.12
1.08
2.27
1.39
10.5
10.0
9.5
9.0
8.5
8.0
7.5
7.0
6.5
6.0
5.5
5.0
4.5
4.0
3.5
3.0
2.5
2.0
1.5
1.0
0.5
0.0
-0.5
f1 (ppm)

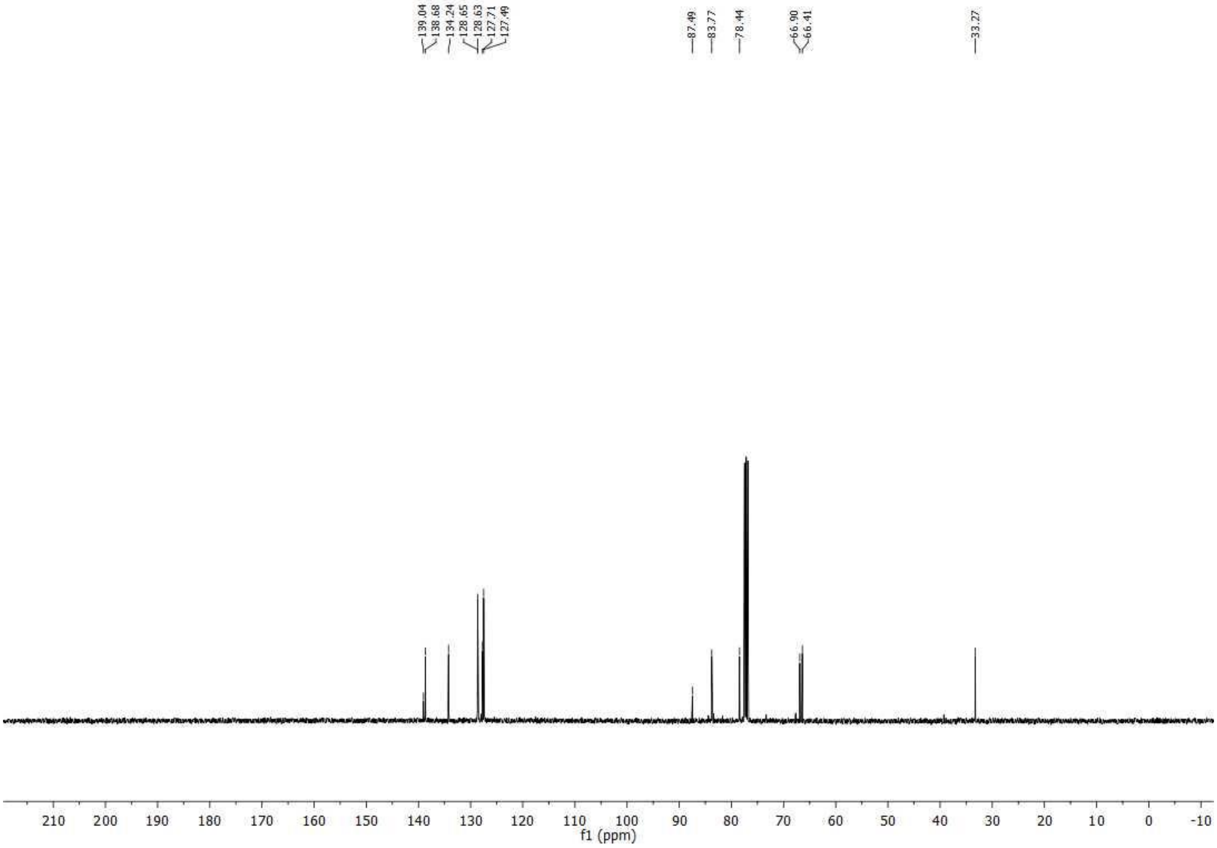
139.04
138.68
134.24
128.65
128.63
127.71
127.49
87.49
83.77
78.44
66.90
66.41
33.27
210
200
190
180
170
160
150
140
130
120
110
100
90
80
70
60
50
40
30
20
10
0
-10
f1 (ppm)

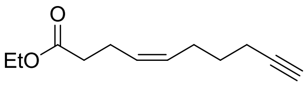
O
EtO

339

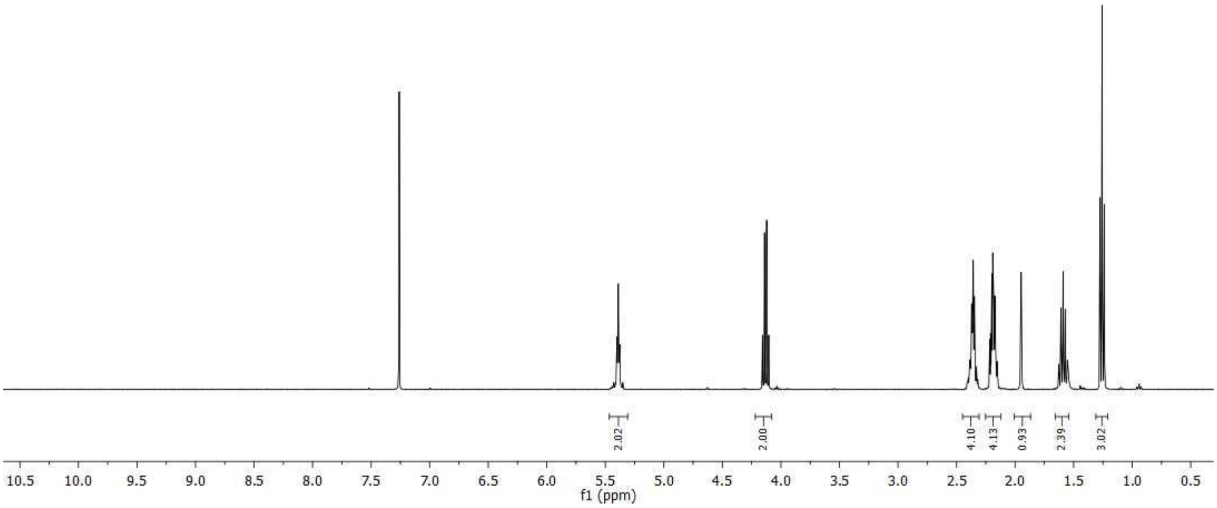
2.02
2.00
4.10
4.13
0.93
2.39
3.02
10.5
10.0
9.5
9.0
8.5
8.0
7.5
7.0
6.5
6.0
5.5
5.0
4.5
4.0
3.5
3.0
2.5
2.0
1.5
1.0
0.5
f1 (ppm)

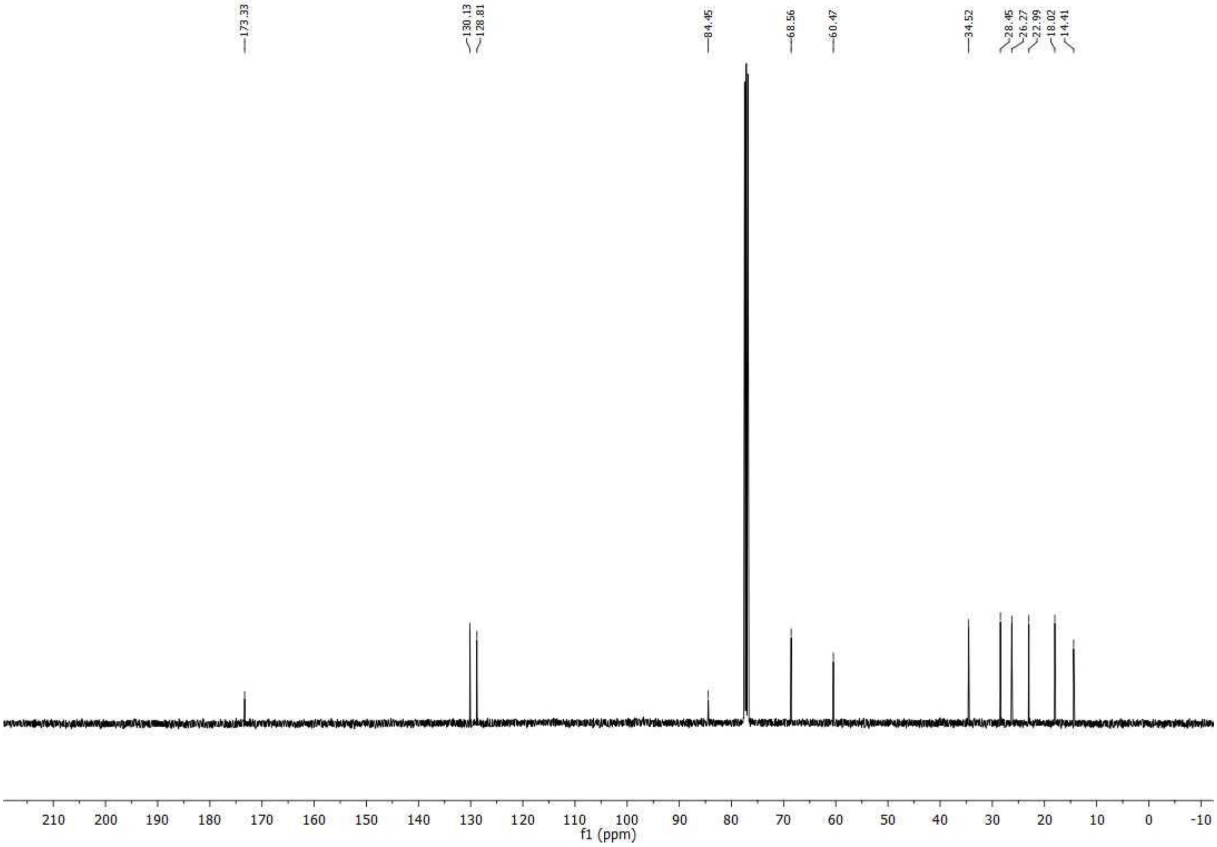
173.33
130.13
128.81
84.45
68.56
60.47
34.52
28.45
26.27
22.99
18.02
14.41
210
200
190
180
170
160
150
140
130
120
110
100
90
80
70
60
50
40
30
20
10
0
-10
f1 (ppm)

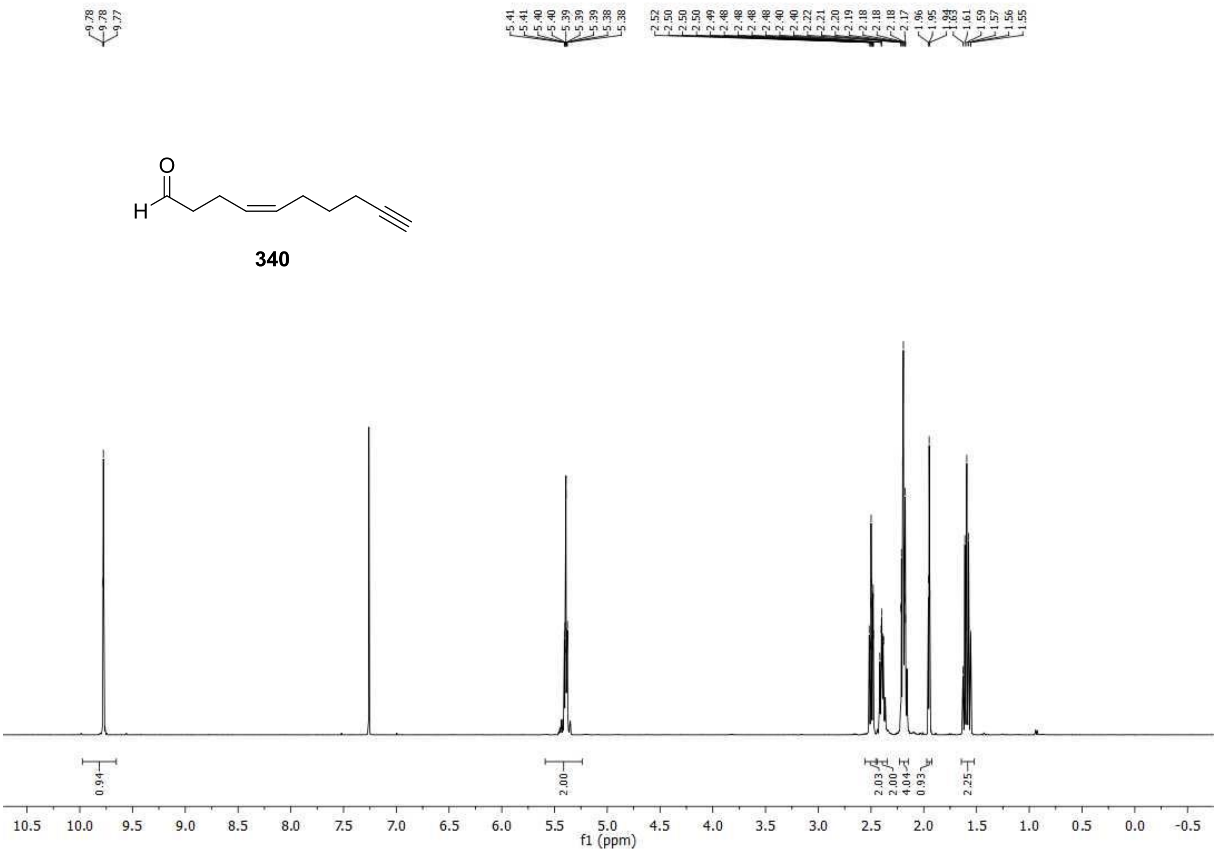
9.78
9.78
9.77
5.41
5.41
5.40
5.39
5.39
5.39
5.38
5.38
2.52
2.50
2.50
2.50
2.49
2.48
2.48
2.48
2.48
2.40
2.40
2.22
2.21
2.20
2.19
2.18
2.18
2.18
2.17
1.96
1.95
1.94
1.93
1.61
1.59
1.57
1.56
1.55
O
H
0.94
2.00
2.03
2.00
4.04
0.93
2.25
10.5
10.0
9.5
9.0
8.5
8.0
7.5
7.0
6.5
6.0
5.5
5.0
4.5
4.0
3.5
3.0
2.5
2.0
1.5
1.0
0.5
0.0
-0.5
f1 (ppm)

340

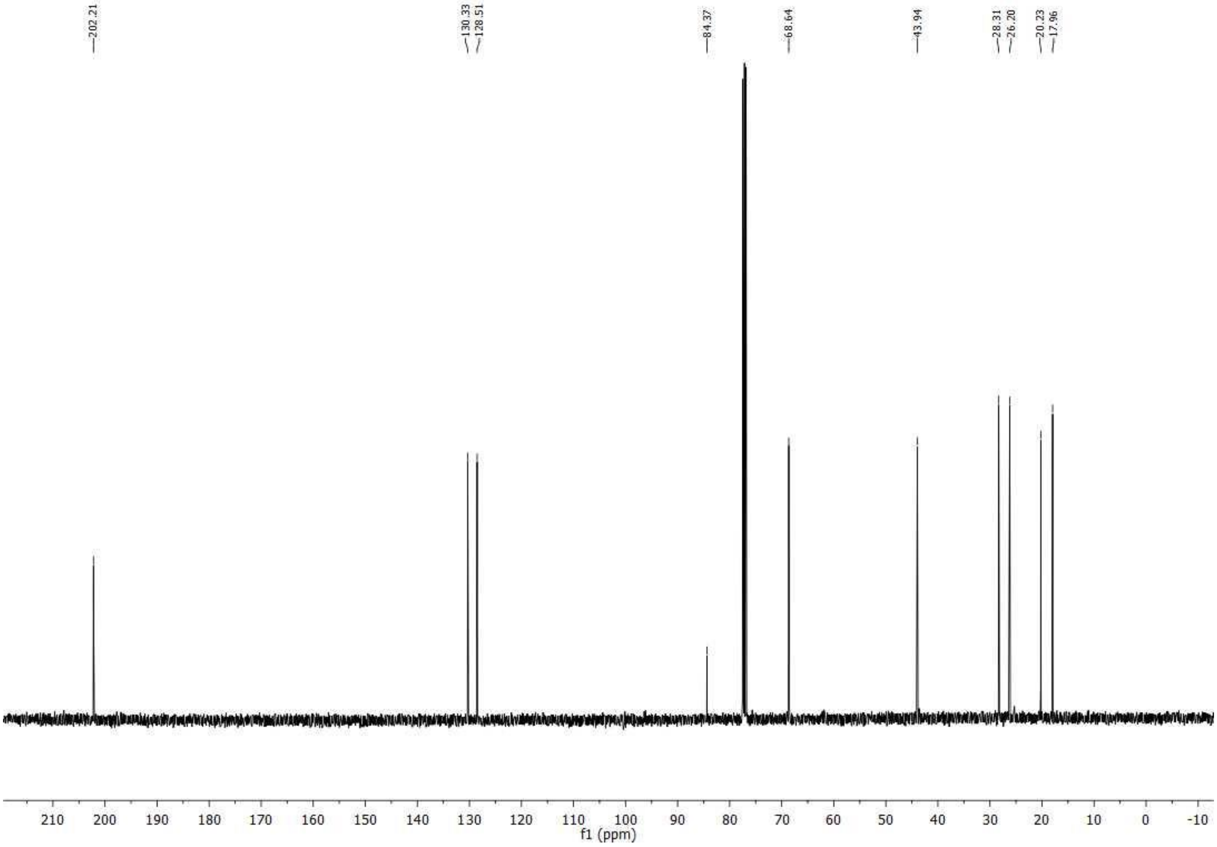
202.21
130.33
128.51
84.37
68.64
43.94
28.31
26.20
20.23
17.96
210
200
190
180
170
160
150
140
130
120
110
100
90
80
70
60
50
40
30
20
10
0
-10
f1 (ppm)

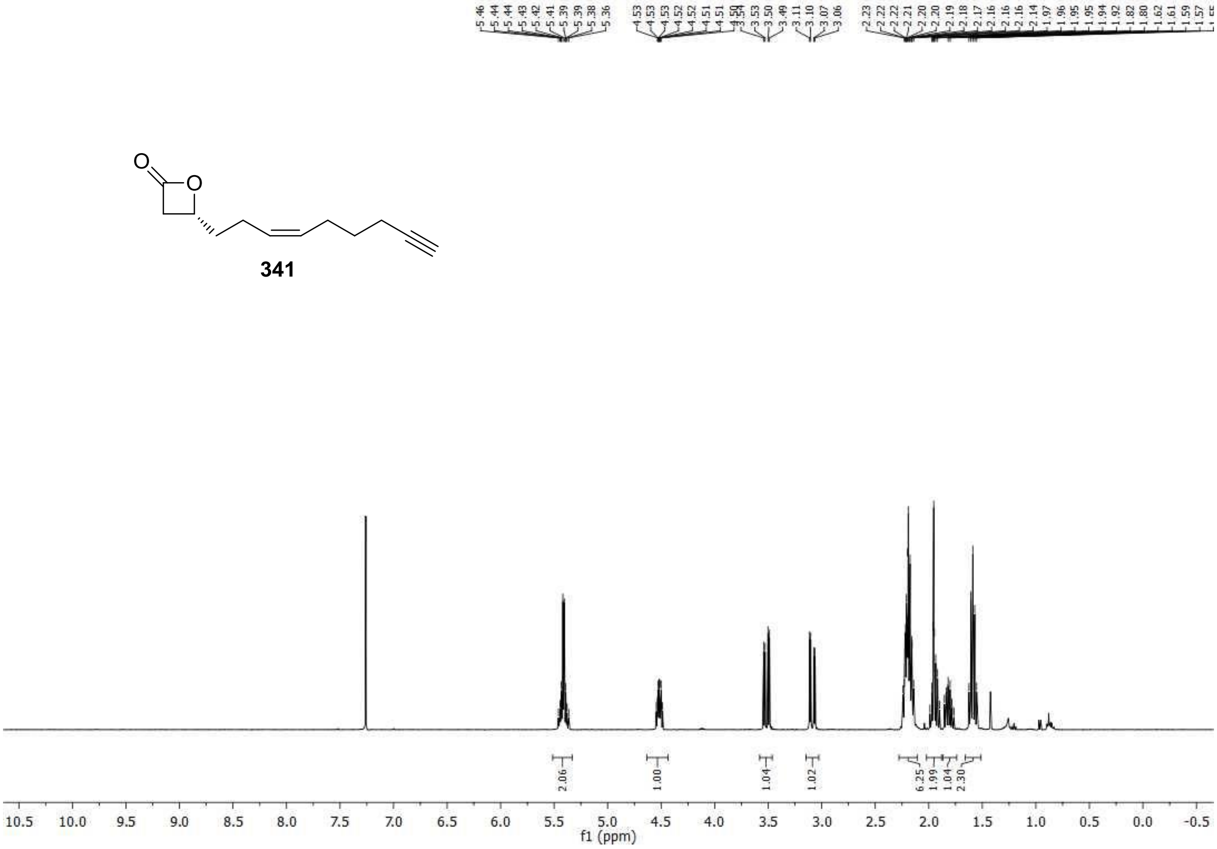
O
O

341

5.46
5.44
5.43
5.42
5.41
5.39
5.39
5.38
5.36
4.53
4.53
4.53
4.52
4.52
4.51
4.51
3.54
3.53
3.50
3.49
3.11
3.10
3.07
3.06
2.23
2.22
2.22
2.21
2.20
2.20
2.19
2.18
2.17
2.16
2.16
2.16
2.14
1.97
1.96
1.95
1.95
1.94
1.92
1.82
1.80
1.62
1.61
1.59
1.57
2.06
1.00
1.04
1.02
6.25
1.99
1.04
2.30
10.5
10.0
9.5
9.0
8.5
8.0
7.5
7.0
6.5
6.0
5.5
5.0
4.5
4.0
3.5
3.0
2.5
2.0
1.5
1.0
0.5
0.0
-0.5
f1 (ppm)

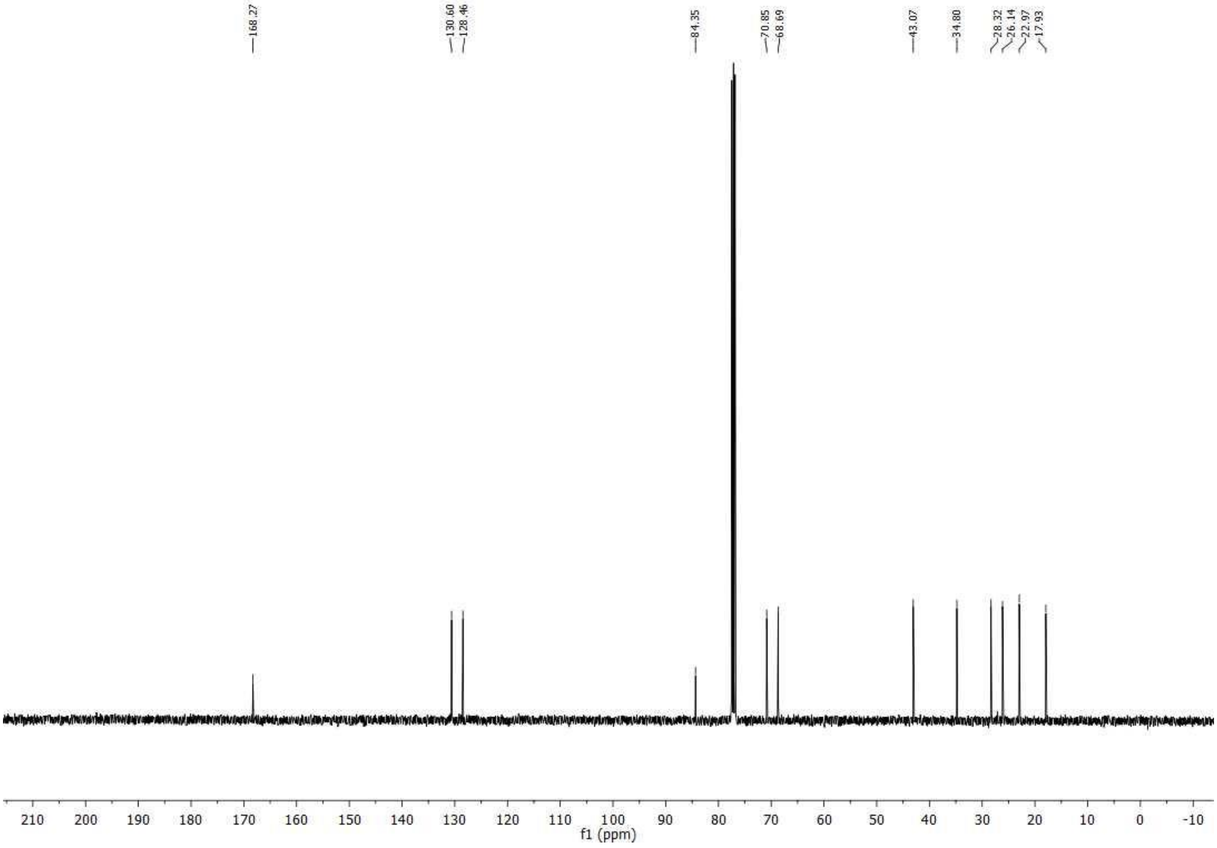
168.27
130.60
128.46
84.35
70.85
68.69
43.07
34.80
28.32
26.14
22.97
17.93
210
200
190
180
170
160
150
140
130
120
110
100
90
80
70
60
50
40
30
20
10
0
-10
f1 (ppm)

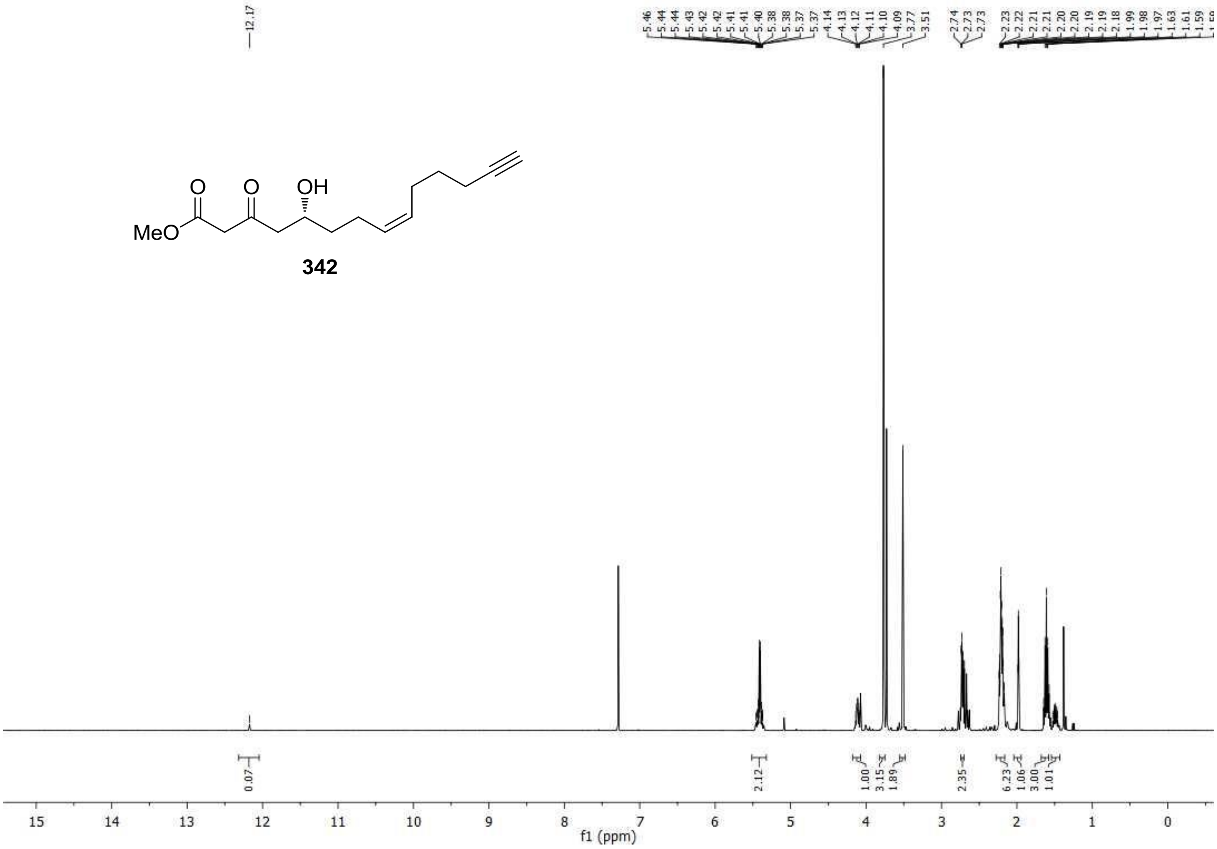
12.17
5.46
5.44
5.44
5.43
5.42
5.42
5.41
5.41
5.40
5.38
5.38
5.37
5.37
4.14
4.13
4.12
4.11
4.10
4.09
3.77
3.51
2.74
2.73
2.73
2.23
2.22
2.21
2.21
2.20
2.20
2.19
2.19
2.18
1.99
1.98
1.97
1.63
1.61
1.59
O
O
OH
MeO
0.07
2.12
1.00
3.15
1.89
2.35
6.23
1.06
3.00
1.01
15
14
13
12
11
10
9
8
7
6
5
4
3
2
1
0
f1 (ppm)

342

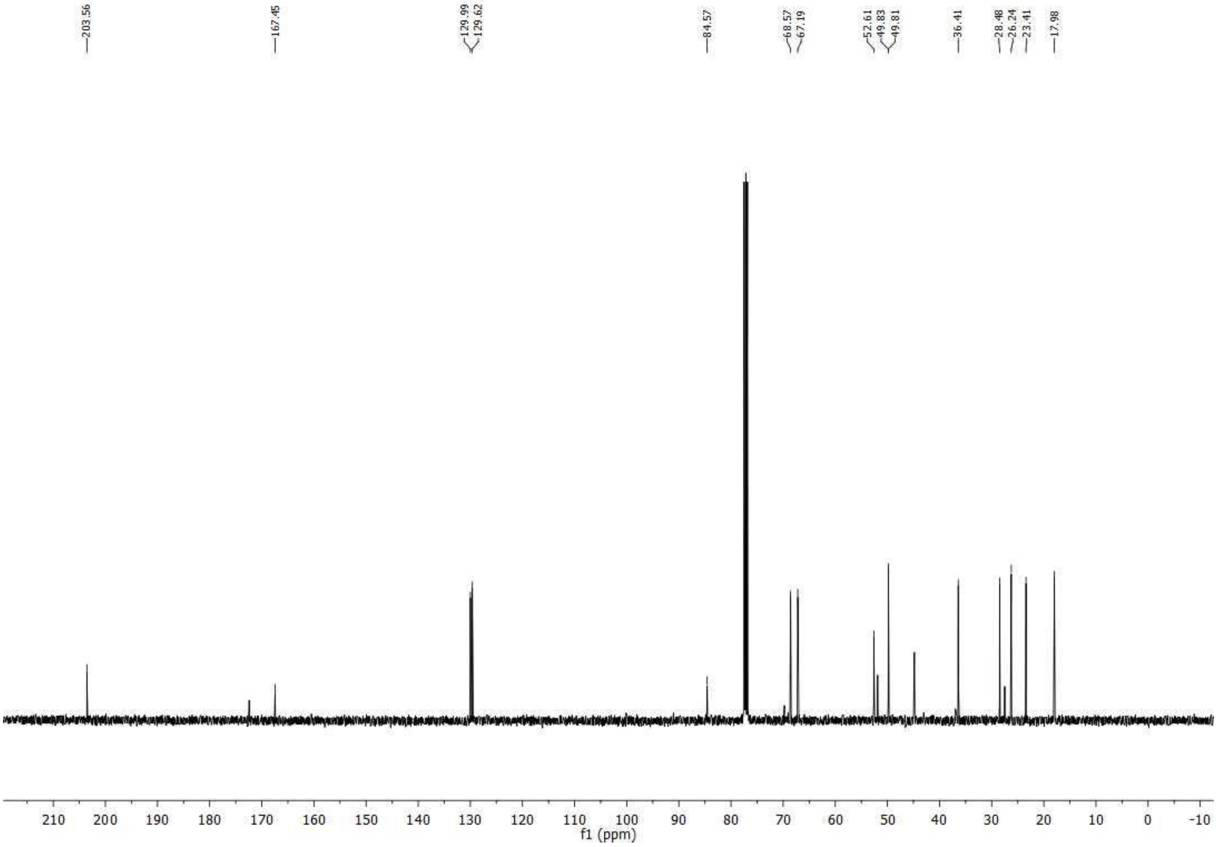
203.56
167.45
129.99
129.62
84.57
68.57
67.19
52.61
49.83
49.81
36.41
28.48
26.24
23.41
17.98
210
200
190
180
170
160
150
140
130
120
110
100
90
80
70
60
50
40
30
20
10
0
-10
f1 (ppm)

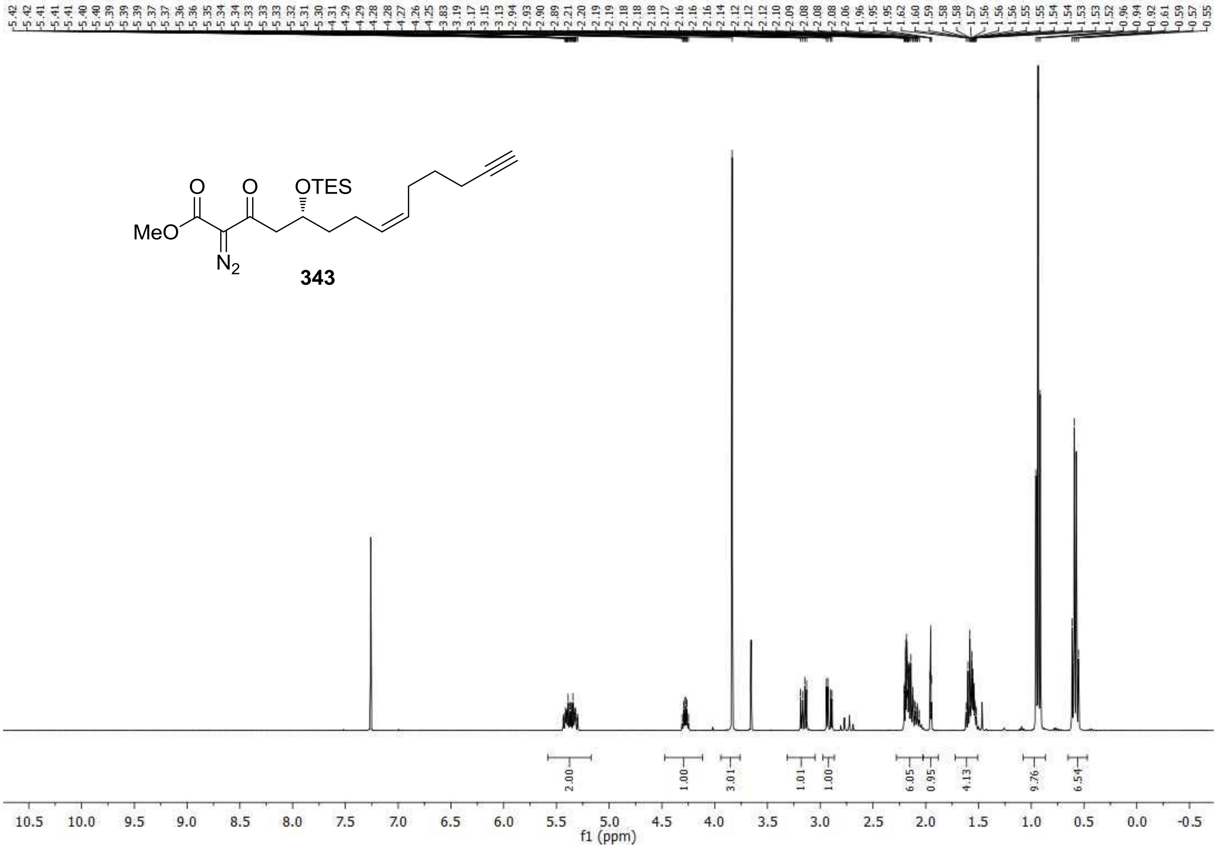
5.42 5.42 5.41 5.41 5.40 5.40 5.39 5.39 5.39 5.37 5.37 5.36 5.36 5.35 5.34 5.34 5.33 5.33 5.33 5.32 5.31 5.30 4.31 4.29 4.29 4.28 4.28 4.27 4.26 4.25 3.83 3.19 3.17 3.15 3.13 2.94 2.93 2.90 2.89 2.21 2.20 2.19 2.19 2.18 2.18 2.18 2.17 2.16 2.16 2.16 2.14 2.12 2.12 2.12 2.12 2.10 2.09 2.08 2.08 2.08 2.06 1.96 1.95 1.95 1.62 1.60 1.59 1.58 1.58 1.57 1.56 1.56 1.56 1.55 1.55 1.54 1.54 1.53 1.53 1.52 0.96 0.94 0.92 0.61 0.59 0.57 0.55
O
O
OTES
MeO
N2
2.00
1.00
3.01
1.01
1.00
6.05
0.95
4.13
9.76
6.54
10.5 10.0 9.5 9.0 8.5 8.0 7.5 7.0 6.5 6.0 5.5 5.0 4.5 4.0 3.5 3.0 2.5 2.0 1.5 1.0 0.5 0.0 -0.5
f1 (ppm)

343

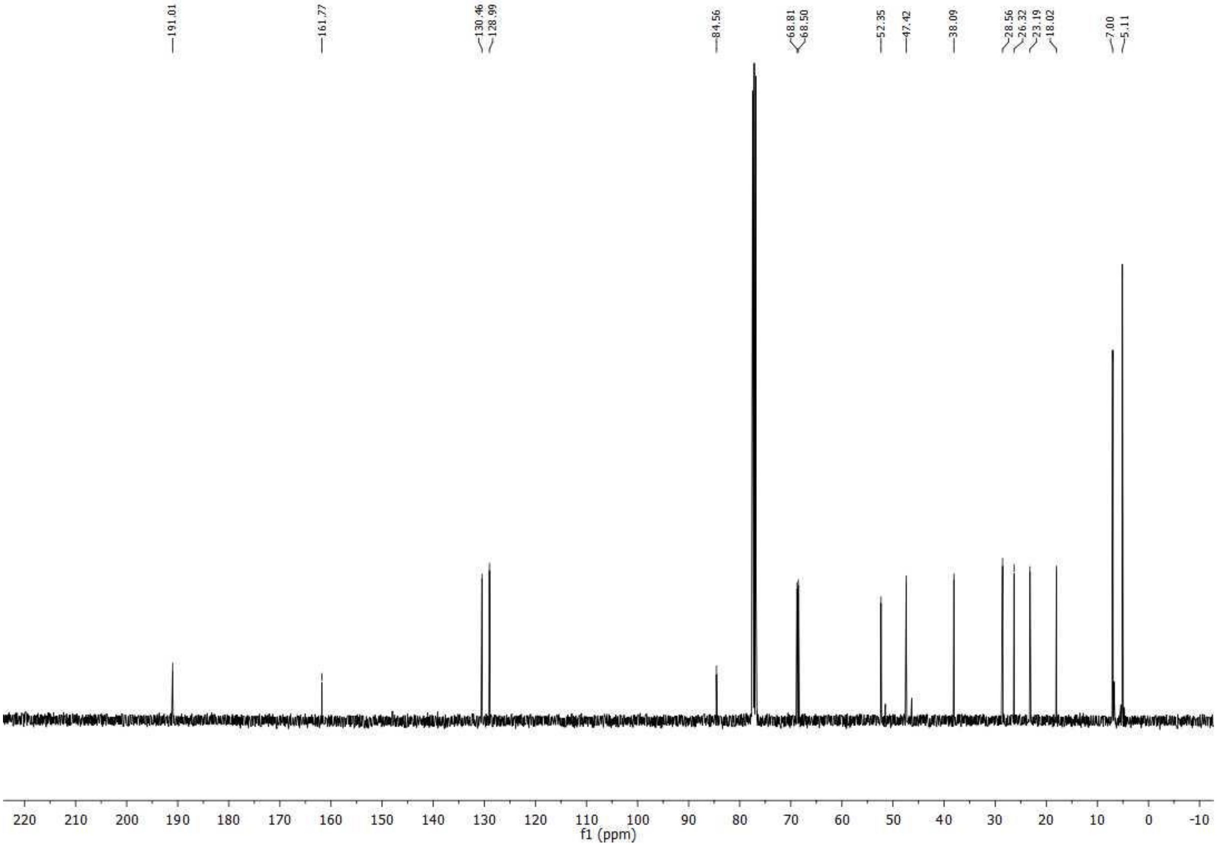
191.01
161.77
130.46
128.99
84.56
68.81
68.50
52.35
47.42
38.09
28.56
26.32
23.19
18.02
7.00
5.11
220 210 200 190 180 170 160 150 140 130 120 110 100 90 80 70 60 50 40 30 20 10 0 -10
f1 (ppm)

O

335

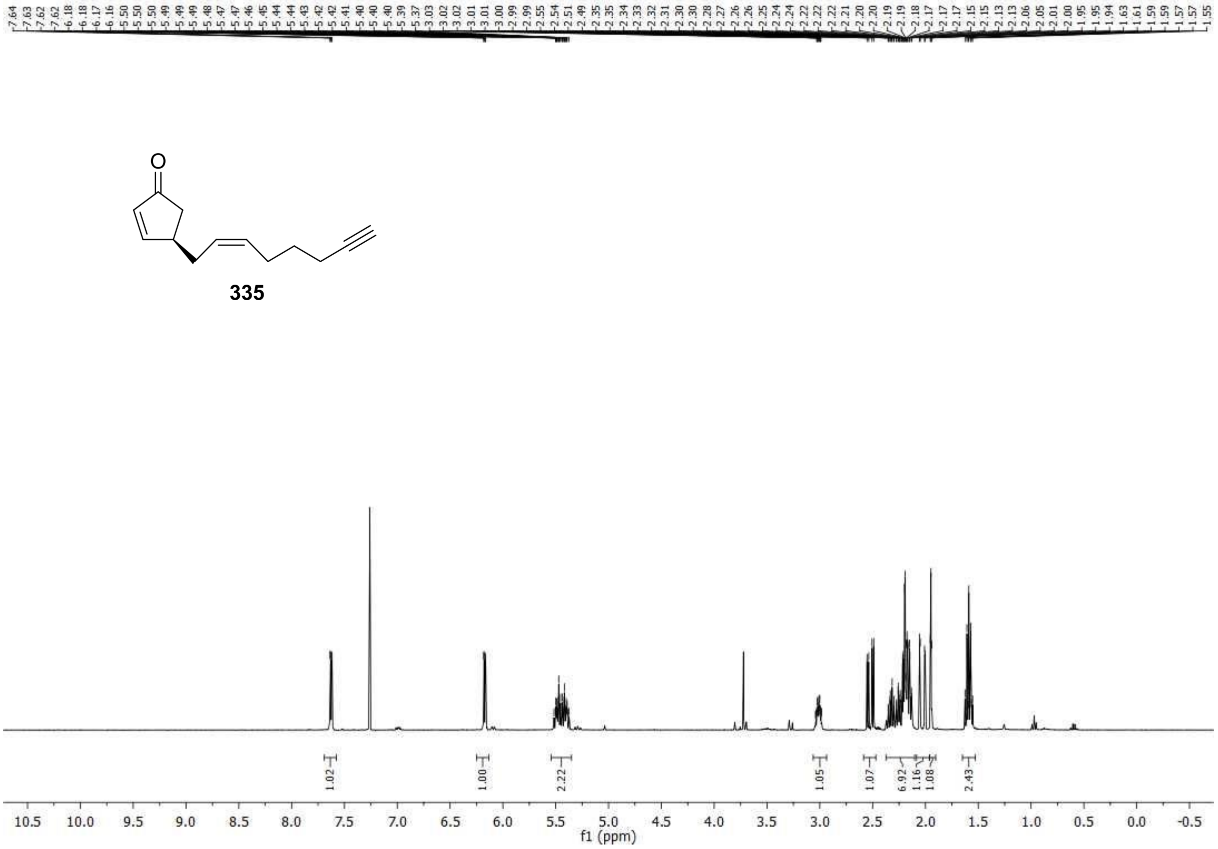
7.64
7.63
7.62
7.62
6.18
6.18
6.17
6.16
5.50
5.50
5.50
5.49
5.49
5.49
5.48
5.47
5.47
5.46
5.45
5.44
5.44
5.43
5.42
5.42
5.41
5.40
5.40
5.40
5.39
5.37
3.03
3.02
3.02
3.01
3.01
3.00
2.99
2.99
2.55
2.54
2.51
2.49
2.35
2.35
2.34
2.33
2.32
2.31
2.30
2.30
2.28
2.27
2.26
2.26
2.25
2.24
2.24
2.22
2.22
2.22
2.21
2.20
2.20
2.19
2.19
2.18
2.17
2.17
2.17
2.15
2.15
2.13
2.13
2.06
2.05
2.01
2.00
1.95
1.95
1.94
1.63
1.61
1.59
1.59
1.57
1.57
1.55
1.02
1.00
2.22
1.05
1.07
6.92
1.16
1.08
2.43
10.5
10.0
9.5
9.0
8.5
8.0
7.5
7.0
6.5
6.0
5.5
5.0
4.5
4.0
3.5
3.0
2.5
2.0
1.5
1.0
0.5
0.0
-0.5
f1 (ppm)

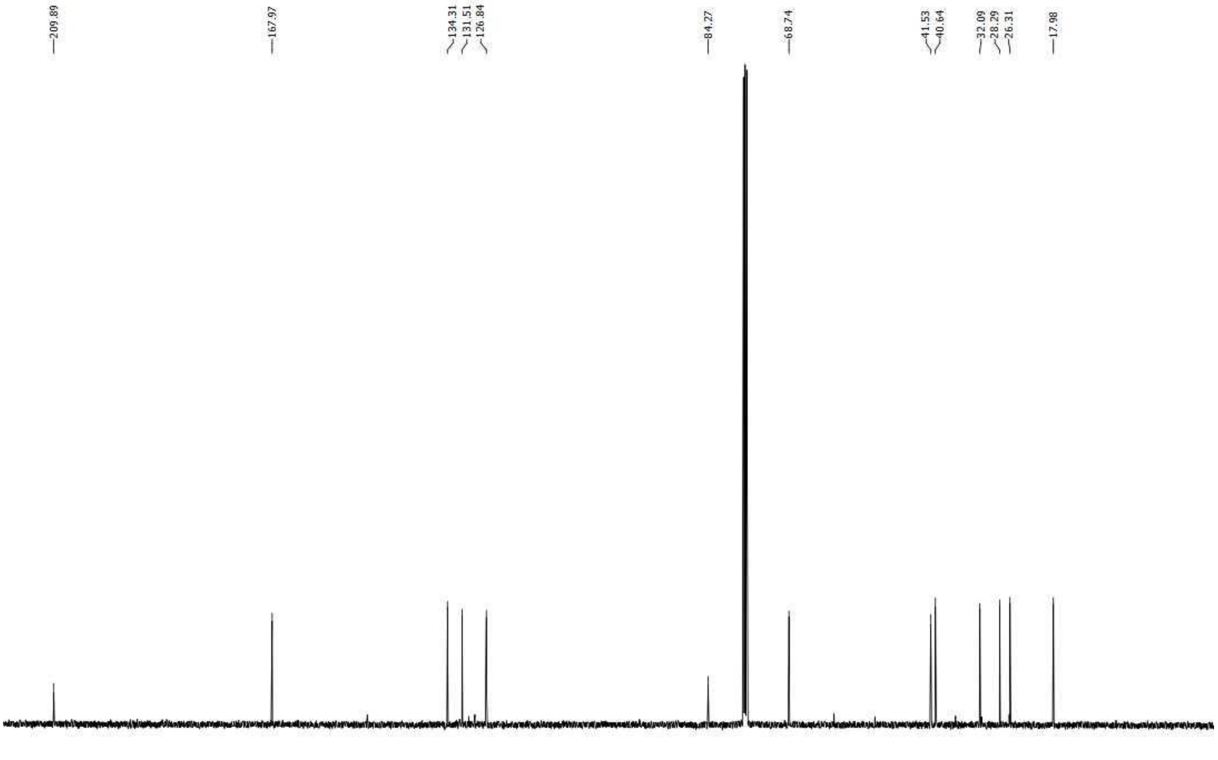
209.89
167.97
134.31
131.51
126.84
84.27
68.74
41.53
40.64
32.09
28.29
26.31
17.98
210
200
190
180
170
160
150
140
130
120
110
100
90
80
70
60
50
40
30
20
10
0
-10
f1 (ppm)

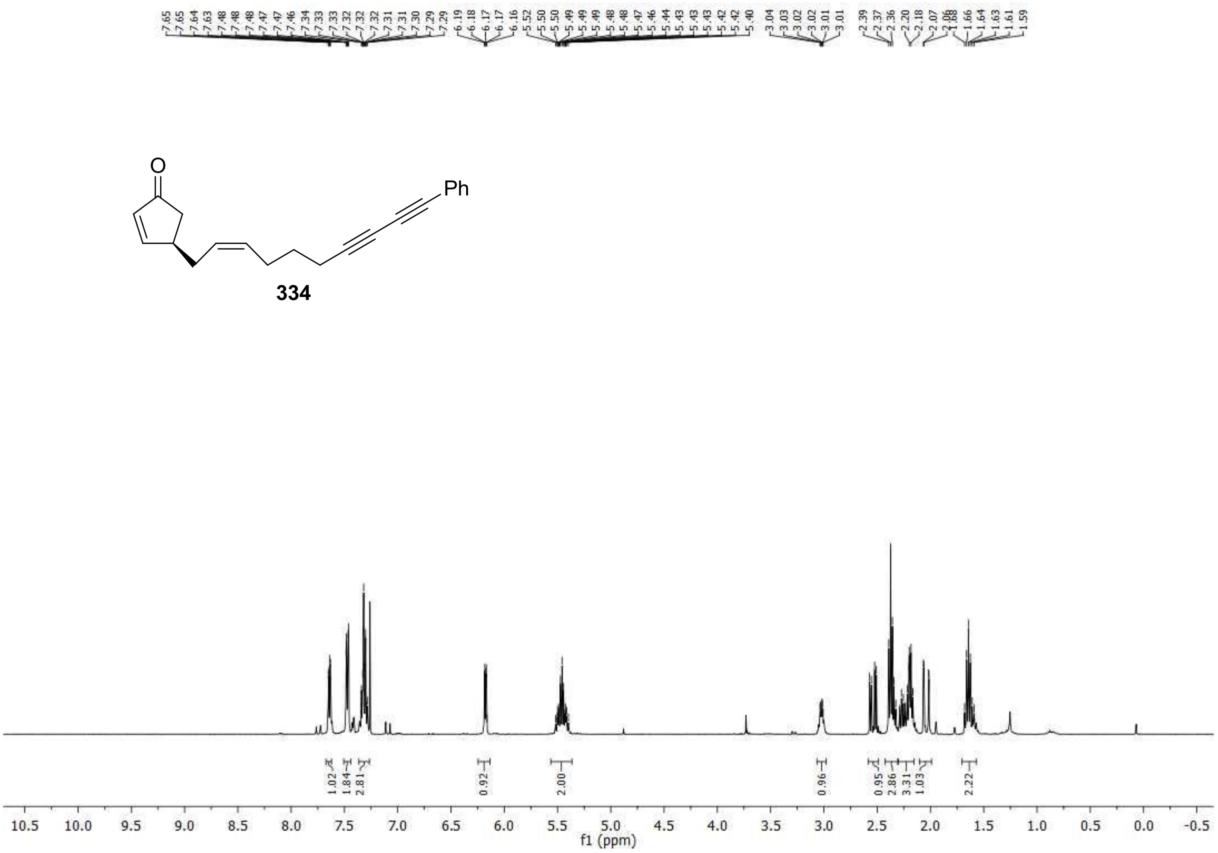
7.65
7.65
7.64
7.63
7.48
7.48
7.48
7.47
7.47
7.46
7.34
7.33
7.33
7.32
7.32
7.32
7.31
7.31
7.30
7.29
7.29
6.19
6.18
6.17
6.17
6.16
5.52
5.50
5.50
5.49
5.49
5.49
5.48
5.48
5.47
5.46
5.44
5.43
5.43
5.43
5.42
5.42
5.40
3.04
3.03
3.02
3.02
3.01
3.01
2.39
2.37
2.36
2.20
2.18
2.07
2.06
1.68
1.66
1.64
1.63
1.61
1.59
O
Ph
334
1.02
1.84
2.81
0.92
2.00
0.96
0.95
2.86
3.31
1.03
2.22
10.5
10.0
9.5
9.0
8.5
8.0
7.5
7.0
6.5
6.0
5.5
5.0
4.5
4.0
3.5
3.0
2.5
2.0
1.5
1.0
0.5
0.0
-0.5
f1 (ppm)

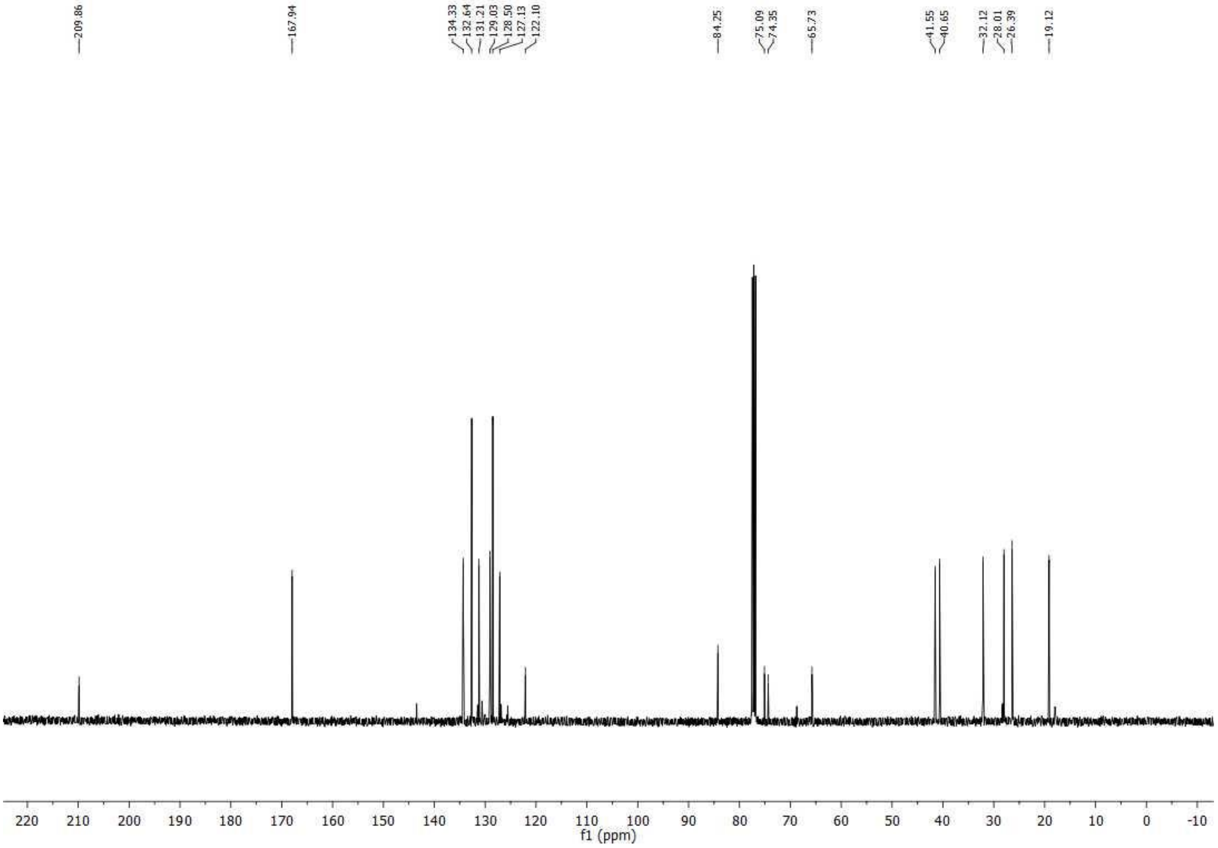
209.86
167.94
134.33
132.64
131.21
129.03
128.50
127.13
122.10
84.25
75.09
74.35
65.73
41.55
40.65
32.12
28.01
26.39
19.12
220
210
200
190
180
170
160
150
140
130
120
110
100
90
80
70
60
50
40
30
20
10
0
-10
f1 (ppm)

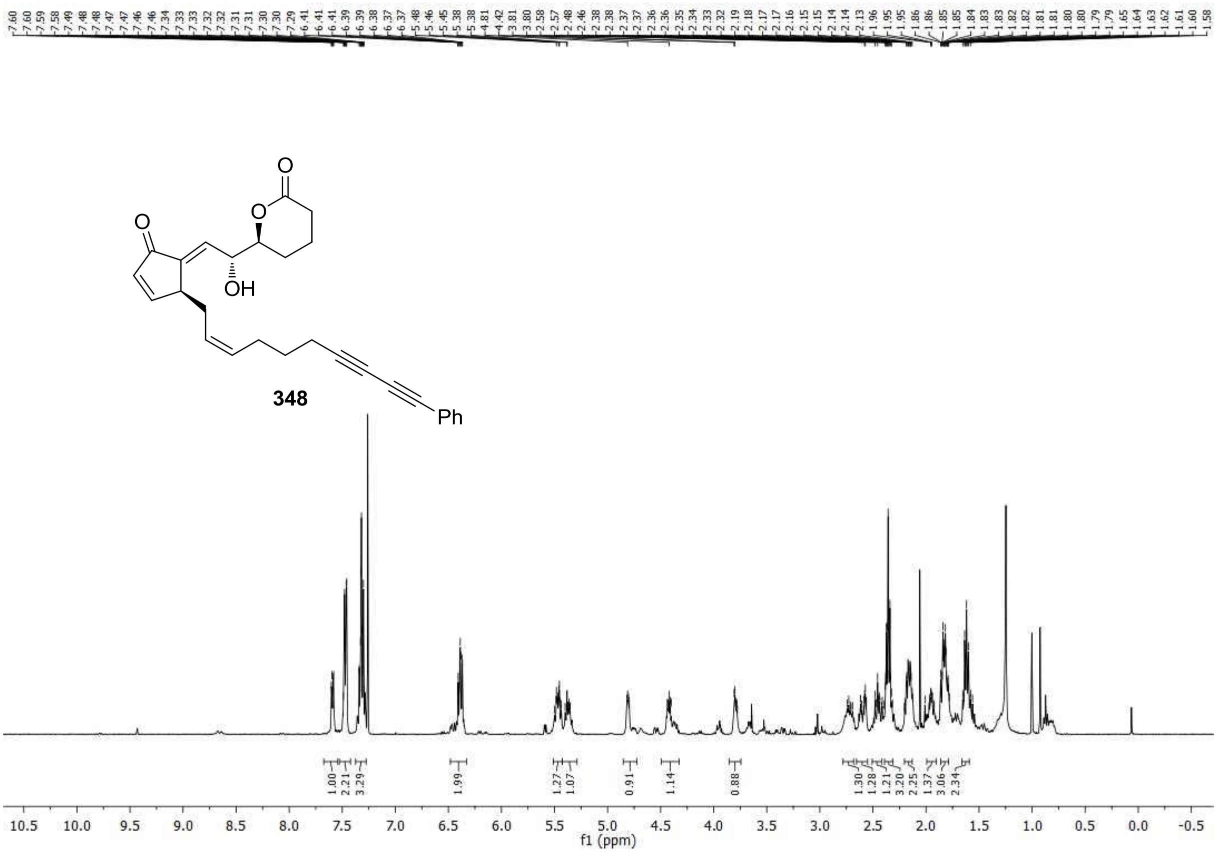

348

7.60 7.60 7.59 7.58 7.49 7.48 7.48 7.47 7.47 7.46 7.46 7.34 7.33 7.33 7.32 7.32 7.31 7.31 7.30 7.30 7.29 6.41 6.41 6.39 6.39 6.38 6.37 6.37 5.48 5.46 5.45 5.38 5.38 4.81 4.42 3.81 3.80 2.58 2.57 2.48 2.46 2.38 2.38 2.37 2.37 2.36 2.36 2.35 2.34 2.33 2.32 2.19 2.18 2.17 2.17 2.16 2.15 2.15 2.14 2.14 2.13 1.96 1.95 1.95 1.86 1.86 1.85 1.85 1.84 1.83 1.83 1.82 1.82 1.81 1.81 1.80 1.80 1.79 1.65 1.64 1.63 1.62 1.61 1.60 1.58
O
O
O
OH
Ph
1.00 2.21 3.29 1.99 1.27 1.07 0.91 1.14 0.88 1.30 1.28 1.21 3.20 2.25 1.37 3.06 2.34
10.5 10.0 9.5 9.0 8.5 8.0 7.5 7.0 6.5 6.0 5.5 5.0 4.5 4.0 3.5 3.0 2.5 2.0 1.5 1.0 0.5 0.0 -0.5
f1 (ppm)

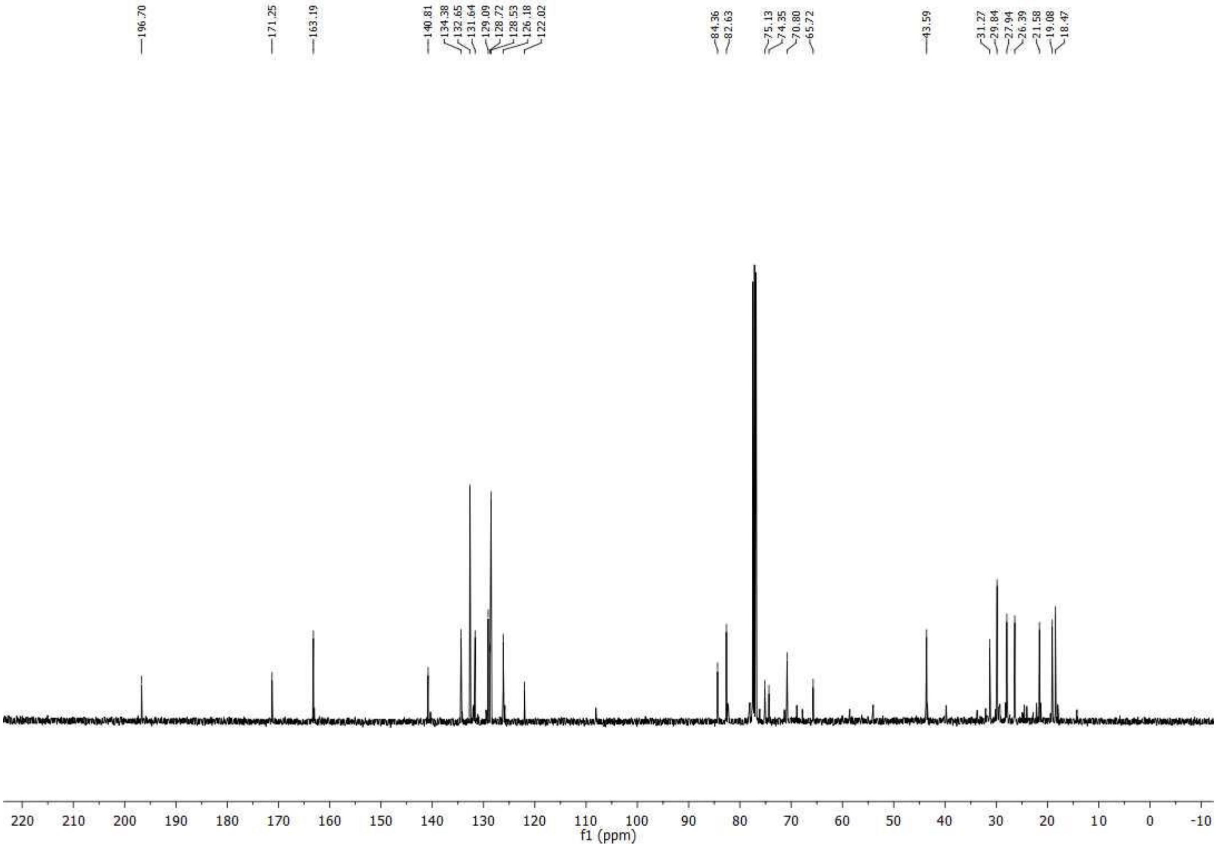

196.70
171.25
163.19
140.81 134.38 132.65 131.64 129.09 128.72 128.53 126.18 122.02
84.36 82.63
75.13 74.35 70.80 65.72
43.59
31.27 29.84 27.94 26.39 21.58 19.08 18.47
220 210 200 190 180 170 160 150 140 130 120 110 100 90 80 70 60 50 40 30 20 10 0 -10
f1 (ppm)

Curriculum Vitae

Born May 5, 1988 in Bad Säckingen, Germany

Education

09/1994 – 05/1998	Grundschule Obersäckingen, Germany
09/1998 – 05/2007	Abitur, Scheffel-Gymnasium Bad Säckingen, Germany
09/2007 – 06/2010	B. Sc. in Chemistry, ETH Zurich, Switzerland
09/2010 – 05/2012	M. Sc. in Chemistry, ETH Zurich, Switzerland
11/2011 – 04/2012	Master Thesis in the Group of Prof. K. C. NICOLAOU The Scripps Research Institute, La Jolla, USA “*Synthesis of Novel Macroheterocycles Through Intramolecular Oxidative Coupling of Furanoid β-Ketoesters*
06/2012 – 10/2016	Ph.D. Studies in the Group of Prof. ERICK M. CARREIRA ETH Zurich, Switzerland “*I. Total Synthesis of Pallambins A and B II. Ti(III)-Mediated Regioselective Epoxide Opening III. Synthesis of Raman-Active Epoxyisoprostane Analogs”*

Teaching Experience

09/2010 – 12/2010	Teaching assistant for introductory-level organic chemistry course, ETH Zurich, Switzerland
09/2013 – 02/2016	Teaching assistant for and advanced-level organic chemistry course, ETH Zurich, Switzerland
07/2015 – 06/2016	Head teaching assistant for an advanced-level organic chemistry course, ETH Zurich, Switzerland
11/2013 – 06/2016	Training of a laboratory technician apprentice, ETH Zurich, Switzerland
09/2012 – 06/2016	Supervision of two undergraduate students in the course of their semester projects, ETH Zurich, Switzerland

Fellowships

09/2011 – 04/2012	Otto-Bayer Fellowship, Bayer Science and Education Foundation, Leverkusen, Germany
10/2012 – 10/2015	Scholarship of the Swiss Chemical Industry, Zurich, Switzerland

Further Experience

06/2013 – 03/2015	Author of *Synfacts* (Thieme Publishing Group)
11/2014 – 03/2015	Head of the Carreira-Group *Synfacts* team